Pole slipping protection for small and medium sized embedded generation

Checksfield, M. J.

Award date:
1997

Awarding institution:
University of Bath

POLE SLIPPING PROTECTION FOR SMALL AND MEDIUM SIZED EMBEDDED GENERATION

Submitted by M J Checksfield,

for the degree of PhD

of the University of Bath

1997.

M J Checksfield

ProQuest LLC
789 East Eisenhower Parkway
P.O. Box 1346
Ann Arbor, MI 48106-1346

SYNOPSIS

This thesis describes a new power based digital protection algorithm which can be used to protect a synchronous embedded generation unit against pole slipping. Pole slipping can cause machine damage and disrupt the quality of supply. The likelihood of embedded generator instability and hence pole slipping has been studied and it is shown that the probability of embedded generator pole slipping is high. The new protection algorithm uses real and reactive power, and rate of change of real power to assess when the generator operates past the 'point of no return' and pole slipping is unavoidable.

An analysis of the conventional techniques used to detect pole slipping is given, along with the changes in plant which can be made to reduce the likelihood of pole slipping. The 'ideal' operating characteristics of a synchronous generator are presented and the changes to these characteristics which occur in embedded generation sets studied. The machine characteristics are used to derive the power based pole slipping algorithm, the basis of which is explained using the Equal Area Criterion method of stability assessment.

The algorithm has been implemented and tested in a commercially available microprocessor relay and has been shown to work correctly for a wide range of power system conditions using computer based simulations, laboratory model power systems, and field trials on three separate generators. The algorithm analysis has included pole slipping, loss of field, short circuit fault, generator synchronisation, loss of prime mover and other tests. The performance of the new algorithm has been compared with conventional pole slipping protection schemes using computer simulation software. The response of standard embedded generator protection schemes during pole slipping conditions has also been examined and it has been shown that the standard schemes will rarely trip when pole slipping occurs.

A summary of the results of the tests performed on the algorithm, conventional techniques and standard protection schemes has been compiled, and is followed by the conclusions. The thesis contains a set of appendices which contain the mathematical derivations of machine and algorithm characteristics, the setting procedures for conventional relays, embedded generator simulation data, published work and details on the implementation of the algorithm into a modern microprocessor relay.

ACKNOWLEDGEMENTS

I would like to express my gratitude to Miles Redfern for his supervision throughout the course. Thanks is also given to Professor A T Johns for allowing me to use the facilities of the School of Electronic and Electrical Engineering.

I also wish to thank Martin Balchin, Rod Dunn, Jim Barrett, Jerzy Grzejewski, Alexon 'AAW' Chiwaya, Rich Liewet, David Briggs, Chris Groom, Phil Sapiano Matt Collins and everyone in the school office and workshop. My special thanks is expressed to James Hodgeson who had the questionable pleasure of proof reading the thesis.

My thanks also extends to my sponsoring company, GEC Alsthom, T & D, Protection and Control, Stafford for providing financial and technical support as well as their resources. Thanks is given specifically to Geoff Weller, Tony Yip, Paul Hindle, Dave Banham, Les Denning, Peggy Ling, Margaret Leese, Mike Tweed, Andy Ellis, Denise Shed, and Ivor Scott .

Thanks is also given to Scottish Power, Scottish Hydro, Midlands Electricity and ECC/Dale Machines. My gratitude is also expressed to Alex Wallis of SWE plc for providing 'real world' information. My gratitude also extends to the Engineering and Physical Sciences Research Council and the Royal Academy of Engineers, who both have provided financial support to enable me to complete this work in addition to attending international conferences.

CONTENTS

Chapter 1
INTRODUCTION

Chapter 2
CONVENTIONAL TECHNIQUES FOR DETECTING AND METHODS FOR PREVENTING POLE SLIPPING

Chapter 3

SYNCHRONOUS GENERATOR CHARACTERISTICS

Chapter 4

THE NEW POWER BASED POLE SLIPPING ALGORITHM

Chapter 5

ALGORITHM EVALUATION STUDIES

Chapter 6

RESULTS OF ALGORITHM EVALUATION TESTS

Chapter 7
SUMMARY OF RESULTS

Appendix A

DERIVATION OF THEORETICAL IMPEDANCE, POWER VARIATIONS AND ALGORITHM SETTING EQUATIONS

Appendix B

SETTING OF CONVENTIONAL IMPEDANCE RELAYS

Appendix C

DATA FOR GENERATORS AND SYSTEMS USED FOR ALGORITHM TESTS

Appendix D

PUBLISHED WORK

Appendix E

IMPLEMENTATION OF THE POWER BASED POLE SLIPPING ALGORITHM INTO A COMMERCIAL MICROPROCESSOR RELAY

Appendix F

EXAMPLES OF COMPUTER FILES USED TO TEST THE POLE SLIPPING ALGORITHM

LIST OF SYMBOLS AND ABBREVIATIONS

'lag'	The number of samples between check points in 'Pm' estimation function
$(\Delta P/\Delta t)$	Rate of change of power
$(\Delta P/\Delta t)_{min}$	pole slipping algorithm rate of change of power trip setting
$(\Delta P/\Delta t)_{tran}$	Transient saliency rate of change of power setting
$(\Delta P/\Delta t)_{fact}$	Minimum magnitude value for $(\Delta P/\Delta t)_{min}$
ϕ_a	Armature flux
ϕ_d	Direct axis flux
ϕ_f	Field flux
ϕ_q	Quadrature axis flux
ANN	Artificial Neural Network
ATP	Alternative Transients Program
AVR	Automatic Voltage Regulator
CCT	Critical Clearing Time
CHP	Combined Heat and Power
CSP	Critical Stability Point
CT	Current Transformer
δ	Load angle
δc	Critical Clearing Angle
DC	Direct Current
δ_m	Machine angle (angle between E and Vg)
δ_o	Initial load angle
DSG	Dispersed Storage and Generation
E	Generator steady state internal voltage
Ed	Direct axis voltage
Eg	Generator voltage behind impedance
Eg/Es	Ratio of source (Es) to generator (Eg) internal voltages
EMF	Electro Motive Force
EMTP	ElectroMagnetic Transients Program
EPRI	Electric Power Research Institute
EPROM	Erasable Programmable Read Only Memory
Eq	Quadrature axis voltage

Eq'	Voltage behind transient reactance
$ErIr^*$	Apparent power
Er	Relay voltage
Es	Source voltage behind impedance
f	System frequency (Hz)
GPS	Global Positioning System
H	Generator inertia constant
HP	Horse Power
HV	High Voltage
I	generator stator current (RMS value)
I"	Sub-transient fault current
i_a, i_b, i_c	instantaneous a,b,c line current
Ic	Cosine fourier filter output of signal, i
Id	Generator direct axis current
IDMT	Inverse Definite Minimum Time
In	Relay nominal current
Iq	Generator quadrature axis current
Ir	Relay current
Is	Sine fourier filter output of signal, i
Ld	Direct axis synchronous inductance
Lff	Field winding inductance
LOE	Loss of Excitation
LOF	Loss of Field - identical to loss of excitation
m	Zg/Ztot
mmf	MagnetoMotive Force
NFFO	Non Fossil Fuels Obligation
OT	Over Torque, a type of pole slip
P	Real power
$P_{(n - lag)}$	Sample value of real power 'lag' samples ago
$P_{(n - (2*lag))}$	Sample value of real power '2 * lag' samples ago
$P_{(n)}$	Present sample value of real power
P_a	Accelerating power on generator rotor
$P_{add\text{-}loss}$	Additional losses which occur as a result of generator transient operation

P_{as}	Generator asynchronous real power output
PC	Personal Computer
Pfact	coefficient used to calculate Pt from estimate of Pm
P_{loss}	Losses in generator during steady state operation
Pm	Prime mover input power
PPSS	Programmable Power System Simulator
PS	Pole Slip
PSM	Plug Set Multiplier
Pt	Pole slipping algorithm real power trip setting
Ptol	Real power tolerance band in Pm estimation function
pu	Per Unit
θ	$\sin^{-1}$ (R/Z) (for generators)
Q	Reactive power
Q_{as}	Generator asynchronous reactive power output
Qtrip	Pole slipping algorithm reactive power trip setting
r	External resistance, between generator terminals and infinite bus
R	Generator stator resistance
REC	Regional Electricity Company
Rf	Field winding resistance
RLC	Resistance, Inductance, Capacitance model of cable or overhead line
RX	Resistance/Reactance (used with reference to impedance diagrams)
S	Apparent Power (VA)
s	generator rotor slip
SCADA	Supervisory Control and Data Acquisition
SF6	Sulphur hexaflouride
Sgen	Generator rating
t	time
Ta	Generator armature time constant
Td'	Direct axis short circuit time constant
Td"	Direct axis sub-transient short circuit time constant
Tdo'	Direct axis open circuit time constant
Tdo"	Direct axis sub-transient open circuit time constant
Te	Machine air gap torque

TMS	Time Multiplier Setting
Tq"	Quadrature axis sub-transient short circuit time constant
Tqo"	Quadrature axis sub-transient open circuit time constant
V	infinite busbar voltage
v_a, v_b, v_c	Instantaneous a,b,c phase voltage
Vg	Generator terminal voltage
VT	Voltage Transformer
ωr	Rotor angular speed
ωs	Synchronous angular speed
X	External reactance between generator terminals and infinite bus
X_{comb}	Combined value of synchronous reactance plus any external reactance.
Xd	Direct axis synchronous reactance
Xd'	Direct axis transient reactance
Xd"	Direct axis sub-transient reactance
Xq	Quadrature axis synchronous reactance
Xq'	Quadrature axis transient reactance
Xq"	Quadrature axis sub-transient reactance
Z	$\sqrt{(R^2 + Xq^2)}$
Zd'	Generator transient impedance
Zg	Generator operational impedance
Zo	Zero sequence impedance
Zr	'Apparent' impedance as seen by a protection relay
Zs	Source impedance
Ztot	combined impedance of generator and source

Chapter 1
INTRODUCTION

1.1 EMBEDDED GENERATION

Embedded generation or Dispersed Storage and Generation units (DSG) is that generation which is connected in parallel with a utility's distribution network. Until recently, the bulk of electricity was generated in large power stations and transferred to consumers via the transmission network and utility distribution system. Recent changes in legislation in the UK[1,2] and the USA[3] have granted permission for local embedded generation to operate in parallel with utility networks. This has resulted in some of the electricity generation occurring adjacent to the loads and within the distribution networks.

There are several factors which have contributed to the increased number of small and medium sized embedded generation units being commissioned. The past two decades have seen increased economic, political and environmental pressures on the production of electricity which have increased interest in incorporating embedded generation into public utility networks [4,5,6]. Combined Heat and Power Schemes improve the overall efficiency of plant by using waste heat from industrial processes to run generators, or vice versa. The current trend in alternative energy sources such as landfill gas, waste incineration and renewables like wind, tidal, solar, mini-hydro and bio-fuel schemes has resulted in a large number of embedded generators being installed. The Non Fossil Fuel Obligation (NFFO) acts as an incentive since it entitles alternative energy schemes to receive premium prices for their electricity.

1.2 PROBLEMS ASSOCIATED WITH EMBEDDED GENERATION

Connecting a small or medium sized generator to operate in parallel with a utility distribution network causes problems concerning safety, quality of supply, earthing and stability[7,8,9,10,11,12,13]. Safety problems result because in a traditional network, disconnecting the main source of supply de-energises the network, if embedded generation is connected, part of the network may remain energised. Quality of supply concerns voltage regulation,

frequency regulation, and harmonics. Regional Electricity Companies (REC's) have to maintain their supplies within pre-defined voltage and frequency limits, and the operation of an embedded generator can create difficulties since the generator may corrupt the utility supply if operated incorrectly. Short circuits on the utility distribution system, and faults in a synchronous embedded generator's control equipment can cause the generator to become unstable. This instability will result in pole slipping, which may compromise the quality of utility supply as well as causing plant damage.

Special precautions are therefore required to prevent the embedded generator degrading the quality of supply to other utility customers. The regulating authorities require the utilities to ensure that the embedded generators will not detract from the quality of supply to other customers and have produced guidelines which define the general protection requirements for protection against all types of faults and abnormal operating conditions. These guidelines are published as 'G59' [14] and 'ET113' [15] in the UK and 'ANSI 1001' [16] in the USA. It is the embedded generator operator's responsibility to supply the necessary level of protection and control equipment for the embedded generator. The utility to which the generator is connected will specify the level of protection that they require. Meeting these protection specifications[17,18,19,20,21,22] can be time consuming and expensive for the embedded generator operator. There is therefore a need for the availability of in-expensive relays which offer the required level of protection and do not require complicated settings.

A widespread complaint from potential operators of embedded generation that the conventional utility grade relays are too expensive. For a small scheme, the protection costs can be comparable to that of the generator itself. To make any small generation scheme economically viable, a low cost multi-functional protection package is therefore required[23,24,25,26,27,28,29,30]. Using a microprocessor based relaying platform provides numerical computing power which can be used to enhance existing protection algorithms or devise completely new algorithms which were not possible with conventional static or electro-mechanical relays[31]. The new pole slipping detection algorithm presented in this thesis is one such algorithm which takes advantage of the computing power available in a modern microprocessor relay platform.

1.3 POLE SLIPPING

A potential difficulty with the operation of an embedded generator is to ensure that the electrical system can absorb the electrical power produced from the mechanical power provided to the generator. If too much mechanical power is provided to the generator and it is unable to deliver that power to the system, instability results. This is referred to as pole slipping.

Pole slipping occurs when the rotor of a synchronous machine slips one pole pitch with respect to the stator magnetic flux, which is synchronised to the stator electrical supply. Two or more machines operating in parallel are required for a pole slip to occur. If there is just one machine then the rotor speed changes result in a change in the frequency of the electrical supply produced by the machine. Pole slipping results from the mismatch in frequencies of two or more machines. For the case of an embedded generator pole slipping, the other machine can be regarded as the utility infinite bus[15]. If the infeed capacity at the terminals of the embedded generator is more than 40 to 50 times the rating of the generator, then the utility infeed can be considered infinite.

The term 'pole slipping' is used only when the field coil on the rotor is excited. Field coil excitation produces a magneto-motive force (mmf) which drives a flux that links the stator and rotor. The points where the magnetic flux leaves and enters the rotor structure can be thought of as magnetic poles, similar magnetic poles will be formed on the stator due to the three phase alternating current flowing in the stator windings. Figure 1.1a shows the magnetic poles perfectly aligned in a machine operating at no load. When the machine is operating as a generator, the generator rotor runs ahead of the rotating flux field produced by the stator, as shown in Figure 1.1c, and in the phasor diagram of Figure 1.1d. In this state, the magnetic poles move out of alignment and an electromagnetic torque, Te, results which rotates at speed ωs, thus producing power. During normal stable operation, the 'north' pole of the rotor is attracted to the 'south' pole of the stator, and vice versa. During pole slipping the generator rotor speed, ωr is different to the electrical supply angular speed, ωs, and the rotor magnetic poles therefore 'slip' past the stator poles, and this is the origin for the term 'pole slipping'. This explains the large fluctuations in torque which result from pole slipping since for the first half of the pole slip cycle ($0° < \delta < 180°$), the magnetic poles attract each other producing a generating torque, whilst for the other half of the pole slip cycle ($180° < \delta < 360°$), the

magnetic poles repel each other, producing a motoring torque.

If the machine's field coil is not excited, the machine operates 'asynchronously'. Since there is no excitation on the rotor, there can be no rotor magnetic poles and hence no pole slipping. This mode of operation is referred to as 'asynchronous running' [32].

Technically speaking, pole slipping is classed as asynchronous running. The term 'asynchronous running' will be used in this thesis to refer only to operation out of synchronism with the rotor winding un-excited. This condition may occur during a loss of field, or loss of excitation condition, or the generator may even be operated in this mode as a means of absorbing reactive VArs from the power system [33,34]. In reality, the rotor will still have weak magnetic poles when there is no excitation, due to residual flux and the magnetic and electrical asymmetry in the rotor. The difference in the use of the two words is justified due to the radical difference between the two modes of operation. With pole slipping, the excitation on the rotor causes severe voltage, power, and reactive loading surges to occur. Asynchronous operation on the other hand, results in relatively small fluctuations in the generator voltage and currents in round rotor synchronous machines. Salient pole machines will produce larger fluctuations in voltage and current during asynchronous operation, due to the reluctance torque component produced by their saliency.

1.4 THE CAUSES OF POLE SLIPPING AND ASYNCHRONOUS RUNNING

Pole slipping occurs when there is insufficient electromagnetic torque to hold the rotor in synchronism with the stator magnetic flux. There are several reasons why the electromagnetic torque produced by the interaction of stator and rotor flux is not strong enough to counteract the driving torque of the prime mover and therefore stop the rotor accelerating to a speed above synchronous speed. Equation 1(1) gives the relationship between generator output power, P, and machine load angle, δ, for a machine operating on an infinite bus of voltage, V, during steady state operation.

$$P = \frac{EV}{Xd}\sin(\delta) + \left(\frac{1}{Xq} - \frac{1}{Xd}\right)\frac{V^2}{2}\sin(2\delta) \qquad 1(1)$$

Where E is the steady state excitation speed voltage, Xd is the direct axis synchronous

reactance, and Xq is the quadrature axis synchronous reactance. It can be seen that if E or V is decreased the maximum amount of power and therefore torque that the machine is capable of producing decreases. If this maximum amount of electromagnetic torque falls below the prime mover's mechanical input torque, then a net accelerating torque will result causing the rotor to rise above synchronous speed and the machine to pole slip. When the generator rotor travels above synchronous speed, the machine load angle, δ, increases. Equation 1(1) shows that once the machine load angle exceeds 90°, the generator output power decreases with an increase in machine load angle. If the machine load angle has exceeded 90° and the electromagnetic torque is less than the prime mover input torque, then the generator is operating in an unstable manner and a pole slip will result.

The discussion so far has only involved steady state operation, most pole slips which occur result from a transient disturbance on the generator such as a power system short circuit fault, or line switching operation.

1.4.1 The Equal Area Criterion

The Equal Area Criterion is one of the simplest methods for assessing generator stability for a given transient disturbance. If the power/machine load angle curves for all states of power system operation are known, then generator stability and hence the possibility of pole slipping can be ascertained for a given disturbance.

Consider the case where a transient disturbance results from a three phase fault on one side of a double circuit line as shown in Figure 1.2a [35]. The fault is removed by disconnecting the faulty circuit, leaving the healthy side of the line to transfer power at a reduced capacity. The power/load angle curves and equal area representation of this scenario is shown in Figure 1.2b.

The pre-fault curve corresponds to the initial operating condition, where both lines are transferring power. In this condition the embedded generator's power transfer capability is at its maximum. The fault duration curve represents the generator's power/load angle characteristic during the fault period. The three phase fault severely reduces system voltage so that power transfer is impaired. The post fault curve depicts the power transfer capability once the faulty line has been disconnected, the power transfer capability is reduced due to an increase in the interconnecting impedance.

The generator's prime mover input power is shown by the line Pm. The interception of the pre-fault output curve and prime mover input curve gives the initial machine load angle $\delta 1$. When the fault occurs the generator's output power characteristic drops down to the fault duration curve. The resulting discrepancy between input and output powers produces a net accelerating torque on the generator rotor. As the rotor accelerates to a speed above synchronous speed, the machine load angle increases.

In this example, when the fault is removed, corresponding to a load angle of $\delta 3$, the generator's output power jumps up above the line Pm to the post fault curve. This occurs because the system voltage is restored. This mismatch in generator input and output powers results in a net retarding force on the generator rotor. Since the rotor is now travelling above synchronous speed, the initial action of the retarding force is to remove kinetic energy from the rotor, and return the rotor towards synchronous speed. If the rotor is returned to synchronous speed before machine load angle δc is reached, then the generator will remain stable for that disturbance. Once the generator rotor is at synchronous speed, any extra retarding force will slow it to below synchronous speed, causing the machine load angle to decrease back towards its new operating angle, $\delta 2$.

If the rotor does not reach synchronous speed by machine load angle δc, then the generator rotor will again start to accelerate because beyond δc, the electrical energy out is less than the mechanical energy in, causing an accelerating torque once more. This is the unstable situation which results in the rotor travelling above synchronous speed and the generator pole slipping. If the generator is not able to counteract the accelerating forces during the pole slipping cycle it will continue to pole slip until the generator governor decreases the input torque, Pm, or the generator is disconnected from the power system.

The Equal Area Criterion [36,37] states that the accelerating energy on the rotor due to a disturbance can be represented by area 'A', whilst the decelerating energy is represented by area 'B'. For synchronism to be lost, the net accelerating energy for a given disturbance must exceed the net decelerating energy, i.e a pole slip will occur if area 'A' is greater than area 'B'. It can be seen from Figure 1.2b that the limiting point for stability occurs when the generators output power falls below its input power, this point is known as the *Critical Stability Point* (CSP) and occurs at the load angle δc. If the generator operates past this point, then stability cannot be maintained, and a pole slip will occur.

Figure 1.3a shows the same Equal Area Diagram as in 1.2b, and also shows the generator load angle characteristic for a generator losing synchronism following a sudden transient shock to the generator [35]. It can be seen that once the generator operates past the CSP, it accelerates quickly into the pole slip because in addition to the prime mover power accelerating the rotor, the generator also draws power from the utility supply as it travels through its motoring region.

The limiting case for stability occurs when the acceleration energy area equals the deceleration energy area, resulting in zero net accelerating torque for the disturbance. In this instance, the rotor will swing up to load angle δc, and then swing back down. The duration of the three phase fault which causes this condition is referred to as the Critical Clearing Time (CCT) since any fault whose duration is longer than this will cause generator instability.

The three phase fault discussed in this example is the most severe fault possible in terms of generator stability because the generator terminal voltage is reduced to a very low value, preventing any electrical power transfer from the generator. At its most extreme, the three phase fault when located close to the generator's terminals will reduce the generator's voltage to zero and no power transfer out of the generator will be possible.

Other faults can produce instability, however an increased fault duration is necessary compared with the three phase fault since some load is still maintained, and therefore there is less accelerating energy going into the rotor. In terms of a fixed fault duration, one study found [38] that the rotor displacement with a phase to phase fault is one quarter that of a three phase fault. Similarly, a phase to ground fault only produces one seventh of the rotor swing, whilst a two phase to earth fault gives five eighths displacement. It is important to note that these figures do not dictate the stability of a generator to a disturbance entirely, since stability is also dependent on the post fault impedance.

Pole slipping can also be invoked by a sudden change in transfer impedance between generator and load, since an increase in transfer impedance will cause a decrease in the maximum output power of the machine. More commonly, pole slipping of embedded machines will be caused by long fault clearance times. The fault clearance times are necessary on distribution systems protected by IDMT type relays to provide adequate grading [17,39,40]. One study [41] found that the minimum clearing time for industrial feeder

short circuits was 0.5 seconds, whilst another [42] stated typical clearing times in the range 0.5 to 1 second.

Faulty excitation systems may also cause the generator to pole slip since they may weaken the field so that the generator is unable to maintain synchronism. Figure 1.3b shows the Equal Area Diagram for a pole slip resulting from a loss of steady state stability. This situation may arise due to insufficient excitation, which takes the peak output power of the generator below the input power. It could also be caused by increasing the prime mover input power without a corresponding increase in excitation. Both of these conditions may result from operator error, or faulty control systems[43].

Complete loss of field is more likely however, since faults can develop in many different locations in the excitation circuit, such as slip rings, field windings and exciter windings. Operator error may also cause a loss of field condition due to the field breaker being accidentally tripped[28,44]. The generator AVR may counteract a partial field fault by boosting field current, in this condition the generator will not lose synchronism, but may sustain damage through over-heating or vibration[45]. Complete field failure will eliminate all synchronous torque except reluctance torque, and asynchronous running will therefore result. An exception to this occurs with a lightly loaded salient pole generator where the reluctance torque component may be sufficient to hold the rotor in synchronism.

The effects of asynchronous running are not usually as severe as pole slipping. With no field on the rotor, the electromagnetic torque pulsations produced as a result of the rotor and stator magnetic field slipping past one another are dictated only by the electrical and magnetic asymmetry in the machine producing a reluctance torque. The Equal Area Diagram for the loss of field condition is shown in Figure 1.3c, note that unlike Figures 1.3a and 1.3b the diagram only contains the first half of the power load angle characteristic. When a short circuit occurs in the field circuit, the generator flux decays slowly, resulting in the generator synchronous output power falling to zero. It should be noted that this diagram does not show the asynchronous component of torque generated from the rotor travelling above synchronous speed. This can be significant in some generators, allowing the machine to continue to generate a significant amount of power.

If a generator loses its field from full load, then it is vital that it be disconnected quickly, since the generator will operate at values of slip as high as 5 %. At this rate of slip high

levels of induced currents can flow in the rotor, and the stator current can rise to above twice its rated value. With such high currents, rotor and stator over-heating can occur quickly, and the generator will draw excessive reactive power from the system. This may depress system voltages and thus adversely effect the performance of nearby machines and generators[42,46] . The depression in system voltage can cause instability in other machines, and in extreme cases, cause a cascading loss of synchronism of machines nearby [24,47].

1.5 DAMAGE CAUSED BY POLE SLIPPING

The damage caused by pole slipping to the machine is dependent on the amount the machine has been over designed, if the machine has a sufficient reserve in terms of shaft rating and thermal capacity, then a pole slipping event may cause no machine damage at all. However, if the machine does not have sufficient reserves, damage can result.

1.5.1 Machine Damage Resulting from Pole Slipping

The extent of the damage caused to the machine is dependent on the rating of the bus which the generator is connected to, the speed of the pole slip, and the overcapacity rating of the machine. When the fault level of the utility system is high in comparison to the generator rating, the currents experienced during pole slipping will be of a higher magnitude than three phase fault levels. Since machine windings are only braced for three phase fault levels, the mechanical forces on the windings produced by these higher current levels during pole slipping will loosen and deteriorate the windings[42].

In addition to the high stator currents produced as a result of synchronising forces, an additional component of stator current will be produced as a result of the machine acting as an induction generator. These currents are highest when the speed of the machine has risen above the peak of it's torque/slip curve[35, 48].

Synchronous machines are not designed to be operated as induction generators, the induced slip frequency currents that flow in the rotor body, damping circuits and excitation windings can result in serious overheating if prolonged operation is permitted[49]. The rotor body and damper circuits are especially prone, since deep current penetration due to low frequency currents contributes a high heating component. In one pole slipping test performed on a 60 MW machine[50], slight blueing of the rotor end rings had occurred

after one minute of operation, indicating that the conditions had taken the machine close to its safe operating limits.

In most machines, stator end region overheating is also likely to result from prolonged operation, due to an increased axial component of leakage flux[48]. Investigations into the type of end ring material showed that a magnetic end ring will experience a greater temperature rise than a non-magnetic end ring[50].

Pole slipping can also cause damage to excitation systems. Pole slipping induces large currents in the field winding, which compensate the high mmf of the stator windings[49]. The magnitude of these currents peaks as the load angle approaches 180°, because the rotor and stator become magnetically disconnected at this point. The field winding will try to maintain constant flux linkage and will therefore compensate for the missing flux contribution from the stator. Once past the 180° point, the currents drop rapidly as the stator and rotor flux begin to link once more, but in the opposite sense (in a motoring condition) and the rotor current must decrease rapidly to maintain the mmf balance. Rectifier excitation systems will not permit the rotor current to reverse, thus ending the mmf balance and producing a rapid flux change. This high rate of change of flux induces a large reverse voltage across the rectifiers which can cause reverse breakdown if they are not sufficiently over rated[51].

Recently, concern has increased over the effect power system disturbances have on generator shafts, out of phase re-closures and pole slipping can both produce potentially damaging shaft torques. During pole slipping, if the frequency of the high currents and pulsating torques produced fall upon a natural frequency of the shaft, then the shaft will be torsionally excited into a resonance condition, exposing the shaft to oscillatory stress. Particularly at risk are turbine generator shafts[52] since the bladed rotating parts of the turbine interact with the couplings and reduced diameter shaft extensions to form a torsionally resonant system. One study[53], found that the generator-exciter shaft section experiences the highest stresses. It was found that all of the fatigue life of this shaft section was used after one pole slip for a shaft over design rating of two. For an over design rating of five, no significant damage occurred.

The study indicated that the maximum torques and torsional stresses occur during the first period of oscillation after each torsional impulse, and it is this period where the shaft

damage usually occurs. It is therefore advantageous to disconnect the generator from the system *before* a pole slipping event occurs in the hope that the torsional impulse will be prevented. It was also indicated that the cumulative effects of smaller disturbances taken together, due to less severe transients, might in the long run lead to significant shaft damage.

1.5.2 The Impact of Pole Slipping on the Rest of the Power System

The 'system centre' is an expression often used to describe the point in the power system where the contribution from the generator equals that from the rest of the system. At this point the voltage fluctuations produced by pole slipping will be at their most severe, the voltage may even fall to zero. For the normal generator/infinite bus situation the system centre appears inside the generator, or its step up transformer. However, if the utility infeed is low, then the system centre may appear in the load network. The location of the system centre is not fixed, and it will move around as the effective impedance of the generator and nearby machines changes. The generator terminal voltage will normally drop during pole slipping as the load angle approaches 180°. Most generators located on industrial sites will have loads connected electrically close to them, and these loads will therefore be susceptible to the voltage disturbances. Since the minimum voltage will occur when the load angle is 180°, it is desirable to disconnect the generator before this load angle is reached.

Drives in industrial plants are generally supplied via starter contactors, which have an instantaneous release time[41] of typically 40 ms. The voltage fluctuations produced can cause these contactors to open, causing unnecessary loss of plant. If system voltages are depressed for a sufficiently long time induction motors may stall and this will further depress system voltage. Synchronous motors may also pole slip in response to a voltage depression, making them subject to any of the effects described in section 1.5.

The location of the system centre determines how much disturbance a pole slipping generator will cause to the rest of the system. If the system centre occurs inside the generator, which occurs when the generator is connected to a 'stiff' bus, then the resultant voltage fluctuations will not be that severe. Unfortunately, the action of AVR's pushes the system centre away from the generator, therefore moving the voltage depressions away from the generator terminals into the distribution system. AVR action will tend to raise machine flux when pole slipping occurs, thus increasing the voltage contribution that the

generator makes to the rest of the system[49].

Power system protection may also suffer from the effects of pole slipping, because the voltage and current variations at the system centre appear the same as a three phase short circuit[36,54,55,56]. At the system centre, the voltage will be a minimum, whilst the current will be at its maximum value. The relays most affected are under-voltage, over-current and impedance type relays.

1.5.3 Legal Obligations

Embedded generator operators have to ensure that their generators do not contravene the recommendations set by the Electricity Council. Engineering Recommendation G59[14] provides recommendations on the requirements that should be met for the connection of private generating plant to an electricity board's distribution system. This states that with reference to the 1937 Electricity Supply Regulations, 'the private generator must not operate his plant in such a way that the electricity board is unable to fulfil its obligations under these regulations'. This makes it unlawful for a private generator to allow their generator to continuously pole slip or operate asynchronously. In addition to this statement, section 6.4 states, 'the board requires protective equipment to be provided by the generator in order to disconnect the generator from the system when a system abnormality occurs that results in an unacceptable deviation of the voltage or frequency at the point of supply'. This also demonstrates that if some form of protection is not fitted which will disconnect the generator when pole slipping or asynchronous running occurs, then the private generator will be in violation of the electricity boards interconnection requirements.

In addition to 'G59', Electricity Council Technical Report 113[15] provides notes of guidance for the production of private generating plant of up to 5 MW for operation in parallel with an electricity board's distribution network. This report shows the detrimental effect on system voltage of a pole slipping generator which is not promptly disconnected. In this instance the system voltage was reduced to an unacceptable mean value of 0.9 p.u. The minimum protection requirements for generators in the range 250 kVA to 5 MVA are also given. The minimum protection scheme comprises of Under/Over Voltage/Frequency, Loss of Mains, Over-current, Earth Fault, Reverse Power, and Neutral Voltage Displacement. The author of this technical report suggests that this type of scheme would be effective at tripping the generator for all pole slipping and asynchronous running

conditions. Later in this thesis, it will be shown that this is not true.

Technical Report 113 also includes a stability study which demonstrates the effects of using different interconnection impedances, and governor action. The study showed that for the 4.5 MVA generator studied, the Critical Clearance Time (CCT) ranged from 84 ms to 222 ms. Since fault clearance times of up to one second are possible on distribution circuits, any generators which are not disconnected as a result of the fault are likely to pole slip.

1.6 MICROPROCESSOR RELAYING PLATFORMS

Nearly all new generator protection is provided by microprocessor based integrated relaying schemes[23,25,27,30,31,57,58,59]. A microprocessor relay is comprised of a microprocessor and memory arrangement, which uses digitally filtered sampled power system waveform data to execute the protection algorithms stored in its memory.

Microprocessor relays offer many advantages over conventional electromechanical relays. As well as containing all of the generator protection functions in one unit, the microprocessor relaying platform allows programmable tripping logic, events recording, signalling, self-monitoring, test facilities and interface with SCADA systems. A greater reliability and availability can be achieved as all of the protection functions and supplementary functions can be factory standardised and housed together in one pre-tested single unit. Installation is also made easier as only one unit needs connecting to the instrument transformers, circuit breaker tripping coils and SCADA system. This reduces the amount of wiring required thereby reducing cost and improving reliability.

The computing power inherent to this type of relay creates numerous opportunities for developing new protection techniques which were not possible with electromechanical or static techniques. Pole slipping protection is especially suitable for development in a digital relaying environment because the phenomenon is relatively slow allowing long window algorithms to be used. Benefits can also be gained from the calculation of machine operating conditions. In addition trajectory tracking in conjunction with a-priori and initial disturbance information allows a faster more secure analysis[31]. The long time frame also means that low burdens are placed on the microprocessor. An IEEE committee

quoted on the subject of digital pole slipping protection "A design challenge is to make such a sophisticated relay easy for utility engineers to apply and set". Apart from the improvement in tripping performance, creating an easy to set pole slipping relay would greatly reduce the time and effort involved in applying pole slipping protection.

1.7 SUMMARY OF PROPOSED TECHNIQUE FOR DETECTING POLE SLIPPING

The new pole slipping protection algorithm proposed in this thesis has been designed to take advantage of the processing power of a modern microprocessor relay and uses power measurements to ascertain whether the generator will remain stable or not. In designing a pole slipping algorithm, the protection should trip when it observes conditions which will produce a pole slip, or correspond to an actual pole slip, but remain stable during fault conditions and other system abnormalities. Most pole slipping protection schemes are designed to detect pole slips in the range of 0.1 to 10 % slip[60]. Like pole slipping, asynchronous running is detrimental to the generator and the system, and in many cases the distinction between asynchronous running and pole slipping can become vague due to saliency and residual flux effects. An algorithm which detects both conditions would therefore be desirable because the generator should be disconnected from the power system in both cases.

By being able to recognise conditions where a pole slip is inevitable, the algorithm offers the prospect of disconnecting the generator before a pole slip actually occurs, thereby disconnecting the machine before it can be damaged, or cause voltage disruption to other consumers.

The new power based algorithm works by detecting if the generator load angle is still increasing once the CSP has been exceeded. It uses condition monitoring techniques to ascertain the generator operating point, and its mode of operation, i.e steady state or transient, it then adjusts its trip settings based on this information. Generator real and reactive power are used to check if the generator is operating beyond the CSP. Generator rate of change of real power is then used to check whether the generator load angle is still increasing in an unstable manner. If it is, the algorithm issues a trip command for the generator to be disconnected as it is operating in an unstable manner and a pole slip is

therefore inevitable. By changing its trip settings according to the generator operating point, the algorithm is able to use sensitive trip settings to quickly detect slow steady state pole slips, whilst having more secure settings to avoid nuisance tripping during stable power swings.

It is important to highlight the distinction between a pole slipping generator and a system out-of-step or power swing condition[61,62]. With generator pole slipping, the system centre appears in, or close by the generator or its step up transformer. This implies that the generator is 'out of step' with the rest of the system. When a system is out of step, and a power swing results, then the electrical centre will appear in between groups of generation, i.e it will appear in a transmission or distribution line. Detection of system out of step conditions is primarily a task for the transmission line protection relays[36,54,55]. This research concentrates on generator pole slipping, it is therefore primarily concerned with generators operating against infinite buses, or at least buses whose infeed is significantly greater than the rating of the generator.

The algorithm proposed in this scheme has been designed to detect 'generator' pole slips, i.e pole slips where the generator rotor speeds up above synchronous speed. It will not detect 'motor' pole slip i.e pole slips where the generator rotor slows down below synchronous speed. Since this research work is aimed at generators operating against buses with a rating larger than their own, only 'generator' pole slips will occur. It is only when considering system out of step protection, or synchronous motor protection, that 'motor' pole slips also need to be detected. Later in the thesis, it will be shown that the new algorithm can easily be modified to detect motor pole slipping.

1.8 RESEARCH OBJECTIVES AND PREVIOUS WORK

The main objective of the research was to gain a thorough understanding of the subject of pole slipping and asynchronous running, in addition to enhancing and testing the pole slipping algorithm which was first proposed in previous work[63,64]. The previous work had formed a basic algorithm which had been shown to work using a dynamic computer based power system simulation package[65], and a laboratory model power system[66].

The computer based power system simulation package did not simulate sub-cycle

phenomena and used a reduced order model for its synchronous machines. More detailed simulations therefore needed to be performed in order to reliably validate the performance of the algorithm. The laboratory power system model provided useful real life data for testing the algorithm, however, the generation set up used did not replicate a real life embedded generation environment exactly[67]. More appropriate data from a real life embedded generation unit was therefore required to test the algorithm more thoroughly. The results of field tests are reported in this thesis.

The initial algorithm assumed that the generators would be working at full load, and therefore one of the main objectives was to develop the algorithm so that it would work over the whole of the generator's operating range. It was also desirable to design an algorithm which required minimal setting, since existing pole slipping protection can be difficult to set reliably.

The final aim of this research project was for a field tested algorithm to be included in a microprocessor based protection relay.

1.9 PRESENTATION FORMAT OF THE THESIS

The thesis covers the work done in designing a new power based pole slipping algorithm. Although initially designed for embedded generators, the new technique is equally applicable to large 'grid' type generators. The causes and consequences of pole slipping, the presently available protection schemes, and the plant modifications required to reduce the likelihood of pole slipping are presented. A study into the operating characteristics of synchronous machines was used as a basis on which to derive the new power based algorithm. The new algorithm was then comprehensively tested using a range of test platforms from laboratories through computer simulations to full field trials. The algorithm's performance was then analyzed and compared with conventional techniques and conclusions drawn. Six appendices are also provided so that the main body of the thesis is concise. These contain; theoretical derivations of power system and algorithm characteristics, the techniques used to set conventional pole slipping relays, data on the power systems simulated, general embedded generator data, the practical implementation of the algorithm in a commercial microprocessor relay, the publications produced as a result of this work, and examples of ATP and 'C' files used in the testing and analysis of

the different pole slipping protection schemes.

Chapter 1 provides an introduction to embedded generation. Where commonly available material is required, numerous references have been given to provide the reader with a wealth of sources which support the concepts given. The problems associated with pole slipping and its causes are also discussed. The opportunities which enabled this project to come to fruition that are provided by modern micro-processor relays are presented and a summary of the proposed pole slipping protection technique given. The research objectives are then described.

Chapter 2 gives a summary of the many various approaches to pole slipping protection giving the benefits and disadvantages of the different schemes with respect to embedded generation. The standard protection schemes used with embedded generators such as under voltage and over current protection are presented and their effectiveness at detecting pole slipping discussed. A study of the changes in plant which can be made to reduce the likelihood of pole slipping is also included.

Chapter 3 presents the 'ideal' characteristics of synchronous generators, then discusses the aspects of practical operation which cause distortion. A study into embedded generator stability has been performed in order to indicate the likelihood of pole slipping. This study highlights the factors which make embedded generators more likely to suffer from pole slipping than conventional large 'grid' type machines. .

Chapter 4 presents the new power based pole slipping protection technique. The basis of the algorithm, the necessary filtering techniques, fault blocking, adaptive trip setting techniques, limits of operation, and other protection functions provided by the algorithm are all given.

Chapter 5 contains details on the different test platforms used in validating the operation of the algorithm. A laboratory model power system, real time dynamic simulator (POWSIM), Alternative Transients Program (ATP), 625 kVA industrial diesel generator, 26.5 MVA hydro-generator, and 353 MVA turbo-generator have all been used as test beds. Most of the data used in constructing the test beds has been placed in Appendix C and Appendix E

Chapter 6 discusses the performance of the new algorithm for each of the tests. For many of the tests, the results and graphs produced are identical. Plots that are virtually identical have not been repeated, only one example of each plot is given for the test bed being discussed.

Chapter 7 summarises the results and conclusions of the tests presented in chapter 6. The reader may wish to read chapter 7 first as it provides a complete and condensed version of the most extensive chapter of the thesis.

Chapter 8 provides the conclusions, and suggestions for further work. Chapter 9 lists the references.

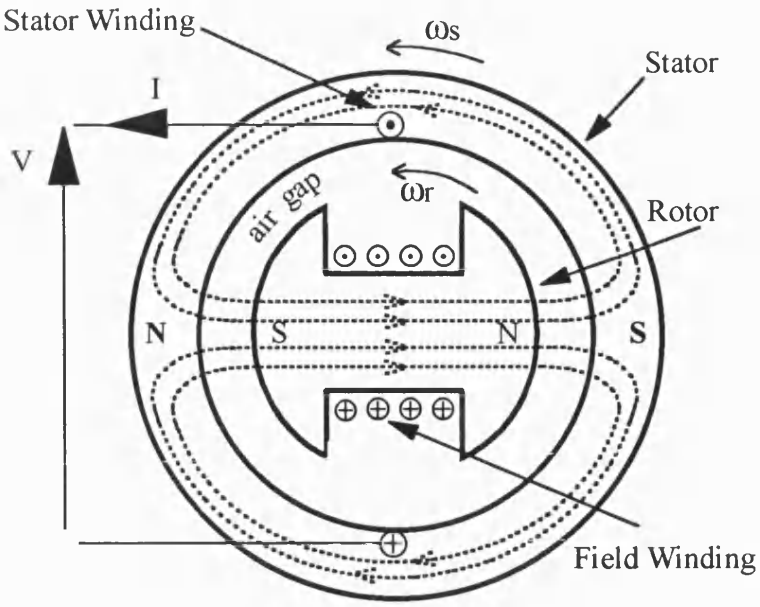

Figure 1.1a
Diagram Showing Stator and Rotor Field 'Poles' for an Underexcited Synchronous Generator at No Load.

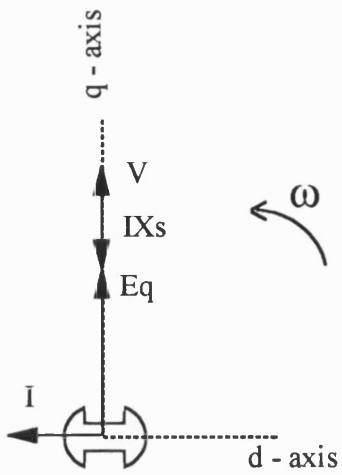

Figure 1.1b
Phasor Diagram for an Underexcited Synchronous Generator at No Load.

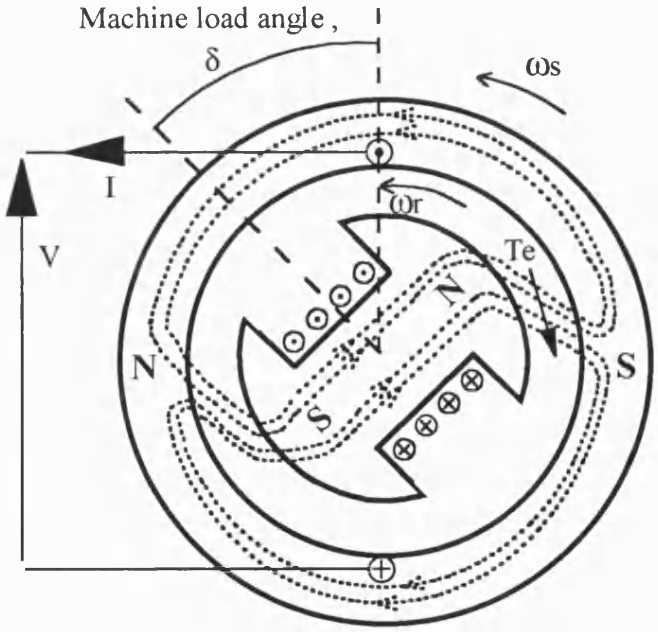

Figure 1.1c
Diagram Showing Stator and Rotor Field 'Poles' for an Underexcited Synchronous Generator Operating at a Machine Load Angle δ of 45 degrees.

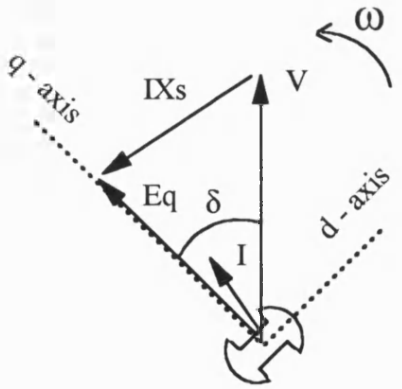

Figure 1.1d
Phasor Diagram for an Underexcited Synchronous Generator with δ = 45 degrees.

NOTE: The stator winding shown on this diagram is a hypothetical coil which would produce the same resultant mmf distribution as a 3 phase winding.

ωs - angular speed of rotating flux produced by a three phase winding on the stator.

ωr - angular speed of generator rotor

Te - electromagnetic air gap torque

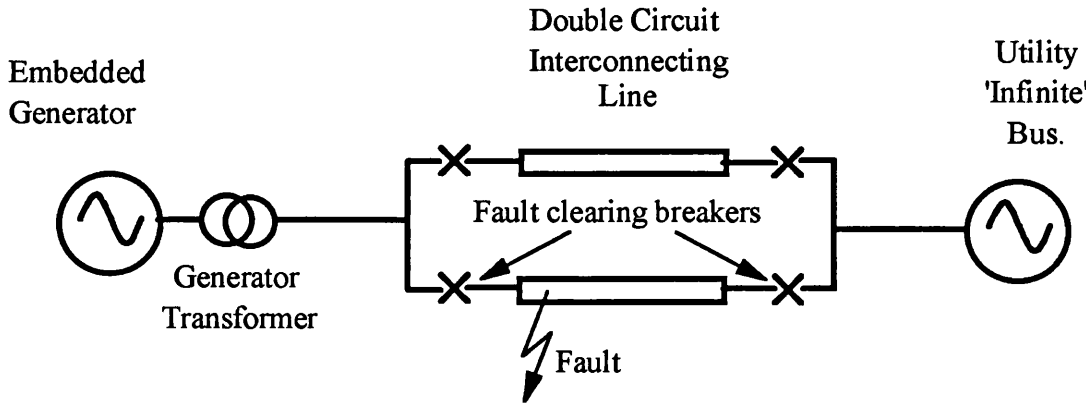

Figure 1.2a
Embedded Generator - Utility Connection.

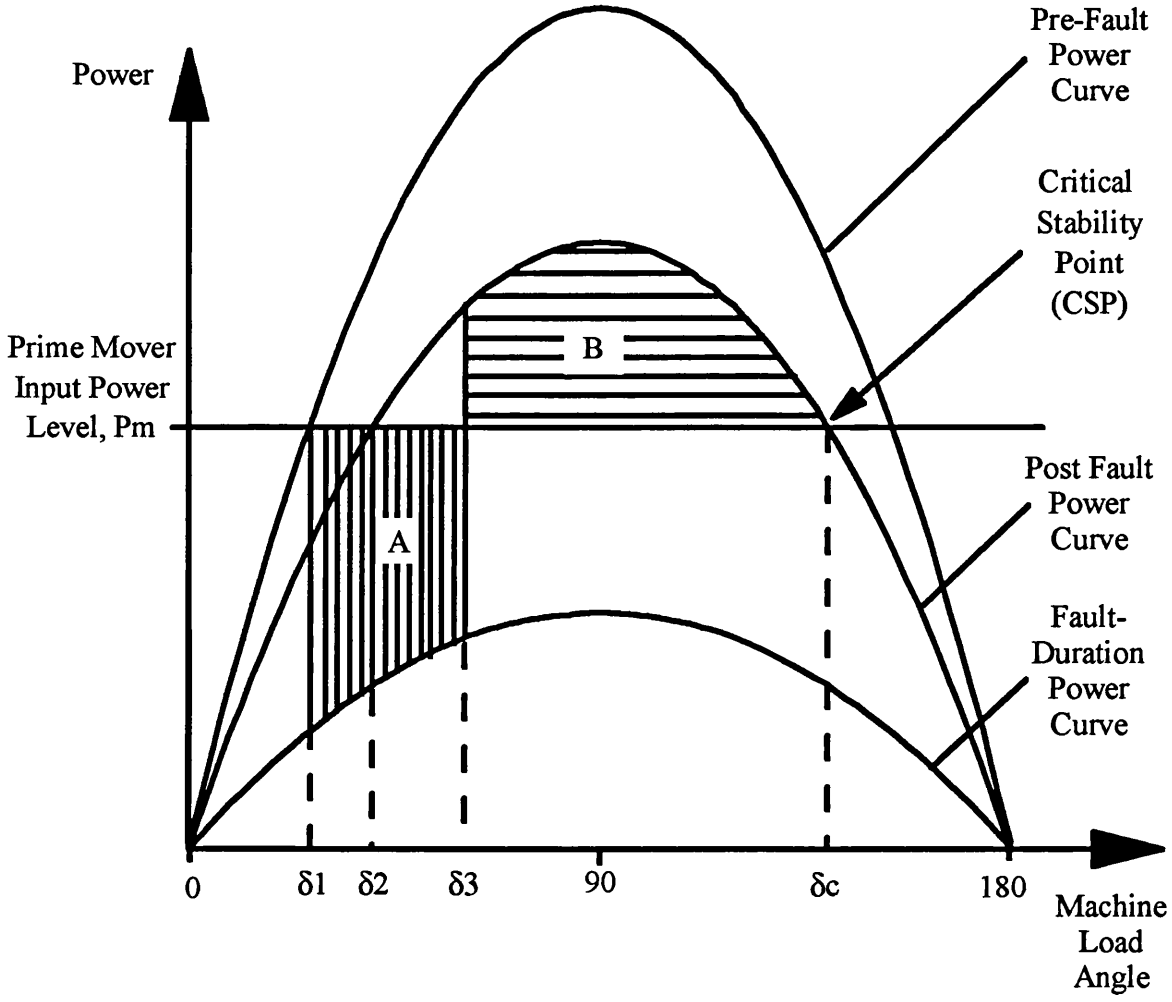

Figure 1.2b
Equal Area Diagram for Clearing of Short Circuit Fault Shown in Figure 1.1a.

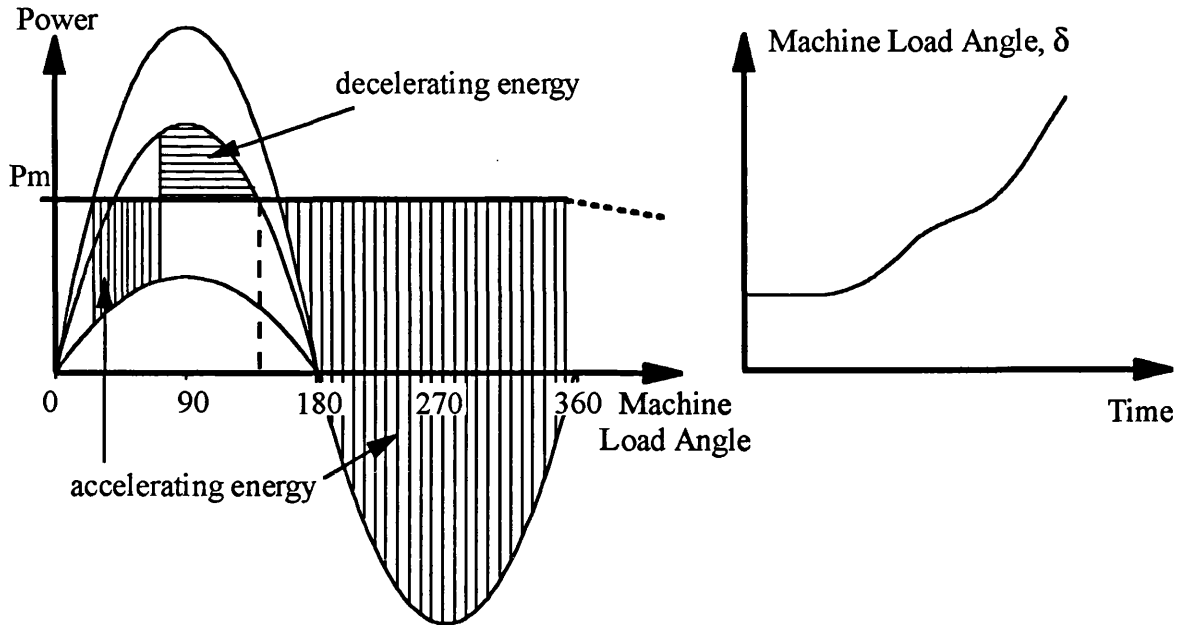

Figure 1.3a
Equal Area Representation of Loss of Transient Stability Caused by a Fault.

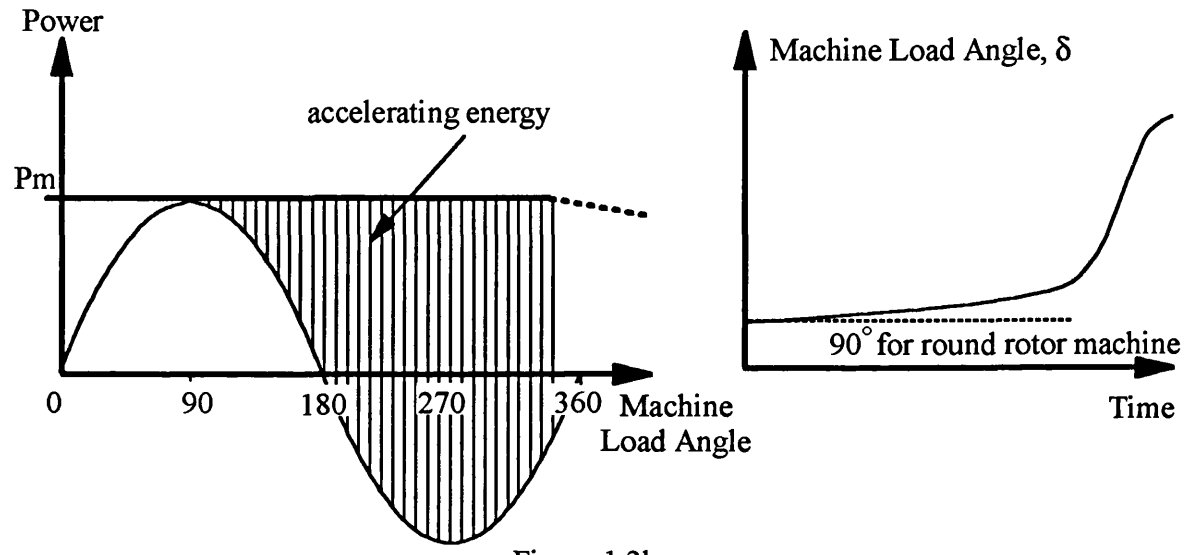

Figure 1.3b
Equal Area Representation of Loss of Steady State Stability Caused by Insufficient Excitation.

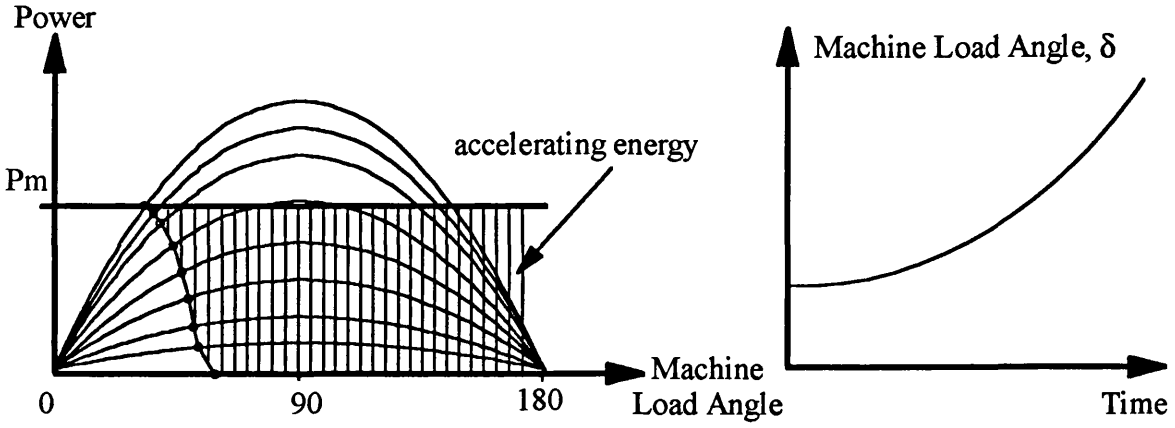

Figure 1.3c
Equal Area Representation of Asynchronous Operation Caused by Loss of Excitation.

Chapter 2
CONVENTIONAL TECHNIQUES FOR DETECTING AND METHODS FOR PREVENTING POLE SLIPPING

This chapter discusses the conventional techniques used for detecting pole slipping, as well as the changes in plant which can reduce the likelihood of pole slipping. The basis for most of the relays commonly used to detect pole slipping is the measurement of the apparent impedance at the generator's terminals. Most of the commonly used designs were conceived around 40 years ago and were based on the work of Edith Clark [185].

Some terms commonly used in this subject area will now be defined. The term 'power swing' refers to the swings in power output which occur when a generator, or group of generators undergoes load angle swings. The generators do not need to become unstable for a power swing to occur. Any oscillation in load angle will cause a power swing. A 'stable' or 'recoverable' power swing therefore occurs when a generator does not lose stability. A pole slip is therefore a form of power swing, but the term refers to power swings where a generator has lost stability.

Some pole slipping schemes have two distinct tripping zones so that they can differentiate between 'stage 1' and 'stage 2' pole slips. A 'stage 1' pole slip is defined as a pole slip where the system centre occurs inside the generator or its transformer. A 'stage 2' pole slip is defined as a pole slip where the system centre occurs beyond the HV terminals of the generator's step up transformer. For most embedded generators, 'stage 1' pole slips will occur because the system centre appears inside the generator.

2.1 IMPEDANCE TYPE POLE SLIPPING RELAYS

Impedance relays respond to the variations in apparent impedance as seen at the generator or high voltage transformer terminals during the pole slip and make their trip decision based on this measurement . Figure 2.1b shows the theoretical variations in impedance during pole slipping for the system shown in Figure 2.1a. These impedance loci are derived using the assumptions that the ratio of generator to source electromotive forces,

Eg/Es, remains constant. It is also assumed that generator saliency is neglected, generator damper effects are neglected, transient fault impedance effects have decayed, shunt loads and shunt capacitance effects are ignored, effects of automatic voltage regulators and governors are neglected, and the source voltages behind their equivalent impedances are sinusoidal and at fundamental frequency[36,68,69,70]. The derivation of these curves is given in Appendix A.

For the case where the ratio Eg/Es = 1, the impedance locus will be a straight line, PQ, which is the perpendicular bisector of the system impedance line GS. When a generator pole slip occurs, the load angle, δ, increases causing the impedance to travel from right to left across the R-X plane. When the load angle reaches 180°, the loss of synchronism point has been reached and the apparent impedance will lie on the system impedance line GS. The point on the system impedance line where the impedance locus appears for δ = 180° is known as the system centre, at this point the impedance gives the appearance of a three phase fault. As the pole slip cycle is completed and δ approaches an in-phase value of 360° the impedance locus will travel to the left of the system impedance line before returning to the load area of the R-X plane.

Figure 2.1 also shows impedance loci for the cases where the ratio Eg/Es < 1 and Eg/Es > 1, which cause the impedance locus to take on a circular arc form. These curves show that as the generator internal voltage is increased, the system centre is pushed away from the generator, out into the system. AVR field forcing action will have this effect.

For the majority of situations, the combined impedance of the generator and its transformer will be larger than the combination of line and equivalent source impedances[62,68,69]. This will result in the system centre appearing inside the generator or its transformer during pole slipping. If the system centre appears out on a transmission or distribution line, then power swing detection/blocking relays should be employed to separate the two systems, since this is not a generator pole slipping problem.

The assumptions made in deriving these theoretical curves do not always apply for embedded machines. Nearby synchronous machines and induction machines can cause the impedance trajectory to follow a less than smooth path across the R-X plane which can make secure installation of relays difficult. Generally the ratio Eg/Es will be in the range[71] 0.8 to 0.9, causing the impedance locus to travel through the generator or the

generator transformer if one is present, i.e the locus would cross the section labelled Zg in Figure 2.1b. Small embedded machines generally complete their pole slip cycles relatively quickly due to their low inertias, the high values of slip this produces can cause difficulty to relays since it can interfere with the fault blocking characteristics required by some schemes. Careful analysis of the embedded system must be made[42] before deciding on the appropriate settings for impedance based pole slipping relays, since standard application procedures developed for large machines are generally inadequate.

It is generally recommended[42,62,68,69] that transient stability studies are performed so that the impedance loci are known and the most appropriate relaying scheme can be selected. These simulations are necessary to enable correct setting of conventional impedance relays. It is important to note that there are no industry standards or commonly used practises for generator pole slipping protection[70].

2.1.1 Loss of Field Scheme

Figure 2.2 shows the loss of field characteristic which sometimes doubles as pole slipping protection[68,69]. This type of relay will provide a degree of pole slipping protection, since it will provide a trip command if the pole slipping impedance locus enters one of the circular characteristics during the slip cycle. Both of the loss of field characteristics are time delayed[40,42,69,72,73], typically values of 0.5 to 1 second are used.

There are a number of possible flaws in this approach. A pole slipping locus that passes through the generator transformer will go undetected because the loss of field relay characteristic only reaches as far as the generator terminals. Due to the time delay inherent in loss of field relays, tripping will only occur for pole slips whose impedance locus stays within the locus for a sufficient time. If a time delay of 0.5 seconds is used, then a generator which is pole slipping a rate of 2 Hz or above will not be tripped. Small embedded generators are likely to pole slip at high rates[42]. If the loss of field relay has an integrating timer arrangement[74], enabling a delay in relay drop off, then higher rates of pole slipping can be detected. Several pole slip cycles will be required to make the relay operate however.

The recommended settings for loss of field usually have an offset equal to Xd'/2 for both distance relay zones[44,46,72], whilst the time delayed zone used for detecting loss of excitation from low generator loadings has a diameter equal to Xd. The faster operating

zone used for detecting loss of field from high initial loadings has a recommended diameter of 1 pu on the generator base. A delay of 4 to 5 cycles is also used[46,75] in order to eliminate nuisance trips due to relay vibration.

Small generators will normally have a single Mho unit with an offset of Xd'/2 and diameter Xd. To ensure nuisance trips do not occur for stable power swings, a time delay of 0.5 to 0.6 seconds is normally used [46].

2.1.2 Mho Element Scheme

This is the simplest pole slipping protection scheme, its characteristic is shown in Figure 2.3. If the impedance locus enters the circle, a trip signal is issued immediately[68,69]. This can be a problem if the relay is too sensitive because a trip signal can be given for a recoverable power swing. Figure 2.3 shows a recoverable power swing impedance locus, for such a swing the impedance locus will travel towards the equivalent system impedance line, then head back towards the load area of the R-X plane as the machine load angle decreases after reaching its maximum value.

The stable power swing locus[60,62] shown in Figure 2.3 would not cause the Mho scheme shown to nuisance trip as it does not enter the Mho circle. However, if the relay were more sensitive, resulting in a larger Mho characteristic, then the power swing locus may have entered the circle causing a nuisance trip. This type of relay is usually set to a sensitivity of 120° load angle[68], accepting that this can cause nuisance tripping since stable swings of up to 155° are possible[38].

One advantage of the scheme is that tripping can occur before the load angle reaches 180°. This is the point where maximum current occurs and therefore the point of maximum mechanical stress on the generator windings. Another advantage is the scheme's ability to provide backup protection for multiphase faults occurring in the generator and a portion of the unit transformer. It also provides inadvertent energisation protection when properly set.

The main disadvantage of the scheme is that a large characteristic circle is liable to cause nuisance tripping during stable swings. If a smaller circle is used, it may fail to detect some pole slips. If it does detect a pole slip, the trip command will be issued to the generator circuit breaker as the load angle approaches 180°. This subjects the generator

circuit breaker to a maximum recovery voltage during arc interruption. If a longer time delay is used to prevent false tripping during stable swings, then the scheme will fail to detect the fast pole slips. If the scheme is not supervised by an over-current fault detector, a trip may occur during a voltage transformer (VT) failure[68].

2.1.3 Single Blinder Scheme

It is important to note that there are several possible variations of this scheme[70]. The basic scheme consists of two impedance elements (referred to as 'blinders' or ohm units) and a supervisory Mho relay, one example of a commonly used scheme is shown in Figure 2.4. The relay is supervised by a Mho element, to restrict the operation of the scheme to swings appearing in the generator or transformer, and to prevent operation for recoverable power swings that pass through both blinder elements. This also stops tripping for oscillations in reactive flow after synchronising[68,76,77].

The angle of the blinder units can be adjusted so that they are parallel to the equivalent system impedance. In this scheme[68,69,76,77] for a trip condition to occur, the locus must originate outside of the mho relay, then enter the Mho characteristic, and cross from one blinder to the other over a period of around two power system cycles. It is important to note that the pole slipping locus must enter from one side and leave from the other for a trip to occur. The scheme is inherently more stable than the mho scheme. Careful setting of the supervisory mho characteristic is still necessary, because if the mho circle is too large, nuisance tripping can occur for recoverable swings which cross both of the blinder elements[60,68] or for system out of step conditions where the electrical centre lies out on a transmission line. An example of a recoverable swing locus is shown in Figure 2.4.

The scheme will issue a trip command either when the impedance locus crosses the left hand blinder function, or upon reset of the supervisory Mho element. This provides a means of controlling the load angle at which tripping occurs, the arc interruption duty on the circuit breaker can therefore be minimised. This scheme will detect both motor and generator pole slips.

A motor pole slip occurs when a synchronous motor's mechanical load exceeds the electrical power it is able to draw from the supply. This causes the machines rotor to decelerate and pole slip relative to the stator flux. The impedance locus will travel across the RX plane from right to left during a motor pole slip.

The single blinder scheme is the most secure of the conventional impedance schemes, the above scheme does have some limitations however. A complete pole slip cycle is required for the scheme to operate, the scheme will therefore not trip until the pole slip has occurred. Although, the scheme is inherently more stable against recoverable power swings and faults, detailed computer based simulations are still required in order to find the correct blinder, mho, and timer settings which will guarantee reliable operation[42,60,68,69].

Sometimes an additional offset mho unit is applied to the scheme which reaches out across the system impedance characteristic[60,78,79]. With an additional directional relay fitted at the HV terminals of the generator step up transformer, stage 2 pole slips can also be detected. The additional mho and directional elements provide a means of differentiating between 'stage 1' and 'stage 2' pole slips.

A much more secure scheme is suggested by Goody[79] for a pumped storage motor/generator. Studies had showed that the scheme suggested above could nuisance trip for unbalanced faults and developing faults as well as circuit breaker pole scatter. It was also shown that CT saturation could have a detrimental effect to the scheme. The modified scheme developed to overcome these problems uses the following modifications to the above scheme. For a trip command to be issued, the supervisory mho element only needs to be in an operated state when the last ohm element operates. In addition the current must also be greater than 10 % of rated during the operation of the scheme. These two measures ensure that the first pole slip cycle is always reliably detected. To stop incorrect operation during developing faults, more criteria were added. Whilst in the generating mode, only loci moving from right to left would be detected as a pole slip. When in motoring mode only the loci moving from left to right would be detected as pole slipping loci. This logic was implemented using auxiliary switches on phase reversal disconnecters. The final criteria was that the pick up operation of each ohm element must be delayed such that its minimum operating time is 20 ms. Note that with this scheme the ohm elements were set to face the opposite direction to that shown in Figure 2.4. This new scheme solved many of the above problems, there were still some potential problem areas however. Developing faults with a development period of around 60 ms may cause a stage 2 nuisance trip. This could be overcome if stage 2 tripping only occurred after the second pole slip. CT saturation during certain faults may cause nuisance tripping. This could be overcome by ensuring that the protection CTs do not saturate during fault

conditions.

The above scheme therefore provides a trip signal after the first pole slip, and is also capable of detecting out of step conditions on the system referred to as 'stage 2' pole slips. This type of detection is necessary in systems with weak transmission, where the system centre may appear out on transmission lines[80]. It is beneficial in this situation, to delay tripping giving the line relays a chance to separate the system at a more beneficial location during out of step conditions. It still requires a detailed system analysis to be set properly however, and does not provide a trip signal until after the pole slip has occurred. In many situations tripping can only be initiated when the system load angle is much less than, or much greater than 180°, since the circuit breaking duty on the breaker is too much at load angles around 180°. The trip command therefore needs to be issued significantly before 180°, or significantly after. Alternatively, a generator circuit breaker must be selected which is capable of breaking out of phase fault current levels.

2.1.4 Double Blinder Scheme

A supervisory Mho element is used in this scheme to provide the same security as in the single blinder scheme. The difference between this approach and the single blinder scheme is that the blinder logic of the relay functions in a different manner. The impedance characteristics of the relay are configured as shown in Figure 2.5. A pole slip is recognised if the impedance remains between the outer and inner blinder elements for longer than a pre set time.

After the first time constraint is satisfied, a portion of the logic circuitry is 'sealed in' if the impedance locus enters the area between the inner elements. When the locus leaves the inner element zone, its traverse time must exceed a preset time before it reaches the outer characteristic. A trip condition exists when the impedance locus leaves the supervisory Mho element.

The important distinction between this scheme and the single blinder scheme is that once the impedance locus has entered the zone made by the inner blinder characteristics and the Mho element, the impedance locus can leave the inner and outer characteristics in either direction for successful operation. The recoverable power swing locus shown on Figure 2.5 would cause the scheme to nuisance trip, the inner blinder elements need moving closer in to prevent this nuisance trip.

The inner element setting must therefore be such that it will only pick up for non-recoverable swings. For this reason the single blinder scheme is inherently more secure than this scheme. The double blinder scheme is therefore more sensitive to its settings than the single blinder scheme, computer based simulations are required to provide the correct blinder, Mho and timer settings.

This scheme has the added disadvantage that if the impedance locus crosses the inner and outer blinders without first picking up the Mho element, then the scheme will not trip for that pole slip cycle. This locus is shown in Figure 2.5 and could happen when pole slipping follows a multiphase power system short circuit fault. During the fault the impedance locus enters the Mho circle between the inner elements and rests on the system impedance line. For the time that the fault is applied, the relay will only see the fault's effect even if the generator is accelerating towards a pole slip. When the fault is cleared the generator load angle may have reached a high value, which causes the impedance to remain between the inner characteristics. The generator will then complete the rest of the pole slip cycle as normal, however the scheme will not trip, since the first stages of the scheme logic have not been 'sealed in'. A trip signal will only occur when the complete second pole slip cycle has occurred, by which time system disruption and machine damage may have occurred.

2.1.5 Lenticular Type Scheme

Several schemes exist which use lenticular type characteristics rather than blinder and Mho elements[60,68,69,81]. The single lens scheme operating characteristic is shown in Figure 2.6. This scheme has similar operating principles to the single blinder scheme. The scheme shown in Figure 2.6 can detect both 'stage 1' and 'stage 2' pole slips[60]. This scheme was originally designed for generators where the system centre would often occur out on the transmission system.

A trip signal is issued when the impedance locus enters from one side, remains inside the lens for a specified time, and leaves via the opposite side. Typical time settings require the impedance locus to stay in each side of the lens for at least 25 ms [79,82]. The suggested generator reach, denoted as Zg in Figure 2.6 is 0.5 Xd [60]. This was chosen to co-ordinate with the loss of excitation relay, so that pole slips with a ratio of Eg/Es greater than 0.66 p.u. would be detected by the lens scheme. The reach of the HV directional relay is chosen to detect swings which appear on the generator side of the step up transformer.

The other important setting is the lens angle, δ. This is chosen according to the maximum percentage slip rate, s which the scheme must detect, and is related to the timer setting, t of the scheme by the following equation [60];

$$\delta = 180 \left(1 - \frac{st}{2} \right) \qquad 2(1)$$

The reactance element and HV directional characteristic shown in Figure 2.6 are provided as a means of discriminating between stage 1 and stage 2 pole slips. This scheme has similar attributes to the single blinder scheme.

2.1.6 Double Lens,Triple Lens and Concentric Circle Schemes

The operating characteristic for the double lens scheme is shown in Figure 2.7. It functions in exactly the same manner as the double blinder scheme, it therefore has the same strengths and weaknesses.

Triple lens schemes have also been devised, which have four steps in detecting a pole slipping condition. This makes the scheme inherently more secure than the double blinder scheme. The logic circuitry required to achieve this higher level of reliability is much more sophisticated than that used in the double lens scheme.

The concentric circle scheme uses two distance elements and operates in the same manner as the double blinder or double lens schemes.

All of the above schemes suffer from similar problems to the double blinder scheme. Careful setting of zones is required to ensure that a recoverable swing locus will not enter the inner zone and cause a nuisance trip. The majority of the impedance based schemes are able to provide satisfactory pole slipping protection if set correctly. Deriving correct settings requires a detailed simulation of the generator and power system to be protected. Collecting sufficient data and adequate models to perform such a simulation can be a time consuming and expensive process. With the exception of the single Mho scheme, all of the other schemes trip after the pole slip has occurred, this generally means that the worst stress point for the generator, and greatest disturbance to the system has already occurred. A pole slipping detection technique which can disconnect the generator before the first pole slip has occurred offers the advantage of reducing the ill effects to an absolute minimum.

2.2 POWER BASED POLE SLIPPING PROTECTION

Only one power based pole slipping detection method is to be found in the literature. This uses the repeated reversal of real power as the generator alternates between a generating and motoring condition to detect pole slipping[36,81,83]. The power reversal is indicated by the alternate closing of the contacts of a duo-directional watt relay. The scheme is secured against faults by the use of a counter, several pole slip cycles are therefore required before a trip decision is given. Nuisance tripping due to hunting at light loads is prevented by the use of an over-current relay in series with the power relay. This approach's main disadvantage is that several pole slip cycles are required before the generator is disconnected. It is also possible that full power reversal may not occur for some pole slips.

2.3 MICROPROCESSOR BASED POLE SLIPPING PROTECTION

The recent pole slipping techniques proposed have all been microprocessor based. All existing microprocessor based pole slipping protection schemes which have been designed with a low computational burden in mind are impedance based. The first designs were just conversions of the conventional electromechanical relay characteristics into a digital domain. The flexible nature of microprocessor systems has meant that characteristics other than circles, lines and lens can be implemented easily, and the more recent relays have used quadrilateral characteristics[84,85,86].

The non-impedance type microcomputer relays at present have a high computational burden and require information not readily available to most embedded generation protection engineers. The highly computational and data intensive nature of these schemes makes them unsuitable for protection of embedded generators because they require a stand alone relay which makes the cost of the scheme too high. Additionally, complete generator, control equipment and system data is often difficult to find[87].

2.3.1 Rate of Change of Apparent Resistance Relay

One proposed scheme[88] uses the apparent resistance and its rate of change to predict an out-of-step condition. This scheme is intended for out of step protection of transmission lines, but could be used for a generator pole slipping scheme. The scheme initiates

tripping 'on the way in' to a pole slip, and therefore the circuit breakers used for system separation in this case need to operate before the angular difference between the systems is greater than 120°. The rate of separation of the systems is also a factor when considering circuit breaker duty because of the time lag between relay operation and circuit breaker clearing.

Apparent resistance is used rather than apparent impedance as this makes the relay insensitive to the location of the system centre. Use of rate of change of apparent resistance provides an indiction of how quickly the systems are separating. The relay can use sensitive settings so that tripping can occur close to the 120° criterion when the rate of separation is slow, whilst tripping can occur earlier at angles around 100° when the systems are separating quickly. The relay settings are therefore not restricted by the three phase fault condition, which produces the highest rate of separation, unlike conventional relay types. The relay can therefore be set closer to actual stability limits. The scheme also has an adaptive feature, which enables the overall settings to be changed when an intertie disturbance occurs. The flag that an intertie disturbance is occurring is provided by other substation control equipment. This also enhances the relays sensitivity since worst case considerations do not dictate the relay settings.

The scheme is prevented from operating for power system faults by recording the time it takes the apparent resistance locus to cross two pre-specified resistance values. If the locus crosses these values very quickly, scheme tripping is blocked as this indicates a fault situation. The reactive reach of the scheme is limited by allowing tripping to occur only if the apparent impedance is less than a set value, in a similar manner to how the Mho circle limits operation in the blinder schemes.

The main limitation of this scheme is the problem of finding correct settings. This scheme is devised for a specific 500 kV intertie where the system parameters are well known. Applying this type of scheme to an embedded generator would involve the same problems encountered with the blinder pole slipping schemes. Finding the correct apparent resistance settings for fault blocking requires detailed simulations.

2.3.2 Multiple Zone Impedance Based Microcomputer Based Protection

One scheme developed by Shiwen[89] uses the single blinder principle to produce a relay that is stable against faults and power swings and operates towards the end of the first

pole slip cycle. The relay breaks the R-X plane into five zones, as shown in Figure 2.8, with each zone's boundary being parallel to the equivalent system impedance line.

A trip signal is given when the impedance locus has passed through each zone in turn, and remains in each zone for a specified time. This time must be greater than the time the impedance would stay in a zone for a short circuit condition, but less than the minimum time it would stay in any zone for a pole slipping condition. The angle at which tripping occurs can be controlled by selection of the zone reach so that more favourable arc interruption is obtained. Tripping therefore occurs towards the end of the first pole slip cycle. In addition, the scheme provides control signals for pole slipping prevention. These signals are derived when the impedance locus satisfies the trip requirements of the first two zones. The signals are intended for use with a large generator with a fast valving or breaking resistor scheme.

The relay offers the advantage over the conventional schemes that it provides preventative control signals before load angles of 180°, and is inherently more stable due to the increased number of zones. Problems still exist with choosing the correct timing settings for the scheme, the scheme may also fail to operate for pole slips where the real power does not sufficiently reverse, since the impedance locus may fail to enter zone 4.

2.3.3 Square Impedance Based Relay Characteristics

Comparisons between square impedance based characteristics and circular or lens type schemes suggest that using a square impedance characteristic is more reliable than the conventional lens, circles or blinder schemes[85,90,91]. The main advantage is that the scheme is less sensitive to the direction in which the impedance locus travels as illustrated in Figure 2.9.

An 'ideal' pole slipping locus travels horizontally across the impedance plane, and most impedance based schemes are set to detect such an impedance locus. If the locus does not take the 'ideal' trajectory, the single blinder type scheme will fail to detect the pole slip because the locus would not cross both of the blinder units. The quadrilateral scheme uses the single blinder principle, in conjunction with the flexibility of having a quadrilateral detection characteristic to enhance pole slipping detection. The locus must enter on one side and leave on the other, taking longer than the preset time 'T1'. The scheme has the flexibility to detect impedance loci such as those shown in Figure 2.9.

Shunt capacitance[36], induction motor loads and other power system equipment[42] can all change the nature of the impedance locus as seen by the impedance relay. Shunt capacitors inject current into the network, they therefore cause the out of step behaviour of a network to deviate from that predicted by the classical two machine model[92].

2.3.4 Multiple Algorithm Pole Slipping Protection

This approach[93] uses three different methods to detect static, dynamic and transient instability. The static stability monitoring scheme is not impedance based, it monitors the generator real power and load angle variations, the generator is considered unstable if :

$$\frac{dP}{d\delta} < 0 \qquad P \geq K_p.P_{MZD} \qquad 2(2)$$

are both satisfied, where $dP/d\delta$ is the synchronising power coefficient, K_p is a coefficient dependent on the number of generators and lines working, and P_{MZD} is the threshold of static stability when all generators and lines are operating, and is entered as a relay setting particular to the system considered. The positive phase sequence values of V and I are found which are then used to calculate active power. δ is calculated from the voltages known at either end of the line and the line impedances. The connecting impedances of the line are determined within the relay according to switch status. This method therefore requires data that is not normally available to an embedded generator protection relay, and would therefore be difficult and expensive to implement.

For the transient stability monitoring, the Equal Area Criterion[36,37] is used in a quantitative manner. If the calculated accelerating area is greater than the decelerating area then a trip is issued. To calculate these areas, $\Delta\delta$ must be calculated and then applied to the power load angle characteristics. To accurately know all of the power load angle characteristics requires detailed information on the system configuration as well as generator and plant data. Such detailed data is often not available, this method is therefore very susceptible to nuisance tripping due to inaccuracies in the data causing incorrect calculation of the accelerating and decelerating areas. This method also relies on the assumption that the mechanical power during steady state is equal to the electrical output power, and that the governor action is ineffective during the transient period.

The dynamic instability prediction acts as a back up to the previous two schemes, and it

detects if an out of step condition is occurring, and whether it is a generator or motor pole slip. It uses resistance and rate of change of resistance to predict pole slipping. For a generator pole slip, a trip signal is initiated if the measured resistance lies between two preset values related to the load angle at the CSP, and the rate of change of resistance is less than zero. The resistance measurand is a combination of actual apparent resistance and a predictive term based on the rate of change of resistance. This assumes that the rate of change of resistance and hence load angle is constant, it therefore trips before the CSP has been reached. In doing this, the scheme may nuisance trip for recoverable swings following faults whose duration is just less than the CCT. With such a swing, the rate of change of load angle decreases as the CSP is reached and it is equal to zero at the CSP.

Both the transient and steady state methods may be effective at providing an early warning system so that fast valving or breaking resistors can be used. The scheme requires detailed system data and is therefore impractical for embedded generators.

2.3.5 Artificial Neural Network Pole Slipping Protection

Several pole slipping and loss of excitation schemes have been devised which use an Artificial Neural Network (ANN) to detect pole slipping or system out of step conditions. One such approach[94] uses the prime mover input power, kinetic energy deviation and the average acceleration during the fault as inputs to an ANN. After the network was trained on a system using 162 samples, it successfully performed for 99 % of the tests conducted. The problem with this approach is that the inputs used are not readily available, or easy to derive in a protection relaying environment. The network also needs to be trained 'off line' using simulations of the power system to be protected. This is too time intensive for application to embedded generators. These restrictions make this approach impractical for pole slipping protection of embedded generators.

Another proposed scheme[95] uses the results of a discrete fourier transform on machine load angle and speed deviation, generator current, voltage, power and admittance and their cross spectra as inputs to an ANN. It relies on using 'sophisticated system models and accurate parameters to enhance the speed and accuracy of the relaying scheme'. It also uses online pattern recognition techniques to enhance its performance. The scheme successfully differentiated between loss of excitation, and transient loss of synchronism 80 % of the time. This approach has the same problems as the scheme above however, and is not suitable for protection of embedded generation.

2.3.6 Pattern Recognition Pole Slipping Scheme

Research has been conducted into using pattern recognition to detect generator out of step conditions[96]. This is the same as using an ANN. The proposed scheme requires generator output power, and mechanical speed as inputs, it also requires the machine inertia. Using this input data, it identifies an out of step condition by using these variables to derive the mechanical input power at the instant of fault initiation, the generator kinetic energy at the instant of fault clearing, and the average acceleration during the fault. These variables are then entered into a pattern recognition algorithm which classifies the situation as stable or unstable. There are several problems in applying this approach to embedded generation. The inclusion of a speed measuring device would make the scheme too expensive, in addition, an accurate value of the machine inertia is not always known. This approach also assumes there is no governor action, no damper windings on the generator, and that all loads are constant impedance loads. The scheme is only aimed at detecting a loss of transient stability, it would therefore be unable to detect pole slips resulting from dynamic or steady state loss of synchronism.

2.3.7 Out of Step Voltage Phase Comparison Schemes

This approach is applied for system out of step problems, where it is vital that the power system be separated into two individual power islands if an out of step condition is likely to, or is actually occurring. The advantage of this approach is that unlike impedance based schemes, the location of the system centre does not effect its operation. The basic principle is that the phase difference between the voltage phasors at either end of the line connecting the power system is calculated. If this phase difference is about to, or actually has exceeded a preset value, then the interconnection is disconnected either at a pre-determined location, or at the system centre. The aim of separating the systems is to create two individual 'in step' power systems where load and generation are balanced.

One approach[97] uses sampled voltage information from four locations on the power system to calculate the phase difference. It then predicts what the phase difference will be in 200 ms time, by approximating the voltage phase difference oscillation to a sinusoid. If the predicted value is greater than a preset value, then a trip signal is given to break the system up at a specific location. This system is very expensive, the cost being justified in the instance of its application because if the system were to fall out of step, the whole power system would fail.

Another scheme[84] uses central and remote apparatus linked by high speed data transmission systems to make an out of step detection based on voltage phase comparison. The internal generator EMF's are calculated from the generator terminal voltage, current and impedance. The adopted value of impedance used is the average of the synchronous and transient reactance. The phase difference is calculated and a trip signal issued if the difference exceeded 180°. This approach may be prone to errors, since the generator impedance varies between the sub-transient value, Xd" and the synchronous value, Xd. The method was claimed to have worked when used for phase comparison of several groups of generation, however, it may become ill-conditioned if applied to an embedded generator to calculate its load angle.

2.3.8 Microcomputer Based Generator Modelling Protection Techniques

Lyapunov methods have also been used to assess overall system stability for use in power system contingency planning. Lyapunov methods use the phase plane domain to determine the critical stability point of the system and assess generator stability. This approach has been applied to individual synchronous generators[98]. The algorithm uses external circuit information, machine data, accelerating power, load angle and slip are required as inputs to a complex, computationally intensive algorithm. This type of algorithm is difficult to instigate on a small integrated protection relay. Two schemes are proposed, the simple one requires all of the system impedances, and machine and system inertias and calculates the load angle, slip, acceleration, voltage magnitude, mechanical input power, and peak transient generator output power. From this information, it calculates the stability limits for the machine, and trips if the generator operates outside its stability boundary. The second, more detailed scheme requires additional data on the generator AVR, governor, saturation, damping and saliency. The scheme also relies on accurately determining when the generator is disturbed by a fault, and it will therefore not trip for steady state pole slips. Loss of dynamic stability may also go undetected. The amount of data required by the scheme is impractical for embedded generation systems.

Another interesting scheme uses time tag, voltage and current phasors and circuit breaker status information from the rest of the system[86,190]. Sample synchronisation is obtained with the aid of the Global Positioning System (GPS). Using this information, the system load angle is derived, and used as a continual update for a simulation of the protected system performed by the relay. The relay models the protected power system as a two machine network. If the simulation predicts instability then the relay will initiate a trip

signal. This relay is intended for installation on a 500 kV interconnection where the consequences of out of step operation are dire. The hardware intensive nature of this scheme is therefore justified. Again, such a scheme can not be justified for smaller machines.

Other instability predicting algorithms[99,100,101] developed are based on similar principles. These can be set to operate before the load angle reaches 180°. However, they are unable to discriminate between stable and unstable swings under all system conditions.

Algorithms based on an exact calculation of the equal area criterion for the generator concerned have been developed. One scheme uses a communications link to calculate the phase angle between points of generation. The areas of the equal area criterion are then calculated based on estimated machine quantities, and a decision on stability made [102].

Any scheme which relies on accurate plant data for prediction of instability is unsuitable for protection of the majority of generators, as the accuracy of the plant data is always questionable, and changes to the power system will affect their performance. These changes therefore need taking into account which requires communications capabilities. The only situation where this approach is justified is out of step protection of important inter-ties, where accurate data is known, and it is imperative to disconnect the inter-tie quickly whenever instability is imminent.

2.4 EMBEDDED GENERATOR STANDARD PROTECTION SCHEMES

In the UK, Engineering Recommendation 'G59'[14], and Engineering Technical Report 113[15] specify the minimum protection requirements for embedded generators. The USA has similar documents including ANSI 1001[16,21]. Figure 2.10 shows a comprehensive protection scheme that may be used on embedded generators greater than 250 kVA. On simpler schemes functions 46N, 51V, 40, 87G, 32R, and 67N may be omitted. Usta[103] and Barrett[104] both provide a comprehensive analysis of these schemes. This thesis will discuss only the relays' ability to detect pole slipping conditions.

Pole slipping is a balanced phenomenon, and therefore functions which are related to phase imbalance conditions do not require consideration when discussing pole slipping

detection. Pole slipping will therefore have no effect on negative phase sequence, neutral voltage displacement, current differential, stator earth fault, and directional earth fault protections.

The basic protection scheme, which does contain the loss of excitation function, is insufficient for detecting all pole slipping conditions. The main problem is caused by the oscillatory effect that pole slipping has on most power system variables. The standard scheme will provide only a limited amount of pole slipping protection cover.

2.4.1 Effect of Pole Slipping on Over & Under Frequency Relays

This form of protection operates when the measured frequency exceeds a preset limit in a preset time. Engineering recommendation G59 states that the over-frequency limit is +1 %, and the under-frequency is -4%, both with a time delay of 0.4 seconds. The time delay requirement comes from the need to detect an abnormal operating condition following a loss of grid before any auto reclose schemes may reconnect the grid to the embedded generator. If the generator is not disconnected before the auto-reclose, an out of phase re-closure may occur which could cause further supply disruption and generator winding and shaft damage[52,105]. Most re-close schemes have a dead time of 0.5 seconds or greater before their first re-closure, a time delay of 0.4 seconds was therefore chosen in order to allow 100 ms for circuit breaker operation.

When a generator pole slips, its real and reactive power output oscillates wildly. This makes the voltage phase angle at the generator terminals oscillate wildly, which causes the measured electrical frequency to oscillate also. Pole slipping will not normally cause under or over-frequency functions to trip, due to the frequency oscillating above and below the trip settings in a time much below the time delay setting.

2.4.2 Effect of Pole Slipping on Under & Over Voltage Protection

This protection operates when the measured voltage exceeds preset limits for a specified time. Engineering recommendation G59 states that the over-voltage limit is +10 %, and the under-voltage limit is -10%, both with a time delay of 0.4 seconds. The time delay is chosen to ensure co-ordination with auto-reclose schemes (see 2.4.1). If the embedded generator is connected to a system with no auto-reclose schemes, then a longer time delay of up to six seconds may be used, which is useful for preventing nuisance tripping of the embedded generator when system faults are cleared by time delayed protections[15].

Depending upon the grid infeed at the terminals of the generator, the under-voltage protection may operate for a pole slipping condition, since pole slipping can depress system voltage far below the trip setting of 0.9 pu. A problem can occur if an integrating timer arrangement is not used on the under-voltage relay because the generator terminal voltage oscillates from a low value to a normal voltage level during pole slipping. The period where the voltage is normal may reset the relay, preventing it from tripping during pole slipping. Under-voltage protection provides a degree of pole slipping protection, but it will not successfully detect every pole slipping condition.

The 'G59' recommendation for under-voltage relays may cause nuisance tripping following system faults due to a slow voltage recovery. During the fault, the system voltage is depressed and the generator load angle increases. This voltage depression can cause the under-voltage element to pick up. When the fault is cleared, in a time of 350 ms for example, the reactive power demand of the generator has increased substantially, because the generator load angle has increased to a high value. This reactive power demand causes a further depression of system voltage, which may be sufficient to cause the under-voltage protection to trip, even though the generator may remain stable, and no pole slipping occurs. There is clearly a co-ordination problem between under-voltage relays and other system relays. Co-ordination problems also exist with loss of field relays, due to the 0.5 to 0.6 seconds time delay normally employed[40].

2.4.3 Effect of Pole Slipping on Rate of Change of Frequency Relays

Rate of change of frequency and phase displacement relays[15] will both experience oscillations in their relaying quantity during pole slipping (section 2.4.1). Engineering technical report 113[15] quotes a manufacturers recommended setting of 12° over 30 cycles. This equates to an average rate of change of frequency of 0.055 Hz/s over 0.6 seconds. This setting is very sensitive and may cause nuisance tripping during disturbances on the utility grid system. Other sources quote a setting of 0.3 Hz/s with a time delay of 0.3 to 0.5 seconds [103].

The oscillations in frequency and hence rate of change of frequency may prevent the rate of change of frequency based relay from tripping during pole slipping, due to the relay continually resetting before the time delay requirements have been satisfied. This is dependent upon the time delay used, and the speed of pole slipping. A very sensitive setting would improve the relays chances of detecting pole slipping, but also increase the

chances of nuisance tripping during recoverable power swings.

2.4.4 Effect of Pole Slipping on Voltage Dependent Over-current Relays

Voltage dependent over-current protection is necessary for synchronous generators because of the decaying fault current response to a short circuit fault[45]. Two types of voltage dependent over-current protection are commonly used. Voltage controlled over-current relays are only permitted to operate as a fault over-current relay if the measured voltage falls below a set minimum value[24,45], otherwise they function as an over-load relay. The voltage value used varies between 0.8 and 0.3 per unit depending upon the type of earthing that the generator has. One type of voltage controlled IDMT over-current relay multiplies its plug scale multiplier setting by 0.4 if the voltage falls below 60 %[106]. A typical setting value is a PSM setting of 2*In, with a TMS setting of 0.1 using a standard inverse IDMT characteristic and a control voltage of 80 %[23,42]. If co-ordination with short circuit clearance times on adjacent system feeders is required, then higher settings may be required, resulting in longer fault clearance times[40]. Intertie over-current protection may be set to a more sensitive level than the generator over-current scheme, so that when a fault occurs, the generator and site load remain connected together. This prevents any discontinuity of site load supply [40].

A voltage restrained over-current relay changes its IDMT characteristic according to the voltage at the machine terminals. It may therefore be regarded as an impedance type relay with a long dependent time delay[45]. The relay therefore operates more or less independently of the current decrement which occurs in the generator.

Pole slipping may cause an IDMT over-current relay to operate. The magnitude of current, speed of pole slipping and the relay settings determine the likelihood of such an event. The current may exceed three phase levels during pole slipping, but only during the period when the load angle approaches 180°. If the relay does not drop off between pole slip current maximums, then a trip condition may result after several pole slips due to the integrating action of the over-current relay[74]. If instantaneous over-current relays are used, then pole slipping may cause them to operate[36].

Over-current relays have more of a role in preventing pole slipping since they can disconnect the generator from the utility when a fault occurs whose duration is long enough to cause pole slipping. If the embedded generator protection scheme philosophy

is to disconnect the generator for all external faults, then in theory, pole slipping should not result from faults. If the over-current relay settings have to be graded with those on adjacent feeders however[40], then the fault clearance times are likely to be in excess of the critical clearance time[42] and pole slipping may occur following faults..

2.5 TECHNIQUES TO REDUCE THE LIKELIHOOD OF POLE SLIPPING

While it is possible to fit relays to disconnect generators when they pole slip, there are numerous other ways of improving power system transient stability which will reduce the risk of pole slipping. The following sections detail the various modifications that can be made to the power system to improve transient stability, as well as machine design changes which alleviate the machine from the phenomenon of pole slipping.

2.5.1 Reducing Fault Clearance Times

Reducing the duration of a fault reduces the accelerating energy which goes into increasing the machine rotor angle and this therefore decreases the load angle swing for the fault and increases the likelihood of maintaining stability. This is one of the most effective methods of increasing transient stability, but reducing the fault clearance time requires costly changes to the existing utility's protection, in addition to protection changes within the neighbouring plants[42]. The cost of such changes generally makes this method impracticable. In order to decrease fault clearance times, the non unit based IDMT over-current protection predominantly used by utilities has to be changed to unit based current differential protection[45]. Differential protection requires relays at either end of the feeder, and a means of passing data from one end to the other. This makes the cost significantly higher than using IDMT over-current type protection, since this only requires one relay and no communications facility. Improvements could also be made using distance protection, this has not been favoured by utilities to date for distribution system protection, due to problems in setting it satisfactorily for short feeders.

Improvements in fault clearance times can also be made by upgrading circuit breakers. An oil circuit breaker may have a total operating time of 100 ms or more[45], whereas an SF6 or vacuum circuit breaker may have an operating time of 50 ms[107].

2.5.2 Resonant Links

Figure 2.11 shows one form of resonant link, known as the short-circuit limiting coupler[51]. The capacitor and linear series reactor are chosen to be in resonance with each other at power system frequency. They therefore present almost zero impedance to load currents.

Under normal operating conditions, the circuit shunted across the capacitor has a high impedance, making the link appear to have nearly zero impedance. When a fault occurs, the voltage across the capacitor rises, causing the main saturable reactor to saturate in less than one system cycle. This results in a large current flowing through the damping resistor which serves to reduce the fault current asymmetry. The voltage produced by this current across R, causes the auxiliary reactor to saturate also, diverting the current away from the resistor and through the auxiliary reactor. The overall combination of inductance of the saturable reactors and the capacitor adds to the impedance of the linear series reactor to limit the fault current and improve system stability. The system takes one to two power system cycles to reset which therefore improves the post fault impedance as well. The link would normally be installed on the utility/industrial plant intertie, and is therefore only of use for faults occurring out in the utility system.

2.5.3 Fast Acting Voltage Regulators

Voltage regulators can apply field forcing to the generator for the fault period which increases the machine's power output when the fault is removed, thereby increasing the amount of decelerating energy available and enhancing stability for a given fault duration[108]. During a fault, the effect of armature reaction will decrease flux linkage, especially if the reactive power output of the generator is large[109]. A decrease in machine flux linkage causes a decrease in output power and a corresponding decrease in machine stability. A fault duration of a few hundred milliseconds will cause a significant decrease in flux linkage[110].

Fast AVR's may serve to improve first swing transient stability, but in doing so reduce the dynamic stability margins for subsequent swings. If the reduction in damping is severe enough, then the generator may maintain stability for the first swing, and then lose synchronism in subsequent swings. This dynamic instability requires incorporation of additional stabilising feedback signals into the AVR to cure the problem[111].

A fast AVR will serve to force the levels of excitation during the fault, and therefore maintain flux levels which would have otherwise decayed. Even though AVR's can significantly improve the flux levels during faults, their effect on the magnitude of the first swing in load angle is generally a reduction of just a few degrees. The situation where they are most beneficial is with long fault clearance times.

Increasing excitation performance also results in more severe pulsations when the machine actually pole slips, as well as increasing the voltage disturbances to other consumers[50]. The AVR tends to 'push' the system centre away from the generator and out into the utility system, because it raises the machine internal voltage level[49]. One method of excitation control proposed known as 'bang-bang' control[112], claims to reduce the impact of pole slipping. With fast excitation systems, the field forcing action will create a make or break type situation where the forcing action will either provide enough retardation energy to maintain synchronism or if it fails in doing this, and the point of no return is past, the excitation will accelerate the rotor into the pole slip, causing a more severe pole slip. A bang-bang excitation control system would remove excitation as the pole slip is entered, and reinstate it after the pole slip at a desirable load angle, thus removing the strong synchronising forces produced by the interaction of stator and rotor magnetic fields.

2.5.4 Turbine Fast Valving

This method increases the speed of response of steam turbine prime mover systems by significantly reducing the mechanical input power to the generator during a fault[113]. It therefore decreases the accelerating power into the rotor and correspondingly increases the decelerating power. During a fast valving operation, the steam valves are completely shut in around 80 to 200 milliseconds, thereby decreasing the output power of the steam turbines[108,114,115,116]. This approach requires a method of detecting rotor acceleration. If a control signal related to acceleration can be derived, then the method does provide a significant increase in transient stability for steam turbine generators.

2.5.5 Fast Governing Systems

A fast response governing system can help to increase the critical clearing time, but will never be able to fully prevent transient instability and hence pole slipping. One stability study showed[15] that inclusion of the governor into the model improved the critical clearing time for a gas turbine generator by 40 ms. The time constants of prime mover and governor systems can vary enormously depending upon the type and sophistication of the

system being considered. Although governors can not completely prevent pole slipping, they are the single most important factor when considering the re-synchronisation of a unit once pole slipping has occurred. A fast governing system will cause a pole slipping generator to re-synchronise after one pole slip cycle if it is not first disconnected.

2.5.6 Braking Resistors

Braking resistors act as a substitute to the load lost due to a fault on the power system therefore 'braking' the generator over the fault period, and decreasing the degree of load angle advance. The resistors are switched off when there is a rotor deceleration[114,116,117]. One problem with braking resistors is determining the instant of switching in and out of the resistors so that transients are controlled most effectively. A sophisticated control scheme is required to enable optimum switching.

When considering embedded generation, the cost of installing a braking resistor and the necessary control schemes would be prohibitive. Braking resistors are normally used with large grid generators in order to meet design stability requirements[118]

2.5.7 Coordinated Control Schemes

Fast AVR's, fast valving, and braking resistors can all be employed at the same time. If they are all controlled by one integrated device, then the transient and steady state stability limits can both be significantly improved[113,116].

2.5.8 Changes in Machine Design

Changes can be made to the parameters of the machine at the design stage which will improve the machine's transient stability. Several novel machine designs have been proposed which produce synchronous machine like output characteristics, but alleviate the transient stability problem.

2.5.8.1 Machine Parameter Changes

The main changes that can be made are to the machine inertia constant and the transient reactance. An increase in the machine inertia constant results in a 'stiffer' machine since more energy is stored in the rotating mass. More acceleration energy will therefore be required to obtain a given deviation in load angle. A higher inertia constant requires a heavier and therefore more expensive machine rotor.

A lower transient reactance will increase the power output of the machine during and after transient disturbances such as faults, providing more deceleration energy. The transient saliency produced by the difference in transient reactances in the direct and quadrature axes causes a further increase in machine output power, as well as shifting the load angle at which the peak occurs to a value greater than 90° [119]. A low value of transient reactance will increase rotor length and therefore the size and cost of the generator[108].

Increased damping will also improve stability, since the resultant asynchronous torque produced by the damper windings and rotor iron will provide a higher real power output for increasing load angles[120]. High damper performance may cause other problems however, since the machines fault current contribution may increase to unacceptable levels, or poor voltage regulation may result due to the damper circuit limiting the rate of change of flux[108].

Embedded machines can sometimes have high values of stator resistance, due to their small size. This causes a decrease in inherent stability[121], low per unit stator resistance is therefore also a virtue. Section 3.5.3 discusses this in more detail.

2.5.8.2 Novel Machine Designs

One development[112] allows the machine load angle to be kept constant irrespective of load power factor, allowing the machine to absorb reactive power up to the thermal limit of the stator without compromising transient stability. It achieves this by using a divided-winding rotor, one half of which is responsible for providing the torque necessary to hold the rotor in synchronism. The other half is responsible for the reactive power control of the machine, applying positive or negative excitation depending on the power factor of the load supplied. The machine load angle can be kept at a constant value of 40°. Transient stability is improved because when load angle increase occurs during a fault, the position of the resultant rotor mmf can be held constant by altering the reactive excitation level. The down side of the scheme is the additional cost of the excitation system, since thermal differential expansion and contraction problems result due to the separate rotor windings carrying different levels of excitation current.

Another machine development removes the problems of synchronous stability and hence pole slipping by relieving the rotor magnetic field from being fixed to the rotor[122]. A polyphase excitation winding is used on the rotor, which is excited with polyphase slip

frequency voltages of proper sequence and phase. In doing this the desirable features of synchronous and asynchronous machines can be realised. The machine's output power characteristics are similar to those of a conventional generator, yet the asynchronised synchronous machine is capable of operating with slip. Machine stability is related to the performance of the excitation system, and the benefits of the new scheme are accounted for in the increased cost of the excitation system required.

2.5.9 Induction Machines

An obvious way of eliminating pole slipping is to use induction machines instead of synchronous machines. An induction machine rotor does not rotate in synchronism with the stator electromagnetic field and therefore can not lose synchronism. Although the initial cost of an induction machine may be less than that of a synchronous machine, induction generators require additional design considerations that synchronous generators do not[7]. The savings in equipment purchases may easily be swamped by more expensive operating costs if the situation is not fully analyzed. Induction machines only operate efficiently at full load. At part load exciting VAr's are required from the system, worsening the operator's power factor and increasing the tariff set by the utility. Induction machines can not be used to operate an independent power island, whereas synchronous machines can. Synchronous generators can also be used to offset a site's reactive and real power demand.

2.6 CHAPTER SUMMARY

All of the suggestions given in this chapter for improving transient stability are expensive and are more applicable to large 'grid' generators rather than small and medium sized embedded machines. All such methods improve transient stability, and therefore reduce the risk of pole slipping, but they do not eliminate it completely however.

The alternative is to install relays that will disconnect the generator from the system when a threatening situation occurs, preventing the generator from the damage caused by pole slipping and the possible disturbance to the power system. The established techniques generally offer a level of pole slipping protection, the single blinder scheme being the most reliable. This scheme requires a complete pole slip cycle to operate however, it is not able to disconnect a generator before a pole slip occurs. Another problem with the

impedance based schemes is that they are difficult to set so that they will operate correctly for all conditions. A detailed computer based simulation study is necessary in order to set the relays with a high degree of confidence.

The majority of new pole slipping protection schemes proposed rely on data being available on the generator and the power system to which it is connected. Data acquisition can be difficult, time consuming and therefore expensive. Even if all of the data is available, techniques which use a quantitative approach to predicting generator instability may fail due to inaccuracies in the data, or in the measurements of the generator's state of operation.

The design challenge is to devise a pole slipping relay which can detect all asynchronous conditions, restrain for all other operating conditions, is easy to set, and inexpensive to realise.

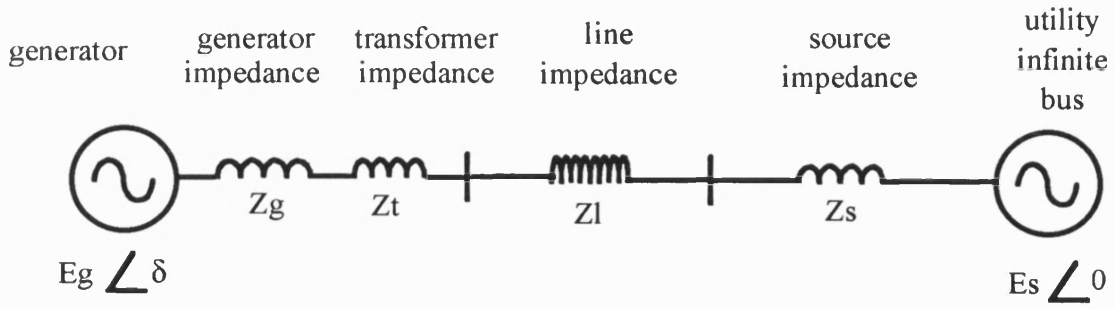

Figure 2.1a
Two Machine Representation of a Power System.

KEY

Zsys, System impedance (Zl+Zs)
Zt, Transformer impedance
Zg, Generator impedance (Xd')
Zl, Line impedance
Zs, Source impedance

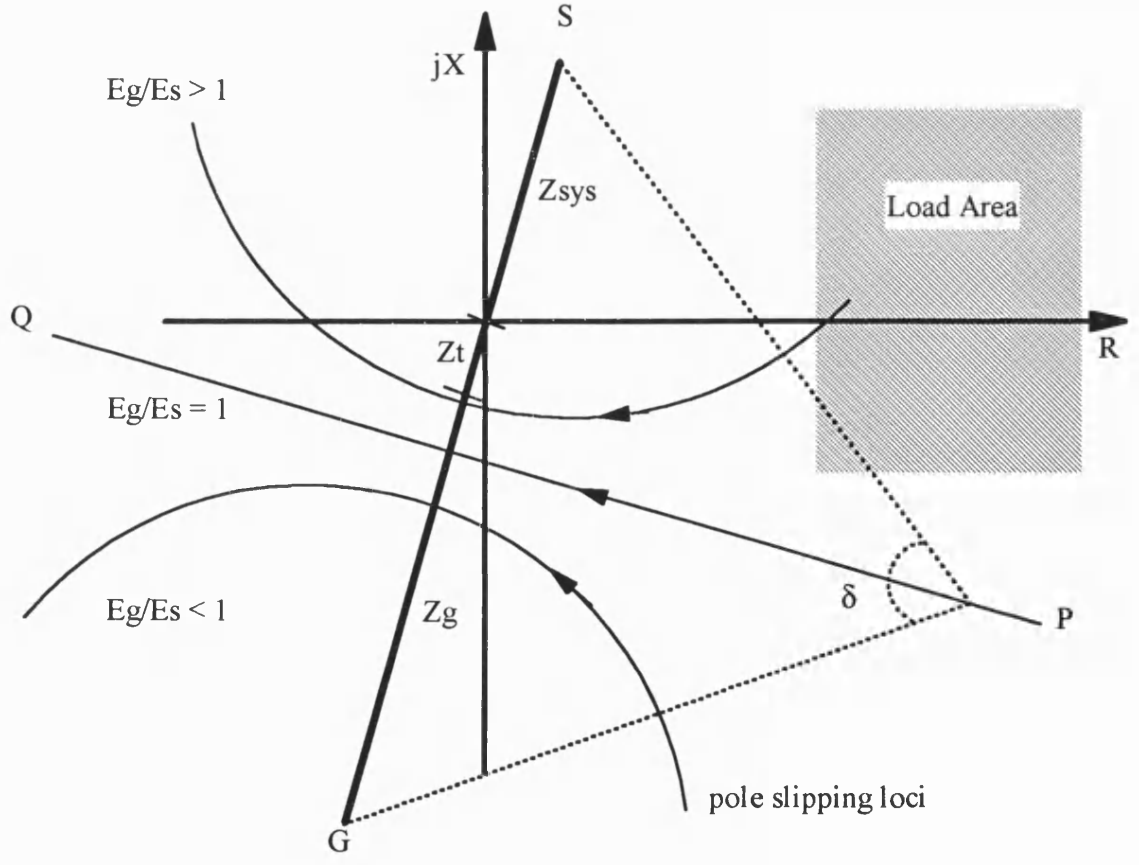

Figure 2.1b
Classical Pole Slipping Impedance Loci.

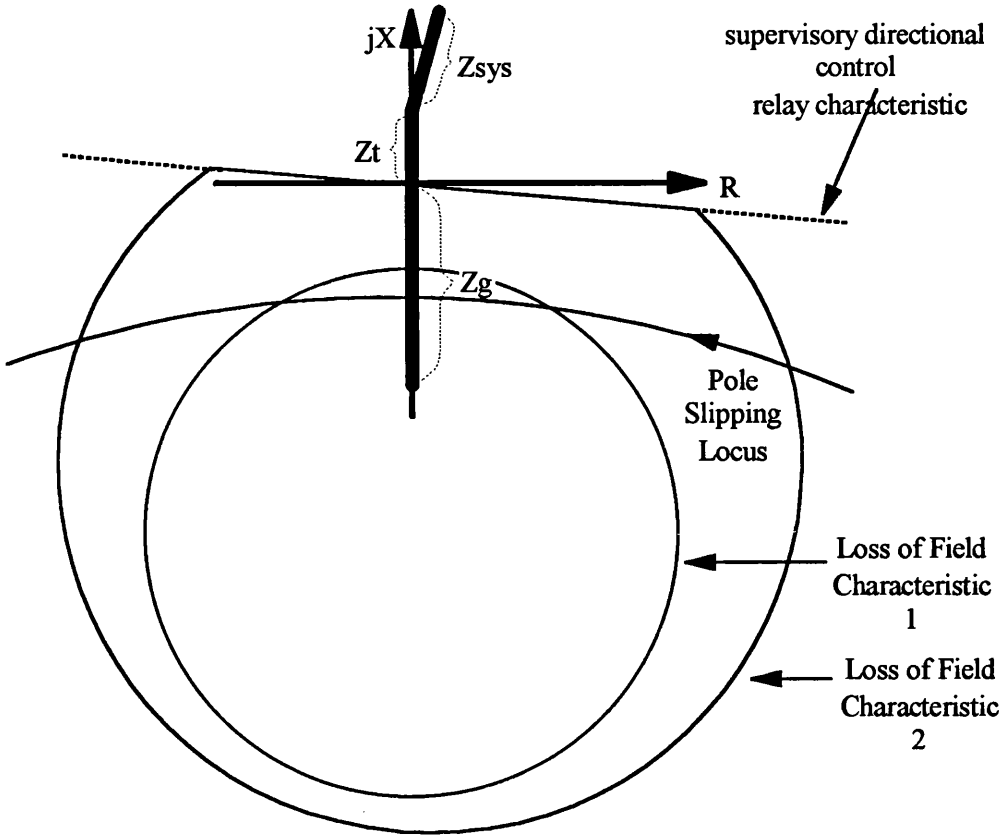

Figure 2.2
Loss of Field Relaying Scheme also used for Pole Slipping Protection.

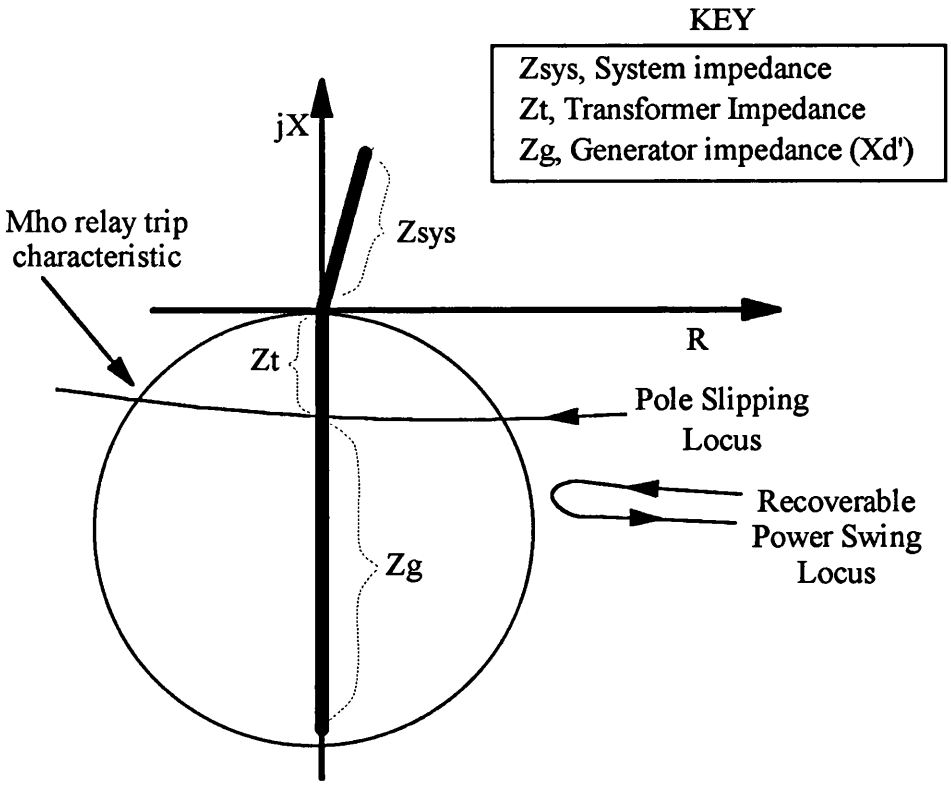

Figure 2.3
Mho Element Pole Slipping Protection Scheme

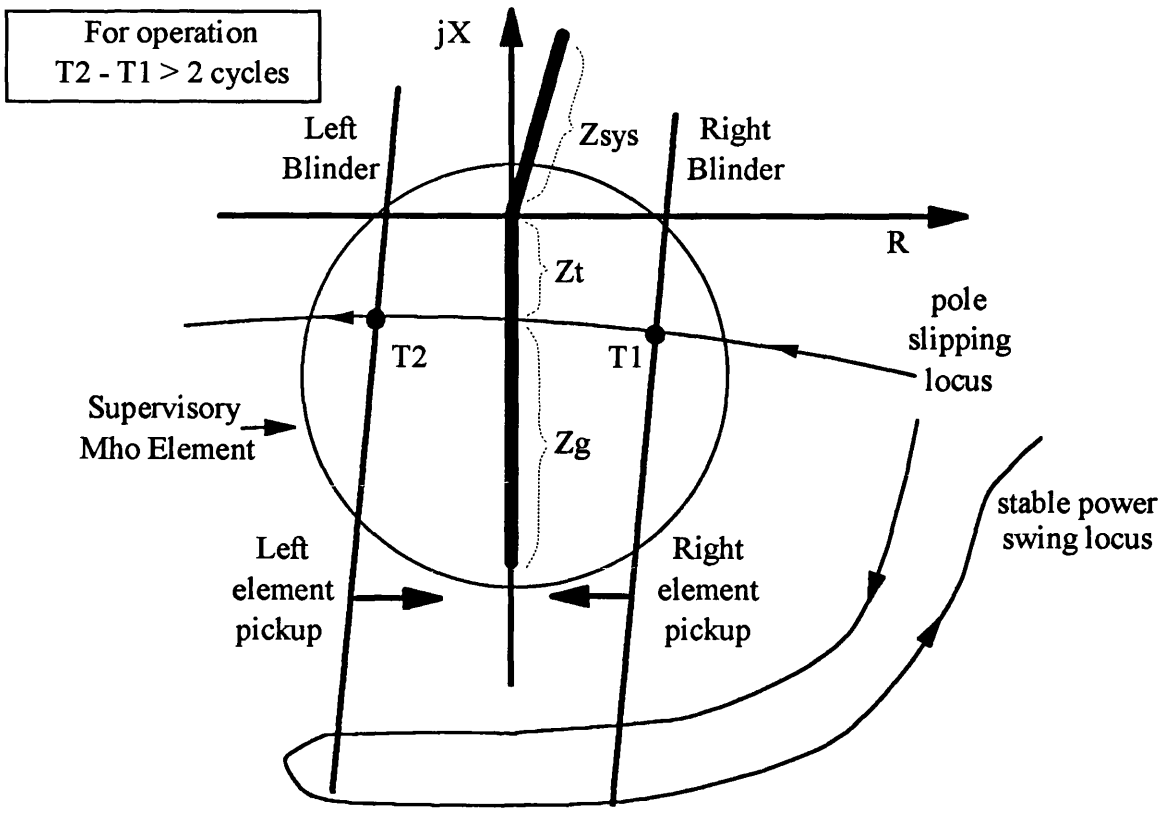

Figure 2.4
Single Blinder Pole Slipping Detection Scheme

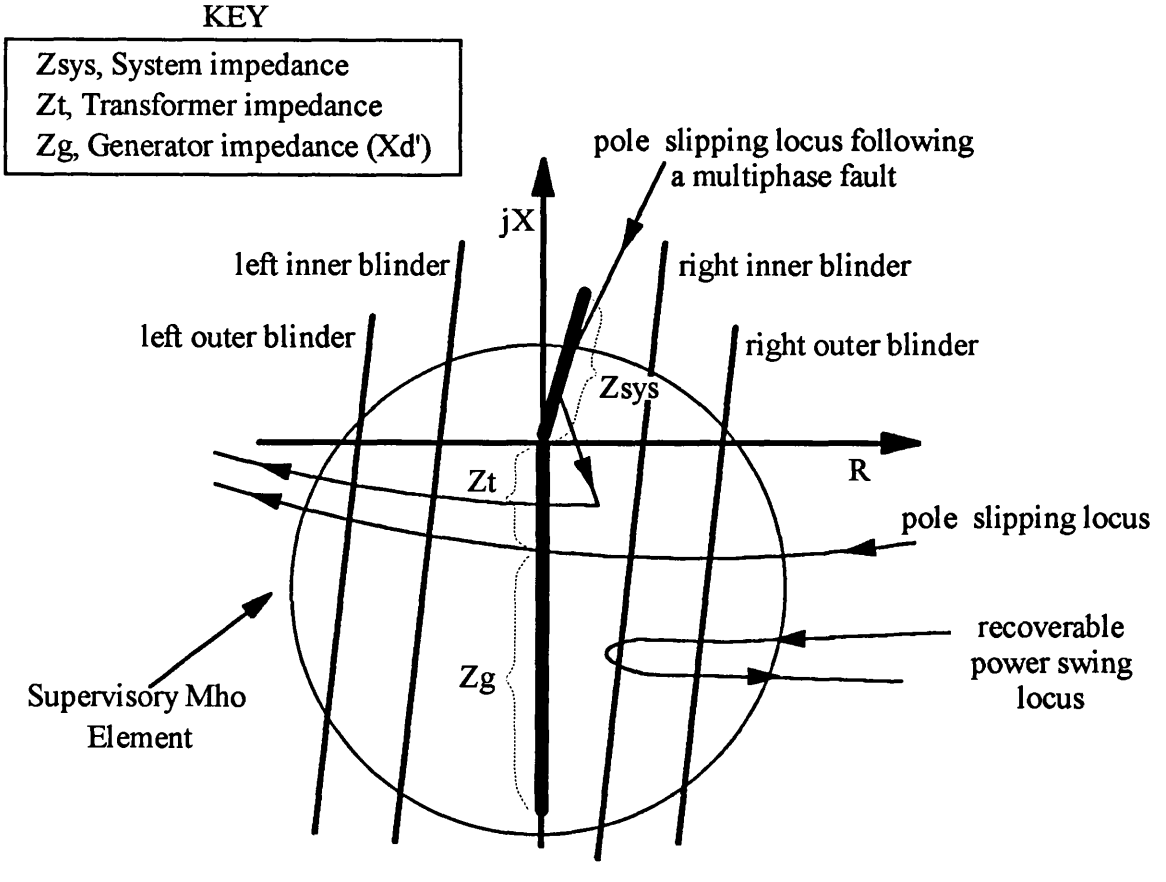

Figure 2.5
Double Blinder Pole Slipping Protection Scheme.

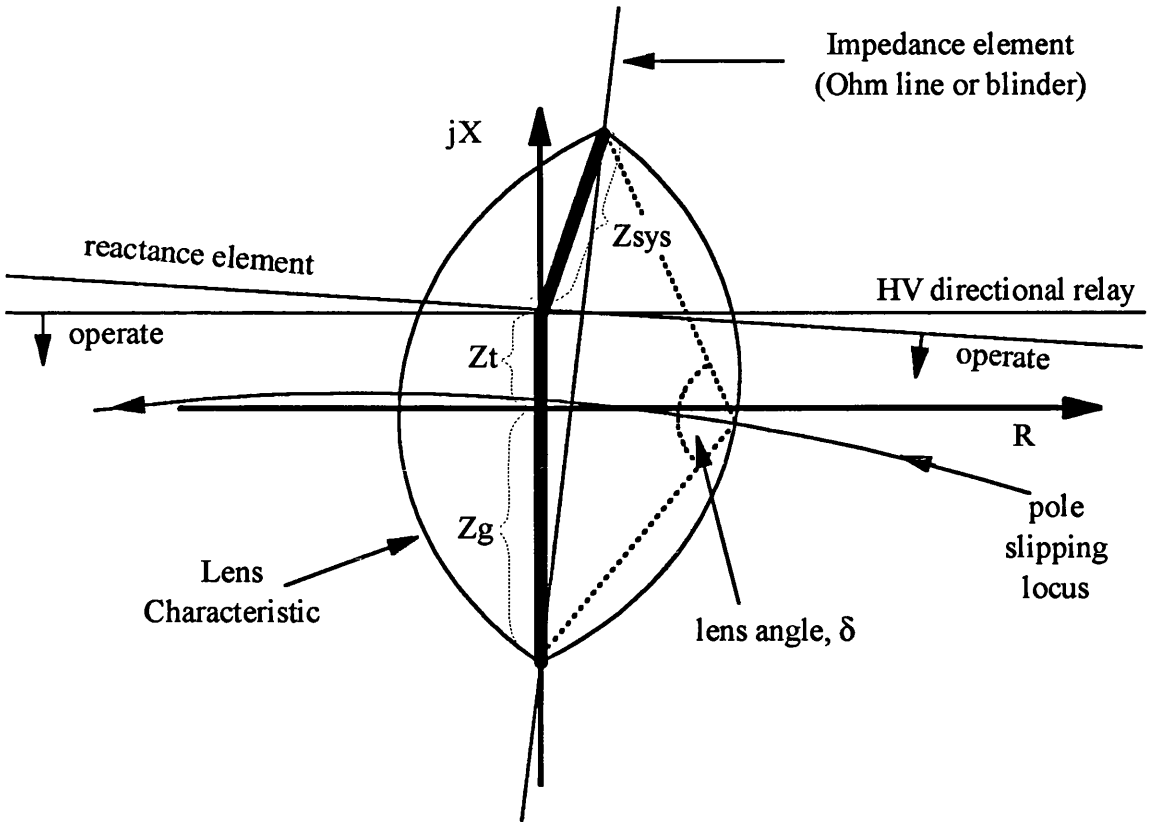

Figure 2.6
Lenticulare Type of Pole Slipping Detection Scheme

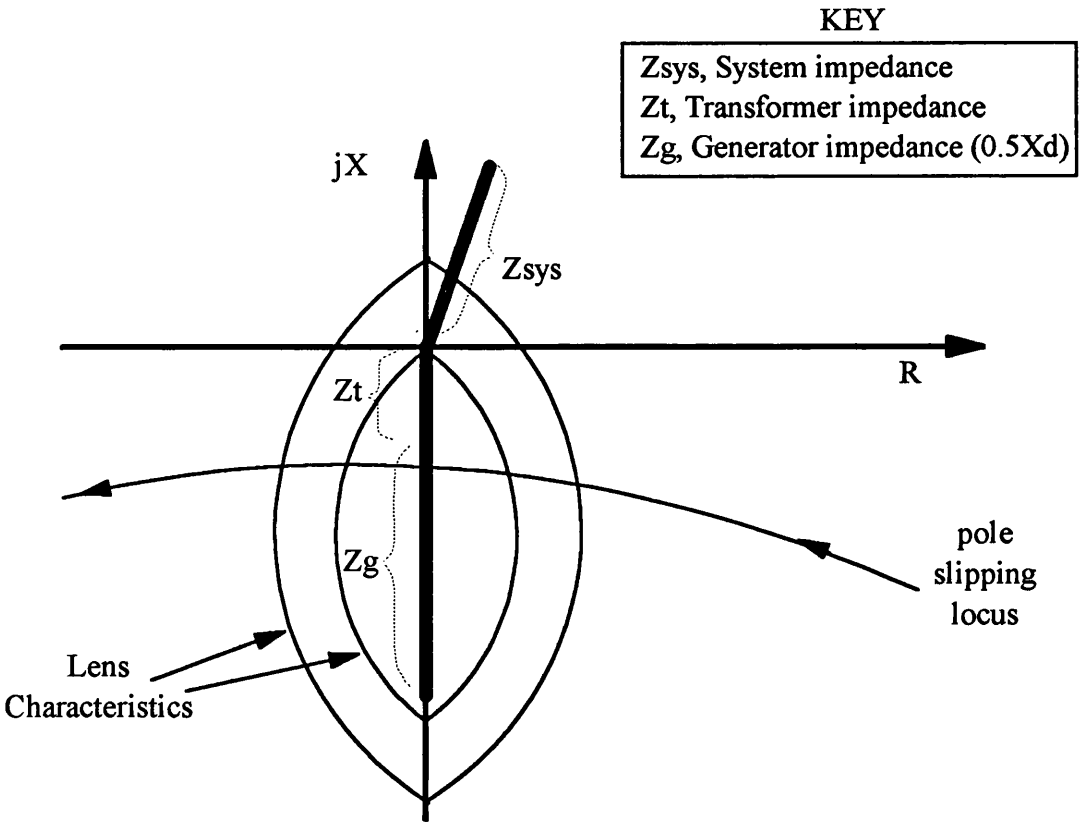

Figure 2.7
Double Lens Type of Pole Slipping Detection Scheme

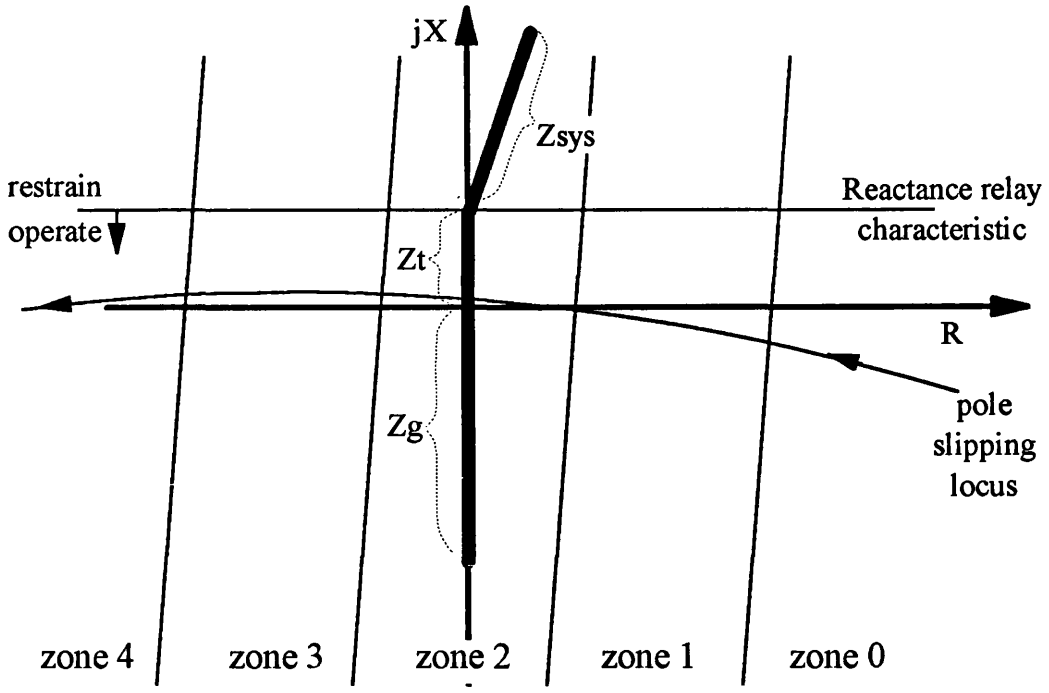

Figure 2.8
Multiple section Microprocessor Based Pole Slipping Protection.

KEY

Zsys, System impedance
Zt, Transformer impedance
Zg, Generator impedance (Xd')

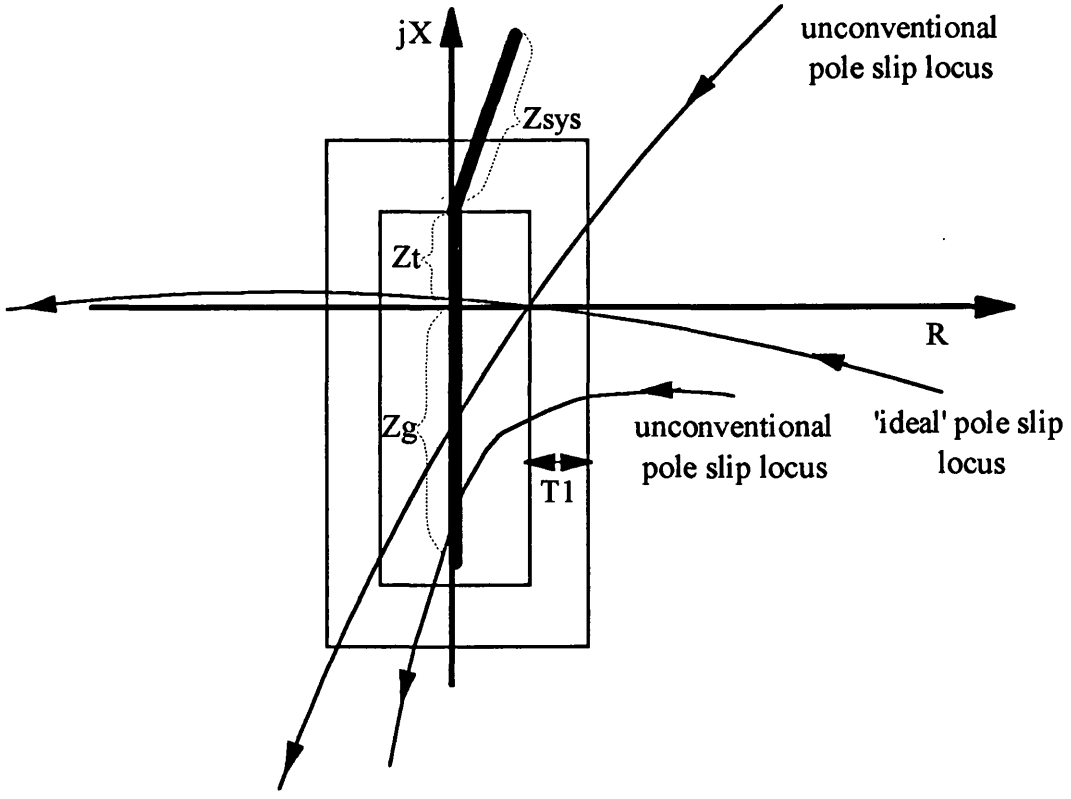

Figure 2.9
Quadrilateral Impedance Relay Characteristic.

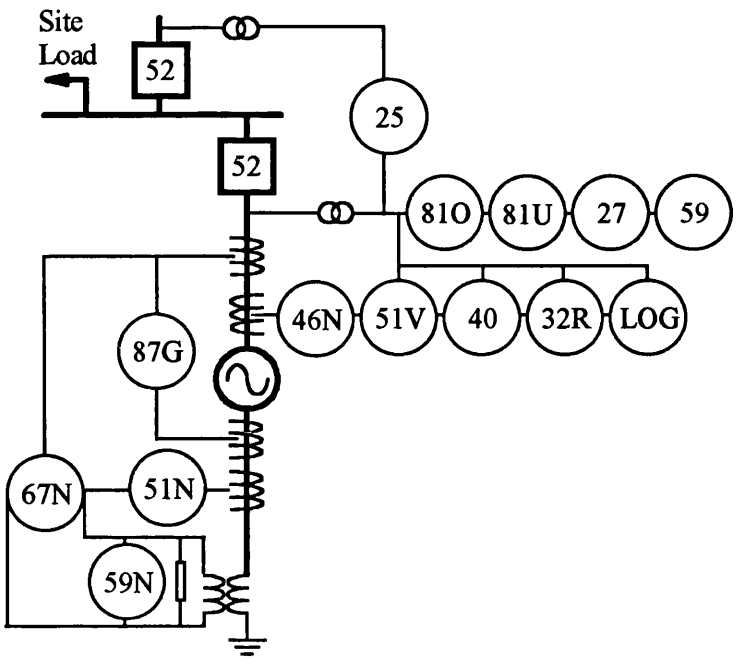

81O	Over Frequency Relay.
81U	Under Frequency Relay.
59	Over Voltage Relay.
27	Under Voltage Relay.
25	Check Sync Relay.
46N*	N.P.S. Overcurrent.
51V*	Voltage Dependent Overcurrent.
59N	Neutral Displacement.
40*	Loss of Excitation.
87G*	Differential Relay.
32R*	Reverse Power.
51N	Stator Earth Fault.
67N*	Directional Earth Fault.
LOG	Loss of Grid Protection.
52	Circuit Breaker.

* these functions may be ommitted

Figure 2.10
Comprehensive Embedded Generator Protection Scheme.

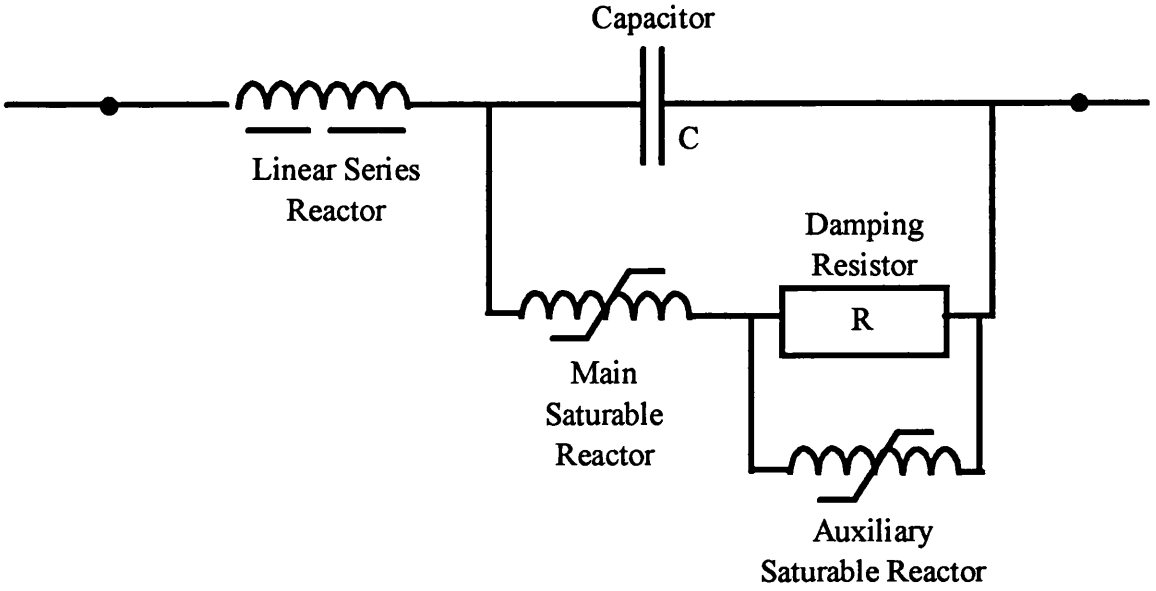

Figure 2.11
Resonant Link Used for Improving Stability.

Chapter 3
SYNCHRONOUS GENERATOR CHARACTERISTICS

3.1 IDEAL SYNCHRONOUS POWER CHARACTERISTICS

The characteristic response of synchronous machines is dominated by the interaction between the field winding flux and the stator flux. This results in a sinusoidal power/load angle characteristic. For a machine connected to an infinite bus, supplying a balanced set of voltages, the steady state real and reactive power load angle characteristics are given by;

$$Pss = \frac{1}{R^2 + XdXq}\left[V^2\left(\left(\frac{Xd - Xq}{2}\right)\sin(2\delta) - R\right) + EVZ\sin(\delta + \theta)\right] \qquad 3(1)$$

$$Qss = \frac{1}{R^2 + XdXq}\left[EVZ\cos(\delta + \theta) + V^2\left(\left(\frac{Xd - Xq}{2}\right)\cos(2\delta) - \left(\frac{Xd + Xq}{2}\right)\right)\right] \qquad 3(2)$$

where $Z = \sqrt{(R^2 + Xq^2)}$ and $\theta = \sin^{-1}(R/Z)$. Appendix A covers the derivation of the effective generator voltage, E for various machine loadings.

Due to the small field resistance, the field flux linkage will generally remain constant following a change in operating condition[123]. When a sudden change in stator current occurs, due to a short circuit for example, the resulting current transient can be broken down into two components[36,124,125,126]. The first component is referred to as the sub-transient component, the second the transient component. The sub-transient component occurs due to circuits other than the field winding on the machine rotor. In salient pole machines, these circuits are provided by damper windings, whilst in round rotor machines, the solid steel rotor provides the circuits for induced eddy currents to flow.

The circuits formed by the field winding and the damper windings form two coupled circuits. These are at rest with respect to each other, but both rotate with respect to the stator. These two circuits have two time constants, a short sub transient time constant, and a longer transient time constant. Both of these time constants are effected by the impedance of the stator. If the stator is short circuited, the time constants are given by their short circuit values Td' and Td", whilst they take on their open circuit values, Tdo'

and Tdo" if the stator is open circuited.

The magnitude of the stator current during the sub transient period is determined by the direct axis sub transient reactance, Xd", whilst the transient magnitude is determined by the direct axis transient reactance, Xd'. Typical values for Tdo" and Td" are 0.125 and 0.035 seconds[110]. Since pole slipping has a considerably longer time period than these values, the sub transient period is of less interest than the transient period. The sub transient period is important for the short circuit characteristics of the machine when setting protection relays or calculating plant ratings. Typical values for Tdo' and Td' are 6 and 1.5 seconds[110], the transient period is therefore of major interest when considering pole slipping characteristics. The transient real and reactive power machine angle characteristics are given by;

$$Ptr = \frac{1}{R^2 + Xd'Xq}\left[V^2\left(\left(\frac{Xd' - Xq}{2}\right)\sin(2\delta) - R\right) + Eq'VZ\sin(\delta + \theta)\right] \qquad 3(3)$$

$$Qtr = \frac{1}{R^2 + Xd'Xq}\left[Eq'VZ\cos(\delta + \theta) + V^2\left(\left(\frac{Xd' - Xq}{2}\right)\cos(2\delta) - \left(\frac{Xd' + Xq}{2}\right)\right)\right] \qquad 3(4)$$

Appendix A contains details on how to calculate the voltage behind transient reactance, Eq', for various machine loadings. Equations 3(1,2,3,4) are for a general synchronous machine.

In general two types of synchronous machine need to be considered. The round rotor and the salient pole type. Round rotor design is typically used for high speed, two pole generators driven by steam turbines. Salient pole designs are used for lower speed multiple pole pair generators such as hydro generators. The real and reactive power characteristics for both types of generators will be discussed in the following sections.

3.1.1 Round Rotor Machine Real Power Characteristics

Figure 3.1a shows the real and reactive power rotor angle plots for a 200 MVA round rotor machine operating at no load and full load in steady state and transient modes. The steady state curves show the fundamental component, produced by the interaction between the field winding and the stator mmf's. This is the sinusoidal characteristics on the no load curves. The real power reaches its peak at a rotor angle of 90°, and stable steady state generator operation can therefore only be maintained between 0 and 90°.

The transient curves have an additional 2δ component, due to transient saliency. This occurs due to the absence of a field winding on the quadrature axis. During transients, the direct axis reactance changes from its synchronous value, Xd, to its transient value, Xd', whilst the quadrature axis reactance stays at its synchronous value. The effect of this 2δ component is to shift the peak of the real power curve past 90°. The peak of the real power curve increases during transient conditions, and this helps the machine to maintain stability following power system disturbances such as short circuits faults. The additional power output capability during transient conditions enables the generator to produce more decelerating energy, which helps retard the rotor towards synchronous speed.

When a pole slip occurs, the machine real power output follows the characteristic given in Figure 3.1a. This shows that at the 120° rotor angle point, the machine is generating five times its rated power, whilst at 240°, it is importing five times its rated power. Note that the difference between the no load and full load curves is small. The main difference is that during full load, there is more mechanical input power into the generator, which promotes faster, more violent pole slips. A pole slip is unlikely to occur from no load because there is virtually no mechanical input power to accelerate the rotor into a pole slip.

3.1.2 Round Rotor Machine Reactive Power Characteristics

Figure 3.1b shows the reactive power/rotor angle curves for steady state and transient, no load and full load conditions. This is also sinusoidal with the difference between this and the real power plot being a phase shift of 90°. The transient curves have been raised from the steady state curves for load angles between 40 to 90° and 270 to 320°, whilst they are much lower than the steady state curves between 90 and 270°. At a value of 90°, all of the curves converge. Equations 3(2) and 3(4) show that at 90°, the equation simplifies to;

$$Q = \frac{-1}{R^2 + XdXq}\left(EVZ\sin(\theta) + V^2Xd\right) \qquad 3(5)$$

This is correct for steady state conditions, during transient conditions, Xd must be replaced by Xd', and E by Eq'.

3.1.3 Salient Pole Generator Real Power Characteristics

Figure 3.2a shows the real power rotor angle characteristics for the 625 kVA salient pole diesel generator described in appendix A, section A3.1.3. The most obvious difference

between the round rotor and salient pole generator curves is the rotor angle at which the peak in steady state real output power occurs. The 2δ term in equation 3(1) causes the peak to occur at load angles below 90°. The transient peaks also occur at lower load angles for salient pole machines, but will still occur at load angles greater than 90°.

3.1.4 Salient Pole Generator Reactive Power Characteristics

Figure 3.2b shows reactive power rotor angle characteristics for the 625 kVA salient pole generator. The main difference between these curves and the round rotor generator curves are that the steady state curves flatten off as they approach rotor angles of 180°. The common point where all of the curves converge is the same for salient pole and round rotor generators, and is given by 3(5).

3.2 GENERATOR ASYNCHRONOUS POWER CHARACTERISTICS

When the generator rotor travels at speeds other than synchronous speeds, real and reactive power is also produced due to induction machine action. The output power characteristics are therefore not only dependent upon the rotor angle, but also on the time rate of change of rotor angle. The asynchronous component of real power, P_{as}, depends upon the asynchronous constants of the generator, the applied voltage, rotor angle, and its time rate of change, referred to as the slip, s. This is defined as;

$$s = -\frac{d\delta}{dt} \qquad 3(6)$$

Slip is negative for speeds above synchronous speed. The asynchronous power, P_{as} which is produced during steady asynchronous operation, is given by;

$$P_{as} =$$

$$-\frac{V^2}{2}\frac{Xd-Xd'}{Xd.Xd'}.\frac{sTd'}{1+(sTd')^2}.\left((1+\sqrt{1+(sTd')^2}).\sin\left(2\delta_o-\tan^{-1}\left(\frac{1}{sTd'}\right)-2st\right)\right)$$

$$-\frac{V^2}{2}\frac{Xd'-Xd''}{Xd'.Xd''}.\frac{sTd''}{1+(sTd'')^2}.\left((1-\sqrt{1+(sTd'')^2}).\sin\left(2\delta_o-\tan^{-1}\left(\frac{1}{sTd''}\right)-2st\right)\right) \qquad 3(7)$$

$$-\frac{V^2}{2}\frac{Xq-Xq''}{Xq.Xq''}.\frac{sTq''}{1+(sTq'')^2}.\left((1-\sqrt{1+(sTq'')^2}).\sin\left(2\delta_o-\tan^{-1}\left(\frac{1}{sTq''}\right)-2st\right)\right)$$

Where δ_o is the initial rotor angle, and the values of the $\tan^{-1}$ terms lie between 0 and 180° [35]. The first term is produced as a result of the direct axis field winding, whilst the

second and third terms are produced as a result of the damper windings. If the generator is operating on a non infinite bus, than the reactances of the tie line can be added to the leakage reactance of the generator when calculating the generator reactances and time constants. The asynchronous reactive power, Q_{as} is given by;

$$Q_{as} =$$

$$-\frac{V^2}{2}\frac{Xd-Xd'}{XdXd'}\cdot\left(\frac{(sTd')^2}{1+(sTd')^2}+\frac{sTd'}{\sqrt{1+(sTd')^2}}\cdot\cos\left(2st-\tan^{-1}\left(\frac{1}{sTd'}\right)\right)\right)$$

$$-\frac{V^2}{2}\frac{Xd-Xd''}{XdXd''}\cdot\left(\frac{(sTd'')^2}{1+(sTd'')^2}+\frac{sTd''}{\sqrt{1+(sTd'')^2}}\cdot\cos\left(2st-\tan^{-1}\left(\frac{1}{sTd''}\right)\right)\right) \qquad 3(8)$$

$$-\frac{V^2}{2}\frac{Xq-Xq''}{XqXq''}\cdot\left(\frac{(sTq'')^2}{1+(sTq'')^2}-\frac{sTq''}{\sqrt{1+(sTd')^2}}\cdot\cos\left(2st-\tan^{-1}\left(\frac{1}{sTq''}\right)\right)\right)$$

Both the real and reactive power asynchronous equations consists of a steady component plus a pulsating component. It is important to note the units used in these equations. Units of slip are in absolute values so that a slip of 1 % corresponds to 0.01. The reactances are all in per unit, whilst the time constants and time are in radians, where $t_{[rad]} = \omega_o\, t_{[sec]}$. ω_o is the electrical angular frequency of the generator [127].

The expressions for synchronous and asynchronous power can be added to give the complete output power of the generator, noting that effects such as saturation have not been taken into account. The equations are useful for gaining an understanding of synchronous machine characteristics. If more accurate characteristics are required a computer based simulation should be used because the mathematics can become too complicated for easy use.

3.3 PRACTICAL SYNCHRONOUS GENERATOR CHARACTERISTICS

The characteristics discussed in sections 3.1 and 3.2 are ideal. For the operation of practical machines, other phenomena need to be considered. The discussions in this chapter relate mainly to generator power characteristics because the algorithms developed use power as their basis. References [110,123,128,129,130] all contain good discussions of generator operating current and voltage characteristics. There are three additional characteristics which are caused by non constant flux linkage, and trapped flux in the

stator. Stator resistance also effects the characteristics, although to a lesser extent.

3.3.1 Non Constant Flux Linkage - The Direct Axis Open Circuit Transient Time Constant, Tdo'

In section 3.1, it was assumed that the field flux linkage remained constant following a transient[123,126,131]. For a sudden application of a step change in field voltage, the time constant of the field during stator open circuit conditions is given by Tdo'. Since the open circuit stator terminal voltage is proportional to the field current in an unsaturated machine, the stator voltage will also change with this time constant. This time constant is given by [110];

$$Tdo' = \frac{Lff}{Rf} \qquad 3(9)$$

Where Lff is the field inductance, and Rf is the field resistance. Most discussions involving synchronous generators are related to large generators which have ratings of hundreds of megawatts. These will have a very high field inductance to resistance ratio and so have a long field time constant, the assumption of constant field flux linkage is therefore valid for at least the first second of a transient. Small embedded generators have much higher per unit resistances, and consequently have much shorter field time constants, the assumption of constant flux linkage is therefore not valid. Tables C1 and C2 of Appendix C contain values of Tdo' for generators ranging from 5 kVA up to 384 MVA. For typical embedded generators, rated below 3 MVA, Tdo' ranges between 1 and 2 seconds, whilst for the larger grid type machines with ratings above 10 MVA, Tdo' ranges between 4 and 7 seconds. Small and medium sized embedded generators generally have shorter time constants than grid connected generators.

Tdo' is applicable to a generator with an open circuited stator, a similar measure known as Td', the short circuit time constant, is applicable when the stator is short circuited. Td' is related to Tdo' by the following equation;

$$Td' = \frac{Xd'}{Xd} Tdo' \qquad 3(10)$$

Tables C1 and C2 show that for small embedded generators, Td' is typically between 100 and 200 ms, whilst for the larger 'grid' type generators, Td' is typically above 1 second. When the generator is connected to balanced external impedances, the field time constant will lie between Tdo' and Td'. Td' is useful when considering generator stability following

a short circuit fault, since it indicates how long the field flux will remain constant, and therefore how long the generator reactance will remain at Xd' and the internal emf at Eq'. When the flux linkage starts to decay, the generator operating characteristic will move from that defined by equation 3(3) to that of 3(1). Having short values of Td' therefore has implications for generator stability, it also affects the performance of conventional impedance based protection schemes. Figure 3.3a shows the real power against time output for three simulations of a diesel driven generator following a close up short circuit fault[132]. In two of the simulations, the generator time constant, Tdo' is equal to 2 and 6 seconds and the generator AVR and governor have been disabled. For the other simulation, Tdo' was set to 2 seconds with a slow acting AVR enabled. The generator parameters are given in Appendix C. For all three simulations, the fault duration was such that stability was just maintained, i.e the generator swung up to the critical stability point (CSP)

The generator is initially operating at full power, which is 80 % of rating. Referring to Figure 3.3a, when the fault begins a small oscillation occurs before the power falls to almost zero. This occurs due to trapped flux in the stator and will be discussed in section 3.3.3. The load angle then begins to increase until it reaches a value of around 135°, the fault is then cleared and the power jumps up to 3 pu. The peaks of the curves A1, B1, and C1 are all at different heights. The highest is the Tdo' = 6.0 s curve, then the Tdo' = 2 s, AVR included case, and then the Tdo' = 2 seconds with no AVR. The Tdo' = 6 s curve jumps the highest because the field flux has decayed the least during the fault. The simulation with the AVR included out performs the manual AVR simulation due to the field forcing action of the AVR during the fault. This has the effect of increasing machine flux. The peaks of the curves did not reach the level predicted in Figure 3.2a due to external circuit reactance and field flux linkage decay. Kimbark[110] gives details on how to calculate the exact change in field flux and states that for generators with a value of Tdo' of around 5 seconds, the assumption of constant flux linkage is a reasonably accurate one unless the clearing time for severe faults is greater than 0.2 sec. A large amount of faults that an embedded generator experiences will be longer than 200 ms, due to the IDMT type over-current protection used on distribution feeders. This coupled with the fact that Tdo' for embedded generators is much less than 5 seconds means that a significant flux linkage decay will occur for faults. This has implications for stability and the operation of conventional pole slipping schemes.

Referring back to Figure 3.3a, the curves then continue towards the CSP, which is roughly at the input power level of 0.8 pu. The CSP's for each simulation are not exactly at 0.8 pu because the fault clearance time was adjusted in one millisecond steps to determine the CSP. After the CSP, the curves head back towards their original steady state operating points. Again the curves all attain different maximum swings in output power, A2, B2, and C2 for the same reason as above. The A2 curve flattens off much earlier than the others because of the decaying flux, this reduces the synchronising coefficient, making the system less oscillatory. It therefore can not be assumed that the flux linkage is constant for embedded generators.

3.3.2 Effects of High Stator Resistance on Generator Operation

Equations 3(1,2,3,4) show the effect of high stator resistance, R, on generator operation. A high stator resistance has two effects on the real power characteristics. It shifts the peak of the power rotor angle curve back by a value, θ, so that it is less than 90°. It also shifts the whole curve downwards by a value $R/(R^2+XdXq)$. In general, unless the generator is less than 50 kVA, the stator resistance will have little effect on the steady state operating characteristics. Tables C1 and C2 of Appendix C give data for a range of synchronous machines. The stator resistance is typically 0.05 pu in small machines, which is negligible compared to a value of Xd between 1 and 2 pu. The greatest effect which resistance has on generator operation is with regard to stability. This will be discussed in section 3.5.8.

3.3.3 Armature Time Constant, Ta

When there is a sudden change in stator current following a fault or large load change, there exists dc, fundamental, and second harmonic components in the phase current. The dc and second harmonic components arise from flux trapped in the stator circuits at the instant of the fault. This flux decays to zero in a time governed by the armature time constant, Ta[110,123]. The stationary trapped stator flux induces a fundamental frequency current in the rotor, which then induces a second harmonic flux back into the stator. The armature time constant is dependent upon the ratio of stator short circuit inductance to resistance. Typical values range between 0.04 and 0.4 seconds[109].

3.3.4 Three Phase Short Circuit Torques and Powers

During and after a three phase short circuit, the generator torque and therefore real power, can be broken down into three components. A dc component due to i^2r losses in the stator and rotor, a fundamental frequency component due to trapped stator flux, and a double frequency component dependent upon the sub transient saliency[123]. The double frequency terms during balanced faults are usually negligible compared to those generated during unbalanced conditions.

As well as the above components, the components due to equation 3(3) also occur at a reduced level because the fault reduces the generator terminal voltage. The fundamental frequency component decays according to the value of armature time constant, Ta. It is important that the existence of such oscillations in torque are known when designing power based protection algorithms.

3.3.5 Unbalanced Short Circuit Torques and Powers

Unbalanced short circuit faults will cause all of the components in torque and power discussed above, the main difference is that the second harmonic component is much greater due to the unbalance. This introduces a 'saliency' in the stator which in addition to any rotor saliency results in double frequency terms in generator real power. An unbalanced load will also produce twice power system frequency terms in power.

3.3.6 The Effect of External Impedance on Generator Operating Characteristics

The equations presented above apply to a generator operating against an infinite bus. The external reactance between generator terminals and bus is by definition, zero. This does not occur practically, however in most cases the external impedance is negligible compared to the generator impedances and the generator can therefore be regarded as operating on an infinite bus. In situations where this is not the case, the real and reactive power equations and time constants can be modified to take the external impedance into account by adding the external impedance to the stator leakage value[35,127]. This approach has been dealt with in Appendix A4.1, for a general synchronous machine.

3.4 GENERATOR CAPABILITY CHARTS

The generator capability, or operating chart is used by generator operators to show the limits of operation of the generator[120,129,130,133,134]. It uses real and reactive power as its two axis. Figure 3.4a shows a round rotor generator operating chart, whilst figure 3.4b shows the under-excited section of a salient pole generator operating chart.

Figure 3.4a and 3.4b shows that the theoretical stability limit is determined by Xq. Figure 3.4a has been labelled Xd since this parameter is most commonly used when referring to round rotor machines. In a round rotor machine Xd and Xq are approximately equal. The practical stability limit line on both diagrams shows that, the generator is always operated to the right of the theoretical stability limit. This allows for fluctuations in load and improves the transient stability margin following power system short circuit faults[135].

3.4.1 Reactive Power Limits

Figure 3.4a shows that with a fast, high performance AVR fitted, it is possible for the generator to operate beyond the theoretical stability limit. Depending upon the impedance of the intertie connecting the generator to the system, it is possible to operate the generator at load angles of up to 130° [120]. This improves the generator's reactive power absorbing capability beyond the theoretical stability limit level of $-V^2/Xd$. If the AVR is capable of supplying negative field current the theoretical no load level becomes $-V^2/Xq$ [123]. However, operation beyond the stability limit does not occur in practice because the generator is likely to become unstable following power system short circuit faults. Some generators are not required to have any reactive power absorbing capability[13], and it is common practice to fit minimum excitation limiter circuitry[136] to embedded generator AVRs to prevent absorption of high amounts of reactive power during high system voltages. This prevents the generator from pulling out of step and thermal overloading during high grid voltages.

Large generators are also fitted with minimum excitation limiters, which are set so that the machine can not operate past the practical stability line[137]. In practice the reactive power absorbing capability of the generator may be less than predicted by theory due to shorted rotor field turns. Many synchronous generators are shipped with one or more shorted turns[137].

Figure 3.4b shows an excitation margin, at the low power region of the capability chart. This is required because the excitation system on some generators is not capable of reducing the field voltage to zero, they therefore have circuitry fitted which limits the field voltage to 5 % of the full load value[133].

3.4.2 Saturation Effects

At low values of excitation, saturation effects are at their lowest, and the synchronous reactance remains constant. The synchronous reactances will therefore be at the manufacturer's values at low excitations, because the open circuit characteristic almost coincides with the air gap line. The unsaturated value of synchronous reactance is normally quoted by manufacturers. As field current is increased, saturation decreases the value of synchronous reactance[130]. Saturation effects are most dominant in the lagging power factor region. In the leading VAr operating area, the effect of saturation is to flatten the normal power angle curve and at the same time, push the maximum power angle above 90°. This drift of the stability limit increases with excitation; at low excitations which correspond to low output powers close to the theoretical stability limit, the effect is negligible. The extent of the drift of the theoretical stability limit depends on the degree of saturation, but even in extreme cases, the overall effect is quite small and shifts the maximum power angle up by 5 to 10° at full load[32]. The effect of stator resistance is the opposite to that of saturation, and the two effects will therefore cancel each other to some extent.

3.5 EMBEDDED GENERATOR STABILITY - THE LIKELIHOOD OF POLE SLIPPING

Embedded generators which operate in parallel with utility distribution systems are more likely to suffer transient instability than the larger grid type generating sets which are connected to transmission circuits. This is due to their low inertias, low time constants and the long fault clearance times associated with utility distribution systems.

Transient stability is the ability of the generator to produce forces which act to restore the generator back to a state of equilibrium following a transient disturbance. Transient disturbances can be produced by load changes, switching operations and electrical faults. Section 1.4 explains the process of losing stability following a transient disturbance to the

generator using the Equal Area Criterion .

The time taken for the load angle to swing from its initial value to the critical clearing angle for a 3 phase short circuit fault, is referred to as the Critical Clearing Time (CCT). Faults must therefore be cleared within this time in order to maintain stability. In most cases of transient stability assessment, if the machine does not lose stability during the first swing in load angle, it will maintain stability for that disturbance. If the generator loses stability during subsequent swings in load angle, this is referred to as dynamic or small signal instability, because the loss of stability is a result of insufficient damping.

For most embedded generators, the point of connection to the REC's distribution system can be thought of as a connection to an infinite bus, that is a bus whose frequency and voltage remain unaffected by the embedded generator's operation. This simplifies the discussion of stability because the one machine-infinite bus model is the most basic system for stability analysis. If the REC's bus is not infinite, then the system can be represented as a two machine system, which can also be analyzed without too much difficulty.

The factors which affect synchronous generator stability can be split into two different categories, those which are determined by the generator and its control equipment, and those which are dependent upon the configuration and operation of the system to which the generator is connected.

The two main generator parameters which have the most affect on stability are the inertia of the generator, and the direct axis transient reactance. The most useful measure of generator inertia is the inertia constant, H in units of kWs/kVA. The main advantage of using H compared with other measures of rotational inertia is that its value is fairly constant for a wide range of generator sizes and types, it therefore makes comparisons between machines easier.

3.5.1 Inertia Constant, H & Transient Reactance Xd'

From a stability viewpoint the higher the generator's value of H, the more stable it will be. For a given fault clearing time, the machine load angle at which the fault is cleared decreases with an increase in inertia. The machine requires more acceleration energy to make its rotor advance and therefore appears less responsive and more able to withstand

a mismatch between generator input and output powers.

The direct axis transient reactance, Xd' is also a vital measure of transient stability because it determines the amplitude of the generator's transient power load angle characteristic. Equation 3(3) shows that the lower the transient reactance, the more output power the generator can produce. This serves to provide a greater decelerating force on the generator rotor following a transient disturbance, assisting stability.

Tables C1 and C2 of appendix C contain values of H for a range of generator sizes. For generator sizes above 9 MVA, the inertia constant is above 2.6 seconds, whilst for those generators below 9 MVA, the inertia constant is below 1.8 seconds. Embedded generators are generally more 'twitchy' than large grid generators, and therefore accelerate faster for a given fault duration. The tables also show Xd' which is similar regardless of the size of the generator. The duration for which the generator reactance is equal to Xd' following a fault does vary however .

3.5.2 Short Circuit Time Constant, Td'

Section 3.3.2 discusses the effect that the value of Tdo' and Td' have on the generator power characteristics. When considering short circuit faults, the parameter Td' is more useful, since this time constant is appropriate for short circuit conditions. Equation 3(10) gives the relationship between Tdo' and Td'.

Td' determines the time taken for the reactance of the machine to change from the transient value Xd' back to the synchronous value Xd following a transient. With this change comes a corresponding decrease in the output power capabilities of the generator and hence its potential to produce decelerating forces in response to a disturbance. It follows from equation 3(9) that the higher the resistance compared with the inductance of the field, the shorter the time constant, and the less time the generator has for producing high output powers. If the generator is exposed to a severe fault, which is cleared in a time of around a few hundred milliseconds the constant flux theorem does not hold because of the decrease in flux caused by the fault[110]. Embedded generators have higher per unit resistances than the larger grid type generators, this results in them having smaller time constants.

Tables C1 and C2 of Appendix C show that for generator sizes above 9 MVA, the time

constant Td' is typically greater than 1 second, whilst for the generators below 9 MVA, Td' is typically in the 100 to 200 ms range. This shows that as well as having lower inertias, embedded generators are unable to maintain the high transient output powers which provide stabilising decelerating forces. In terms of the Equal Area Criterion, this reduces the decelerating energy and increases the accelerating energy for a given disturbance, resulting in a shorter CCT and therefore a higher likelihood of instability and hence pole slipping.

3.5.3 Damping Power Provided by Generator and AVR

Another factor which can influence stability is the damping power produced by the generator. This is dependent mainly upon the type of damper winding in the machine, the magnitude of armature/tie-line resistance and the AVR parameters. A positive damping coefficient will aid stability by producing a decelerating force on the rotor when it is accelerating.

The effect that the combined value of armature and tie line resistance has on the damping coefficient is dependent upon the AVR used[138]. If the AVR is not in service, then an increase in resistance will result in a decrease in the damping coefficient, to the point where the machine can become negatively damped[125]. This damping is the natural damping of the machine. If the AVR is in service, then an increase in the resistance increases the damping resulting from the AVR. The damping provided by the AVR is dominant over the generator natural damping, and therefore a high resistance can improve damping overall.

However, a poorly tuned AVR can make the damping worse. If the loop gain of the AVR is too high, the damping can become negative. If the AVR does not have a suitable value of stabilising derivative feedback signal[37], then the high gain necessary to produce a small steady state voltage error will remain high during transient disturbances. This can result in rotor oscillations which increase in magnitude until the generator becomes unstable and pole slipping occurs. This is known as dynamic instability and additional stabilising feedback signals often need to be incorporated into the AVR to prevent it[111].

3.5.4 AVR Field Forcing Action During Short Circuit Faults

The effect of high fault current and therefore armature reaction during a fault tends to decrease flux linkage, especially if the reactive power output of the generator is large[109].

If the generator has an AVR in operation, the action of the AVR tends to force the excitation system to boost the exciter's mmf and therefore maintain flux levels. Anderson[109], states that the dominant factor with AVRs in maintaining stability is the ability to offset the effects of armature reaction during faults. Even though AVRs can significantly improve the flux levels during faults, their effect on the magnitude of the first swing in load angle is generally only a reduction of a few degrees. They are most beneficial with long clearance time faults. It is therefore advantageous to have a high performance AVR. Unfortunately embedded generator AVRs are often basic due to the size of the generator and the application. High performance from an AVR is not seen as a pre-requisite since embedded generators are too small to affect system voltages. AVRs are normally used on embedded generators to provide constant power factor operation in order to meet the site real and reactive power demand[7,12,71].

3.5.5 Generator Governors

Depending upon the type of governor/prime mover set used, the governor may offer a significant improvement in the CCT. If the governor and prime mover system has a small overall time lag, the CCT can be increased by governor action. In many transient stability texts, the effect of governor action is neglected on the grounds that the governor will not respond in the one second period of the transient under consideration. This may be true for a three stage high, medium, and low pressure steam turbine combination, but the assumption is invalid for fast valved steam turbines, gas turbines, and diesel generators. Hydro prime movers are different because their characteristics produce a power increase before a power decrease during an over-speed condition.

Studies conducted[15] on a 4.51 MVA gas turbine generator show that the governor can increase the critical clearance time by approximately 40 ms. The critical clearance times found with this study were in the region of 200 ms. If the governor and prime mover system has a long time lag, it's time constants will render it practically in-active during the first swing of a transient disturbance, and it will therefore have little effect on the CCT[139].

3.5.6 Protection Characteristics of the System Connected to the Generator

The two main external factors which affect the transient stability margins of a generator are the effective transfer impedance between generator and infinite bus and the protection clearance times for faults.

Protection clearance time is the most important factor in maintaining stability, because the longer the fault exists on the system, the longer the power transfer capabilities of the generator are disrupted. The protection clearance times normally associated with high power transfer transmission circuits are usually in the region of several power system cycles. This means that only a small amount of accelerating energy is produced as a consequence of the fault. The generator rotor should therefore not accelerate much.

The protection associated with distribution feeders can have clearance time in excess of one second where graded IDMT over-current relays are employed[21,41,42,140]. With this long clearance time, the load angle increases so much that the likelihood of the generator maintaining stability is low. Embedded generator CCT's are generally between 200 and 400 ms. Since distribution circuit breakers can take up to 100 ms to operate, this leaves only 100 to 300 ms for fault detection. This figure is hard to achieve with IDMT type over-current relaying .

Engineering recommendation G59[14,141] states in section 6.4 that the generator should be disconnected from the system "when a system abnormality occurs that results in an unacceptable deviation of the voltage or frequency at the point of supply". Power system faults can produce unacceptable deviations at the point of supply, G59 therefore requires that the generator be disconnected for all short circuit faults. If this is achieved, then pole slipping should not occur following short circuit faults. However, in practice the generator is not disconnected for all external short circuit faults. Pole slipping may therefore occur. Additionally, the above definition also demands that a pole slipping generator be disconnected due to the voltage or frequency disruptions which may occur.

Engineering Technical Report 113[15] also specifies that over-current protection should be fitted to the generator and gives methods for deriving the fault current contribution from the generator. The amount of fault current contribution from the generator depends upon the generator reactances, time constants and AVR parameters. A low value of sub transient and transient reactance will result in high fault currents, whilst the longer the time constants, the longer the transient components of fault current will last. Because embedded generators generally have short time constants, these transient currents will therefore be short-lived. The AVR ceiling voltage determines the steady state fault current. If this ceiling limit is low, then the generator fault current contribution may not be sufficient to operate an IDMT type over-current relay. Generator manufacturers supply

as standard, generators fitted with static excitation systems without terminal current boost[42]. The fault current in this type of generator will quickly fall to zero because the excitation system will not supply any field voltage during the fault.

Fielding[140] states that voltage controlled IDMT over-current protection is used on embedded generators. The generator protection coordination is such that the generator relays grade with the utility distribution relays, the generator would therefore not be disconnected for faults on the utility feeders. Such faults would be cleared in around 500 ms. If the clearance of the fault does not result in the disconnection of the generator network from the utility grid supply, then pole slipping will occur.

3.5.7 Transfer Reactance Between Generator and Infinite Bus

The value of connecting impedance between the generator and the infinite bus has a crucial affect on generator stability. The study conducted on the 4.5 MVA gas turbine generator in reference[15] revealed that the CCT rapidly decreases once the utility source impedance reaches the sub-transient infeed. With source impedances below the sub transient level, the CCT ranged from 200 to 220 ms, for impedances above the sub transient level, the CCT dropped to 150 ms.

Any reactance between the terminals of the generator and the infinite bus can be added to the reactance of the generator, including that of a step up transformer. It follows that a large external impedance reduces the synchronising power transfer capability. The generator therefore cannot produce the decelerating forces necessary to maintain synchronism. As a general rule[15], the critical clearing time is related to inertia and inter tie or external reactance in the following manner;

$$CCT \;\alpha\; \sqrt{\frac{H}{(Xd' + X)\,(Xd + X)}} \qquad 3(11)$$

Where X is the external or 'transfer' reactance. The situation may be worse following the clearance of a fault because one of several parallel interconnections would be disconnected to clear the fault, resulting in a higher post fault transfer impedance.

3.5.8 Effect of Resistance on Stability

Section 3.5.3 stated that high stator and inter-tie resistances may reduce the natural damping capabilities of the generator, lessening the stability margin. The greatest concern

with high resistance values in an embedded generation environment is the effect on dynamic stability. A high value of resistance found in a long length of cable, combined with a poorly damped machine, low performance AVR and poorly damped governor could result in a negative value of damping[111,121,142,143]. This could cause the machine to oscillate with the amplitudes of the oscillations increasing until the generator loses stability.

Increased resistance can also be beneficial to stability for close up short circuit faults because the power dissipated in the resistance provides some load for the generator, reducing the accelerating power going into the rotor.

3.5.9 Affect of Fault Type on Stability

A decrease in fault impedance reduces the power transfer from the generator, causing a lower stability limit for a given fault duration. In order of fault severity, the most severe fault is the 3 phase fault. This is followed by 2 phase to earth, two phase, and single phase to earth faults. Kimbark[139] states that the difference in severity of faults becomes smaller as the fault duration is decreased, however, with a fault of 200 ms there is a significant difference.

3.5.10 Affect of Earthing on Stability

The grounding of the system affects it's zero sequence impedance, Zo which in turn affects the impedance of unbalanced faults and therefore the level of power mismatch caused by the fault. As Zo increases with reference to the fault location, the severity of an unbalanced fault decreases. If the extreme of an infinite value of Zo is considered, it can be seen that a two phase to earth fault would transform into a two phase fault. It is therefore beneficial from a stability viewpoint to ground through impedances rather than using solid grounding techniques. Grounding resistors close to generators are more beneficial than reactors as they provide an additional braking effect to the generator during unbalanced faults.

Embedded generators are normally un-earthed when operating in parallel with a utility supply. This therefore improves stability with respect to unbalanced faults.

3.5.11 Effects of Embedded Generation System Configuration on Stability

Some embedded configurations have multiple embedded generators located at one site. If the generators are connected to the same bus, they can be grouped together, their behaviour appearing as one larger generator. From a stability viewpoint, adding extra generation to a site will reduce the ratio of infinite bus to machine ratios. If the ratio becomes too low, the synchronising power following disturbances will decrease and the generators will be more prone to instability.

Step up transformers also affect stability, the impedance of the transformer can be added to that of the generator's stator circuit. If the transformer has a high impedance, the interchange of synchronising power between generator and grid will be reduced, causing a decrease in the stability margin. The transformer may improve stability for close up terminal faults because the transformer will partially load the generator.

3.5.12 Summary of Embedded Generator Stability Discussion

Embedded generators connected to distribution systems using over-current protection are much more prone to instability than large 'grid' style generators connected to transmission systems. The long fault clearance times associated with utility IDMT style over-current protection, coupled with low generator inertias and short time constants substantially decreases their stability margins.

Prolonged disturbance to the surrounding power system may result following a fault, due to the effects of a synchronous generator operating in an unstable manner. These problems can only be remedied by either reducing fault clearance times so that the generator remains stable, or installing protective relays to disconnect the generator when it becomes unstable.

If the generator has over-current protection set to operate for any external short circuit fault, then pole slipping due to faults will not occur because the fault which would cause the pole slip will cause the generator to be disconnected. If the over-current protection is set to grade with protection on adjacent feeders, then pole slipping is likely to occur following faults.

The Critical Clearance Time (CCT) for small and medium sized embedded generation has been found in most studies to be between 200 and 300 ms[12,15,144,145]. When compared with

the 0.5 to 1 second fault clearance times typically produced by over-current relays, it can be concluded that there is a high likelihood that embedded generators will suffer instability and pole slip.

3.6 SYNCHRONOUS GENERATOR POLE SLIPPING CHARACTERISTICS

This section presents the voltage, current, flux and power characteristics for pole slipping generators. Impedance is not discussed because it has already been discussed in chapter 2. Appendix A gives full derivations of impedance and power variations during pole slipping for a range of power system models.

3.6.1 Variation in Voltage and Current During Pole Slipping

The voltage and current variations are most easily explained if the synchronous machine/utility connection is represented as the classical one machine/infinite bus[146], as shown in Figure 2.1a. The machine and utility are represented by a voltage behind a reactance, and are connected via the distribution line impedance.

As a generator falls out of step, the phase difference between the two voltages increases, and when this difference is 180°, the voltages are in direct opposition. This produces a point between the two machines where the voltage will fall to almost zero. This point is known as the system centre. It's location is fixed by the relative impedances of the two machines and the interconnecting equipment between. If the combination of generator and transformer impedance equals the utility source impedance in Figure 2.1a, the system centre would occur at the geometric centre of the connecting line.

If the generator rating is decreased, its impedance Zg would increase, and the system centre will move towards the generator. For embedded machines, the rating of the machine is small in relation to the rating of the system it is connected to. The system centre will therefore normally occur inside the machine or its transformer unit. With a system centre inside the generator, local loads will be affected by the voltage fluctuations produced by pole slipping. If the generator voltage, Eg, were increased using a higher excitation level, the system centre, and therefore the point of worst voltage fluctuations would move away from the generator, causing more of a voltage disturbance to other consumers.

The current produced when the voltages are 180° in opposition is high, giving the appearance of a short circuit at the system centre. Figure 3.5 shows generator terminal voltage and current plots in relation to load angle for two consecutive pole slips, followed by re-synchronisation. These plots were produced by POWSIM,[107] using the power system model described in Chapter 5. The 588 MVA generator modelled had a 220 ms three phase fault placed at its terminals which resulted in two pole slip cycles. The source capacity at the terminals of the generator was 4.5 times that of the generator. The source impedance was equal to 72 % of Xd'. This resulted in the system centre appearing just inside the generator.

Figure 3.5b shows the voltage fluctuations for the pole slips, which at a time of 1.1 seconds fall to 0.4 pu at the machine terminals. This voltage minimum coincides with the point where the load angle is at 180° and the machine voltages are in complete phase opposition. As the load angle increases past 180°, the two voltages oppose each other less until they are back in phase again, resulting in normal system voltages and currents.

The current plot shows the current maximum produced during pole slipping at a time of 1.1 seconds to be higher than the sub transient fault level which occurs at the fault on point. This demonstrates the strain which pole slipping can place on the generator windings. The pole slipping current is at the sub transient fault level for much longer than the sub transient time constant. Consider a generator[147] with typical values of reactance such that Xd' = 0.3 and Xd'' = 0.2. The maximum level of sub-transient current for a solid three phase terminal fault is given by;

$$I'' = \frac{V}{Xd''} = \frac{1}{0.2} = 5pu \qquad 3(12)$$

For pole slipping, the worst case is where the generator is connected directly to an infinite bus. The source impedance is therefore negligible when compared to the transient reactance. The current level when the voltages are 180° apart is then given by;

$$I_{max\,(poleslip)} = \frac{2V}{Xd' + X} = \frac{2}{0.3 + 0} = 6.67pu \qquad 3(13)$$

The situation will be worse if generator AVR field forcing raises the generator EMF to above 1 p.u. This shows that the currents experienced during pole slipping may be substantially higher than three phase fault levels.

3.6.2 Pole Slipping Explained in Terms of Magnetic Flux

If all of the magnetic effects due to induced currents in the field, rotor iron and damper windings are neglected, then a simpler explanation of the process of losing synchronism is possible. This assumption is valid when pole slipping results from a slow loss of synchronism, such as a loss of steady state stability. In this situation, the whole pole slip can take one second or more, and at this rate of slip, the induced effects are negligible.

As the load angle starts to increase from its steady state value, the air gap flux will decrease due to the demagnetising effect of armature reaction[45,148]. The demagnetising effect results from currents flowing in the stator, which create an mmf that opposes the rotor mmf, thus weakening the resultant air gap mmf. With further load angle increase, the flux linking the stator and the rotor together will begin to unlink, taking leakage flux paths instead. This causes a weakening of the magnetic coupling between the stator and rotor. The point where the magnetic coupling between the stator and the rotor becomes zero is defined as the loss of synchronism point[148] and at this point the air gap flux will be at its minimum and the resultant restraining torque on the rotor is negligible. In an 'ideal' machine this point would correspond to a load angle of 180°.

With no magnetic coupling, the rotor does not oppose the driving force of the prime mover, and the load angle will increase rapidly, as the machine moves from generating to motoring. The flux between rotor and stator will again start to link. However, it will link with the rotor pole next to and behind of the pole it used to link with, and the machine will be in a motoring condition. With the machine in a motoring condition, power is drawn from the electrical supply, as well as the prime mover. Most of this power is used to accelerate the rotor. The rotor will therefore travel quickly through the motoring region until once more, the rotor and stator flux link in a generating condition. The machine will only re-synchronise if the strength of the magnetic coupling between stator and rotor is sufficient to overcome the extra kinetic energy in the rotor produced by it travelling above synchronous speed. If the machine is to re-synchronise, all of the excess kinetic energy must be removed before the CSP for that slip cycle is reached.

3.6.3 Direct and Quadrature Axis Flux Variations with Load Angle Increase

For low load angles ($<< 90°$), the major proportion of the air gap flux is comprised of the direct axis component, with the quadrature axis contributing very little. As the load angle increases, the flux produced by the stator, ϕ_a begins to lag further behind ϕ_f, the

field flux. As the phase angle between ϕ_a and ϕ_f increases, a corresponding increase in armature current occurs, causing an increase in braking torque, and thus balancing the accelerating torque that produced the load angle increase. The magnitude of the quadrature component of flux, ϕ_q, changes with variations in load angle. The upper limit[149] on ϕ_q is set by V/X_{comb}, this peak occurs at a load angle of 90°, beyond this point, it decreases again. V is the infinite bus voltage, and X_{comb} is the combined value of synchronous reactance plus any external reactance. The direct axis component of flux, ϕ_d, will reach its minimum at a load angle of 180°. For the process of losing synchronism, the direct axis component will gradually decrease as the rotor is accelerated, accompanied by an increase in quadrature axis component. The quadrature axis component provides an increasing amount of braking torque as the load angle approaches 90°. Once the load angle exceeds 90°, ϕ_q, will begin to decrease along with ϕ_d, resulting in an unstable decrease in braking torque with load angle increase. When the load angle approaches 180°, ϕ_q will vanish and ϕ_d will be at its lowest level. This causes the lowest magnetic coupling between stator and rotor, and with no flux interaction to provide a braking torque, the rotor will accelerate further and the machine will pole slip into a motoring condition.

References [148] and [149] provide a finite element analysis of the process of losing synchronism, and contain figures showing the change in flux paths as the machine loses synchronism.

3.6.4 Real and Reactive Power Pole Slipping Characteristics

The main real and reactive power characteristic during pole slipping are determined by the sinusoidal terms in equations 3(3) and 3(4). If the slip rate during the pole slip is above 0.33 %, then the generator reactance will be less than twice the value of Xd'[45]. The transient saliency terms will therefore contribute a significant amount to the fundamental sinusoidal characteristics resulting from the interaction of stator and rotor flux.

As the load angle completes a 360° cycle, one sinusoidal variation in real and reactive power will occur. Any asynchronous power generated during the pole slip will shift the sinusoidal variation in power up. A detailed analysis of the power characteristics during pole slipping are given in Chapter 6.

3.7 CHAPTER THREE SUMMARY

This chapter presents the steady state and transient power characteristics of a generator. These have a sinusoidal power load angle characteristic, with a second harmonic component caused by saliency. Embedded generators are far from 'ideal' however and the constant flux linkage assumption normally used for large 'grid' type generators can not be used. Embedded machines have short time constants which for long duration faults, cause a significant decay in the field flux. This distorts the sinusoidal variations in power, because the reactance of the generator changes from Xd' to Xd as the flux decays. Field flux decay can cause a decrease in embedded generator transient stability margins.

Power system frequency oscillations and second harmonics can also occur in the generator's real power during and after short circuit faults, due to trapped flux in the generator stator. These oscillations decay at a rate determined by the armature time constant.

When the generator rotor travels above synchronous speed, the induced slip frequency currents in the field structure enable the generator to generate asynchronous power in the same way as an induction machine. Reactive power is absorbed by the generator during asynchronous operation as this provides the necessary magnetising VArs.

A fast acting AVR enables the operation of a generator beyond its steady state stability limit, at machine rotor angles greater than 90°. Although this type of operation is possible, it is never practised, because the reserve in hand for transient stability is generally too low.

Embedded generators are more likely to pole slip than 'grid' type machines because they have short time constants, low inertias, and are exposed to long fault clearance times. Their CCT is typically between 200 and 400 ms, whereas the fault clearance time exhibited by the typical over-current protection used on distribution feeders is between 0.5 and 1.0 seconds.

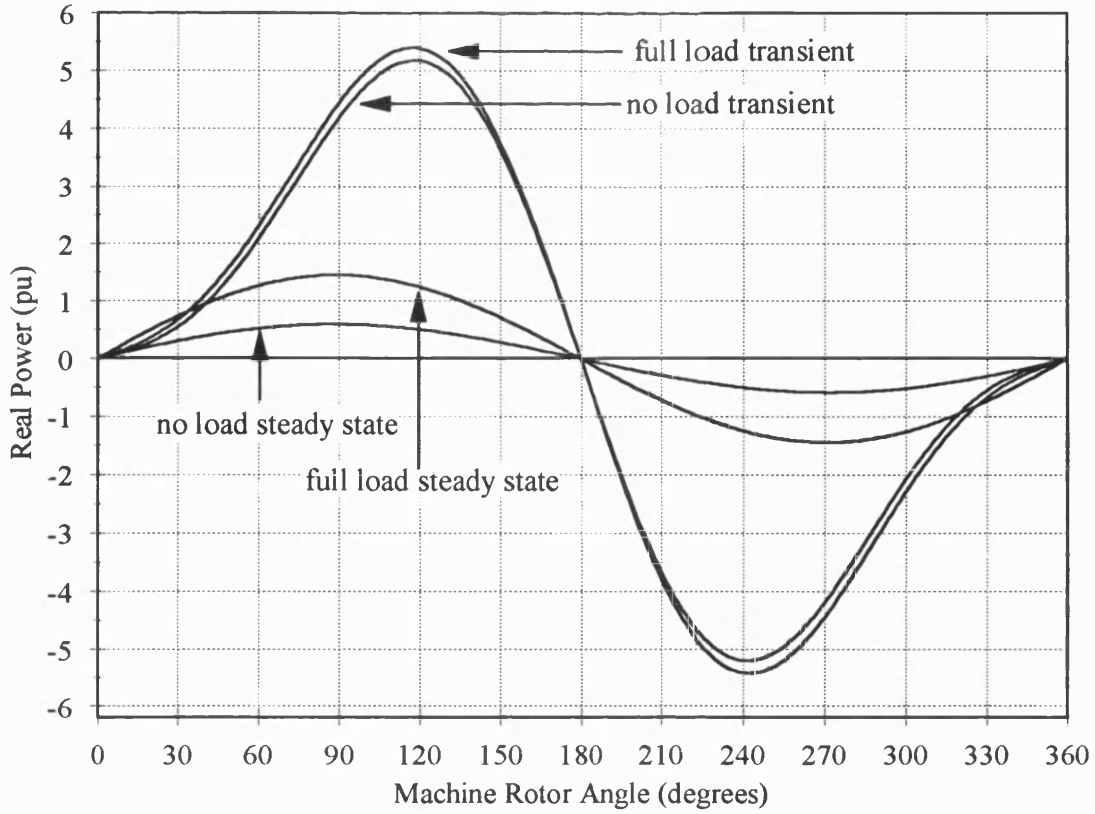

Figure 3.1a
Real Power Load Angle Characteristic for a 200 MVA Round Rotor Steam Turbine Generator.

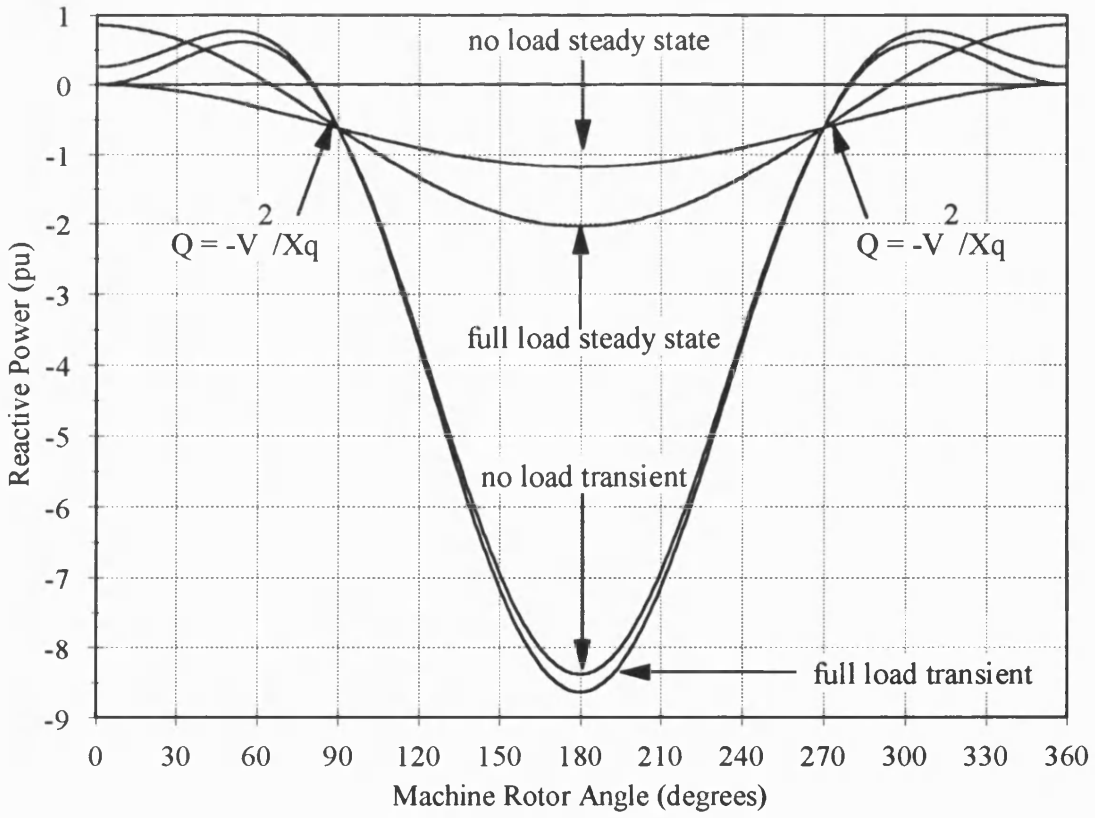

Figure 3.1b
Reactive Power Load Angle Characteristic for a 200 MVA Round Rotor Steam Turbine Generator

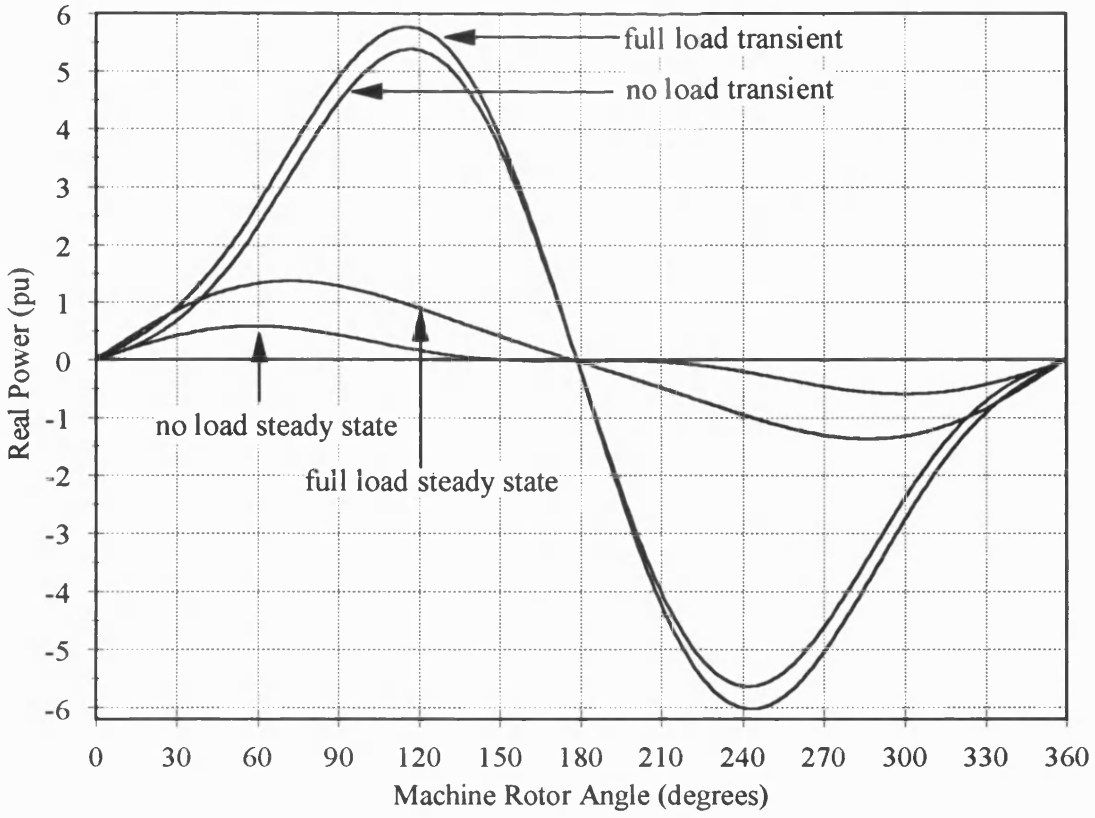

Figure 3.2a
Real Power Load Angle Characteristic for 625 kVA Salient Pole Diesel Generator.

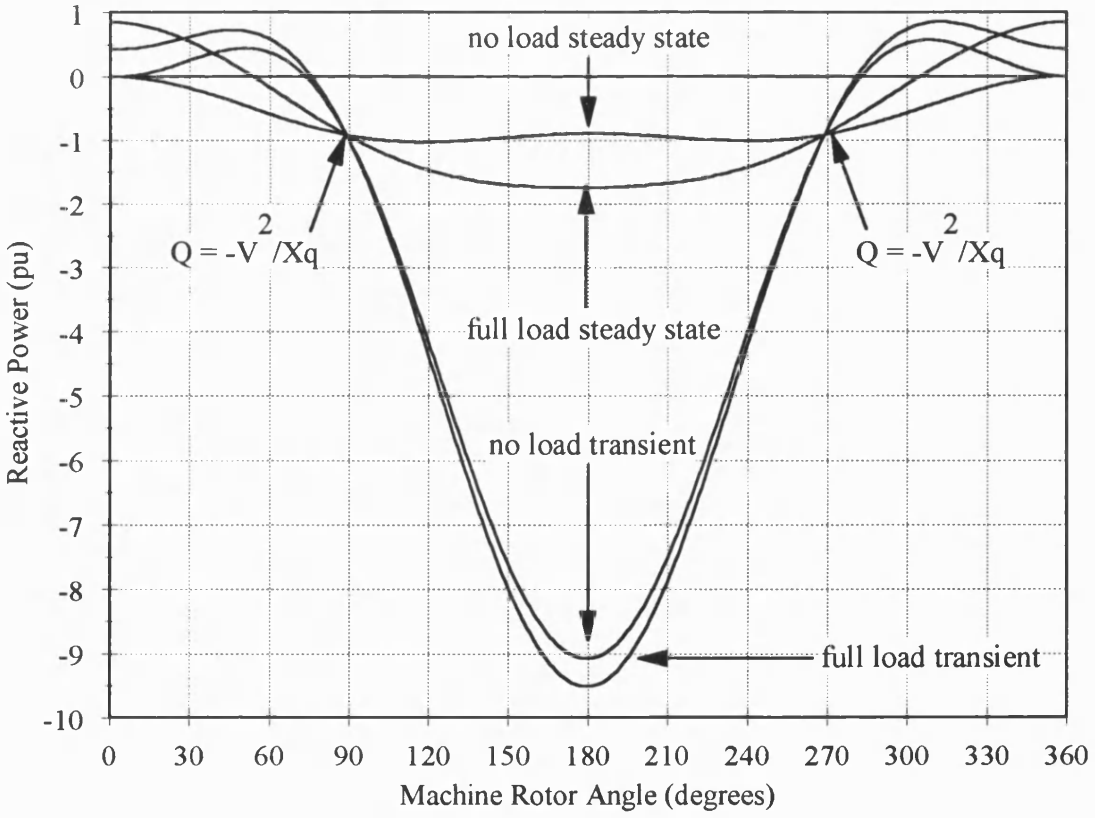

Figure 3.2b
Reactive Power Load Angle Characteristic for 625 kVA Salient Pole Diesel Generator.

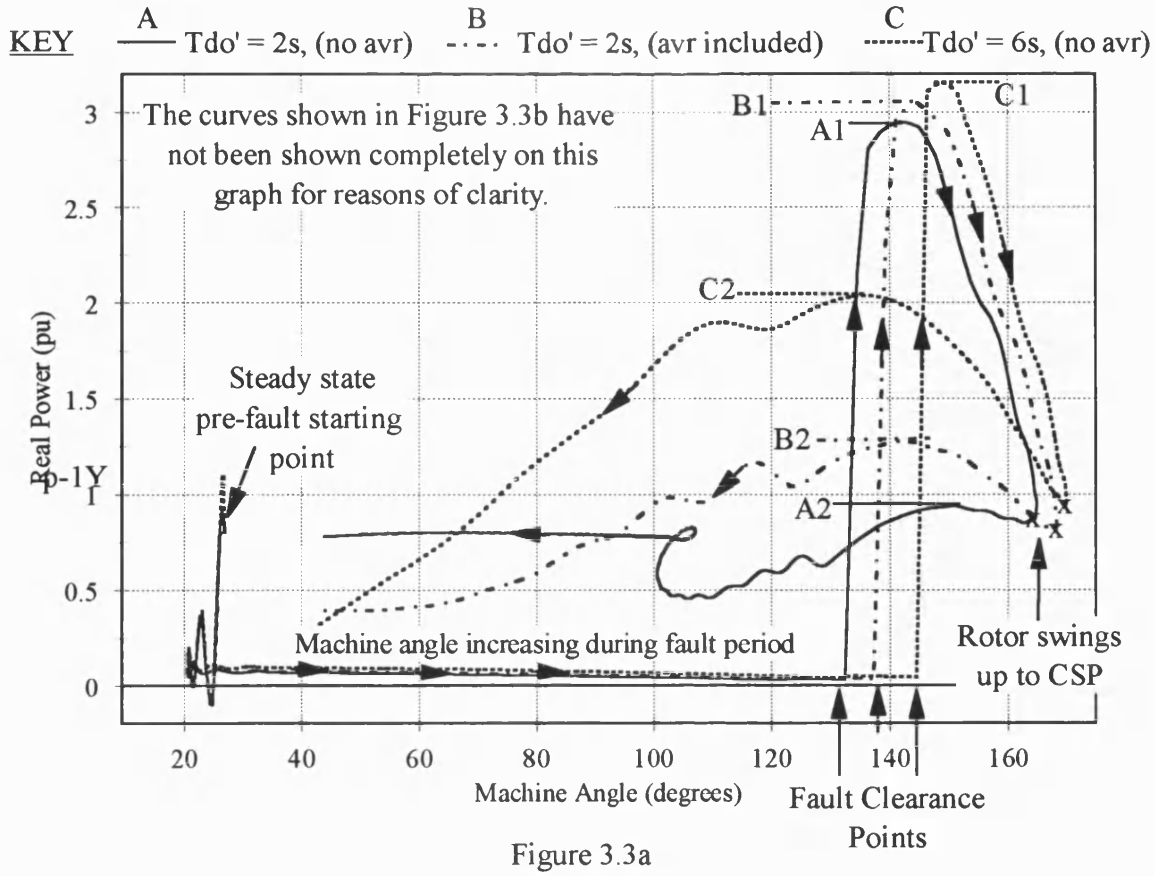

Figure 3.3a
Real Power / Machine Angle Plot for Three Phase Fault Simulations with Various Values of Tdo' on a Diesel Generator, Governor Disabled.

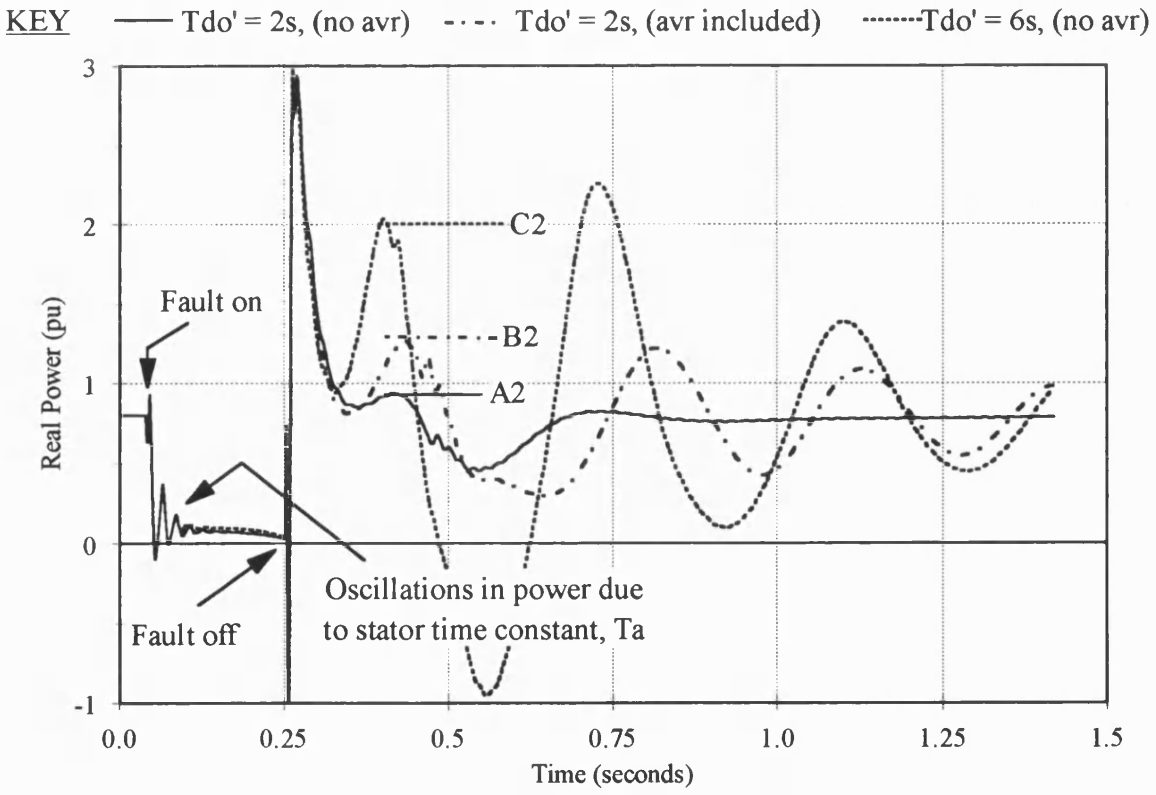

Figure 3.3b
Real Power/Time Plot for Three Phase Fault Simulations on a Diesel Generator, Governor Disabled.

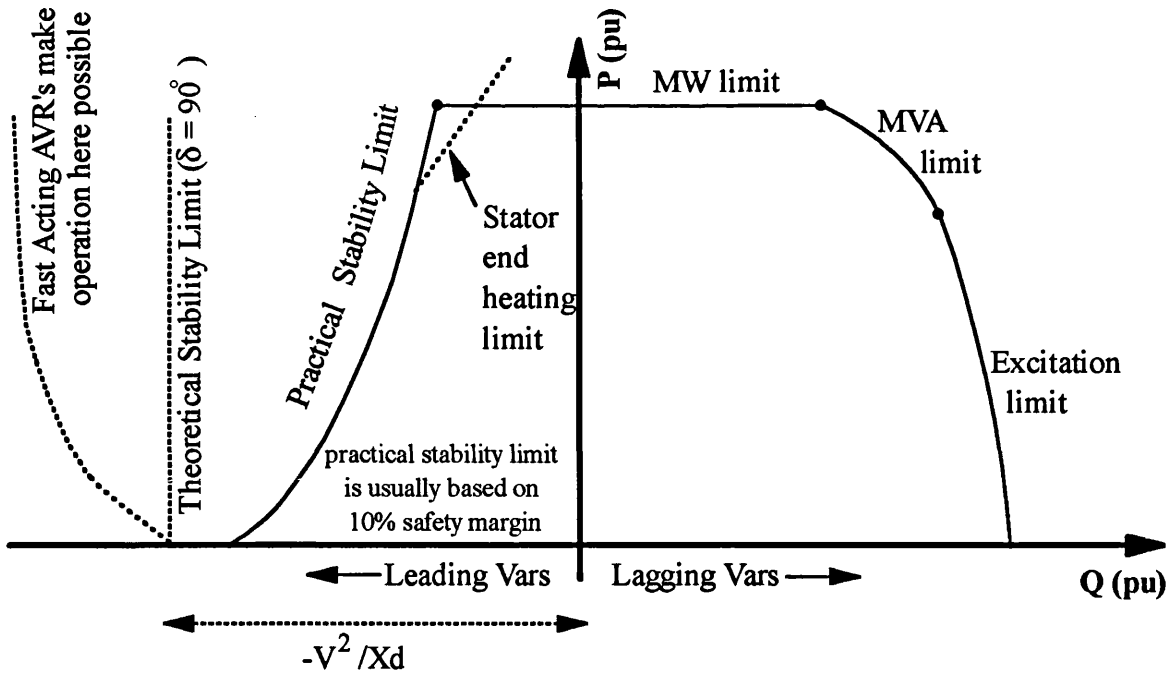

Figure 3.4a
Round Rotor Generator Operating Chart.

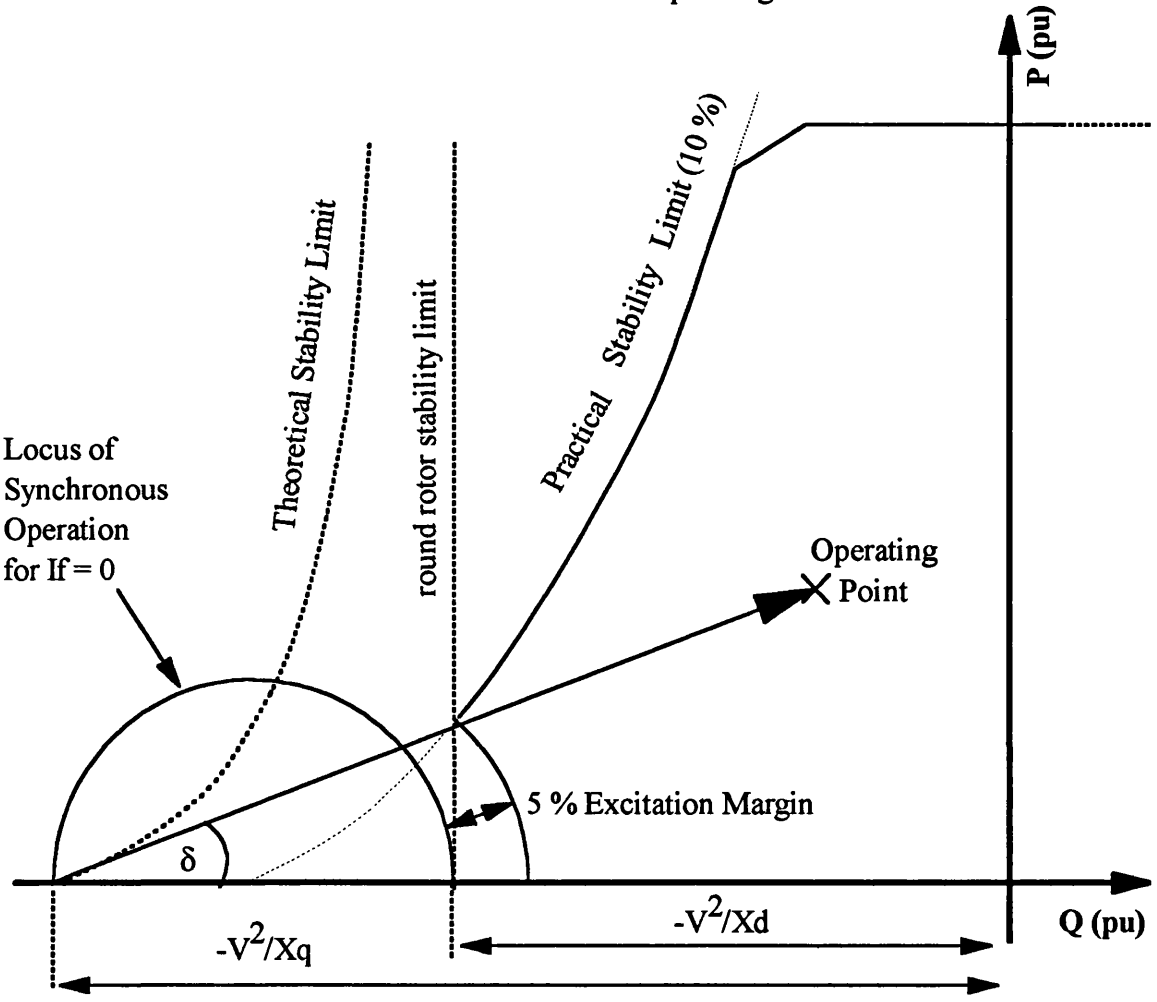

Figure 3.4b
Under-Excited Section of Salient Pole Generator Operating Chart

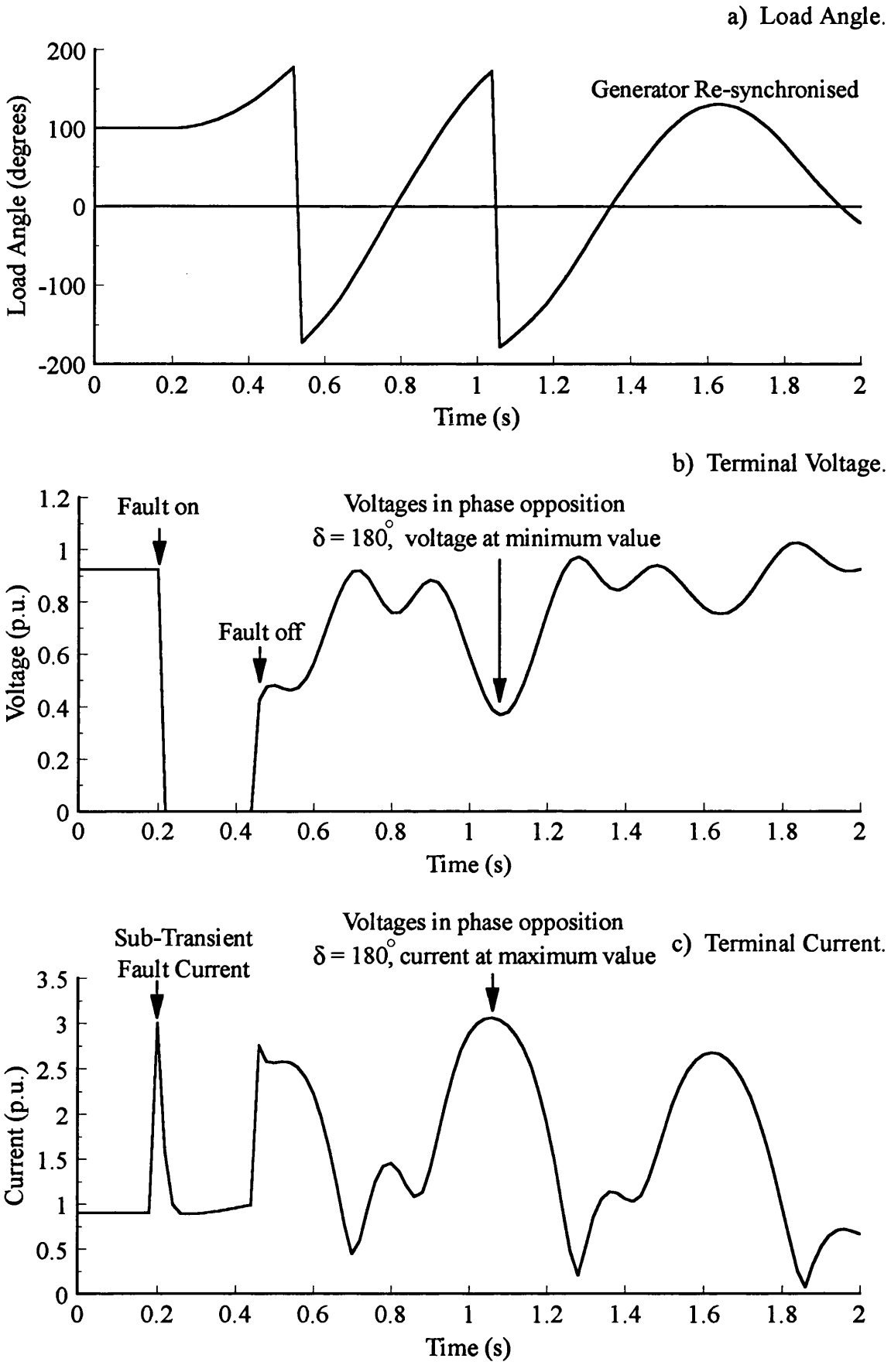

Figure 3.5

Voltage and Current Variation During Pole Slipping for a 588 MVA Generator with A Terminal Source Capacity 4.5 Times its Rating. (Source Impedance = 72 % Xd')

Chapter 4
THE NEW POWER BASED POLE SLIPPING ALGORITHM

In designing a pole slipping algorithm, it must be able to predict when a generator is committed to a pole slip or actually is pole slipping. It must also remain stable for all other power system conditions, including faults and power swings. The algorithm has been designed for use in a multi-function microprocessor based relaying environment[23,27,28,29,30,31,57,91,150]. A limited amount of computer processing power is therefore available. An IEEE committee report on 'Experience with Generator Protection and Prospects for Improvements Using Digital Computers' reported that respondents from a utility engineer survey stated that "generator protection can be improved by providing out-of-step relays that detect loss of synchronism for conditions that do not cause the apparent impedance to move through the conventional blinder characteristics". This confirms that conventional pole slipping relays can be difficult to set and suggests a need for improved pole slipping relay design.

The paper reports that out-of-step relaying can benefit most from micro-processor based relaying since sophisticated algorithms can be developed which take advantage of the computing power and long time frames involved with pole slipping. The paper also stated that "A design challenge is to make such a sophisticated relay easy for utility engineers to apply and set". This point has been given much consideration when designing the new power based pole slipping algorithm, since there is little point in designing an algorithm which is too complicated for utility protection engineers to easily set.

The protection functions found in a micro-processor relay are generally independent; there is therefore little difficulty in using a common hardware system. An entire suite of protection functions necessary for protection of a synchronous generator can therefore be included into one microprocessor relay, thus providing the economy required to meet modern requirements. This is especially true for embedded generators because they are

relatively inexpensive. They therefore require inexpensive protection schemes. Other protection functions intended for embedded generators[103,104,151,152] also require real and reactive power calculations. The software overhead for this task can therefore be shared, minimising the demand on the processor made by the algorithm.

Using power in this type of environment has an advantage over reactance and resistance measurement, since exact point on wave synchronisation is not required and the voltage and current samples do not have to be resolved into direct and quadrature components. Generator real power, P, and reactive power, Q, can be calculated from instantaneous voltage and current samples using[153];

$$P = v_a * i_a + v_b * i_b + v_c * i_c \qquad 4(1)$$

$$Q = \frac{1}{\sqrt{3}} (v_a * (i_c - i_b) + v_b * (i_a - i_c) + v_c * (i_b - i_a)) \qquad 4(2)$$

where v_a ,v_b ,v_c are the sampled values of phase to earth voltages, and i_a ,i_b ,i_c are the sampled values of line current. Alternatively, if the relay only measures two line to line voltages then the 'two wattmeter' method can be used;

$$P = v_{ab} * i_a + v_{bc} * i_c \qquad 4(3)$$

$$Q = \frac{1}{\sqrt{3}} (v_{ab} * (i_c - i_b) + v_{bc} * (i_a - i_b) \qquad 4(4)$$

Note that the sign convention used for reactive power is that reactive power will be negative at the terminals of an under-excited generator.

4.1 BASIS OF THE ALGORITHM

The algorithm predicts pole slipping by detecting if the generator's load angle is still increasing once the Critical Stability Point (CSP) has been exceeded. Section 1.4.1 explains the Equal Area Criterion and Figure 1.2b shows the Equal Area Diagram and the CSP for the clearance of a short circuit fault. It is important to note that the new pole slipping algorithm does not use the equal area criterion in a quantitative manner. The Equal Area Criterion is used to explain the concept of the CSP.

Inspection of Figure 1.2b shows that at, or beyond the CSP, two conditions apply. The load angle is greater than 90°, and the generator real power output, P is equal to, or less than the prime mover input power, Pm. Section 3.1.2 states that the reactive power characteristics for a generator are such that they always take on the same value at 90° and 270°. For load angles between 90° and 270°, the reactive power will be less than the value at 90°, and for load angles from 270° to 90°, the reactive power will always be greater. If resistance is neglected, then from equation 3(5) the reactive power at 90° is given by;

$$Q_{(at\ 90°)} = -\frac{V^2}{Xq} = Qtrip \qquad 4(5)$$

This quantity is referred to as Qtrip, and is used to identify operation at or beyond the CSP. The unsaturated value of Xq is used because saturation effects are negligible when a generator's reactive power output is close to Qtrip. The manufacturer normally supplies unsaturated values of reactances. Figure 1.2b shows that the generator electrical power output can also be less than the prime mover input power, Pm, for load angles of less than 90°. This could occur at load angle δ1 in Figure 1.2b. Generator reactive power output is therefore used to reveal when the generator is operating in the potentially unstable area when the load angle is greater than 90°. The real power measurement is then used to determine if the generator is operating at, or beyond the CSP. Operation at, or beyond the CSP therefore occurs when;

$$Q < Qtrip$$
$$P < Pt \qquad 4(6)$$

Where Pt is the algorithm real power trip setting, that is based on the prime mover input power, Pm.

The criteria of equation 4(6) could predict that pole slipping will occur, since pole slipping is inevitable if the generator operates past the CSP. However, Chapter 3 shows that synchronous generators do not behave in an ideal manner. Effects such as asynchronous power generation, prime mover dynamics and measurement errors would result in too many false trip conditions if only equation 4(6) was used to predict pole slipping. To overcome this problem, generator rate of change of power is used to determine whether or not the load angle is still increasing once the CSP has been exceeded. If the load angle is still increasing when the generator operates beyond the CSP, then pole slipping is inevitable. If the generator just maintains stability after reaching the CSP, then the load angle will be temporarily static, or decreasing.

Figure 1.2b shows that if the load angle is increasing at the CSP, then the generator real power output will be decreasing, and therefore the time rate of change of real power will be negative. Load angle increase at the CSP is therefore identified when;

$$(\Delta P/\Delta t) \; < \; (\Delta P/\Delta t)_{min} \qquad 4(7)$$

Where $(\Delta P/\Delta t)_{min}$ is a margin for error, allowed for in this expression to ensure algorithm mal-operation due to measurement errors and non-ideal machine effects does not occur. The theoretical form of the power based algorithm therefore takes the form;

$$\text{TRIP IF:} \quad \begin{array}{l} Q \; < \; Qtrip \\ \quad and \\ P \; < \; Pt \\ \quad and \\ (\Delta P/\Delta t) \; < \; (\Delta P/\Delta t)_{min} \end{array} \qquad 4(8)$$

4.2 FILTERING TECHNIQUES

The algorithm has been implemented and tested in a commercial micro-processor based relaying platform[74]. Several different filtering techniques have been used to remove noise, or enhance algorithm security. This section explains the different techniques and the reasons for their use.

4.2.1 Anti-Aliasing Filters

The sampling theorem states[154,155] that the sampling frequency must be greater than twice the highest frequency to be sampled. If this is disobeyed, then aliasing effects will distort the sampled waveform, since the higher frequencies will impersonate the lower ones and cause distortion.

The pole slipping algorithm has been designed to work for frequencies 10 Hz above or below the nominal 50/60 Hz system frequency, i.e from 40 to 70 Hz. To avoid the effects of aliasing, a first order passive low pass filter with a cut of frequency of 132 Hz is used. This ensures that any frequencies above half the maximum sampling frequency of 840 Hz are filtered out before they reach the analogue to digital converters. This ensures that only the 50 Hz power system frequency and its second and third harmonics are used by the relay. Note that a 'gentle' first order filter cut off has been used to minimise the effects of group delay, thus speeding up relay response for functions which require very fast

response times[154].

4.2.2 Voltage and Current Fourier Full Cycle Cosine Filters

The relay uses a sampling rate of 12 samples per power system cycle, this is achieved by the use of a frequency tracking algorithm[74]. The Fourier filter extracts the fundamental frequency component of the voltage and currents. The pole slipping algorithm should use only balanced three phase fundamental frequency components of voltage and current, since pole slipping is a balanced phenomenon.

A Fourier cosine filter provides the in phase component of a signal, a sine filter provides the quadrature phase component. The cosine Fourier filter signal, Ic of a sampled signal, i takes the form;

$$Ic = \frac{2}{N}\left[\frac{I_0}{2} + \frac{i_N}{2} + \sum_{n=1}^{N-1} i_n \cos(\omega n \Delta t)\right] \qquad 4(9)$$

whilst the sine Fourier filter signal, Is of a sampled signal, i takes the form;

$$Is = \frac{2}{N}\left[\sum_{n=1}^{N-1} i_n \sin(\omega n \Delta t)\right] \qquad 4(10)$$

where N is the number of samples per power system cycle, i_n is the instantaneous value of voltage or current sampled at time $n\Delta t$, ω is the system angular frequency, i_0 is the instantaneous value of signal, i, sampled at time 0, and i_N is the instantaneous value of signal, i, sampled at time $N\Delta t$ [156]. Equations 4(3) and 4(4) use only the cosine filter components to calculate real and reactive power. The sine component is required for sample error compensation. The relay has only one analogue to digital converter, the voltage and current samples are therefore each delayed by 20 μs. The fourier sine and cosine filter components are used with pre-determined multiplicative constants to 'rotate' the voltage and current vectors so that they are all effectively sampled at the same time.

The frequency response characteristics of the 1 cycle fourier filter are shown in Figure 4.1a. The response of the filter to the 11th harmonic is the same as the response to the fundamental components, due to the effects of aliasing. However, the anti-alias filter attenuates these harmonics significantly, and the combined response of the anti-alias and full cycle fourier filters is shown in figure 4.1b.

Figure 4.1b shows that the fundamental frequency component passes through almost

unchanged, whilst all harmonics up to the 10th harmonic are removed. This removes distortion in the calculated power signals due to harmonics. Embedded generators are exposed to harmonics because they are located at distribution levels where high levels of harmonics are more likely to exist.

DC components are also removed. This is desirable since it reduces the power system frequency oscillations which occur in the real power signal during faults. These are produced as a result of DC current components interacting with power frequency voltage components. These oscillations are discussed in section 3.3.4.

4.2.3 Moving Average Filters

After filtering the voltage and current signals, the algorithm processing rate is reduced from 12 to 4 samples per power system cycle. This significantly reduces the demand which the algorithm places on the relay's processor. Processing at a rate of 4 samples per cycle also has some advantages from a filtering viewpoint.

Power system unbalance produces double power frequency components in the calculated real and reactive power signals[152,157]. This can interfere with the operation of the algorithm, because the algorithm may use the top or bottom of the unbalanced signal, as shown in Figure 4.2a. Using the top or bottom of the unbalanced signal could result in a significant error. Applying a two point, half cycle moving average filter removes this problem completely. A half cycle moving average filter removes the second harmonic, and also attenuates the fundamental, whilst allowing DC through.

Figure 4.2b shows the effect that the moving average filter has on the power signal for an unbalanced fault. The level of unbalance on the 'raw' value of instantaneous power can be seen to increase to a maximum over one power system cycle. The moving average filtered signal suffers a small oscillation, then settles on the average value of power within a half cycle of the unbalance reaching a steady state. The mathematical equation for a moving average filter is given below;

$$y_{(n)} = \frac{1}{N} \sum_{r=0}^{N-1} x_{(n-r)} \qquad 4(11)$$

Where $y_{(n)}$ and $x_{(n)}$ are the n^{th} output and input respectively, and N is the window size. With a processing rate of 4 samples per cycle, the equation used for a half cycle moving average filter becomes;

$$y_{(n)} = \frac{x_{(n)} + x_{(n-1)}}{2} \qquad 4(12)$$

This places a small burden on the relay's processor because with the correct internal scaling, the calculation can be reduced to a simple addition.

4.2.4 Calculation of the Rate of Change of Power Signal

The rate of change of power signal, ($\Delta P/\Delta t$), is calculated using the following equation;

$$\Delta P/\Delta t = \frac{P_{(n)} - P_{(n-2)}}{2\Delta t} \qquad 4(13)$$

Note that this method uses the previous but one sample to calculate ($\Delta P/\Delta t$), instead of the previous sample. This technique was originally proposed by Barrett[104] as a method of removing unbalance. However, the half cycle moving average filter applied to the real power signal achieves this. The effect of using this technique is shown in Figure 4.2c. This figure shows the half cycle moving average filtered power of Figure 4.2b, and the two rate of change of power signals. The advantage of the alternate sample method is that less disruption is caused to the ($\Delta P/\Delta t$) signal. The alternate sample method only causes two 'spikes' in the ($\Delta P/\Delta t$) signal when a change in the level of unbalance occurs.

4.3 THE COMPLETE ALGORITHM

The combined criteria specified in equation 4(8) will successfully predict and detect pole slipping. However, they can also occasionally be satisfied during power system short circuit faults. The faults which have been found to cause problems are three phase and two phase to earth faults. The problem arises at the fault off point. Additional fault blocking constraints are therefore required to stop algorithm operation for faults. Section 3.3.4 discusses the short circuit torques which occur during faults. The discussion also applies to electrical output power since at synchronous speed, torque equals power. This section states that double power frequency terms will occur in the instantaneous power signal during unbalanced faults, whilst power frequency terms will occur in the power signal during balanced faults. These power frequency terms will be reduced by the dc rejection characteristics of the fourier filters, although a small amount will still occur since the fourier filters still allow low frequencies through.

Section 4.2 showed that unbalanced faults will cause a positive and a negative peak in ($\Delta P/\Delta t$) at their fault on and fault off points.

Empirical analysis has shown that if a time delay of one and a quarter power system cycles is used on the algorithm trip criteria of equation 4(8), the algorithm successfully restrains for all power system faults. All of the faults tested did not cause the criteria of 4(8) to be satisfied for more than one power system cycle. Choosing one and a quarter cycles therefore introduces an extra safety margin. The complete pole slipping algorithm is therefore;

$$\begin{aligned} Q &< Qtrip && \} \text{ Satisfied} \\ &and && \} \text{ Continuously} \\ P &< Pt && \} \text{ For} \\ &and && \} \text{ 1.25 Power} \\ (\Delta P/\Delta t) &< (\Delta P/\Delta t)_{min} && \} \text{ System} \\ & && \} \text{ Cycles} \end{aligned} \qquad 4(14)$$

4.3.1 The Condition Monitored Real Power Trip Setting, Pt

The real power trip setting, Pt is based on the value of prime mover input power, Pm, as shown in Figure 1.2b. In an embedded generation relaying environment, the only signals available are the voltage and current signals from the VT's and CT's. Information such as the governor position or prime mover output power are not available. The value of Pm is therefore estimated from an on-line analysis of the generator electrical power output, P. The input power, Pm is estimated by observing the output power of the generator to see whether it remains constant for a specific amount of time. If the output remains constant it can be concluded that the generator is in a steady state and the output power will approximately equal the input power, except for losses. The function which is used by the relay to do this is given below;

$$\begin{aligned} &if \quad |P_{(n)} - P_{(n-lag)}| \; and \; |P_{(n)} - P_{(n-(2*lag))}| < Ptol \; ; \\ &then \quad Pt = P_{(n)} * Pfact \end{aligned} \qquad 4(15)$$

where $P_{(n)}$ is the present real power sample value, $P_{(n - lag)}$ is the sample value of 'lag' samples ago, $P_{(n - (2*lag))}$ is the sample value of '2*lag' samples ago, and Ptol is a tolerance band, chosen as nominally 5% of machine rating. Pfact is a coefficient to take into

account the losses and inaccuracies inherent in measuring machine input power from output power. The algorithm processing rate is 4 times per power system cycle, the nominal value of 'lag' typically chosen is 200 which equates to 1 second, Pfact is nominally set to 0.9. This results in a safety margin of 10 % to allow for losses and prime mover response times. The effects of synchronous machine losses on the algorithm are discussed in Appendix A. Figure 4.3 shows the flowchart for the function in the algorithm. Note that Pt can never take on a negative value, i.e. the function will not work for motoring conditions, it has only been designed as a *generator* pole slipping protection. Section 4.6 states how the algorithm can be adapted for synchronous motor pole slipping protection.

The algorithm implemented in the commercially available hardware platform had several settings which were included for algorithm development purposes only. These enabled 'fine tuning' of the algorithm during field trials, without having to make costly modifications to the software placed into the relay's EPROM. Section 4.7 contains the settings used, their ranges, and the settings necessary if the algorithm were released commercially.

4.3.2 The Adaptive Rate of Change of Power Trip Setting, $(\Delta P/\Delta t)_{min}$

The rate of change of power trip setting, $(\Delta P/\Delta t)_{min}$ is calculated by the algorithm according to the external relay setting, slip, and two internal real power parameters, Pt and Pmax. The method for determining Pmax, the maximum generator output power is presented in section 4.3.3.

The margin for error, $(\Delta P/\Delta t)_{min}$ used in the $(\Delta P/\Delta t)$ criterion is based on the theoretical value of $(\Delta P/\Delta t)$ at the CSP, it is given by;

$$(\Delta P/\Delta t)_{min} = -s * Pmax * \cos(\delta_c) \qquad 4(16)$$

where s is the slip and δ_c is given by;

$$\delta_c = 180° - \sin^{-1}\left(\frac{Pt}{Pmax}\right) \qquad 4(17)$$

the derivation of $(\Delta P/\Delta t)_{min}$ is given in appendix A5.2. The value of slip chosen will not be the exact value at which the relay trips, due to effects not taken into account in the derivation of 4(16), such as damping power. Equation 4(16) is used by the algorithm to continuously update the trip setting $(\Delta P/\Delta t)_{min}$ according to what the variables Pmax and

Pt dictate.

Pmax is a measure of the maximum output power that the generator has produced in the last second. It enables the algorithm to adjust its setting according to whether transient or steady state conditions are prevailing. With 'steady state' pole slips, a gradual loss of synchronism occurs, and the resulting power output waveforms change gently to begin with, as shown in Figure 1.3b. This produces low values of ($\Delta P/\Delta t$), a sensitive trip setting is therefore required. If the generator has been transiently disturbed, its output during the first swing in load angle, be it stable or unstable, will be much greater than its nominal output, because the power load angle characteristics change to the transient curves. This results in a greater magnitude in ($\Delta P/\Delta t$) at the CSP. The algorithm therefore needs to adjust its setting $(\Delta P/\Delta t)_{min}$ accordingly. The algorithm adjusts the setting, $(\Delta P/\Delta t)_{min}$ according to 4(18);

$$\begin{aligned} &If \quad \frac{Pt}{Pmax} < 0.6 \\ &then \quad (\Delta P/\Delta t)_{min} = (\Delta P/\Delta t)_{min} + (\Delta P/\Delta t)_{tran} \end{aligned} \qquad 4(18)$$

where $(\Delta P/\Delta t)_{tran}$ is an external relay setting based on the degree of transient saliency in the generator. Transient saliency arises due to differences in the values of Xd' and Xq'. In a salient pole generator, the changing stator flux produced by a transient can pass sideways through the field coils without linking them and inducing current. Consequently, for salient pole machines, Xq' is equal to Xq[110]. In a solid round rotor machine, a value of Xq' does exist due to eddy currents in the solid rotor structure. Typically the value of Xq' is 2 to 4 times larger than Xd', and has a time constant, Tqo' which is typically 10 times shorter than the field time constant, Tdo' [109]. For the purpose of deriving the setting, $(\Delta P/\Delta t)_{tran}$, it is assumed that Xq' is equal to Xq. $(\Delta P/\Delta t)_{tran}$ is given by;

$$(\Delta P/\Delta t)_{tran} = \left(\frac{1}{Xq} - \frac{1}{Xd'} \right) * Sgen \qquad 4(19)$$

This approach has the advantage that algorithm security against power swings is inherently increased because a greater magnitude of ($\Delta P/\Delta t$) is required before tripping will occur. For a 'steady state' pole slip, no peak will occur in the power output before the pole slip. The algorithm trip setting should therefore be at its most sensitive level to detect the pole slip because low values of ($\Delta P/\Delta t$) will result.

4.3.3 The Maximum Generator Output Power Monitor, Pmax

The value of Pmax used by equations 4(16), 4(17) and 4(18) is nominally set to 1.4 * Pt, so that the ratio Pt/Pmax equals 0.71. Equation 4(18) shows that $(\Delta P/\Delta t)_{tran}$ is not included in the calculation of $(\Delta P/\Delta t)_{min}$ during steady state conditions. If the generator's power output rises above the existing value of Pmax for longer than one power system cycle, the value of Pmax is updated to the new maximum for a duration of one second. The one second limit is used so that the new value of Pmax is only used for the period where a pole slip or recoverable power swing associated with that value is likely to occur. The one cycle constraint is necessary to prevent updates in Pmax for spurious spikes in the power waveform. Figure 4.4 shows the Pmax function flowchart.

4.3.4 Minimum Setting Value for $(\Delta P/\Delta t)_{min}$, Setting $(\Delta P/\Delta t)_{fact}$

If the generator was operating at a low value of output power, then it would be possible that the setting $(\Delta P/\Delta t)_{min}$ calculated by equation 4(16) could almost be zero. This may reduce algorithm security because if a fault causes a stable power swing, the $(\Delta P/\Delta t)_{min}$ setting may be too sensitive. The setting $(\Delta P/\Delta t)_{fact}$ is used so that if the magnitude of $(\Delta P/\Delta t)_{min}$ calculated by 4(16) falls below this setting, then $(\Delta P/\Delta t)_{min}$ is set to $(\Delta P/\Delta t)_{fact}$. At this development stage, this setting can be adjusted externally. If the algorithm were released commercially, it would not be provided as an external setting, a value would be chosen which would be embedded into the algorithm code. The nominal value chosen is given by;

$$(\Delta P/\Delta t)_{fact} = -0.25 * Sgen \qquad 4(20)$$

i.e 25 % of the generator rating. Using equation A(57) from appendix A and equation 4(20), the theoretical operating power at which $(\Delta P/\Delta t)_{fact}$ is used for the value of $(\Delta P/\Delta t)_{min}$ is given by;

$$Pt_{(at\ which\ (\Delta P/\Delta t)_{fact}\ is\ used)} = \frac{-0.255 * Sgen}{Slip(\%) * \pi} \qquad 4(21)$$

The factor of pi is necessary to convert slip from units of percent to absolute units which are in the time frame of the generator. This equation has been calculated assuming a power system operating frequency of 50 Hz. With the default setting of slip of -0.5 %, $(\Delta P/\Delta t)_{fact}$ is used when Pt falls below 16 % of generator rating.

4.3.5 Implementation of the Power Based Pole Slipping Algorithm into a Commercial Relay Platform

The algorithm has been implemented in a commercial micro-processor relay[74]. This enabled the testing of the algorithm in several ways;

a) It confirmed that the algorithm was suitable for inclusion into a microprocessor based relaying platform.

b) It made the testing of the algorithm in an industrial environment easier because the disturbance recorder function of the relay could be used to store the algorithm measurands and trip levels.

c) It permitted continuous field trials to be conducted on the algorithm since the relay could be interrogated remotely with a modem. This served to increase the confidence in the algorithm's ability to restrain for non-pole slipping conditions since the algorithm was installed on two generators which were regularly taken on and off load. One of these generators was a salient pole hydro set, the other a round rotor steam turbine set. The algorithm was therefore tested with both types of synchronous generator.

Figure 4.5 shows a flowchart for the complete algorithm. The flowchart also shows how relay output chatter has been prevented. Relay output chatter occurs when an algorithm measurand continuously crosses back and forth across its trip setting. This is undesirable as it causes excessive output contact wear. The problem is usually overcome by including some hysteresis in the trip level, so that after it is first satisfied, the trip level is reduced to prevent the output contact chatter.

Relay output chatter in the pole slipping algorithm was prevented by keeping the algorithm in a 'tripped' state until the reactive power criterion was no longer satisfied. This results in only one trip output per pole slip cycle.

Appendix E contains the document written for the practical implementation of the algorithm in a commercial relay hardware platform[74]. This document contains practical information such as simplification of algorithm equations in order to reduce processor power, numerical overflow considerations, setting ranges, default settings and disturbance recorder operation.

4.4 THEORETICAL OPERATING RANGE OF ALGORITHM

The theoretical operating range of the algorithm is dictated by;

a) The minimum value of system infeed at the generator terminals which permits the reactive power criterion to operate correctly and the algorithm to function successfully.

b) The fastest rate of pole slipping which can be detected.

c) The slowest rate of pole slipping which can be detected.

4.4.1 Minimum Value of System Infeed For Algorithm Operation

If the system infeed at the generator terminals is too low, the reactive power criterion will not be satisfied. The algorithm will therefore fail to detect poleslips. Put another way, if the system centre does not appear sufficiently inside the generator, the algorithm will fail to work. For most embedded generators, the infeed is high enough for the algorithm to operate correctly. For situations where the system centre appears out in the transmission/distribution network, the algorithm will fail to operate. This is not considered a problem however, because this is generally thought of as a job for the transmission line relays. To determine the point where the algorithm will no longer operate, a detailed analysis was performed using the equations for real and reactive power developed in Appendix A, section 4.1. These equations are too complicated for a simple equation to be derived that shows how the limit for system infeed changes with generator parameters. The mathematics software package, 'Mathcad' was therefore used to derive graphs which can be applied to any synchronous machine, showing the limits of operation. The method used to produce the graphs is given in Appendix A, section A5.3.

Four graphs were derived, one showing the effect of varying the external resistance, r, the others showing the effect of varying Xd' for different values of Xq and E. Figure 4.6a shows the setting graphs for different values of tie line resistance. This graph shows that the effect of tie line resistance is small and a high tie-line resistance aids algorithm operation.

Figures 4.6b, 4.7a and 4.7b show the setting graphs for varying values of Xq, Xd', and E. To use the graphs the maximum expected value of internal generator voltage, E is chosen. This determines which graph is used. For most applications the highest value of E is 1.25 pu[79]. The graph of Figure 4.6b should therefore be used. In communications with

a private protection consultant, it was stated that the practical values for Eg/Es range between 1.1 pu and 0.8 pu. In rare cases, the maximum value of E can be 1.5 pu, and if an extremely fast, high ceiling AVR is used, then E may reach 1.75 pu. Once the graph has been selected, Xd' is calculated as a fraction of Xq. The appropriate curve on the graph is then selected, and the maximum value of external reactance, X, looked up for the corresponding value of Xq.

If the value of X taken from the graph is greater than the actual value of external reactance for the system to be protected, the algorithm will work correctly. The value of external reactance used should be the largest value possible, i.e the situation of lowest capacity infeed. The external reactance should include the source reactance, transformers, and inter-connecting lines. The setting lines were calculated for the case where the external resistance, r, was equal to 10 % of the external reactance, X. This introduces a margin for error because it is a pessimistic outlook.

If the relay's VT's are located on the system side of the generator step up transformer, the transformer reactance should not be included in the external reactance value. Instead, the transformer reactance should be added to the values of Xd' and Xq of the generator. This enables the algorithm to detect pole slips that it could not otherwise detect because the system centre does not lie sufficiently inside the generator.

4.4.2 Fastest Rate of Pole Slipping Detected by Algorithm

Most pole slip schemes specify that slip rates of up to 10 % should be detected[60,79,147]. The one and a quarter cycle tripping constraint used in the algorithm sets the limit on the fastest pole slip which the algorithm can detect. It is assumed that the reactive power criterion, Qtrip is satisfied for machine angles between 90° and 270°. For the fastest rate of pole slipping to occur, the generator must be operating at full power, the real power trip setting will therefore equal 0.9 pu if the default value of Pfact of 0.9 is used. The peak in real power, Pmax is assumed to occur at a load angle of 90°, and equal two times rated power. This assumption is based on empirical values. Using a value for Pt of 0.9 pu, and Pmax of 2 pu, and assuming a sinusoidal power/load angle curve, the CSP when the real power criterion will be satisfied will occur at an angle, δ_c given by (equation 4(17));

$$\delta_c = 180 - \sin^{-1}(0.9/2) = 153° \qquad 4(22)$$

The real power criterion will therefore be satisfied between the load angles of 153 and

297°. Using the default value for $(\Delta P/\Delta t)_{tran}$ of -3.0 pu (see table 4-1), a value of δ_c of 153°, and the nominal slip setting of -0.5%, equations 4(16) and 4(18) give a value for the rate of change of power trip setting, $(\Delta P/\Delta t)_{min}$ of -5.72 pu. Assuming a slip rate of 10 %, and using equations A(54) and A(55) of Appendix A, the equation for rate of change of power is given by;

$$(\Delta P/\Delta t) = 10\% * \pi * \frac{d}{dt}(2 * \sin(\delta)) = 62.8\cos(\delta) \qquad 4(23)$$

Using the value for $(\Delta P/\Delta t)_{min}$ and equation 4(23), the load angles at which the rate of change of power trip setting is satisfied are 95 and 265°.

The final assumption made is that the 90 to 270° section of the pole slip occurs at twice the speed of the 270 to 90° section. This assumption is made because the machine accelerates using power from the prime mover and power from the utility during this period.

All three trip criteria are satisfied between the load angles of 153 and 265°, i.e they are satisfied for 112°. The algorithm requires 25 ms to trip. The fastest pole slipping rate which the algorithm can detect is therefore calculated as follows;

1) the 90 to 270° section of the slip cycle requires 25 ms * 180/112 = 40 ms
2) the mean time to complete 360° is therefore 40 ms * 3 = 120 ms
3) A period of 120 ms equates to 8.3 Hz, i.e 16 % slip at 50 Hz.

This is greater than the 10 % specification which most other pole slipping schemes use, and is therefore sufficient.

4.4.3 Slowest Rate of Pole Slipping Detected by Algorithm

Very slow pole slips occur rarely. They can occur during times of low excitation, when a generator is at low load. It is possible that one pole slip cycle can take a minute to complete[51]. Other pole slipping schemes are specified to operate down to a pole slipping rate of 0.1 % [60,79]. At a system frequency of 50 Hz, this translates to a single pole slip cycle taking 20 seconds. It is difficult to give a theoretical basis showing the slowest pole slip rate which the algorithm could detect because it is dependent upon the generator characteristics. The setting which determines the limit for detection of slow pole slips is $(\Delta P/\Delta t)_{min}$. At very slow pole slip rates, the rate of change of power may not be sufficient to operate the relay. However, although the whole pole slip may take 20 seconds, the part of the pole slip where the generator passes the CSP, and the algorithm operates will occur

at a speed much faster than the mean rate of pole slipping indicates because the generator rotor accelerates at this point. The algorithm should therefore trip. A simulation has been performed to confirm this theory, details of which can be found in Chapter 5.

4.5 OTHER ALGORITHM CONSIDERATIONS

This section discusses considerations which are secondary to the theoretical basis of the algorithm, such as circuit breaker operating duty, and post fault analysis.

4.5.1 Circuit Breaker Switching Duty

Conventional pole slipping schemes such as the single and double blinder impedance schemes are generally set to trip at a system load angle of 270°. This reduces the switching duty placed on the generator circuit breaker, since it is exposed to a maximum voltage across its poles at a load angle of 180°. The application engineer must decide which is more important, minimising the damage to the generator and disturbance to the system, or minimising the switching duty on the generator circuit breaker. This is dependent upon the over-rating of the generating plant and the rating of the local system.

Flurscheim[158] states that an important requirement for inter-connectors between generating stations is the ability of the circuit breaker to open satisfactorily under asynchronous conditions. In this case the recovery voltage across an opening circuit breaker may be much higher than under short circuit conditions and the duty may be more severe in some respects than the short circuit duty. If no special provision is made to relate the opening with phase displacement, it must be assumed that a circuit breaker may open at any phase angle. For a solidly earthed system, the recovery voltage has a maximum value of twice the phase to neutral voltage at a phase angle of 180°. IEC Document 56 calls for an asynchronous switching capability of interrupting 25 % rated short circuit current at 2.0 times normal voltage. However, the asynchronous switching duty is decreased because the severity of the transient recovery voltage is small compared with that arising during short circuit switching. This is due to the damping provided by the impedances either side of the circuit breaker. Westinghouse[61] state that if the circuit breaker has insufficient dielectric strength to withstand the asynchronous recovery voltage, re-ignitions will continue until a more favourable load angle is reached.

The micro-processor relaying environment enables several additional facilities which can overcome the switching duty problem. The theoretical point where the algorithm trip signal is reset occurs when the reactive power criterion is no longer satisfied. This results in only one trip output per pole slip cycle, and for an ideal system, this occurs at a load angle of 270°. A facility can therefore be provided whereby the tripping is delayed until this point is reached, thus minimising the duty on the circuit breaker. This can be provided within the relay as a setting option so that immediate tripping, or delayed tripping can be chosen. It is possible during loss of excitation conditions, that the reactive power criterion may not be reset, a timer must therefore be included so that if, after a specified time, the reactive power criterion had not been set, the trip command would be issued anyway. A suitable time would be 100 ms after the algorithm originally tripped. This would allow 90° of load angle increase for a mean pole slipping rate of 2.5 Hz. This ensures that the algorithm would always trip once it had detected a pole slipping condition.

4.5.2 Minimum Number of Pole Slips Before Tripping

For some applications, it is desirable to trip the generator only if continued pole slipping occurs. A facility should therefore be provided within the relay which delays circuit breaker tripping until a specified amount of pole slips have occurred. For instance, the decision to trip could be delayed until a second pole slip is detected. This may be useful for situations where it is possible for the generator to re-synchronise after the first pole slip. There would be little point in dis-connecting the generator if it is about to re-synchronise and commence normal stable operation. This decision can therefore be left to the applications engineer by providing an 'n' pole slips until trip setting.

4.5.3 Differentiation Between 'Steady State' and 'Transient' Pole Slips

The causes of 'steady state' and 'transient' pole slips are quite different, the protection engineer may therefore find it useful to know what type of pole slip caused the algorithm to trip. In the case of a 'transient' pole slip, the pole slip is normally due to a short circuit fault close to the generator. A 'transient' pole slip does not occur due to a failing in the generator or its control system. The generator can therefore be re-synchronised as soon as the disturbance which caused the pole slip has been removed. A 'steady state' poleslip may be caused by a defect in the generator's AVR or governor. It is therefore useful to know which type of pole slip occurred so that any corrective work required can be conducted.

Section 4.6 states that the power based pole slipping algorithm also detects some loss of excitation conditions. There is a grey area where generator pole slipping and loss of excitation overlap because during loss of excitation, the generator can commence asynchronous operation before the field flux has fully decayed. The remaining field flux gives the generator a degree of excitation. It can therefore have the appearance of a generator which has pole slipped due to insufficient excitation. Loss of excitations occurring from a high initial generator power output can therefore have the same appearance as a steady state pole slip.

The generator maximum power output monitor provides one means of differentiation between the types of pole slips. A steady state pole slip or loss of excitation will not cause a peak in real power output. The Pmax measurement can therefore be used to differentiate between the two. If Pmax has been updated to greater than the nominal value of 1.4 * Pt, then the pole slip would be a transient pole slip. The simplest way of implementing this in the algorithm code would be to check the ratio Pt/Pmax at the instant of tripping. If this is below the default level of 0.7, then Pmax is not at its nominal level.

Monitoring the magnitude of ($\Delta P/\Delta t$) also provides a complimentary method. Loss of excitation or steady state pole slips do not cause an abrupt change in real power before the trip command is issued. If the magnitude of ($\Delta P/\Delta t$) exceeds a specified level before the algorithm trips, it can be inferred that a transient disturbance has occurred on the network, and that the pole slip is a 'transient' type. Checking if a variable exceeds a specified level requires little additional processor time. Such checks therefore do not impose a large computational burden. A ($\Delta P/\Delta t$) level of five times the rating of the generator would be suitable for detecting a transient disturbance. If the algorithm is installed alongside fault detection algorithms, then information from their starter elements could also be used to improve reliability.

The steady state or transient pole slip information may also be used to implement an adaptive tripping scheme within the algorithm. Pole slips caused by faults will generally accelerate quickly into the pole slip. The algorithm typically produces a trip signal at a load angle of approximately 160° because the CSP does not occur until 140°. This inevitably means that the circuit breaker is forced to open at load angles of 180°, the worst place for circuit breaker opening duty. This problem can be overcome by delaying tripping as described in section 4.5.1 for 'transient' pole slips.

For steady state pole slips, the algorithm generally produces a trip signal at much lower load angles, typically 110°. Since the process of losing synchronism is much slower during steady state pole slips, the load angle does not increase as quickly as for transient pole slips. Circuit breaker tripping can therefore be initiated the instant the algorithm has predicted the 'steady state' pole slip, i.e pole slips which the algorithm detected when Pmax was at nominal value and ($\Delta P/\Delta t$) had not exceeded its preset level.

4.6 ADDITIONAL ALGORITHM DEVELOPMENTS - MOTOR POLE SLIPPING PROTECTION

The algorithm has been specifically developed for embedded generators. However, it is simple to extend its operation to motor pole slipping protection. This is especially important for hydro generator pumped storage schemes, as they are particularly prone to pole slipping when operating in the pumping mode[60,80,82,147]. One stability analysis[145] showed that the CCT was 120 ms whilst in the pumping mode. It was also stated that "generator manufacturers usually don't want to guarantee the asynchronous operation period of their synchronous machines when they are excited. The machine protection should consequently detect and prevent such kind of operation".

Synchronous motor protection is based on either impedance measurement, with a time delayed offset mho characteristic, or a power factor relay, which operates if a very low power factor occurs with a high current[45,159]. The single and double blinder schemes can also provide motor pole slipping protection.

To adapt the algorithm to enable motor pull out protection, the signs of the real power and rate of change of power trip settings need reversing. To provide motor and generator pole slipping protection in one algorithm, the algorithm would need to ascertain whether the machine was in a motoring or generating condition. This is easily done by monitoring the sign of the real power trip criterion, Pt. If this is negative, then the machine is motoring and the $(\Delta P/\Delta t)_{min}$ calculation needs changing so that the sign of $(\Delta P/\Delta t)_{min}$ is positive. The maximum power output measuring function would also need changing so that maximum negative powers are measured. The motor pole slipping algorithm would take the following form;

$$
\left.\begin{array}{rcl}
Q & < & Qtrip \\
& and & \\
P & > & Pt \\
& and & \\
(\Delta P/\Delta t) & > & (\Delta P/\Delta t)_{min}
\end{array}\right\}
\begin{array}{l}
\} \\
\} \text{ continuously} \\
\} \text{ for 1.25 power} \\
\} \text{ system} \\
\} \text{ cycles} \\
\}
\end{array}
\qquad 4(24)
$$

where Qtrip remains the same, Pt will be negative instead of positive, and $(\Delta P/\Delta t)_{min}$ will be positive instead of negative.

4.6.1 Performance for Detecting Loss of Excitation

The algorithm will also detect the most damaging of loss of excitation conditions because essentially, the algorithm is an asynchronous operation detection unit. The algorithm will successfully detect loss of excitations from high initial powers because the field flux has not fully decayed at the onset of asynchronous operation. The necessary fluctuations in real power required to operate the real power and rate of change of power portions of the algorithm are therefore produced.

In round rotor machines, the difference in Xd' and Xq' results in a transient saliency which also produces oscillations in power causing the algorithm to trip. At very low initial output powers. There is not enough variation in real power and hence $(\Delta P/\Delta t)$ to satisfy the $(\Delta P/\Delta t)$ trip criterion. To offer full loss of excitation cover from zero to full power, the algorithm would need supplementing by an additional algorithm which would provide detection of the low initial power loss of excitations[160].

With salient pole machines, a different problem can occur. The (2δ) term in equation 3(1) shows that a significant reluctance torque can be generated, due to the differences in Xd and Xq. Assuming Xq to equal one half of Xd, a quarter of rated power can be generated by a salient pole generator with no excitation, whilst still maintaining synchronism. A large amount of embedded generators have salient pole construction because they can be operated at much slower speeds, and are easier to manufacture. Even if a salient pole generator operates synchronously without a field, it still requires immediate disconnection because it will be consuming a large amount of reactive power which may depress system voltage. The power based algorithm will not detect this condition, because a loss of synchronism has not occurred. The algorithm described in reference [160] could be used

to supplement the power based algorithm.

If a salient pole generator does operate asynchronously, the power based algorithm will detect this condition as large oscillations in real power will occur due to the saliency.

4.7 ALGORITHM SETTING PROCEDURE

Table 4-1 provides the equations used for setting the algorithm. It is important to note that if the algorithm were released commercially, it is envisaged that the only settings required by the algorithm would be Xq, Xd' and the generator rating. A setting program within the relay would then be used to calculate the internal settings. More settings are used at present since at the development stage, greater control of the settings is required to fine tune the algorithm if required. If settings such as slip were 'hard coded' into the algorithm code, then any modification would require modifications to the processor board within the field trial relays, which can not be achieved remotely.

Table 4-1 Summary of Settings for Pole Slipping Algorithm

Setting	Formula	Default Value	Minimum Setting	Maximum Setting
Qtrip	-1/Xq * Sgen	Xq = 1.5 pu	Xq = 2.5 pu	Xq = 0.3 pu
Ptol	x %/100 * Sgen	x = 5 %	x = 1 %	x = 20 %
Pfact	none	0.9	0.7	1.0
$(\Delta P/\Delta t)_{fact}$	y %/100 * Sgen	y = -25 %	-10 %	-50 %
$(\Delta P/\Delta t)_{tran}$	(1/Xq - 1/Xd') * Sgen	-3 * Sgen	Xq = 2.5 pu Xd' = 0.1 pu	Xq = 2 pu Xd' = 2 pu
slip	none	-0.5 %	-0.1%	-0.5%
lag	none	1 s	0.1 s	10 s

In some instances, the only data available on the generator may be Xd, Xd' and its rating. If the generator has round rotor construction, then a value of Xq can be estimated using;

$$Xq_{(round\ rotor)} = 0.97 * Xd \qquad 4(25)$$

This value is an average value, based on data from 18 round rotor generators[109]. If the generator has salient poles, then Xq can be estimated using;

$$Xq_{(salient\ pole)} = 0.6 * Xd \qquad 4(26)$$

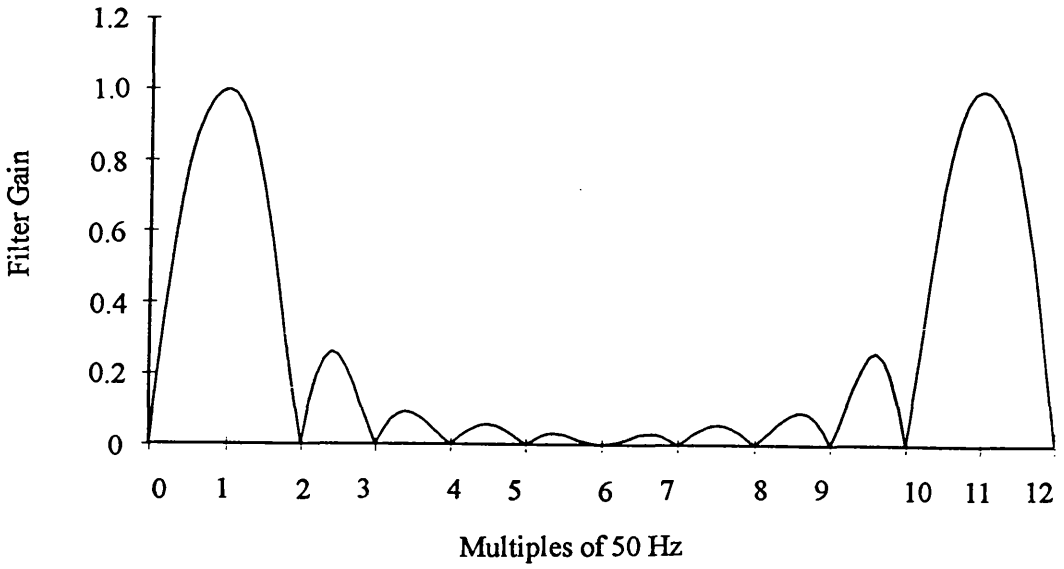

Figure 4.1a
Frequency Response of 12 Point, One Cycle Fourier Cosine Filter [74].

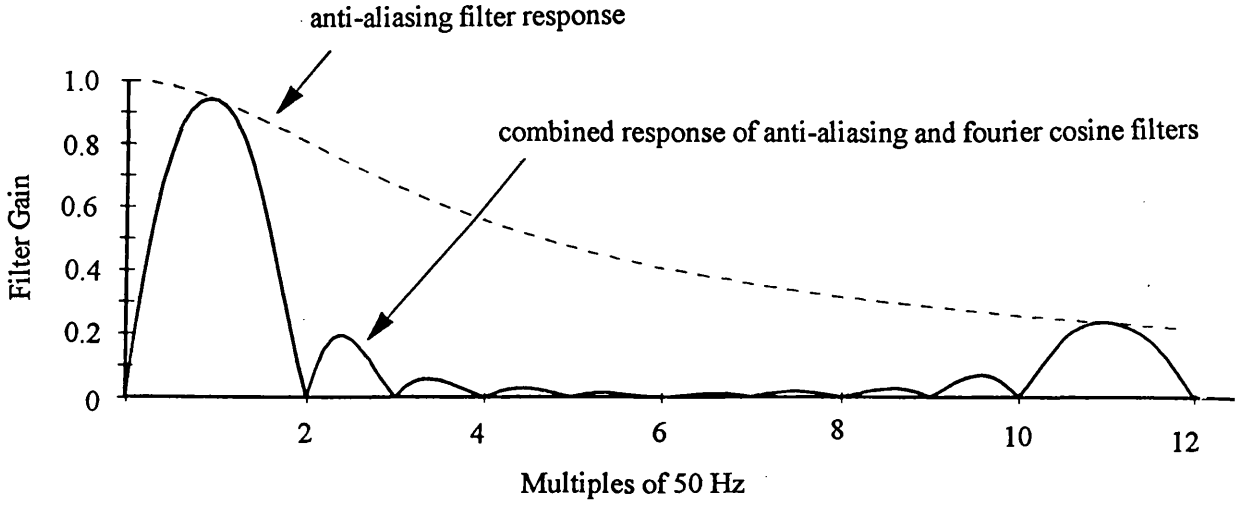

Figure 4.1b
Frequency Response of Anti-Aliasing Filter and Fourier Cosine Filter [74].

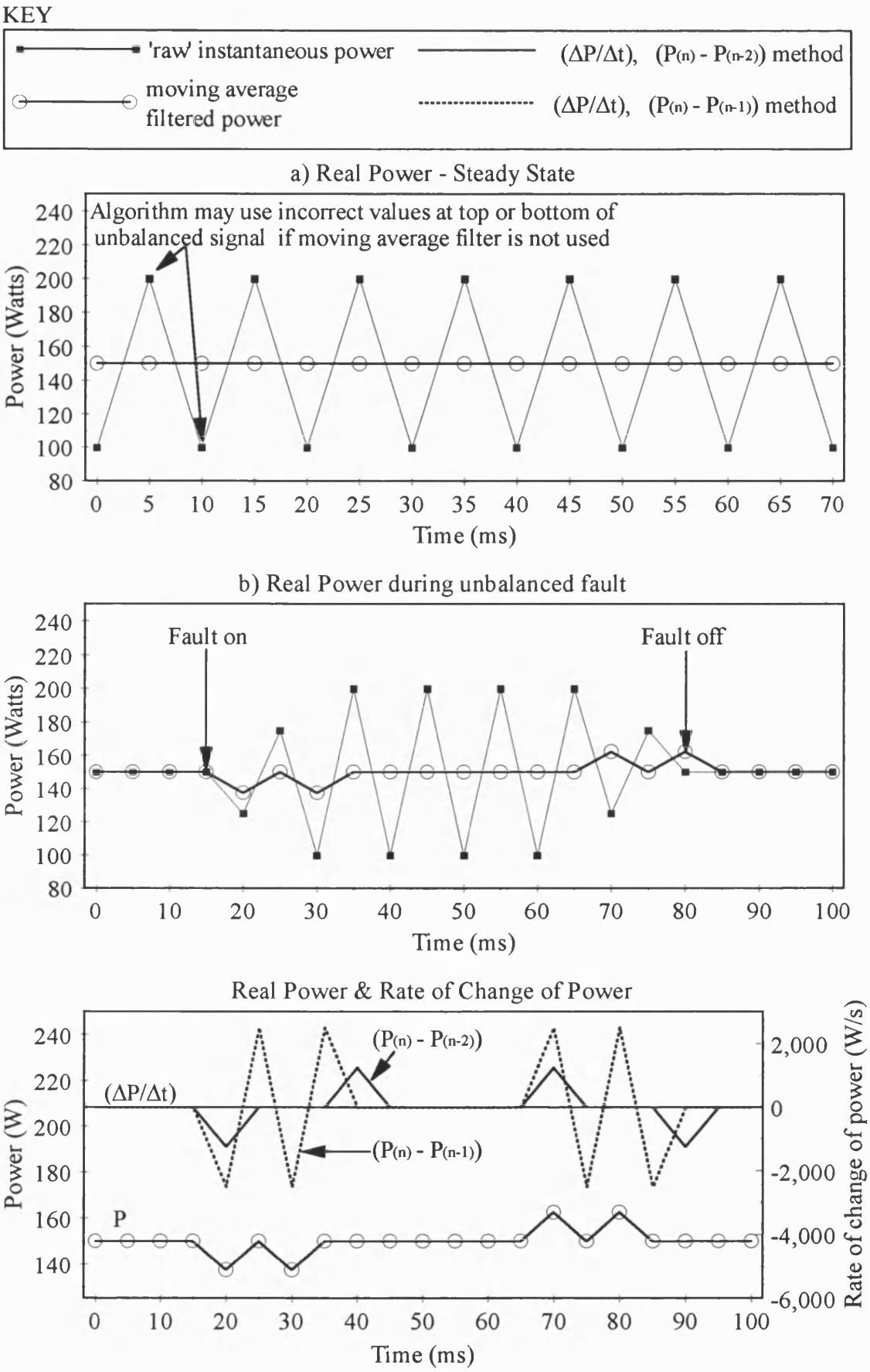

Figure 4.2
Graphs Showing Two Point Moving Average Filter Effect on Power Signals, and Effect of Two Point Rate of Change of Power Calculation Method

Pt Calculation Function.

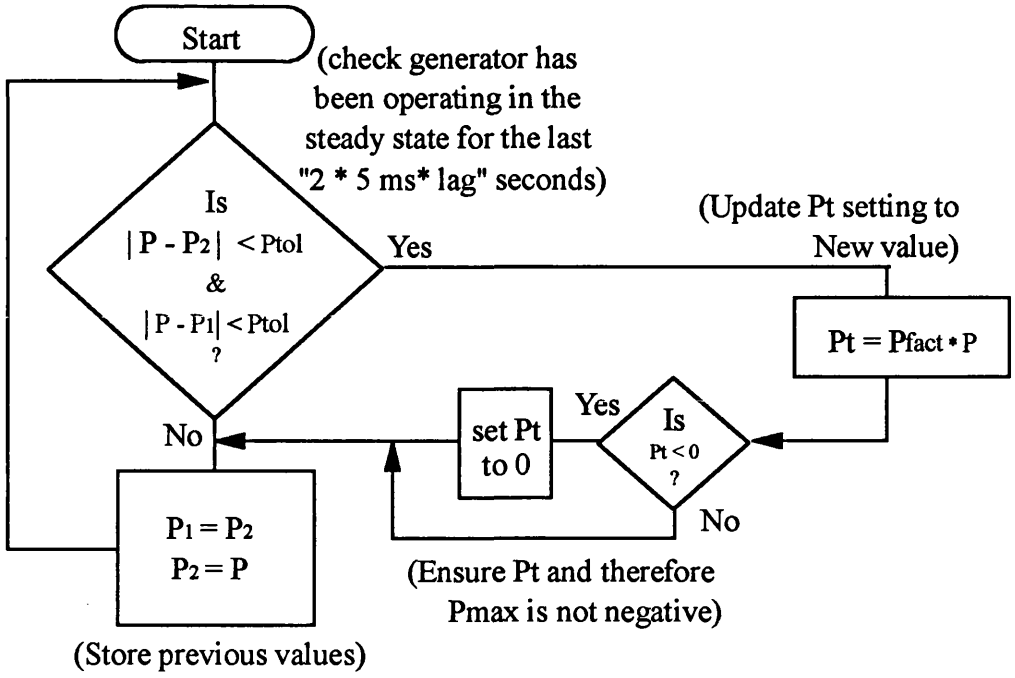

NOTE

1) The Pt calculation function is called every '5 ms * lag' seconds, which for a 'lag' setting of 200, equates to 1 second. The most recent value of moving average filtered real power calculated at the time the function is called is set to 'P'. This function is separate from the rest of the algorithm and is performed asynchronously, all of the other algorithm functions are called synchronously every quarter of a power system cycle. This serves to reduce processor demand.

2) P_1 is the value of P used '2*5 ms * lag' seconds ago, whilst P_2 is the value of P used '5ms * lag' seconds ago.

3) Pfact is the scaling factor used to introduce a safety margin in the Pt estimation. Nominally, it is set to 0.9 in absolute terms. It can be externally set from 0.7 to 1.0 in 0.1 increments.

4) Ptol is the tolerance band which the generator output power must stay within over the time period ' 2* 5ms* lag' seconds for the value of Pt to be updated.

Figure 4.3
The Generator Input Power Estimation Function (Calculates Trip Setting, Pt.)

Pmax Calculation Function.

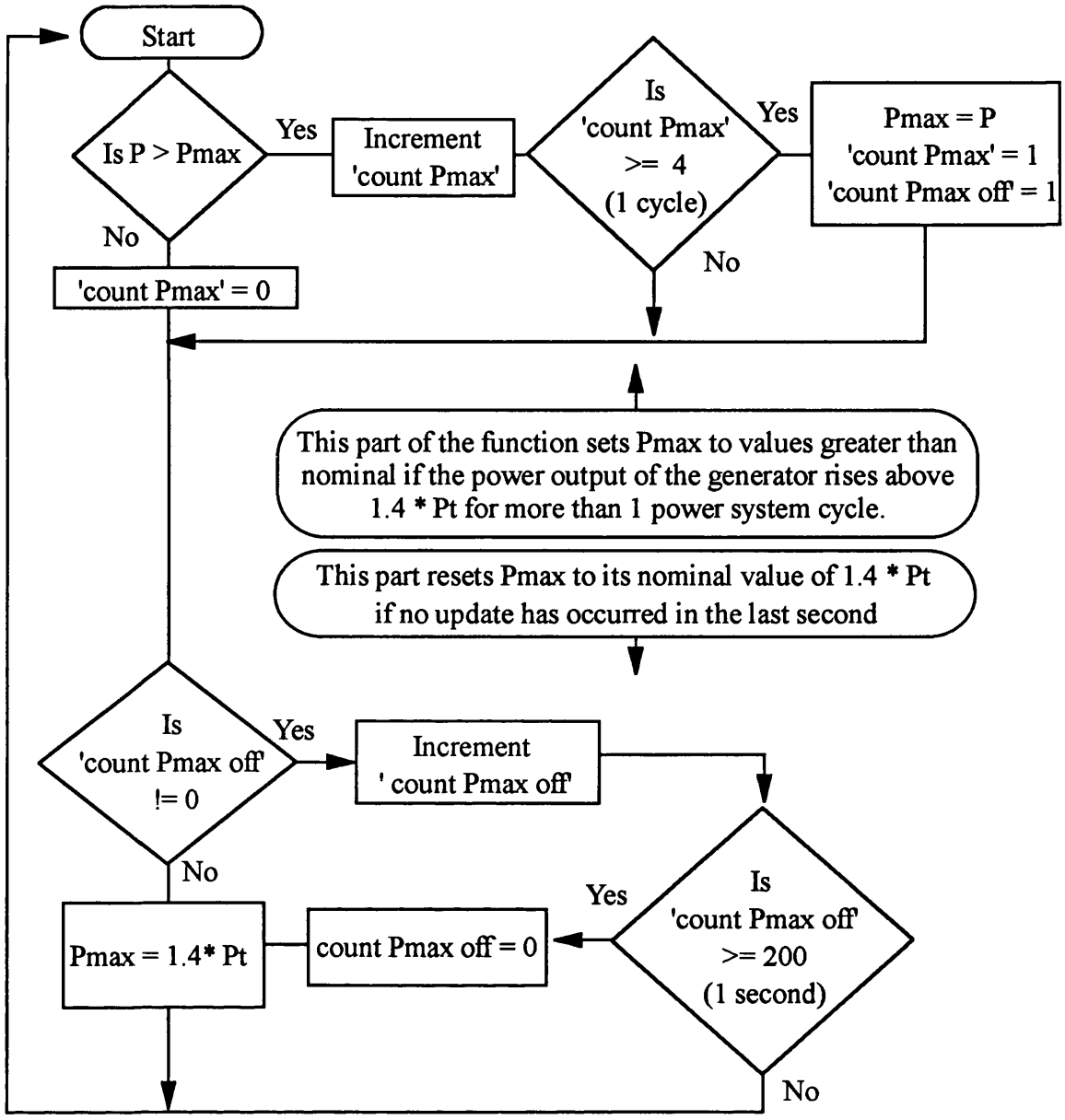

NOTE

1) The function tracks any slow changes in power output from the generator which are greater than the nominal value of 1.4 * Pt. It will reject any spikes produced by disturbances such as faults, this is why the moving average filtered power, P has to be greater than Pmax for one power system cycle before an update occurs. Once an update occurs, the updated value is 'held' for one second, Pmax is then reset to its nominal value.

2) The variables 'count Pmax' and 'count Pmax off' are counters used in the c code to count the necessary time constraints. Since the function is called every quarter power system cycle, a count of 4 is equivalent to one power system cycle.

Figure 4.4
Generator Maximum Output Power Monitor (Pmax Measuring Function).

The Power Based Pole Slipping Algorithm.

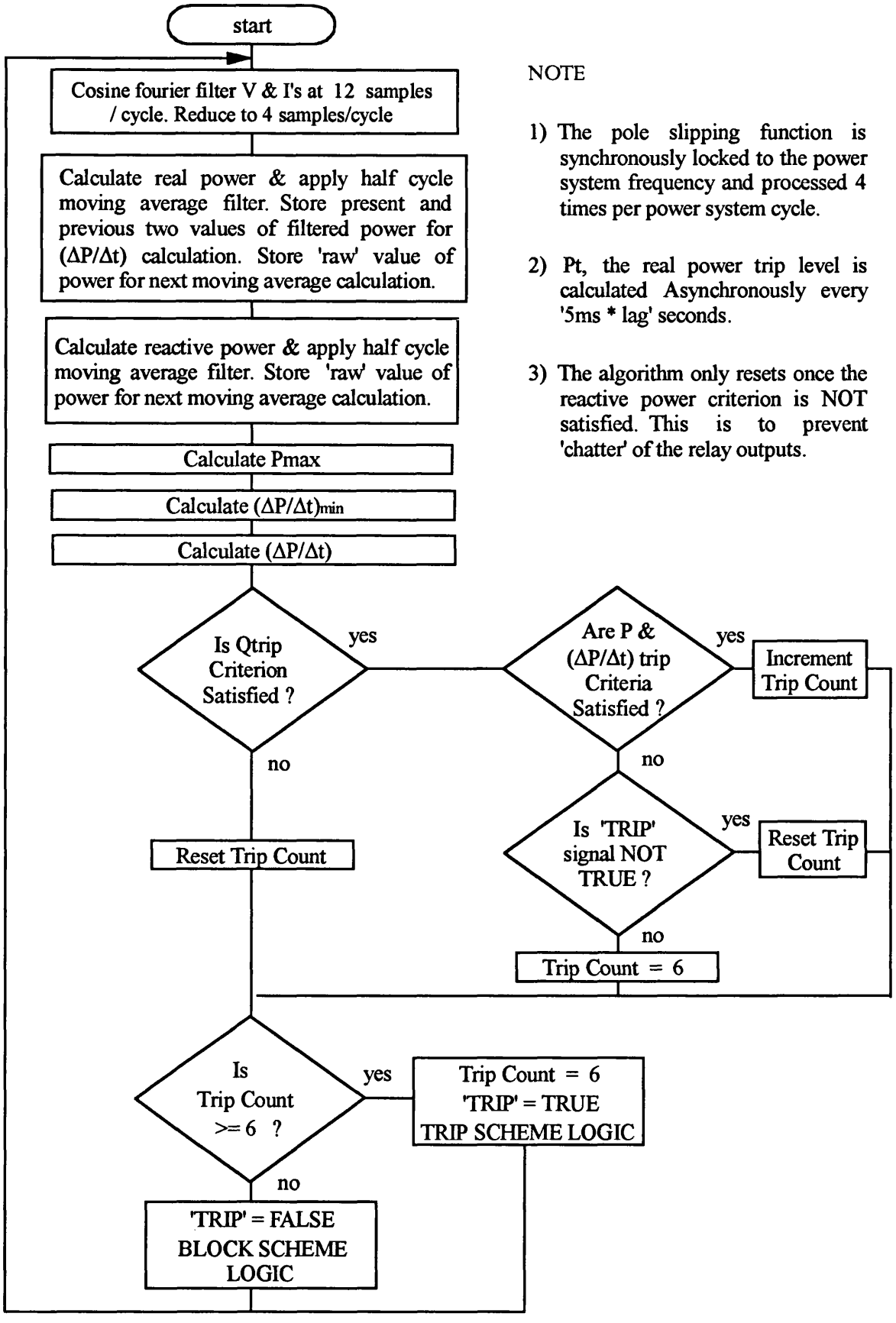

NOTE

1) The pole slipping function is synchronously locked to the power system frequency and processed 4 times per power system cycle.

2) Pt, the real power trip level is calculated Asynchronously every '5ms * lag' seconds.

3) The algorithm only resets once the reactive power criterion is NOT satisfied. This is to prevent 'chatter' of the relay outputs.

Figure 4.5
Flowchart Showing Operation of The Pole Slipping Algorithm

KEY ———— r = 0.1 * X ..... r = X

4.6a - Setting Limits for Pole Slipping Algorithm (Xd' = 0.1Xq)

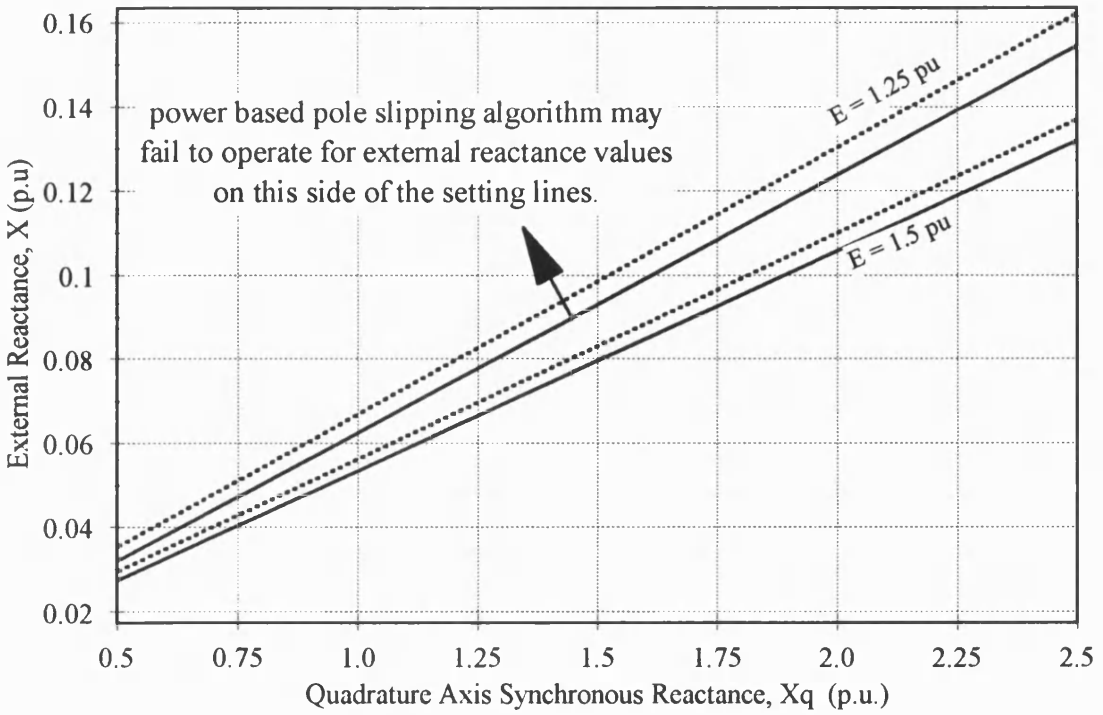

4.6b - Setting Limits for Pole Slipping Algorithm (E = 1.25 pu, r = 0.1X)

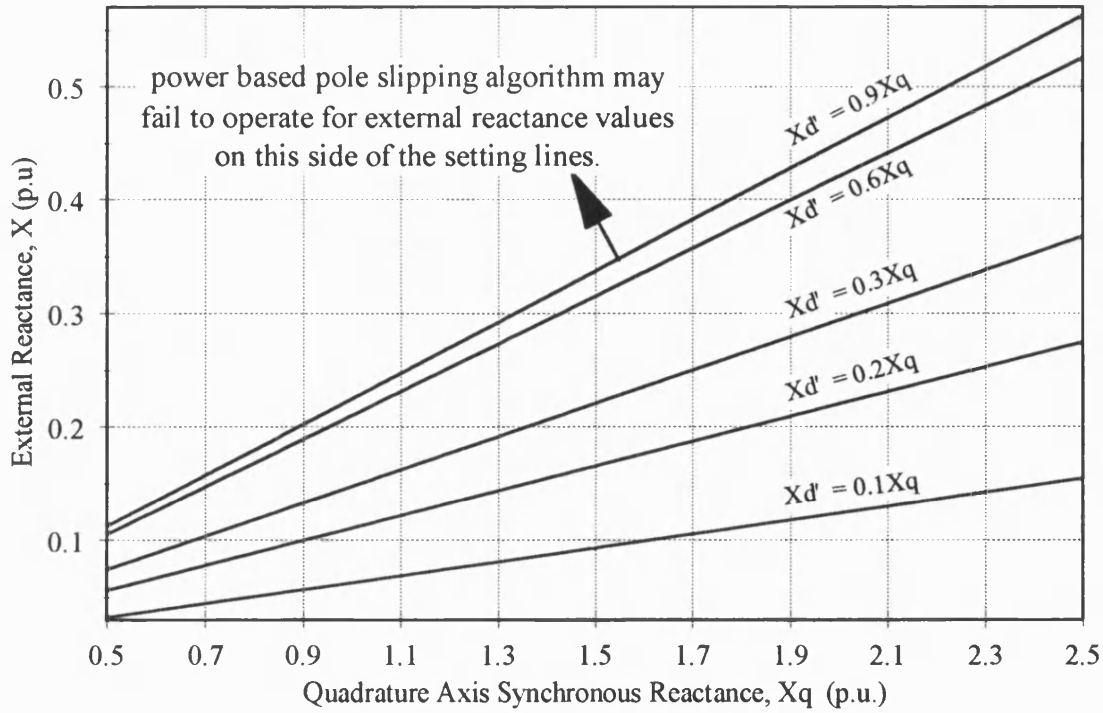

Figure 4.6
Graphs Showing Maximum Amount of External Reactance,
for which the Pole Slipping Algorithm Can Still Operate.

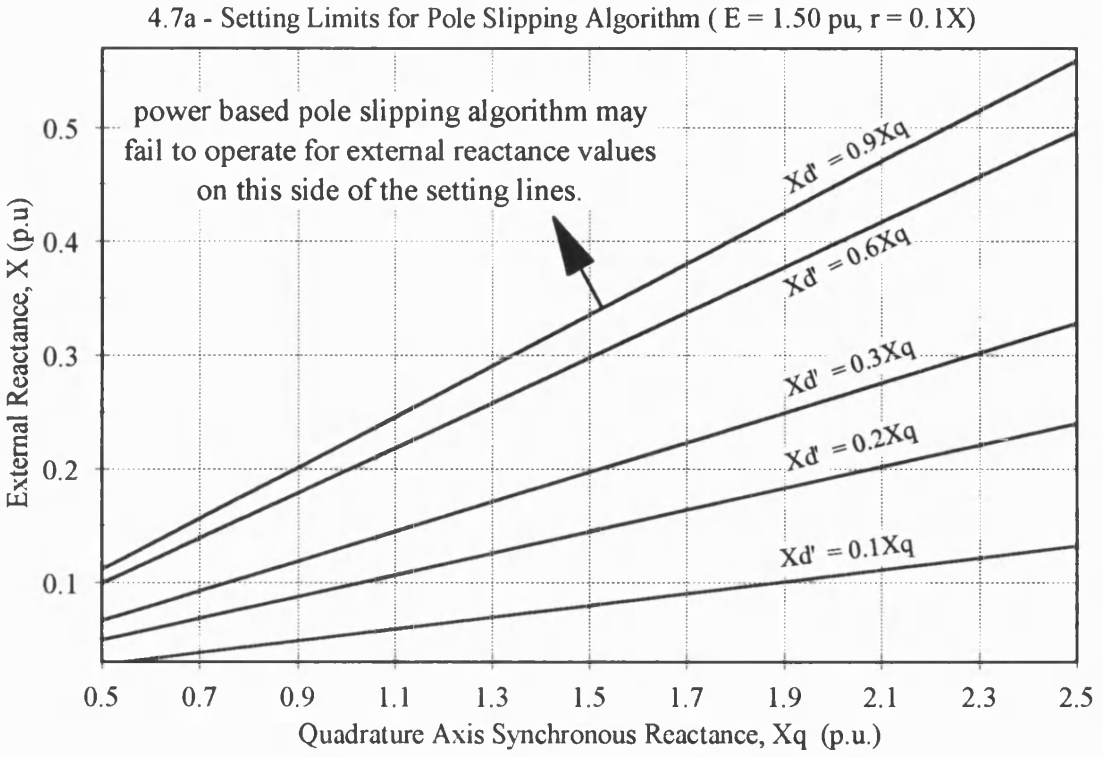

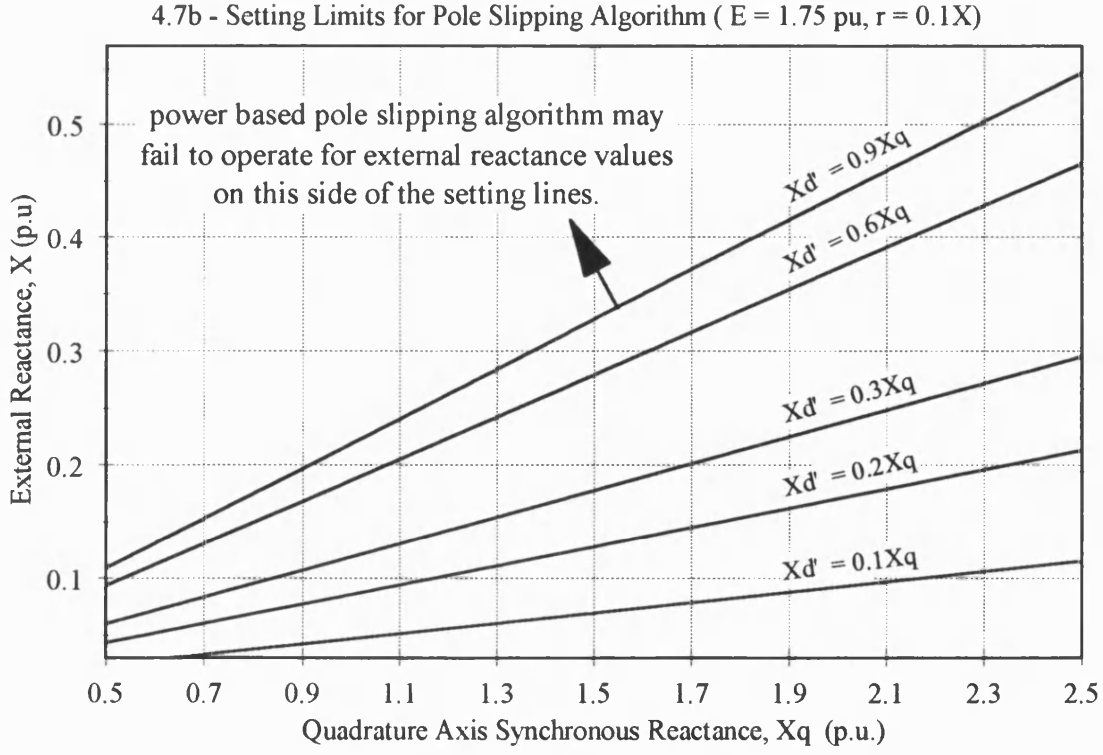

Figure 4.7
Graphs Showing Maximum Amount of External Reactance,
for which the Pole Slipping Algorithm Can Still Operate for E = 1.5 and 1.75.

Chapter 5
ALGORITHM EVALUATION STUDIES

A variety of methods were used to verify the operation of the algorithm. Initially the algorithm was proved off-line using data from computer based simulations performed using POWSIM[161], and data taken from tests performed on a laboratory power system model. The algorithm was then implemented in a microprocessor relay[162] and tested using the laboratory power system model. The algorithm was then implemented into a commercially available relay platform[74] and tested using a Programmable Power System Simulator (PPSS) [45]. The data files used by the PPSS were created using the PC based Alternative Transients Program (ATP) version of the ElectroMagnetic Transients Program (EMTP). An off-line software version of the algorithm was also used to test the algorithm using results directly from the ATP. This was particularly useful for testing various power system operating conditions because the only equipment required to perform the tests was a PC.

The algorithm correctly operated within the commercial relay for all of the tests conducted. To test the algorithm's operation in an industrial environment, the commercial relay containing the power based pole slipping algorithm was installed on a 625 kVA industrial diesel generator. In addition to this, two relays were installed in power stations. Both relays were installed with modems so that the relays could be interrogated remotely. These relays were commissioned in October 1996, one on a 26.5 MVA salient pole generator and the other on a 353 MVA turbo-generator. The field trials were intended to test the algorithm to ensure that it did not nuisance trip.

5.1 REAL TIME POWER SYSTEM SIMULATOR (POWSIM)

POWSIM[65,161] is a real-time electro-mechanical transient power system simulator. It uses a partitioned approach to solve the sets of equations which describe the behaviour of the machines, control systems and transmission network. The differential equations for each machine group are solved independently to calculate the current injection into the transmission network. The algebraic network equations are then solved and the whole calculation repeated until the required accuracy is obtained.

The machine model used is based on Park's transformation[169,170]. Damper winding and eddy current effects are represented by a short circuited winding on both the direct and quadrature axis. POWSIM is not suitable for simulating asynchronous operation, since it assumes that speed changes are negligible. The machine flux linkages are therefore not altered by a change in speed. The simulations will therefore be acceptable until synchronism is lost. The algorithm should operate before the loss of synchronism point. The simulations were therefore suitable for testing the algorithm. POWSIM also cannot simulate the effects of unbalance because it is a three phase simulation package. However, it is useful in testing and illustrating the basic theory behind the new algorithm, since the results it produces are of an 'ideal' nature and contain the fundamental characteristics of pole slips and power swings.

The classical single machine infinite bus model shown in Figure 5.1 was used. This is similar to most embedded generation sets because their rating is small compared with the system infeed. The rating of the 'infinite bus' used was one hundred times the rating of the machine.

Pole slipping was triggered by applying a three phase fault on the generator transformer busbar with a fault duration just greater than the critical clearance time (CCT). This is the maximum fault duration allowable before instability occurs. This technique was also used to trigger a power swing but for this the fault duration was chosen to be just less than the CCT. This will produce the largest possible load angle swing for a given operating condition and therefore provide the most testing conditions for the algorithm.

Both the pole slip and power swing tests were preceded by a reduction in generator loading from full to half power, this was done in order to test the condition monitoring section of the algorithm.

5.2 THE LABORATORY MODEL POWER SYSTEM

Section C1.2 of appendix C contains a schematic diagram of the laboratory power system model and data on the generator, prime mover and utility infeed. A variety of tests were conducted to test the algorithm's ability to detect pole slipping and restrain for faults.

5.2.1 Pole Slip Tests

For health and safety reasons, it was not possible to apply solid three phase faults at the terminals of the generator. Pole slipping was therefore induced using other methods.

In one of the pole slipping tests conducted, pole slipping was induced by switching a resistor in parallel with the field winding. This reduced the field's strength and hence the synchronising torque which holds the rotor in synchronism with the stator magnetic flux. The generator excitation was initially set to its full load value, with the generator operating at a low initial power. The generator's power input was then increased by increasing the power output of the DC machine. The instant the generator was operating at full power, the resistor was switched in parallel with the field, causing the generator to pole slip. Apart from the fluctuations in ammeter readings, a strobe directed at a marker on the generator's rotor was used to verify that the generator was pole slipping. The test was performed with a local load of 4 kW. These tests served to verify the operation of the condition monitored real power trip setting, Pt as well as the algorithm. Due to the limited length of the disturbance recording equipment, the time setting, 'lag', in the algorithm's prime mover power estimation function was set to 0.5 seconds instead of the normal 1 second. This was necessary so that the algorithm could be seen to operate correctly over the time span of the disturbance record.

Pole slipping was also induced by a sudden increase in the input torque to the generator. This type of poleslip will be referred to as an 'over torque' pole slip. Such a pole slip could happen if a microprocessor prime mover control system failed or due to operator error. A variety of tests were performed, at varying levels of excitation and local load. In addition tests were performed with another generator operating on the same bus. Pole slipping and loss of excitation tests were performed on this generator to check whether the algorithm remained stable during disturbances occurring on adjacent generators. Table 5-1 contains details of the tests conducted.

Table 5-1 Pole Slipping Tests Performed on 5 kVA Generator.

OT - Over Torque, PS - Pole Slip, LOE - Loss of Excitation.

Test letter	type of test	local load	Excitation
C	Weak Field PS	4 kW	PS caused by inserting a resistor in parallel with field
E	OT PS	4 kW	low (3 Amps)
F	OT PS	4 kW	medium (6 Amps)
G	OT PS	4 kW	high (9 Amps)
H	OT PS	none	low (3 Amps)
I	OT PS	none	med (6 Amps)
J	OT PS	none	high (9 Amps)
K	Adjacent OT PS	4 kW	high (9 Amps), protected machine in steady state.
L	Adjacent LOE	4 kW	high (9 Amps), protected machine in steady state

5.2.2 Fault Tests

The data for the fault tests was taken from tests which Barrett[104] performed when developing a micro-processor based loss of grid relay. To limit the fault current, a 'fault resistance' was used at the fault point. Three phase to earth, three phase, two phase to earth, two phase, and phase to earth faults were applied at position CB2 in Figure C4 of Appendix C. The tests were performed with and without the generator neutral solidly earthed. Embedded generators generally operate with an isolated neutral, this is a requirement of the REC's single point earthing regulation.

One three phase fault was of particular interest as it caused the generator to pole slip, giving data which tested the algorithm's ability to restrain for faults and trip for a pole slip shortly after. Table 5-2 contains details on the fault tests.

Table 5-2 Fault Tests Performed on 5 kVA Generator.

Test	Fault Type	Generator Neutral Connection	Generator Initial Operating Point
1A	A-E	Earthed	P = 3.5 kW, Q = 250 VAr
1B	A-E	Isolated	P = 3.75 kW, Q = 250 VAr
2A	A-B	Isolated	P = 3.6 kW, Q = 500 VAr
3A	A-B-E	Earthed	P = 3.5 kW, Q = 0 VAr
3B	A-B-E	Isolated	P = 3.7 kW, Q = 400 VAr
4A	A-B-C	Isolated	P = 4 kW, Q = 0 VAr
5A	A-B-C-E	Earthed	P = 3.9 kW, Q = 0 VAr
5B	A-B-C-E	Isolated	P = 3.8 kW, Q = 0 VAr

5.3 PROGRAMMABLE POWER SYSTEM SIMULATOR (PPSS) TESTS

The power system model used to generate the PPSS test data was taken from an EPRI transient stability model[163] of a 200 MVA generator. The commercial relay implementation of the algorithm was used for the tests. Appendix E contains details on the techniques used to install the algorithm in a microprocessor relaying environment. Appendix C, section C1 contains details of the power system, AVR and governor models used in the simulations. The ATP was used to simulate pole slips, power swings, faults, circuit breaker pole scatter, operation at machine load angles in excess of 90°, loss of excitation, and loss of prime mover conditions. Details of all of the tests conducted can be found in Tables 5-3, 5-4, and 5-5.

The performance of the conventional pole slipping schemes described in chapter 2 was compared with the power based pole slipping algorithm. The impedance based relays were modelled using a PC. Section 5.7 contains details of the techniques used to model the impedance relays.

Table 5-3 Details of PPSS Pole Slipping Simulation Tests

Test Name (Code)	Description of Pole Slipping Test
PSL1NN (A1)	Pole Slip (following a 940 ms, 3 Phase to Earth Fault), no governor or AVR modelled, 20 % initial load, Fault on point staggered by 10 ms for each phase.
PSL2NN (A2)	Pole Slip (following a 650 ms, 3 Phase to Earth Fault), no governor or AVR modelled, 50 % initial load.
PSL3NN (A3)	Pole Slip (following a 350 ms, 3 Phase to Earth Fault), no governor or AVR modelled, 100 % initial load
PSL1GN (A4)	Pole Slip (following a 1180 ms, 3 Phase to Earth Fault), governor modelled, AVR not modelled, 20 % initial load
PSL2GN (A5)	Pole Slip (following a 950 ms, 2 Phase to Earth Fault), governor modelled, AVR not modelled, 50 % initial load
PSL3GN (A6)	Pole Slip (following a 950 ms, Phase to Phase Fault), governor modelled, AVR not modelled, 100 % initial load
PSL1NA (A7)	Pole Slip (following a 1170 ms, 3 Phase to Earth Fault), no governor modelled , AVR modelled, 20 % initial load
PSL2NA (A8)	Pole Slip (following a 750 ms, 3 Phase to Earth Fault), no governor modelled, AVR modelled, 50 % initial load
PSL3NA (A9)	Pole Slip (following a 290 ms, 3 Phase to Earth Fault), no governor modelled, AVR modelled, 100 % initial load
PSL1GA (B1)	Pole Slip (following a 1170 ms, 3 Phase to Earth Fault), governor & AVR modelled, 20 % initial load
PSL2GA (B2)	Pole Slip (following a 650 ms, 3 Phase to Earth Fault), governor & AVR modelled, 50 % initial load
PSL3GA (B3)	Pole Slip (following a 330 ms, 2 Phase to Earth Fault), governor & AVR modelled, 100 % initial load
PSL1GAF (B4)	Pole Slip (due to faulty avr action - Vf reduced by 95 %), governor & AVR modelled, 20 % initial load
PSL2GAF (B5)	Pole Slip (due to faulty avr action - Vf reduced by 50 %), governor & AVR modelled, 50 % initial load
PSL3GAF (B6)	Pole Slip (due to faulty avr action - Vf reduced by 20 %), governor & AVR modelled, 100 % initial load

Table 5-4 Details of PPSS Stable Power Swing Simulation Tests

Test Name (Code)	Description of Stable Power Swing Test
PSW1NN (B7)	Stable Power Swing (following a 900 ms, 3 Phase to Earth Fault), no governor or AVR modelled, 20 % initial load.Fault on phases staggered by 10 ms, fault off by 20 ms.
PSW2NN (B8)	Stable Power Swing (following a 610 ms, 3 Phase to Earth Fault), no governor or AVR modelled, 50 % initial load
PSW3NN (B9)	Stable Power Swing (following a 263 ms, 3 Phase to Earth Fault), no governor or AVR modelled, 100 % initial load
PSW1GN (C1)	Stable Power Swing (following a 1155 ms, 3 Phase to Earth Fault), governor modelled, AVR not modelled, 20 % initial load
PSW2GN (C2)	Stable Power Swing (following a 810 ms, 2 Phase to Earth Fault), governor modelled, AVR not modelled, 50 % initial load. Fault off phases staggered by 5 ms.
PSW3GN (C3)	Stable Power Swing (following a 820 ms, 2 Phase Fault), governor modelled, AVR not modelled, 100 % initial load. Fault off phases staggered by 10 ms.
PSW1NA (C4)	Stable Power Swing (following a 1150 ms, 3 Phase to Earth Fault), no governor modelled, AVR modelled, 20 % initial load
PSW2NA (C5)	Stable Power Swing (following a 630 ms, 3 Phase to Earth Fault), no governor modelled, AVR modelled, 50 % initial load
PSW3NA (C6)	Stable Power Swing (following a 280 ms, 3 Phase Fault), no governor modelled, AVR modelled, 100 % initial load
PSW1GA (C7)	Stable Power Swing (following a 1150 ms, 3 Phase to Earth Fault), governor & AVR modelled, 20 % initial load
PSW2GA (C8)	Stable Power Swing (following a 630 ms, 3 Phase to Earth Fault), governor & AVR modelled, 50 % initial load
PSW3GA (C9)	Stable Power Swing (following a 320 ms, 2 Phase to Earth Fault), governor & AVR modelled, 100 % initial load

Table 5-5

Details of PPSS AVR Assisted High Load Angle, Loss of Field and Loss of Prime Mover Simulation Tests

Test Name (Code)	Description of Loss of Excitation or Loss of Prime Mover Test
AVR4NA (D1)	Operation at $\delta > 90°$, no governor modelled , AVR modelled, 87.5 to 44 % initial load. Tdo' reduced from 6.2 to 4.2 s, AVR gain reduced from 400 to 200.
AVR5NA (D2)	Operation at $\delta > 90°$, no governor modelled , AVR modelled, 50 to 0 % initial load. Tdo' reduced from 6.2 to 4.2 s, AVR gain reduced from 400 to 200.
AVR6NA (D3)	Operation at $\delta > 90°$, no governor modelled , AVR modelled, 87.5 to 70 % initial load. Tdo' reduced from 6.2 to 4.2 s, AVR gain reduced from 400 to 200.
LOF1GA (D4)	Loss of Field , governor modelled, Field voltage reduced to 0, 20 % initial load. Tdo' reduced from 6.2 to 2.2 s.
LOF2GA (D5)	Loss of Field , governor modelled, Field voltage reduced to 0, 50 % initial load. Tdo' reduced from 6.2 to 3.8 s.
LOF3GA (D6)	Loss of Field , governor modelled, Field voltage reduced to 0. 100 % initial load.
LOP1NA (D7)	Loss of Prime Mover , AVR modelled, Input power reduced to -3 % rated power, 20 % initial load
LOP2NA (D8)	Loss of Prime Mover , AVR modelled, Input power reduced to -3 % rated power, 50 % initial load
LOP3NA (D9)	Loss of Prime Mover , AVR modelled, Input power reduced to -3 % rated power, 100 % initial load

Note: For the tests involving operation at load angles in excess of 90°, the forward path gain of the AVR had to be reduced from 400 to 200 in order to improve the damping. In addition, the generator open circuit time constant, Tdo' was changed

from 6.2 to 4.2 seconds. This was necessary to improve the speed with which the AVR was able to cause changes in the generator's field excitation.

Note: The maximum time which the PPSS can simulate is 6 seconds. The time constant, Tdo' was therefore adjusted for the low initial power loss of excitation tests so that the generator lost synchronism within the 6 second time period.

The PPSS uses the data from ATP simulations to re-create the voltage and current waveforms which would normally come from the generator VTs and CTs. These waveforms are then injected into the relay to test the algorithm. Reference [45] contains details on the PPSS which was used for the tests.

5.3.1 Suitability of the ATP Simulation Package for Generator Simulations

This section discusses the suitability of the ATP for performing simulations which will test the power based algorithm. There are many different methods and models available for simulating synchronous machines, and it is important to choose an approach which will model the synchronous generator accurately as it pole slips. It is also important to model the effects of the generator control systems. In many studies, it is assumed that the effect of the generator governor can be neglected because the time constants involved are several seconds[108]. This assumption is invalid. The stator, field, damper windings, AVR and governor all need including in the model. This section will not give a detailed discussion of synchronous machine simulation, this subject has been well covered in many other texts[37,103,109,123,164,165]. This section will discuss the synchronous machine model used, and the reasons for its use.

The model used[166,167,168] assumes that the electrical part of the machine has three armature windings, connected 120° apart, one field winding, which produces flux in the direct axis when excited, one hypothetical winding on the direct axis which represents damper bar effects, one hypothetical winding on the quadrature axis which represents damper bar effects, and one hypothetical winding on the quadrature axis which represents slowly changing fluxes in the quadrature axis, which are produced by deeply flowing eddy currents (negligible in salient pole machines). The model is in the form of the general synchronous machine equations derived by Park[169,170]. These hold for any variation of the speed of the machine, and any kind of transient change in currents and voltages[103].

The ATP model was originally developed to investigate sub-synchronous resonance (SSR). The electrical and mechanical shaft torsional dynamics are therefore represented. One paper[168] states with reference to the application of the model that, "Other typical applications include transmission line re-closure, independent pole switching, load rejection, loss of synchronism and multi-machine interaction problems".

To simulate a pole slipping machine, it is necessary to take into account the effects of changes in rotor speed. Changes in rotor speed cause two main effects. Firstly a change in rotor speed will result in a change in the flux linkage, this change therefore needs including in the model. Secondly, as the rotor speed departs from synchronous speed, induction machine effects also need modelling because induced currents will flow in the field and damper windings. Additionally, flux cannot be assumed constant, since the simulations are of a long duration and embedded generators can have short time constants. The model used by the ATP includes all of these effects, as well as including saturation, and modelling of AVR's and governors. It is therefore suitable for performing simulations which can be used to test the algorithm.

Examples of the ATP simulation files can be found in Appendix F.

5.3.2 Simulation of Overhead Lines and Cables

Another modelling consideration is the way in which lines, transformers and sources are simulated. As shown in Figure 4.1b, the relay is sensitive to frequencies below 200 Hz. Effects such as travelling waves do not require representation in the power system model, since they will not be seen by the relay. In addition, embedded generators are generally connected to short cables or overhead lines. The lumped parameter mutually coupled pi model of a transmission line can therefore be used[37,164,166]. It is impractical to use a distributed parameter model for such short lines because the travel time of such a line would require an unsuitably small simulation time-step. The important consideration when modelling lines is to adequately represent the positive, negative and zero phase sequence components so that balanced and unbalanced faults can be simulated. The ATP type 1,2,3 mutually coupled RLC pi model[166] is suitable for representing unbalanced faults. The parameters can be entered manually, or derived by the ATP cable or line constants program.

5.3.3 Simulation of Transformers

Transformers have been represented in two different ways. In the PPSS simulations, the transformer model was taken directly from an EPRI transient stability study model[163]. This uses the ATP internal saturable transformer model called TRANSFORMER, which models transformers using the classical model shown in Figure 5.2. This uses leakage reactance and resistances on both the primary and secondary side, an ideal transformer, and a resistor in parallel with a saturable non-linear reactor representing the magnetisation circuit. This model will simulate the losses found in a transformer as well as the zero sequence trap which occurs in delta connected windings. It is therefore suitable for simulation of unbalanced faults.

The second technique uses the ATP supporting routine 'BCTRAN' to derive a six by six impedance matrix which represents the transformer. This uses standard transformer test data and is therefore a convenient way of converting manufacturer's data into a usable format. This is the recommended approach for simulating the zero sequence capabilities of transformers[163]. Examples of BCTRAN simulation files can be found in Appendix F.

5.3.4 Simulation of Source Impedances

It is impractical to represent in detail, the entire power system. It is necessary to derive a thevenin equivalent of the system at some point and it is important to properly represent the source impedance which represents the 'utility' when performing embedded generation simulations[171]. If the three phase and phase to earth fault currents for that and only that part of the system are known, then a thevenin equivalent impedance can be derived as follows[171];

$$Z_1 = \frac{1}{Ifault_{(3\ ph)}} \qquad 5(1)$$

where Z_1 is the per unit positive sequence impedance, and $Ifault_{(3\ ph)}$ is the per unit three phase fault current of the section of power system to be represented. The per unit zero sequence thevenin impedance, Z_0 is given by;

$$Z_0 = \frac{3}{Ifault_{(1\ ph\text{-}E)}} - \frac{2}{Ifault_{(3\ ph)}} \qquad 5(2)$$

where $Ifault_{(1\ ph\text{-}E)}$ is the per unit single phase to earth fault current of the section to be represented. This approach can be used only if there is no significant capacitance or transmission lines at the bus which is being converted to a thevenin equivalent.

5.4 625 kVA INDUSTRIAL DIESEL GENERATOR FIELD TESTS

The 625 kVA diesel generator used to perform field tests is a salient pole machine. Appendix C contains the data available on the generator and utility connection. The commercial relay implementation of the algorithm was installed for the tests. An additional relay was installed in parallel with the pole slipping relay so that raw samples of voltage and current could be taken. This enabled comparison between conventional pole slipping schemes and the new approach. Pole slipping, loss of excitation, steady state, and local load change tests were performed, the details of which are given in tables 5-6, 5-7, and 5-8.

Pole slipping could not be induced by placing short circuit faults close to the generator, as this was not permitted. Instead, pole slipping was induced in two ways. One method involved weakening the field excitation until the generator lost synchronism, the other involved suddenly increasing diesel engine output torque until a pole slip occurred. This type of pole slip could occur due to control system mal-function, or operator error. There was also a 593 kVA diesel generator next to the test machine, this was forced to pole slip and to lose excitation in order to test the algorithm's ability to restrain for nearby disturbances.

Loss of excitation was invoked by disconnecting the field supply. This effectively short circuited the field winding. The largest local load which could be switched on and off at one discrete point was a compressor. This caused an abrupt load change when switched on, but not when switched off. Large local load disconnections therefore could not be performed. The compressor rating was 120 HP.

The relay was operational throughout the whole test period. Generator run-up and synchronisation tests were effectively performed, though no disturbance records were taken.

Table 5-6

Pole Slipping Tests Conducted on 625 kVA Diesel Generator.

Test	Protected Generator (625 kVA)	Adjacent Generator (593 kVA)	Notes
A1	Pole Slip (100 kW)	Not in Operation	*Tried* to induce pole slip by weakening the field. But field would not weaken enough.
A2	Pole Slip (250 kW)	Not in Operation.	*Tried* to induce pole slip by weakening the field. But field would not weaken enough.
A3	Pole Slip (500 kW)	Not in Operation.	Induced pole slip by weakening the field.
A4	Steady State. (100 kW), (-200 kVAr)	Pole Slip (474 kW).	Induced pole slip by weakening the field.
A6	Pole Slip . (100 kW), (-200 kVAr)	Not in Operation.	*Tried* to induce pole slip by suddenly increasing input power.
A7	Pole Slip (0 kW) (- 200 kVAr)	Not in Operation.	Induce pole slip by suddenly increasing input power.

Note: The figures given in brackets are the initial generator output powers. The first figure is the real power output, the second the reactive power output. The reason pole slips did not occur in tests A1, A2 and A6 is that the control which adjusted the field excitation could only be decreased to a certain level. An open circuit, un-synchronised test was performed to see what this level corresponded to. In the middle position, the generator open circuit terminal voltage was 440 volts. This is above the no load value of excitation, which should produce a voltage of 415 volts. With the excitation set to a minimum, the open circuit terminal voltage was

380 volts, i.e 8 % less than the no load value. This limit combined with the effect of the generator AVR meant that pole slipping could not be induced for low levels of generator loading

Table 5-7

Loss of Excitation Tests Conducted on 625 kVA Diesel Generator.

LOE - Loss of Excitation

Test	Protected Generator
B1	LOE from 20% load. (100 kW), under-excited (-200 kVAr)
B2	LOE from 20% load. (100 kW), over-excited (200 kVAr)
B3	LOE from 50% load. (250 kW), under-excited (-160 kVAr)
B4	LOE from 50% load. (250 kW), over-excited (200 kVAr)
B5	LOE from 100% load. (500 kW), under-excited (-130 kVAr)
B6	LOE from 100% load. (500 kW), over-excited (200 kVAr)

Table 5-8

Steady State and Local Load change Tests Conducted on 625 kVA Diesel Generator.

Test	Protected Generator (625 kVA)	Notes
C1	Steady State. 30 % load (150 kW), under-excited (-200 kVAr)	Steady State Operation.
C2	Steady State. 30 % load (150 kW), level-excited (0 kVAr)	Steady State Operation.
C3	Steady State. 30 % load (150 kW), over-excited (200 kVAr)	Steady State Operation.
C4	Steady State, 100 % load (500 kW), under excited (-130 kVAr).	Switch compressor on.
C6	Steady State, 20 % load (100 kW), under excited (-200 kVAr)	Switch compressor on.

5.5 STEAM TURBINE AND HYDRO GENERATOR FIELD TRIALS

Two relays were also installed in power stations in a purely supervisory role in order to test whether the algorithm would operate correctly. Capturing a pole slip on one of these generators would be a considerable bonus because the trials were primarily conducted to ensure that the algorithm did not nuisance trip for power system conditions other than pole slipping or loss of excitation.

The relays had been installed for three months at the time of writing this thesis, it is intended that they will remain connected to the generator for a period of one year. Both of the relays had modems connected to their serial communications ports so that they could be interrogated remotely. As well as the pole slipping algorithm, a voltage controlled over-current protection function[74] with sensitive settings was enabled so that the relays disturbance recorder would be triggered for any power system faults. The disturbance recorder was also set to trigger if the algorithm tripped, or if the reactive power criterion was satisfied.

5.5.1 Steam Turbine Generator Set

The turbo-generator used for the field trials is a coal fired 353 MVA machine. It generated at 17 kV giving a full load current of 12000 Amps. The generator was a round rotor type, with the following parameters;

Xd = 2.52 pu
Xq = 2.40 pu
Xd' = 0.268 pu.

5.5.2 Hydro Turbine Generator Set

The hydro-generator used for the field trials is a 26.5 MVA machine. It generated at 11 kV giving a full load current of 1390 Amps. The generator was a salient pole type. The only data on the machine available was measured at 50 % rated volts;

Xd = 1.148 pu
Xq = 0.700 pu
Xd' = 0.358 pu.

The reactances at 100 % voltage will be lower than at 50 %, since synchronous machines are designed to operate in the saturated region. The amount by which these reactances change is largely dependent upon the design of the machine. In one machine, the reactances were typically 10 % larger at 50 % volts compared to rated volts[130]. Other studies show that this figure is typically between 10 % and 20 % [129]. Assuming a higher percentage change will result in a more secure reactive power trip level because the magnitude of Qtrip becomes larger as Xq decreases.

A 10 % drop was assumed for this particular machine, the resultant figures used for deriving the algorithm settings were therefore;

Xd = 1.03 pu
Xq = 0.63 pu
Xd' = 0.322 pu.

The algorithm settings were derived for both machines as defined by table 4-1 of Chapter 4.

5.6 ATP SIMULATIONS OF EMBEDDED GENERATORS

Some additional simulations were required so that aspects of generator operation which had not been addressed by any of the other tests were investigated. Section 3.3.2 of Chapter 3 showed that the 'ideal' sinusoidal power-load angle characteristics predicted if a constant field flux linkage was assumed may not occur with embedded generators, due to a very low value of time constant, Tdo'. Stable power swing and pole slip simulations with low values of Tdo' were therefore performed in order to verify that the algorithm operated correctly. The 750 kVA generator described in table C1 of Appendix C was used for these simulations. A slow AVR model was used because a fast one would have offset the effect of a short value of Tdo'. No governor was modelled in these tests, it was assumed that a slow acting type was used. A slow acting governor would not respond in the short time window of the simulation.

A fast diesel governor was also simulated to ensure that the algorithm did not nuisance trip. This test was important because the algorithm assumes that the generator input power

remains constant during a disturbance. A 4 % droop governor was represented using a first order lag, with a time constant of 40 ms. The diesel engine was modelled as a 15 ms time delay[172,173,174,175,176,177,178,179,180]. This is the fastest prime mover/governor combination likely to occur in practice, and is appreciably faster than steam turbines, gas turbines, and hydro turbines[180,181,182,163]. It therefore presents the most onerous conditions for testing the algorithm. Appendix F contains an example of the ATP file used in the simulation.

Section 4.6 of Chapter 4 stated that theoretically, the algorithm should detect synchronous motor pole slipping with little modification. A hydro-generator in pumping mode was therefore simulated to see if the modified algorithm of equation 4(22) would work. A fast hydro governor was simulated[163], using the same 750 kVA generator model as in the above tests. A stable power swing and a pole slip were simulated. The CCT for such a generator was 75 ms, which shows the vulnerability to instability that hydro-generators have when they are in their pumping mode.

The AVR was disabled from the hydro-generator model, and another pole slip simulated by decreasing the machines terminal voltage by 80 %. This is a steady state motor pole slip.

A simulation was also performed using the PPSS test system. The 200 MVA generator was initially operating under-excited, with an initial output power of 20 %. The generators excitation was then reduced so that a pole slipping rate of approximately two pole slips/minute was achieved. This tested the algorithm against slow pole slips, and conformed the theory of section 4.4.3.

Table 5-9 contains details of the tests conducted.

Table 5-9

Details of the Additional ATP Simulations Performed to Test the Power Based Pole Slipping Algorithm.

Test	Type	Governor	AVR	Generator Details / Type of Disturbance
LT1	Stable Swing	None	Slow	Tdo' set to 1.0 s / 170 ms 3 Ph. fault
LT2	Stable Swing	None	Slow	Tdo' set to 2.0 s / 200 ms 3 Ph. fault
LT3	Stable Swing	None	Slow	Tdo' set to 3.0 s / 210 ms 3 Ph. fault
LTP1	Pole Slip	None	Slow	Tdo' set to 1.0 s / 200 ms 3 Ph. fault
LTP2	Pole Slip	None	Slow	Tdo' set to 2.0 s / 230 ms 3 Ph. fault
LTP3	Pole Slip	None	Slow	Tdo' set to 3.0 s / 250 ms 3 Ph. fault
FG1	Stable Swing	Fast	Slow	Tdo' set to 1.0 s / 260 ms 3 Ph. fault
FG2	Stable Swing	Fast	Slow	Tdo' set to 3.0 s / 370 ms 3 Ph. fault
MOT1	Stable Swing	Hydro	Slow	Tdo' set to 3.0 s / 70 ms 3 Ph. fault
MOT2	Pole Slip	Hydro	Slow	Tdo' set to 3.0 s / 80 ms 3 Ph. fault
MOT3	Pole Slip	Hydro	None	Tdo' set to 3.0 s / Infinite bus voltage reduced to 80 %.
SLW	Pole Slip	PPSS	PPSS	generator at 20 % initial load / pole slipping rate of 2 cycles/minute.

5.7 PC BASED SIMULATION OF IMPEDANCE RELAYS

The apparent impedance at the generator terminals was calculated using half cycle moving average filtered, three phase values of real power, reactive power and voltage. Before the variables were calculated, the voltages and currents were pre-filtered using a full cycle fourier cosine filter, as described by equation 4(9). For the analysis of the 200 MVA generator PPSS tests, the processing rate used was 1000 Hz. For the 625 kVA diesel

generator tests, a processing rate of 12 samples per power system cycle was used. The 'three phase' voltage was calculated using;

$$V_{(3\,Ph.\,RMS)} = \sqrt{\overline{Va}^2 + \overline{Vb}^2 + \overline{Vc}^2} \qquad 5(3)$$

The real and reactive power was calculated using the three phase technique described in Chapter 4. All three signals were then half cycle moving average filtered as described in Chapter 4, to remove unbalance and smooth the calculated value of impedance. Apparent resistance, R, and reactance, X were then calculated as follows;

$$R = \frac{P * V^2}{P^2 + Q^2} \qquad 5(4)$$

$$X = \frac{Q * V^2}{P^2 + Q^2}$$

The proof of these equations is simple, the denominator is equal to the apparent power squared , S^2. The term V^2/S gives the impedance, Z, whilst the term P/S is equal to $\cos(\theta)$, and Q/S is equal to $\sin(\theta)$.

The mho, loss of field, single blinder and double blinder relays were all simulated using the logic described in Chapter 2. An example of the C code used to simulate the commonly used single blinder scheme is given in Appendix F.

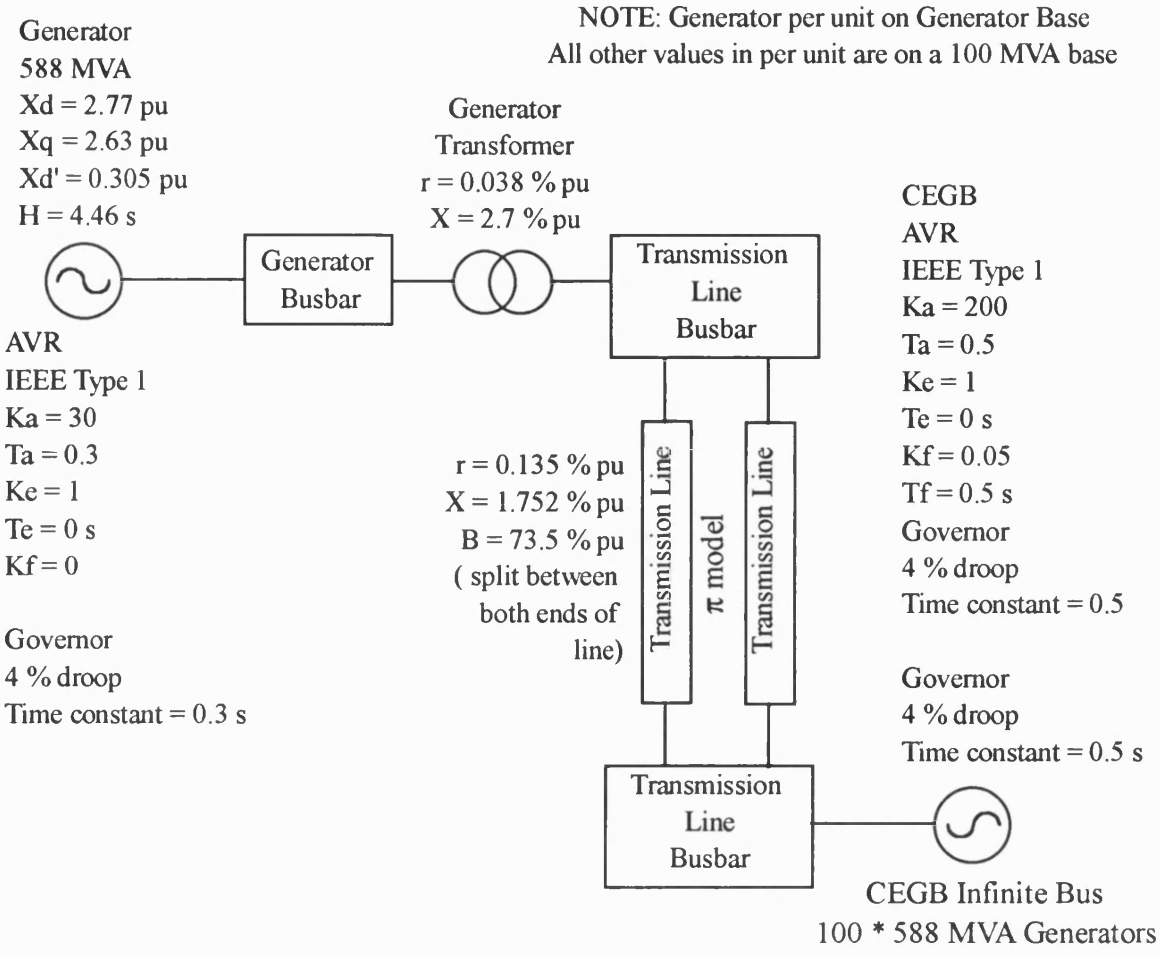

Figure 5.1
Classical One Machine/ Infinite Bus Power System Model Used in POWSIM

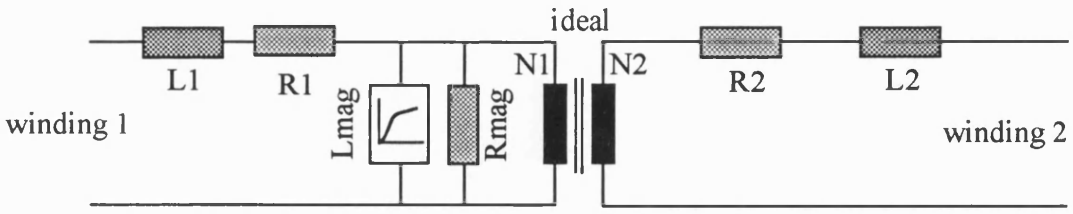

Figure 5.2
Classical Transformer Model used by ATP's 'TRANSFORMER' Component.

Chapter 6
RESULTS OF ALGORITHM EVALUATION TESTS

In the tests conducted, the algorithm successfully operated for all pole slipping conditions, and restrained for all other power system conditions apart from loss of excitation. The algorithm provided limited loss of excitation protection, the amount of cover depending upon the initial operating power and the type of generator. The concept of tripping time cannot be applied to pole slipping in the same way as it is for faults, since the point at which the algorithm trips depends upon the load angle. Tripping times are therefore expressed in terms of load angle, where load angle information is available, or generator real power output. When the real power reverses sign during a pole slip, the load angle will equal 180° if asynchronous effects are neglected.

6.1 POWSIM TEST RESULTS

The algorithm successfully detected the pole slip, also successfully categorising it as a 'transient' pole slip. If delayed tripping had been required due to circuit breaker operating duty, then tripping would have been delayed until the load angle was approaching the optimum switching point.

The algorithm successfully restrained for the stable power swing test.

6.1.1 Response to Pole Slip Test

Figure 6-1 shows the algorithm's response to the simulated pole slip. The algorithm predicted that a pole slip would occur at a load angle of 168°, i.e. just before the machine actually slipped. The reactive power criterion was satisfied first, followed by the rate of change of power criterion, then the real power criterion. 25 ms after all three criteria had been satisfied, a trip signal was issued.

The reactive criterion was satisfied the instant the fault was cleared, this indicates that the load angle was greater than 90°, the load angle plot confirms this. The fact that the rate of change of power criterion was satisfied next indicates that the generator rotor was

travelling above synchronous speed, i.e the load angle was increasing. This is also confirmed by the load angle plot, which wraps around at load angles of +/- 180°. Finally with both the Qtrip and $(\Delta P/\Delta t)_{min}$ criterions satisfied, the real power falls below its criterion, Pt, indicating that the CSP had been reached and no further decelerating energy was available. Instability was therefore unavoidable and the algorithm tripped.

The 'Q criterion satisfied' curve shows the point at which the trip signal would have been reset, this is at 1 second on the record. The maximum output power measuring function, Pmax was greater than its nominal value at the time of tripping, the ratio Pt/Pmax was less than 0.6 and the pole slip was classified as a 'transient' pole slip. The rate of change of power signal also reached a magnitude of 50,000 MW/s before the trip output, this served as another indicator that the pole slip was a 'transient' type.

If tripping was delayed until reset of the reactive power criterion, due to concern over the generator circuit breaker operation duty, then the 'trip circuit breaker' command would have been issued at a load angle of -100°, i.e as the generator was approaching the 'in phase' position. This would have been the ideal time for the circuit breaker to commence arc interruption, and would have placed minimum duty on the circuit breaker.

The algorithm successfully detected the second pole slip, at a time of 1.4 seconds. However, by this time, the speed of pole slipping had considerably increased and the algorithm tripped at a load angle of 188°.

6.1.2 Response to Stable Power Swing Test

The simulated power swing which produced the largest possible stable load angle swing of 152° is shown in Figure 6-2. For the time period between 0.3 and 0.8 seconds the reactive power is less than Qtrip, indicating that the load angle is greater than 90°, as the load angle plot confirms. However, during this time, the real power does not satisfy its trip setting Pt, the algorithm therefore restrained from operation. This condition indicates that decelerating energy is still available, and that the CSP has not yet been reached. The section marked AB represents the generator swinging up to its maximum load angle. The rate of change of power curve is zero at point 'B', showing that the rotor is once again at synchronous speed. This is confirmed by the load angle plot which is at a maximum at this point. The section BC occurs when the generator rotor backswings towards a stable operating point. In doing so, the peak of the real power load angle curve is crossed once

more, resulting in a rise in the power output of the machine between points B and C. As the load angle swings back from its maximum value, the reactive power rises above Qtrip. This causes the algorithm to restrain and ensures that no nuisance tripping occurs. The algorithm therefore restrained during the recoverable power swing.

6.2 LABORATORY MODEL POWER SYSTEM TEST RESULTS

The algorithm successfully operated for all of the pole slipping tests, whilst restraining for all of the fault tests.

6.2.1 Weak Field Pole Slip - Test 'C'

Figure 6.3 shows the pole slipping algorithm response to the pole slip caused by insertion of a resistor in parallel with the generator field winding. The time limit on the disturbance recorder meant that the algorithm time setting, lag, which is used in the prime mover output power measuring function was set to 0.5 seconds rather than the 1.0 second recommended in table 4-1 of chapter 4. This was necessary so that the algorithm would update its settings over the duration of the disturbance record.

Plots a and b of Figure 6.3 show that the generator was initially operating overexcited at low power. The $(\Delta P/\Delta t)_{min}$ curve in plot c shows that the $(\Delta P/\Delta t)_{min}$ setting was initially determined by $(\Delta P/\Delta t)_{fact}$, because of the low real output power of the generator. This ensures that there is always an adequate margin for error in the rate of change of power trip criterion. For the 5 kVA generator, this value was set to 25 % of the generator rating, as defined in table 4-1.

At a time of 1 second on the record the power input to the generator was increased from 150 W to 2.75 kW. The maximum output power monitor, Pmax tracks this increase in output power, causing a corresponding increase in $(\Delta P/\Delta t)_{min}$. The trip setting $(\Delta P/\Delta t)_{min}$ gradually increased in magnitude as Pmax increased because a high value of generator output power results in high values of $(\Delta P/\Delta t)$, a less sensitive trip level should therefore be used. This change in Pmax also caused the ratio Pt/Pmax to fall below 0.6, the transient saliency factor $(\Delta P/\Delta t)_{tran}$ was therefore included in the $(\Delta P/\Delta t)_{min}$ calculation, de-sensitising the algorithm further.

At 3 seconds, the real power trip setting, Pt is updated to the new prime mover input power. Shortly after this, Pmax is updated to its default level of 1.4 * Pt. This causes the $(\Delta P/\Delta t)_{min}$ level to become more sensitive, because the transient saliency scaling factor, $(\Delta P/\Delta t)_{tran}$ is no longer included in the calculation because the generator is in a steady state.

At 3.2 seconds, the resistor was inserted in parallel with the field winding, causing the generator to pole slip. The reactive power plot shows that this criterion was satisfied at 3.75 s, indicating that the load angle had increased to a value above 90°. A further update in Pt occurs at 4 seconds, this would not have occurred if the setting, lag, had been set to its default value of 1.0 second. The effect of this update was to decrease the real power trip setting sensitivity, but increase the rate of change of power setting sensitivity. The setting Ptol limits the extreme to which this can occur. The default setting ensures that Pt can only update to within 5 % of the generator rating when compared to the previous value.

At 4.4 seconds, the real power trip criterion is satisfied, leaving just the $(\Delta P/\Delta t)$ criterion to be satisfied. The $(\Delta P/\Delta t)$ criterion is satisfied at a time of 4.85 seconds, and therefore all three criteria were satisfied for the one and a quarter cycles required. The algorithm therefore tripped at this point. The trip signal is included on the real power plot. The trip command was issued a significant time before the generator real power went negative. The algorithm therefore tripped before the pole slip. The usual point where a pole slip is said to have occurred is when the machine goes from generator to motor action, i.e when the power output of the machine goes negative. Unfortunately, the whole pole slip could not be recorded, due to limitations in the data acquisition system.

The pole slip was classified as a 'steady state' pole slip because the ratio Pt/Pmax was at its nominal value at the time of tripping. There was however, a large deviation in $(\Delta P/\Delta t)$ of -37,500 W/s before the algorithm tripped which resulted from the switching of the field resistor. This caused conflicting information. If fault starter element information was also available to the algorithm, then there would be no doubt that this was a 'steady state' pole slip because the starter elements would not have picked up. The protection engineer would therefore know that the pole slip was caused by a problem with the generator.

6.2.2 'Over Torque' Pole Slip - Tests 'E,F,G,H,I,J'

The results to low, medium, and high excitation 'over torque' pole slips, with local load connected are given in Figures 6.4, 6.5, & 6.6 respectively. The results to tests H, I, & J were nearly identical. Local load has little effect on pole slipping characteristics.

The algorithm successfully detected all of the pole slips, producing one trip output per pole slip cycle. Two pole slips occur in Figure 6.4, the first being a much slower pole slip than the second. The high levels of noise in the ($\Delta P/\Delta t$) are due to problems with the data acquisition system. These problems did not occur in the algorithm implemented in the commercial micro-processor relay.

The main difference between the three graphs is the fluctuations in algorithm measurands. As the generator excitation is increased, the magnitude of the fluctuations also increases. This is due to a higher level of effective generator internal voltage. In all cases, the algorithm tripped before the pole slip occurred. In Figures 6.5 and 6.6 an update in Pt occurs after the prime mover input torque was increased. This was due to the 0.5 second 'lag' setting. These updates would not have occurred if the nominal value for 'lag' of 1.0 second had been used. This information is useful because it shows the effect of using a smaller 'lag' setting. The update produces a more sensitive real power trip setting, resulting in an earlier algorithm trip. It must be emphasised however, that this is not desirable as the algorithm may incorrectly update during a power swing. It would therefore use an incorrect value for the prime mover input power. The 'over torque' pole slip tests do not produce typical pole slipping characteristics. The tests were repeated with the 'lag' setting set to 1 second, and the algorithm still successfully detected all of the pole slips. These tests show that having a short 'lag' setting can make the algorithm prone to incorrect trip level updates, which may result in nuisance tripping. It is therefore recommended that the default level of 1.0 second for lag is used.

6.2.3 Adjacent Generator Pole Slip and Loss of Excitation - Tests 'K, L'

Figure 6.7 shows the algorithm measurands for the test where a generator connected to the same bus as the protected generator was forced into 'over-torque' pole slipping. It pole slipped four times at a rate 2 Hz before it was re-synchronised. The algorithm remained stable for this disturbance. The reactive power output actually increases and moves further away from the trip setting, Qtrip, when the adjacent generator begins to pole slip. The algorithm was therefore less likely to operate. This occurs because of the inherent

regulation characteristics of the machine. The adjacent generator consumed a large amount of reactive power during its pole slipping, thus depressing system voltage. The protected generator therefore increased its reactive power output in an attempt to maintain its terminal voltage. This test shows that the algorithm is stable when operating alongside a pole slipping generator.

Figure 6.8 shows the algorithm response to the adjacent machine loss of excitation test. The algorithm successfully restrained for this test, for the same reasons as with the adjacent generator pole slipping test. None of the three criteria were satisfied for the one and a quarter power system cycles required for the algorithm to operate.

6.2.4 Generator Fault Tests

The algorithm did not nuisance trip for any of the fault tests. Graphs for the isolated generator neutral tests have been included. The graphs for the solidly earthed tests are similar and have therefore not been included.

Figure 6.9 contains the algorithm response to the single phase to earth fault test (1B). The fault causes the real and reactive power to rapidly fluctuate at the fault on and off points, but causes no significant change during the fault period. Neither of the real and reactive power trip criterions were satisfied during the fault test. It can be concluded that the algorithm remains very secure for single phase to earth faults.

Figure 6.10 contains the phase to phase fault test results (Test 2A). A significant amount of distortion occurs in the algorithm measurands, this was due to an increase in the harmonic content of the voltage and currents. The reactive power criterion was not satisfied during the test, the algorithm therefore restrained. The reactive power changed to a negative value after removal of the fault. This occurred because the generator load angle increased during the fault. After the initial change in reactive power at the fault off point, the reactive power returns to its original value as the generator returns to its original operating position. The harmonic distortion in the algorithm measurands shows that the algorithm in unaffected by this type of interference. This aspect of the laboratory model power system is useful for testing protection algorithms. The voltage and current waveforms are far from ideal. If the algorithm can operate successfully under these conditions, then it should operate for any other conditions.

Figure 6.11 shows the algorithm response to the two phase to earth fault, test '3B'. The reactive power criterion was satisfied at the fault off point for this test. This indicates that the generator load angle increased to a value above 90° during the fault. However, at the instant the reactive power criterion is satisfied, the real power jumps above its trip level, blocking algorithm operation. This provides decelerating energy to the generator rotor, indicating that the CSP had not been reached. The algorithm therefore restrained from tripping.

The three phase fault test (test 4A) results are given in Figure 6.12. Once more, the fault off point is the most testing part of the fault test for the algorithm, due to the reactive power criterion being satisfied. This shows that the generator load angle increased to above 90° during the fault. When the fault was cleared the real power jumps above its trip level, showing that the CSP has not yet been reached. This prevented the algorithm from tripping. Additionally, the ($\Delta P/\Delta t$) criterion was only satisfied for half a power system cycle.

After the fault has been cleared, the generator real and reactive power continue to decrease, as the generator loses stability. The sign of the ($\Delta P/\Delta t$) signal is continuously negative after the fault has been cleared, indicating that load angle increase is occurring. The real power starts to decrease more rapidly as the generator accelerates into a pole slip, and the algorithm trips. This occurs at an output power of 2 kW. The algorithm therefore tripped before the pole slip. The pole slip was diagnosed as 'transient' in nature because of the large fluctuations in ($\Delta P/\Delta t$) produced by the fault. If the algorithm's slip setting had been lower, the algorithm would have tripped much earlier. A slip setting of -0.25 % rather than the nominal -0.5 % would have resulted in an algorithm trip at a real power value of 3 kW.

The algorithm response to the three phase to earth fault (test 5B) is shown in Figure 6.13. The algorithm did not trip for the same reasons as for the other faults. The fundamental basis of the algorithm, which ensures that tripping does not occur until the CSP has been reached, blocks algorithm operation during power system faults.

6.2.5 Observations from the Laboratory Power System Model Tests

The main observation is that the algorithm detected three different types of pole slips, namely 'weak field', 'over-torque' and 'fault induced'. The algorithm was secure for all

possible fault types. The 'over-torque' tests showed that reducing the 'lag' timer setting below 1.0 second can result in updates in the algorithm trip levels which increase algorithm sensitivity. Although the updates in Pt during the over-torque pole slip tests were correct, because the prime mover input power had been increased, it is safer to use the 1.0 second 'lag' setting so that incorrect updates do not occur during stable power swings, where the prime mover output power has not increased. Most generator prime movers increase their torque outputs at a much slower rate than the rates used in these tests. This is one of the inaccuracies of the laboratory power system model. Prime movers are normally constant torque devices, whereas the DC machine used as the prime mover is a constant speed device. The laboratory tests do however provide proof that the algorithm operates satisfactorily in a real power system environment, and are therefore useful. The parameters of the 5 kVA generator are also atypical, due to the very high value of transient reactance. This in conjunction with all of the other tests performed strengthens the value of the tests, as it proves that the algorithm works for a wide variety of machines.

6.2.6 Analysis of Pole Slipping Impedance Loci for the 5 kVA Laboratory Generator

Inspection of the real power plots for the pole slipping tests also shows that the real power does not go as negative as theory suggests. This is mainly due to the asynchronous power generated during the pole slip, which shifts the whole real power characteristic up. This effects the path of the apparent impedance locus and therefore it affects impedance based pole slipping relays. Using the single blinder characteristic derived in Appendix B for the 5 kVA generator, the response of the scheme to the pole slip tests was analyzed. The scheme operated for two of the 6 'over torque' pole slipping tests. Figure 6.14 shows several impedance loci for differing tests, along with the single blinder relay characteristic.

Figure 6.14a is for the pole slip which occurred following the three phase fault test. The power based pole slipping algorithm response to this test is shown in Figure 6.12. If the most commonly used single blinder scheme is chosen, as described in chapter 3, the scheme would have failed to detect the pole slip. This scheme requires the supervisory mho to have picked up before the impedance crosses the blinder element. Figure 6.14a shows that the impedance locus crosses the blinder elements before the mho element picks up. This problem can be remedied by increasing the size of the mho characteristic. This

highlights the intricacies required in setting the single blinder scheme. The mho pole slipping scheme would have successfully detected this pole slip. The double blinder scheme would not have detected it. Details on this and the mho scheme can be found in Appendix B.

Figure 6.14b shows the response to the low excitation over-torque pole slip test. The power based algorithm response for this test is given in Figure 6.4. The single blinder scheme did not operate for this pole slip, and could not be modified so that it would. One of the quadrilateral impedance based pole slipping protection characteristics described in section 2.3.3 could have detected this condition however. The real power does not reverse sufficiently in this test to make the impedance locus traverse from right to left across the impedance plane. Consequently the locus does not cross both blinder elements, and the scheme therefore failed to trip. The mho scheme would have detected this pole slip, as would a loss of field scheme. The double blinder scheme described in Appendix B would not have detected the pole slip. If the size of the supervisory mho characteristic used in the double blinder scheme had been doubled it would have detected this slip. Increasing the size of the supervisory mho characteristic must be performed cautiously however, since too large a mho characteristic may result in nuisance tripping during stable power swings.

Figure 6.14c shows the impedance locus for the high excitation over torque pole slipping test. The single blinder scheme successfully detected this pole slip, the double blinder scheme did not however, because the impedance locus left the supervisory Mho circle before crossing the blinder. Again a larger supervisory mho characteristic would have remedied this problem.

The above analysis highlights some of the problems with conventional impedance based pole slipping schemes. It is not intended as a thorough analysis of these schemes. A more thorough analysis will be given when discussing the PPSS and 625 kVA diesel generator tests.

6.3 PPSS TEST RESULTS

The commercial relay implementation of the algorithm successfully detected all pole slipping conditions, and restrained for all of the recoverable power swing tests. It also detected all of the loss of field conditions, and restrained for the loss of prime mover simulations. The algorithm did operate for the tests where the generator was operated at load angles above 90° with the aid of a fast AVR. This was expected and as stated in chapter 4, does not cause a problem because generators are never practically operated in this manner.

As well as using the ATP simulations to run the PPSS, a comparison with the conventional impedance based protection techniques was performed using PC models of the relays. Details of these models can be found in appendix F.

6.3.1 Pole Slipping Algorithm Response to PPSS Pole Slip Tests

Test 'PSL1GA'

Figure 6.15 contains the algorithm response to the pole slipping test 'PSL1GA'. In this test, pole slipping was caused by a 1170 ms, 3 Phase fault. A long fault duration was required because the generator was initially operating at 20 % load. The algorithm successfully restrained for the duration of the fault, and tripped at a time of 1.5 seconds on the record. The pole slip was diagnosed as a 'transient' pole slip. The generator slipped one pair of poles before re-synchronising. The ATP machine angle plot is not a plot of the machine load angle, or the system load angle, the angle is measured relative to a reference point and is given here to show the overall increase of 360° which occurs during a pole slip. These curves were produced using a PC based simulation of the algorithm because this file was unavailable when the PPSS tests were conducted.

Pole slipping caused by faults from such a low initial generator output power is unlikely in practice, since the fault would be cleared much faster than 1170 ms, unless a stuck circuit breaker situation occurred. The test is still required because the algorithm must be tested for all operating conditions.

Test 'PSL2GA'

Figure 6.16 shows the variables down-loaded from the relay's disturbance record for PPSS test PSL2GA. All of the graphs are given in terms of relay secondary quantities. The generator terminal voltage on the secondary side of the VT is 110 Volts (phase to phase rms), whilst nominal or full load current is 1 Amp (rms). The relay secondary rating for the generator is therefore 190.5 VA. For this test, the generator was initially at 50 % load. It pole slipped twice before re-synchronisation. The algorithm detected both pole slips, which were correctly diagnosed as 'transient' pole slips. The reactive power plot shows that Qtrip was satisfied three times during the test, and the real power plot shows that during the third time, the generator developed enough decelerating power to re-synchronise. The generator therefore stopped short of the CSP after the second pole slip. This is shown as point A on the real power plot.

Test 'PSL3GA'

Figure 6.17 shows the algorithm response to test PSL3GA. The generator failed to re-synchronise for the duration of the test because it was initially operating at full load. The algorithm detected the first pole slip, but failed to detect subsequent pole slips because of AVR field forcing action pushing the system centre away from the generator. The effects of field forcing can be observed in the real and reactive power plots. In the reactive power plots, the reactive power criterion is satisfied for the first pole slip, but not for any subsequent slips because the mean level of reactive power drifted up above the reactive power trip level, Qtrip. In the real power plots, the magnitude of the positive and negative peaks which occur during every slip cycle increases. The peaks reach a value of 650 W, which is almost 3.5 times the generator rating.

Section 4.4.1 of Chapter 4 provided graphs which show the theoretical operating range of the algorithm. For the PPSS test generator, the value of external reactance, X given in Appendix C is 0.133 pu, whilst Xq = 1.64 pu, and Xd' = 0.238 pu. Expressed as a fraction of Xq, Xd' = 0.145*Xq. If these figures are applied to the setting graphs 4.6b and 4.7a then the graph for an effective generator voltage, E of 1.25 pu shows that the algorithm should just work; the maximum value of external reactance from this graph is 0.145 pu, whilst the value from the E = 1.5 pu graph is 0.125 pu. This simulation therefore confirms that the setting graphs are correct. The algorithm detected the first pole slip, before the reactive power criterion was no longer satisfied, and would therefore have disconnected the generator avoiding damage. This system is close to the operational limits

of the algorithm, and was chosen to confirm the theoretical setting limits.

The PPSS has a pre-fault cycling function which enables you to continuously cycle the first power system cycle of the simulation file. If the first cycle is at a steady state, then the initial steady state period at the start of the simulation can be extended almost indefinitely. This function was used because the maximum PPSS simulation time was 6 seconds. The algorithm requires at least 3 seconds before the real power trip level, Pt is updated. A pre-fault cycling period of 3 seconds was therefore used with all of the PPSS tests. The update in Pt in this case occurs just before 500 ms. This implies that at the instant the PPSS simulation started, the Pt function must have been approximately half way between its sample check points, which are 'lag' seconds apart. The default value of 'lag' is 1 second, the update before 500 ms therefore confirms that Pt is updating correctly.

The Pmax function shown in Figure 6.17b was reset to its nominal value just before the update in Pt occurred. Since Pt at this point was 0, Pmax was reset to zero for one power system cycle before tracking back onto the power waveform. This produces a temporary drop in the magnitude of $(\Delta P/\Delta t)_{min}$. This does not cause a significant increase in algorithm sensitivity however, because the trip level is changed for a period of less than the 1.25 cycles required by the algorithm to trip.

Note that once Pt is updated, the $(\Delta P/\Delta t)_{min}$ trip level does not reset to its lower 'steady state' level. This is a result of computer code 'bomb-proofing'. If the ratio Pt/Pmax is greater than 0.7, or less than 0, when $(\Delta P/\Delta t)_{min}$ is calculated, the algorithm automatically uses the 'transient' value $(\Delta P/\Delta t)_{tran}$ in the calculation of $(\Delta P/\Delta t)_{min}$. Pmax does not update to its nominal value of 1.4*Pt the instant Pt is updated because once an update in Pmax occurs, Pmax is not updated for another second, unless an even higher value of real power occurs. This provides an additional amount of algorithm security.

Test 'PSL3GN'

Figure 6.18 shows the algorithm response to test 'PSL3GN'. This is identical to the above test, except that the AVR was on 'manual' control. No field forcing action therefore occurred and the algorithm successfully detected all of the pole slips. The reactive power shows that with no field forcing action, the reactive power criterion was satisfied for every slip cycle. Note that the peaks in real power during pole slipping are much less severe with the AVR on manual control. This shows that once a generator is pole slipping, AVR

action generally increases the severity of the pole slips, and does nothing to aid the re-synchronisation process. The single most important factor for re-synchronisation is the speed of the governor and prime mover system.

Test 'PSL3NN'

Figure 6.19 shows the results to test 'PSL3NN'. In this test the effects of AVR and governor action were not modelled The prime mover input power and generator excitation therefore stay at their initial steady state values through the entire test. The algorithm successfully detected the first 7 pole slips, and then failed to detect the next 3. This was a result of the high speed at which the generator was pole slipping. The algorithm trip criterions are not satisfied for a sufficient duration. After failing to detect the three pole slips, the algorithm trips again, and remains tripped. This occurred because the reactive power criterion was continually satisfied.

Figure 6.20 contains an expanded section of the real power and rate of change of power plots, showing why the algorithm failed to detect the later pole slips. The real power and rate of change of power are only satisfied for five consecutive sample points. Six consecutive sample points are required for the algorithm to trip.

This confirms the performance predicted in section 4.4.2. If the time between consecutive peaks in real power is measured, it gives a mean pole slipping rate of 8 Hz. Section 4.4.2 predicted that the algorithm would detect a maximum pole slip rate of 8.3 Hz.

A glitch in the reactive power plot of Figure 6.19 occurs just before 2000 ms. The glitch is a jump in reactive power to zero exactly. It is therefore thought to be a result of a problem in the computer code. It is impossible to say if the glitch occurred when converting the 32 bit integer variables used by the algorithm to 16 bit variable for storage in the disturbance record, or if it occurred in the calculation of reactive power by the algorithm. This was the only glitch seen in over 100 disturbance records which have been down-loaded from the commercial relay.

Test 'PSL1GAF'

Figure 6.21 shows the algorithm measurands for the 'PSL1GAF' test. This pole slip was caused by a 'fault' in the generator AVR, which reduced the AVR's reference voltage from unity down to 0.05 per unit. The generator was initially operating at 20 % load, the entire

6 seconds of the PPSS test was therefore required for the generator to lose synchronism. If the reference voltage had been reduced less, the generator would not have lost synchronism in the 6 second limit. The incredibly low AVR reference voltage practically makes this a loss of field test. The algorithm tripped before the pole slip occurred, then shortly after, the simulation ended. The pole slip was correctly diagnosed as a 'steady state' pole slip. The graph shows the levels of noise found on the ($\Delta P/\Delta t$) signal. This was higher than expected, and is power system frequency noise. This suggests that the source of the noise is due to an offset in either the voltage or currents. A DC offset in one of the signals, when multiplied by the power system frequency alternating component of the other, superimposes a power system frequency oscillation onto the mean level of the calculated power signal.

Without performing more steady state tests with varying amounts of real and reactive power, the exact cause of the noise can not be found. There was no opportunity to do this, and since the noise levels do not effect the algorithm operation, no further investigations were conducted. The noise may be due to timing errors in the analogue to digital converters. It is not due to a drift in the analogue component tolerances, since several different data acquisition boards have been used in the relay, all of which produce the same level of noise.

The noise caused a small time delay in algorithm tripping in this test because the 1.25 cycle trip criterion was not satisfied until the mean level of ($\Delta P/\Delta t$) fell below the $(\Delta P/\Delta t)_{min}$ trip setting by the peak amplitude of the noise. This pole slip was the most demanding for the algorithm to detect. The low levels of ($\Delta P/\Delta t$) produced as a result of the generator pole slipping slowly meant that the $(\Delta P/\Delta t)_{min}$ criterion was barely satisfied. Neglecting the effect of the minium setting value, $(\Delta P/\Delta t)_{fact}$, if the slip setting had been reduced from -0.5 % to -0.25 %, then the algorithm would have tripped at a time of 1724 ms rather than 1844 ms. It would therefore have tripped 120 ms earlier. The -0.25 % slip trip point is shown as the dotted line in Figure 6.21.

Test 'PSL2GAF'

Figure 6.22 shows the curves for the 'PSL2GAF' test. For this test, the AVR reference voltage was set to 0.5 per unit, the generator was initially operating at 50 % load. The higher initial load resulted in much higher values of ($\Delta P/\Delta t$). The noise in the signal therefore had much less effect on the tripping time than with the 20 % initial generator

loading case. The algorithm tripped before the pole slip occurred, and the pole slip was diagnosed as a 'steady state' pole slip. The pole slip shown took 4.0 seconds to occur, the next pole slip would have occurred in another 5 to 6 seconds. The mean pole slipping rate was therefore 0.2 Hz. This shows that the algorithm can detect slow pole slips. With slow pole slips, the increase in load angles to 100° takes a long time, as does the period when swinging from 270° to 100°. The part of the pole slip cycle where the generator load angle moves from 90 to 180° occurs quickly, producing sufficient rates of change of power for the algorithm to trip. The mean rate of pole slipping may therefore be low, and the algorithm will still detect the pole slip, because of the fast rate at which part of the pole slip occurs.

If the slip setting had been reduced from -0.5 % to -0.25 %, the algorithm would have tripped earlier. The lower slip setting trip point is shown on Figure 6.22 as the dotted trip line. The algorithm tripped at a time of 2004 ms, this was 60 ms before the -0.5 % slip setting trip point.

Test 'PSL3GAF'

Figure 6.23 shows the algorithm response to test 'PSL3GAF'. The AVR reference voltage was reduced to 0.8 per unit to induce the pole slip, which occurred quickly because the generator was initially operating at 100 % full load. The algorithm tripped before the generator pole slipped. The pole slip was correctly diagnosed as a 'steady state' pole slip. This would inform the protection engineer that a fault in the generator or its controls was the cause of the pole slip.

The speed at which the pole slipping took place meant that additional reactive power was drawn from the system to supply exciting VArs for asynchronous induction generation. This resulted in the reactive power remaining below Qtrip for the first few pole slips, and consequently the algorithm produced one long trip signal for several pole slip cycles. The real power also shows the amount of asynchronous power generated, since the positive peaks in real power are much greater than the negative peaks. The mean value of real power generation was shifted up by 100 Watts. The generator was therefore generating approximately 50 % of rated power asynchronously.

After three or four pole slips, the AVR responded to the voltage depression caused by the excessive reactive power demand, and increased excitation. This pushes the system centre

away from the generator and causes the reactive power to oscillate either side of Qtrip.

If the slip setting had been reduced from -0.5 % to -0.25 %, then the algorithm would have tripped 35 ms earlier. This shows that the gain in tripping time decreases as the generator loading increases, due to higher values of ($\Delta P/\Delta t$).

The graphs for the other tests have not been included because they are practically identical to the graphs already presented.

6.3.2 Pole Slipping Algorithm Response to PPSS Stable Power Swing Tests

The power based pole slipping algorithm successfully restrained for all of the stable power swing tests.

Test 'PSW1GA'

Figure 6.24 shows the pole slipping algorithm response to test 'PSW1GA'. This was a severe stable power swing, induced by a 1150 ms three phase fault. The generator was initially operating at 20 % output power. The algorithm remained very secure during the fault because the reactive power criterion was not satisfied. It is rare for the reactive power criterion to be satisfied during a fault because faults are normally inductive. The instant the fault was cleared, the reactive power criterion was satisfied because the generator load angle had risen above 90°. For the duration that Q was less than Qtrip, the generator's real output power was greater than the trip setting, Pt. This indicated that there was decelerating power available. The algorithm therefore restrained from tripping.

After this initial period, the reactive power criterion was no longer satisfied because the generator load angle had swung back to a stable operating point below 90°. The algorithm therefore remained stable for the duration of the entire stable power swing.

Test 'PSWL2GA'

Figure 6.25 shows the pole slipping algorithm response to test 'PSW2GA'. This was a severe stable power swing, induced by a 630 ms three phase fault. The generator was initially operating at 50 % output power. The algorithm did not trip for the above reasons.

Test 'PSW3GA'

Figure 6.26 shows the response to test 'PSW3GA'. This was a severe stable power swing, induced by a 320 ms two phase to earth fault. The generator was initially operating at 100 % output power. Again the algorithm did not trip for above reasons.

Test 'PSW1GN'

In the above three tests, the generator AVR was in service, Figure 6.27 shows the algorithm response to test 'PSW1GN', when the AVR was set to manual control. The stable power swing was caused by a 1155 ms three phase fault. The real and reactive plots show that without the AVR in service, more dramatic fluctuations occur in the algorithm measurands. Without the AVR in service, the overall damping of the rotor oscillations is decreased, because of the high value of impedance between the generator and infinite bus. This condition is made worse by the fault clearance. This disconnected the 235 MW load which also assisted damping. In addition, the initial generator excitation was low because the generator was initially operating at a low output power. This results in low synchronising torques, which can be over-shadowed by the asynchronous torques produced during the swing. The operating characteristic of the generator is no longer dominated by the sinusoidal load angle variations produced as a result of field excitation. The flux due to field excitation will also be weakened by the long fault duration, due to the de-magnetising effects of armature reaction. The end result is that the generator rotor swings more violently compared with the case when the AVR is in service. The reactive power criterion is therefore satisfied four times rather than the one time which occurred with test 'PSW1GA'. This increases the number of occasions where algorithm operation may occur. The real power plot shows the points where the reactive power criterion was satisfied, and the rate of change of power plot shows when both the real and reactive power criteria were satisfied.

The purpose of the transient saliency scaling factor, $(\Delta P/\Delta t)_{tran}$ can be seen. This de-sensitises the algorithm during severe power swings so that it does not operate. The non-sinusoidal variation in real and reactive power results in the real and reactive power criterions being satisfied more times than if the components of power were only produced due to synchronising torques. A de-sensitised rate of change of power trip criterion is therefore required to improve algorithm security. The additional component in $(\Delta P/\Delta t)_{min}$ caused by $(\Delta P/\Delta t)_{tran}$ ensures that the rate of change of power criterion is not satisfied, and that the algorithm restrains. If one sensitive setting had been used for $(\Delta P/\Delta t)_{min}$ which

detected the slow 'steady state' pole slips, the algorithm would have nuisance tripped for this stable power swing test.

Test 'PSW2GN'

Figure 6.28 shows the algorithm measurands for test 'PSW2GN'. The AVR was also set to manual control on this test. This resulted in the reactive power criterion being satisfied twice. The first time, the real power was above Pt, showing that decelerating power was available. The second time that the reactive power fell below Qtrip, the real power criterion was also satisfied. This occurred when the machine angle was at a minimum. It was therefore a result of asynchronous induction generation effects. Inspection of the rate of change of power plot shows that the algorithm was prevented from operating due to the large magnitude of $(\Delta P/\Delta t)_{min}$. This test illustrates the advantages of having an adaptive rate of change of power setting.

Test 'PSW3GN'

Figure 6.29 shows the results to test 'PSW3GN'. The AVR was also set to manual control on this test. In this test the reactive power criterion is only satisfied during the period of the swing when the load angle is above 90°. The machine characteristics are dominated by the effects of field excitation, because the initial value of excitation was much higher. The algorithm measurands therefore behaved in the 'ideal' way predicted by basic synchronous generator theory, and the algorithm restrained from tripping with relative ease when compared to the 'PSW2GN' and 'PSW1GN' tests.

The 'PSW1GN' and 'PSW2GN' tests are very severe power swing tests. They would happen rarely in practice, since they require a fault duration of at least 800 ms, coupled with a generator AVR set to manual, and an initial low value of generator operating power. They are however, possible and are more likely to happen in an embedded generation environment, where long IDMT fault clearance times exist. There are several reasons why an embedded generator may not be operated at full load. The generator may be used to offset a site load, or may use excess steam from an industrial process in a CHP scheme. It is also possible that the AVR may be set to manual. The tests are useful because they provide the severest power swing test conditions possible. If the pole slipping algorithm does not operate for these stable power swings, it is unlikely that it will operate for any others.

The graphs for the other tests have not been included because they are practically identical to the graphs already presented.

6.3.3 Pole Slipping Algorithm Response to PPSS Tests Where the Generator is Operated in its Dynamic Stability Region - at Load Angles Greater than 90°

The algorithm operated for all three of these tests, as predicted in Chapter 4. When a fast AVR is used to operate the generator at load angles above 90°, the generator is effectively being operated beyond its conventional CSP. This 'fools' the algorithm when a sudden input power decrease occurs because the reactive power criterion is satisfied due to the load angle being above 90°. The real and rate of change of power criteria are also satisfied as a result of the load decrease.

However, as stated in chapter 4, this is not considered a problem, since generators are never practically operated in this area because the reserve in hand for transient stability is too low. These simulations have been included for completeness.

Test 'AVR5NA'

Figure 6.30 shows the algorithm variables for test 'AVR5NA'. The curves were produced by the PC based version of the algorithm code, in order to see the full 16 second duration of the test. The generator is initially operated in the over-excited region. The AVR voltage reference is then reduced, which results in the generator moving over into the under-excited region. This causes the load angle to increase above 90°, and results in the reactive power criterion being satisfied. A period of steady state operation is then simulated to allow the generator to settle. At 10 seconds, the generator input power is reduced from 0.5 pu to 0 pu. This causes the load angle to decrease and the reactive power to increase. Before the reactive power rises above its trip level, the real and rate of change of power trip levels are satisfied, and the algorithm nuisance trips.

It is important to note that this is a worst case simulation. In practice, the output power of a generator prime mover is not instantaneously reduced or increased. A slower change in output power will produce lower values of ($\Delta P/\Delta t$). The algorithm may therefore not nuisance trip for some forms of generation. For example, hydro generators are normally loaded up or down over a period of 30 seconds. At this rate of change the algorithm real power trip level, Pt may track the change in output power, and the algorithm would not

nuisance trip.

6.3.4 Pole Slipping Algorithm Response to PPSS Loss of Field Tests

The algorithm tripped for all of the loss of excitation tests performed.

Test 'LOF1GA'

The algorithm response to test 'LOF1GA' is shown in Figure 6.31. This was a generator loss of field test from 20 % initial load. The algorithm successfully tripped before the generator lost synchronism. The trip was diagnosed as a 'steady state' pole slip. Comparison of these test results with those of test 'PSL1GAF' shown in Figure 6.21 shows the two tests to be almost identical. This occurred because the field voltage was reduced to such a low value that the generator would lose synchronism in the 6 second time window of the PPSS.

Test 'LOF2GA'

The algorithm measurands for test 'LOF2GA' are shown in Figure 6.32.. This was a generator loss of field test from 50 % initial load. The algorithm tripped before synchronism was lost. Comparison between these results and those produced by test 'PSL2GAF' in Figure 6.22 shows the similarity between the two tests. The AVR reference voltage in test 'PSL2GAF' was reduced to 50 % per unit, whilst the field voltage in the loss of field test was reduced to zero. The similarity occurs because the generator AVR reduces the field voltage to zero in both tests.

Test 'LOF3GA'

Figure 6.33 shows the results to test 'LOF3GA', a loss of field from an initial load of 100 %. The algorithm tripped before the generator lost synchronism. The trip was diagnosed as a 'steady state' trip. These results are different to those of test 'PSL3GAF' shown in Figure 6.23, but only after the initial algorithm trip. The effects of AVR action are apparent in the latter test, as the peaks in real power increase in magnitude once synchronism is lost. With the loss of field case, the peaks become smaller due to a decaying generator flux.

6.3.5 Pole Slipping Algorithm Response to PPSS Loss of Prime Mover Tests

Figure 6.34 shows the algorithm measurands for the loss of prime mover test 'LOP3NA'. The algorithm successfully restrained for this operating condition. The algorithm

remained very secure.

6.3.6 Effect of Altering the Pole Slipping Algorithm 'Slip' Setting

The effect of altering the algorithm's 'slip' setting has been discussed in some of the above tests. A reduction in the slip setting results in earlier tripping times during 'steady state' pole slips. These pole slips produce very low values of ($\Delta P/\Delta t$) as the generator loses synchronism. The ($\Delta P/\Delta t$) criterion is the last criterion to be satisfied. It therefore determines the point at which the algorithm will trip. With 'transient' pole slips, the real power criterion determines the tripping point because the ($\Delta P/\Delta t$) and reactive power criteria are satisfied as the real power begins to decrease from its maximum value, Pmax.

The power system frequency noise experienced in the commercial relay implementation of the algorithm further delayed the tripping point because the mean value of ($\Delta P/\Delta t$) must exceed the trip level $(\Delta P/\Delta t)_{min}$ by the peak value of the noise. The noise in the PPSS tests was typically +/- 50 W, which for a generator secondary rating of 190.5 VA, is approximately equal to 25 % of the generator rating. It is therefore feasible that the slip setting can be reduced. The noise will effectively counteract the increase in sensitivity which occurs by decreasing the magnitude of the trip level, $(\Delta P/\Delta t)_{min}$. The PPSS ATP tests were run through the PC based simulation of the algorithm, with a slip setting of -0.25 %. No nuisance trips occurred. The only tests where the trip time was improved were the 'PSL?GAF' , and the 'LOF?GA' tests because all of the pole slips in these tests were 'steady state' pole slips.

The PPSS 'steady state' pole slip test disturbance records were also analyzed with a slip setting reduced from -0.5 % to -0.25 %. The analysis showed that a lower slip setting would improve the steady state pole slip trip times, without compromising algorithm security.

Table 6-1 contains the improvements in trip times for a reduction in the 'slip' setting. The figures in brackets are where $(\Delta P/\Delta t)_{fact}$, the minimum set value for $(\Delta P/\Delta t)_{min}$ was reduced from 25 % of generator rating to 10 %. This occurred because it was inhibiting any effect that a reduction in the slip setting might have on $(\Delta P/\Delta t)_{min}$ at low levels of Pt.

The PC based simulations show the theoretical gain, whilst the PPSS disturbance record tests show the practical gain. In the 50 % and 100 % initial load tests, denoted by the

tests with a 2 or 3 in the title, the theoretical gain is greater than the practical gain, because of the noise in the practical system. For the 20 % initial load cases, the real power criterion Pt inhibits tripping because an update in Pt occurs just before the real power begins to fall as the generator loses synchronism. This effect can be seen on Figure 6.31. Figure 6.35 shows the change in $(\Delta P/\Delta t)_{min}$ and trip points for test 'PSL1GAF'.

This analysis shows that an appreciable gain in 'steady state' pole slip tripping times can be achieved by reducing the slip setting to -0.25 %. This must also be accompanied by a decrease in the setting $(\Delta P/\Delta t)_{fact}$ so that the new slip setting can take effect at low values of Pt.

Table 6-1

Improvement in trip times for a reduction in the 'slip' setting from -0.5 % to -0.25 %. (figures in brackets are where $(\Delta P/\Delta t)_{fact}$ has also been reduced from 25 % to 10 % of generator rating.)

Test	PC Based Algorithm (ms)	PPSS Disturbance Record (ms)
PSL1GAF	0 (60)	0 (120)
PSL2GAF	80	60
PSL3GAF	55	35
LOF1GA	15 (110)	0 (140)
LOF2GA	85	40
LOF3GA	70	60

The change in slip setting does not effect the algorithm security for 'transient' pole slips because the setting $(\Delta P/\Delta t)_{tran}$ compensates for this.

6.3.7 Comparison of the Performance of the New Power Based Pole Slipping Algorithm with Conventional Impedance Based Pole Slipping Schemes

The performance of the new and conventional approaches to pole slipping protection was analyzed using the PPSS test simulation files and PC based models of the relays. The

tripping times for the power based algorithm are for when the ATP generator voltage and current output files were passed through the PC 'relay simulator' code. They are not related to the PPSS disturbance records given in the previous sections. Tables 6-2, 6-3 and 6-4 contain the trip times for all of the tests.

Table 6-2

Results of Comparisons Between Conventional and New Pole Slipping Protection Methods for PPSS Pole Slipping Simulation Tests.

Test	Loss of Field Trip (s)	Mho Scheme Trip (s)	Single Blinder Trip (s)	Double Blinder Trip (s)	Power Algorithm Trip (s)
PSL1NN	NT	1.227	NT*	NT*	1.305
PSL2NN	NT	0.929	1.357	1.364	0.995
PSL3NN	NT	0.633	0.882	0.887	0.655
PSL1GN	NT	1.456	NT*	NT*	1.560
PSL2GN	NT	1.119	1.608	1.617	1.565
PSL3GN	NT	1.158	1.503	1.253	1.255
PSL1NA	NT	1.451	NT*	NT*	1.545
PSL2NA	NT	1.290	1.377	1.386	1.330
PSL3NA	NT	0.635	0.978	0.982	0.670
PSL1GA	NT	1.451	NT*	NT*	1.540
PSL2GA	NT	0.932	1.592	1.602	1.030
PSL3GA	NT	0.664	1.031	1.036	0.705
PSL1GAF	3.232	NT*	NT*	NT*	5.225
PSL2GAF	2.589	NT*	NT*	NT*	3.115
PSL3GAF	1.677	2.000	2.253	2.255	1.465

* - signifies that the relay did not operate as required.

6.3.7.1 Comparison of Impedance Relays with New Power Based Protection Algorithm for Pole Slipping Conditions

Table 6-2 shows that the new power based pole slipping algorithm tripped for all of the pole slipping conditions, whilst some of the conventional schemes failed to trip. The Mho scheme failed to detect all of the 'faulty AVR' pole slips, whilst the single and double blinder schemes failed to detect some of the pole slips which occurred from 20 % initial generator load. The setting procedure used to set the impedance based relays is given in Appendix B. The loss of field scheme operated for all of the 'faulty AVR pole slips'.

Test 'PSL3GN'

Figure 6.36 contains the single blinder scheme characteristic and the impedance trajectory for test PSL3GN. The single blinder scheme failed to detect the first pole slip for this test, but correctly detected the subsequent pole slip cycles. For the scheme to operate, the impedance locus must first enter the supervisory mho characteristic, cross one of the blinders, remain in between the blinders for 40 ms, then cross the opposite blinder. The mho element must remain energised for this entire sequence. During the fault, the impedance locus crossed the right hand blinder with the mho element dropped out. This resulted in the scheme failing to trip for the first pole slip cycle when the impedance locus crossed the left hand blinder. If the right hand blinder had been placed a fraction more to the left, the scheme would have detected the first pole slip. The scheme successfully detected the subsequent pole slip cycles because the impedance locus took the classical trajectory.

The double blinder scheme detected the first pole slip cycle because its supervisory Mho circle was located higher up the R-X plane.

Test 'PSL1GA'

Figure 6.37 shows the single blinder scheme and the pole slip impedance locus for test 'PSL1GA'. The single and double blinder schemes failed to detect the pole slip because the impedance locus crossed the right hand blinder unit during the fault when the supervisory Mho unit was dropped out. The generator was operating at 20 % initial load, and therefore re-synchronised after the first pole slip. A full pole slip impedance locus, with no alteration due to fault effects was therefore not produced. It is sometimes argued that pole slipping schemes should not trip if only one pole slip occurs. However, the

author believes it is desirable to detect the first pole slip cycle, even if tripping does not occur until the second cycle. The decision of when a pole slipping scheme should trip can then be left to the protection engineer.

The common single blinder scheme described in chapter 2 fails because the supervisory Mho unit must have picked up before the impedance locus crosses the blinder units. An enhanced scheme used for a pumped storage generator, which is also described in chapter 2 would not have suffered these problems, but would still suffer the same setting dilemmas as the commonly used scheme.

A stable swing impedance locus can also be seen on Figure 6.37. This occurred after the generator re-synchronised. This shows that care must be taken when setting the Mho and double blinder schemes; if the mho characteristics, and blinder locations are set so that they reach too far out to the right of the R-X plane, then they can nuisance trip for stable swings.

'Test PSL3GA'

Figure 6.38 shows the mho scheme characteristic and the pole slipping loci produced by test 'PSL3GA'. The Mho scheme tripped for the first three pole slip cycles. It failed to trip for the subsequent cycles because the pole slipping impedance locus did not remain inside the Mho characteristic for the 20 ms delay necessary for it to trip. After the sixth pole slip cycle, the impedance locus was pushed above and outside of the Mho characteristic by the field forcing action of the AVR.

The single blinder scheme only detected the second and third pole slip cycles. It did not detect the first cycle and the fourth and subsequent cycles because the impedance locus crossed the right hand blinder unit before entering the supervisory mho characteristic.

The double blinder scheme did not detect the first pole slip cycle for the same reasons as the single blinder scheme. It did detect all subsequent cycles because its supervisory Mho characteristic was located higher up the R-X plane compared to the single blinder scheme.

Test 'PSL3NN'

Section 6.3.1 stated that the power based algorithm detected the first seven pole slips, failed to detect the next three, then detected the subsequent pole slips. Analysis of the

Mho scheme's response to this test showed that it detected the first eight pole slip cycles, then failed to detect any further pole slips.

The single blinder scheme operated for only the second and third pole slip cycles. The double blinder scheme operated for the second, third, and fourth cycles. All of the impedance based approaches failed to operate for the fast pole slips because the impedance locus travelled through their trip characteristic too quickly.

'Test PSL2GAF'

Figure 6.39 contains the Mho pole slipping protection scheme characteristic, the loss of field characteristic, and the pole slipping locus for test 'PSL2GAF'. The Mho, single and double blinder schemes failed to detect the pole slip because the impedance locus passed underneath their trip characteristics. This occurred because the generator dynamic impedance during the pole slip was greater than Xd', and the generator internal voltage was less than unity. The loss of field protection did trip for the pole slip however. The times when the impedance entered and left the loss of field characteristic are shown in Figure 6.39. The impedance locus entered the loss of field characteristic for a duration of 1.48 s. This satisfied the 0.6 second time delay used to stop nuisance tripping during stable power swings. The power based algorithm also tripped for this simulation, approximately 0.5 seconds after the loss of field scheme.

'Test PSL3GAF'

Figure 6.40 contains the Mho pole slipping protection scheme characteristic, the loss of field characteristic, and the pole slipping loci for test 'PSL3GAF'. The Mho, single and double blinder schemes failed to detect the first pole slip because the impedance locus passed under their trip characteristics. The mho, single and double blinder schemes successfully detected the second and subsequent pole slips, which are labelled 2,3...7 on Figure 6.40.

The loss of field scheme operated for the first pole slip cycle, labelled '1' on Figure 6.40. It failed to trip for the subsequent cycles, because a portion of the impedance locus occurred outside the loss of field characteristic. This is shown as point 'A' on Figure 6.40. This portion of the locus prevented the 0.6 s loss of field time delay from being satisfied. If a 'delay on reset' function was included in the loss of field scheme, as used in some modern relays[74], the relay would have detected the subsequent pole slips.

6.3.7.2 Comparison of Impedance Relays with New Power Based Protection Algorithm for Stable Power Swing Conditions

Table 6-3 shows the results for the recoverable power swing simulations. The power based pole slipping scheme and single blinder scheme successfully restrained for all of the stable power swing simulations. The Mho scheme nuisance tripped for 8 of the 12 simulations. The double blinder scheme nuisance tripped for 1 of the 12 simulations. The loss of field scheme remained stable for all of the simulations, showing that the 0.6 s time delay blocked relay operation during such conditions.

Table 6-3

Results of Comparisons Between Conventional and New Pole Slipping Protection Methods for PPSS Stable Power Swing Simulation Tests

Test	Loss of Field	Mho Pole slipping	Single Blinder	Double Blinder	Power Based Algorithm
PSW1NN	NT	1.188*	NT	NT	NT
PSW2NN	NT	NT	NT	NT	NT
PSW3NN	NT	NT	NT	NT	NT
PSW1GN	NT	1.431*	NT	NT	NT
PSW2GN	NT	1.094*	NT	NT	NT
PSW3GN	NT	1.176*	NT	NT	NT
PSW1NA	NT	1.431*	NT	NT	NT
PSW2NA	NT	NT	NT	NT	NT
PSW3NA	NT	0.670*	NT	0.846*	NT
PSW1GA	NT	1.431*	NT	NT	NT
PSW2GA	NT	NT	NT	NT	NT
PSW3GA	NT	0.702*	NT	NT	NT

* - signifies that the relay did not operate as required.

'Test PSW3GA'

Figure 6.41 shows the Mho characteristic and the stable power swing impedance locus for test PSW3GA. The impedance locus entered the Mho characteristic at a time of 0.683 s, and remained inside until 0.745 s. It was therefore inside the characteristic for 62 ms. This was ample time to satisfy the 20 ms time delay applied to the scheme to enhance its security towards stable power swings. If the time delay had been increased to 65 ms to prevent the nuisance trip, the scheme would fail to detect fast pole slips because the impedance locus would pass through the characteristic in under 65 ms. If the Mho circle size is reduced to prevent the nuisance trip, some pole slips may go undetected.

The Mho scheme nuisance tripped in the same way for 7 of the other stable power swing tests. This confirms the weaknesses of the Mho scheme stated in Section 2.1.2.

Test 'PSW3NA'

A section of the double blinder characteristic, and the impedance locus for test 'PSW3NA' are shown in Figure 6.42. The double blinder scheme nuisance tripped for this simulation. After fault clearance at a time of 0.52 s, the impedance trajectory travels from inside the two inner elements to outside the right outer blinder element. At 0.57 s, the supervisory Mho element is picked up, but the two right hand blinder units are not. The locus then heads back to the left and crosses both of the blinders with a time delay of approximately 0.13 s. This 'seals in' the first stage of the double blinder logic. The locus then stays in between the inner blinder elements for long enough to seal the next stage of the scheme's logic. It then crosses back over the two right hand blinder units in 0.12 s, satisfying the final stage of the scheme logic, and issues a trip signal at a time of 0.85 s.

The small 'oval' in the impedance trajectory is produced as the generator swings up to the CSP. After the fault clearance, the generator swings up to the CSP, and in doing so passes over the peak of its real power load angle curve. It then swings back towards a stable operating point, and again passes over the peak of its power output curve. In terms of time, the CSP is reached at 0.70 s on the record.

Although the double blinder scheme only nuisance tripped once for the 12 stable power swing tests conducted, this nuisance trip highlights one of the problems with the double blinder scheme. Careful setting is required to ensure that this kind of nuisance trip does not occur. The 'oval' which occurred in the impedance locus often occurs during severe

stable power swings. The inherent security of the double blinder scheme is much lower than for the single blinder scheme, because the double blinder scheme does not require the impedance locus to enter from one side and leave from the other.

6.3.7.3 Comparison of Impedance Relays with New Power Based Protection Algorithm for Other Power System Conditions

Table 6-4 contains the results of the performance comparison tests for the loss of field, loss of prime mover, and operation of the generator in the dynamic stability region tests.

The loss of field and power based relays both operated for all of the loss of field tests. The single and double blinder schemes did not operate. The Mho scheme operated for the loss of field from 100 % initial load test.

The loss of field scheme and the new power based algorithm nuisance tripped for the simulations where the generator was operated at load angles of greater than 90°. This is not considered a problem because generators are never operated in this way in practice because the reserve in hand for transient stability is too low.

All of the protection relays remained stable during the loss of prime mover tests.

Test 'LOF3GA'

Figure 6.43 shows the impedance locus and loss of field relay operating characteristic for test 'LOF3GA'. The impedance locus stays within the operating characteristic almost continuously for this test. The circle which occurs in the impedance locus is due to the effects of magnetic saliency in the generator rotor structure.

The loss of field relay operated before the power based relay because it only required the generator to import large amounts of reactive power to trip. The power based algorithm on the other hand, requires the onset of asynchronous operation before it will trip. The difference in tripping times is most pronounced at low initial operating powers. If the generator was operating at zero initial operating power, the power based algorithm would not trip because the generator would not lose synchronism. An additional power based algorithm, requiring almost no additional relay processor time could be used alongside the power based pole slipping algorithm to provide full loss of excitation protection[160].

Test 'AVR5NA'

Figure 6.44 contains the impedance locus for test 'AVR5NA' . The generator was initially operating at point 'A'. The AVR reference voltage was then reduced, causing a reduction in generator excitation in an attempt to regulate the terminal voltage to the new reference point. This resulted in the generator importing reactive power, which moved the impedance locus to point 'B'. The loss of field relay therefore tripped because point 'B' is located inside the relay trip area. At a time of 10 seconds into the simulation, the generator prime mover input power was reduced from 0.5 pu to zero. The change in power moved the impedance locus from point 'B' to point 'C'. Point 'C' was still inside the loss of field relay trip zone. After several seconds of operation at point 'C', the AVR reference voltage was returned to unity, causing the impedance locus to return to the positive reactive power region.

Table 6-4

Results of Comparisons Between Conventional and New Pole Slipping Protection Methods for PPSS AVR Assisted High Load Angle, Loss of Field and Loss of Prime Mover Simulation Tests.

Test	Loss of Field	Mho Pole slipping	Single Blinder	Double Blinder	Power Based Algorithm
AVR4NA	1.796*	NT	NT	NT	10.345*
AVR5NA	2.406*	NT	NT	NT	10.330*
AVR6NA	1.796*	NT	NT	NT	10.385*
LOF1GA	3.488	NT	NT	NT	6.825
LOF2GA	3.716	NT	NT	NT	4.870
LOF3GA	2.910	3.384	NT	NT	3.030
LOP1NA	NT	NT	NT	NT	NT
LOP2NA	NT	NT	NT	NT	NT
LOP3NA	NT	NT	NT	NT	NT

* - signifies that the relay did not operate as required.

6.3.8 Analysis of the Performance of Current, Voltage and Frequency Relays to the PPSS Pole Slipping Conditions

The performance of under and over-voltage, under and over frequency, and over-current relays for detecting pole slipping conditions was analyzed using the PPSS test simulation files and PC based models of the relays. Table 6-5 contains the results for all of the PPSS pole slip tests. For all of the tests, the effects of the fault on the relays which caused the pole slip have been neglected, since a large majority of the faults used to induce pole slipping caused the relays to operate. The analyses performed in this section will solely concentrate on the effects that a pole slipping generator will have on these relays.

Table 6-5
Response of Current, Voltage and Frequency Relays to
Pole Slipping Conditions in PPSS Test Files

Test	Over-Current trip	Under-Voltage trip	Over-Frequency trip
PSL1NN	no trip	no trip	no trip
P2SL2NN	no trip	no trip	no trip
PSL3NN	TRIP	TRIP	no trip
PSL31GN	no trip	no trip	no trip
PSL2GN	no trip	no trip	no trip
PSL3GN	no trip	no trip	no trip
PSL1NA	no trip	no trip	no trip
PSL2NA	no trip	no trip	no trip
PSL3NA	TRIP	no trip	no trip
PSL1GA	no trip	no trip	no trip
PSL2GA	no trip	no trip	no trip
PSL3GA	no trip	TRIP	no trip
PSL1GAF	no trip	TRIP	no trip
PSL2GAF	no trip	TRIP	no trip
PSL3GAF	no trip	TRIP	no trip

The analysis shows that these relays do not provide protection against pole slipping conditions, as suggested by Engineering Technical Report 113[15]. Although this study system has not focused specifically on embedded generators, the results apply equally to embedded machines. The main difference between the two environments is that pole slipping is more likely to occur with embedded generators.

6.3.8.1 Response of Over-Current Relay to Pole Slipping Conditions

The PC based 'C' code model of the Voltage Controlled IDMT over-current relay[45] used in the analysis can be found in Appendix F. The over-current relay operated for 2 of the 15 pole slipping tests. The following settings were used;

Plug Set Multiplier Setting (PSM) = 1.5 * Generator Full Load Current
Time Multiplier Setting (TMS) = 0.1
Voltage Control Setting = 70 % Nominal Voltage
IDMT Curve Type = Standard Inverse.

These settings are sensitive, yet the IDMT relay still failed to detect most of the pole slipping conditions. Figure 6.45 contains the Phase A RMS currents and IDMT trip points for tests PSL3NN, PSL2GA, and PSL3GA. The phase B and C currents will be identical for the pole slipping section of the plot because pole slipping is a balanced phenomenon.

Figure 6.45a shows the current for test 'PSL3NN'. The first trip occurs as a result of the fault, the second occurs due to the pole slipping. A total of 17 pole slip cycles were required to operate the relay. Although the mean level of current was 2.75 pu, and the maximum level around 4 pu, the IDMT relay did not trip until the minimum current level approached the relay pick-up current setting of 1.5 pu. The minimum current is the important quantity when considering the performance of IDMT relays at detecting pole slipping conditions. The relay simulated used a 5 cycle exponential reset function[57]. This meant that for the first 10 pole slip cycles, the relay reset after every cycle. One pole slip cycle is not sufficient to operate the relay, the relay therefore failed to trip until a reset did not occur at the end of each cycle.

Figure 6.45b shows the current for test 'PSL2GA'. The over-current relay failed to trip for the three pole slip cycles that occurred, for the same reasons as above. The peak current during the pole slip cycle lasted for much longer in this test, but was still not

sufficient to operate the over-current relay. A current level of 4 pu, in conjunction with the relay settings used would require the current to remain at this level for 700 ms before the relay will trip. If the voltage control element operates, the PMS setting would be adjusted by a factor of 0.4, changing it from 1.5 to 0.6*In. With the new PMS setting of 0.6*In, a fault duration of 362 ms is still required. This was just longer than the current duration that occurred during the test.

Figure 6.45c shows the current for test 'PSL3GA'. The overcurrent relay did not operate because the IDMT relay was reset after each pole slip cycle.

The above analysis shows that unless very sensitive settings are used, IDMT type over-current relays do not provide effective pole slipping protection because the relay is reset between pole slip cycles. A long delay on reset function would alleviate this problem..

6.3.8.2 Response of Under-Voltage Relay to Pole Slipping Conditions

The under-voltage relay operated for 5 of the 15 pole slipping tests conducted. The relay trip setting was 90 % of rated volts, with a time delay of 0.5 seconds. The time delay enables the relay to 'ride through' most short circuit faults. Figure 6.46 shows the phase 'A' RMS voltage for tests 'PSL3NN', 'PSL2GA', and 'PSL3GAF'. The 200 MVA generator used in the PPSS model is connected to an infinite bus through a relatively weak tie line. The system centre is therefore close to the terminals of the generator, rather than far inside the generator. This results in large fluctuations in voltage during pole slipping, or when excessive amounts of reactive power are drawn from the system.

Figure 6.46a shows the voltage, under-voltage trip, and trip level for test 'PSL3NN'. The under-voltage relay tripped after 25 pole slip cycles. As with the over-current relay, the under-voltage relay is inhibited from tripping because it is reset during every pole slip cycle. For this test, the reactive power consumption becomes so large that eventually no resets occur, and the relay trips. Figure 6.19a shows the reactive power for part of this test, which decreases as the pole slipping continues. If the generator had been connected to a 'stiffer' bus, the under-voltage relay may not have tripped because it would have reset during the 'in phase' part of each pole slip cycle.

Figure 6.46b shows the response for test 'PSL2GA'. This test has a slower rate of pole slipping, and shows the extent to which pole slipping can disturb the system voltage.

However, the disturbances are still insufficient to cause the relay to trip for the pole slip. It did trip during the fault however.

Figure 6.46c shows the response for test 'PSL3GAF'. This pole slip was caused by a faulty AVR. As the reactive power absorbed by the generator increases, the terminal voltage decreases. Figure 6.23a shows a plot of the reactive power for this test. The decreasing terminal voltage causes the under-voltage relay to trip before the generator starts to operate asynchronously. The relay remains tripped for the first 4 pole slip cycles, and is then reset. The voltage fluctuations increase towards the end of the test as a result of the field forcing action of the AVR. Although faulty, the AVR still responds to the voltage depression.

6.3.8.3 Response of Over-Frequency Relays to Pole Slipping Conditions

The over-frequency relay did not operate for any of the 15 pole slipping tests conducted. The relay was set to trip at 1 % above the nominal frequency of 50 Hz, with a time delay of 0.4 seconds. The PC based 'C' code model of the frequency measuring device[182] used in the analysis can be found in Appendix F. As with the under-voltage and over-current relays, the over-frequency relay was inhibited from tripping because of the cyclic fluctuations in measured frequency which occur during pole slipping.

Figure 6.47a shows the measured frequency for test 'PSL3NN'. A glitch occurs in the measured frequency during the fault on and fault off points. This occurs because the position of the voltage waveform's zero crossing changes rapidly. The frequency measurement soon returns to its correct value. The frequency can be seen to rise during the fault because the generator rotor accelerates. Once the fault has been cleared, the frequency oscillates wildly at the rate of pole slipping. Although the actual generator rotor is travelling at least 1 % above synchronous speed, the measured frequency does not show this. The fluctuations in frequency are produced because of the fluctuations in voltage phasor which occur due to the large fluctuations in real and reactive power, as shown in Figure 6.19. If the input to the frequency relay was derived from the generator rotor speed, the relay would have tripped.

Figure 6.47b shows the result for test 'PSL2GA'. The frequency can be seen to rise during the fault period, then fluctuate at the rate of pole slipping afterwards. The fluctuations are less severe than in test 'PSL3NN' because the fluctuations in real and reactive power are

not as severe. Note that even after the generator has re-synchronised, at a time of 2 seconds on the record, small fluctuations in frequency still occur. Figure 6.16 shows the real and reactive power fluctuations for this test.

Figure 6.47c shows the frequency plot for test 'PSL3GAF'. There is no fault in this test. The fluctuations observed in frequency are therefore solely due to pole slipping. The frequency remains at 1 pu until the generator loses synchronism. It then begins to fluctuate as the oscillations in real and reactive power build up, as shown in Figure 6.23. The magnitude of the frequency fluctuations increases with the magnitude of the real power fluctuations. The fluctuations make the over-frequency relay reset very often, the 0.4 second time delay is therefore never satisfied.

6.4 625 KVA DIESEL GENERATOR FIELD TRIAL RESULTS

The power based pole slipping algorithm successfully tripped for all of the pole slipping conditions. For the loss of excitation tests, the algorithm detected the loss of excitations from high initial operating powers, but failed to detect those which occurred from 50 % and 20 % load because the generator did not lose synchronism over the duration of the test period. The algorithm restrained for all other operating conditions, such as synchronisation, local load changes, adjacent generator pole slipping, and all generator load and excitation changes.

6.4.1 625 kVA Diesel Generator Pole Slip Tests

Figure 6.48 shows the algorithm response to test 'A2'. An attempt was made to induce pole slipping from 50 % initial load by weakening the field excitation. However, the excitation could not be sufficiently weakened to do this. The generator therefore did not pole slip, and the algorithm did not trip. Figure 6.48a shows that the reactive power criterion was satisfied, but the real and rate of change of power trip criteria were not.

4 Hz oscillations occurred in the real power for this test. Their magnitude was 10 kW peak. This is equal to 1.6 % of generator rating, the setting Ptol is nominally set to 5 %. The oscillations did not cause any problems to the adaptive real power trip setting section of the algorithm. Oscillations in real power are common in diesel generators, and take two forms, either forced or natural. Forced oscillations occur as a result of the periodic

torque produced by the diesel engine. Generator-diesel units are normally designed to minimise the effects of such oscillations[183]. Natural oscillations can occur for a variety of reasons, such as poor AVR or governor performance. An adequate explanation for the oscillations in real power for this 625 kVA diesel generator has not been put forward. Anderson[184] suggests that these oscillations may be due to poor quality fuel.

It is important for the algorithm to track the output power, regardless of the oscillations. It is equally important that the algorithm does not track the oscillations caused by power swings. The field trial tests therefore provide data on this subject.

Figure 6.49 shows the power based pole slipping algorithm measurands for test 'A3'. The plots are made up of two disturbance records which were taken consecutively. A pole slip was induced by decreasing field excitation. The algorithm tripped before the generator pole slipped, at a real power of 306 kW.

The algorithm also tripped during the oscillations in real power which occurred after the pole slip. These do not normally cause a problem. However, the reactive power plot shows that the load angle was increasing and a pole slip was about to occur. The increase in load angle resulted in the reactive power criterion being satisfied. The oscillations in real power satisfied the remaining two criteria. This trip is not seen as problematic, since the generator was close to pole slipping again. The problem could easily be overcome by increasing the duration of time for which Pmax is held before being reset to its nominal value. This would increase algorithm security, without effecting sensitivity towards detecting steady state pole slips. A period of two seconds would ensure that this type of problem would not occur because the damping in most synchronous machines is such that most oscillations have abated in this period.

Figure 6.50 shows the disturbance records for test 'A4', where an adjacent generator was forced to pole slip. The algorithm remained stable for this test. The reactive power plot has the reactive power demands of the adjacent pole slipping generator translated onto it. As the demand for reactive power by the pole slipping machine increases, the protected generator supplies some of the increased demand. This takes the reactive power output further away from the trip level, Qtrip. This test demonstrates that the algorithm is not liable to trip for adjacent generators which are pole slipping.

The real power plot contains the 4 Hz oscillations, which appear to be triggered by the disturbances from the adjacent generator. This suggests that the oscillations are triggered via some form of voltage feedback mechanism, since the generators were completely independent apart from being connected to the same busbar. The peak to peak amplitude of the oscillations was 100 kW, which equates to 16 % of generator rating. The algorithm still successfully updated Pt, the setting for a value of Ptol of 5 %. This setting is therefore adequate. It is unlikely that oscillations more severe than this would occur.

Figure 6.51 shows the combined disturbance records for test 'A7'. Pole slipping was induced by increasing the diesel engine's output power. The increase in real power from 250 to 575 kW over 3 seconds was the fastest rate possible; the servo-mechanism in the governor limited it to this rate. The algorithm correctly updated its Pt setting just after the maximum power output had been reached. The algorithm then tripped at a power level of 428 kW. It therefore tripped before the pole slip occurred. After the first pole slip, the machine's output power rose to 2.6 MW, which is equivalent to five times the rating of the generator. Allowing for a circuit breaker interrupting time of 100 ms, the algorithm would have disconnected the generator before the power reversed sign, the algorithm would therefore have avoided the potentially damaging variation in output power.

The generator slipped another pair of pole before re-synchronising. The algorithm tripped for this pole slip also.

6.4.2 625 kVA Diesel Generator Loss of Excitation Tests

The algorithm tripped for both of the loss of excitation from 100 % initial load tests, but did not trip for the 25 % and 50 % initial load cases. It did not trip for the low initial load tests because the generator did not lose synchronism. The saliency in its rotor structure provided enough reluctance torque to maintain synchronism. An additional power based algorithm, using a rectangular setting characteristic in the PQ plane tripped for the lower power loss of excitations[160]. If this type of algorithm is used to compliment the power based pole slipping algorithm, then full loss of excitation protection, which covers the generator's entire operating range, can be achieved.

Figure 6.52 shows the algorithm measurands for test 'B2', loss of excitation from 20 % initial load. The reactive power does not satisfy the Qtrip criterion because the load angle

has not increased to 90°. The real power criterion was not satisfied either. The algorithm therefore did not trip.

Figure 6.53 shows the results to test 'B3', loss of excitation from 50 % initial load. The reactive power criterion was satisfied, indicating that the load angle had advanced beyond 90°. The real power only dropped by 10 kW however, which was insufficient to satisfy the criterion, the algorithm therefore did not trip. It is possible for the generator to temporarily maintain a level of output power above the level predicted from the steady state saliency term of equation 3(1). Inspection of equation 3(3) shows that the transient saliency term may be sufficient to temporarily hold the rotor in synchronism. A simulation was performed to confirm this, the results of which are shown in Figure 6.54. The ATP file used for the simulation can be found in Appendix F. The power remained constant for 12 seconds, and then the generator lost synchronism. The field trial loss of excitation tests were run for 8 seconds or so. The generator was disconnected after this time. The generator may therefore have lost synchronism if the test had been continued for longer. Figure 6.54d shows the effect that the excessive reactive power demand can have on generator terminal voltage.

Figure 6.55 shows the algorithm response to test 'B6', loss of excitation from 100 % initial load. The algorithm successfully tripped for this test because the generator lost synchronism before the generator was disconnected. Note that even during loss of field conditions, the power pulsations produced still reach 1.5 MW. The loss of excitation was correctly diagnosed as a 'steady state' trip.

6.4.3 625 kVA Diesel Generator Steady State and Load Tests

The algorithm remained stable for all of the steady state and load change tests. Figure 6.56 shows the algorithm measurands for steady state test 'C3'. The reactive power plot shows the quantisation levels as a result of the disturbance recorder storage mechanism. The 'C' code for the algorithm uses 32 bit integers for its variables such as the reactive power, but to optimize storage space, 16 bit integers are used for the disturbance records. Details can be found in Appendix E.

Figure 6.57 shows the measurands for load change test 'C6'. The load change can be seen in the reactive power output, which step changes by 5 kVAr. The load change did not cause the algorithm to come even close to tripping.

6.4.4 Comparison of Conventional Impedance Based Pole Slipping Relays with Power Based Relay for 625 kVA Diesel Generator Pole Slip Tests

The relay models described in section 6.3.6 were used for this analysis. Details on the settings used can be found in Appendix B. The mho, single blinder, and double blinder pole slipping schemes all failed to detect either of the pole slips which occurred in field trial tests 'A3', and 'A7'.

Figure 6.58a shows the single blinder pole slipping scheme and the impedance locus for test 'A3'. The pole slip occurs between the time of 0 and 0.2 on the RX plot. The impedance locus shows that the single blinder scheme failed to detect the pole slip because the impedance locus passed underneath the scheme's characteristic. Inspection of Figures B10, B11, and B12 of Appendix B, which contain the mho, single and double blinder schemes trip characteristics, shows that they all occupy approximately the same area on the R-X plane. This is the area bounded by the generator impedance, Xd'. This confirms that the mho and single blinder schemes would also fail to operate for this pole slip, because the impedance locus passed beneath their operating characteristics. Comparison between this figure and Figure 6.49, which shows the power based pole slipping algorithm response for the same test provides a means of correlation between the power, current and voltage produced during pole slipping.

Figure 6.58b and 6.58c show the generator terminal voltage and current for the same test. The effect of pole slipping on the terminal voltage can clearly be seen. The voltage is almost depressed to 90 % of its nominal value. If the generator were to continually pole slip, the voltage depressions would continuously remain at this level. The current plot shows the high current levels which occur during pole slipping, which in this case reached 2.5 pu.

Figure 6.59a shows the single blinder characteristic, and impedance locus for test pole slip 'A7'. All of the conventional impedance based pole slipping schemes failed to detect either of the pole slips for the same reason as in test 'A3'. The impedance locus passed underneath their operating characteristic. The first pole slip occurs between 0 and 0.2 seconds, whilst the second occurs between 0.4 and 0.6 seconds.

The voltage and current for this test are shown in Figures 6.59b and 6.59c. The voltage depression which occurs leading up to and during the pole is a 10 % depression, whilst the current approaches 3 pu. After the pole slips occurred, the peak in current reaches 5 pu. This could cause cumulative damage to the machine windings.

6.5 STEAM TURBINE AND HYDRO GENERATOR FIELD TRIAL RESULTS

At the time of writing, the two field trial relays had been in place for 10 weeks. Neither relay nuisance tripped during this period showing that the power based algorithm is stable. No pole slips have been reported for either generator, the algorithms ability to trip has therefore not been demonstrated.

Three disturbance records have been triggered by the over-current element on the turbo-generator, one of these records is shown in Figure 6.60. The over-current element showed this to be a phase to phase fault, which was remote from the generator because it caused little disturbance to the generator's output power. The reactive power did not fall even near to the trip level, Qtrip. The algorithm therefore remained very secure for this fault. The disturbance records for the other two faults were virtually identical, and were therefore not included.

Figure 6.61 shows a disturbance record taken when the turbo-generator was in steady state. Figure 6.62 shows a steady state disturbance record taken from the hydro-generator relay. These plots show that the oscillations experienced during the diesel generator field trials did not occur for either type of machine. Since the Pt section of the algorithm worked with the diesel generator, it has no problem whatsoever with these types of generator.

The noise levels in the ($\Delta P/\Delta t$) signal were +/- 6 MW, which equates to the same magnitudes experienced with the diesel generator and PPSS tests; the level was 23 % of generator rating.

6.6 ADDITIONAL ATP SIMULATION TEST RESULTS

The pole slipping algorithm tripped for all the generator and motor pole slipping tests, and restrained for all the stable power swing simulations.

Figure 6.63 shows the algorithm measurands for test 'LT1', a simulated power swing with a generator open circuit time constant, Tdo' of 1.0 second. This is very low, and distorts the 'ideal' sinusoidal power load angle characteristics produced if a constant field flux linkage is assumed. The distortion is most evident in the real power plot. The algorithm remained stable for this simulation because the reactive power criterion was only satisfied when the real power was above its trip level, Pt.

Figures 6.64 and 6.65 shows the plots for the stable swing tests where Tdo' was set to 2 and 3 seconds. The algorithm remained secure for these tests for the same reasons as above.

Figure 6.66 shows the power plots for test 'LTP1', pole slipping with the value of Tdo' set to 1 second. The generator pole slipped one pair of poles before re-synchronising. The algorithm successfully detected this pole slip, which would have been diagnosed as a 'transient' pole slip due to the large fluctuations in ($\Delta P/\Delta t$) caused by the fault which induced pole slipping.

Figures 6.67 and 6.68 show the results for tests 'LTP2' and 'LTP3'. The algorithm successfully tripped during these tests, and diagnosed the pole slips as 'transient'. Note that the higher the value of Tdo', the more pole slips occurred before the generator re-synchronised. Equation 3(7) of chapter 3 shows that as the time constant, Tdo' increases, the amount of asynchronous power which is generated decreases. A shorter time constant therefore enables the generator to generate more asynchronous power. This provides the necessary additional retardation energy required for the generator to regain synchronism.

Figures 6.69 and 6.70 show the results for the fast governor simulations. The algorithm did not trip for either of these simulations because the reactive power criterion reset before the real power criterion was satisfied. These tests show that the algorithm will work with fast governors. It is unlikely that governors with a faster response will be used in practice.

Figure 6.71 shows the modified 'motor' power based pole slipping algorithm measurands for the stable power swing for a hydro-generator in pumping mode test. The reactive power criterion plot is identical to that produced by the 'generator' pole slipping algorithm. The real and rate of change of power plots are different however. They both have been reflected across the x-axis so that Pt and Pmax are now negative numbers, and $(\Delta P/\Delta t)_{min}$ is a positive number. The algorithm did not trip for this test because when the reactive power criterion was satisfied, indicating that the motor's load angle had reached 90°, the real power was less than its trip setting Pt. This indicated that there was still accelerating power left, and that the motor's CSP had not been reached.

Figure 6.72 shows the modified 'motor' pole slipping algorithm's response for the hydro-machine pole slip from pumping mode. The algorithm tripped for the pole slip, and diagnosed it as the 'transient' variety. The algorithm did not reset between pole slip cycles due to the reactive power being constantly below the trip level Qtrip,

Figure 6.73 shows the plots for test 'MOT3', the pole slipping of a hydro-generator in pumping mode due to a 20 % decrease in terminal voltage. The algorithm tripped for all of the 11 pole slip cycles which occurred before the machine governor reduced the motor load torque so that the motor could re-synchronise. The pole slip was diagnosed as 'steady state', which in conjunction with information about the voltage depression that occurred before the pole slip, would have enabled the protection engineer to ascertain the cause.

Figure 6.74 shows the algorithm response to the slow pole slipping rate test 'SLW'. The generator pole slipped at a mean rate of 2 to 3 pole slips per minute. A pole slip rate of 3 cycles/minute equates to a mean slip of 0.1 %. The algorithm successfully tripped for the slow pole slip, and diagnosed it as a 'steady state' type. This simulation shows that the algorithm meets the 0.1 % slip specification used by most other pole slipping schemes.

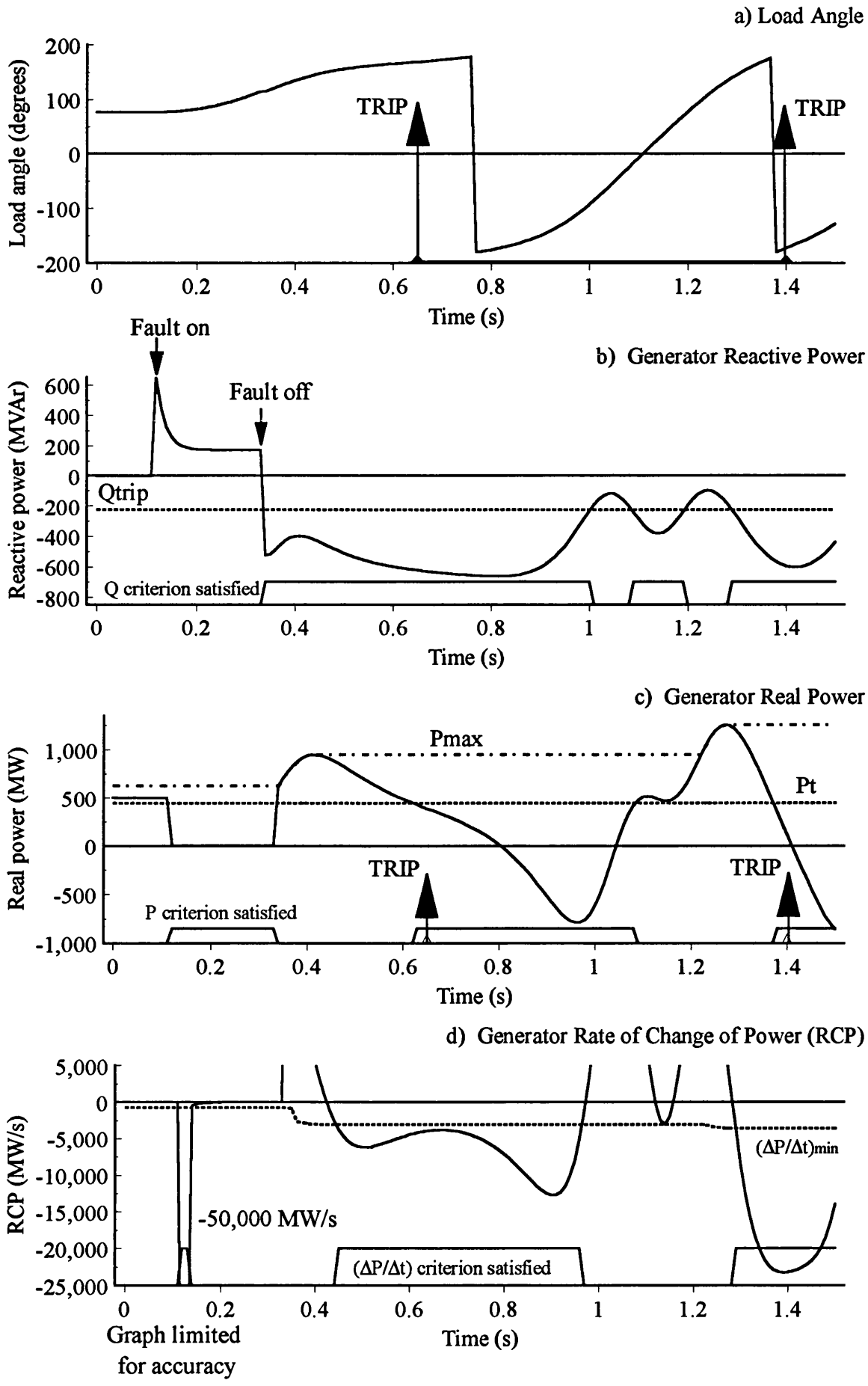

Figure 6.1
Pole Slipping Algorithm Response to Simulated Pole Slip Using POWSIM.

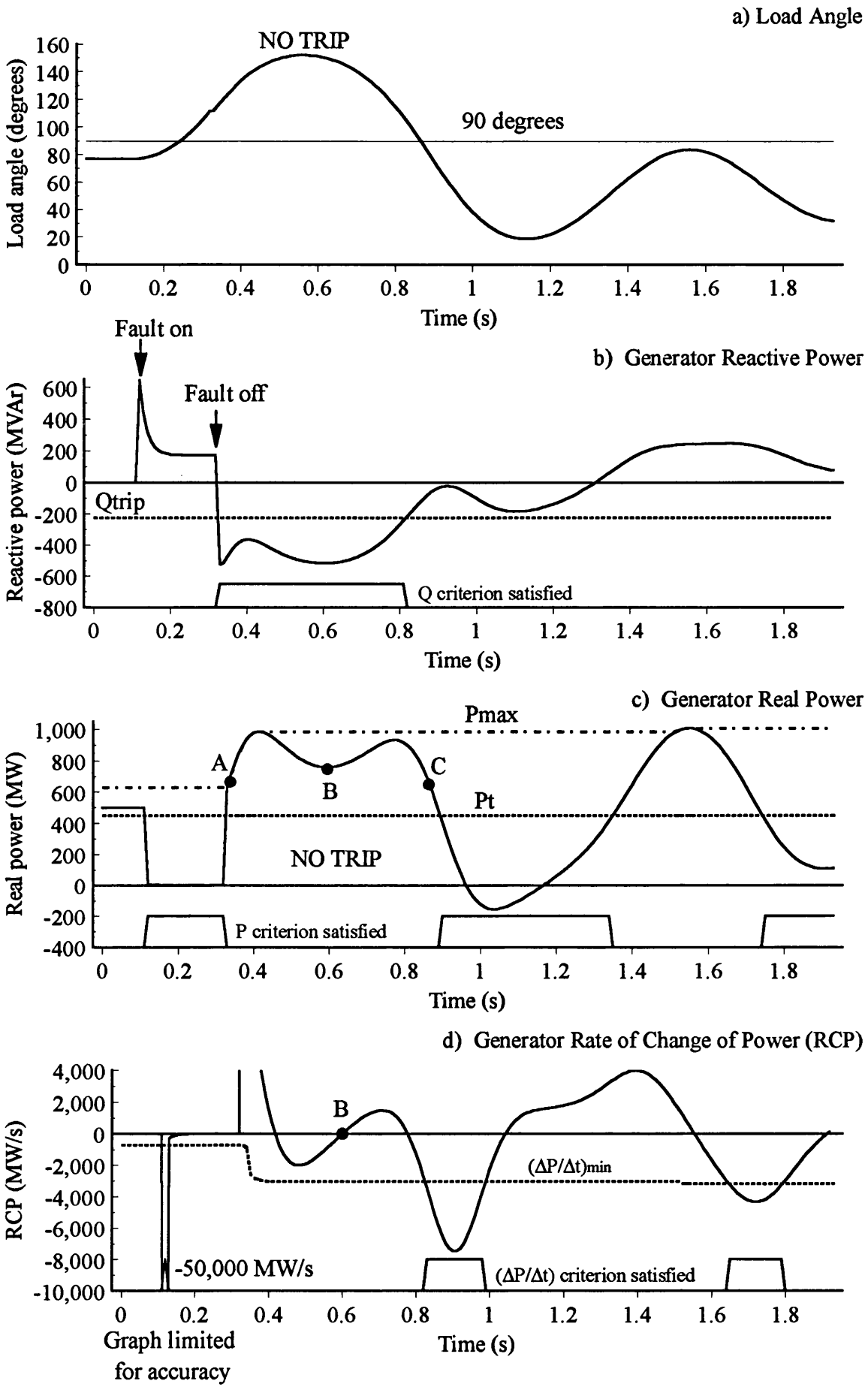

Figure 6.2
Pole Slipping Algorithm Response to Simulated Stable Power Swing Using POWSIM.

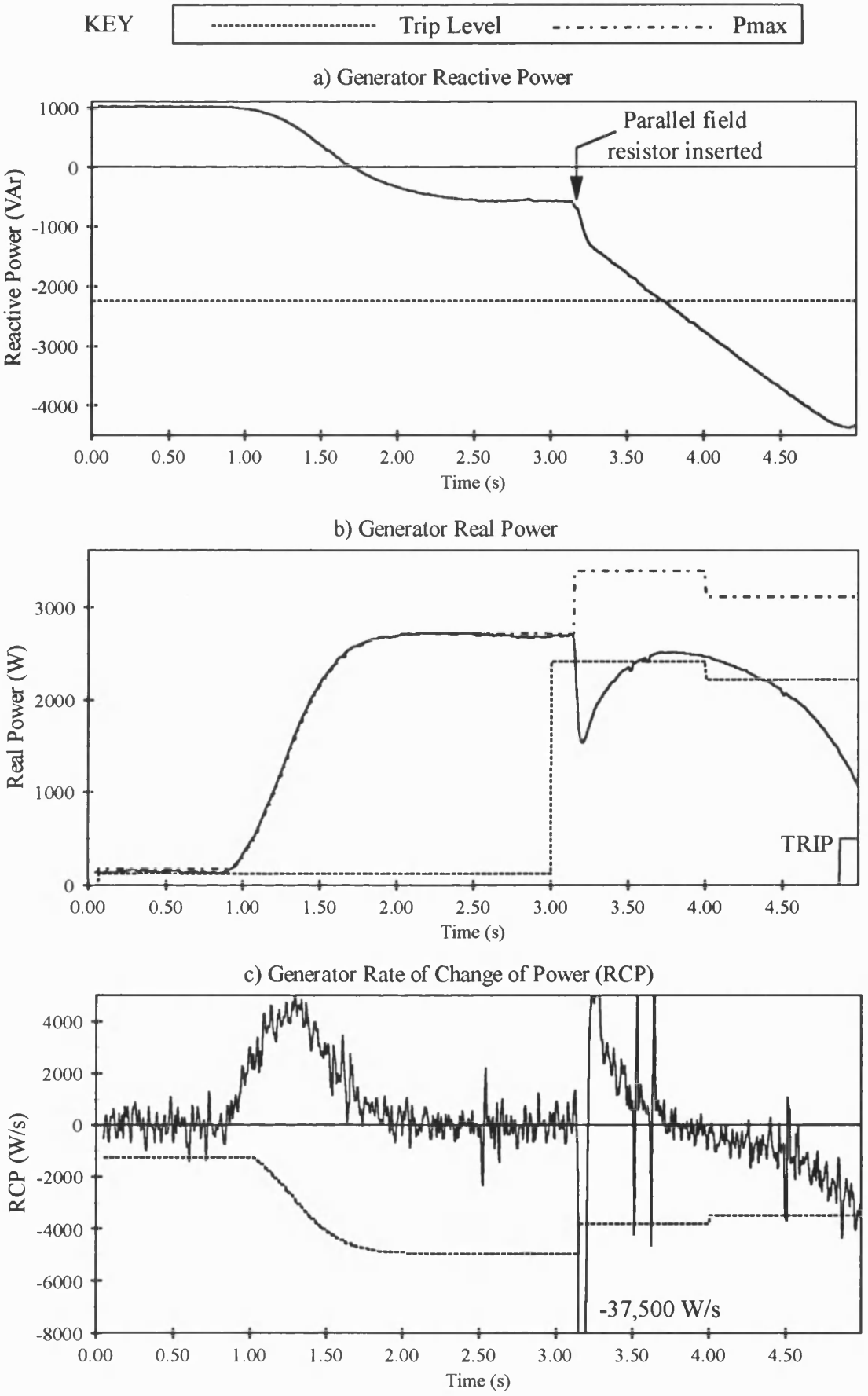

Figure 6.3
Pole Slipping Algorithm Response to a 'Weak Field' Pole Slip on
the Laboratory Model Power System 5 kVA Generator - Test 'C'

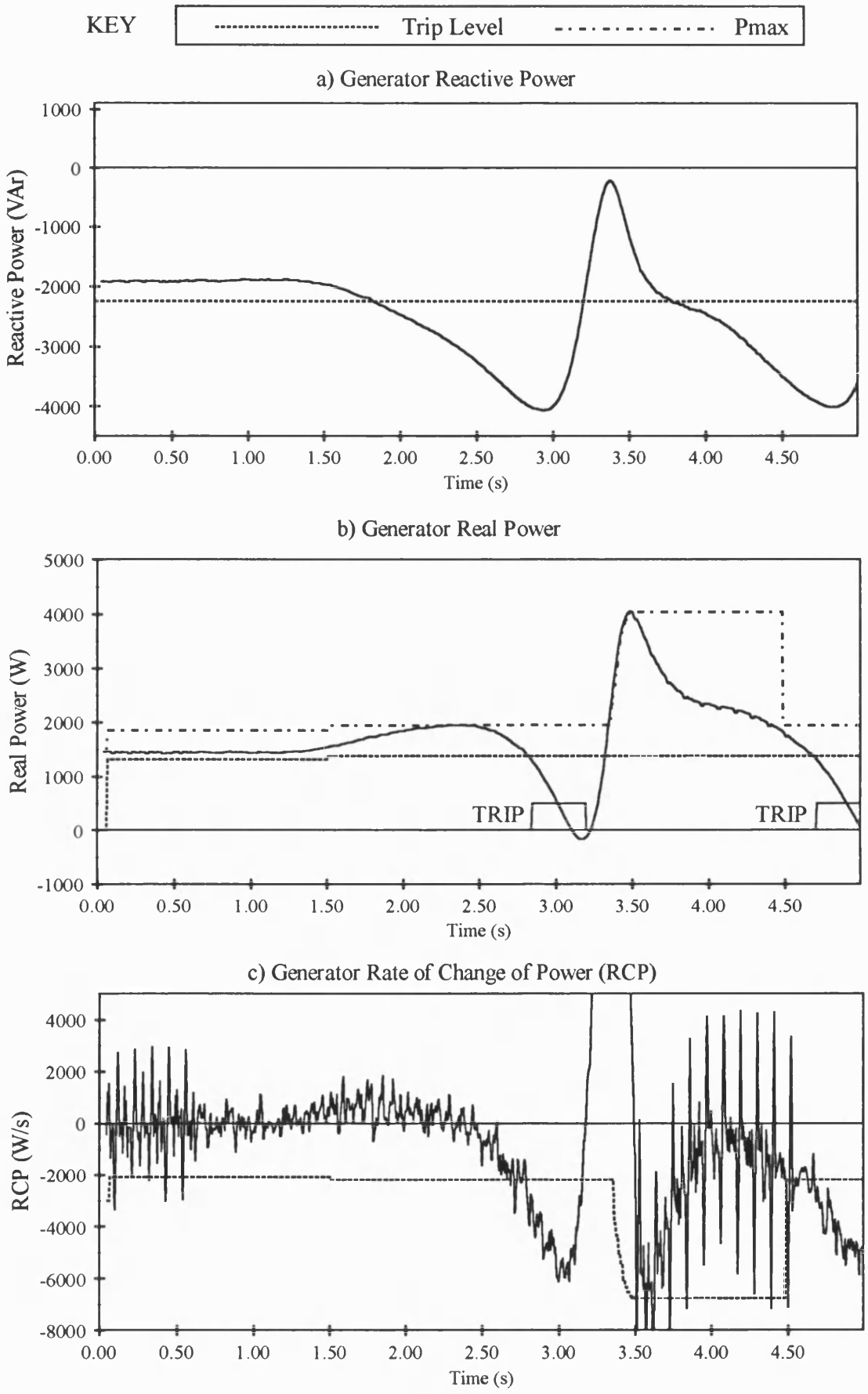

Figure 6.4

Pole Slipping Algorithm Response to an 'Over Torque' Pole Slip on the Laboratory Model Power System 5 kVA Generator - Test 'e' (low excitation, 4 kW of local load)

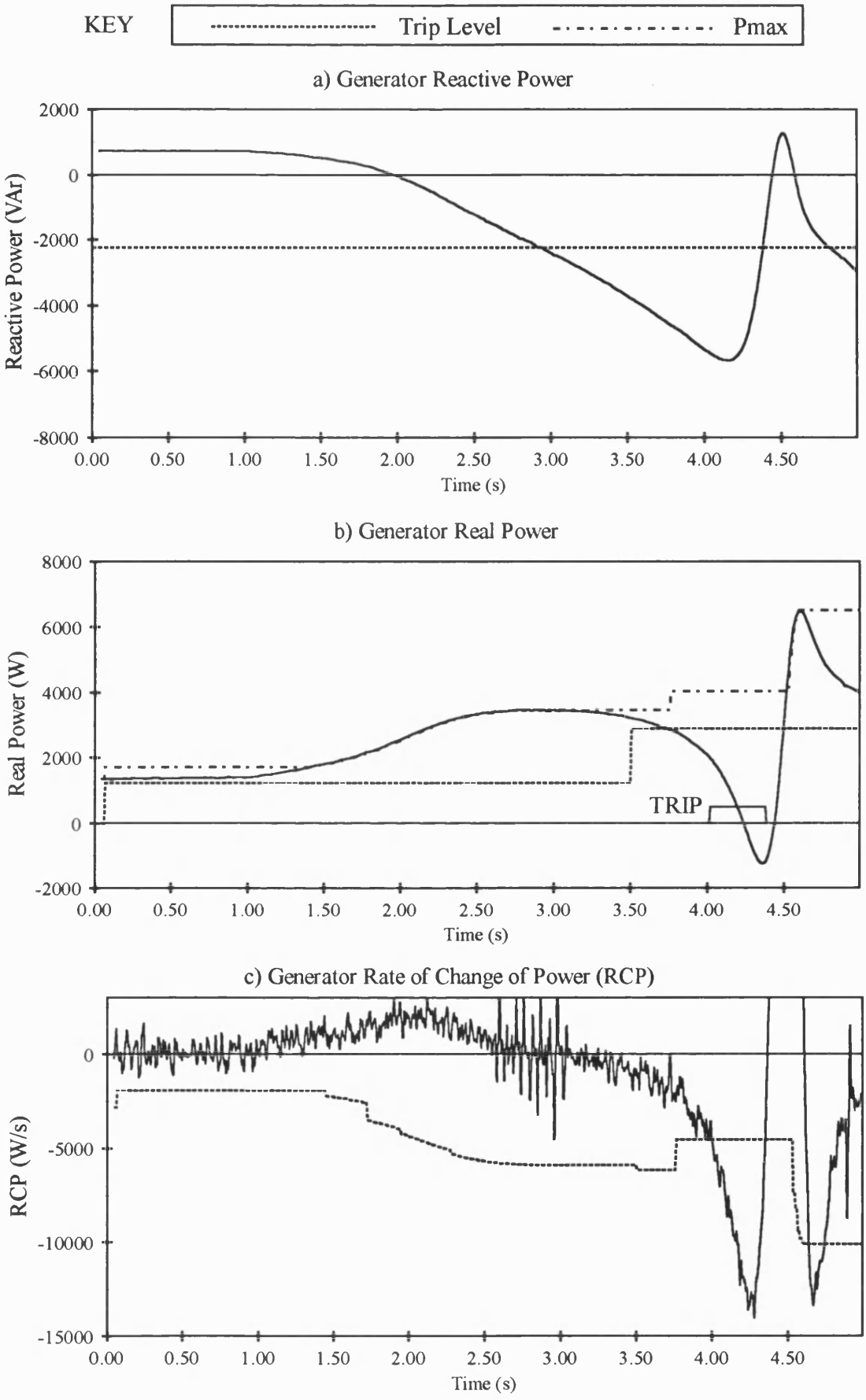

Figure 6.5

Pole Slipping Algorithm Response to an 'Over Torque' Pole Slip on the Laboratory Model Power System 5 kVA Generator - Test 'F' (medium excitation, 4 kW of local load)

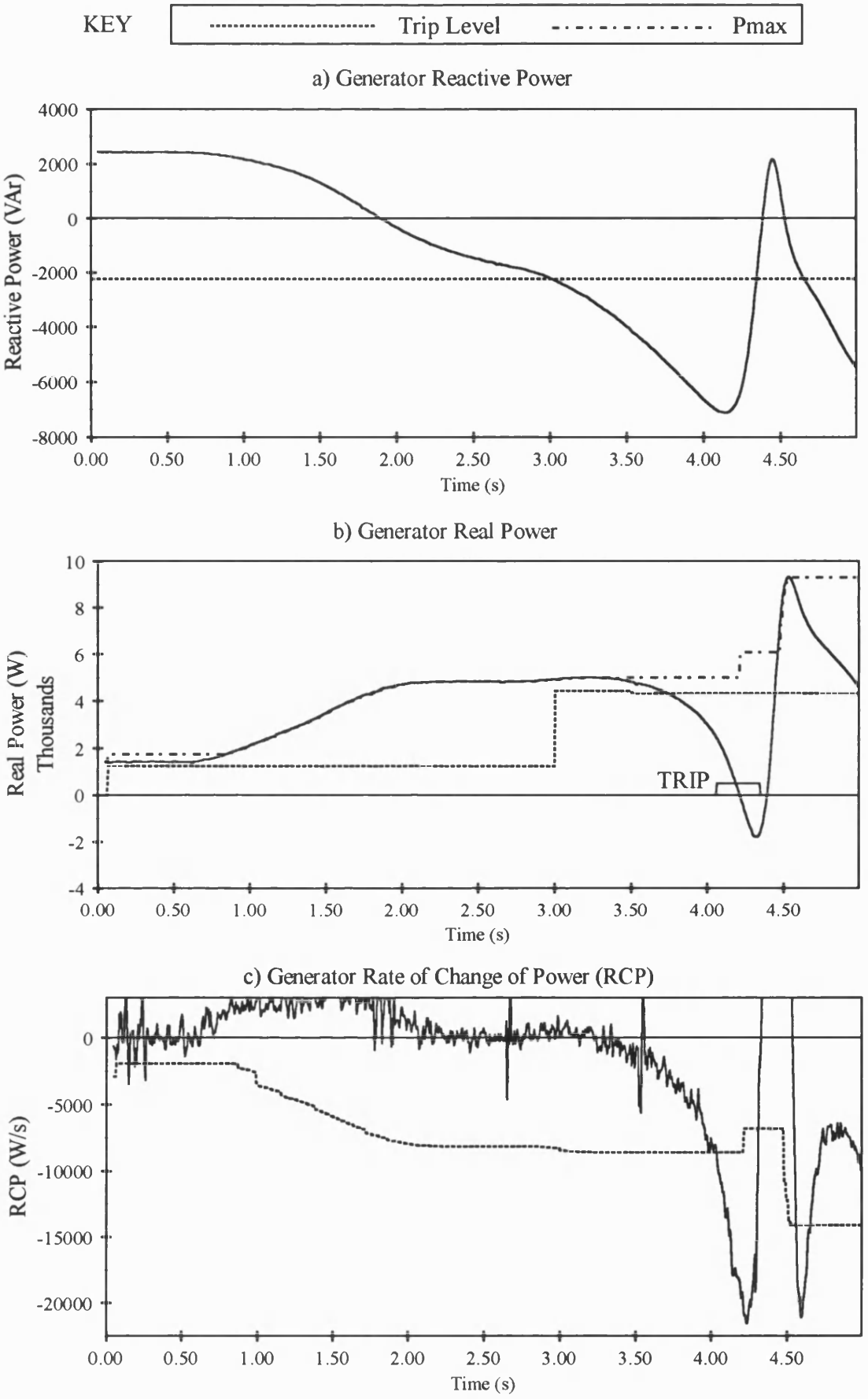

Figure 6.6

Pole Slipping Algorithm Response to an 'Over Torque' Pole Slip on the Laboratory Model Power System 5 kVA Generator - Test 'G' (high excitation, 4 kW of Local Load)

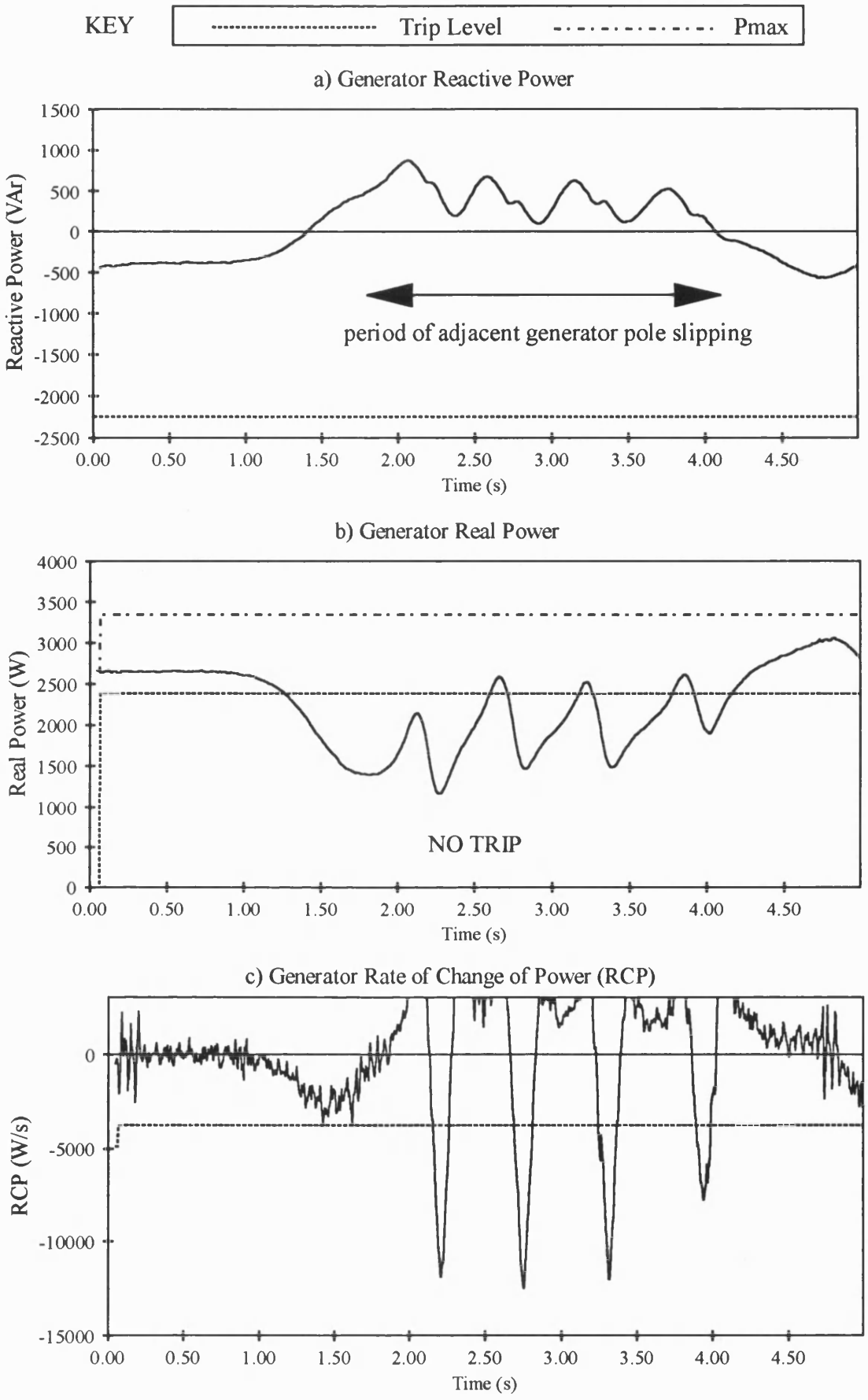

Figure 6.7

Pole Slipping Algorithm Response to an Adjacent 5 kVA Generator Suffering an 'Over Torque' Pole Slip on the Laboratory Power System Model - Test 'K'

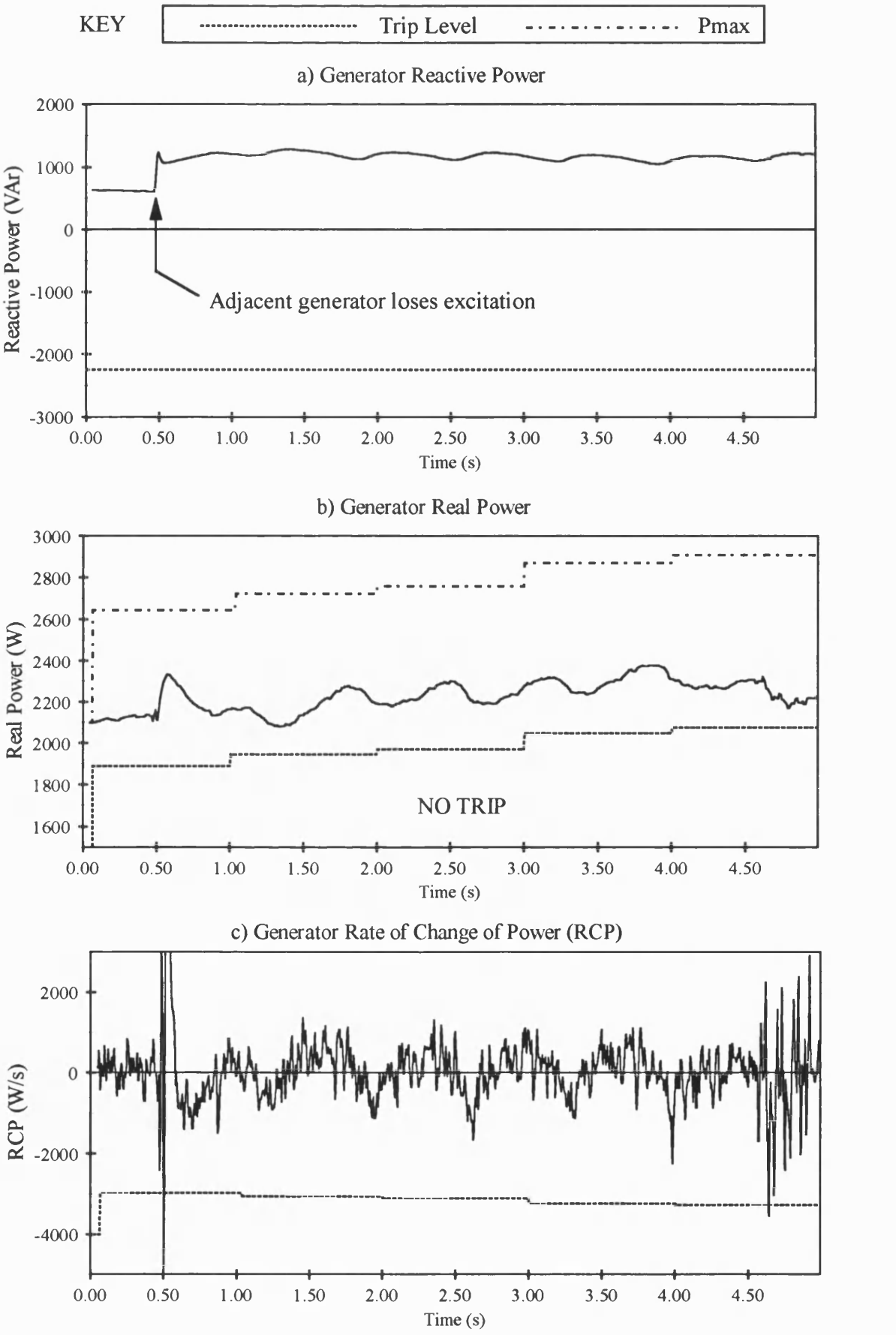

Figure 6.8
Pole Slipping Algorithm Response to an Adjacent 5 kVA Generator Loss of Excitation on the Laboratory Model Power System 5 kVA Generator - Test 'L'

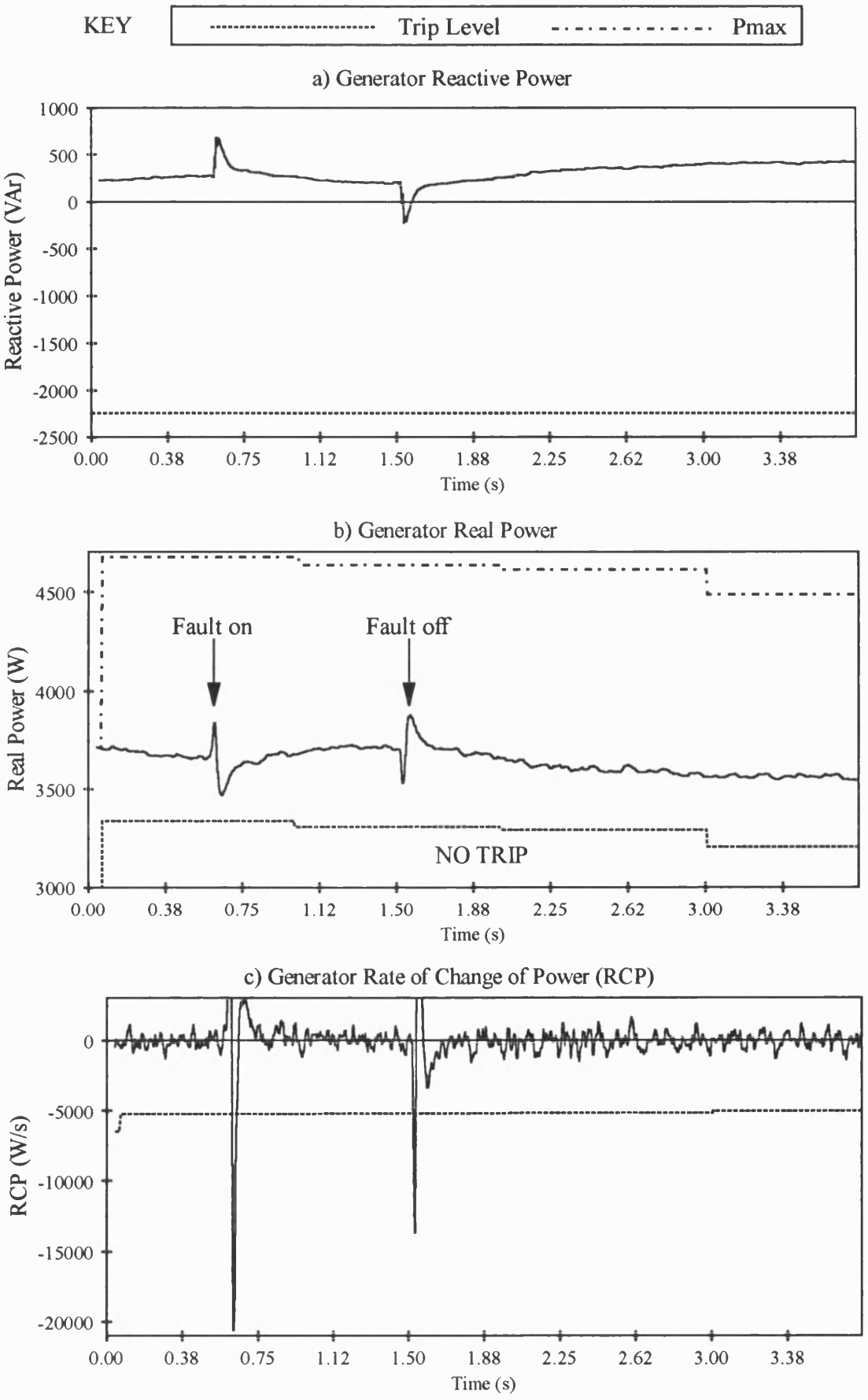

Figure 6.9

Pole Slipping Algorithm Response to a Single Phase to Earth Fault on the Laboratory Model Power System 5 kVA Generator, Generator Neutral Isolated - Test '1B'

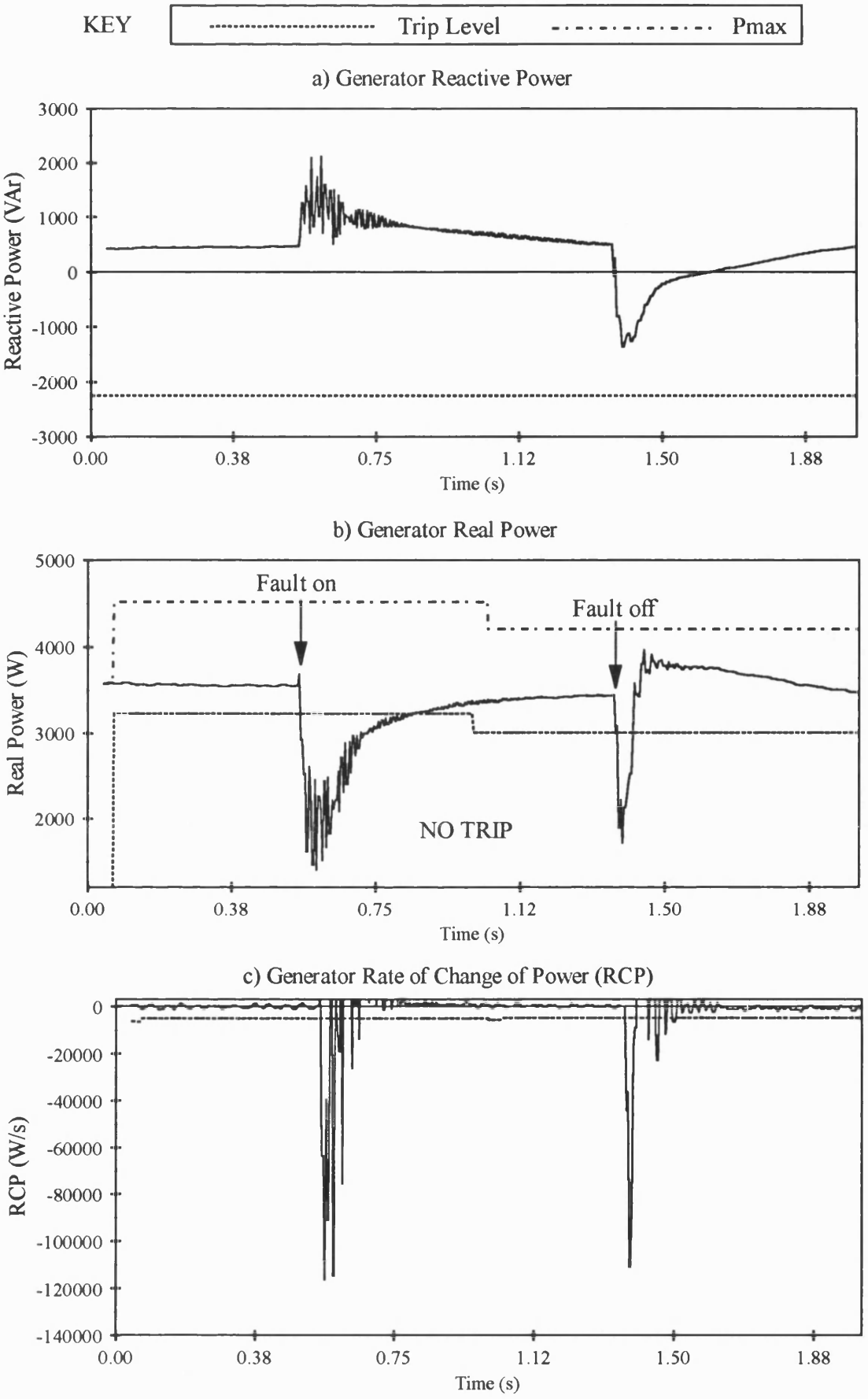

Figure 6.10

Pole Slipping Algorithm Response to a Phase to Phase Fault on the Laboratory Model Power System 5 kVA Generator, Generator Neutral Isolated - Test '2A'

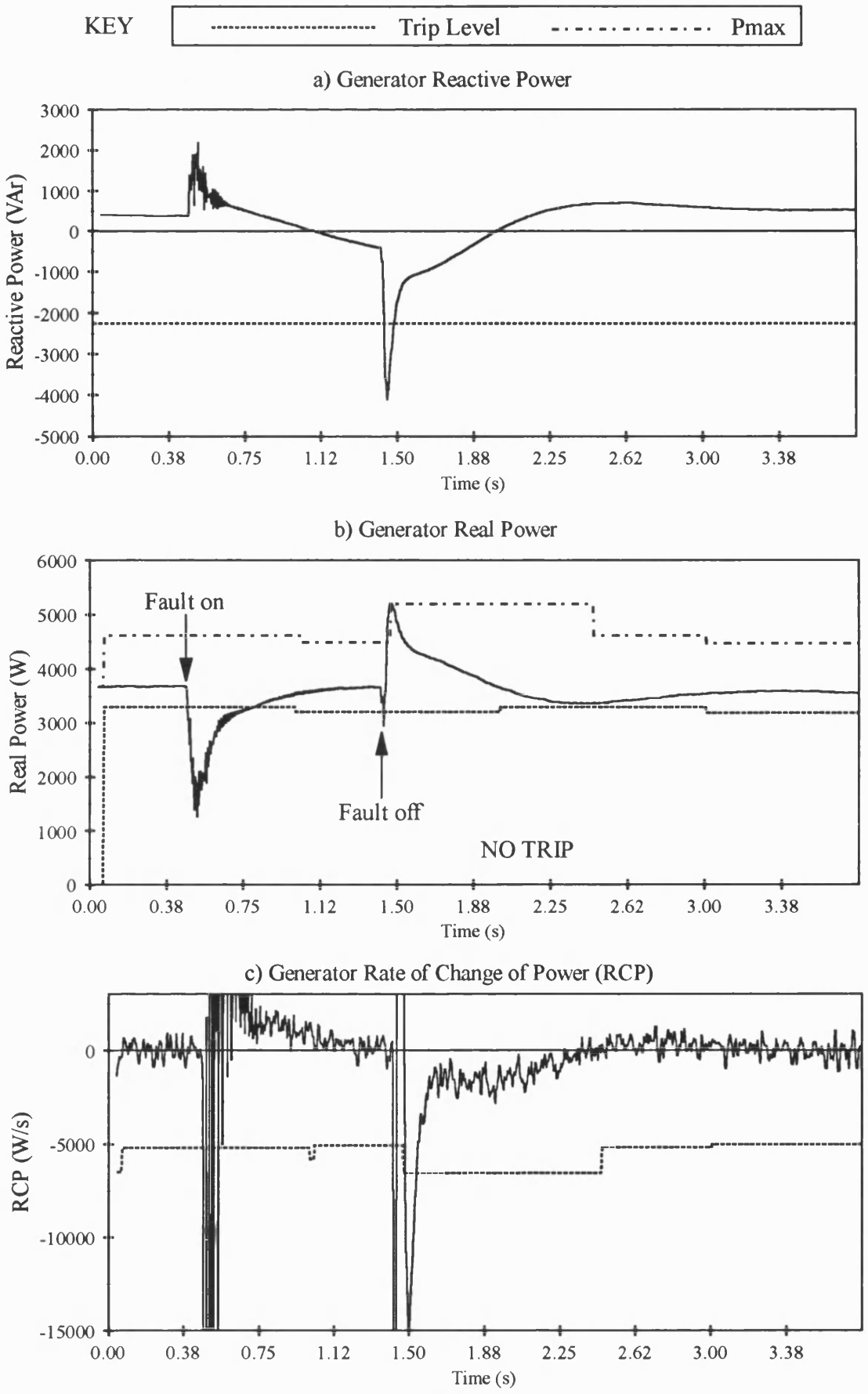

Figure 6.11

Pole Slipping Algorithm Response to a Two Phase to Earth Fault on the Laboratory Model Power System 5 kVA Generator, Generator Neutral Isolated - Test '3B'

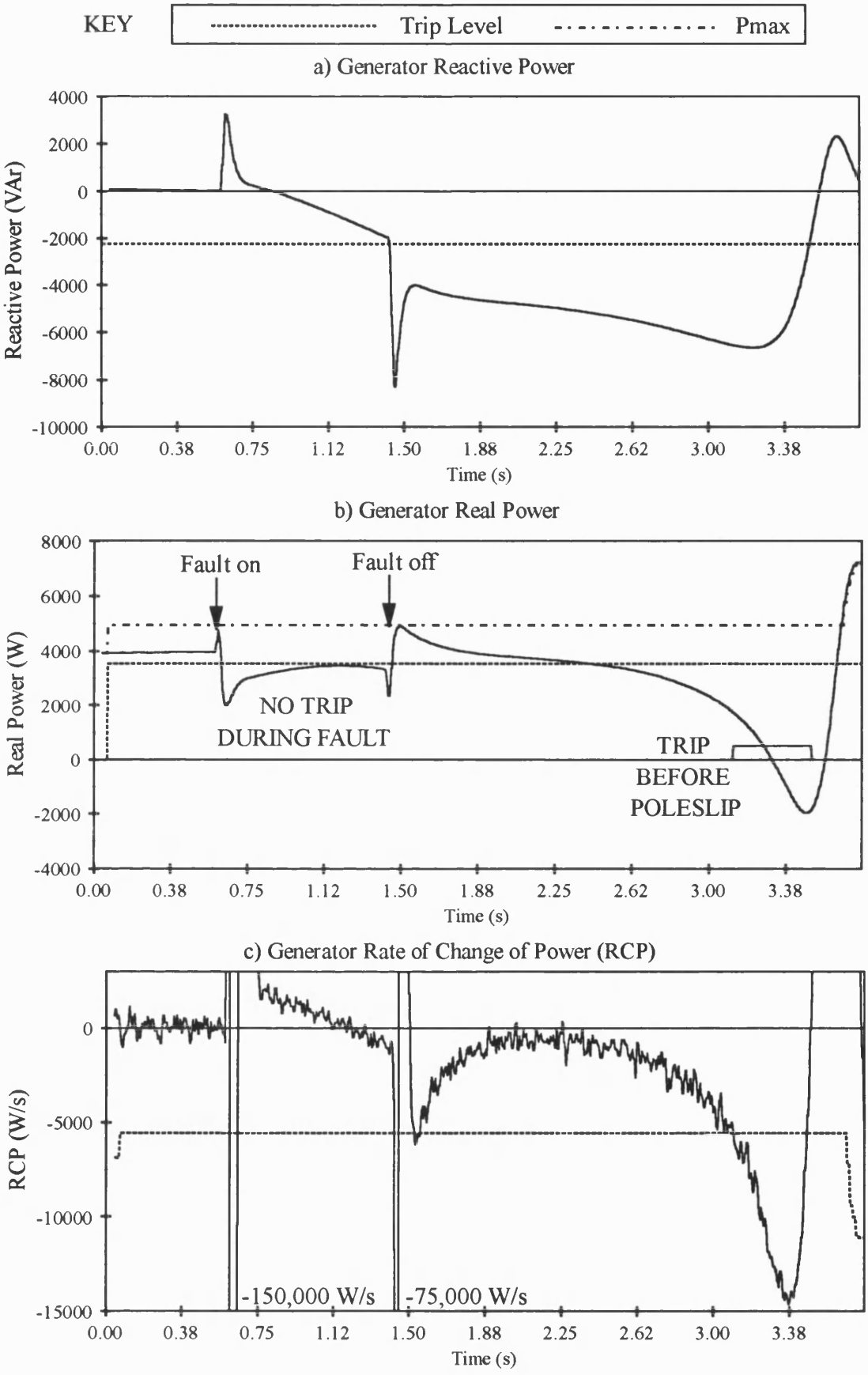

Figure 6.12

Pole Slipping Algorithm Response to a Three Phase Fault on the Laboratory Model Power System 5 kVA Generator, Generator Neutral Solidly Earthed - Test '4A', Fault Resulted in the Generator Pole Slipping.

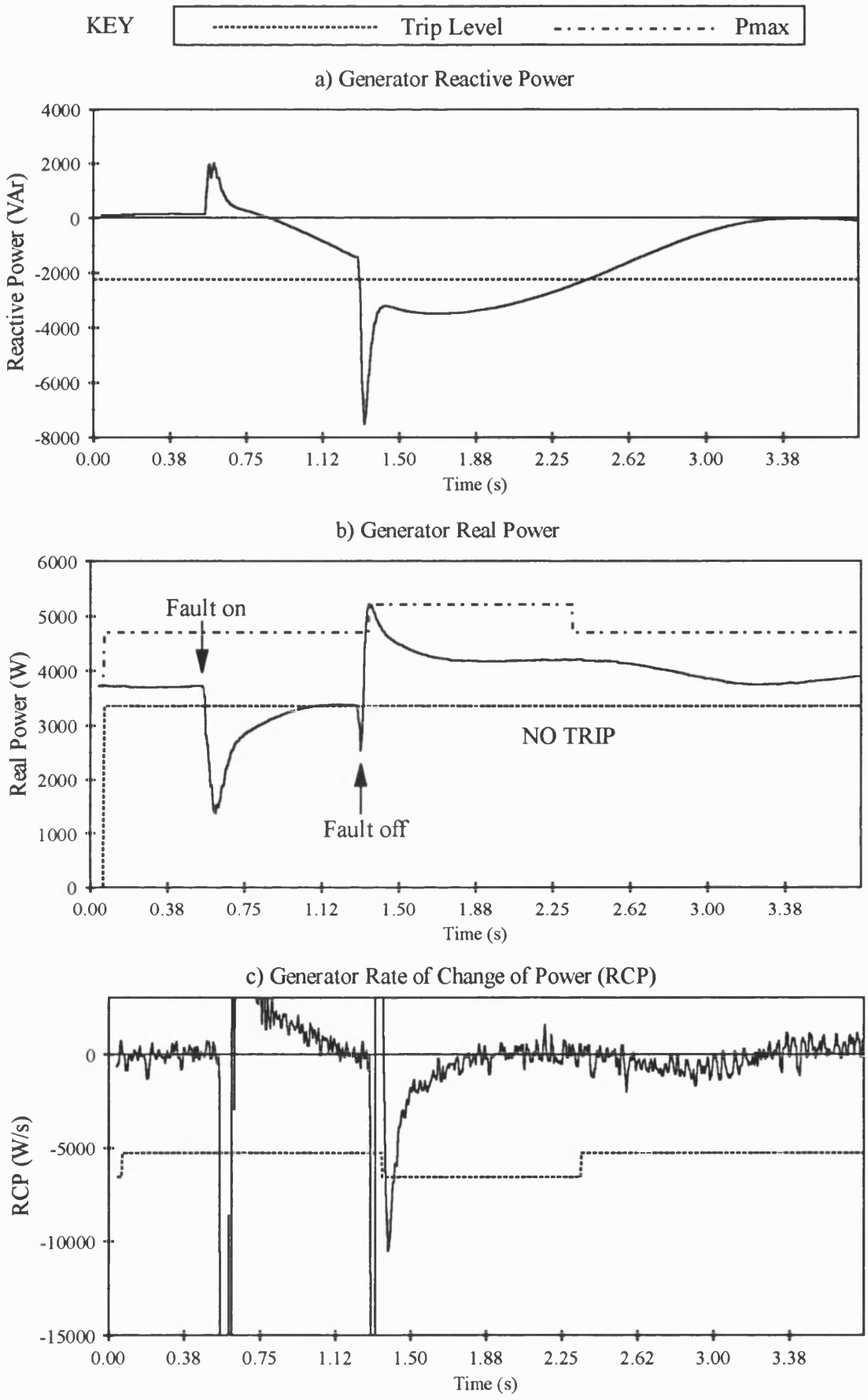

Figure 6.13

Pole Slipping Algorithm Response to a Three Phase to Earth Fault on the Laboratory Model Power System 5 kVA Generator, Generator Neutral Isolated - Test '5B'

6.14a
Impedance Diagram Showing 5 kVA Generator Single Blinder Scheme and Pole Slipping Loci for Test 4A - Pole Slipping After a Three Phase Fault.

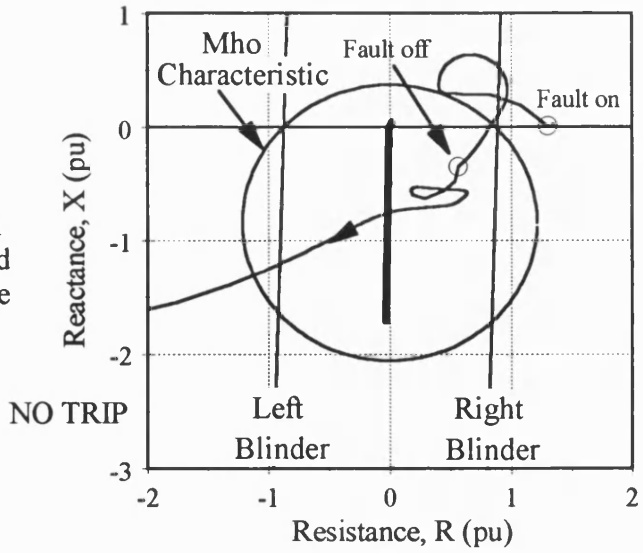

6.14b
Impedance Diagram Showing 5 kVA Generator Single Blinder Scheme and Pole Slipping Loci for Test E - Over Torque Pole Slip (low excitation).

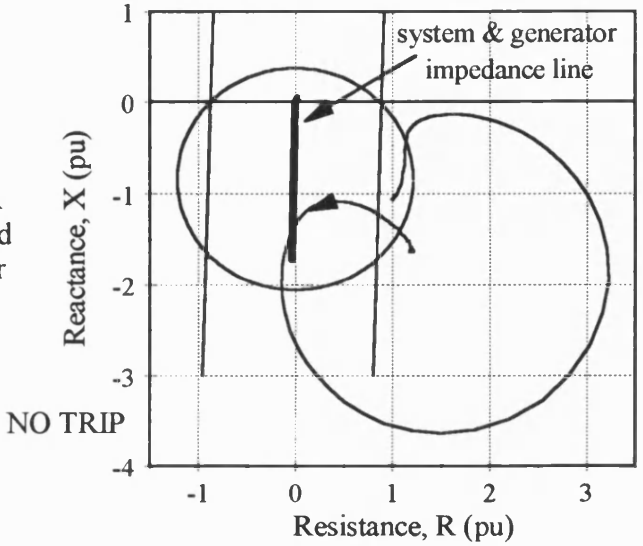

6.14c
Impedance Diagram Showing 5 kVA Generator Single Blinder Scheme and Pole Slipping Loci for Test G - Over Torque Pole Slip (high excitation).

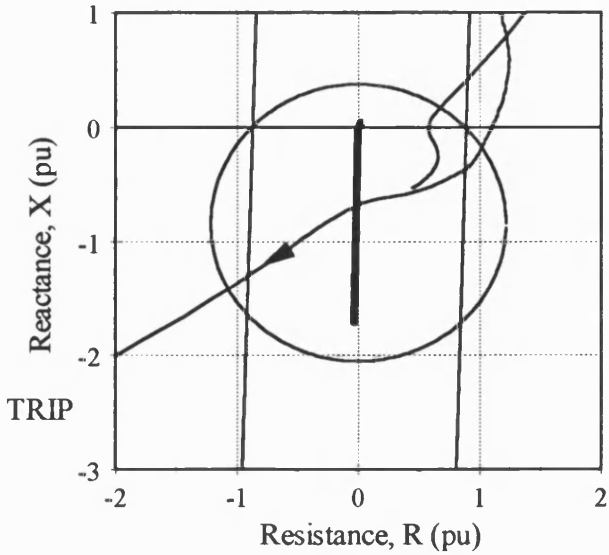

Figure 6.14
Single Blinder Pole Slipping Protection Scheme Characteristic for Laboratory 5 kVA Generator Pole Slipping Tests.

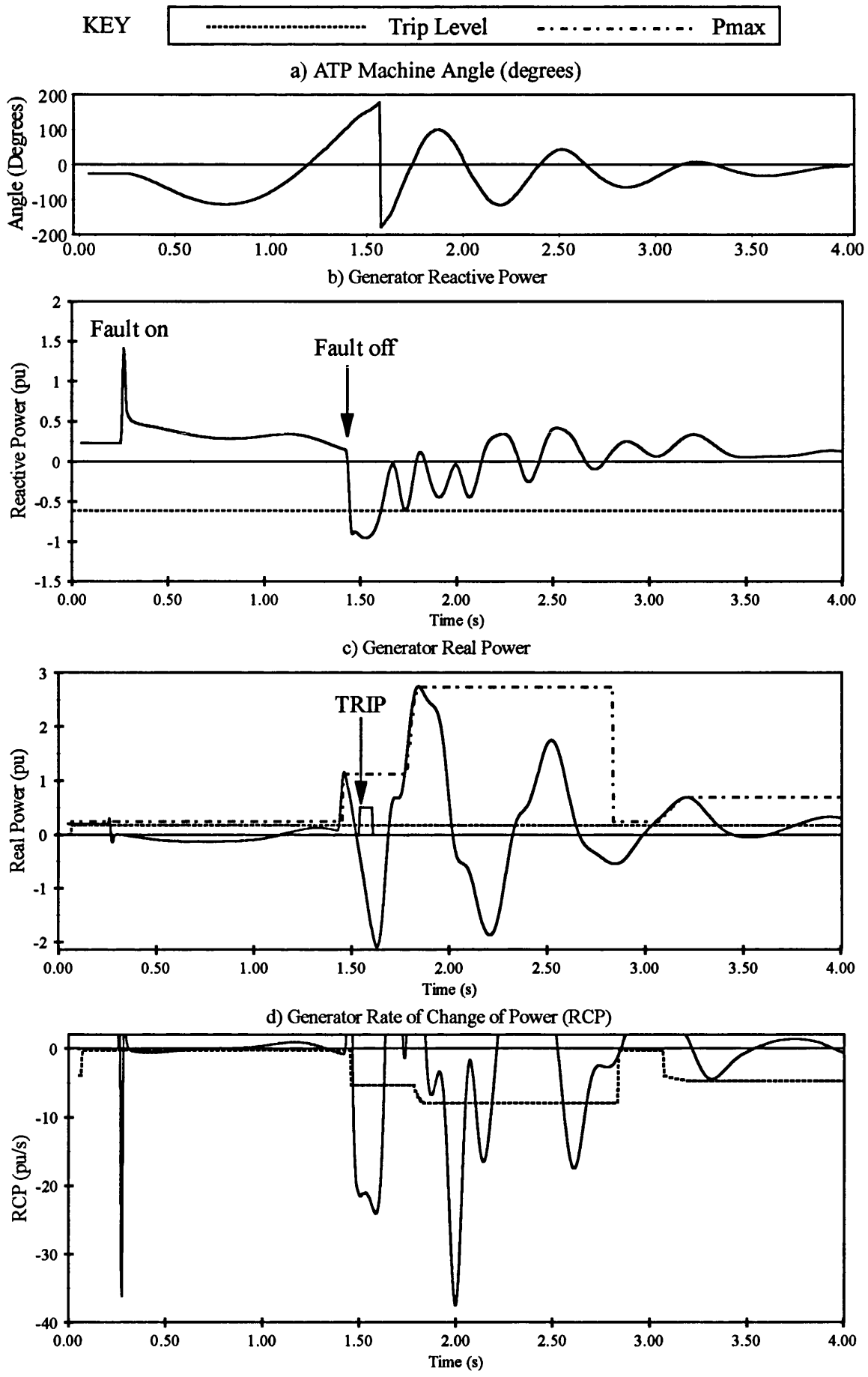

Figure 6.15

Pole Slipping Algorithm Response to Test 'PSL1GA' - Pole Slipping of a 200 MVA Generator Induced by a Fault from 20% Initial Load, AVR and Governor Modelled

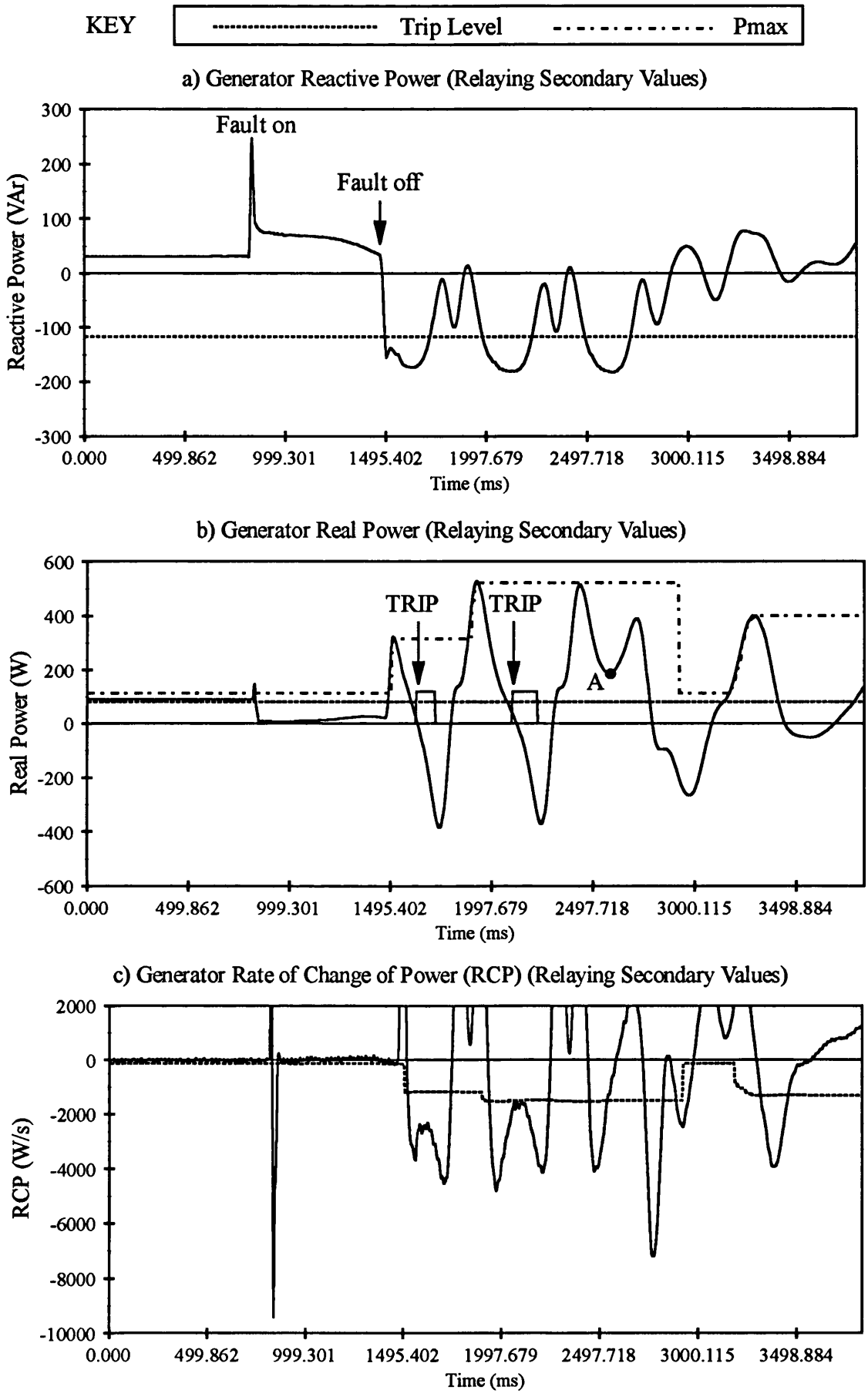

Figure 6.16

Pole Slipping Algorithm Response to PPSS Test ' PSL2GA' - Pole Slipping of a 200 MVA Generator, Induced by a 650 ms Three Phase Fault , Governor and AVR Modelled.

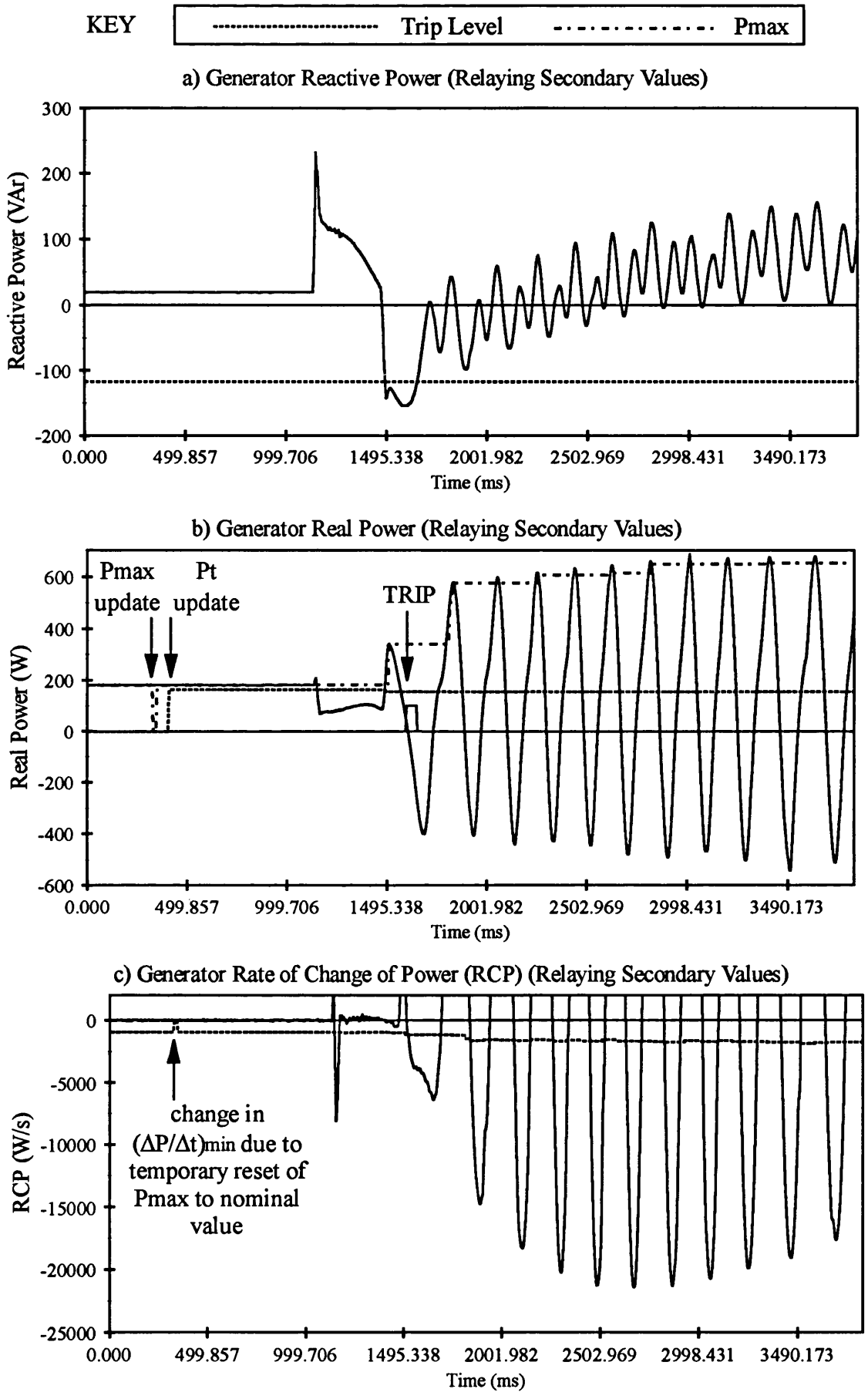

Figure 6.17

Pole Slipping Algorithm Response to PPSS Test ' PSL3GA' - Pole Slipping of a 200 MVA Generator, Induced by a 330 ms Two Phase to Earth Fault , Governor and AVR Modelled.

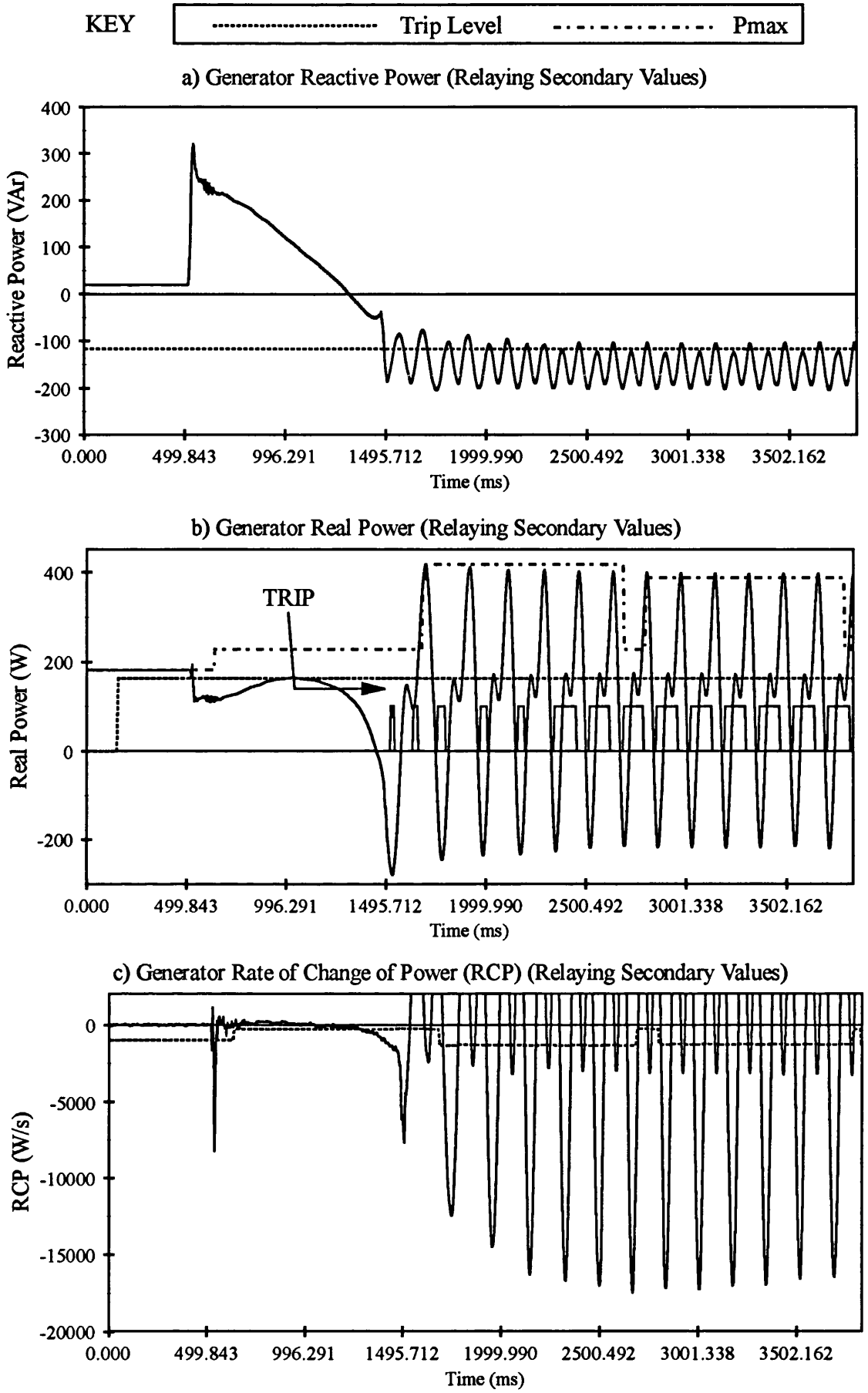

Figure 6.18

Pole Slipping Algorithm Response to PPSS Test ' PSL3GN' - Pole Slipping of a 200 MVA Generator, Induced by a 950 ms Two Phase Fault , AVR not Modelled, Governor Modelled.

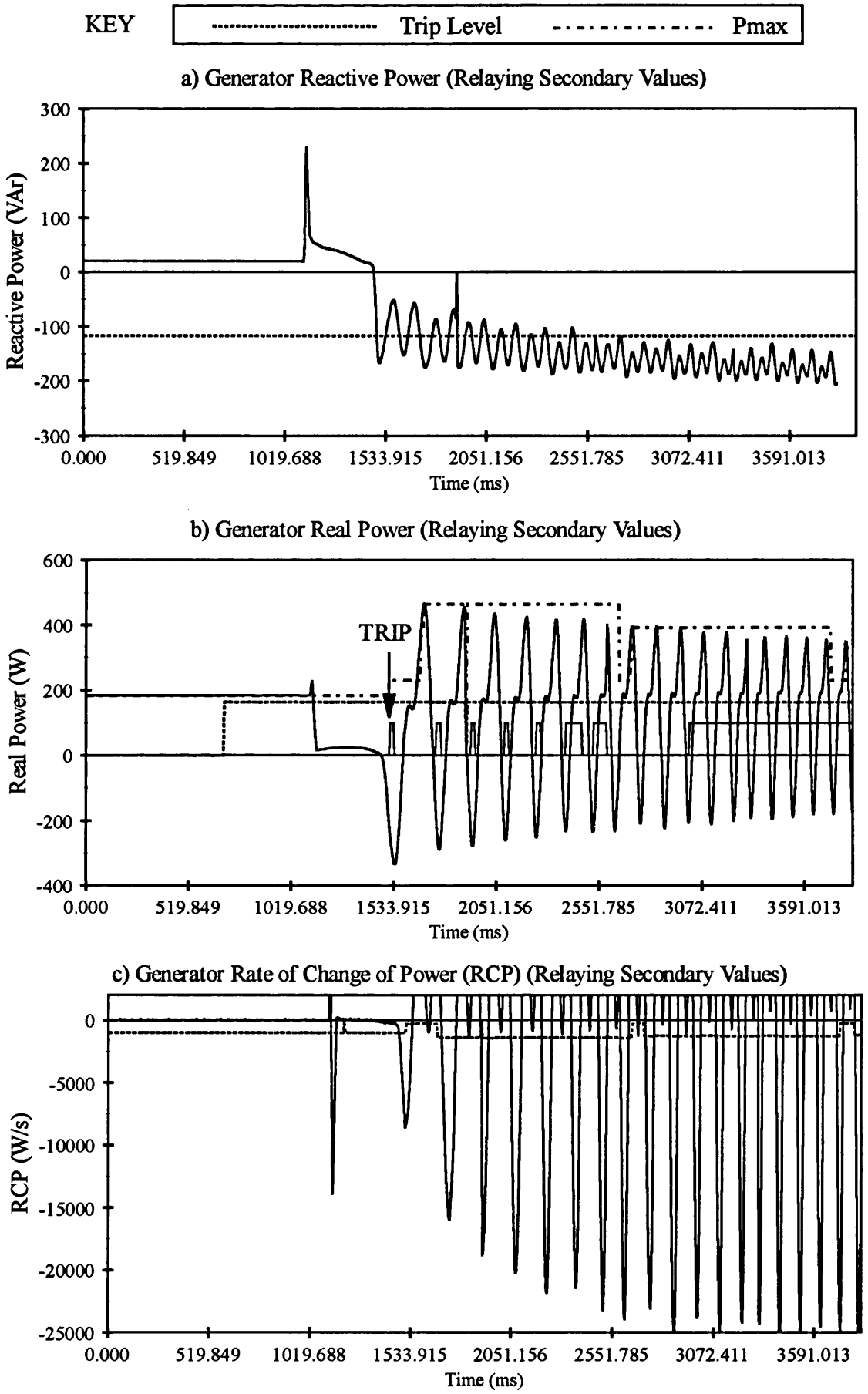

Figure 6.19

Pole Slipping Algorithm Response to PPSS Test ' PSL3NN' - Pole Slipping of a 200 MVA Generator, Induced by a 350 ms Three Phase Fault , No Governor or AVR Modelled.

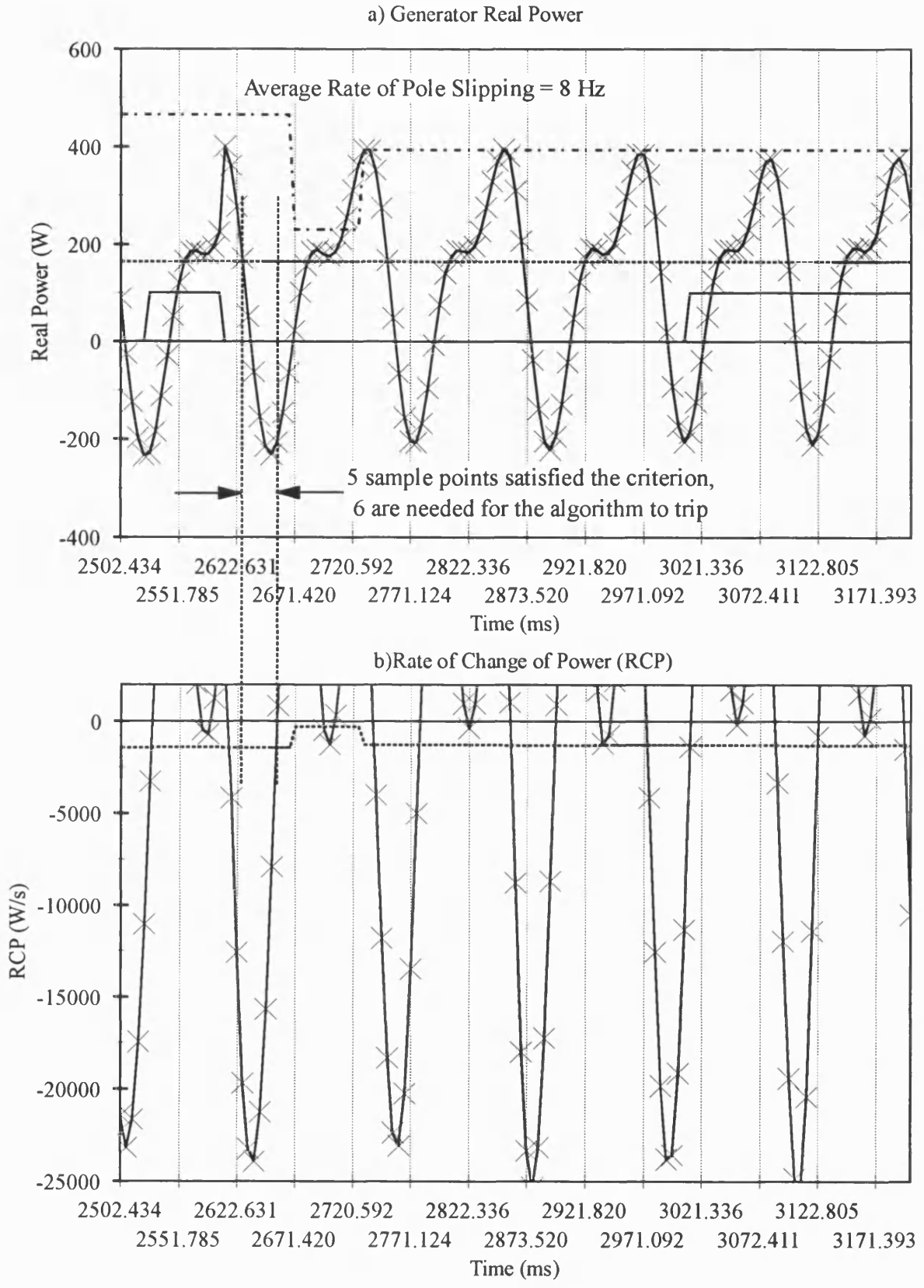

Figure 6.20
Expaned Graphs from PPSS Test ' PSL3NN' Showing That the Algorithm Failed to Detect Some of the Later Pole Slips Due to a Pole Slipping Rate of 8.0 Hz.

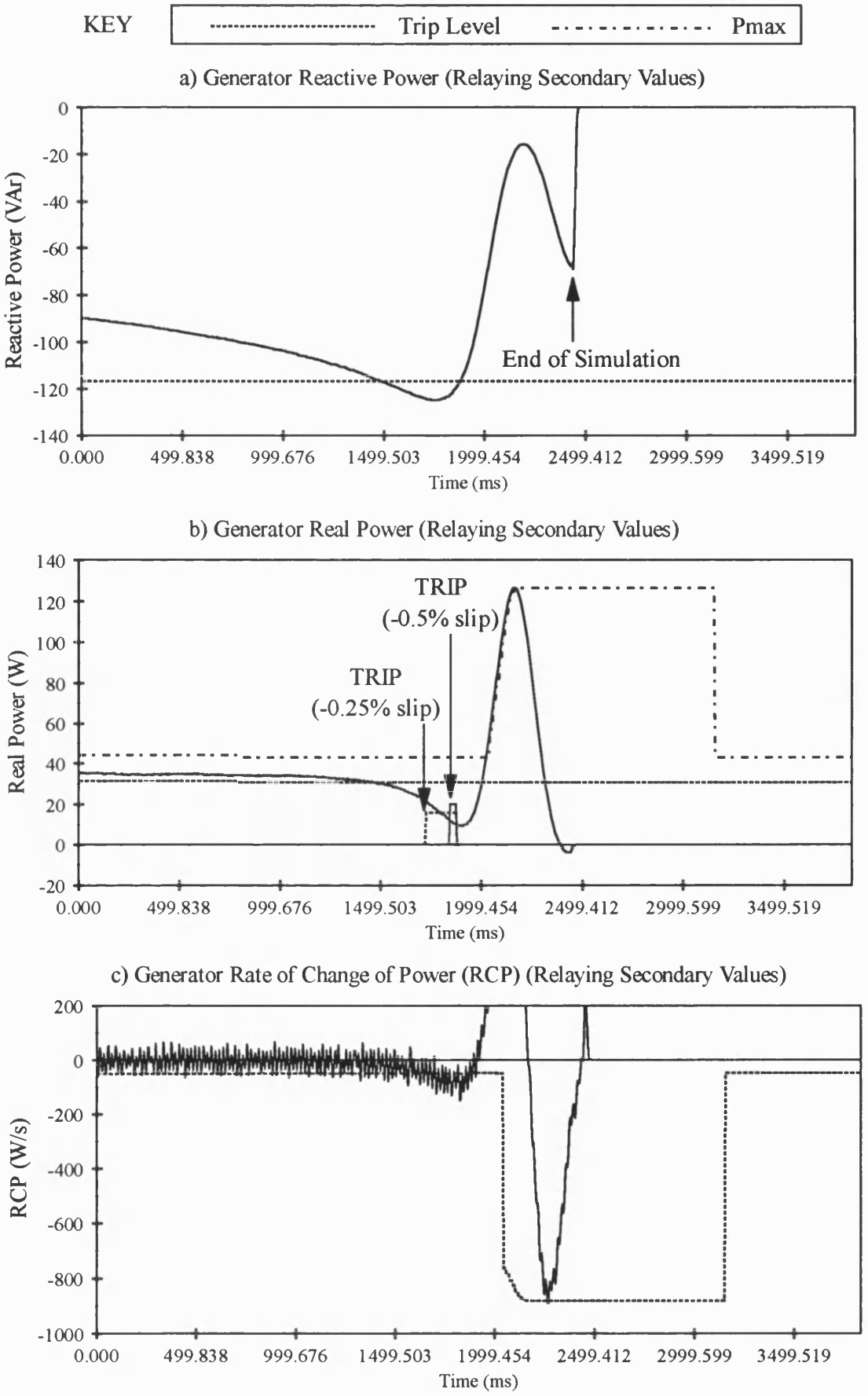

Figure 6.21

Pole Slipping Algorithm Response to PPSS Test ' PSL1GAF' - Pole Slipping of a 200 MVA Generator, Induced by Setting the AVR Reference Voltage to 5% pu, Governor & AVR Modelled.

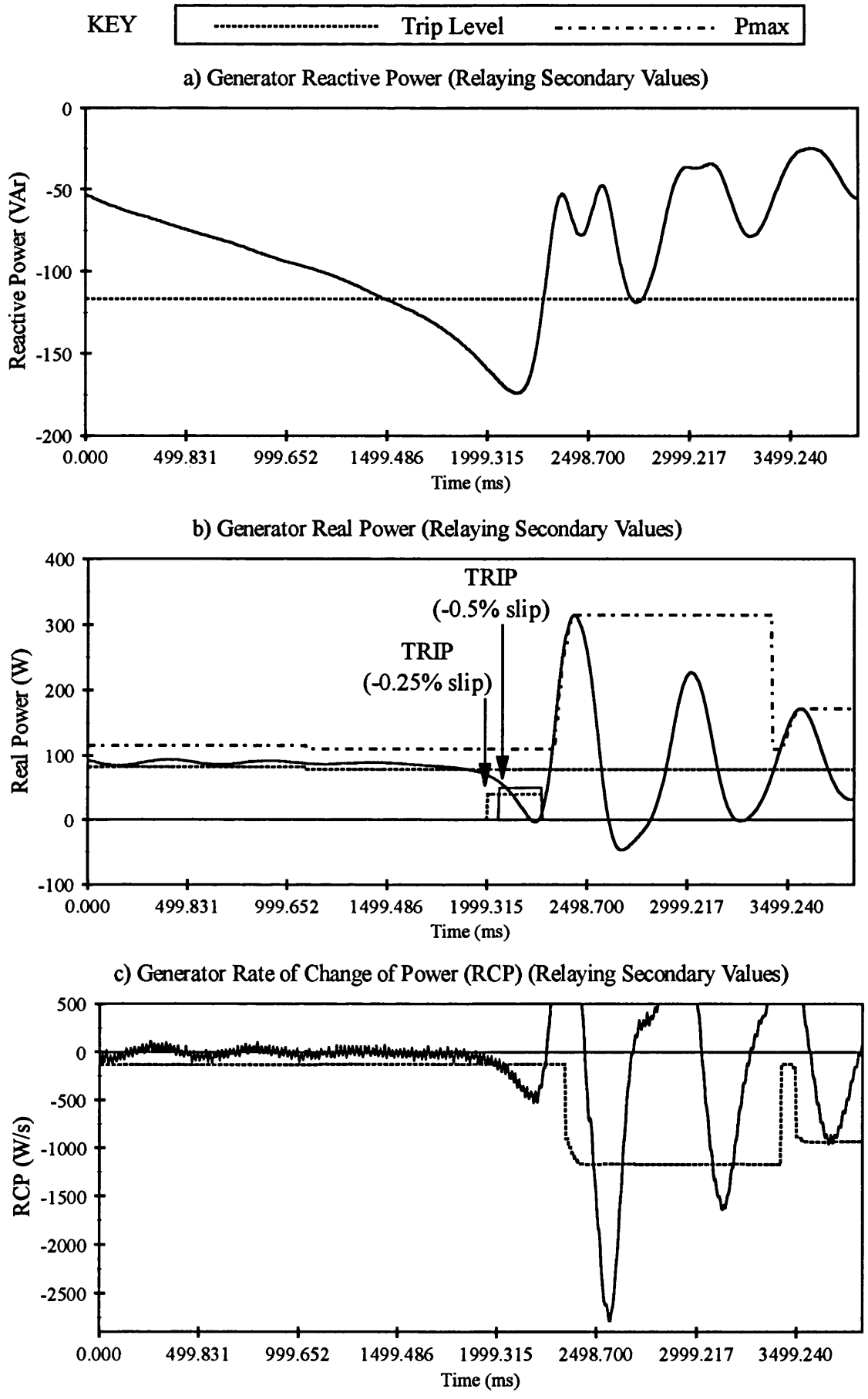

Figure 6.22

Pole Slipping Algorithm Response to PPSS Test ' PSL2GAF' - Pole Slipping of a 200 MVA Generator, Induced by Setting AVR Reference Voltage to 50 % Rated, Governor and AVR Modelled.

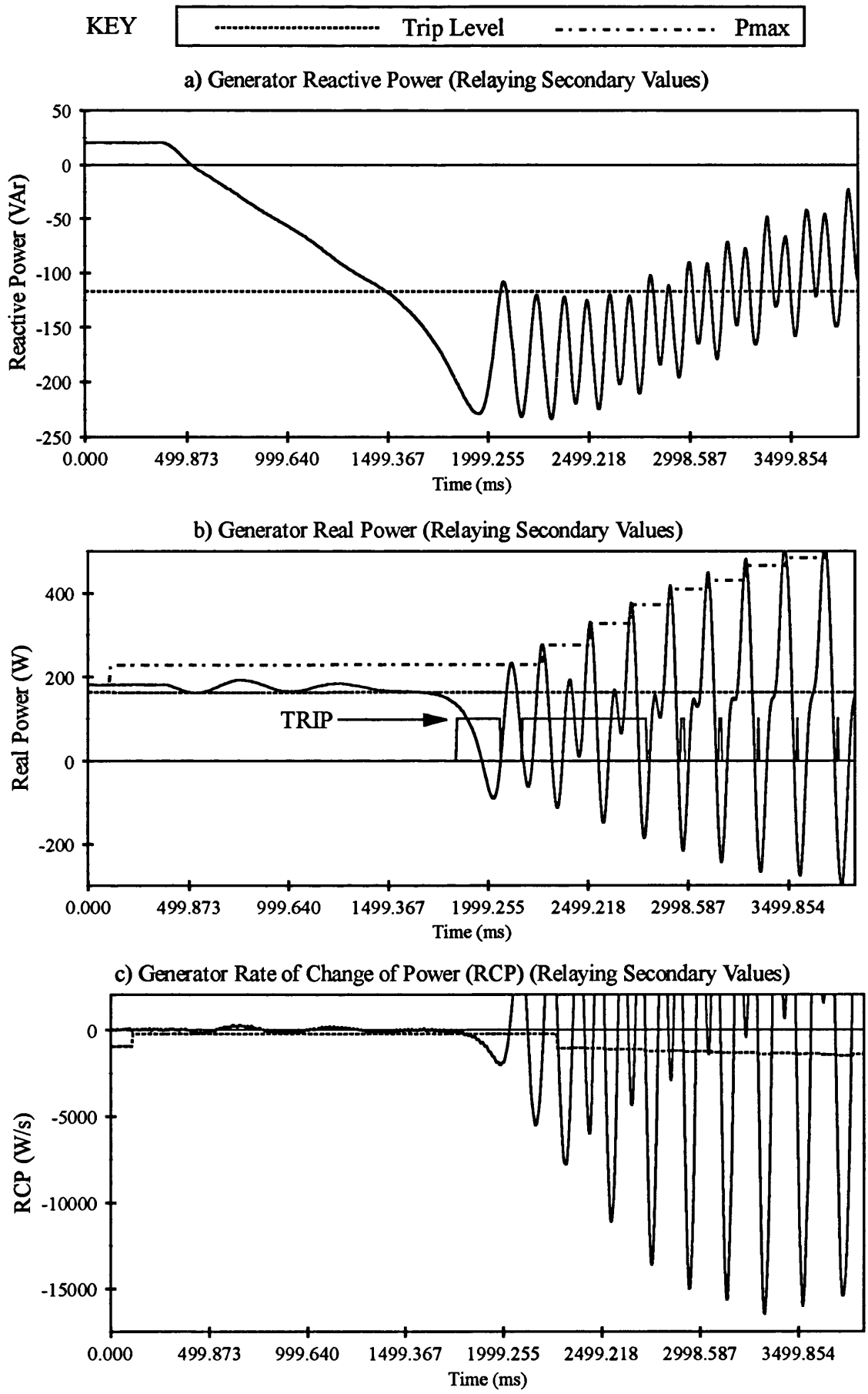

Figure 6.23

Pole Slipping Algorithm Response to PPSS Test ' PSL3GAF' - Pole Slipping of a 200 MVA Generator, Induced by Setting AVR Reference Voltage to 80 % pu, Governor and AVR Modelled.

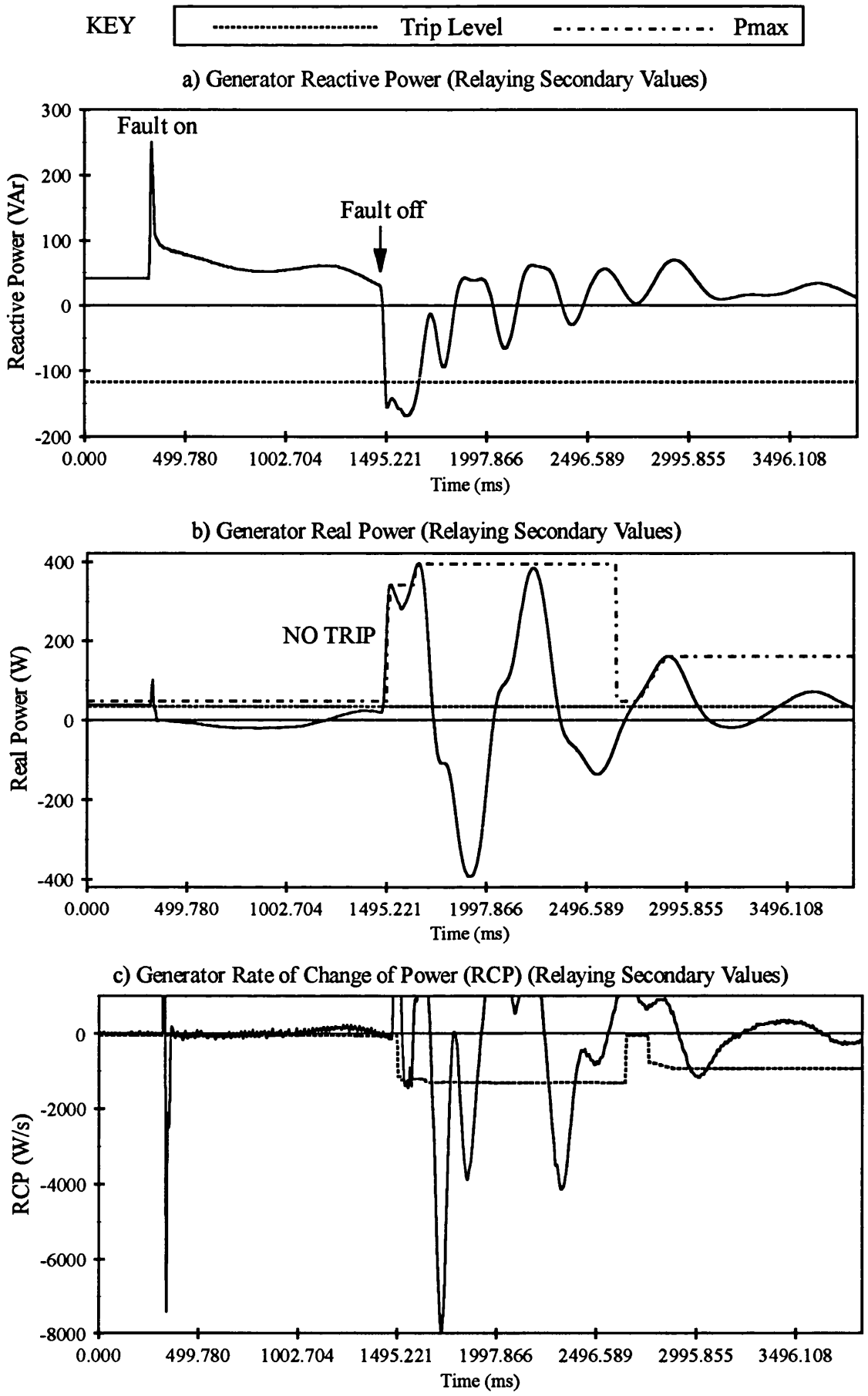

Figure 6.24

Pole Slipping Algorithm Response to PPSS Test ' PSW1GA' - Stable Power Swinging of a 200 MVA Generator, Induced by a 1150 ms Three Phase Fault , Governor and AVR Modelled.

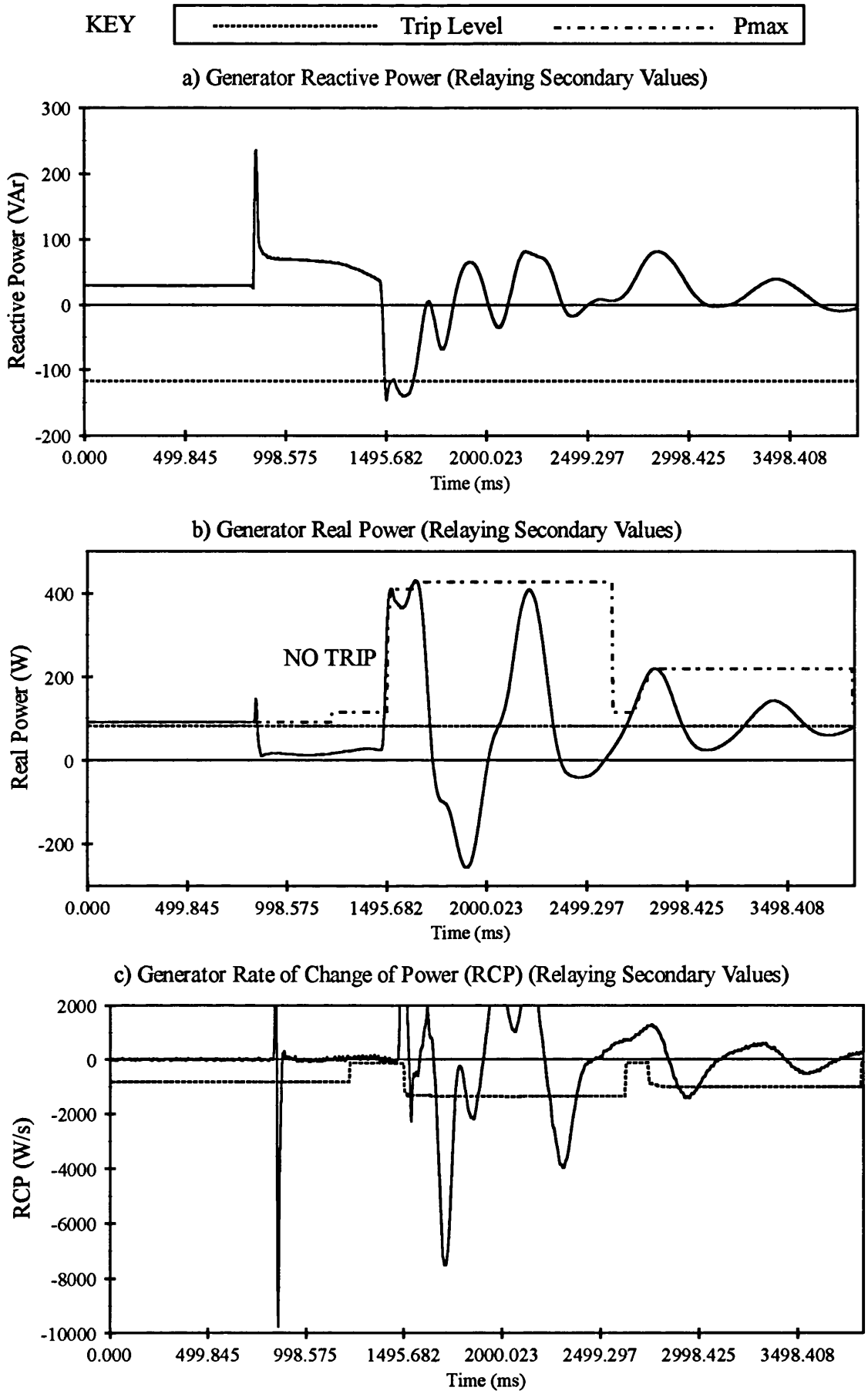

Figure 6.25

Pole Slipping Algorithm Response to PPSS Test ' PSW2GA' - Stable Power Swinging of a 200 MVA Generator, Induced by a 630 ms Three Phase Fault , Governor and AVR Modelled.

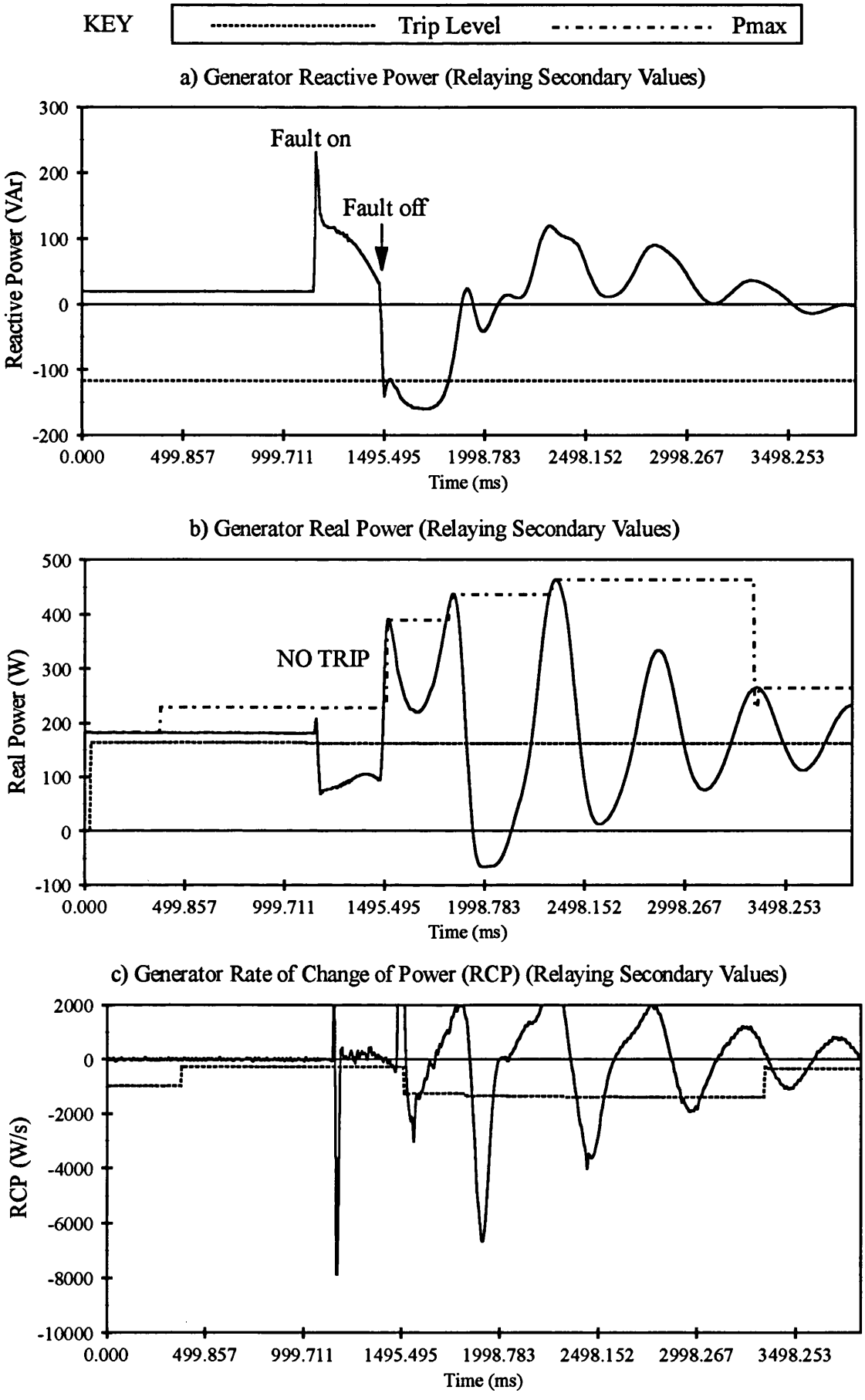

Figure 6.26

Pole Slipping Algorithm Response to PPSS Test ' PSW3GA' - Stable Power Swinging of a 200 MVA Generator, Induced by a 320 ms Two Phase to Earth Fault , Governor and AVR Modelled.

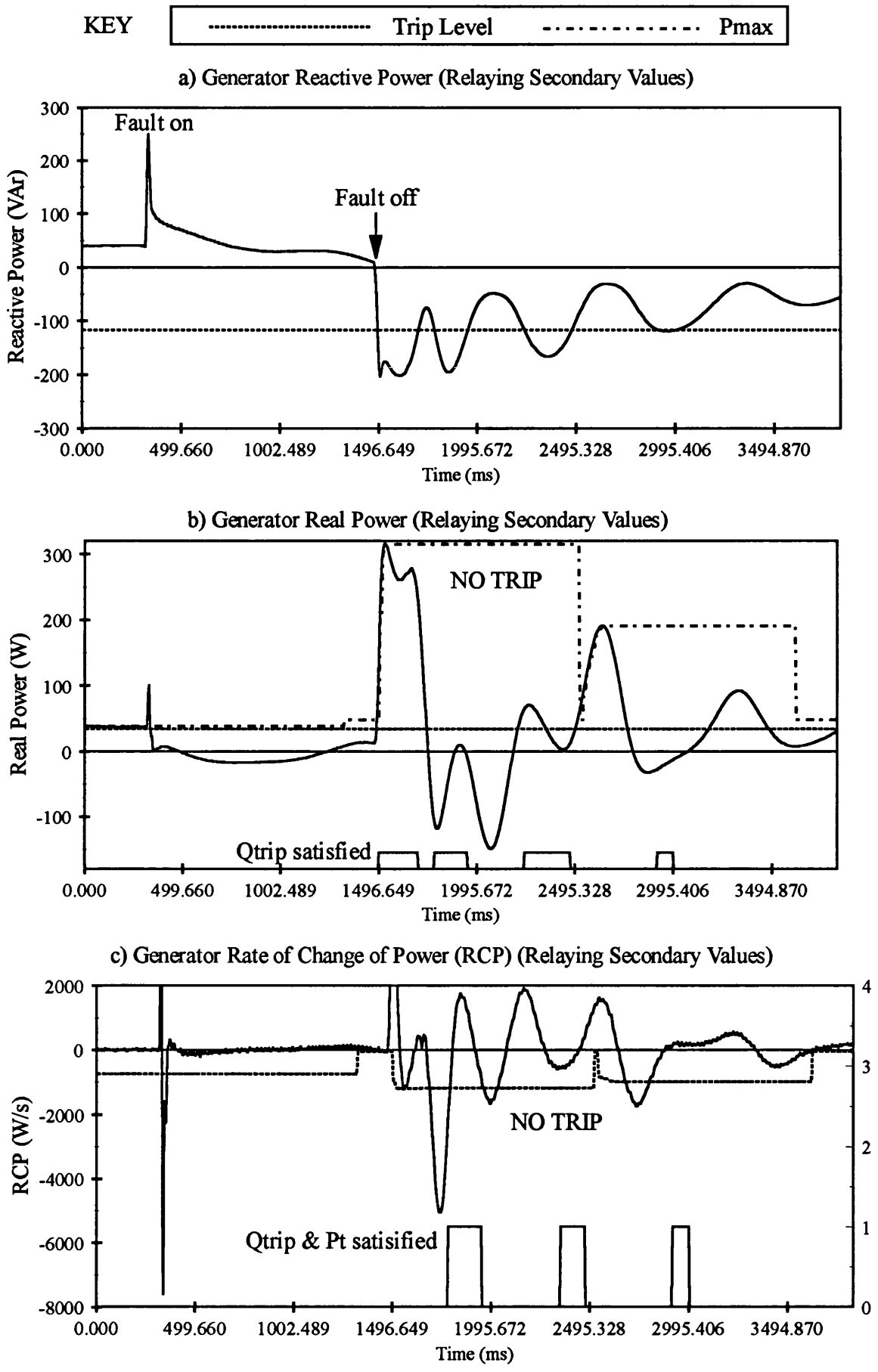

Figure 6.27

Pole Slipping Algorithm Response to PPSS Test ' PSW1GN' - Stable Power Swinging of a 200 MVA Generator, Induced by a 1155 ms Three Phase Fault , AVR Out of Service.

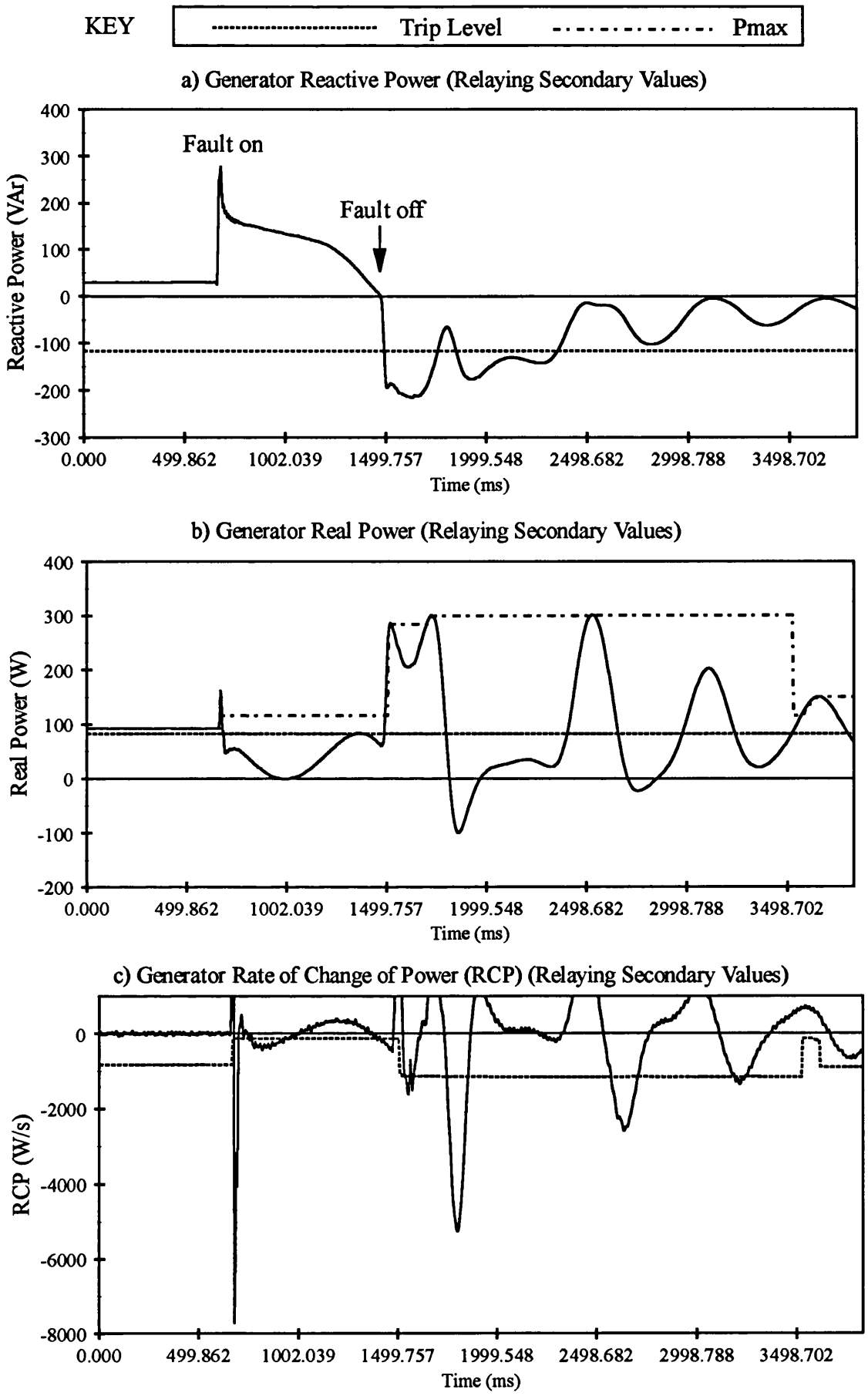

Figure 6.28

Pole Slipping Algorithm Response to PPSS Test ' PSW2GN' - Stable Power Swinging of a 200 MVA Generator, Induced by a 810 ms Two Phase to Earth Fault, AVR Out of Service.

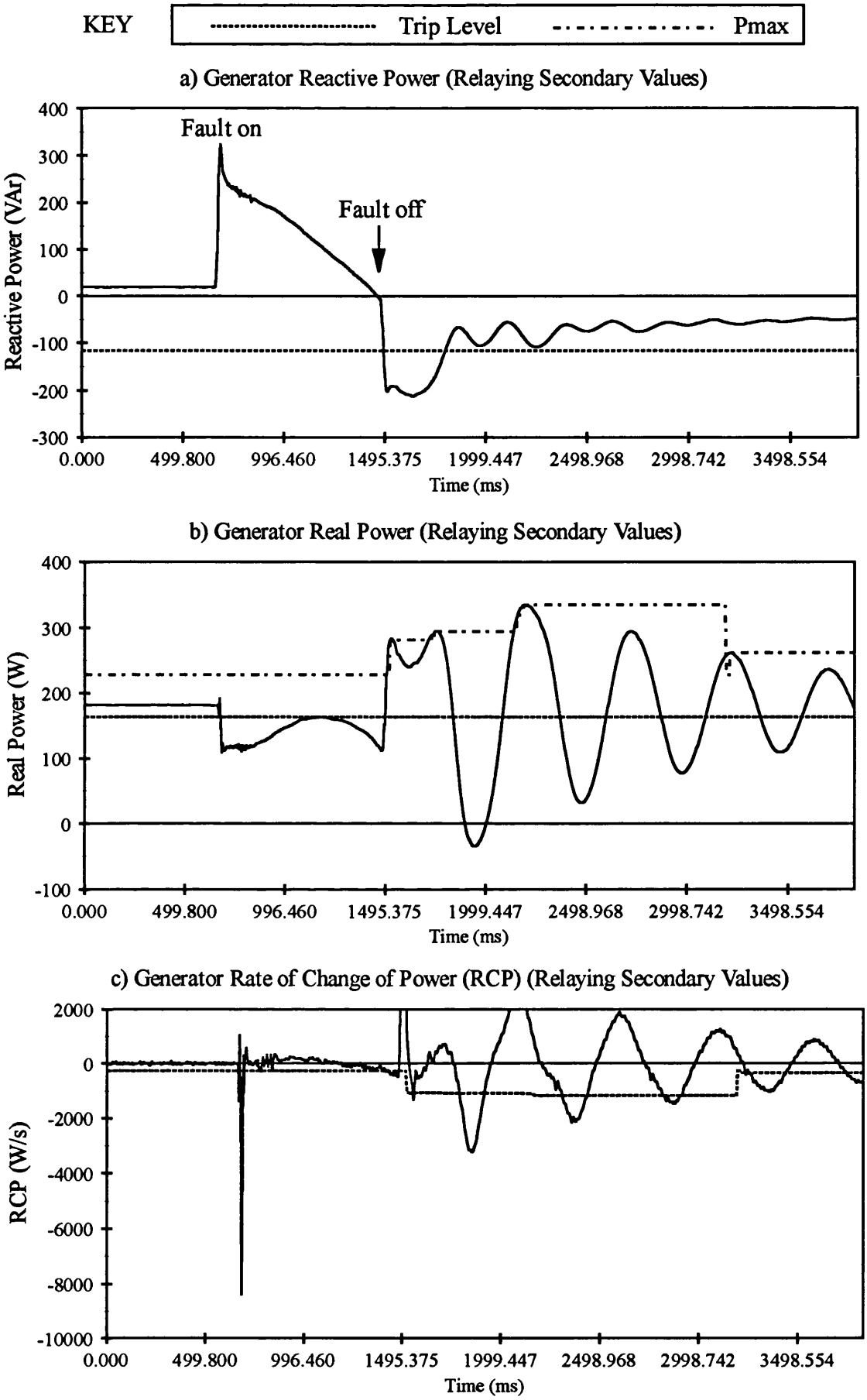

Figure 6.29

Pole Slipping Algorithm Response to PPSS Test ' PSW3GN' - Stable Power Swinging of a 200 MVA Generator, Induced by a 820 ms Two Phase Fault , AVR Out of Service.

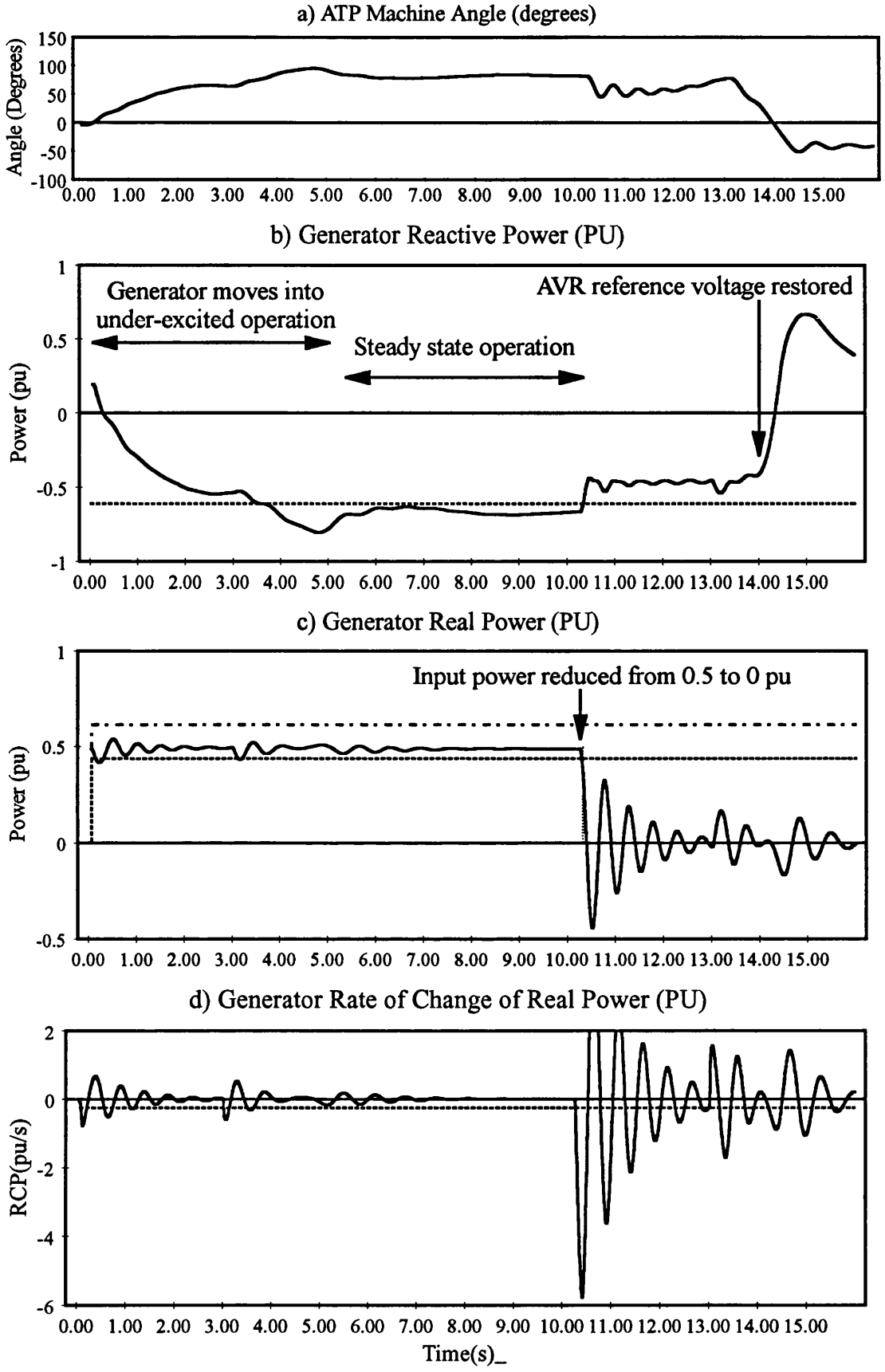

Figure 6.30

Pole Slipping Algorithm Response to Test D2 (AVR5NA) Generator Operation Absorbing System VArs Using A Fast AVR.

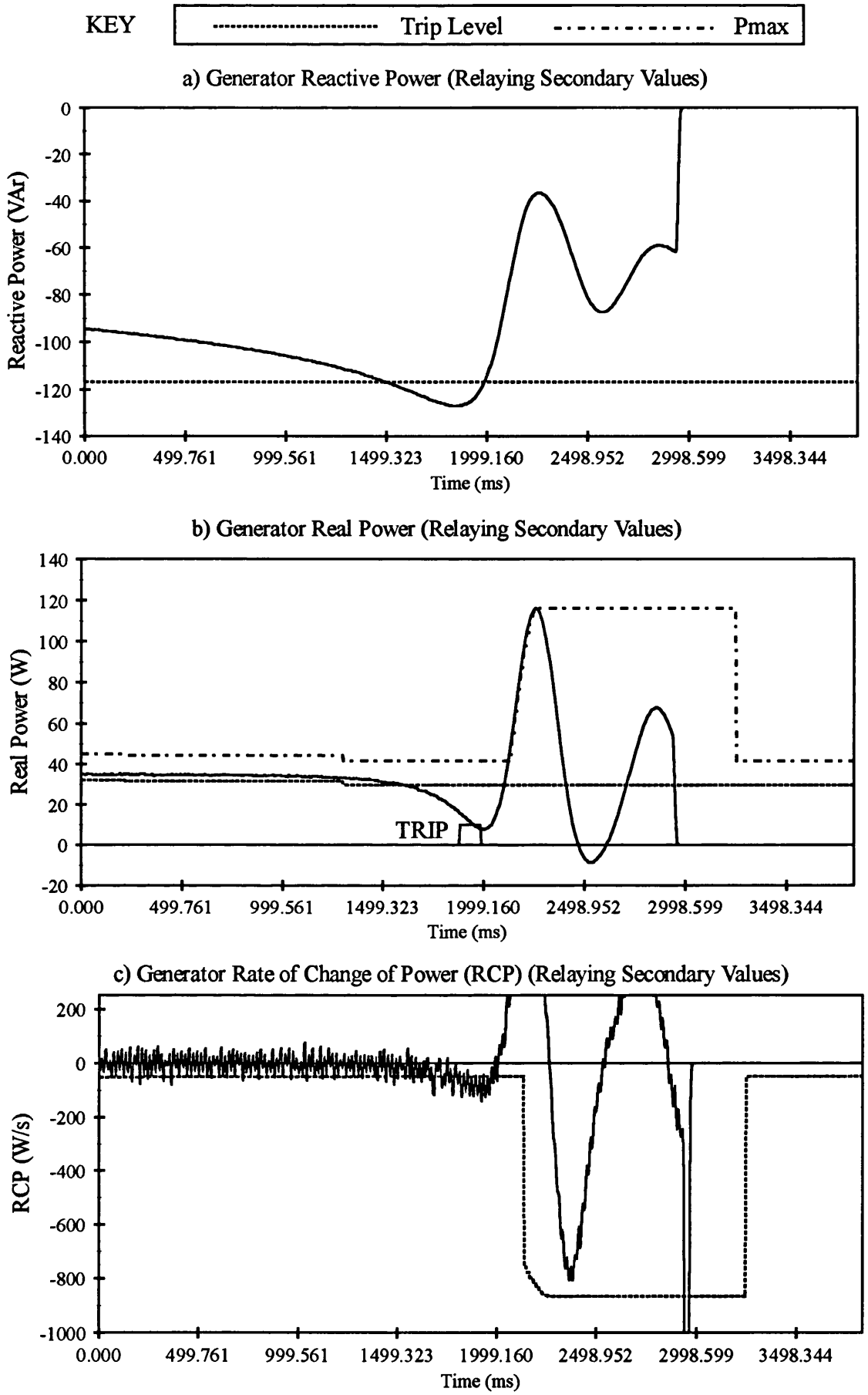

Figure 6.31
Pole Slipping Algorithm Response to PPSS Test ' LOF1GA'
Loss of Field on a 200 MVA Generator, Governor Modelled.

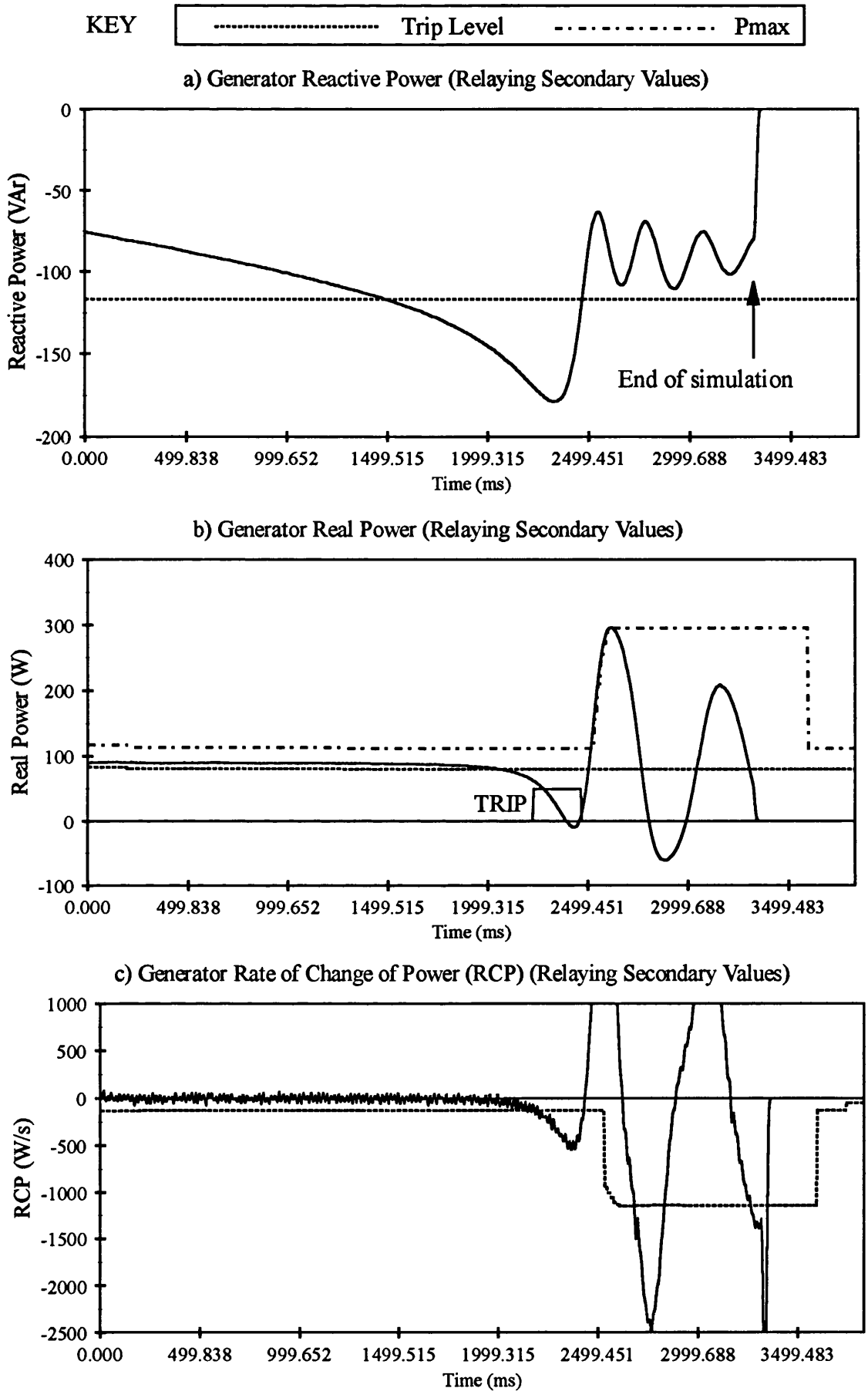

Figure 6.32
Pole Slipping Algorithm Response to PPSS Test ' LOF2GA'
Loss of Field on a 200 MVA Generator, Governor Modelled.

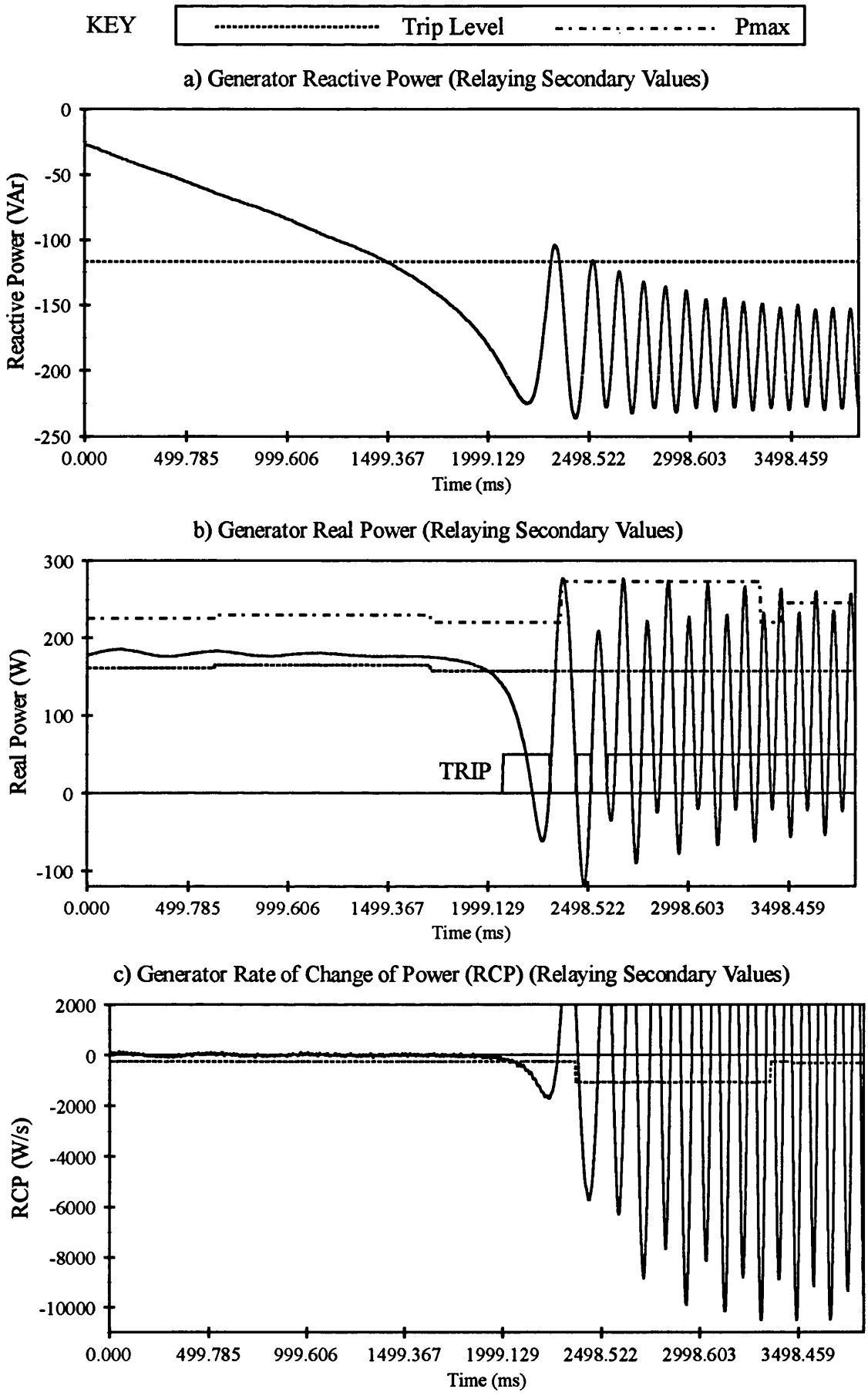

Figure 6.33
Pole Slipping Algorithm Response to PPSS Test ' LOF3GA'
Loss of Field on a 200 MVA Generator, Governor Modelled.

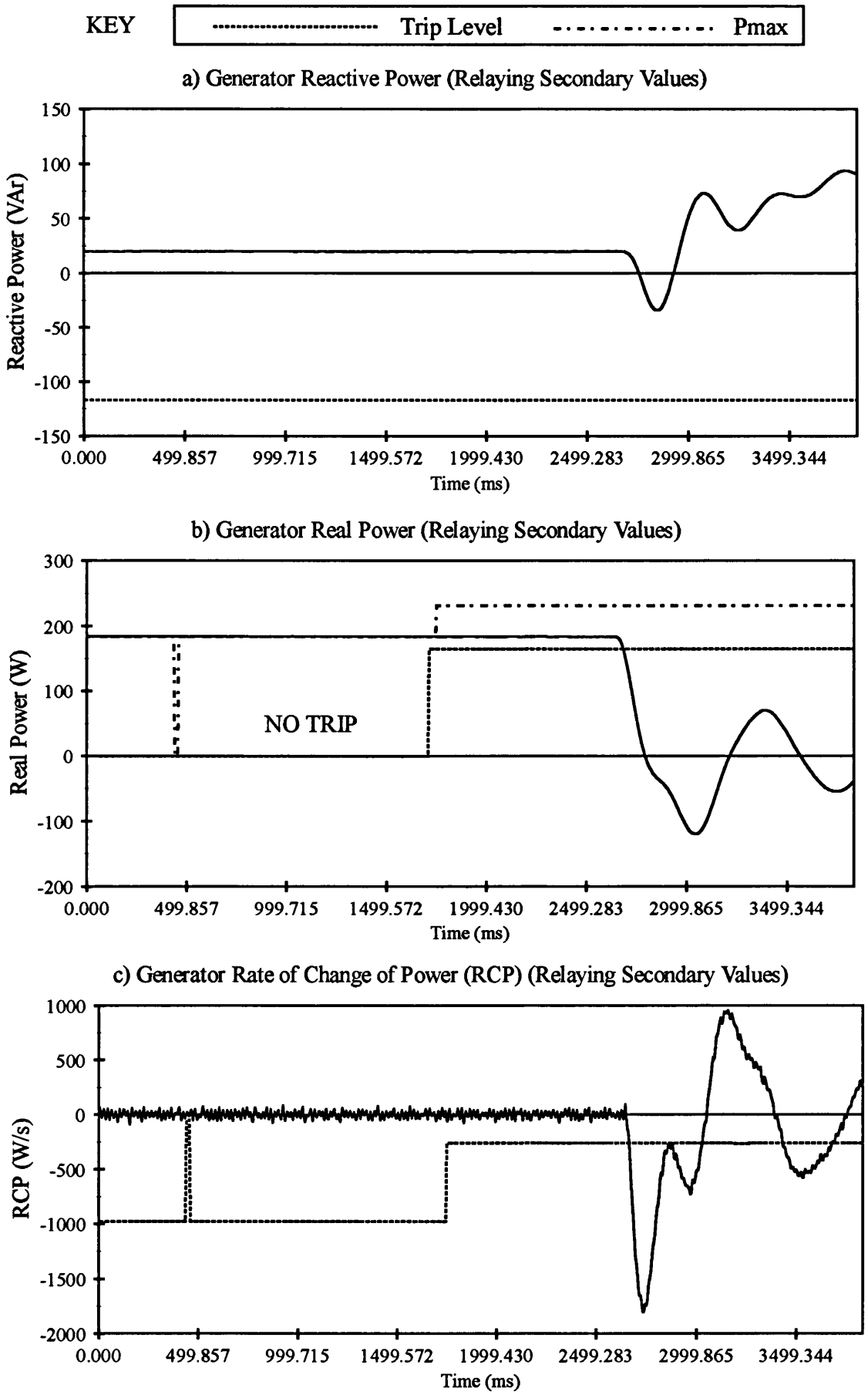

Figure 6.34
Pole Slipping Algorithm Response to PPSS Test ' LOP3NA'
Loss of Prime Mover of a 200 MVA Generator, AVR Modelled.

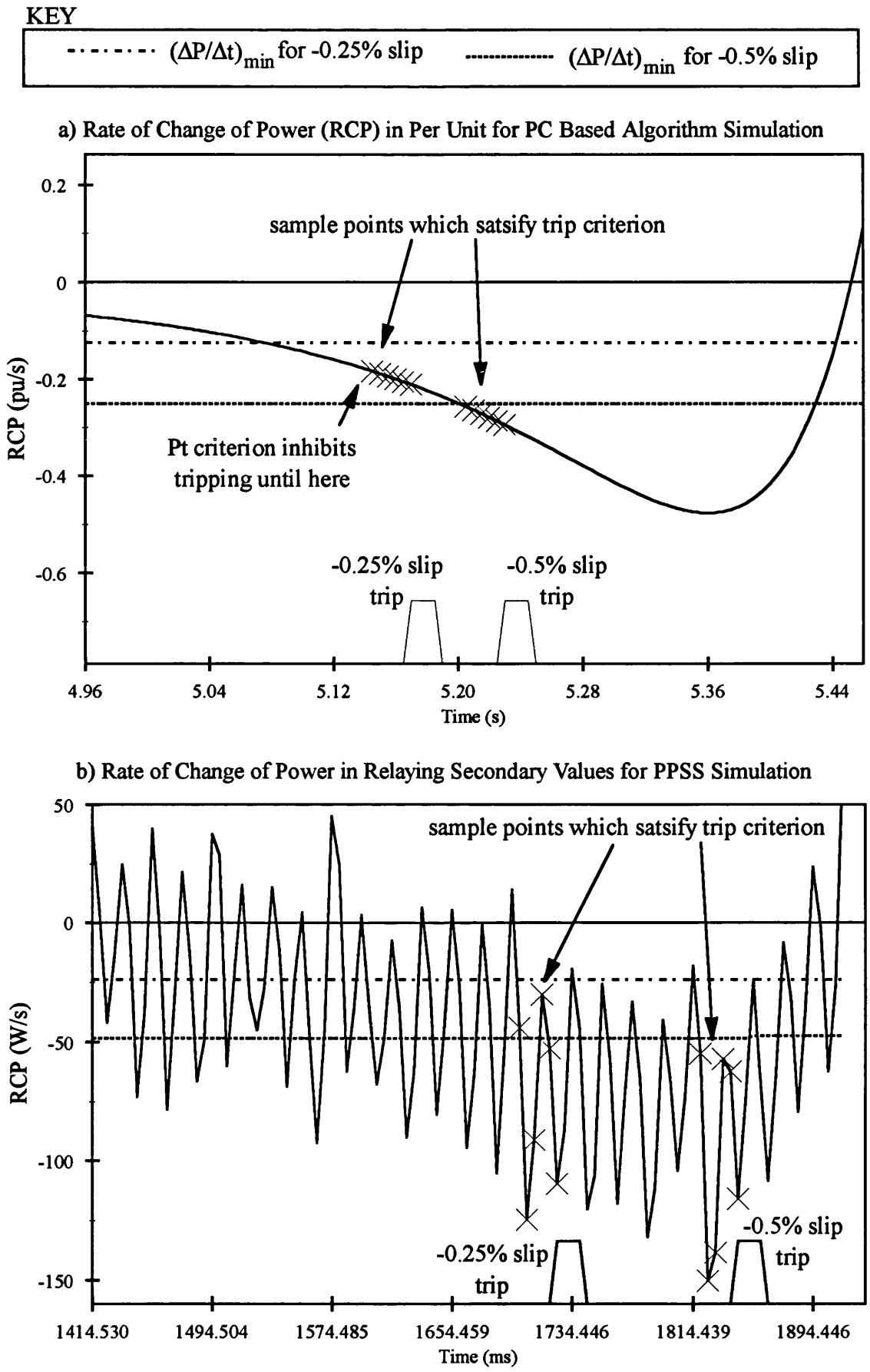

Figure 6.35
Graphs Showing Rate of Change of Power Criterion Trip Points for test 'PSL1GAF' for PPSS and PC Based Algorithm Test Systems.

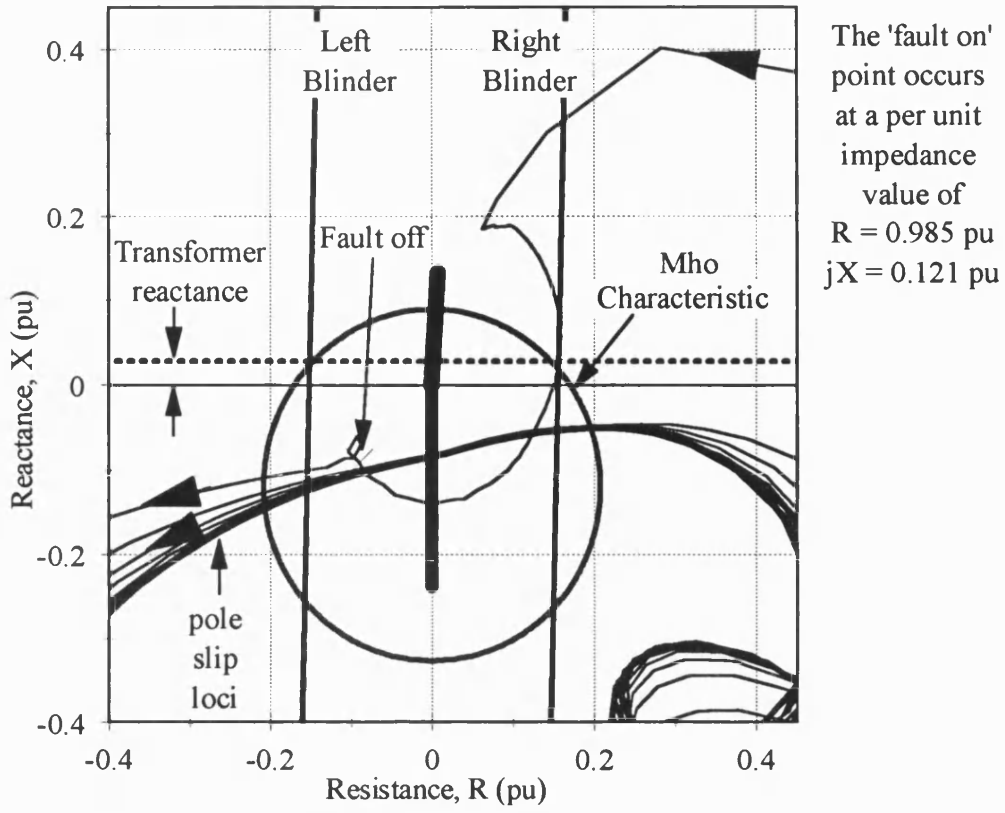

Figure 6.36
Impedance Diagram Showing 200 MVA Generator Single Blinder Pole Slipping Protection Scheme and Pole Slipping Loci for Test 'PSL3GN'

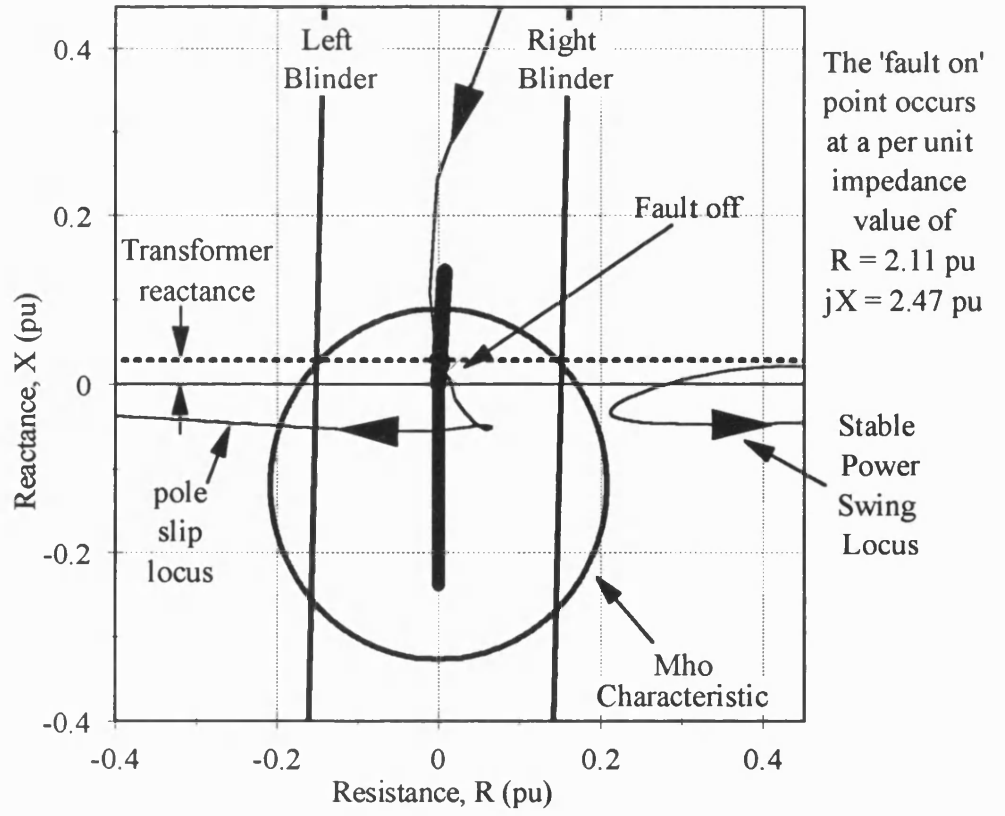

Figure 6.37
Impedance Diagram Showing 200 MVA Generator Single Blinder Pole Slipping Protection Scheme and Pole Slipping Locus for Test 'PSL1GA'

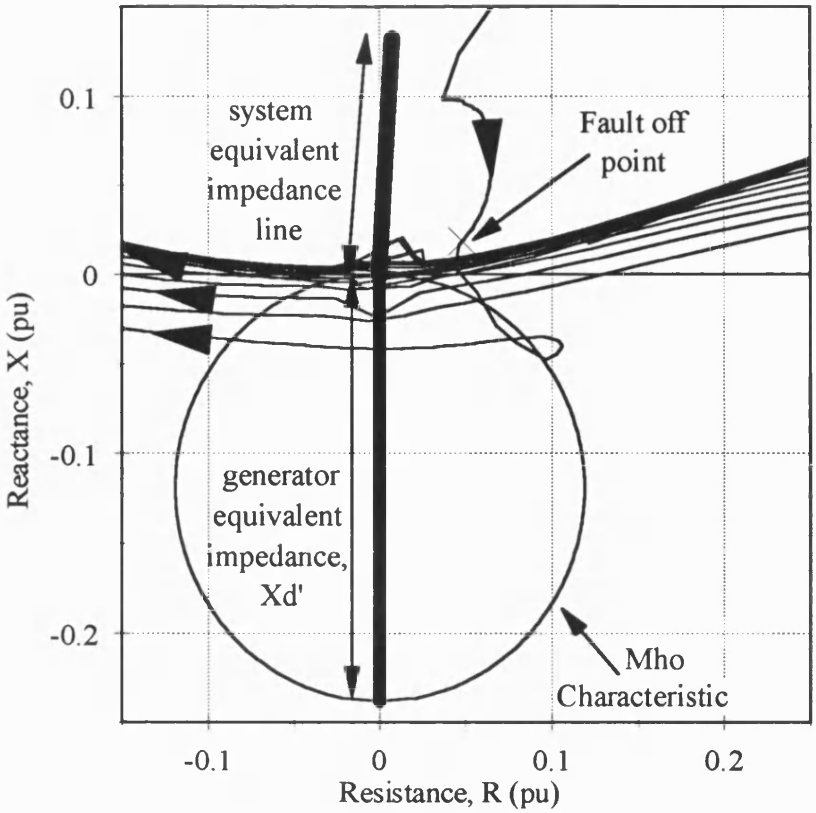

The 'fault on' point occurs at a per unit impedance value of
R = 0.985 pu
jX = 0.121 pu

Figure 6.38
Impedance Diagram Showing 200 MVA Generator Mho Pole Slipping Protection Scheme Characteristic and Pole Slipping Loci for Test 'PSL3GA'

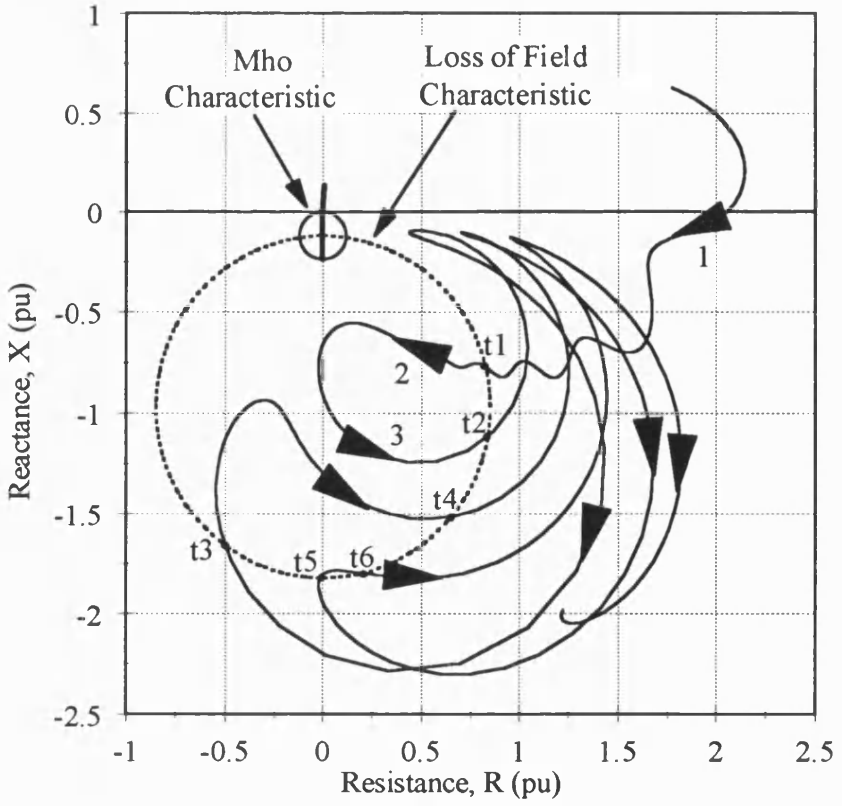

t1 = 1.99 s
t2 = 3.47 s
t3 = 3.79 s
t4 = 4.02 s
t5 = 4.44 s
t6 = 4.48 s

t1 to t2 represents the poleslip locus

t2 to t6 respresent stable power swings

Figure 6.39
Impedance Diagram Showing 200 MVA Generator Mho Pole Slipping Protection Scheme Characteristic and Pole Slipping Locus for Test 'PSL2GAF'

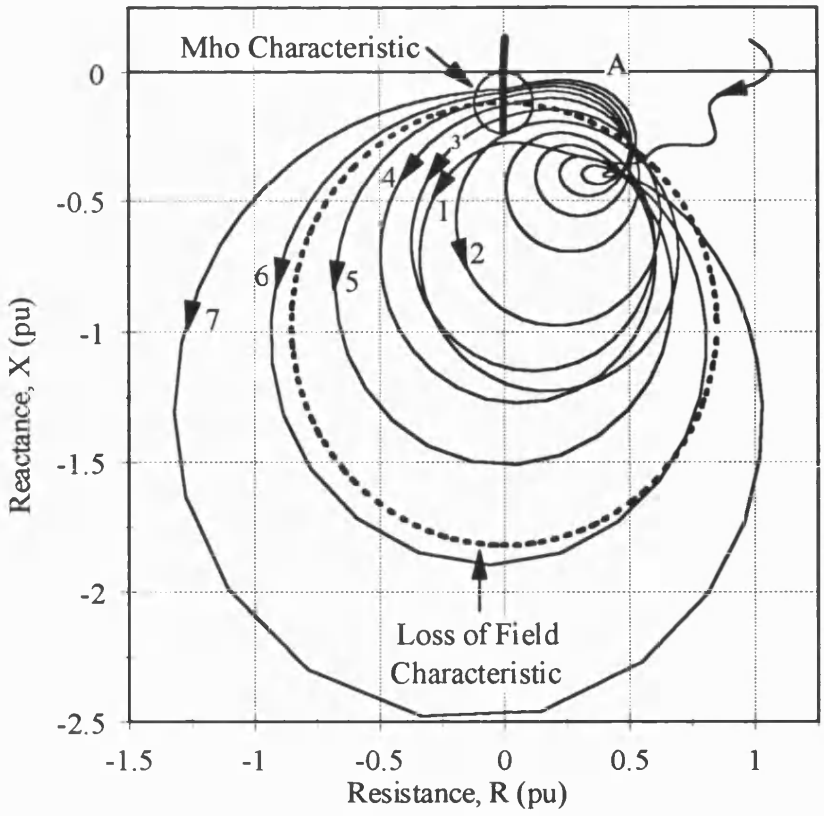

Figure 6.40
Impedance Diagram Showing 200 MVA Generator Loss of Field Protection Scheme Characteristic and Pole Slipping Loci for Test 'PSL3GAF'

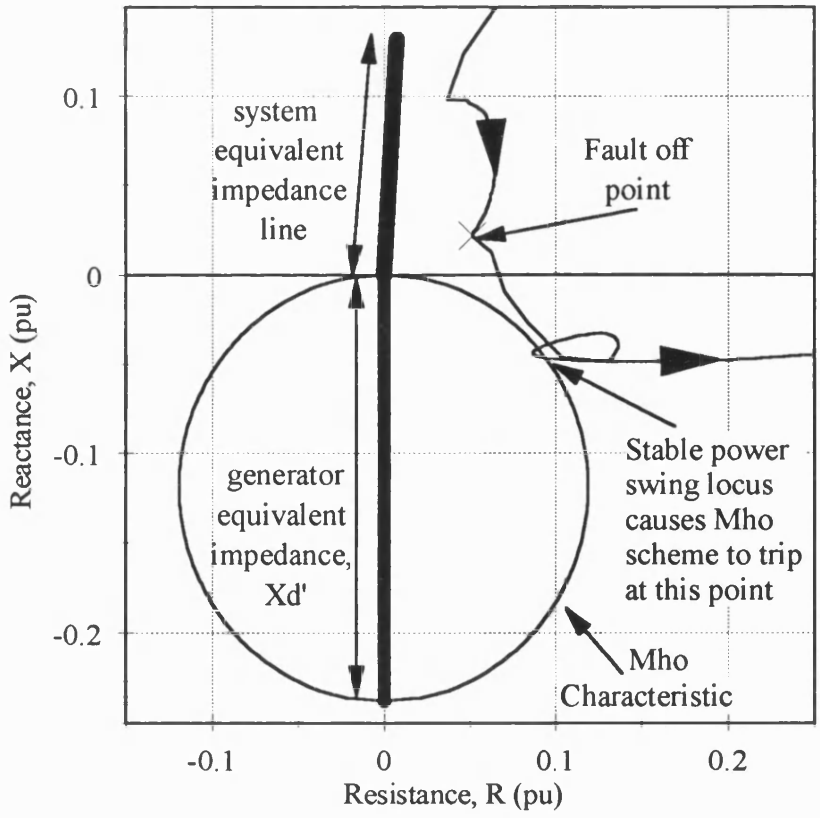

Figure 6.41
Impedance Diagram Showing 200 MVA Generator Mho Pole Slipping Protection Scheme Characteristic and Power Swing Locus for Test 'PSW3GA'

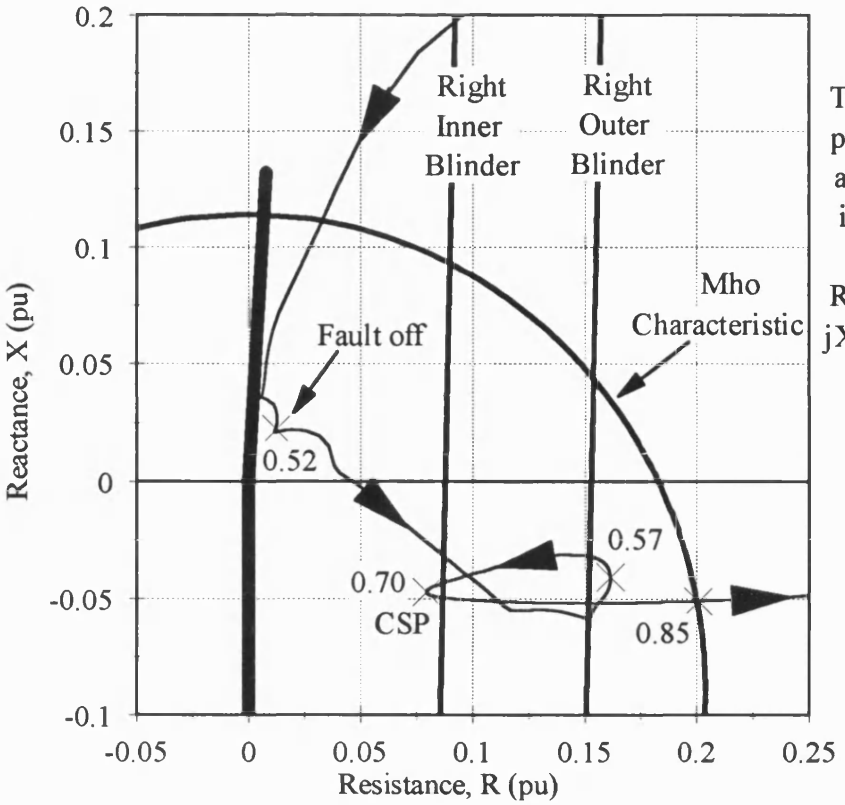

Figure 6.42

Impedance Diagram Showing 200 MVA Generator Double Blinder Scheme and Power Swing Loci for Test 'PSW3NA'

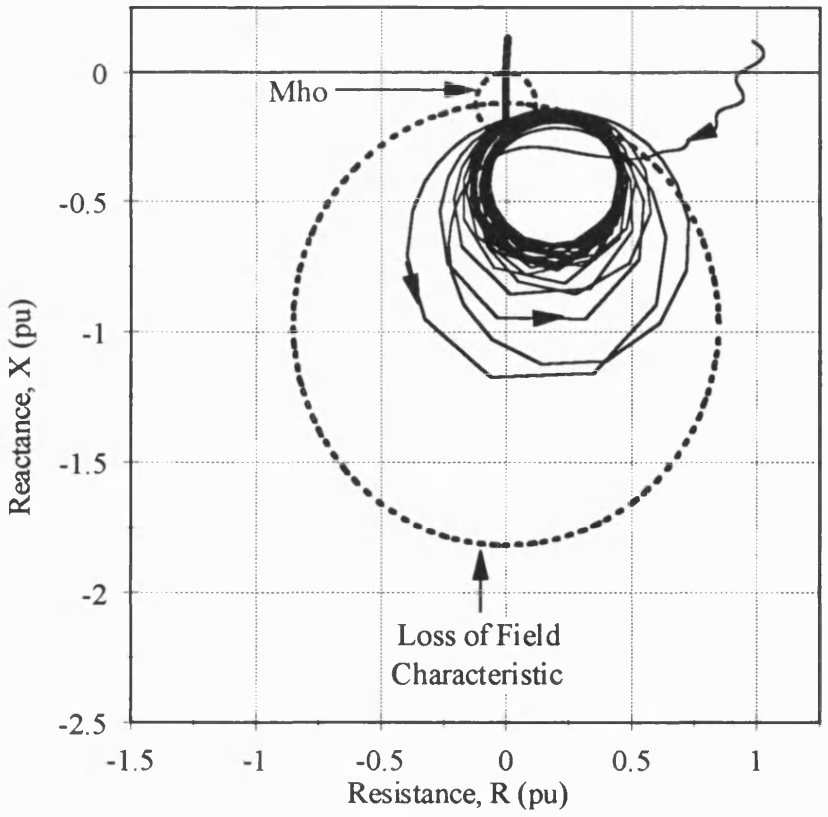

Figure 6.43

Impedance Diagram Showing 200 MVA Generator Loss of Field Protection Scheme Characteristic and Loss of Field Loci for Test 'LOF3GA'

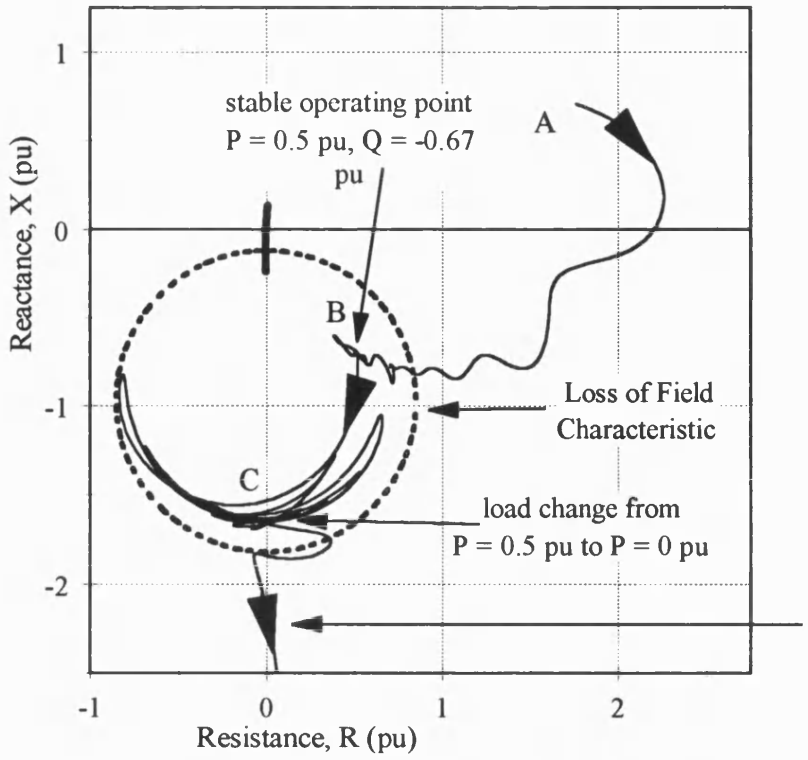

Figure 6.44

Impedance Diagram Showing 200 MVA Generator Loss of Field Protection Scheme Characteristic and Impedance Locus for Test 'AVR5NA'

Figure 6.45a - A Phase RMS Current and IDMT trip for Test PSL3NN

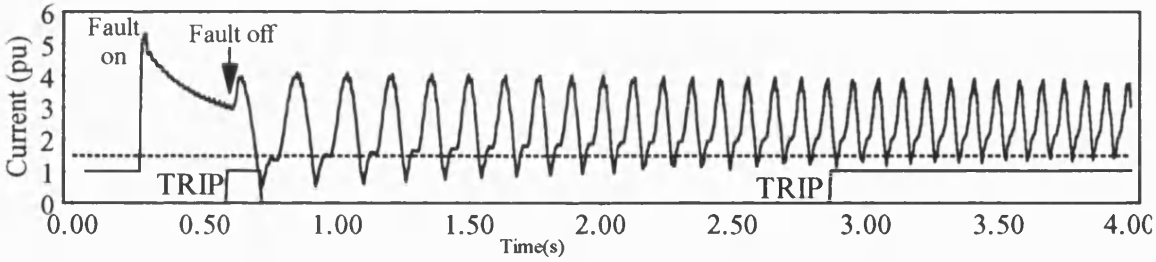

Figure 6.45b - A Phase RMS Current and IDMT trip for Test PSL2GA

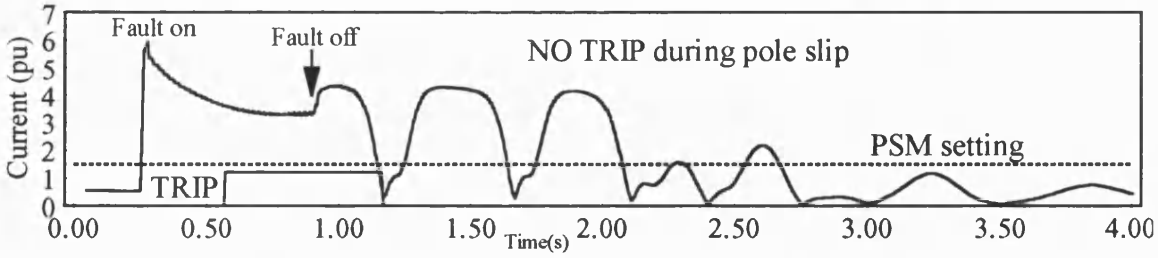

Figure 6.45c - A Phase RMS Current and IDMT trip for Test PSL3GA

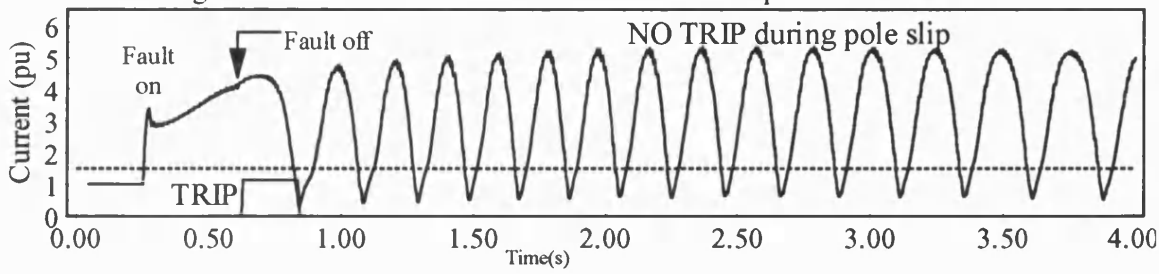

Figure 6.45 - Phase A RMS Current for PPSS Tests PSL3NN, PSL2GA and PSL3GA

NOTE: A time delay of 0.5 seconds was used with the Under-Voltage relay

Figure 6.46a - A Phase RMS Voltage and Under Voltage Trip for Test 'PSL3NN'

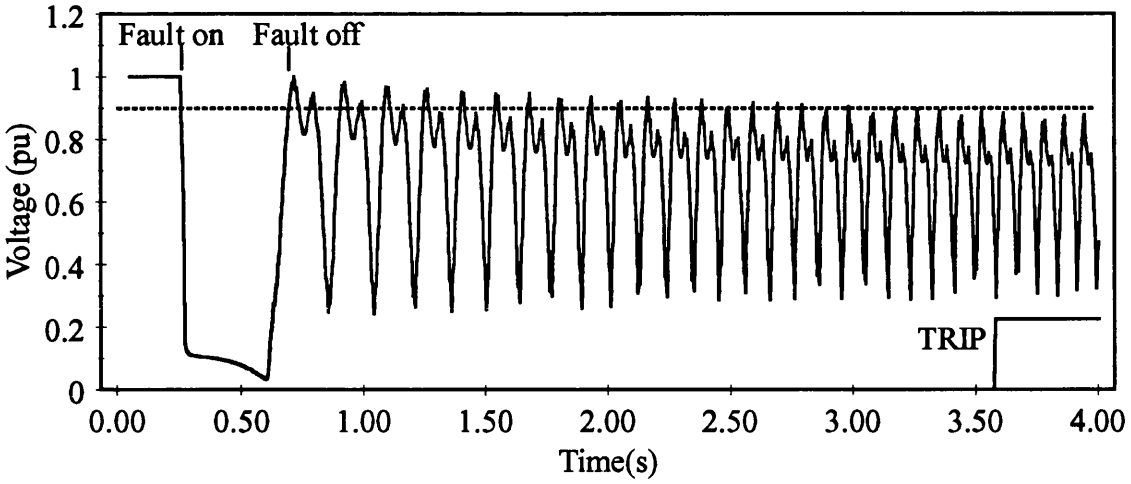

Figure 6.46b - A Phase RMS Voltage and Under Voltage Trip for Test 'PSL2GA'

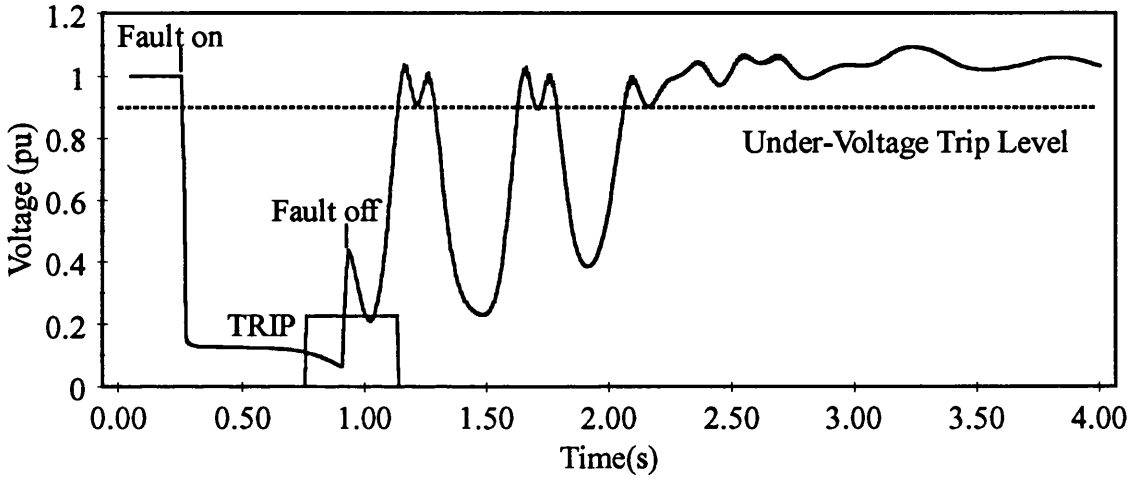

Figure 6.46c - A Phase RMS Voltage and Under Voltage Trip for Test 'PSL3GAF'

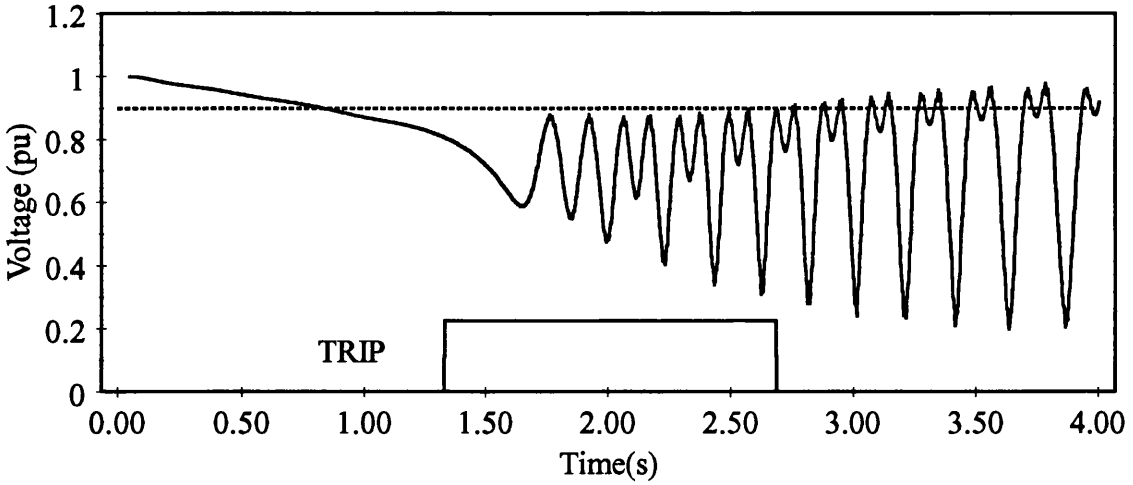

Figure 46
Under-Voltage Relay Response to Tests 'PSL3NN' , 'PSL2GA' , and 'PSL3GAF'

NOTE: A time delay of 0.4 seconds was used with the Over-Frequency Relay

Figure 6.47a - Measured Frequency at Generator Terminals,
and Over Frequency Trip for Test 'PSL3NN'

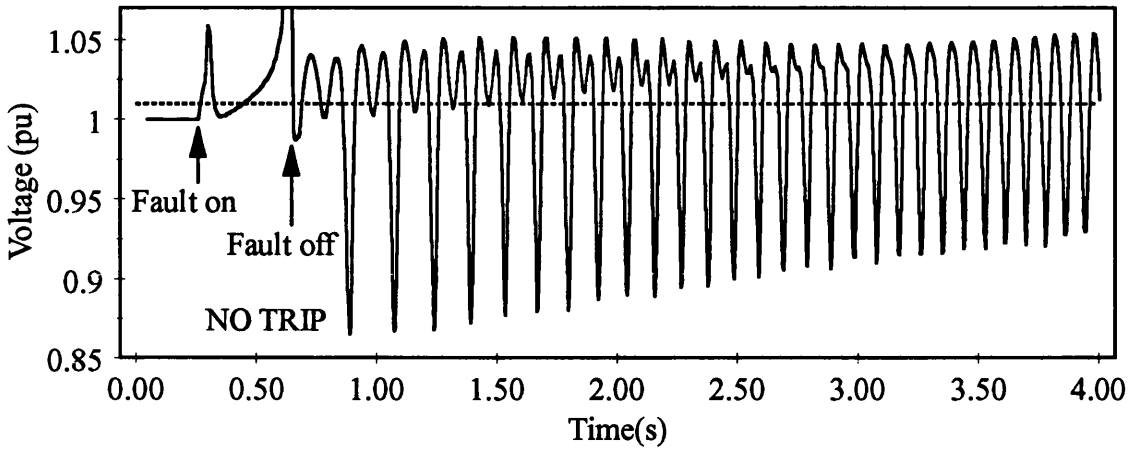

Figure 6.47b - Measured Frequency at Generator Terminals,
and Over Frequency Trip for Test 'PSL2GA'

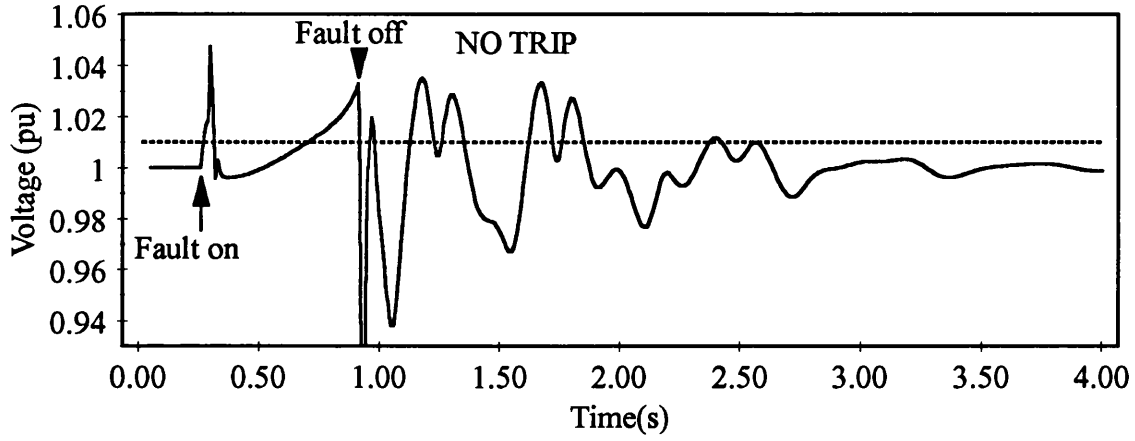

Figure 6.47c - Measured Frequency at Generator Terminals,
and Over Frequency Trip for Test 'PSL3GAF'

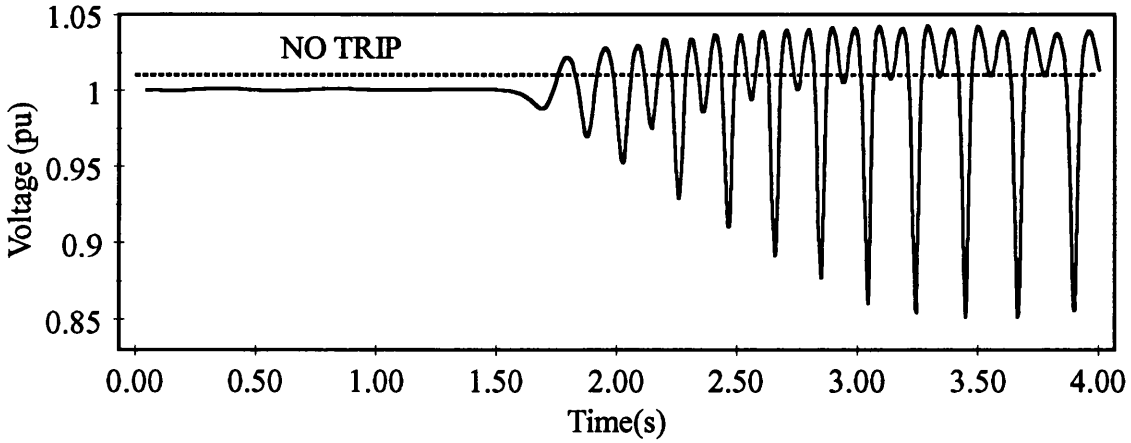

Figure 47
Over-Frequency Relay Response to Tests 'PSL3NN' , 'PSL2GA' , and 'PSL3GAF'

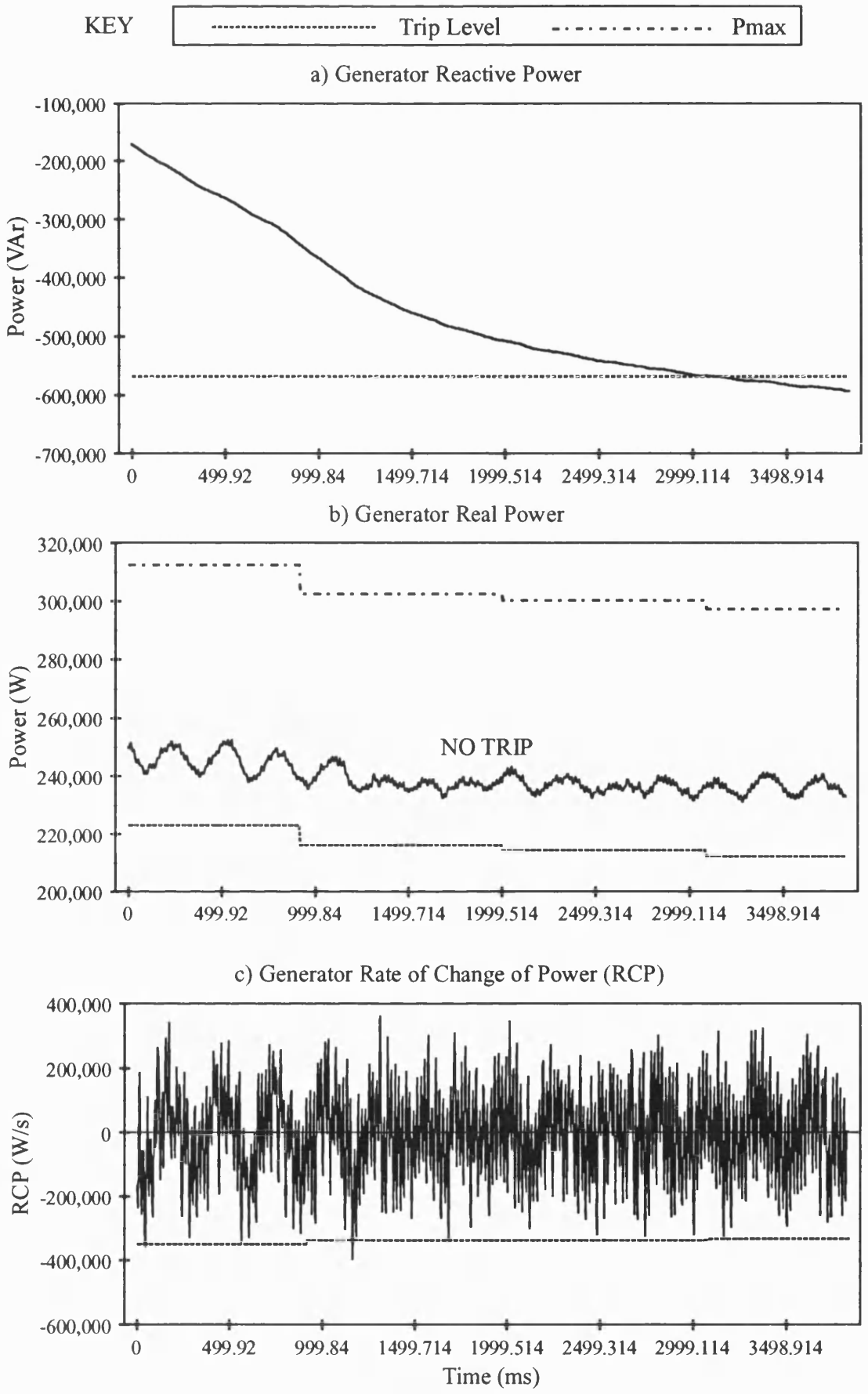

Figure 6.48
Pole Slipping Algorithm Response to 625 kVA Diesel Generator Field Trial Test 'A2'
Unsuccessful Pole Slip Attempt by Weakening the Field Excitation.

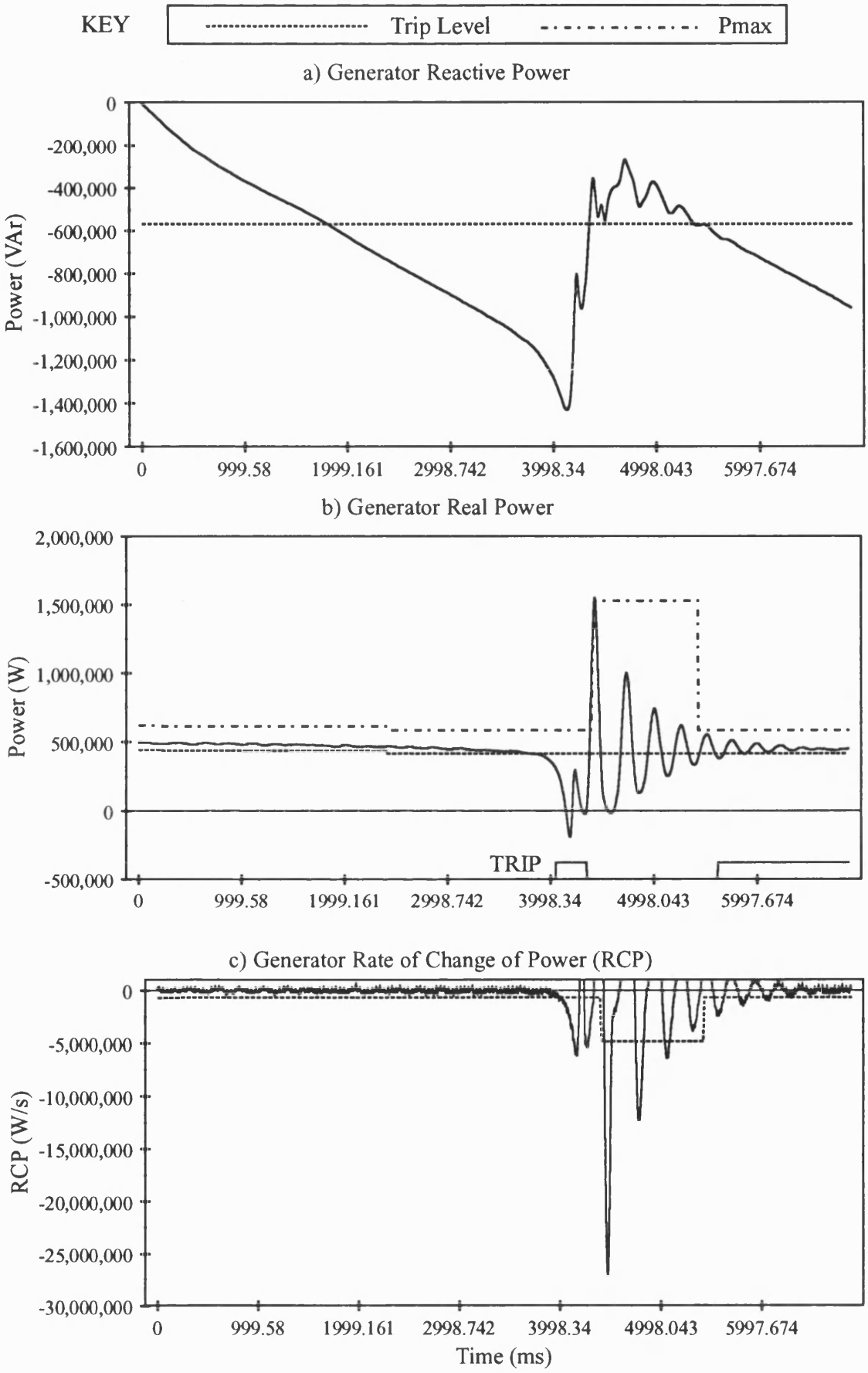

Figure 6.49
Pole Slipping Algorithm Response to 625 kVA Diesel Generator Field Trial Test 'A3'
Pole Slip Induced by Weakening the Field Excitation.

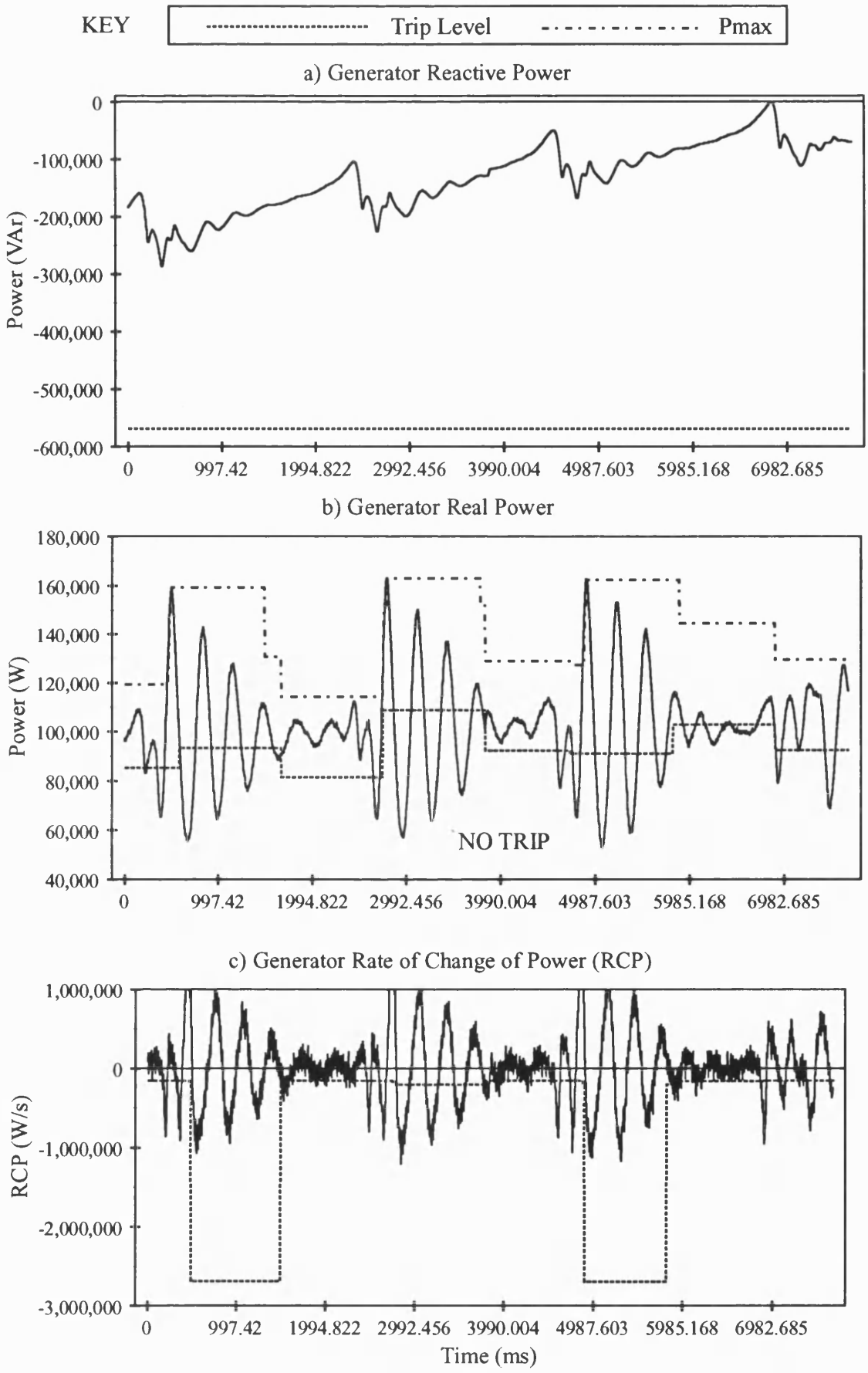

Figure 6.50
Pole Slipping Algorithm Response to 625 kVA Diesel Generator Field Trial Test 'A4'
Adjacent Generator Pole Slip Induced by Weakening the Field Excitation.

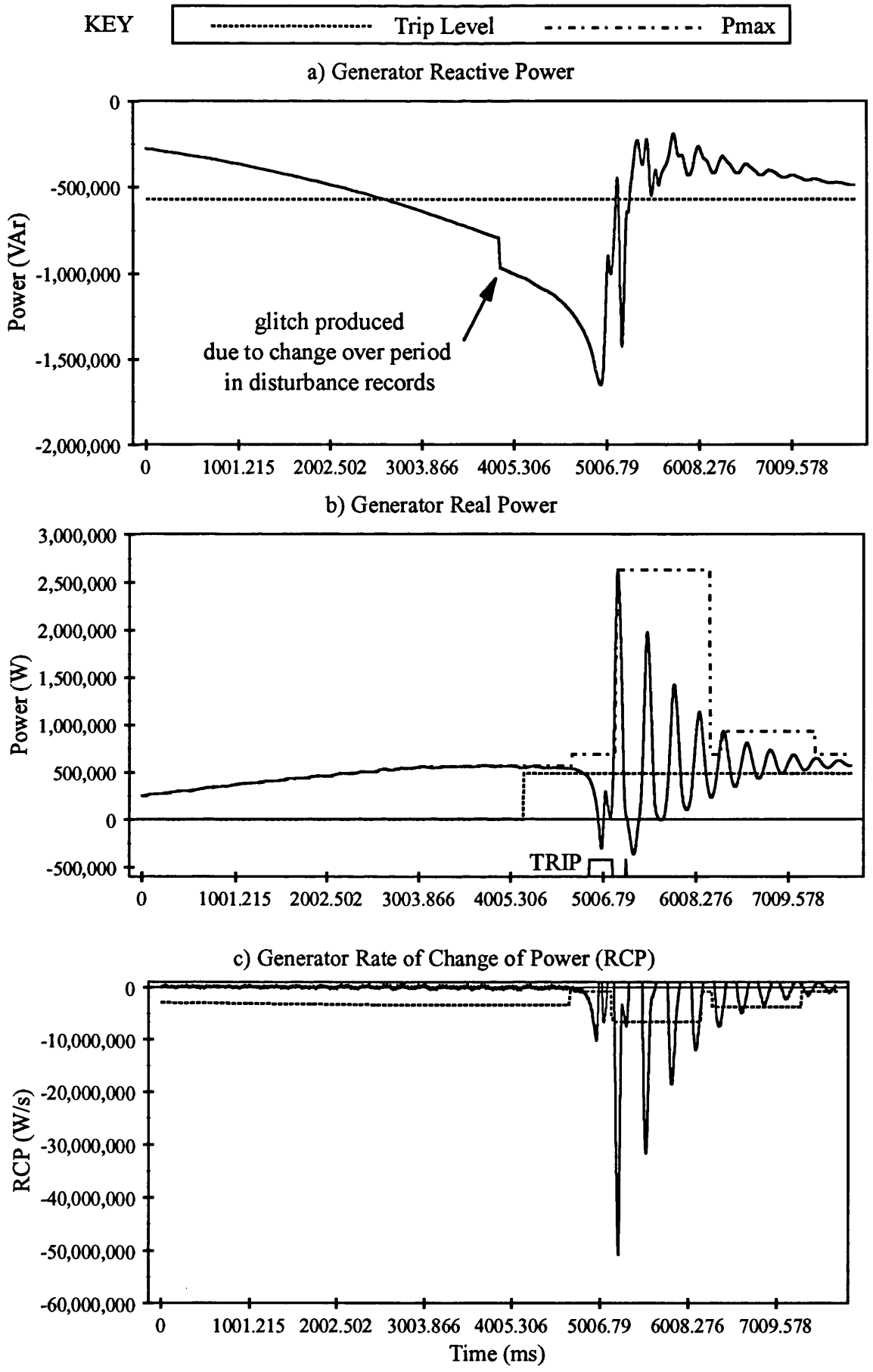

Figure 6.51
Pole Slipping Algorithm Response to 625 kVA Diesel Generator Field Trial Test 'A7'
Pole Slip Induced by Suddenly Increasing Prime Mover Output Power.

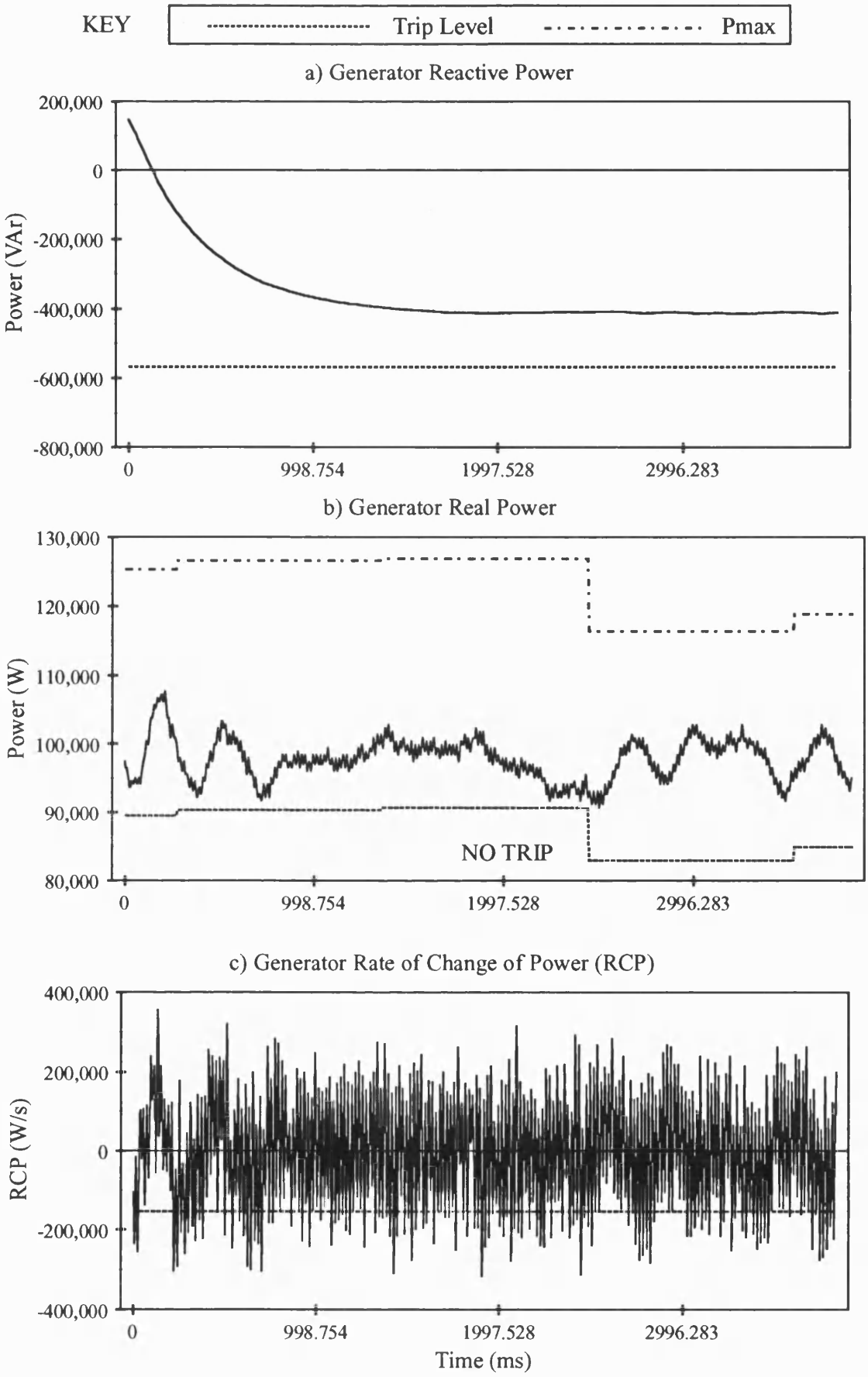

Figure 6.52
Pole Slipping Algorithm Response to 625 kVA Diesel Generator Field Trial Test 'B2'
Loss of Excitation from 20% Initial Load.

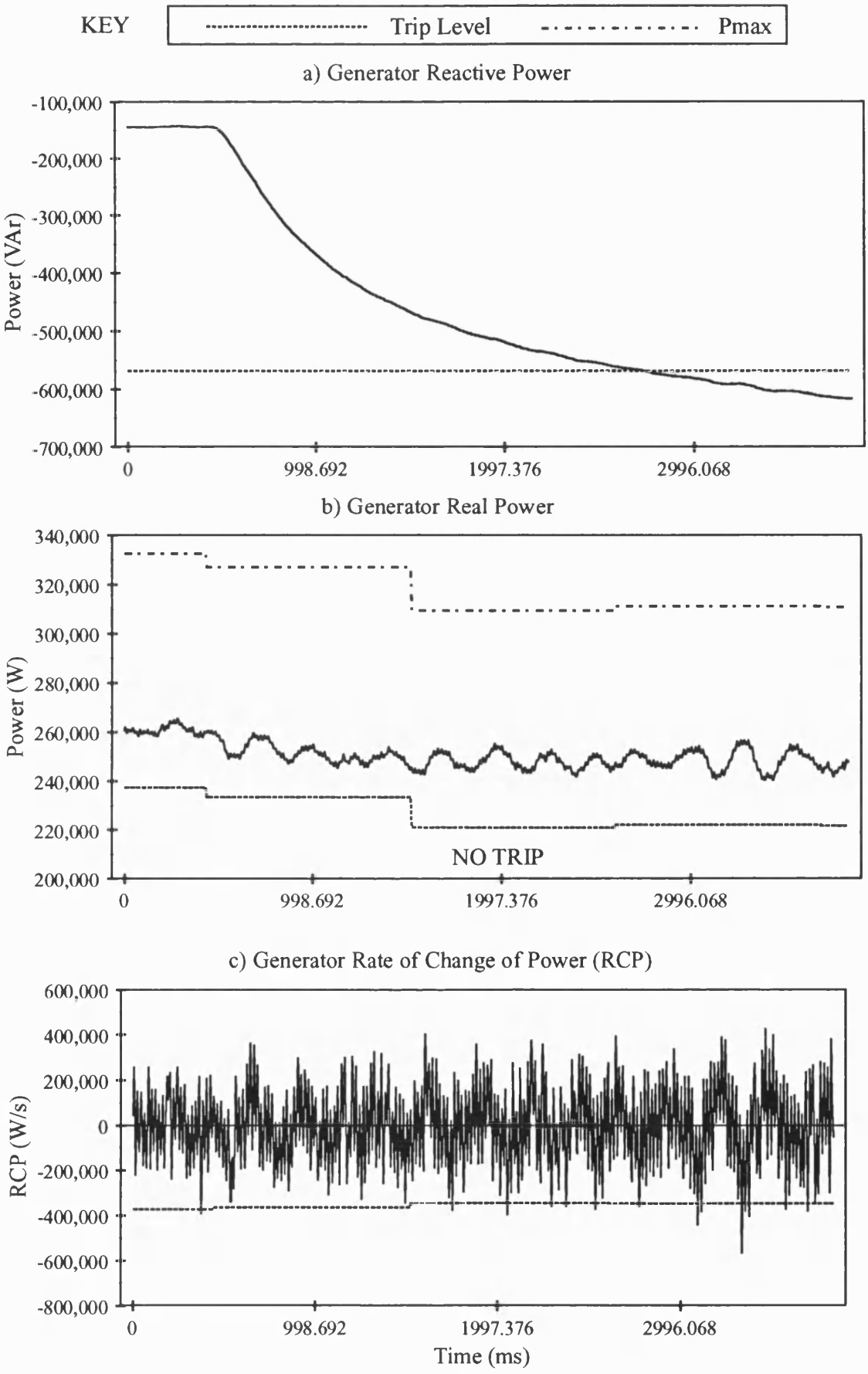

Figure 6.53
Pole Slipping Algorithm Response to 625 kVA Diesel Generator Field Trial Test 'B3'
Loss of Excitation from 50 % Initial Load.

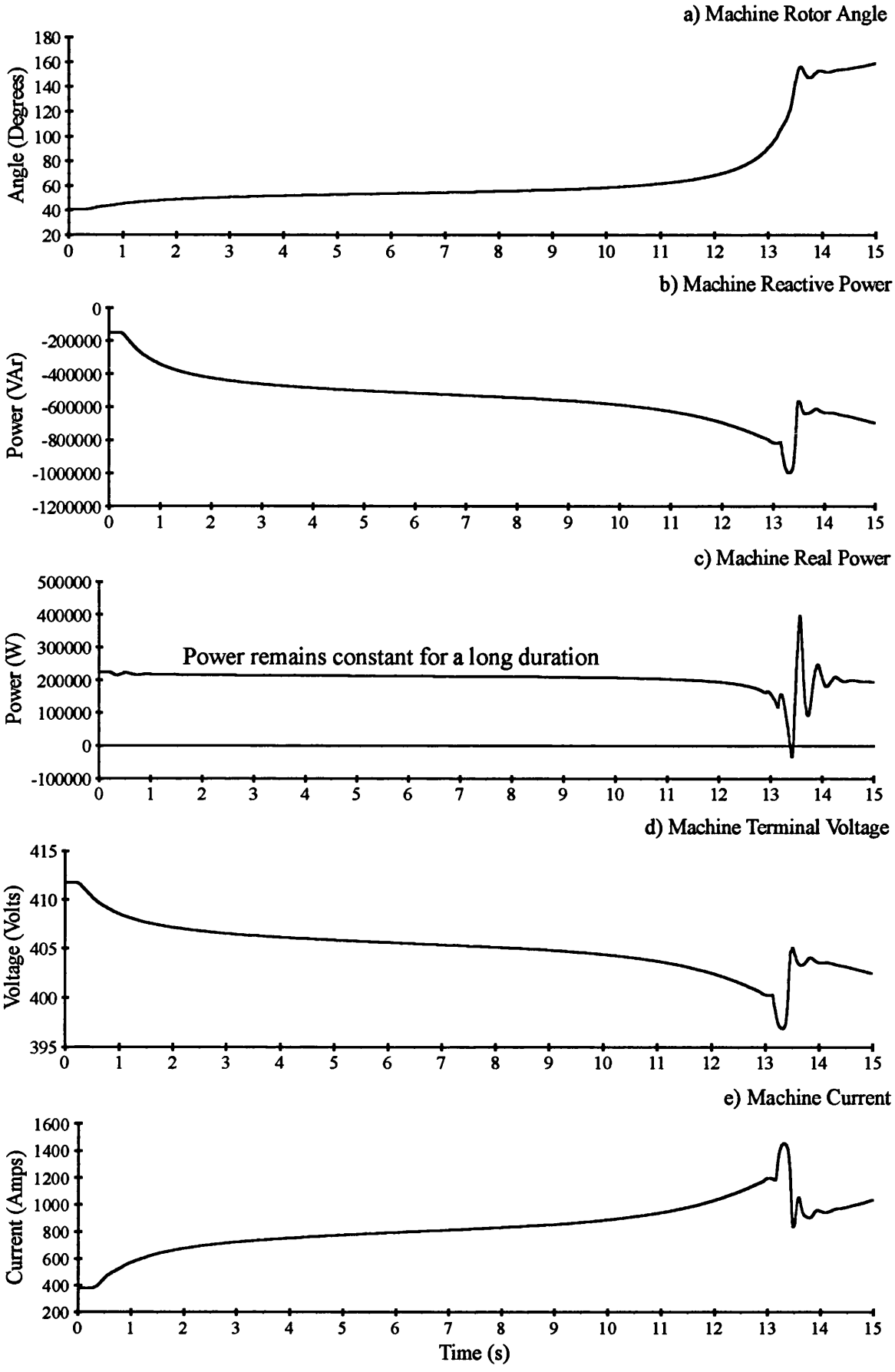

Figure 6.54
Generator Variables for ATP Simulation of a 625 kVA Diesel
Generator Loss of Excitation from 45 % Initial Load.

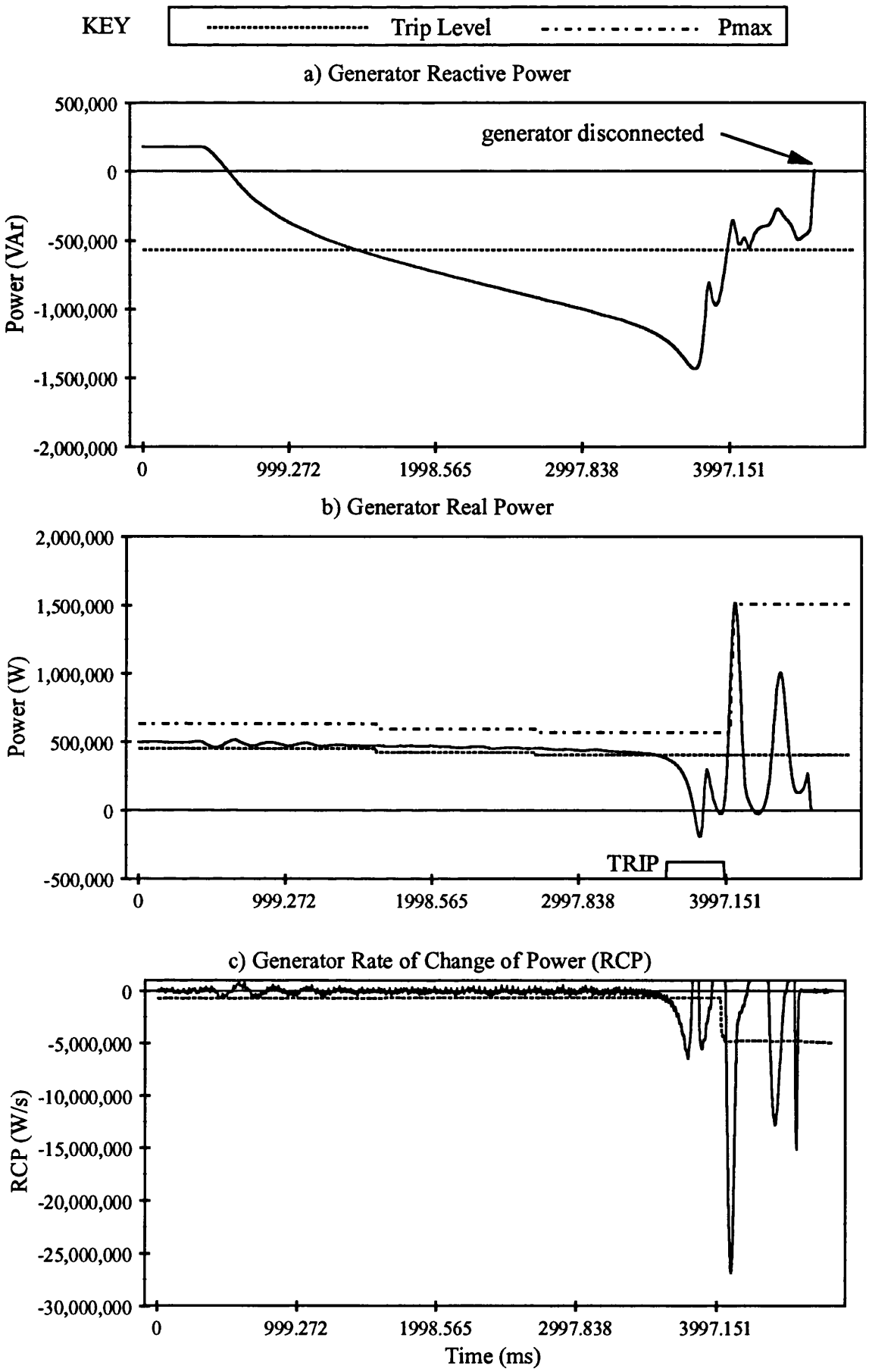

Figure 6.55
Pole Slipping Algorithm Response to 625 kVA Diesel Generator Field Trial Test 'B6'
Loss of Excitation from 100 % Initial Load.

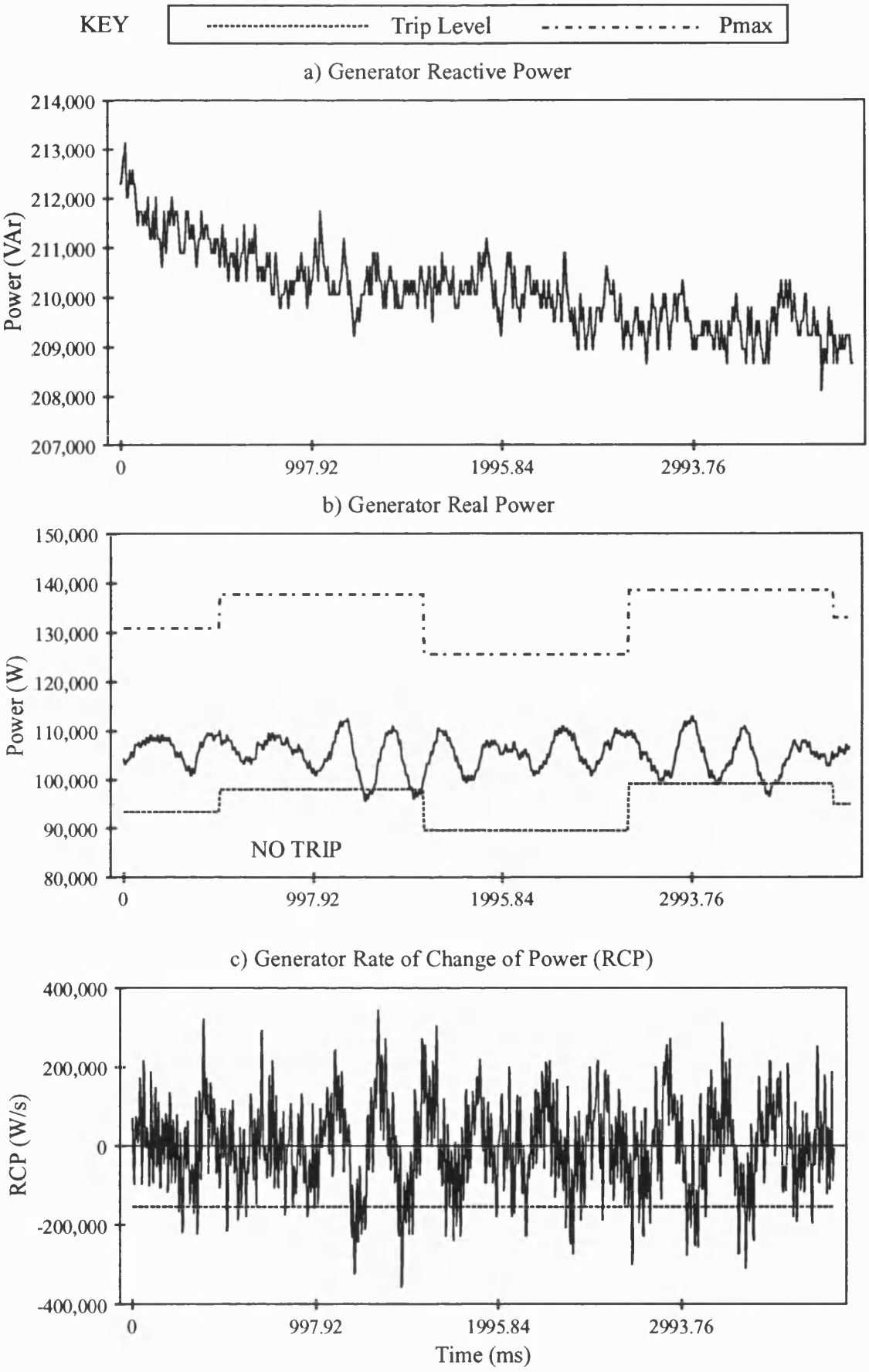

Figure 6.56
Pole Slipping Algorithm Response to 625 kVA Diesel Generator Field Trial Test 'C3'
Steady State Operation at 30 % Load, Over-Excited Exitation.

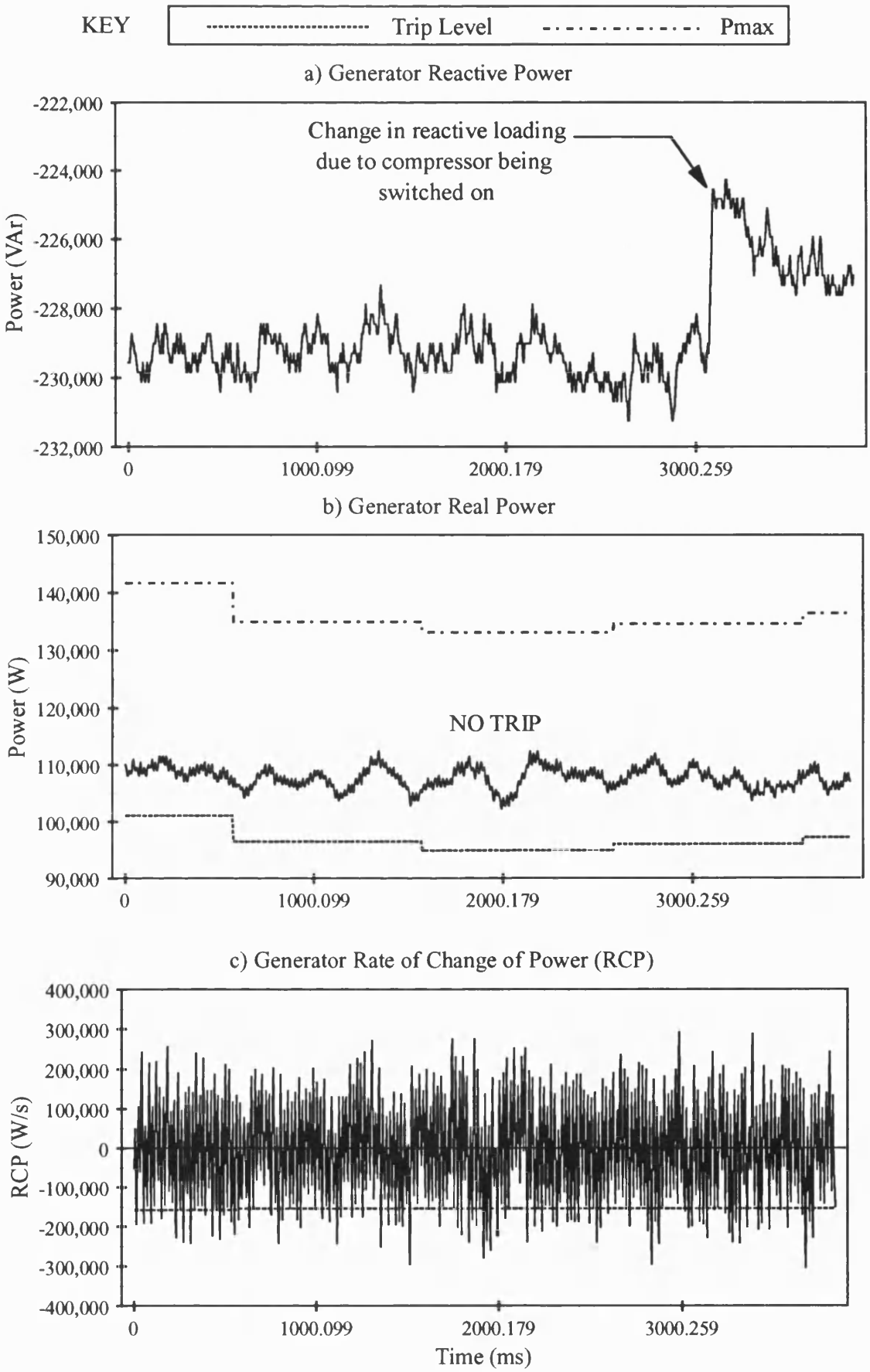

Figure 6.57
Pole Slipping Algorithm Response to 625 kVA Diesel Generator Field Trial Test 'C6'
Compressor Energisation Test at 20% Initial Generator Loading.

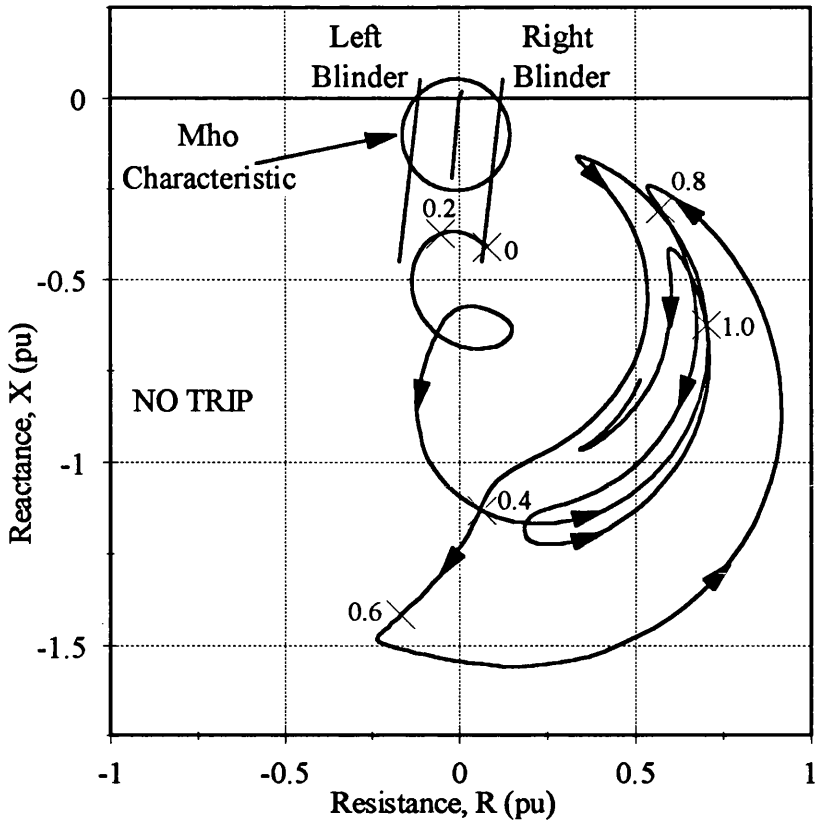

Figure 6.58a
Impedance Diagram Showing 625 kVA Generator Single Blinder Pole Slipping Protection Scheme and Pole Slipping Loci for Test 'A3'

Figure 6.58b - Machine Terminal Voltage for Test 'A3'

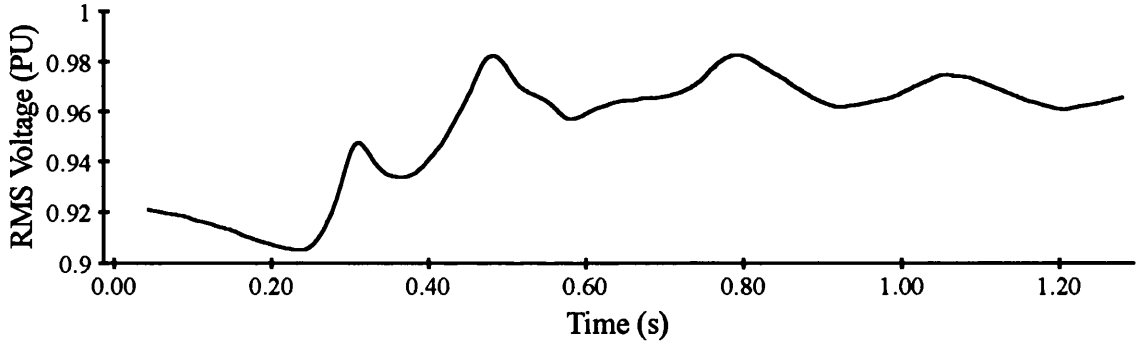

Figure 6.58c - Machine Terminal Current for Test 'A3'

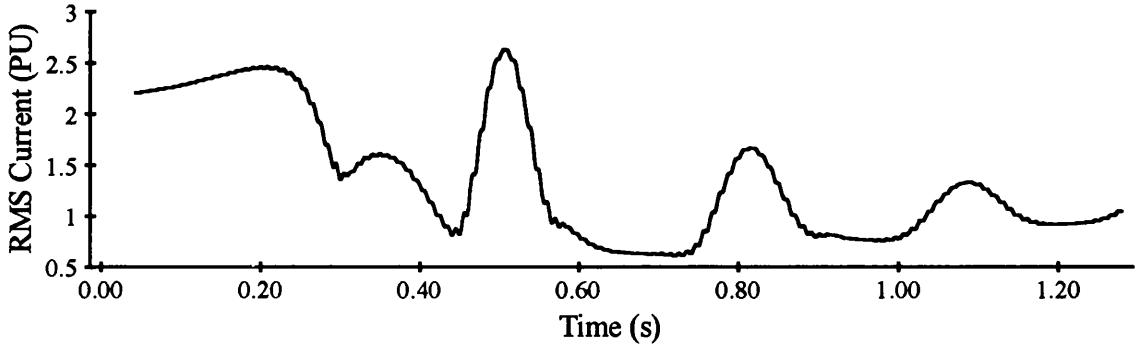

Figure 6.58
Plots Showing Generator Impedance, Voltage and Current Variations for 625 kVA Diesel Generator Field Trial Pole Slip Test 'A3'

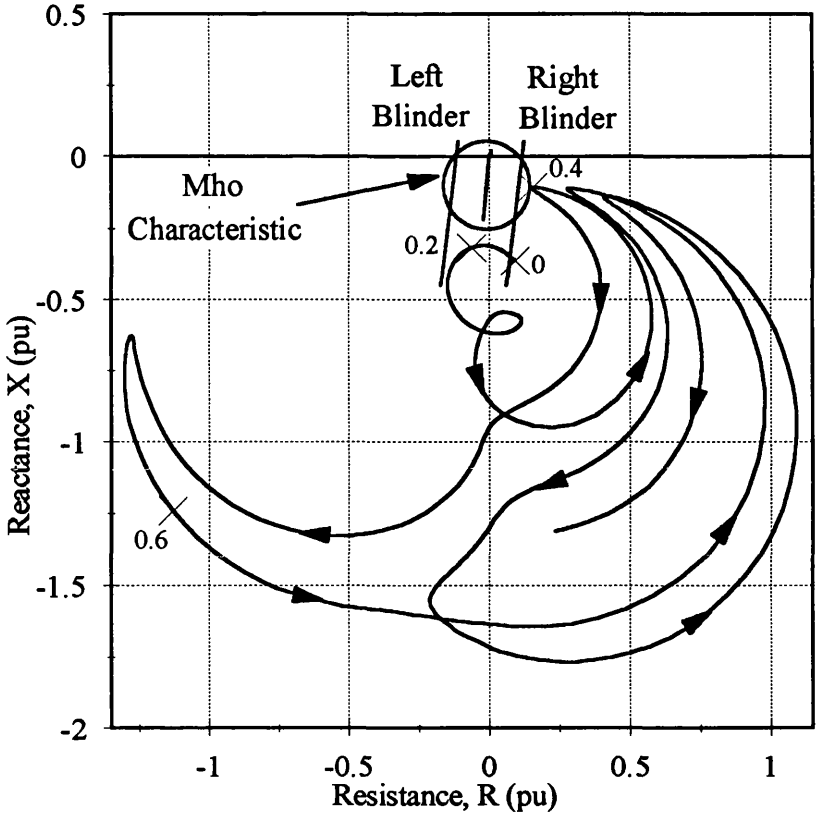

Figure 6.59
Impedance Diagram Showing 625 kVA Generator Single Blinder Pole Slipping Protection Scheme and Pole Slipping Loci for Test 'A7'

Figure 6.59b - Machine Terminal Voltage for Test 'A7'

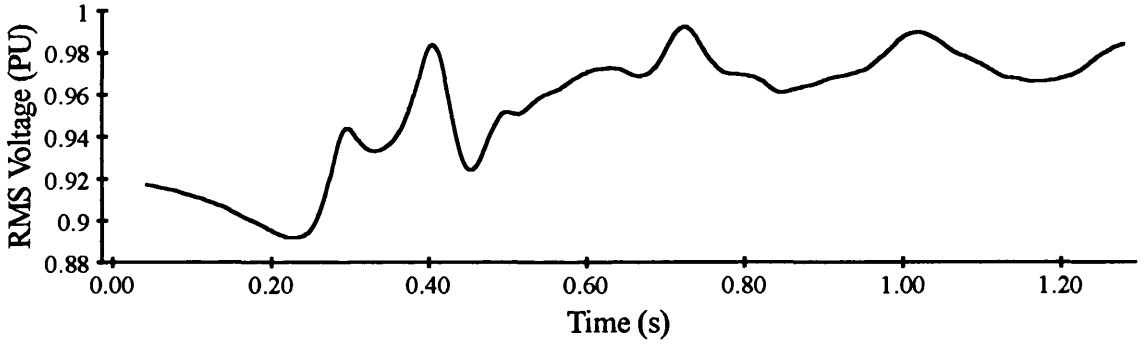

Figure 6.59c - Machine Terminal Current for Test 'A7'

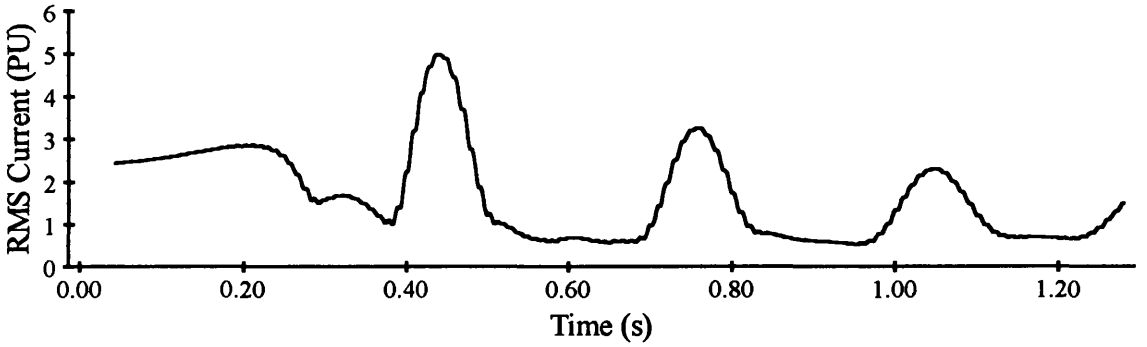

Figure 6.59
Plots Showing Generator Impedance, Voltage and Current Variations for 625 kVA Diesel Generator Field Trial Pole Slip Test 'A7'

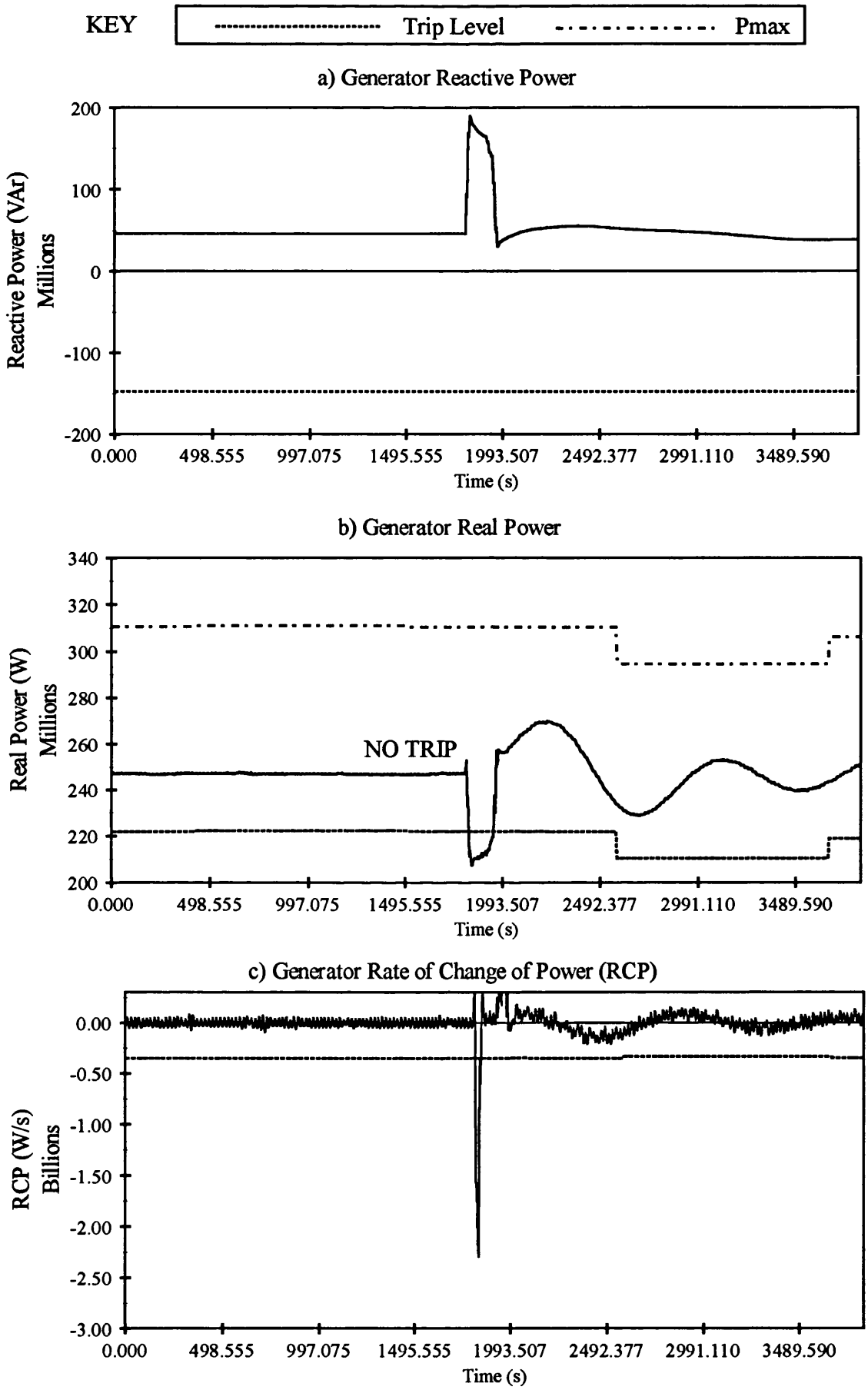

Figure 6.60
Pole Slipping Algorithm Response to a Fault During the
Field Trials on a 353 MVA Turbo-Generator

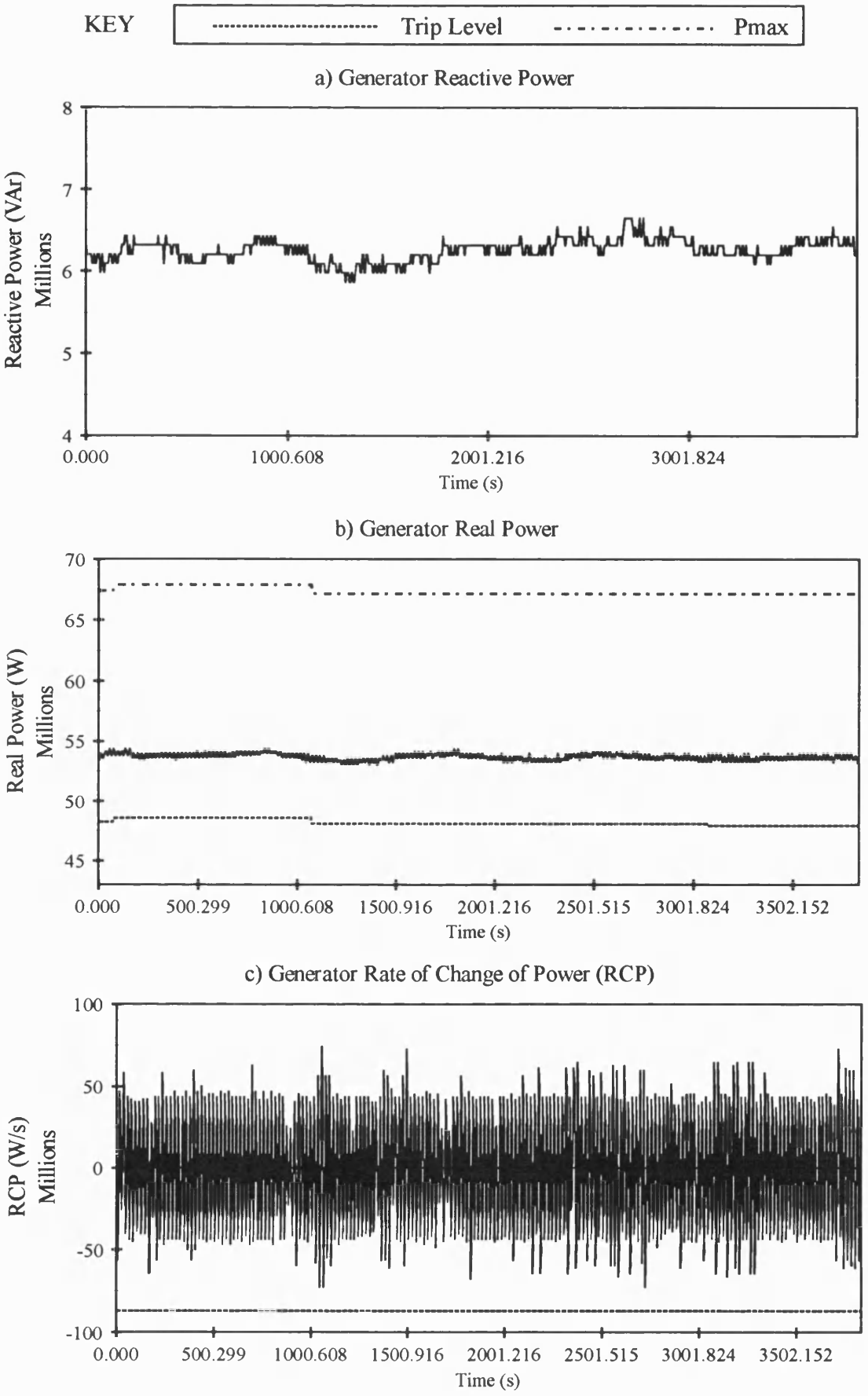

Figure 6.61
Pole Slipping Algorithm Measurands for Generator Steady State Operation During the Field Trials on a 353 MVA Turbo-Generator

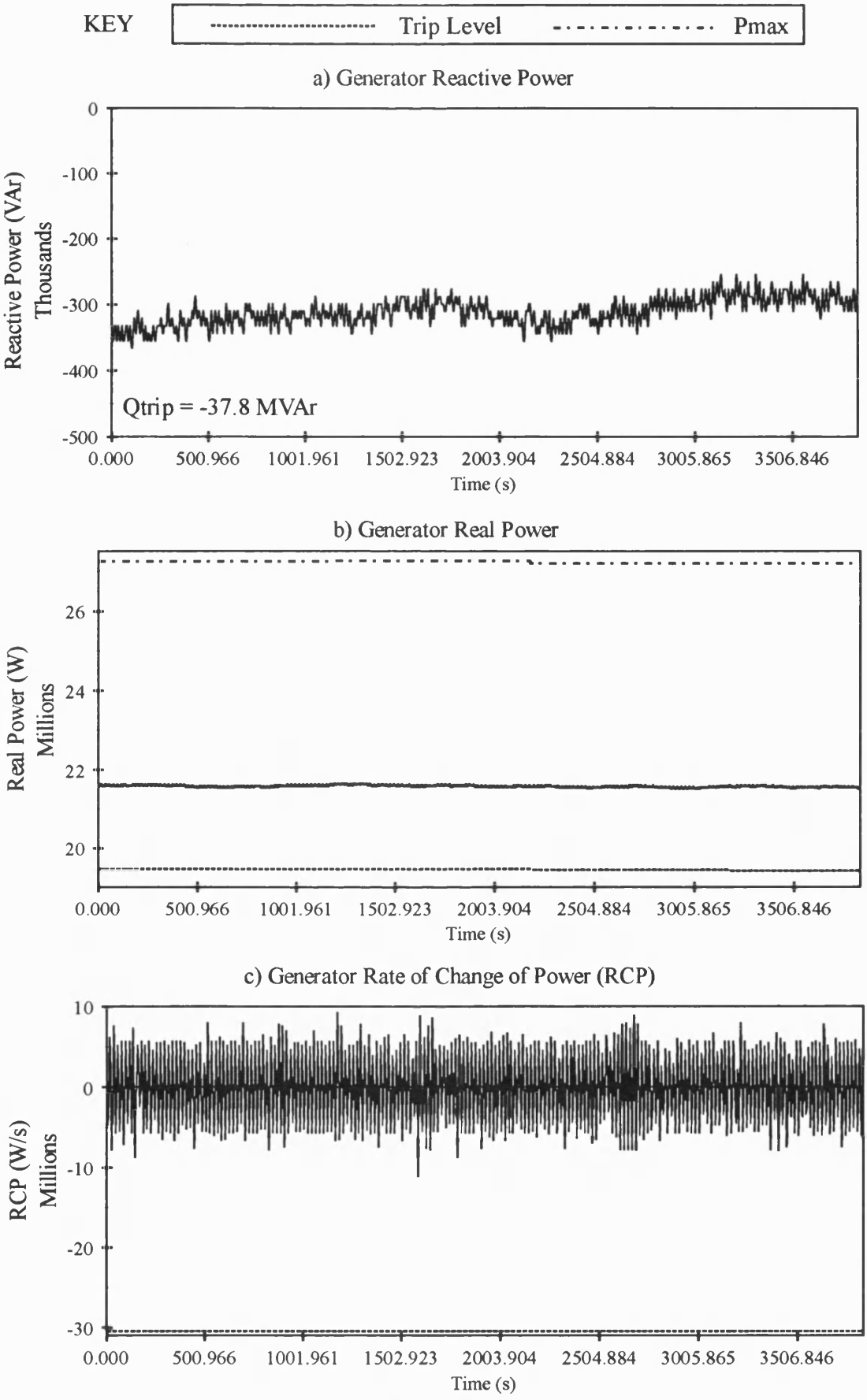

Figure 6.62
Pole Slipping Algorithm Measurands for Generator Steady State Operation During the Field Trials on a 26.5 MVA Hydro-Generator.

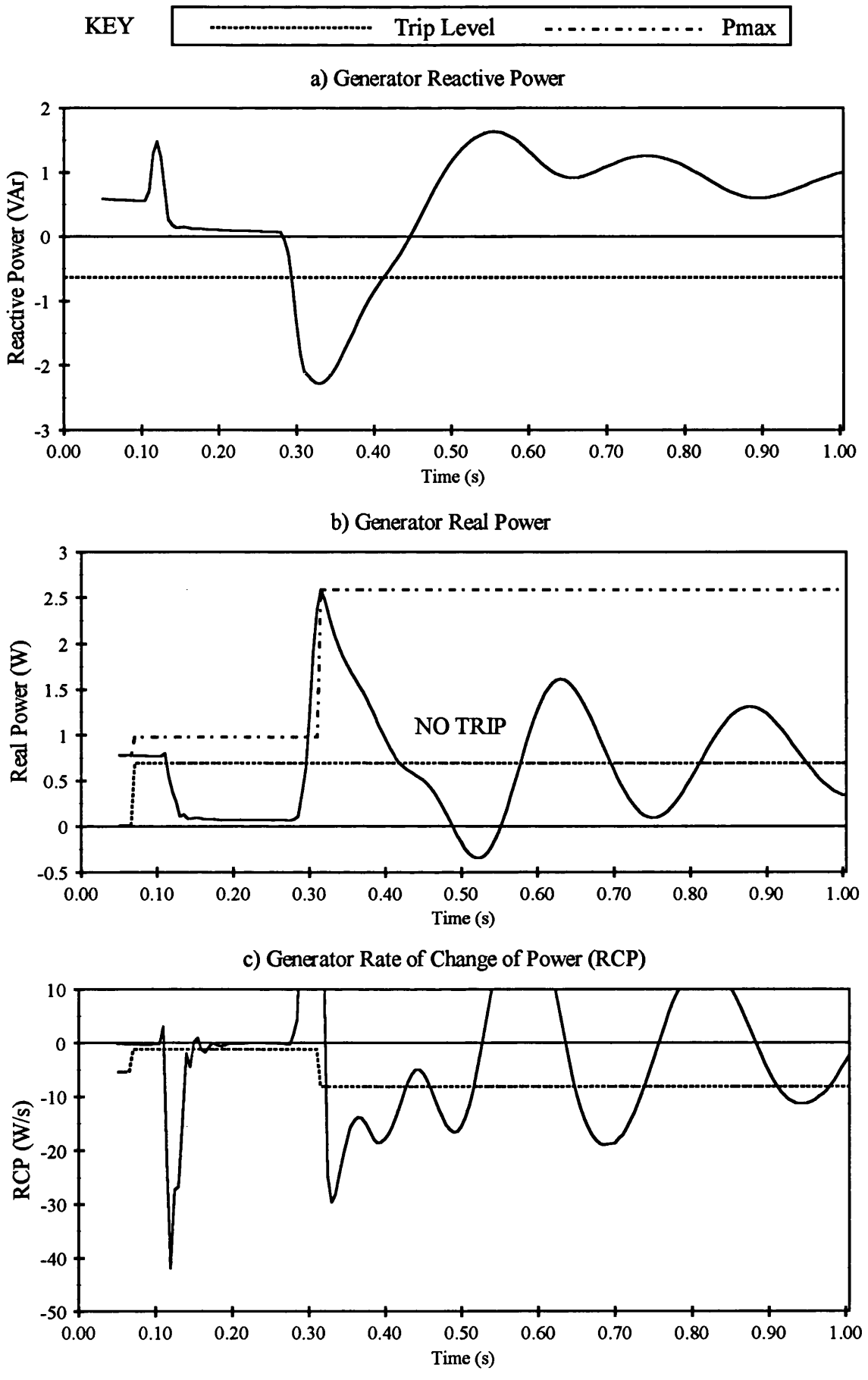

Figure 6.63

Pole Slipping Algorithm Response to an ATP Simulated Stable Power Swing on a 750 kVA Generator with Tdo' = 1.0 s, Slow AVR Model Included, No Governor Model - Test LT1 .

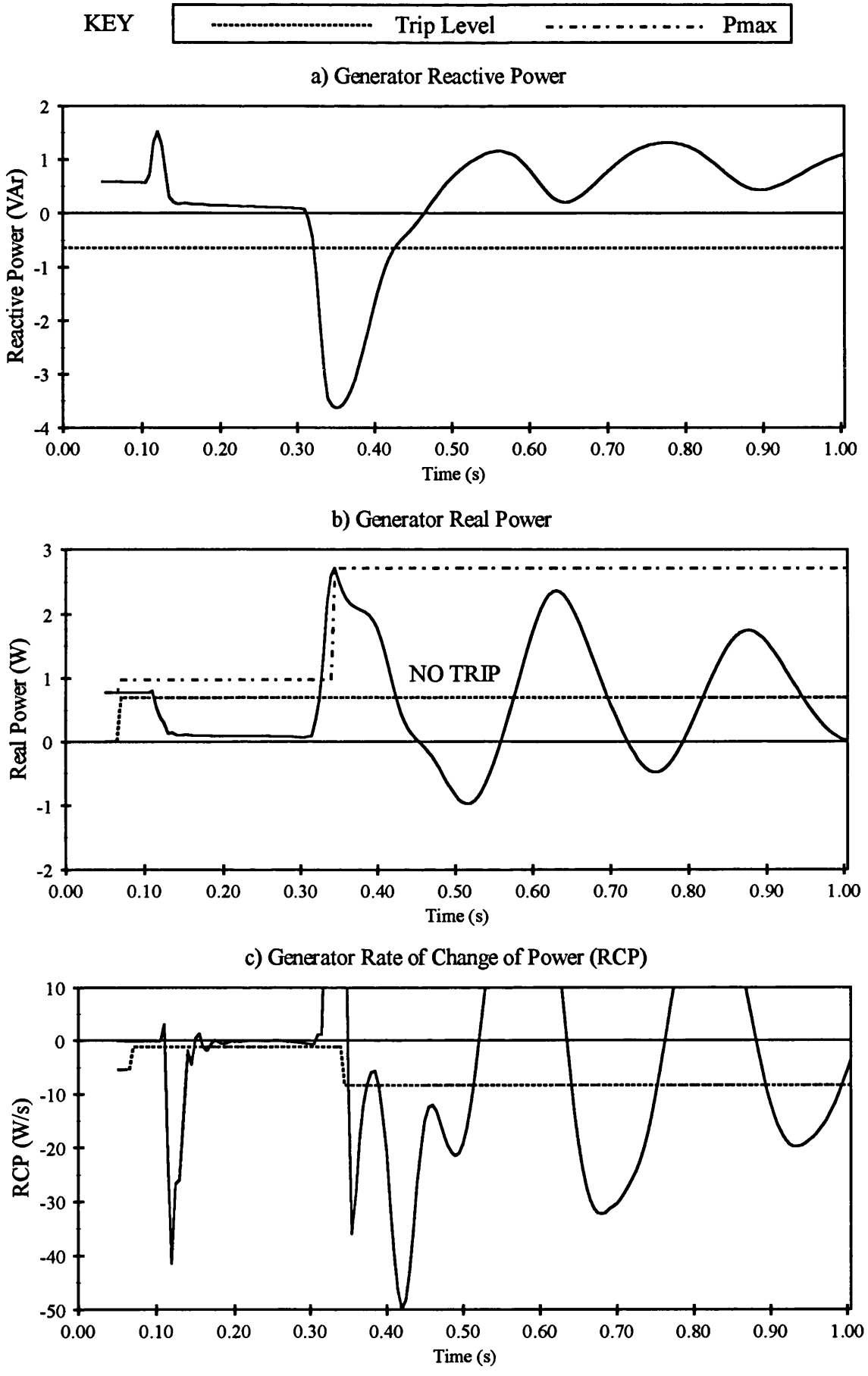

Figure 6.64

Pole Slipping Algorithm Response to an ATP Simulated Stable Power Swing on a 750 kVA Generator with Tdo' = 2.0 s, Slow AVR Model Included, No Governor Model - Test LT2.

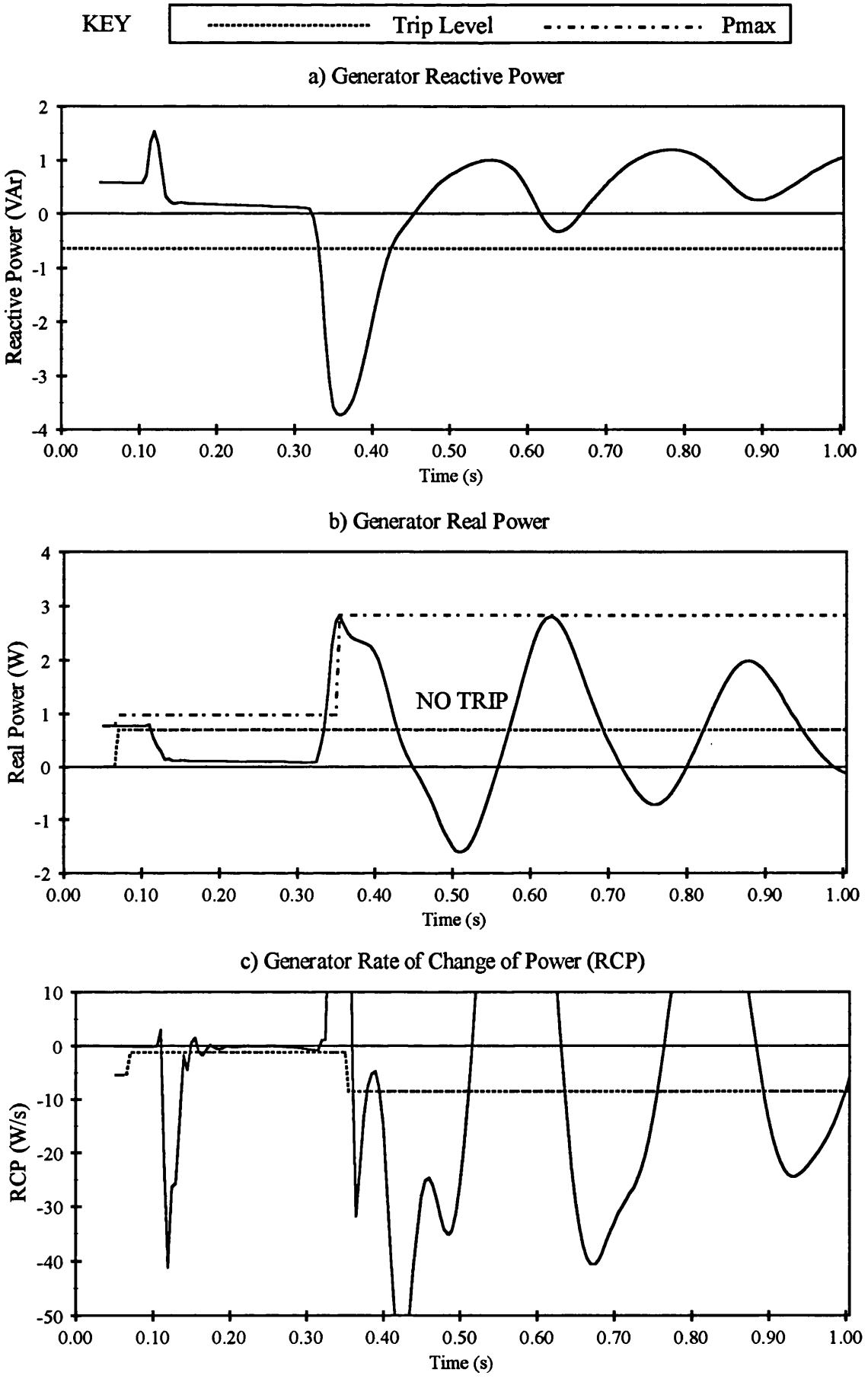

Figure 6.65

Pole Slipping Algorithm Response to an ATP Simulated Stable Power Swing on a 750 kVA Generator with Tdo' = 3.0 s, Slow AVR Model Included, No Governor Model - Test LT3.

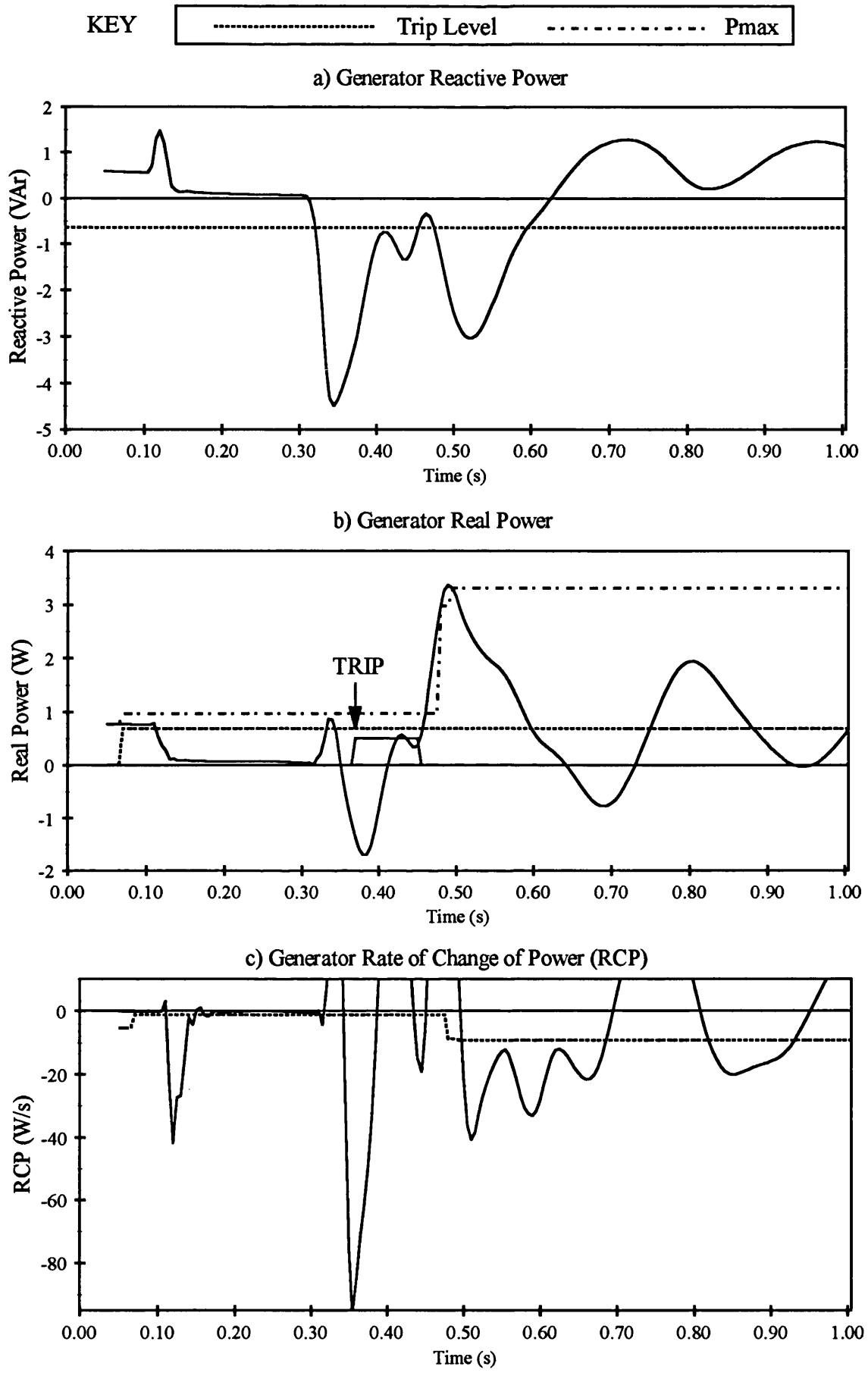

Figure 6.66

Pole Slipping Algorithm Response to an ATP Simulated Pole Slip on a 750 kVA Generator with Tdo' = 1.0 s, Slow AVR Model Included, No Governor Model - Test LTP1.

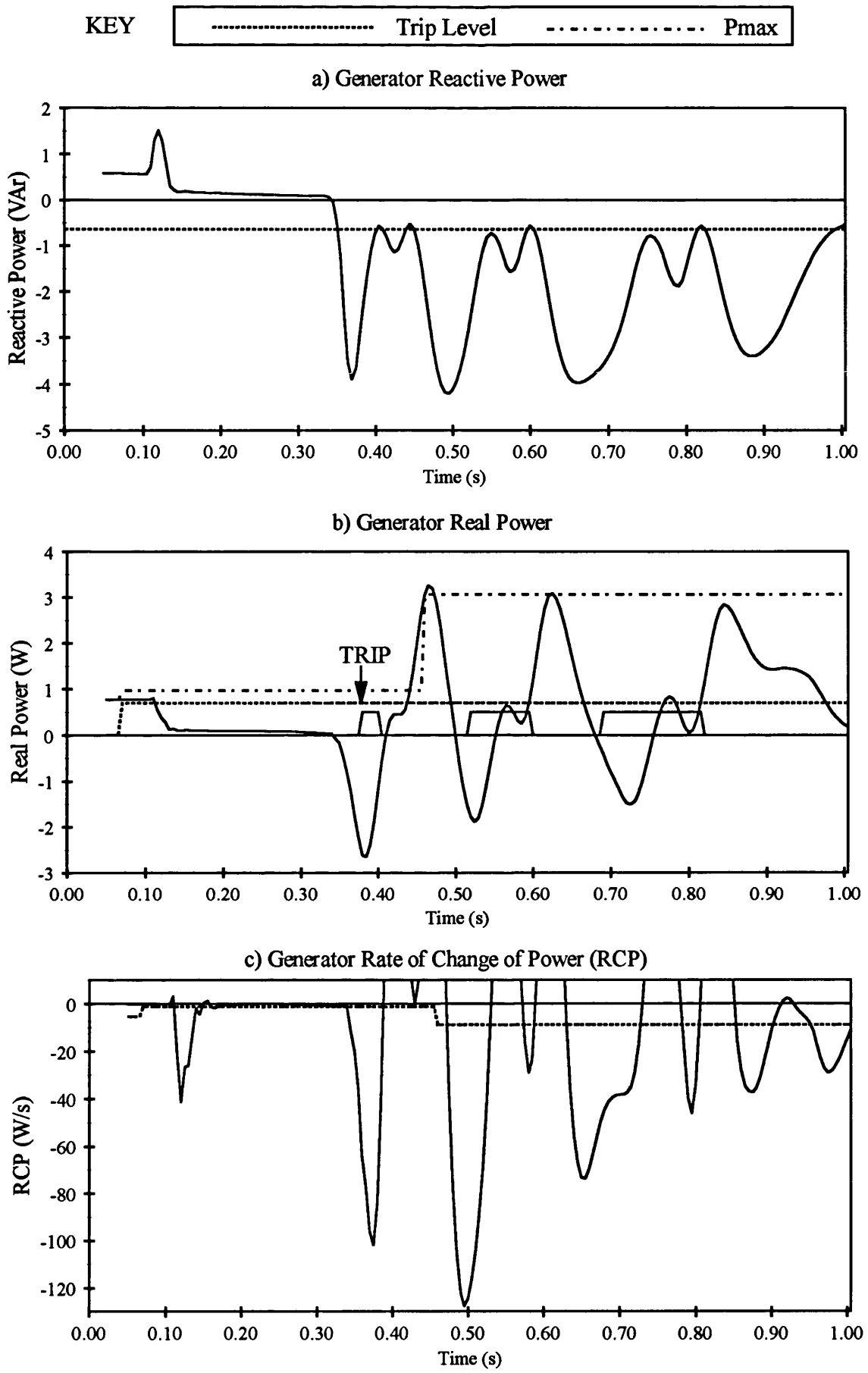

Figure 6.67

Pole Slipping Algorithm Response to an ATP Simulated Pole Slip on a 750 kVA Generator with a value of Tdo' of 2.0 s, Slow AVR Model Included, No Governor Model - Test LTP2.

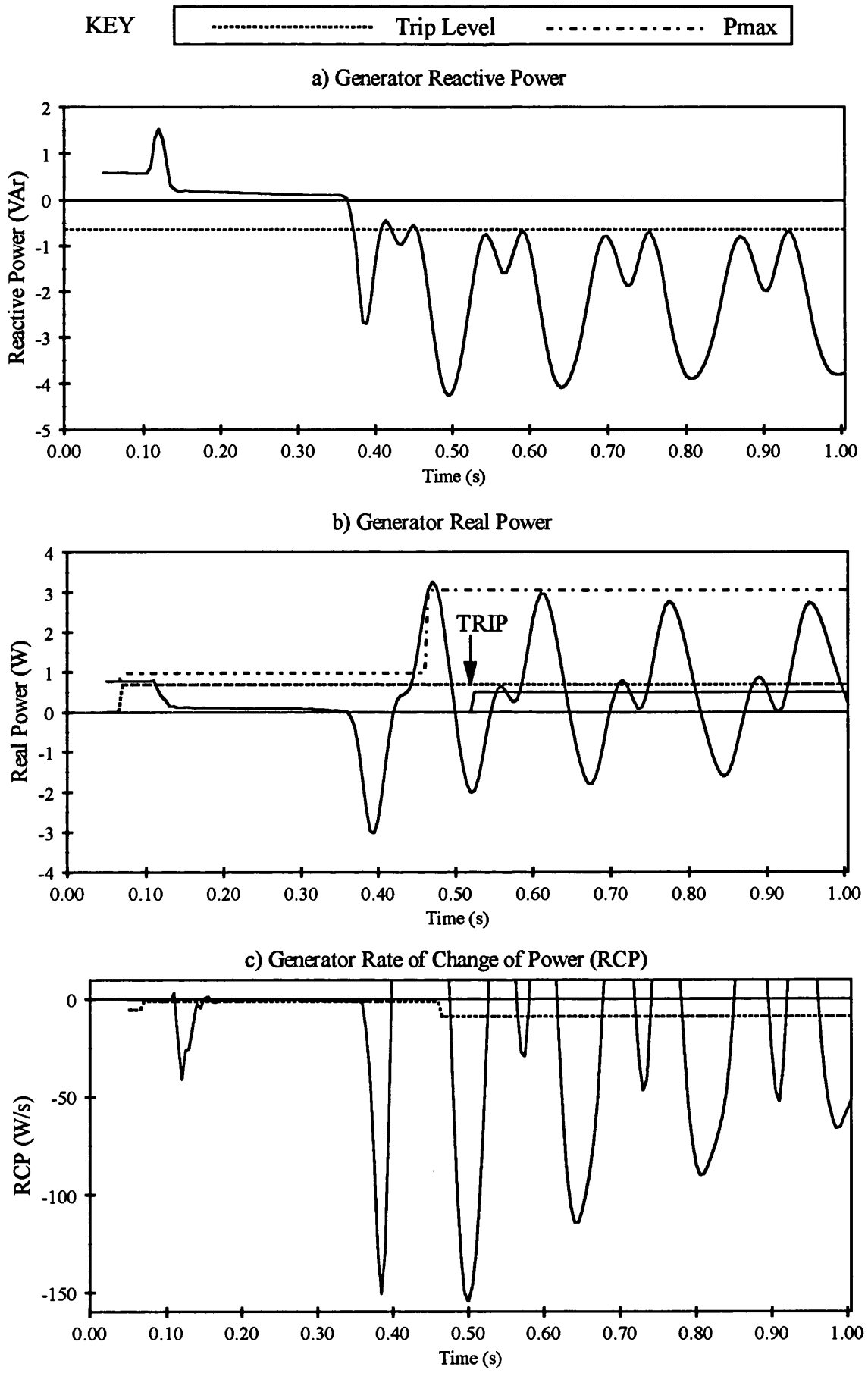

Figure 6.68

Pole Slipping Algorithm Response to an ATP Simulated Pole Slip on a 750 kVA Generator with a value of Tdo' of 3.0 s, Slow AVR Model Included, No Governor Model - Test LTP3.

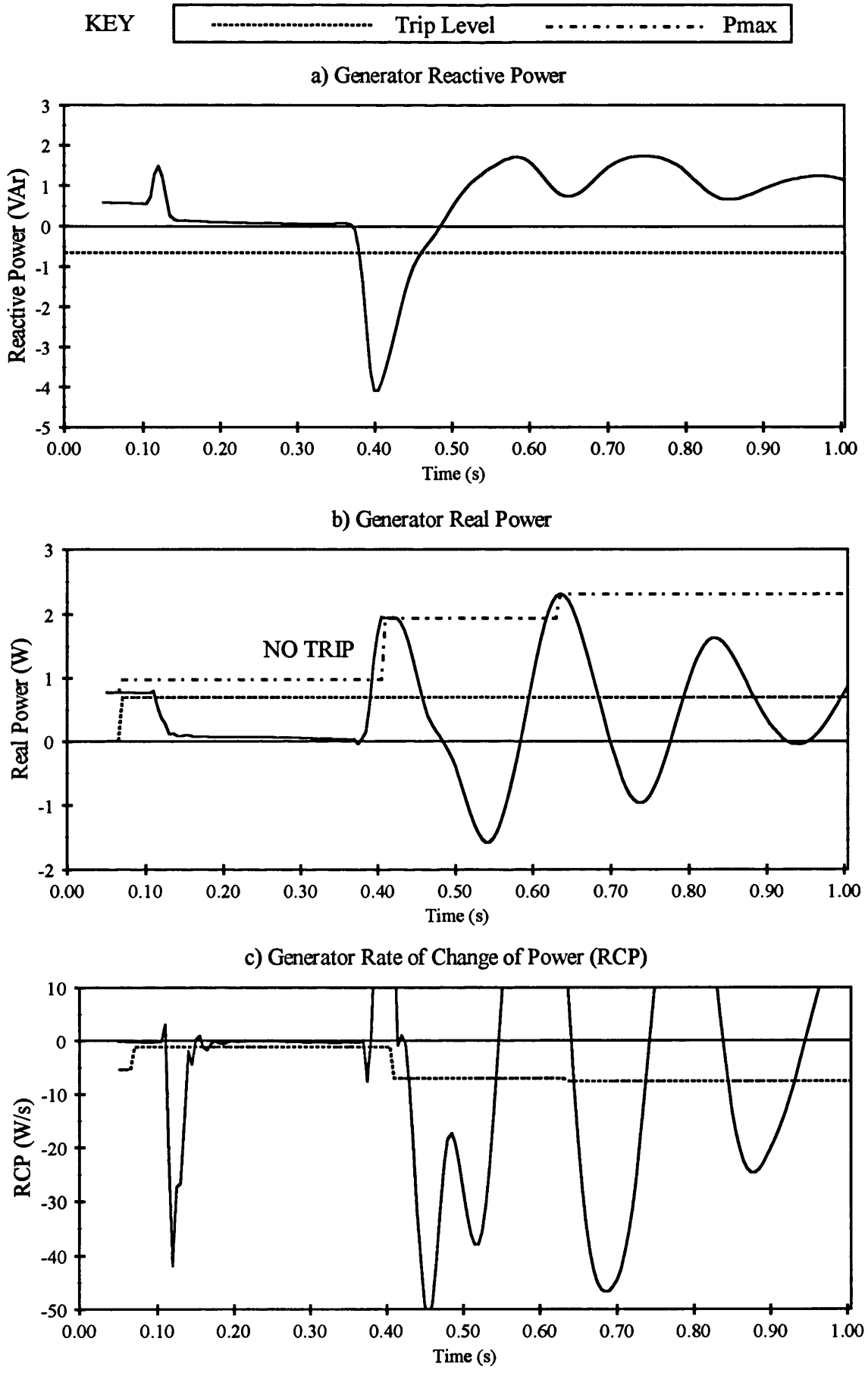

Figure 6.69

Pole Slipping Algorithm Response to an ATP Simulated Stable Power Swing on a 750 kVA Generator with Tdo' = 1.0 s, Slow AVR Model and Fast Governor Model - Test FG1.

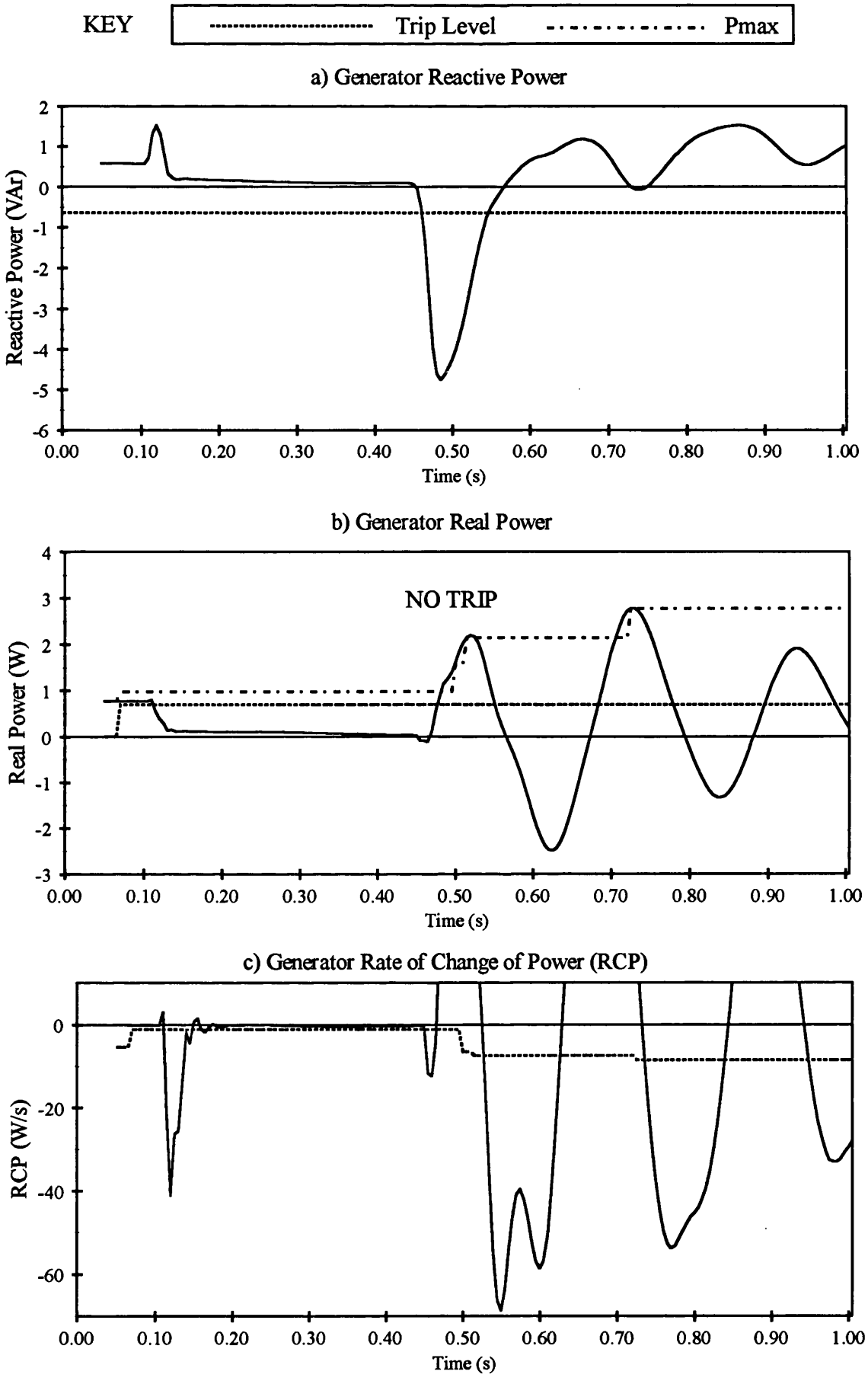

Figure 6.70

Pole Slipping Algorithm Response to an ATP Simulated Stable Power Swing on a 750 kVA Generator with Tdo' = 3.0 s, Slow AVR Model and Fast Governor Model - Test FG2.

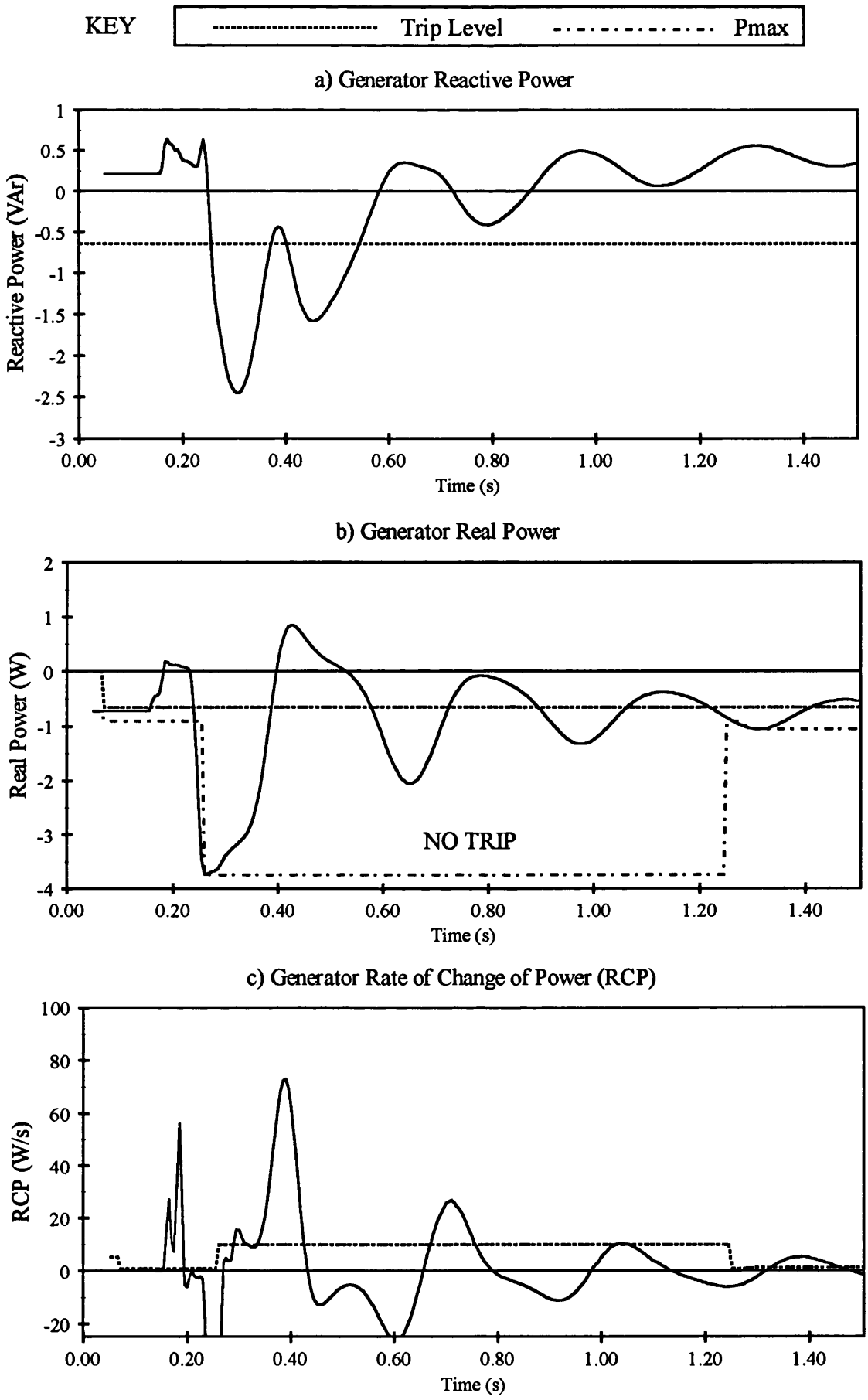

Figure 6.71

Modified Motor Pole Slipping Algorithm Response to an ATP Simulated Synchronous Motor Stable Power Swing on a 750 kVA Hydro Machine in Pumping Mode - Test MOT1

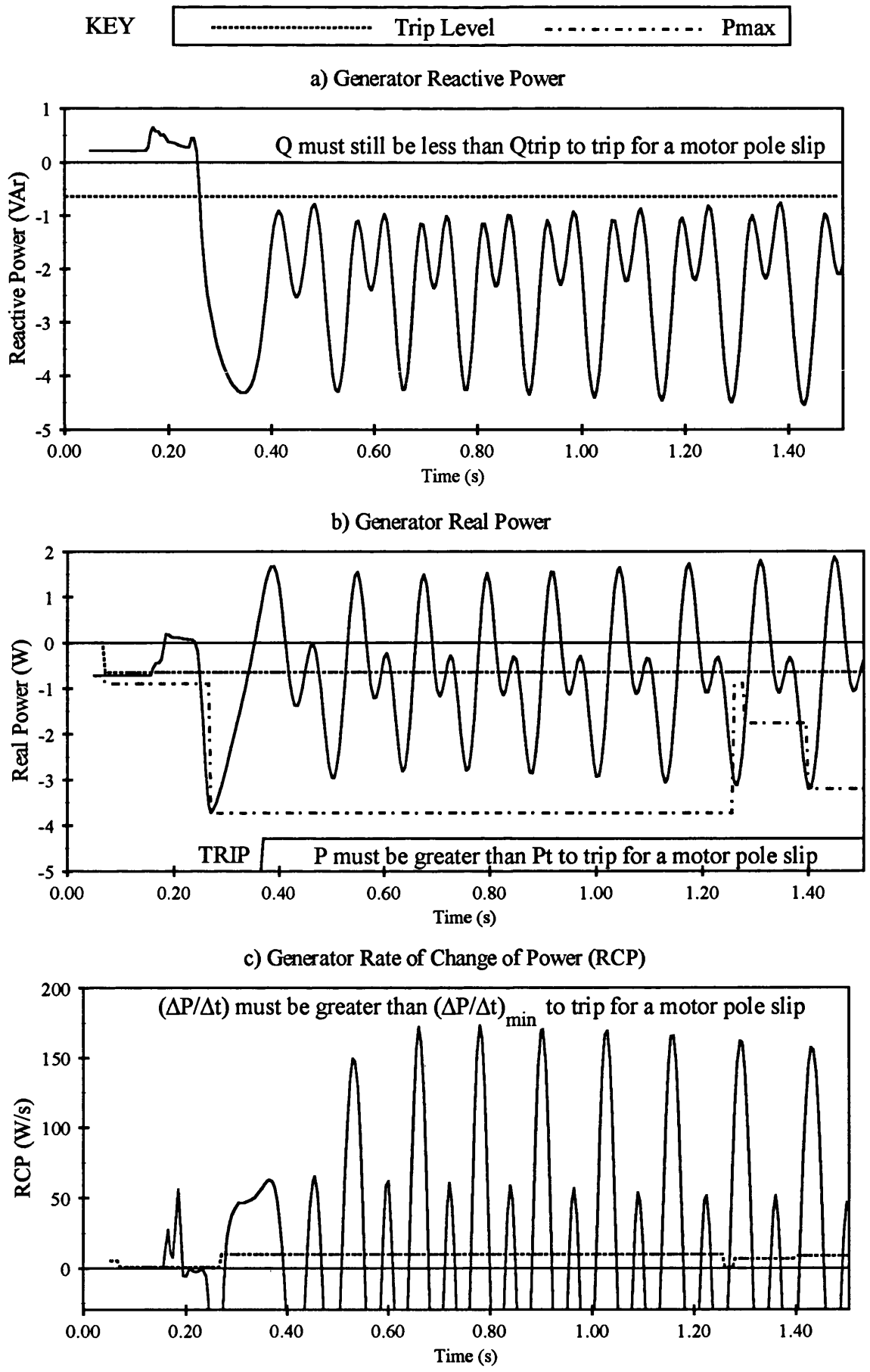

Figure 6.72
Modified Motor Pole Slipping Algorithm Response to an ATP Simulated Synchronous Motor Pole Slip on a 750 kVA Hydro Machine in Pumping Mode - Test MOT2

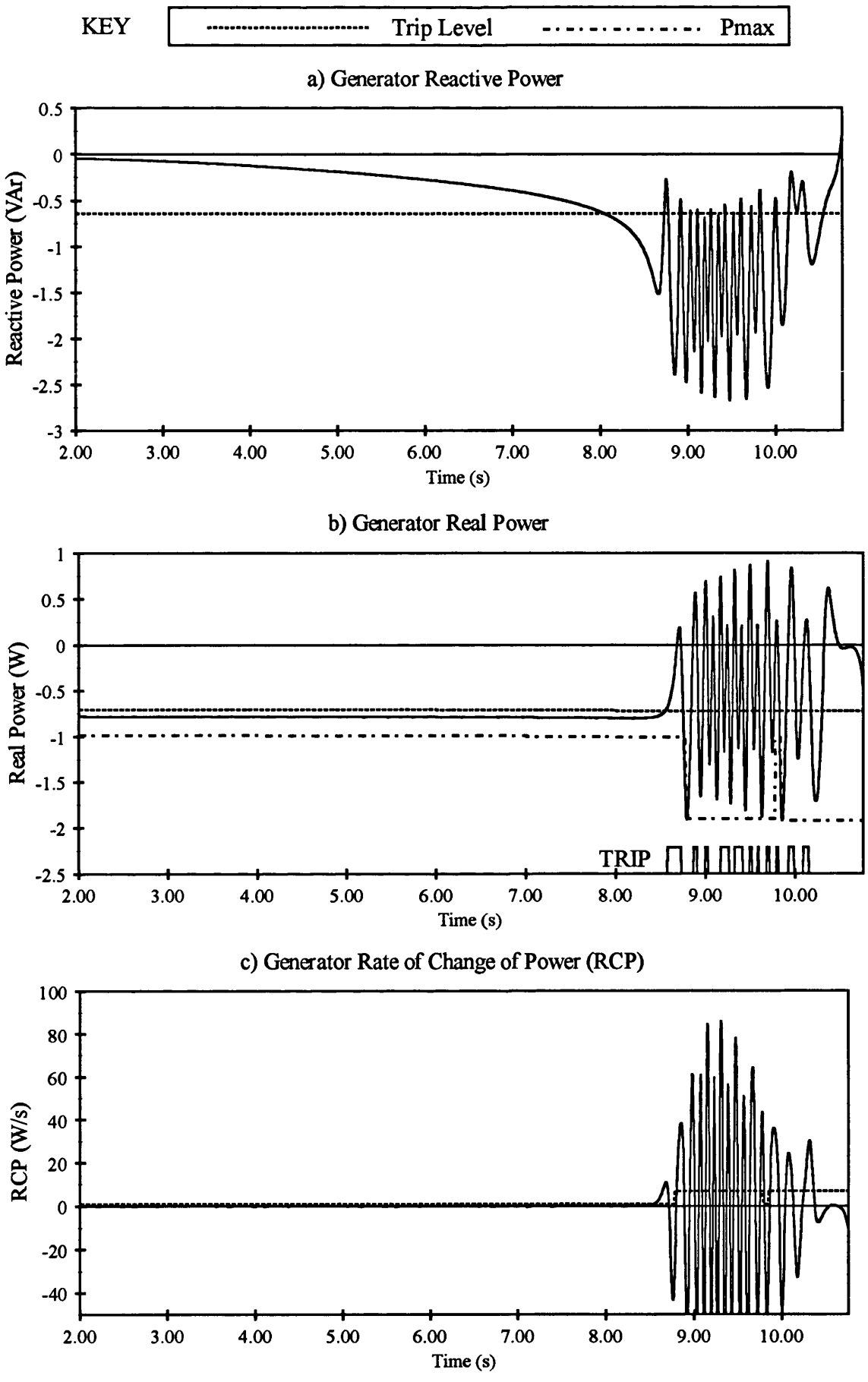

Figure 6.73
Modified Pole Slipping Algorithm Response to an ATP Simulated Pole Slip on a 750 kVA Hydro Motor, Pole Slip Caused by an Redcuction in Machine Terminal Voltage to 80 % - Test MOT3.

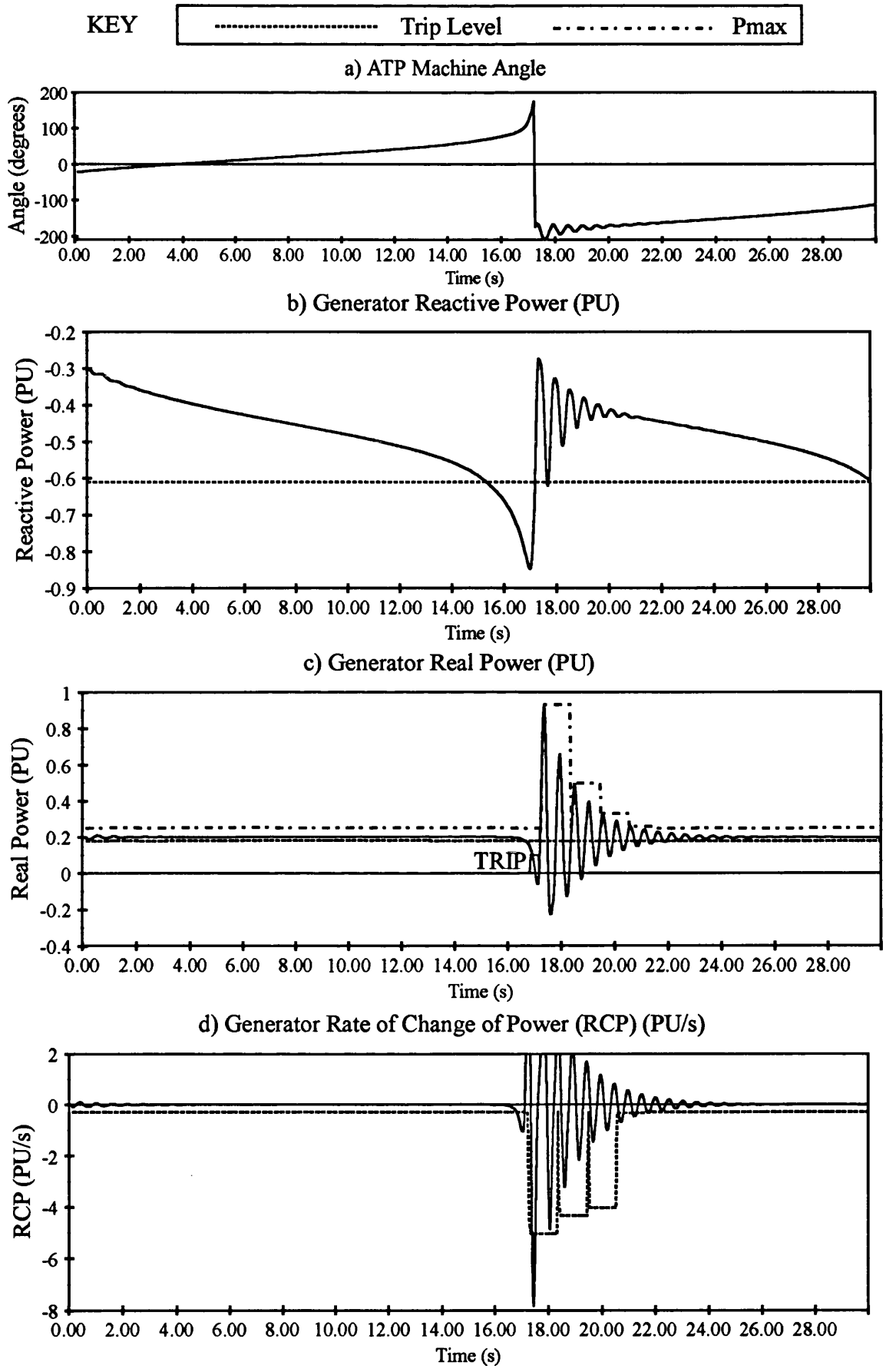

Figure 6.74

Pole Slipping Algorithm Response to Additional Algorithm Test ' SLW' - Slow Pole Slipping of a 200 MVA Generator, Induced by a Weak Excitation, Governor and AVR Modelled, Pole Slipping Rate = 0.05 % slip - Test SLW.

Chapter 7
SUMMARY OF RESULTS

This chapter presents a summary of the test results presented in Chapter six.

7.1 RESPONSE OF THE POWER BASED POLE SLIPPING ALGORITHM

The power based pole slipping algorithm operated for all of the pole slipping tests performed. It successfully restrained for all of the stable power swing, fault, loss of prime mover, synchronisation, load change and adjacent generator pole slip tests. It did not nuisance trip during the field trials conducted on a hydro and a steam turbine generator.

7.1.1 Differentiation Between 'Transient' and 'Steady State' Pole Slips

The algorithm can successfully categorise pole slips as either 'transient' or steady state. Using the magnitude of ($\Delta P/\Delta t$) as well as the ratio Pt/Pmax, the algorithm successfully categorises all transient pole slips. If however, the algorithm only used the ratio Pt/Pmax for the assessment, it could fail to recognise some 'transient' pole slips because it is possible that no peak in output power will occur if the fault which causes the pole slip is cleared at a load angle between 180° and 360°.

7.1.2 Adaptive Tripping Times for Minimising Circuit Breaker Operating Duty

If there is concern over generator circuit breaker switching duty when a generator is disconnected during pole slipping, the algorithm can be set for delayed circuit breaker tripping. This will minimise the asynchronous switching duty placed on the circuit breaker as illustrated by the POWSIM test results. Instead of tripping when the algorithm detects that a pole slip is imminent, the algorithm can delay the "trip circuit breaker" command until the reactive power criterion resets. In an ideal system, this occurs at a load angle of 270°, and ideal point to commence circuit breaker arc interruption.

The delayed switching option can also be used adaptively. During steady state pole slips, the generator loses synchronism slowly and therefore the algorithm can be set to trip the instant it detects that a pole slip is about to occur. This will typically occur at load angles

of 110°, where the switching duty on the circuit breaker is not too high. If the algorithm diagnoses a transient pole slip, tripping can be delayed until the reactive power criterion is reset, corresponding to a load angle of 270°.

7.1.3 Analysis of the Optimum Values for the 'lag' and 'Ptol' Settings

The lag setting used by the algorithm was chosen to be set to one second. The 5 kVA laboratory generator test results show that a shorter setting may result in incorrect updates in Pt. For all of the tests conducted, the one second setting resulted in correct updates.

The default value for Ptol of 5 % of the generator rating worked satisfactorily for all tests. The most demanding test conditions occurred during the 625 kVA diesel generator field tests. Significant oscillations occurred in the real power which could have resulted in the algorithm failing to update Pt because the magnitude of the oscillations exceeded the 'Ptol' setting. However, the algorithm updated Pt correctly for all of the diesel generator field tests. The real output power of the 5 kVA, 26.5 MVA and 353 MVA generators showed no significant oscillations. The diesel generator provided the most testing conditions. Because the algorithm functioned satisfactorily on the diesel generator, it follows that it can be expected to function correctly for all other types of generator.

7.1.4 Algorithm Response to Adjacent Generator Disturbances

The 5 kVA and 625 kVA generator tests showed that the algorithm will remain secure during pole slipping and loss of excitation of an adjacent generator connected to the same bus as the protected generator. During pole slipping, the adjacent generator's reactive power demand increases. The healthy generator will attempt to supply some of the increased reactive power demand and will therefore increase its reactive power output. This increases algorithm security because the protected generators reactive power output moves away from the trip setting, Qtrip.

7.1.5 Algorithm Response to Fault Tests

Fault tests were conducted on the 5 kVA laboratory and 200 MVA PPSS generators, and three fault disturbance records were captured by the 353 MVA steam turbine generator field trial relay. The algorithm remained secure for all of the faults it was subjected to. It was noted that the reactive power criterion is not satisfied at the beginning of, or during a fault. Faults present an inductive load to a generator, the generator's reactive power output is therefore generally positive during a fault, and therefore does not satisfy the

negative reactive power trip setting.

The most testing situation for algorithm security occurs during clearance of short circuit faults which can cause the generator load angle to increase above 90° thus satisfying the reactive power criterion. The fundamental basis of the algorithm ensures that it remains secure. After fault clearance, if the generator is not going to lose synchronism, it will not have reached the CSP, the real power criterion will therefore not be satisfied. This condition has to occur because the generator requires deceleration energy to remain stable. However, for some faults it was observed that the real power criterion may be satisfied for a very short time at fault clearance due to the fast transients which occur. These occur for under one power system cycle, and algorithm operation is therefore blocked by the one and a quarter cycle time delay applied to the algorithm.

7.1.6 Algorithm Operational Limits

The setting curves presented in Chapter four were shown to be correct by the PPSS tests. Test 'PSL3GA' (section 6.3.1) showed that the value of external reactance at which the algorithm's reactive power criterion fails can be read from the setting graphs. The graphs therefore enable the applications engineer to see if the power based algorithm is suitable for the system to be protected. For most generators, the value of external reactance between the generator terminals and the infinite bus is low enough to enable the algorithm to successfully operate.

The PPSS test 'PSL3NN' (section 6.3.1) showed that the algorithm can detect pole slips up to a rate of 8 Hz. This equates to a slip of 16 %. This test confirmed the theory of section 4.4.2, which predicted that the maximum rate of pole slipping that the algorithm could detect was 8.3 Hz.

Test 'SLW' described in section 5.6 demonstrated that the algorithm could also detect slow pole slipping rates. Slow pole slips occur when the generator is operating at low power, with low excitation. The generator pole slipped in this test at a rate of two to three cycles per minute. A pole slip rate of three slip cycles per minute equates to a slip of 0.1 %. This is the lowest slip rate specified in conventional impedance based pole slipping schemes. The algorithm is able to detect such slow pole slip rates because the section of the pole slip cycle where the algorithm will operate occurs quickly. The section of the pole slip which occurs after a load angle of approximately 130° occurs quickly because

even at low mechanical input powers, the combined effect of the prime mover input power and the power which the generator draws from the utility causes a rapid increase in load angle.

7.1.7 Algorithm Response to Stable Power Swing Tests

The PPSS tests provided the most testing stable power swing conditions. The algorithm restrained for all of the stable power swings tested. The severest test conditions occurred when the power swings were caused by a long duration fault at low initial excitation and low power output with the AVR set to manual. Test 'PSW1GN' (section 6.3.2) is an example of such an operating condition. These conditions are severe because the initial low level of excitation is further decreased by the demagnetising effect of armature reaction during the fault. With the AVR set to manual, no field forcing occurs during the fault, which would normally offset the effects of armature reaction. As a result, the generator output power characteristics are no longer dominated by field excitation terms. The field excitation terms cause the sinusoidal power-load angle characteristics. Instead the characteristics have a significant asynchronous induction generation component. The sinusoidal characteristics which the power based algorithm and impedance based protection schemes are based upon therefore do not occur. The resulting asynchronous characteristics produce real and reactive power variations which are very testing for all types of pole slipping protection.

The algorithm did not operate during any of these severe power swing tests. This was attributed to its adaptive $(\Delta P/\Delta t)_{min}$ trip setting which enhances algorithm security without reducing sensitivity. During transient conditions such as stable power swings, a high $(\Delta P/\Delta t)_{min}$ setting is used because large fluctuations in $(\Delta P/\Delta t)$ occur. The setting is increased by the transient saliency scaling factor $(\Delta P/\Delta t)_{tran}$. During steady state conditions, a sensitive value of $(\Delta P/\Delta t)_{min}$ is used because only small fluctuations in $(\Delta P/\Delta t)$ occur.

7.1.8 The Effect of Using a Lower 'Slip' Setting

The PPSS tests showed that a reduction in the 'slip' setting from the default value of -0.5 % to -0.25 % resulted in faster tripping times for steady state pole slips. The highest gain in tripping time occurs for steady state pole slips which occur from low initial operating powers. The largest practical gain in tripping response was 140 ms for test 'PSL1GAF' (section 6.3.1). In order for the change in the 'slip' setting to be effective, the $(\Delta P/\Delta t)_{fact}$ setting had to be reduced from -25 % to - 10 % of the generator rating.

The reduction in slip setting did not result in the algorithm nuisance tripping for any of the tests conducted. The transient saliency setting, $(\Delta P/\Delta t)_{tran}$ provided adequate algorithm security during transient conditions. Care must be taken however, if the slip setting is reduced when a low value of the setting $(\Delta P/\Delta t)_{tran}$ is used. If the algorithm were to be released commercially, the slip setting may no longer be a setting. It could be included in the algorithm code. It would therefore be advisable to use a limit on the value of $(\Delta P/\Delta t)_{tran}$ of twice the generator rating so that the algorithm was always secure during transient conditions.

7.1.9 Algorithm Performance for Detecting Loss of Field Conditions

The algorithm successfully detected all of the loss of field conditions where the generator lost synchronism and operated asynchronously.

The algorithm operated for all of the PPSS loss of field tests. The 200 MVA PPSS generator was of round rotor construction, it therefore had virtually no saliency and could not generate reluctance torque to keep it in synchronism. It would not detect loss of field from zero initial power however. There would be no prime mover power available to accelerate the rotor and cause the generator to lose synchronism.

The algorithm only operated for the high initial operating power 625 kVA diesel generator loss of field tests. It failed to detect the low and medium initial power loss of field conditions because the saliency present in the diesel generator rotor structure provided enough reluctance torque to prevent the generator from losing synchronism in the timescale of the test.

Full loss of field cover could be achieved for all types of generator by complimenting the power based pole slipping algorithm with an additional simple power based algorithm[160].

7.1.10 Algorithm Tripping During Synchronous Operation

As predicted in Chapter four, the power based algorithm nuisance tripped during the tests where the generator was operated at load angles of greater than 90° with the aid of a fast AVR. This is of little concern however, as generators are not operated in this mode in practice due to insufficient transient stability margins.

The algorithm also tripped between pole slips for the 625 kVA diesel generator test 'A3'.

The real power oscillated following the first pole slip which occurred in this test, and these oscillations resulted in the real and rate of change of power criterions being satisfied. Normally this would not cause a problem because the reactive power criterion would not be satisfied. However, in this case the generator was about to slip another pair of poles, the reactive power criterion was therefore satisfied. This trip is not serious because it occurred between two pole slips. It could be a concern if a 'trip after 'n' pole slips' function is implemented in the algorithm.

This trip could have been prevented by increasing the reset time used in the 'Pmax' function. After Pmax has been updated to a value above nominal, it is held at the new value for one second and then returned to its nominal value. The reset in Pmax results in $(\Delta P/\Delta t)_{tran}$ being omitted from the $(\Delta P/\Delta t)_{min}$ calculation. This increases algorithm sensitivity because the algorithm is in its 'steady state' mode. The trip occurred just after a reset in Pmax, if Pmax had remained at its high value, the 'transient' rate of change of power setting would not have been satisfied and the algorithm would not have tripped. It is therefore recommended that the reset time is increased from one to two seconds. This would ensure that any transient disturbances have decayed by the time the reset occurs.

7.1.11 Algorithm Modification to Detect Motor Pole Slipping

The 'MOT' tests described in section 5.6 confirmed the theory of section 4.6; the algorithm can be easily modified to detect synchronous motor pole slips. If the signs of the real power and rate of change of power criterions are reversed, the algorithm successfully detects synchronous motor pole slipping whilst restraining for synchronous motor stable power swings. The algorithm code would only require minor modifications to enable it to provide synchronous motor and generator pole slipping protection in one function. This would be required for pumped storage machines, which are often operated in both modes and are prone to pole slipping because of the low CCT that hydro machines have in the pumping mode.

7.2 RESPONSE OF THE IMPEDANCE BASED POLE SLIPPING RELAYS

Analysis of the impedance based relays showed that they may nuisance trip during stable power swings. The single blinder scheme is the most secure of the schemes, followed by the double blinder, then the mho scheme. The impedance based schemes were also shown to fail to detect pole slips whose impedance locus does not follow the 'ideal' trajectory.

The single blinder scheme will operate correctly with the right settings. However, finding the correct settings requires detailed computer based simulations.

The single blinder scheme requires a full pole slip cycle before it will trip and disconnect the generator. It therefore trips after the pole slip has happened.

7.2.1 The Mho Pole Slipping Protection Scheme

The mho scheme operated for all of the PPSS pole slip tests, but failed to operate for the 625 kVA diesel generator pole slips. For these tests, the impedance locus passed underneath its operating characteristic.

Having detected the first few pole slips, it was shown to fail to detect some of the faster PPSS pole slips because the impedance locus travelled through its characteristic too quickly. This problem is made worse if the locus travels across the top or bottom of the mho circle because the locus will remain inside the trip zone for a shorter time.

The mho scheme nuisance tripped for 8 of the 12 PPSS stable power swing tests. If the reach of the mho scheme had been reduced to prevent these nuisance trips, or a longer time delay applied to the scheme, it would have failed to detect some of the pole slips.

7.2.2 The Single Blinder Protection Scheme

This scheme failed to detect some pole slips because the impedance locus passed underneath its supervisory mho characteristic. If the supervisory mho reach was increased, the scheme may have detected some of the pole slips. However, increasing the size of the mho circle increases the chances of nuisance tripping during recoverable power swings.

For numerous tests, the single blinder scheme also failed to detect the first pole slip cycle

following faults because the impedance locus crossed the right hand blinder element before the supervisory mho element had picked up. The problem could be remedied by increasing the reach of the supervisory mho element, but care has to be taken since this may compromise the security of the scheme. A more complex scheme described by Goody[79] can also be used which overcomes this problem.

Some pole slips satisfied the initial stages of the schemes logic, but then failed to satisfy the final stages. The impedance locus would travel horizontally at first, entering the mho characteristic, then crossing the right hand blinder unit. However, as it reached the jX axis, it would 'bend' downwards, leaving the supervisory mho characteristic before it crossed the left hand blinder. The scheme would therefore fail to trip. This type of problem can be overcome by using a quadrilateral type impedance characteristic.

The scheme also failed to detect some of the fast pole slips because the impedance locus crossed the left and right blinders in under 40 ms. In test 'PSL3NN' (Section 6.3.6.1) the single blinder failed to operate at a mean pole slipping rate of 6.5 Hz.

The scheme did restrain for all of the stable power swing tests, showing that it is the most secure of the conventional impedance based schemes.

7.2.3 The Double Blinder Protection Scheme

This scheme suffered from the same problems as the single blinder scheme. It was also shown to nuisance trip during one of the PPSS stable power swing simulations. After fault clearance, the impedance locus travelled to the right of the right blinder unit, then travelled to the left of the right inner blinder unit before moving back out towards the load area of the RX plane.

This nuisance trip demonstrated that the double blinder scheme does not have the inherent security of the single blinder scheme because the impedance locus does not have to enter and exit its characteristic on opposite sides to cause a trip.

7.3 THE EFFECTIVENESS OF STANDARD PROTECTION SCHEMES AT DETECTING POLE SLIPPING

The response of under-voltage, over-frequency and IDMT over-current relays during pole slipping conditions was analyzed. The analysis showed that none of the relays could be relied on to trip during pole slipping because of the fluctuations in most power system quantities during pole slipping.

All three types of relay were reset at some point in the pole slip cycle, which meant that their time delay criteria were never satisfied. The problem occurs because as the pole slipping generator reaches the in-phase position, its current and voltage return to their normal values, resetting the relays. The problem can be overcome if a delay on reset function is included in the relay. This would enable the relay to 'integrate' over several pole slip cycles until their trip criterion is satisfied, but may cause difficulties for other protection duties.

The fluctuations in real and reactive power cause the generator terminal voltage phasor to swing back and fourth. Frequency measuring devices track these swings in phase angle, which cause the measured frequency to rise and fall with the period of pole slipping. These relays are therefore also reset during every pole slip cycle and are prevented from tripping.

Chapter 8
CONCLUSIONS & FURTHER WORK

8.1 CONCLUSIONS

With the increasing number of synchronous embedded generators being installed to operate in parallel with utility distribution systems, generator stability is being recognised as an area of concern. Generator instability causes pole slipping which can damage the machine and disturb the local power system. Stator winding damage, overheating, excitation system insulation failure and shaft fatigue may occur if a pole slipping generator is not disconnected from the network.

The likelihood of embedded generator pole slipping is much higher than that of large 'grid' type generators because of lower inertias, shorter time constants and longer fault clearance times. The critical clearance time for most embedded generators is between 200 and 300 ms whereas the fault clearance times of the IDMT type over-current protection used on most distribution systems can be up to one second.

The protection requirements of embedded generators are best met by modern multi-function microprocessor relays. Research has therefore been conducted into a new pole slipping algorithm which uses the computing power available in microprocessor relays to enhance the performance provided by conventional pole slipping schemes and reduce the setting complexity.

The traditional technique for detecting pole slipping is to examine the variations in apparent impedance at the terminals of the generator. The simplest protection scheme uses a mho relay. It can trip before the generator load angles reaches 180° and also provides a degree of back up protection for faults occurring in the generator and transformer. However, it can nuisance trip during recoverable power swings and can fail to detect fast pole slips or pole slips whose impedance locus does not take the 'ideal' trajectory.

The single blinder scheme is the most secure of the impedance based pole slipping protections. It requires a complete pole slip cycle to trip and therefore trips after pole slipping has occurred. The main disadvantage with the single blinder scheme is finding

settings which work for all pole slipping conditions.

The double blinder scheme is less secure than the single blinder scheme because unlike the single blinder scheme, it does not require the impedance locus to enter and exit its trip characteristic on opposite sides. It can therefore nuisance trip during stable power swings.

The pole slipping impedance locus of embedded generators can be far from ideal. This can make it difficult to set the impedance based schemes so that they operate for all pole slipping conditions without them nuisance tripping during stable power swings or faults. To obtain reliable settings, detailed computer based simulations of the embedded generator, its control equipment and the local electrical system are required. These can be expensive and time consuming.

The level of protection required for embedded generators is specified in Engineering Recommendation 'G59'[14] and Engineering Technical Report 113[15]. Under-voltage, over-frequency, loss of grid, over-current and other relays are included in this specification. It has been suggested that these relays will disconnect a pole slipping generator[15]. Tests have shown however, that these relays do not generally operate during pole slipping because they are reset once every slip cycle as the generator passes through the in phase position.

The alternative to installing relays to disconnect the generator when pole slipping occurs is to ensure that pole slipping will not occur. However, this requires costly changes to the utility protection systems and generator which make this option unfeasible.

A new power based pole slipping algorithm has been developed which monitors the operating condition of the generator and adapts its settings according to the generator's mode of operation. The algorithm is based on the fact that once the generator operates beyond its Critical Stability Point (CSP), it will become unstable and pole slipping will therefore occur. The algorithm uses real and reactive power and rate of change of real power as inputs. It trips if the generator exceeds its CSP and its load angle is increasing.

The algorithm uses sensitive settings to detect pole slips which occur due to a loss of steady state stability, whilst it automatically selects more secure settings when transient conditions such as recoverable power swings occur. It offers the immediate advantage of

detecting when an embedded generator is committed to a pole slip, rather than has actually pole slipped. It therefore offers the opportunity of disconnecting the machine from the network before possible damage or major disturbance to the power system occurs.

The algorithm's settings are determined from readily available generator data. It is therefore simple to set compared with conventional impedance based relays and obviates the need for power system simulation studies.

The new algorithm has been implemented in a commercially available microprocessor relay and tested using a variety of test platforms such as computer based simulations, laboratory power system models and industrial generators. The algorithm has been shown to operate correctly using computer based simulations of a 588 MVA steam turbine generator, a 200 MVA steam turbine generator and a 750 kVA diesel generator. It has also operated correctly during tests on a 5 kVA laboratory generator, a 625 kVA industrial diesel generator, a 26.5 MVA hydro generator, and a 353 MVA steam turbine generator.

Tests have shown that the algorithm trips before a generator pole slips whilst remaining secure during stable power swings, power system short circuit faults, generator synchronisation, and generator loss of prime mover. Tripping may occur if a generator is operated at load angles above 90°, but this mode of operation is not used in practice because the reserve in hand for transient stability is too low.

The algorithm has also been shown to operate for generator loss of field conditions if the generator operates asynchronously. It will not trip for loss of field conditions where the generator maintains synchronism due to reluctance torque. The algorithm can be complimented by a time delayed PQ trip zone characteristic[160] to provide full loss of field protection.

The tests show that the algorithm can differentiate between 'steady state' and 'transient' pole slips. This information can be used to delay tripping until after the pole slip, if the circuit breaker switching duty is a concern.

Although this research has focused specifically on embedded generators, the algorithm will function correctly on large grid generators.

It has been shown that the algorithm can be easily modified to detect synchronous motor pole slips. This is important for pole slipping protection of pumped storage hydro machines. These machines have short values of critical clearing times which increase the likelihood of pole slipping.

8.2 SUGGESTIONS FOR FUTURE WORK

The pole slipping tests have assumed that the protection algorithm is applied to only one generator. However, embedded generation units can use multiple generators operating in parallel. If the generators are similar, it is expected that one relay could be used to provide pole slipping protection for the whole group of generators. Further simulation studies are required to confirm this theory. This approach would only be used if one overall protection scheme was used for the whole group.

Tests have shown that the algorithm can be modified to detect motor pole slipping protection. However thorough testing of the motor pole slipping algorithm has not been tested.

If the algorithm were to be released commercially, most of the future work required would be development rather than research. At present the algorithm code is written using 32 bit variables for the intel 80186 processor. The code would need optimising by converting to 16 bit variables. The codes efficiency could be further improved, since the calculation of the rate of change of power trip criterion is performed every 5 ms. The variables, Pt and Pmax which are used in the calculation may only change once a second. The code could therefore be written so that $(\Delta P/\Delta t)_{min}$ is only calculated when a change in Pt or Pmax occurs.

A setting calculation program could also be written for a commercial version of the algorithm so that the applications engineer need only enter the generator variables Xd', Xq and the generator rating, and the relay would then calculate the settings itself.

Chapter 9
REFERENCES.

[1] 'The Energy Act 1983', Her Majesty's Stationary Office, London.

[2] 'The Electricity Act 1989', Her Majesty's Stationary Office, London.

[3] 'Public Utility Regulatory Policies Act - PURPA 1978', US Federal Energy Regulatory Commission.

[4] FIELDING G & BRADLEY J, 'Local Generation - The Devolution of Power', IEE Review, March 1990, pp 117-120.

[5] SMITH W P & FISCHER R N, 'Cogeneration: Small Turbine-Generator Case Study', IEEE Transactions on Industry Applications, Vol IA-22, No.1, Jan/Feb 1986, pp 121-125.

[6] HOGWOOD E E & RICE D E, 'The Electrical Aspects of Cogeneration System Design', IEEE Transactions on Industry Applications, Vol IA-23, No.4, July/August 1987, pp 712-722.

[7] DALEY J M, 'Design Considerations for Operating On-Site Generators in Parallel with Utility Service', IEEE Transactions on Industry Applications, Vol IA-21, No.1, Jan/Feb 1985, pp.69-80.

[8] JEWELL T & RIZY TM, 'Interconnection Problems Associated with Small Dispersed Electric Generators and Inverter Devices', ISA Transactions, 1984, Vol 23, No.2, pp 21-26.

[9] POPE J W, 'Parallel Operation of Customer Generation', IEEE Transactions on Industry Applications, Vol IA-19, No.1, Jan/Feb 1983, pp 32-36.

[10] PRINCE W R, 'Current Operating Problems Associated with Non-Utility Generation', IEEE Transactions on Power Systems, Vol.4, No.4, October 1989, pp 1534-1541.

[11] NOBILE P A, 'Power System Studies for Cogeneration: What's Really Needed ?', IEEE Transactions on Industry Applications, Vol IA-23, No.5, Sep/Oct 1987, pp 777-785.

[12] NICHOLS N, 'The Electrical Considerations in Cogeneration', IEEE Transactions on Industry Applications, Vol.IA-21, No.4, May/June 1985, pp 754-761.

[13] DOUGHTY R L, GISE L, KALKSTEIN E W & WILLOUGHBY R D, 'Electrical Studies for an Industrial Gas Turbine Cogeneration Facility', IEEE

Transactions on Industry Applications, Vol.25, No.4, July/August 1989, pp 750-765.

[14] The Electricity Council, 'Engineering Recommendation G59 - Recommendations for the Connection of Private Generating Plant to the Electricity Boards' Distribution System', London, June 1985.

[15] The Electricity Council, 'Engineering Technical Report ET113 - Notes for Guidance for the Protection of Private Generating Sets up to 5 MW for Operation in Parallel with Electricity Boards' Distribution Networks', London, 1989.

[16] American National Standard, 'IEEE Guide for Interfacing Dispersed Storage and Generation Facilities with Electric Utility Systems', ANSI/IEEE Std 1001-1988, February 1989, IEEE New York, USA.

[17] ROOK M J, GOFF L E, POTOCHNEY G J & POWELL L J, 'Application of Protective Relays on a Large Industrial-Utility Tie with Industrial Cogeneration', IEEE Transactions on Power Apparatus and Systems, Vol.PAS-100, No.6, June 1981, pp 2804-2812.

[18] WAGNER C L, FEERO W E, GISH W B & JONES R H, 'Relay Performance in DSG Islands', IEEE Transactions on Power Delivery, Vol.4, No.1, Jan 1989, pp 122-129.

[19] DUGAN R C & RIZY D T, 'Electric Distribution Protection Problems Associated with the Interconnection of Small, Dispersed Generation Devices', IEEE Transactions on Power Apparatus and Systems, Vol.PAS-103, NO.6, June 1984, pp 1121-1127.

[20] FARDANESH B & RICHARDS E F, 'Distribution System Protection With Decentralised Generation Introduced into the System', IEEE Transactions on Industry Applications, Vol.IA-20, No.1, Jan/Feb 1984, pp122-130.

[21] Summary Report of an IEEE Working Group Report, 'Intertie Protection of Consumer-Owned Sources of Generation, 3 MVA or Less', IEEE Transactions on Power Delivery, Vol.5, No.2, April 1990, pp 924-929.

[22] BOWE T R, IQBAL S, DAPKUS D & RIZY D T, 'A Decision Analysis Model to Determine the Appropriate Level of Protection for Small Power Producer/Utility Interconnection', IEEE Transactions on Power Delivery, Vol.PWRD-1, No.3, July 1986, pp 78-89.

[23] HARLOW J H, 'A Multi-function Protective Relay for the Cogeneration Industry', IEEE Computer Applications in Power, October 1990, pp 25-30.

[24] POWELL L J, 'An Industrial View of Utility Cogeneration Protection

Requirements', IEEE Transactions on Industry Applications, Vol IA-24, No.1, Jan/Feb 1988, pp 75-81.

[25] FROMM F, FRANC Z, KULENDIK B & STEINER C, 'Generator Protection with the Digital MODURES 216', Brown Boveri Review 1987, Vol.74, No.12, pp 693-700.

[26] RIFAAT R M, 'Protection Scheme Considerations for Common Generator Bus Configurations used in Cogeneration Plants', IEEE Wescanex 93 - Communications, Computers and Power in the Modern Environment : Conference Proceedings 1993, Ch. 60, pp 1-6.

[27] ZIEGLER G, 'Developments in Generator Protection - Design and Application Aspects of a New Numerical Relay Range', Fifth International Conference on Developments in Power System Protection, IEE Conf Pub 368, 1993, pp 111-114.

[28] PETTIGREW R D, 'Generator Protection Using Multi-function Digital Relays', International Conference on New Developments in Power System Protection and Local Control, May 25 - 28, 1994, Beijing, China, pp 390 - 399.

[29] XUESHEN Z, RONGSHANG G, ZHAOXIN Z, ZHENHUA Z, WEIJIAN W, JUNHONG L, & ZHENHUA L, 'Development of Microcomputer-Based Complete Protection for Large Generator-Transformer Set', International Conference on New Developments in Power System Protection & Local Control, May 25-28, 1994, Beijing, China, pp 110 - 115.

[30] KOULISCHER M, MAUN J C, & HENNIGER K, 'A Multi-Functions Digital Protection for Generators', CIGRE Symposium, Bournmouth 1989, Paper 2A-05.

[31] IEEE Committee Report, 'Survey of experience with Generator Protection and Prospects for Improvements using Digital Computers', IEEE Transactions on Power Delivery, Vol.3 , No.4, Oct 1988, pp 1511-1521.

[32] Modern Power Station Practice: Operation and Efficiency. Volume 7, C.E.G.B, Pergamon Press, Oxford, 1971.

[33] SEETHARAMAN C K, VERMA S P & EL-SERAFI A M, 'Operation of Synchronous Generators in the Asynchronous Mode', IEEE Transactions on Power Apparatus and Systems, Vol.PAS-93, pp 928-934.

[34] CHALMERS B J, 'Asynchronous Performance Characteristics of Turbo-Generators', Proc. IEE Paper No. 3940 S, Vol. 109 A, Aug 1962, pp 300-308.

[35] Transient Phenomena in Electrical Power Systems. VENIKOV V A, Pergamon Press, Oxford, 1964.

[36] Power System Stability Volume 2: Power Circuit Breakers and Protective Relays.

KIMBARK E W, John Wiley & Sons, New York, 1964.

[37] Power System Stability and Control. KUNDUR P, McGraw-Hill Inc, USA 1994.

[38] SHACKSHAFT G & NEILSON R, 'Results of Stability Tests on an Under-exited 120 MW Generator', Proc.IEE, Vol.119, No.2, Feb 1972, pp 175-187.

[39] Industry Survey Analysis, 'Distribution Line Protection Practices', IEEE Transactions on Power Apparatus and Systems, Vol.PAS-102, No.10, Oct 1983, pp 3270-3287.

[40] FIELDING G, 'Specification of Control and Protection Equipment for Independent Generation Systems', IEE Second Annual Conference on Embedded Generation, May 1995.

[41] FIELDING G, EVANS G W, 'Industrial Feeder Protection', Tenth International Conference on Electricity Distribution, Part 1, 5- Consumers Installations, 1989, pp 460 -466.

[42] CLARK H K & FELTES J W, 'Industrial and Cogeneration Protection Problems Requiring Simulation', IEEE Transactions on Industry Applications, Vol 25, No.4, July/August 1989, pp 766-775.

[43] MACKENZIE W F (Chairman), 'Loss-of-Field Relay Operation During System Disturbances - Working Group Report - June 1971', IEEE Trans. on Power Applications and Systems, Vol. PAS-94, No.5, Sept 1975, pp 1464-1472.

[44] YALLA M, 'IEEE Tutorial on the Protection of Synchronous Generators: Loss of Field Protection', IEEE Power System Relaying Committee, 1995, ref 95-TP-102.

[45] Protective Relays Application Guide. GEC Measurements, Third Edition - 1987, pp 316-319.

[46] LANDOLL L E, 'Summary of the Guide for AC Generator Protection', ANSI/IEEE C37.102-1987, IEEE Transactions on Power Delivery, Vol.4, No.2, April 1989, pp 957-964.

[47] SIMPSON R H, 'Protective Relaying for Multi-Source Generator Buses', IEEE Transactions on Industry Applications, Vol.26, No.2, March/April 1990, pp 330-341.

[48] MASON T H, FAIRNEY W, ARNOLD J J & THELWELL M J, 'Asynchronous Operation of Turbo-Generators', CIGRE Vol.1 , 1972, Sec 11-02.

[49] COOPER C B, EASTON V, JOHN M N, PARTON K C, SHACKSHAFT G & WHITELEGG T M, 'Problems Associated with Limited Pole Slipping of Turbo-Generators Following System Faults', CIGRE 1966, Vol.3, No.306, pp 1-16.

[50] MASON T H, AYLETT P D & BIRCH F H, 'Turbo-Generator Performance

Under Exceptional Operating Conditions', Proc. IEE, Vol.106, Jan 1959, pp 357-373.

[51] Electrical Power Systems : GUILE A E and PATTERSON , Vol 2, pp 106-141, Oliver & Boyd, 1969.

[52] ABOLINS A, LAMBRECHT D, JOYCE J S & ROSENRERG L T, 'Effect of Clearing Short Circuits and Automatic Re-closing on Torsional Stress and Life Expenditure of Turbine-Generator Shafts', IEEE Transactions on Power Apparatus and Systems, Vol.PAS-97, No.1, Jan/Feb 1976, pp 14-25.

[53] MASRUR M A, AYOUB A K & TIELKING J T, 'Studies on Asynchronous Operation of Synchronous Machines and Related Shaft Torsional Stresses', Proc.IEE, Part-C, Vol.138, Jan 1991, pp 47-56.

[54] MASON C R, 'Relay Operation During System Oscillations', AIEE Transactions, Vol. 56, July 1937, pp 823-832.

[55] BANCKER E H & HUNTER E M, 'Distance Relay Action During Oscillations', AIEE Transactions, Vol. 53, July 1934, pp 1073-1080.

[56] MECHRAOUI A & THOMAS D W P, 'The Influence of Power Swing on Transmission Line Distance Protection, Measurement of Power Flow and Voltage Phasor Oscillation at the Relaying Point', UPEC 93, Stafford, 1993, pp 585-588.

[57] YALLA M V V S, 'A Digital Multi-function Protective Relay', IEEE Transactions on Power Delivery, Vol.7, No.1, Jan 1992, pp 193-200.

[58] BENMOUYAL G, BARCELOUX S & PELLETIER R, 'Field Experience with a Digital Relay for Synchronous Generators', IEEE Transactions on Power Delivery, Vol.7, No.4, Oct 1992, pp 1984-1992.

[59] STRANNE G, 'Numerical Generator Protection', IEE Discussion Meeting, London, 17 December 1992.

[60] STALEWSKI A, GOODY J L H & DOWNES J A, 'Pole Slipping Protection', Developments in Power System protection, IEE Conference Publication No.185, pp 38-45.

[61] Applied Protective Relaying. Westinghouse Electric Corporation, 1979. Silent Sentinels Publication.

[62] ILAR F, 'Innovations in the Detection of Power swings in Electrical Networks', Brown Boveri Revue, Part 2, 1981, pp 87-93.

[63] CHECKSFIELD M J, 'An Investigation into Pole Slipping Protection for Small and Medium Sized Embedded Generation', Final Year Project Report No. 12/93, University of Bath, 1993.

[64] CHECKSFIELD M J and REDFERN M A, 'An Investigation into Pole Slipping Protection for Small and Medium Sized Embedded Generation', Proc. 28th UPEC, Stafford 1993, Vol 2, pp 957-960.

[65] BERRY T, CHAN K, DUNN R W, and NG F, 'Real Time Power System Training Simulator', Proc. 25th UPEC, University of Bath 1990, pp 671-674.

[66] REDFERN M A, BARRETT J, HEWINGS D & USTA O, 'A Laboratory Facility for Research into Digital Protection Algorithms Used for the Protection of Small and Medium Sized Synchronous Generators', Proc. 27th UPEC. Vol.1, September 1992, pp 16-19.

[67] HEWINGS D B, 'An Investigation into Enhanced Passive Techniques for the Protection of Stator Windings in Small and Medium Sized Generators', MSc Thesis, University of Bath 1992.

[68] IMHOF J A, 'Out of Step Relaying for Generators - Working Group Report', IEEE Transactions on Power Apparatus and Systems, Vol.PAS-96, No.5, Sep/Oct 1977, pp 1556-1564.

[69] SMAHA D W, 'IEEE Tutorial on the Protection of Synchronous Generators: Out of Step Protection of Generators', IEEE Power System Relaying Committee, 1995, ref 95-TP-102.

[70] Power System Stability and Control: Prabha Kundur, EPRI Power System Engineering Series, Mc-graw-Hill Inc, London 1993.

[71] WOODWORTH M, 'Electrical Control Aspects of Small Scale CHP', Presented at a Lecture for the IEE Power Group, London, 26 October 1990.

[72] BERDY J, 'Loss of Excitation Protection for Modern Synchronous Generators', IEEE Transactions on Power Apparatus and Systems, Vol.PAS-94, No.5, Sep/Oct 1975, pp 1457-1463.

[73] MASON C R, 'A New Loss of Excitation Relay for Synchronous Generators', AIEE Trans. Vol 68, pp 1240-1245, 1949.

[74] LGPG 111 Integrated Generator Protection Service Manual R5942. GEC ALSTHOM T & D PROTECTION AND CONTROL LTD. Stafford. July 1995

[75] ARNDT C R & ROGERS M, 'A Study of Loss-of-Excitation Relaying and Stability of a 595-MVA Generator on the Detroit Edison System', IEEE Trans. on Power App. and Systems, Vol. PAS-94, No.5, Sept 1975, pp 1449-1456.

[76] MORRIS W C, 'One Slip Cycle Out of Step Relay', AIEE Trans. Vol 68, pp 1246-1250, 1949.

[77] Applied Protective Relaying: Westinghouse Electric Corporation, 1979. Silent

Sentinels Publication. Out of Step Relaying Chapter, Chapter 19.

[79] GOODY J, 'Overcoming Problems Associated with Impedance Measurements in Pole Slipping Protection for Dinorwig', IEE Proc. Vol 133, Part C, No. 1, January 1986, pp 44-48.

[80] HARKER K, 'The North Wales Super-grid Special Protection Schemes', IEE Electronics and Power, September 1984, pp 719-723.

[81] ILAR M, ZIDAR J, FIORENTIS M, 'Innovations in Generator Protection', Brown Boveri Review, Vol 65, 1978, No 6, pp 379-387.

[82] HABIBULLAH B, 'Wivenhoe Pumped Storage Station - System Protection Against Loss of Synchronism', Electrical and Electronics Journal, Australia, Vol 5, No 2, June 1985 pp 120- 128.

[83] AIEE RELAY SUBCOMMITTEE, 'Interim Report on Application and Operation of Out-of-Step Protection', AIEE Transactions, Vol. 62, Sept 1943, pp 567-573.

[84] AKIYAMA K, SHIRAISHI K, TAMAKI H, MATSUSHIMA T, SAWAI K, ISHIBASHI A, 'Development of a New Out-of-Step Separation System to Balance Supply and Demands After Power System Separation', International Conference on New Developments in Power System Protection & Local Control, May 25 - 28, 1994, Beijing, China, pp 234 - 239.

[85] EYSSEM J and PETROIANU A, 'An Investigation of Characteristics to be Used for Detecting Out of Step Conditions', ESKOM Conference 1995.

[86] CENTENO V, DE LA REE J, PHADKE A G, MICHEL G, MURPHY J, BURNETT R, 'Adaptive Out of Step Relaying Using Phasor Measurement Techniques', IEEE Computer Apps. In Power, Vol. 6, No. 4, Oct. 93, pp 12-17.

[87] GISH W, 'Small Induction Generator and Synchronous Generator Constants for DSG Isolation Studies', IEEE Trans. Power Systems, Vol PWRD - 1, No. 2, April 86, pp 231 - 239.

[88] TAYLOR C W, HANER J M, HILL L A, MITTELSTADT A & CRESAP R L, 'A New Out-of-Step Relay with Rate of Change of Apparent Resistance Augmentation', IEEE Transactions on Power Apparatus and Systems, Vol.PAS-102, No.3, March 1983, pp 631-639.

[89] SHIWEN S, 'Microcomputer Based Out-of-Step Protection for Large Generator', IEE International Conference on Advances in Power System Control, Operation and Management, November 1991, Hong Kong, pp 839-842.

[90] EYSSEN J VAN, 'An Investigation of Characteristics for Tripping Protection Detecting Out of Step Conditions: An ESKOM Case Study', 30th UPEC, Vol 2,

1985, pp 415-418.

[91] WINKLER W, 'A Microprocessor Based Protective System for Generator-Transformer Units', IEE Conf Pub 302. Fourth International Conference on Developments in Power System Protection, pp 56-60.

[92] VILLIERS L N F De, 'Out of Step Operation in A Weakly Interconnected Network', ESKOM Conference 1995.

[93] BAOHUI Z, XIAONING K & YAOZHONG G, 'Out-of -Step Relay Based on Microprocessor', International Conference on New Developments in Power System Protection & Local Control, May 25 - 28, 1994, Beijing, China, pp 320 - 324.

[94] ABDELAZIZ A Y et al, 'Fast Prediction of Out of Step Condition by Artificial Neural Networks for Power System Transient Stability Assessment', 30th UPEC, Greenwich 1995, Vol 2, pp 789-793.

[95] LIE T T, 'A Global Detection Relay for Synchronous Generator Transient and Loss of excitation Stability Using Neural Networks', Third APSCOM, Hong Kong 1995, pp 351-356.

[96] EL-ARABATY A M et al, 'Out of Step Detection Based on Pattern Recognition', International Journal of Electric Power and Energy Systems, 1994, Vol 16(4), pp 269-275.

[97] OHURA Y et al, 'A Predictive Out of Step Protection System Based on Observation of the Phase Difference Between Substations', IEEE Trans. Power Delivery, Vol 5, No 4, November 1990, pp 1695-1704.

[98] ROEMISH W R & WALL E T, 'A New Synchronous Generator Out-of-Step Relay Scheme', Parts 1 and 2, IEEE Transactions on Power Apparatus and Systems, Vol.PAS-104, No.3, March 1985, pp 563-582.

[99] BROWN R D & McCLYMONT K R, 'A Power Swing Relay for Predicting Generation Instability', IEEE Winter Power Meeting, New York, N.Y., Jan/Feb 1965, pp 119-224.

[100] ROEMISH W R, CLEMANS C L, LLOYD L W & SCHLEIF F R, 'An Acceleration Relay for Power Systems', IEEE Trans, PAS 1971, pp 1150- 1154.

[101] SCHLEIF F R, LLOYD L W, WORLD R W & GISH W B, 'A Swing Relay for the East-West Intertie', IEEE Transactions on Power Apparatus and Systems, Vol.PAS-88, No.6, June 1969, pp 821-824.

[102] THORP J S et al,'Some Applications of Phasor Measurements to Adaptive Protection', IEE Proc. Vol 133, Part C, No 1, January 1986, pp 44-48.

[103] A Power Based Digital Algorithm for the Protection of Embedded Generators.

Omer Usta, Ph D Thesis, University of Bath 1992.

[104] A Digital Loss of Grid Protection. James Barrett, Ph D Thesis, University of Bath, 1994.

[105] CUDWORTH C J & SMITH J R, 'Steam Turbine Generator Shaft Torque Transients : a Comparison of Simulated and Test Results', Proc.IEE, Vol.137, Pt.C, No.5, Sep 1990, pp 327-333.

[106] CDV 22,62 Voltage Controlled Over-Current Relays. Manual R 5121, GEC ALSTHOM T & D PROTECTION AND CONTROL LTD. Stafford.

[107] Distribution Switch Gear. R W Blower, Collins, London 1986.

[108] DINELEY J L, 'Power System Stability Part 2 - Hardware, Generators and Their Controls', IEE Power Engineering Journal, July 1991, pp 191-196.

[109] Power System Control and Stability. ANDERSON P M and FOUAD A A, Iowa State University Press. Vol 1, 1977.

[110] Power System Protection Volume 3 - Synchronous Machines. KIMBARK E W, J Wiley & Sons, Inc. London 1956.

[111] DEMELLO F P & CONCORDIA C, 'Concepts of Synchronous Machine Stability as Affected by Excitation Control', IEEE Trans. Vol. PAS-88, No.4, April 1969, pp 316.

[112] Electrical Power Systems: GUILE A E and PATTERSON, Volume 2, pp 304-309. Oliver & Boyd, 1969.

[113] DINELEY J L and FENWICK P J, 'The Effects of Prime Mover and Excitation Control on the Stability of Large Steam Turbine Generators, IEEE Trans. PAS 93, 1974, pp 1613-1623.

[114] BYERLY R T AND KIMBARK E W, 'Stability of Large Electric Power Systems', IEEE Press 1974, New York. pp 459-467, pp 468-478, pp 479-488.

[115] Electric Power Systems. WEEDY B M, Third Edition, J Wiley & Sons, Chichester 1987.

[116] ISHIGURO et al, 'Coordinated Stabilizing Control of Exciter, Turbine and Breaking Resistor', IEEE Trans. on Power Systems, Vol PWRS-1, No 3, August 1986, pp 74-80.

[117] AL-BAIYAT S A & RAHIM A H M A, 'Dynamic Braking Resistor-Reactor Switching Strategies Through A Novel Linear Transformation Technique', Electric Machines & Power Systems, Vol. 21, No. 5, Sept 93, pp 543- 568.

[118] PEELO D F et al, 'Application of a 138 kV 200 MW Braking Resistor', IEE Power Eng Journal, Aug 1994, Vol.8, No.4, pp 188-192.

[119] DINELEY J L, 'Power System Stability Part 3 - Improved Modelling and New York', IEE Power Engineering Journal, January 1992, pp 43-46.

[120] BUSEMANN F & CASSON W, 'Results of Full Scale Stability Tests on the British 132 kV Grid System', Proc. IEE, Paper No.2575S, Feb 1958, pp 347-362.

[121] NICKLE C A & PIERCE C A, 'Stability of Synchronous Machines - Effect of Armature Circuit Resistance', AIEE Transactions, Vol. 49, 1930, pp 338-351.

[122] SESHANNA P, 'Characteristics of an Asynchronized Synchronous Generator', Electric Machines and Electromagnetics 1982 Vol.7 No.1 PP.9-25

[123] Synchronous Machines. Charles Concordia. J Wiley & Sons Inc, London 1951.

[124] NILSSON N E & MERCURIO J, 'Synchronous Generator Capability Curve Testing and Evaluation', IEEE Trans. on Power Delivery, Vol. 9, No. 1, January 1994, pp 414 - 421.

[125] DINELEY J L, 'Power System Stability Part 1 - Fundamental Theory', IEE Power Engineering Journal, January 1991, pp 29-35.

[126] DOHERTY R E & NICKLE C A, 'Synchronous Machines-III - Torque-Angle Characteristics Under Transient Conditions', AIEE Transactions, Vol.46, Jan 1927, pp 1-8.

[127] Transient Phenomena in Electrical Power Systems: Problems and Solutions. VENIKOV V A, Pergamon Press, Oxford, 1964.

[128] The Unified Theory of Electrical Machines. JONES, Butterworth & Co Ltd, London 1967.

[129] Design Operation and Testing of Synchronous Machines. JAIN G C, Asia Publishing House, London 1966.

[130] Advanced Electrical Power and Machines. BROSAN & HAYDEN, Pitman & Sons, London 1966.

[131] CRARY S B & WARING M L, 'Torque Angle Characteristics of Synchronous Machines Following System Disturbances', AIEE Transactions, Vol. 51, 1932, pp 764-773.

[132] REDFERN M A & CHECKSFIELD M J, 'A New Pole Slipping Protection for Numerical Relaying', 11th CEPSI Conference Proceedings, paper 12-29, Kuala Lumpur, Malaysia, October 1996, pp 12.29/1 - 12.29/10.

[133] WALKER J H, 'Operating Characteristics of Salient Pole Machines', IEE Proc. Vol 100, Part 2, 1953, pp 13-24.

[134] SZWANDER W, 'Fundamental Electrical Characteristics of Synchronous Turbo-Generators', Journal.IEE, No.91, Part II, Oct 1943, pp 185-194.

[135] Modern Power Station Practice - Vol.4 - Generator and Electrical Plant, CEGB: 1963 - Permagon Press, pp 126-153, and pp 527-533.

[136] EBERLY T W and SCHAEFER R C, 'Minimum/Maximum Excitation Limiter Performance Goals for Small Generation', IEEE Trans. Energy Conversion, Vol 10, No 4, December 1995, pp 714-721.

[137] NILSSON N E & MERCURIO J, 'Synchronous Generator Capability Curve Testing and Evaluation', IEEE Trans. on Power Delivery, Vol. 9 . No. 1, January 1994, pp 414-421.

[138] ALDEN R T H et al, 'Analysis of Damping & Synchronising Torques, Part 1 - General Calculation Method, Part 2 - Effect of Operating Conditions and Machine Parameters', IEEE Trans, Vol PAS-98, No 5, September 1979, pp 1696-1706.

[139] Power System Stability Volume 1: Elements of Stability Calculations. KIMBARK E W, John Wiley & Sons, New York, 1964.

[140] ELKATEB M M & FIELDING G, 'Coordinating Protection and Control of Dispersed Generation', Tenth International Conference on Electricity Distribution, Part 1, 5- Consumers Installations, 1989, pp 131 -135.

[141] WALLACE A R and STAPLETON S A, 'Renewable Energy Generation Schemes Embedded in Rural Grid Systems', 30th UPEC, Greenwich 1995, Vol 2, pp 609-612.

[142] CONCORDIA C, 'Effect of Prime Mover Speed Control Characteristics on Electric Power System Performance', IEEE Trans. Vol. PAS-88, No. 5, May 1969, p 752.

[143] CONCORDIA C & CARTER G K, 'Negative Damping of Electrical Machinery', AIEE Trans. Vol. 60, March 1941, p 116.

[144] CHECKSFIELD M J & REDFERN MA, Assessment of Embedded Generator Stability when Connected to a HV Utility Distribution System', UPEC 95, Greenwich, September 1995, Vol 1, pp 219-222.

[145] OMAHEN P & PREPELUH F, 'Analysis of the Bulb-Unit Hydro Power Plant Stability and its Protection Scheme Arrangement', UPEC 96, Iraklio, Crete, September 1996, pp 555-559.

[146] CRICHTON L N, 'A System Out-of-Step and it's Relay Requirements', AIEE Transactions, Oct 1937, Vol.56, pp 1261-1267.

[147] GANTNER J & GAILLET B, 'Protection Against Out of Step Operation of Large Synchronous Machines', Electra No. 50, pp 77-93.

[148] MATSUKI J, OKADA T & UENOSONO C, 'Loss of Synchronism Process of a Synchronous Generator Described by its Internal Flux and Force Distributions',

IEEE Transactions on Energy Conversion, Vol.7, No.1, March 1992, pp 177-181.

[149] UENOSONO C, MATSUKI J & OKADA T, 'Analysis of Step-Out Process of a Three-Phase Synchronous Machine by Air Gap Fluxes', Electrical Engineering in Japan, Vol. 100B, No.1, Jan, 1980, pp 41-48.

[150] KHAN K R & CORY B J, 'Developments in Digital Generator Protection', 3rd International Conference on Developments in Power System protection, 1985, Vol.249, Ch.47, pp 223-226.

[151] REDFREN M A, USTA O & FIELDING G, 'Protection Against Loss of Utility Grid Supply for a Dispersed Storage and Generation Unit.' IEEE Paper 92 SM 376-4 PWRD presented at the PES Summer Meeting, Seattle, 1992.

[152] REDFERN M A, HEWETT R J, CHIWAYA A A W, 'An Investigation into Reverse Power Flow Protection for Small and Medium Sized Embedded Generation.' 28 UPEC, Stafford, 1993, pp 109-112.

[153] BONWICK W J & HESSION P J, 'Fast Measurement of Real and Reactive Power in Three Phase Circuits', Proc. IEE, Part.A, Vol.139, No.2, March 1992, pp 51-55.

[154] Power System Protection, Volume 4 - Protection and Signalling. IEE Series, London, UK, 1995, ISBN 0 85296 838 8.

[155] Digital Filters. HAMMING R W, Second Edition, 1983, Prentice-Hall Inc, Engelwood Cliffs, New Jersey.

[156] KWONG W S, CLAYTON M J and NEWBOLD A, 'A Microprocessor Based Current Differential Relay for Use with Digital Communication Systems', GEC Measurements Ltd, UK.

[157] Polarised Polyphase Current Differential Protection for Distribution Feeder Circuits Using a Digital Voice Frequency Communications Channel. CHIWAYA A A W, Ph D Thesis, University of Bath, 1994.

[158] Power Circuit Breaker Theory and Design. FLURSCHEIM C H, IEE Publications, Peter Peregrinus Ltd, 1975.

[159] FISCHER J D, 'Alternatives in Synchronous Motor Pull Out Protection', IEE Conference Record of Industrial and Commercial Power Systems, Technical Conference 1987. pp 48-51.

[160] CHECKSFIELD M J & REDFERN M A, UPEC 96, Iraklio, Crete, September 1996, pp 9-12.

[161] CHAN K W et al, 'Real Time Electro-Mechanical Transient Simulator for On Line Applications', International Conference on Digital Power System Simulators, Texas, USA, April 1995, p 259.

[162] REDFERN M A, BARRETT J and HEWINGS D, 'A Laboratory Facility for Research into Digital Protection Algorithms used for the Protection of Small and Medium Sized Synchronous Generators', UPEC 92, Vol 1, Sept. 1992, pp 16-19.

[163] ElectroMagnetic Transients Program (EMTP) Volume 3, Workboook 3. ALVARADO F L, DOMMEL H and BRANDWAJN V, Ref EL-4651, EPRI Research Project 2149-6, June 1989.

[164] Computer Analysis of Power Systems. ARRILLAGA J & ARNOLD C P, John Wiley & Sons, Chichester 1990.

[165] Electrical Machine Dynamics. GUPTA S & LYNN, Macmillon Press Ltd, 1980.

[166] EMTP Rule Book 1989, MEYER et al.

[167] EMTP Theory Book 1989, MEYER et al.

[168] ROSS G & HALL M C, 'Synchronous Machine and Torsional Dynamics Simulation in the Computation of Electromagnetic Transients', IEEE Transactions on Power Apparatus and Systems, Vol.PAS-97, No.4, July 1978, pp 1074-1086.

[169] PARK R H, 'Two Reaction Theory of Synchronous Machines - Part I', AIEE Transactions, Vol. 48, No. 2, July 1929, pp 716-730.

[170] PARK R H, 'Two Reaction Theory of Synchronous Machines - Part II', AIEE Transactions, Vol. 52, No. 2, June 1933, pp 352-355.

[171] ElectroMagnetic Transients Program (EMTP) Workbook 1. ALVARADO F L, LASSETER R H and LONG W F, Ref EL-4651.EPRI Research Project 2149-6, September 1986.

[172] HASSAN I D, WERONICK R, BUCCI R M & BUSCH W, 'Evaluating the Transient Performance of Standby Diesel-Generator Units by Simulation', IEEE Transactions on Energy Conversion, Vol.7, No.3, Sep 92, pp 470-477.

[173] TANG L and ZAVADIL R M, 'Simulation of the Operational and Control Characteristics of Hybrid Wind/Diesel Energy Systems Using the EMTP', ASME Transactions on Wind Energy, SED - Vol 14, 1993, pp 59-66.

[174] STAVRAKAKIS G S & KARINIOTAKIS G N, 'A general Simulation Algorithm for the Accurate Assessment of Isolated Diesel-Wind Turbine System Interaction', Part 1, A General Multi-Machine Power System Model. IEEE Paper Reference 95 WM 092-7 EC.

[175] STAVRAKAKIS G S & KARINIOTAKIS G N, 'A general Simulation Algorithm for the Accurate Assessment of Isolated Diesel-Wind Turbine System Interaction', Part 2, Implementation of the Algorithm and Case Studies with Induction Generators, IEEE Paper Reference 95 WM 093-5 EC.

[176] Micro-Machine Model Studies of a Ships Power Supply System, HILL B H, Ph D Thesis, University of Bath 1984.

[177] A Real Time Simulation of a Complex Engineering System Incorporating a Diesel Generator. EVANS P A, BSc report No 22/86, University of Bath, 1986.

[178] MALATESTAS P B et al, 'Modelling and Identification of Diesel-Wind Turbines Systems for Wind Penetration assessment', IEEE Trans on Power Systems, Vol 8, No 3, August 1993, pp 1091-1097.

[179] ROY S et al, 'An Adaptive Control Scheme for Speed Control of Diesel Driven Power Plants', IEEE Trans. Energy Conversion, Vol 6, No 4, December 1991, pp 605-611.

[180] The Analysis and Experimental Assessment of the Transient Behaviour of Marine and Off Shore Electro-Mechanical Systems. STRONACH A F, Ph D Thesis, University of Aberdeen, 1980.

[181] HUNG W W et al, 'Dynamic Simulation of Gas-Turbine Generating Unit', IEE Proc. Part C, Vol 138, No 4, July 1991, pp 342-350.

[182] HEYDEMAN J & LULF E N, 'Microprocessor Based Under-Frequency Relaying', IEE Conf Publication No 249, International Conference on Developments in Power System Protection. pp 24-28.

[183] The Diesel Engine - It's Theory, Basic Design and Economics, ARMSTRONG and HARTMAN, Chapter 19, New York, 1959, The Macmillan Company.

[184] ANDERSON P M & MIRHEYDAR M, 'Analysis of a Diesel Driven Generating Unit and the Possibility for Voltage Flicker', IEEE PES Summer Meeting 1994, Paper No. 94 SM 416-8 EC.

[185] CLARKE E, 'Impedances Seen By Relays During Power Swings With and Without Faults', AIEE Transactions, Vol. 64, 1945, pp 372- 384.

[186] Performance & Control of Electrical Machines. O'KELLY D, McGraw-Hill, London, 1991.

[187] St. PIERRE C R, 'Loss-of-Excitation Protection for Synchronous Generators on Isolated Systems', IEEE Transactions on Industry Applications, Vol.IA-21, No.1, Jan/Feb 1985, pp 81-98.

[188] Example 2, Rotating Machines Advance Level Course Notes, 17th European EMTP Meeting, November 6-7, 1989, Leuven.

[189] Circuits, Devices and Systems. SMITH R. John Wiley & Sons, Chichester, 1984.

[190] PHADKE A G, 'Synchronized Phasor Measurements in Power Systems', IEEE Computer Applications in Power, April 1993, Vol. 6, No.2, pp 10-15.

Appendix A

DERIVATION OF THEORETICAL IMPEDANCE, POWER VARIATIONS AND ALGORITHM SETTING EQUATIONS

A1.1 CALCULATION OF THE IMPEDANCE LOCI PRODUCED DURING POLE SLIPPING

The method used to calculate the theoretical impedance locus during pole slipping is well established, it was first published by Clarke[36,185].

If it is assumed that the impedance of all parts of the system have the same angle, then the total impedance between the two voltage sources can be lumped together, as shown in Figure A1. Note that the generator is represented as a voltage source behind transient reactance for these studies. The value of generator impedance, Zg used is therefore Xd' + R = Zd'. The armature resistance, R is relatively small in large synchronous machines. Zd' is normally expressed in generators as a pure reactance, Xd'. Zd' has been used in this analysis for completeness. The source impedance, Zs comprises of the generator transformer impedance, inter-connection impedance, and bus source impedance. Referring to Figure A1, the total combined impedance, Ztot is given by;

$$Ztot = Zg + Zs \qquad \text{A(1)}$$

The value of m is given by;

$$m = Zg / (Zg + Zs) = Zg / Ztot \qquad \text{A(2)}$$

The generator impedance, Zg is given by;

$$Zg = Zd' = mZtot \qquad \text{A(3)}$$

The voltage and current at the relaying point, i.e the generator terminals is given by;

$$relay\ voltage\ ,\ Er = (1 - m)Eg\angle\delta + mEs \qquad \text{A(4)}$$

$$relay\ current\ ,\ Ir = (Eg\ \angle\delta - Es\ ) / Ztot \qquad \text{A(5)}$$

The impedance 'seen' by the relay at the generator terminals, Zr, is therefore given by;

$$Zr = \frac{Er}{Ir} = \left(\frac{(1-m)Eg\ \angle\delta + mEs}{Eg\ \angle\delta - Es}\right) Ztot \qquad A(6)$$

There are three power system conditions which need analysing using equation A(6). These are when the generator internal voltage, Eg is less than, equal to, or greater than the utility source voltage, Es.

Condition 1 Eg = Es = 1.0 pu

With this condition, A(6) can be written;

$$\frac{Zr}{Ztot} = \frac{(1-m)\angle\delta + m}{\angle\delta - 1} = \frac{-m\ (\angle\delta - 1) + \angle\delta}{\angle\delta - 1} = -m + \frac{1}{1 - \angle -\delta} \qquad A(7)$$

$$\frac{Zr}{Ztot} = -m + \frac{1 + \angle\delta}{(1 - \angle -\delta)\ (1 + \angle\delta)} = -m + \frac{1 + \angle\delta}{1 + \angle\delta - \angle -\delta - 1} \qquad A(8)$$

$$\frac{Zr}{Ztot} = -m + \frac{1 + \angle\delta}{\angle\delta - \angle -\delta} = -m + \frac{1 + \cos\delta + j\sin\delta}{2j\ \sin\delta} \qquad A(9)$$

$$\frac{Zr}{Ztot} = \left(\frac{1}{2} - m\right) - j\left(\frac{1 + \cos\delta}{2\ \sin\delta}\right) = \left(\frac{1}{2} - m\right) - j\ \frac{1}{2}\cot\frac{\delta}{2} \qquad A(10)$$

This equation represents a straight vertical line, since the real part is constant, whilst the imaginary part varies as a function of δ, (recall cot = 1/tan). If A(10) is multiplied through by Ztot, to give the relay 'seen' impedance, the lengths are multiplied by the magnitude of Ztot, and the line is rotated anti-clockwise through the impedance angle, α. In an 'ideal' reactive transmission system, the system impedance angle, α, is equal to 90°. Table A1 contains calculated values for the components of A(10) for a unity per unit system.

If the two generators are in phase with each other, the current is zero and the seen impedance is infinite. If they are in complete anti-phase, the voltage becomes zero at the middle of the impedance Ztot, and the current magnitude becomes high, giving the appearance of a three phase short circuit at the mid-point.

For the purpose of setting impedance relays, pole slipping loci for different ratios of Eg/Es are required. The maximum is dependent upon the ceiling limit of the AVR. Consider the case where the system is purely reactive and the value of Ztot is j1 pu, and m is 0.75. Solving A(6) for values of Eg/Es of 2 pu and 0.5 pu will give two curves which will

generally provide a bounds for the theoretical pole slipping impedance locus;

Table A1 - Solution of A(10) for Eg/Es = 1.0, Ztot = $1\angle 90°$ pu, m = 0.75;

δ	cot (δ/2)	Real component of Ztot * A(10)	Imaginary component of Ztot * A(10)
0	∞	∞	-0.25
30	3.732	1.866	-0.25
60	1.732	0.866	-0.25
90	1.000	0.5	-0.25
120	0.577	0.289	-0.25
150	0.268	0.134	-0.25
180	0	0	-0.25
210	-0.268	-0.134	-0.25

Condition 2 Eg = 2.0 Es = 1.0 pu

Applying the above figures to A(6), then;

$$\frac{Zr}{Ztot} \equiv \frac{0.25 * 2.0\ \angle\delta\ + 0.75}{2.0\ \angle\delta\ - 1.0} = \frac{0.5\ \angle\delta\ + 0.75}{2.0\angle\delta\ - 1.0} \qquad \text{A(11)}$$

The maximum value of Zr/Ztot occurs at δ = 0°, and is therefore;

$$\text{maximum Zr/Ztot} = (0.5 + 0.75) / (2.0 - 1.0) = 1.25$$

The minimum value of Zr/Ztot occurs at δ = 180°, and is therefore;

$$\text{minimum Zr/Ztot} = (-0.5 + 0.75) / (-2.0 - 1.0) = 0.25/-3.0 = -0.08333$$

When the ratio of Es to Eg is not equal to unity, the pole slipping impedance locus is no longer a straight line, it is a circle. In this case the impedance does not take on an infinite value when δ = 180°. A proof of this is given in reference[36].

Since the impedance locus is a circle, the centre of the circle must lie midway between the maximum and minimum points, i.e between 1.25 and -0.08333. The centre of the

circle is therefore at;

$$\text{centre of locus} = -0.08333 + (1.25 - -0.08333)/2 = 0.58333$$

The centre of the locus of Zr on the impedance plane is therefore at;

$$0.58333 * Ztot = 0.58333 * j1 \text{ pu} = j0.58333 \text{ pu.}$$

The radius of Zr must be half the difference between the two points. The radius of the impedance locus is therefore;

$$\text{radius of locus} = |Ztot| * (1.25 - -0.08333)/2$$
$$= 1\text{pu} * 0.6666 = 0.6666\text{pu.}$$

Condition 3 Eg = 0.5 Es = 1.0 pu

Using A(6) and the above figures, then;

$$\frac{Zr}{Ztot} \equiv \frac{0.25 * 0.5 \angle\delta + 0.75}{0.5 \angle\delta - 1.0} = \frac{0.125 \angle\delta + 0.75}{0.5\angle\delta - 1.0} \qquad \text{A(12)}$$

The maximum value of Zr/Ztot occurs at $\delta = 0°$, and is therefore;

$$\text{maximum Zr/Ztot} = (0.125 + 0.75) / (0.5 - 1.0) = -1.75$$

The minimum value of Zr/Ztot occurs at $\delta = 180°$, and is therefore;

$$\text{minimum Zr/Ztot} = (-0.125 + 0.75) / (-0.5 - 1.0) = -0.41666$$

Since the impedance locus is a circle, the centre of the circle must lie midway between the maximum and minimum points, i.e between -1.75 and -0.41667. The centre of the circle is therefore at -1.08333. The centre of the locus of Zr on the impedance diagram is therefore at -1.08333 * Ztot = -1.08333 * j1 pu = -j1.08333 pu. The radius of Zr must equal half the difference between the two points, i.e the radius is equal to;

$$1 \text{ pu} * (1.75 - 0.41666)/2 = 0.6667 \text{ pu}$$

A1.1.1 The Affect of Resistance on Impedance Loci

Embedded generators can be connected to the main utility network through cables which have a higher resistive component than overhead lines.

The effect of a resistive component in the impedance, Ztot, is to rotate the loci derived for a purely reactive system clockwise. Consider the same system of section A1.1, but with a value of Ztot of $1\angle 45°$ pu, i.e, $1/\sqrt{2} + j1/\sqrt{2}$ pu. Compared to the original impedance of $1\angle 90°$ pu, there is a 45° difference. The impedance loci for this condition will therefore be those shown in Figure A2, rotated clockwise around the origin by 45°. For convenience, Figure A2 has been repeated in Figure A3c, Figure A3d shows the impedance loci for a value of Ztot of $1\angle 45°$ pu. This shows that the impedance loci for this condition are rotated versions of those in A3c.

A1.1.2 The Affect of Variation in the Generator to Source Impedance Ratio

Figure A3 also shows the effects of changing the ratios of Zg to Zs. Impedance loci for values of m of 1.0, 0.75 & 0.5 have been given. When m is equal to 1.0, the impedance Ztot is determined entirely by the generator impedance, Zg. This scenario occurs when a generator is operating on an 'ideal' infinite bus. When m is equal to 0.5, the generator and source impedances are equal. This situation occurs if two identical machines operate in parallel with each other. A value of m of 0.5 is unlikely to occur in a practical embedded generation environment because the rating of the generator is generally small when compared to the rating of the utility bus.

A2.1 REAL AND REACTIVE POWER TRANSFER CHARACTERISTICS

Using the diagram in Figure A1, the real and reactive power characteristics can be derived from;

$$\begin{aligned} \textit{Real Power, } P &= \textit{Real part of } \; Er\,Ir^* \\ \textit{Reactive Power, } Q &= \textit{Imaginary part of } \; Er\,Ir^* \end{aligned} \qquad \text{A(13)}$$

From A(5) the complex conjugate of Ir is given by;

$$Ir = \frac{(Eg\ \angle\delta\ - Es\ )}{Ztot\ \angle\alpha} = \frac{Eg\ \angle\delta}{Ztot\ \angle\alpha} - \frac{Es}{Ztot\ \angle\alpha}$$

$$\therefore Ir = \frac{Eg}{Ztot}\angle\delta - \alpha - \frac{Es}{Ztot}\angle -\alpha \qquad \text{A(14)}$$

$$\therefore Ir^* = \frac{Eg}{Ztot}\angle\alpha - \delta - \frac{Es}{Ztot}\angle\ \alpha$$

where α is the impedance angle, i.e $\alpha = \sin^{-1}(X/Ztot)$. The total apparent power of the circuit is given by $ErIr^*$, using A(4) & A(14);

$$ErIr^* = \left((1-m)Eg\angle\delta\ + mEs\right) * \left(\frac{Eg}{Ztot}\angle\alpha - \delta - \frac{Es}{Ztot}\angle\alpha\right) \qquad \text{A(15)}$$

$$\therefore ErIr^* = \frac{(1-m)Eg^2}{Ztot}\angle\alpha - \frac{(1-m)EgEs}{Ztot}\angle(\delta+\alpha) + \frac{mEgEs}{Ztot}\angle(\alpha-\delta) - \frac{mEs^2}{Ztot}\angle\alpha$$

Converting from polar to rectangular format, A(15) becomes;

$$\begin{aligned} ErIr^* = {} & \frac{(1-m)Eg^2}{Ztot}\cos(\alpha) + j\frac{(1-m)Eg^2}{Ztot}\sin(\alpha) \\ & - \frac{mEs^2}{Ztot}\cos(\alpha) - j\frac{mEs^2}{Ztot}\sin(\alpha) \\ & - \frac{(1-m)EgEs}{Ztot}\cos(\delta+\alpha) - j\frac{(1-m)EgEs}{Ztot}\sin(\delta+\alpha) \\ & + \frac{mEgEs}{Ztot}\cos(\alpha-\delta) + j\frac{mEgEs}{Ztot}\sin(\alpha-\delta) \end{aligned} \qquad \text{A(16)}$$

Using A(13) and A(16), the real power, P characteristic is given by;

$$\begin{aligned} P = {} & \frac{(1-m)Eg^2}{Ztot}\cos(\alpha) - \frac{mEs^2}{Ztot}\cos(\alpha) \\ & - \frac{(1-m)EgEs}{Ztot}\cos(\delta+\alpha) + \frac{mEgEs}{Ztot}\cos(\alpha-\delta) \\ \therefore P = {} & \frac{(1-m)Eg^2 - mEs^2}{Ztot}\cos(\alpha) - \frac{(1-m)EgEs}{Ztot}\cos(\delta+\alpha) \\ & + \frac{mEgEs}{Ztot}\cos(\delta+\alpha) \end{aligned} \qquad \text{A(17)}$$

Using A(13) and A(16), the reactive power, Q characteristic is given by;

$$Q = \frac{(1-m)Eg^2}{Ztot}\sin(\alpha) - \frac{mEs^2}{Ztot}\sin(\alpha)$$

$$- \frac{(1-m)EgEs}{Ztot}\sin(\delta+\alpha) + \frac{mEgEs}{Ztot}\sin(\alpha-\delta)$$

A(18)

$$\therefore Q = \frac{(1-m)Eg^2 - mEs^2}{Ztot}\sin(\alpha)$$

$$- \frac{(1-m)EgEs}{Ztot}\sin(\delta+\alpha) - \frac{mEgEs}{Ztot}\sin(\delta-\alpha)$$

A(17) & A(18) have been plotted for various values of Eg, Es, m & α in Figure A4. These graphs show how variations in m, and the ratio Eg/Es effect the real power load angle characteristics. This analysis does not allow for generator saliency, a more detailed analysis of the real and reactive power characteristics for synchronous machines is therefore provided below.

A3.1 SYNCHRONOUS GENERATOR REAL AND REACTIVE POWER CHARACTERISTICS WHEN OPERATING ON AN INFINITE BUS

Figure A5 contains the voltage vector diagrams for a synchronous generator operating in the steady state. To derive real and reactive power load angle equations from these vector diagrams, the following assumptions are required[123,128,130,186];

a) a balanced supply to sinusoidally distributed stator windings.

b) saturation is neglected

c) stator slots cause no appreciable variation in rotor inductance with change in rotor angle

d) the generator is operating on an infinite bus.

Figure A5a shows a simplified machine equivalent circuit, showing the conventions used for this derivation. The generator convention has been adopted, the internal machine voltage, E therefore leads the terminal voltage, V. Since the generator is operating on an infinite bus, its terminal voltage is equal to the infinite bus voltage, V. The machine or rotor angle, δ is positive for a generator and the output power will also be positive. Figure A5b shows a method for finding δ and E, given the generator terminal voltage, current, and power factor angle, ϕ, together with the machine constants, Xd, Xq, and R, the armature resistance. The values V, I and ϕ, are drawn, then the vectors IR, IXq, IXd are added. A line is drawn which lies on points 'o' and 'c', then an additional line is drawn

from 'd' so that it is perpendicular to the 'oc' line, meeting it at 'e'. Point 'e' is the tip of the internal machine voltage vector, E.

Figure A5c shows the voltage vector diagram broken down into its quadrature and phase components. Resolving along quadrature and phase axes gives;

$$V\cos(\delta) = E - RIq - XdId \qquad \text{A(19)}$$

$$V\sin(\delta) = XqIq - RId \qquad \text{A(20)}$$

The real and reactive power characteristics at the generator terminals are given by;

$$S = P + jQ = V I^* \qquad \text{A(21)}$$

where S is the apparent power. Solving A(19) & A(20) for Id and Iq gives;

$$Id = \frac{EXq - VXq\cos(\delta) - VR\sin(\delta)}{R^2 + XqXd} \qquad \text{A(22)}$$

$$Iq = \frac{VXd\sin(\delta) + ER - VR\cos(\delta)}{R^2 + XqXd} \qquad \text{A(23)}$$

In complex notation the infinite bus voltage (and terminal voltage) is expressed as;

$$V = V\cos(\delta) - Vj\sin(\delta) \qquad \text{A(24)}$$

The generator current is expressed as;

$$I = Iq - jId \quad \therefore \quad I^* = Iq + jId \qquad \text{A(25)}$$

The apparent power, S is therefore given by;

$$S = \left[V\cos(\delta) - jV\sin(\delta)\right] * \frac{1}{R^2 + XqXd} * \qquad \text{A(26)}$$

$$\left[\, VXd\sin(\delta) - VR\cos(\delta) + ER \quad -jVXq\cos(\delta) - jVR\sin(\delta) + jEXq \,\right]$$

The real power, P is given by the real part of A(26);

$$P = \frac{1}{R^2 + XdXq}\left[V^2\left(\left(\frac{Xd - Xq}{2}\right)\sin(2\delta) - R\right) + EVZ\sin(\delta + \theta)\right] \qquad \text{A(27)}$$

where $Z = \sqrt{(R^2 + Xq^2)}$ and $\theta = \sin^{-1}(R/Z)$. The reactive power, Q is given by;

$$Q = \frac{1}{R^2 + XdXq}\left[EVZ\cos(\delta + \theta) + V^2\left(\left(\frac{Xd - Xq}{2}\right)\cos(2\delta) - \left(\frac{Xd + Xq}{2}\right)\right)\right] \qquad \text{A(28)}$$

A3.1.1 Transient Power Characteristics

When a synchronous generator is perturbed by a power system disturbance such as a fault, load change, or line switching operation, it can be said to pass through three different modes of operation. These are the sub transient, transient, and steady state modes. These modes of operation are a result of the high inductance to resistance ratio in the field and damper windings. This has the effect of keeping the field and damper winding flux linkage constant over a period determined by the time constant of the winding[123]. If an abrupt change occurs in the stator current, the change causes an mmf which tries to establish a flux through the field pole core. If such a flux occurred, it would tend to link the field winding, and since the field winding wants to maintain its flux at a constant zero level, an opposing mmf is produced by induced field current. This tends to maintain the flux linkage of the field at zero. The only flux which can therefore be established immediately is that which does not link the field winding. This flux passes through the low permeance leakage paths, which are mostly in air. The resultant flux per ampere value is low, and the reactance which results is the direct axis transient inductance, Ld'. This value will be much smaller than Ld, the direct axis synchronous reactance due to the flux being forced to travel through air rather than iron. The same process also occurs with the damper windings. However, the time constant of the damper windings is much smaller than the field winding time constant. The sub-transient damper winding effects therefore last for a fraction of the field winding transient time.

Figure 6a shows a voltage vector diagram for the machine in steady state. The diagram shows the quadrature and phase components of terminal voltage, V and terminal current, I. It also shows some additional voltages. This diagram is very similar to Figure A5b. Both diagrams can be used to find the position of the quadrature and direct axes relative to V and I. Eq does not have any simple physical meaning, but is useful because its tip lies on the quadrature axis and therefore identifies the axis position. When drawing IXq and Eq, it is also possible to draw IXd and the corresponding quantity Ed. Once the location of Ed is known, E can be found by drawing a line from Ed which is perpendicular to the quadrature axis. E can then be found at the intersection of the two lines. Figures A5c and A6a show that the value, E can be found from;

$$E = Vq + IdXd + IqR \qquad \text{A(29)}$$

If the field flux linkage is assumed constant, a point on the vector diagram which is proportional to field flux linkage can be identified[123]. Figure A6b shows this point,

which is denoted as Eq'. It can be seen that Eq' is given by;

$$Eq' = Vq + IdXd' + IqR \qquad \text{A(30)}$$

Equations A(29) and A(30) are identical in form, the difference between them is that Xd has been substituted with Xd', and E has been substituted with Eq'. Figure A6b also shows that Eq' can be found from;

$$Eq' = E - (Xd - Xd')Id \qquad \text{A(31)}$$

The above substitutions do not just apply to equations A(29) and A(30). They can also be applied to equations A(27) and A(28) because these equations were derived from the same vector diagram[123]. The transient power load angle equations are therefore given by;

$$P = \frac{1}{R^2 + Xd'Xq}\left[Eq'VZ\sin(\delta+\theta) + V^2\left(\left(\frac{Xd'-Xq}{2}\right)\sin(2\delta) - R\right)\right] \qquad \text{A(32)}$$

$$Q = \frac{1}{R^2 + Xd'Xq}\left[Eq'VZ\cos(\delta+\theta) + V^2\left(\left(\frac{Xd'-Xq}{2}\right)\cos(2\delta) - \left(\frac{Xd'+Xq}{2}\right)\right)\right] \qquad \text{A(33)}$$

Note that an equivalent value of Xq' does not exist since there is no field winding in the quadrature axis. A value of Xq' does exist for solid round rotor machines, but results from flux linking with the iron paths in the solid rotor structure. In such cases the duration of the quadrature axis transient period and the decrease in impedance from Xq to Xq' is much less pronounced than in the direct axis[110].

As well as a transient period following a sudden change in stator currents, a sub-transient period also exists. This sub-transient period is shorter and occurs before the transient period. In defining Xd' it is assumed that no rotor circuits exist except the main field winding. This is not the case as salient pole machines will have damper windings fitted to both axes[110]. If round rotor machines do not have dampers fitted, their steel rotor core acts as a path for eddy currents to flow. When a sudden change in stator currents occurs, induced currents occur in the damper circuits as well as the main field winding. These induced currents serve to oppose the stator mmf, and are able to maintain the flux linkage of the rotor damper circuit constant at zero for a short time. Because the rotor circuits are closer to the air gap than the field winding circuits, the flux is forced into an even lower permeance path than during the field winding transient. The resulting stator flux linkage/amp is lower than the transient field winding case, and this value is defined as the sub-transient reactance. This may occur in both the quadrature and direct axes giving rise

to Lq" and Ld".

The time that the generator direct and quadrature axes reactances remain at their sub-transient values is small due to the low X/R ratios of the damper circuits. The generator reactance will remain at its transient value for much longer due to the higher value of X/R which occurs in the field winding.

A3.1.2 Calculation of Synchronous Generator Steady State and Transient Real and Reactive Power Curves

The following section explains how to derive the quantities necessary for calculating the steady state and transient real and reactive power machine angle characteristics.

A3.1.2.1 No Load Calculations

For no load excitation, the generator is said to be 'floating', and the value of E will therefore be equal to V, the terminal voltage. For this reason the following names are often used for E; 'open circuit voltage', 'no-load excitation', 'excitation e.m.f', 'internal machine voltage', and 'voltage behind synchronous reactance' [186]. Note that at this condition, the angle δ will be zero. The angle δ is known as the 'machine angle', 'rotor angle', 'rotor load angle', or 'pole angle'. If the generator is not operating against an infinite bus, then for the case of a simple tie-line with series resistance, r and reactance, X, the tie line impedance can be added to the stator impedance[123]. The term 'load angle' is used more in the context of the angle between voltages at either end of a transmission line. It is important to know which angle is being referred to when reading texts on the subject.

The values used to calculate the no load characteristics are as follows ;

$$E = 1$$

$$V = 1$$

$$Eq' = 1$$

E and Eq' are also unity at no load since the current I is zero, see A(29) and A(31). The reader is reminded that the generator terminal voltage is equal to the infinite bus voltage, V in this case because the generator is operating on an infinite bus.

A3.1.2.2 Full Load Calculations

The following equations can be used to find E and Eq' for a generator operating at full load excitation[123]. For a generator operating at current magnitude $|I|$, with a power factor, pf, then complex value of the current I is given by;

$$I = |I| \, (pf - \sqrt{1 - pf^2}) \qquad \text{A(34)}$$

The quantity Eq must then be calculated. From Figure A6a, this is given by;

$$(jEq) = V + (R + jXq) \, I \qquad \text{A(35)}$$

The direct axis current, Id must then be found from (Figure A5c);

$$Id = |I| \sin(\delta + \phi) \qquad \text{A(36)}$$

From Figure A5c, the angles δ and ϕ, are given by;

$$\delta = \tan^{-1}\left(\frac{Im(Eq)}{Re(Eq)}\right) \quad and \quad \phi = \tan^{-1}\left(\frac{Im(I)}{Re(I)}\right) \qquad \text{A(37)}$$

From Figure A6a, the value of E can then be found using;

$$E = Eq + (Xd - Xq) \, Id \qquad \text{A(38)}$$

From Equation A(31), the value of Eq' can then be found. Once E and Eq' are known, the power load angle characteristics can be plotted using Equations A(27,28,32,33).

A3.1.3 Calculation of Generator Characteristics for a Diesel Generator

Using the above procedure, the power characteristics for the 625 kVA diesel generator described in Appendix C were calculated. The parameters required for the calculation are given below;

Xd = 2.25 pu, Xd' = 0.22 pu, Xq = 1.1 pu, pf = 0.8, R = 0.02 pu, V = 1.0 pu.

No Load Values.

The no load values for both generators are V = E = Eq' = 1.0 pu.

Full Load Values (all values in pu)

The current, I is given using A(34);

$$I = 0.8 - j0.6$$

The quantity, Eq is given using A(35);

$$jEq = 1 + (0.8 - j0.6)\ (\ 0.02 + j1.1) = \ 1.676 + j0.868 = 1.887$$

The angles δ and ϕ are given using A(37) ;

$$\delta = \tan^{-1}(\ 0.868/1.676) = 27.34° \quad \phi = \tan^{-1}(0.6/0.8) = 36.87°$$

Using (A36) the direct axis current is therefore ;

$$Id = 1 * \sin(27.34 + 36.87) = 0.9$$

The value of E is calculated using A(38);

$$E = 1.887 + (2.25 - 1.1)(0.9) = 2.922$$

The value of Eq' can then be found from A(31);

$$Eq' = \ 2.922 - (2.25\text{-}0.22)(0.9) = 1.095.$$

Applying these figures to equations A(27,28,32,33) gives the following no load and full load, steady state and transient power load angle equations;

$$\begin{aligned}
Pnl(ss) &= 0.444\sin(\delta + 1.04°) + 0.2323\sin(2\delta) - 0.0080 \\
Qnl(ss) &= 0.444\cos(\delta + 1.04°) + 0.2323\cos(2\delta) - 0.6767 \\
Pnl(tr) &= 4.539\sin(\delta + 1.04°) - 1.815\sin(2\delta) - 0.0825 \\
Qnl(tr) &= 4.539\cos(\delta + 1.04°) - 1.815\cos(2\delta) - 2.723 \\
Pfl(ss) &= 1.299\sin(\delta + 1.04°) + 0.2323\sin(2\delta) - 0.0080 \\
Qfl(ss) &= 1.299\cos(\delta + 1.04°) + 0.2323\cos(2\delta) - 0.6767 \\
Pfl(tr) &= 4.970\sin(\delta + 1.04°) - 1.815\sin(2\delta) - 0.0825 \\
Qfl(tr) &= 4.970\cos(\delta + 1.04°) - 1.815\cos(2\delta) - 2.723
\end{aligned} \qquad \text{A(39)}$$

Where 'nl' refers to no load, 'fl' refers to full load, (ss) refers to steady state, and (tr) refers to transient. Figures 3.1 and 3.2 contain plots of these equations. Chapter three discusses the nature of these curves.

A4.1 ANALYSIS OF GENERATOR REAL AND REACTIVE POWER CHARACTERISTICS WHEN OPERATING AGAINST A SIGNIFICANT SOURCE IMPEDANCE, SALIENCY EFFECTS INCLUDED

For reasons of clarity, the analysis of generator real and reactive power characteristics has so far dealt with either operation against a 'finite' bus, with no saliency, or vice versa. This section will provide a full analysis which takes into account the effects of saliency and operation on a 'finite' bus. Such an analysis could not be found in any other texts. This is not surprising however, as the equations derived are complex and are not easy to

use.

Figure A7a shows the schematic representation of a generator operating against a source impedance. Figure A7b shows the corresponding phasor diagram for this scenario, and Figure A7c shows the voltage phasor diagram which relates the generator internal voltage, E, the generator terminal voltage, Vg, and the infinite bus voltage, V. Note that two angles have been used for the machine load angle. The angle between generator internal voltage and terminal voltage, known as the machine angle is denoted as δ_m. The angle between generator terminal voltage and infinite bus voltage, known as the system load angle, is denoted as δ. Using the same form of analysis as in section A3.1, Figure A7b shows that the direct and quadrature axis currents are given by;

$$Id = \frac{E(Xq+X) - V(Xq+X)\cos(\delta) - V(R+r)\sin(\delta)}{(R+r)^2 + (Xq+X)(Xd+X)} \qquad A(40)$$

$$Iq = \frac{V(Xd+X)\sin(\delta) + E(R+r) - V(R+r)\cos(\delta)}{(R+r)^2 + (Xq+X)(Xd+X)} \qquad A(41)$$

In complex notation the generator terminal voltage is expressed as;

$$V_g = V_g\cos(\delta_m) - jV_g\sin(\delta_m) \qquad A(42)$$

The current expressed in complex notation is identical to equation A(25). Resolving along the direct and quadrature axis of Figure A7c gives;

$$V_g\cos(\delta_m) = E - IdXd - IqR \qquad A(43)$$

$$V_g\sin(\delta_m) = IqXq - IdR \qquad A(44)$$

Substituting A(43) and A(44) into A(42), and multiplying by the complex conjugate, as defined by equations A(25), A(40), and A(41) yields the following equations for real and reactive power;

$$\begin{aligned} Q &= EId - Id^2Xd - Iq^2Xq \\ P &= EIq - IdIqXd - Iq^2R + IdIqXq - Id^2R \end{aligned} \qquad A(45)$$

substituting equations A(40) and A(41) into A(45) gives;

$$Q = E\frac{E(Xq+X) - V(Xq+X)\cos(\delta) - V(R+r)\sin(\delta)}{(Xd+X)(Xq+X) + (R+r)^2}$$

$$- \frac{(E(Xq+X) - V(Xq+X)\cos(\delta) - V(R+r)\sin(\delta))^2}{\left[(Xd+X)(Xq+X) + (R+r)^2\right]^2} Xd \qquad \text{A(46)}$$

$$- \frac{(V(Xd+X)\sin(\delta) - V(R+r)\cos(\delta) + (R+r)E)^2}{\left[(Xd+X)(Xq+X) + (R+r)^2\right]^2} Xq$$

$$P = E\frac{V(Xd+X)\sin(\delta) - V(R+r)\cos(\delta) + (R+r)E)}{(Xd+X)(Xq+X) + (R+r)^2}$$

$$- \left[\frac{(E(Xq+X) - V(Xq+X)\cos(\delta) - V(R+r)\sin(\delta))}{\left[(Xd+X)(Xq+X) + (R+r)^2\right]^2}\right].$$

$$\left[(V(Xd+X)\sin(\delta) - V(R+r)\cos(\delta) + (R+r)E)Xd\right]$$

$$- \frac{(V(Xd+X)\sin(\delta) - V(R+r)\cos(\delta) + (R+r)E)^2}{\left[(Xd+X)(Xq+X) + (R+r)^2\right]^2} R \qquad \text{A(47)}$$

$$+ \left[\frac{(E(Xq+X) - V(Xq+X)\cos(\delta) - V(R+r)\sin(\delta))}{\left[(Xd+X)(Xq+X) + (R+r)^2\right]^2}\right].$$

$$\left[(V(Xd+X)\sin(\delta) - V(R+r)\cos(\delta) + (R+r)E)Xq\right]$$

$$- \frac{(E(Xq+X) - V(Xq+X)\cos(\delta) - V(R+r)\sin(\delta))^2}{(Xd+X)(Xq+X) + (R+r)^2} R$$

Since the equations and analysis are in the same form as that of section A3.1, the transient equations can be obtained by substituting Xd' for Xd, and Eq' for E.

A5.1 THE EFFECT OF MACHINE LOSSES UPON THE POLE SLIPPING ALGORITHM AND ASSESSMENT OF THE CORRECT VALUE FOR Pfact

The effect of machine losses must be considered because the fundamental basis of the algorithm relies on power input and output differences. The accelerating power on the generator rotor, P_a for any operating condition can be expressed in the form;

$$P_a = Pm - P - P_{loss} \qquad A(48)$$

where Pm is the mechanical input power, P is the electrical output power, and P_{loss} represents the losses inside the generator. The algorithm estimates the input power from the electrical output power when P_a is zero, (i.e. the generator is in a steady state). If Pfact is set to unity to simplify the argument, the trip setting, Pt is given by;

$$Pt = P = Pm - P_{loss} \qquad A(49)$$

If the losses remained constant for both steady state and transient operation, they would have no effect on the algorithm's operation, because they would be taken into account in the trip setting Pt. However, if the losses increased during transient disturbances, due to increased synchronous and asynchronous current components, the algorithm may be adversely effected. This therefore requires investigation.

Let $P_{add\text{-}loss}$ be the additional component of losses during transient operation, due to higher current levels. The real power criterion is satisfied when P < Pm, i.e. for the situation where P_a goes from negative to positive. The effect of the additional losses on P_a can be seen below;

$$P_a = Pm - P_{loss} - P_{add\text{-}loss} - P \qquad A(50)$$

The extra component $P_{add\text{-}loss}$ can be seen to make the accelerating power more negative. As expected, the additional losses therefore improve stability. This stands to reason, additional losses during a transient provide the generator with an additional load, and therefore decrease the accelerating area as defined by the equal area criterion.

The algorithm however does not take this additional loss component into account. The real power criterion in the algorithm will therefore be satisfied earlier than it actually should be. This shows that in theory, if the losses increased sufficiently during a critical power swing, the algorithm could nuisance trip because the real power criterion was satisfied before it actually should have been.

It is stressed that this is an absolute worst case consideration. With the algorithm having three criteria, and a time dependent criterion, the likelihood of nuisance tripping is decreased considerably. Algorithm security is threatened most during stable power swings where the generator rotor swings up to the CSP, and there is an appreciable increase in

losses. This scenario could cause a threat to algorithm security if 'Pfact' is not chosen correctly.

Jain[129] discusses synchronous machine losses in detail. There are many types of losses, such as iron losses due to main and parasitic fluxes, hysteresis losses, eddy-current losses, I^2r armature losses, friction and windage losses. The loss which increases most during transient operation is the armature I^2r loss, due to the increased armature currents which flow.

The highest value of embedded generator armature resistance can be expected to be around 0.03 p.u. as found in table C1 of appendix C. The highest rise in armature current expected as the generator approaches the CSP is approximately 2 pu. The highest value of additional losses created in the generator during a transient disturbance are therefore approximately equal to 24 % of generator rating. This is a very high figure, since most generators typically have a value of armature resistance far below 0.03 per unit.

The value of Pfact chosen was 0.9, since this allows for 10 % additional losses during the transient. This value for Pfact of 0.9 has worked correctly although it is much lower than the 24 % figure. The algorithm has functioned correctly on machines with a value of stator resistance of 0.032 pu. The development algorithm implemented in the commercial relay hardware had several settings which, if the algorithm were to be released commercially, would not be available. These settings were chosen at the development stage so that the algorithm could be 'fine tuned' if necessary. One such setting was 'Pfact'. It was never necessary to change this from the default setting of 0.9 however.

A5.2 THE VALUE OF RATE OF CHANGE OF POWER AT THE CSP

In order to choose the correct value of margin for error for the rate of change of power trip level, $(\Delta P/\Delta t)_{min}$, an analysis of the factors which determine the rate of change of power at the CSP is required.

The type of pole slip will have a great affect on the magnitude of $\Delta P/\Delta t$. A pole slip which results from a severe fault, will cause the machine power output to reach a high value before the actual pole slip. At the CSP, the real power will be decreasing from this

maximum value. This type of pole slip will therefore produce high values of $\Delta P/\Delta t$, and this must be considered when choosing the setting $(\Delta P/\Delta t)_{min}$.

If the pole slip is a result of insufficient excitation it will be a steady state pole slip, and no peak will occur in the output power before the pole slip. The value of Pmax will therefore be at its nominal value of 1.4 * Pt.

The foregoing discussion shows that there are two ways in which a generator can lose synchronism. These different ways will produce different variations in $(\Delta P/\Delta t)$, an adaptive technique which alters the algorithm setting $(\Delta P/\Delta t)_{min}$ according to which type of pole slip is going to occur will therefore provide a faster acting, more secure algorithm.

A5.2.1 Mathematical Analysis of $(\Delta P/\Delta t)_{min}$ at the CSP

The real power output of the generator can be expressed as a sum of three different expressions. These expressions are related to,

a) the sinusoidal variation in output power with load angle, Ps

b) the added effect transient saliency has on this, Ptrs

c) the effect of induction generator action, i.e. asynchronous effects. , Pasyn

The synchronous parts given by (a) and (b) are described by equations A(27) and A(32), whilst the asynchronous part is given by equation 3(7) of Chapter 3. Equation 3(7) is too complicated to be used in a protection relaying environment because it requires too many generator parameters, as well as information on the state of operation of the generator. The asynchronous parts will therefore be neglected from the analysis.

When the generator is in a steady state, the algorithm assumes a sinusoidal power load angle relationship when calculating the trip setting $(\Delta P/\Delta t)_{min}$. The magnitude of this sinusoid is determined by the algorithm measurement, Pmax. Figure A7 shows such a curve, along with the algorithm variables Pt and Pmax. This derivation of the value of $(\Delta P/\Delta t)$ at the CSP neglects any saliency effects. These effects will be included later. The sinusoidal power load angle relationship is given by;

$$P = Pmax \sin(\delta) \qquad \text{A(51)}$$

The load angle at which P = Pt for load angles greater than 90° (unstable operation) is given by :

$$\delta_c = 180 - \sin^{-1}\left(\frac{Pt}{Pmax}\right) \qquad A(52)$$

The derivative of real power with respect to time, can be expressed as :

$$\frac{dP}{dt} = \frac{dP}{d\delta}\frac{d\delta}{dt} \qquad A(53)$$

The derivative of load angle with respect to time is the slip, s and is defined as;

$$\frac{d\delta}{dt} = -s \qquad A(54)$$

i.e. negative values of slip exist for speeds above synchronous speed. If A(51) is differentiated with respect to load angle then:

$$\frac{dP}{d\delta} = Pmax \cos(\delta) \qquad A(55)$$

The derivative of real power at the algorithm CSP, where P = Pt is given using equations A(52,53,54,55);

$$\left.\frac{dP}{dt}\right|_{@CSP} = -s\ Pmax \cos\delta_c = (\Delta P/\Delta t)_{min} \qquad A(56)$$

The value of $(\Delta P/\Delta t)_{min}$ will therefore change with generator loading. The value of $(\Delta P/\Delta t)_{min}$ becomes more negative as the generator loading increases. This stands to reason, since as the loading increases the values of $(\Delta P/\Delta t)$ occurring at the CSP will increase because the nominal value of Pmax increases with generator loading. With Pmax its nominal value of 1.4 * Pt, $(\Delta P/\Delta t)_{min}$ for steady state operation is given using A(52,56);

$$(\Delta P/\Delta t)_{min}\Big|_{(steady\ state)} = 0.98 * s * Pt \qquad A(57)$$

Equation A(56) is used by the algorithm to calculate the rate of change of power trip setting during non-transient conditions.

In terms of algorithm operation, generator transient conditions are defined as occurring when the ratio Pt/Pmax falls below 0.6. This shows that the generator output power has risen significantly above the nominal value of Pmax. This will only occur when a transient disturbance on the generator has caused the generator output power-load angle curve to take on transient values. Chapter three showed that during transient conditions, the machine output power is much greater than nominal, and transient saliency components occur in the power load angle curve. These effects must be considered if the algorithm is to remain secure during stable power swings.

A5.2.2 Including Transient Saliency Effects in the $(\Delta P/\Delta t)_{min}$ Calculation

When the generator is operating in its transient mode, the effects of transient saliency can be very pronounced. Figures 3.1a and 3.2a in Chapter 3 show the steady state and transient characteristics for both round rotor and salient pole machines. The peak in the transient power load angle curve occurs around 120°, for both types of machines. Transient saliency therefore increases the value of $(\Delta P/\Delta t)$ at the CSP. If resistance is neglected, then A(32) becomes;

$$P = \frac{Eq'V}{Xd'} \sin(\delta) + \left(\frac{1}{Xq} - \frac{1}{Xd'}\right)\frac{V^2}{2}\sin(2\delta) \qquad \text{A(58)}$$

The derivative of A(58) with respect to δ is given by;

$$\frac{dP}{d\delta} = \frac{Eq'V}{Xd'}\cos(\delta) + \left(\frac{1}{Xq} - \frac{1}{Xd'}\right)V^2\cos(2\delta) \qquad \text{A(59)}$$

Using A(53), A(54) and A(59) gives an expression for the rate of change of power, neglecting asynchronous effects, which is given by;

$$\frac{dP}{dt} = -s\left(\frac{Eq'V}{Xd'}\cos(\delta) + \left(\frac{1}{Xq} - \frac{1}{Xd'}\right)V^2\cos(2\delta)\right) \qquad \text{A(60)}$$

The Pmax measuring function within the algorithm measures the peak produced by the two terms contained in A(60). There is no simple way of telling how much each term has contributed to that peak however.

During transient conditions, algorithm security is the greatest concern since recoverable power swings produce massive variations in all of the algorithm measurands, and the machine characteristics become far from ideal. With this in mind a conservative approach has been taken in including the effects of transient saliency into the calculation of $(\Delta P/\Delta t)_{min}$ which is as follows.

If the voltage, V is assumed to be 1 p.u. and it is assumed that the CSP occurs at a load angle which makes the magnitude of $\cos(2\delta)$ equal to unity, then an estimate of the contribution from the transient saliency term to the $(\Delta P/\Delta t)$ signal at the CSP can be made. Figures 3.1a and 3.2a shows that even at full load the intersection of the unity real power line and the transient power load angle characteristic is such that the CSP will occur at around 160°. This makes the $\cos(2\delta)$ term approximately equal to unity. The above

assumption is therefore valid. The above assumptions make the approximate contribution of the transient saliency term to (ΔP/Δt) at the CSP equal to;

$$(\Delta P/\Delta t)_{tran} = \left(\frac{1}{Xq} - \frac{1}{Xd'}\right) * Sgen \qquad A(61)$$

This term is added to the existing value of $(\Delta P/\Delta t)_{min}$ which was calculated by assuming a sinusoidal power load angle characteristic. This additional transient saliency term, $(\Delta P/\Delta t)_{tran}$ is therefore only added to $(\Delta P/\Delta t)_{min}$ when the ratio Pt/Pmax falls below 0.6 as defined by equation 4(18) in Chapter 4.

A5.2.3 Errors Produced by the Assumptions Used to Derive $(\Delta P/\Delta t)_{min}$

An error occurs because steady state saliency is neglected when assuming a sinusoidal power load angle relationship. This is only a consideration in salient pole machines. Neglecting this effect results in a value of $(\Delta P/\Delta t)_{min}$ being estimated which is more negative than it should be. This tends to make the algorithm more secure. The degree of steady state saliency produced in a salient pole generator is small compared to the transient saliency term, the effect of neglecting it is therefore small and does not affect algorithm operation.

The other main error in deriving $(\Delta P/\Delta t)_{min}$ is neglecting asynchronous effects. These are too complicated to be taken into consideration. A qualitative analysis of their effects on the value of (ΔP/Δt) at the CSP will therefore be given. The generator's instantaneous asynchronous power output is given by;

$$P_{as} =$$

$$-\frac{V^2}{2}\frac{Xd-Xd'}{Xd\,Xd'}\cdot\frac{sTd'}{1+(sTd')^2}\cdot\left(1+\sqrt{(}\,1+(sTd')^2\,).\sin\left(2\delta_o-\tan^{-1}\left(\frac{1}{sTd'}\right)-2st\right)\right) \qquad A(62)$$

$$-\frac{V^2}{2}\frac{Xd'-Xd''}{Xd'\,Xd''}\cdot\frac{sTd''}{1+(sTd'')^2}\cdot\left(1-\sqrt{(}\,1+(sTd'')^2\,).\sin\left(2\delta_o-\tan^{-1}\left(\frac{1}{sTd''}\right)-2st\right)\right)$$

$$-\frac{V^2}{2}\frac{Xq-Xq''}{Xq\,Xq''}\cdot\frac{sTq''}{1+(sTq'')^2}\cdot\left(1-\sqrt{(}\,1+(sTq'')^2\,).\sin\left(2\delta_o-\tan^{-1}\left(\frac{1}{sTq''}\right)-2st\right)\right)$$

If the mean components of A(62) (non-sinusoidal components) are differentiated with respect to time, it can be seen that the sign of the dP_{as}/dt term is given in the form;

$$d\frac{(P_{as})}{dt} = -A\frac{ds}{dt} - B\frac{ds}{dt} - C\frac{ds}{dt} \qquad A(63)$$

where the constants A, B, C are all positive. Figure A9 shows the generator rotor angle, slip, s, and rate of change of slip, ds/dt for a stable and an unstable power swing. Figure A9c shows that ds/dt will be positive for a stable power swing as the load angle swings up to and back away from the CSP. The contribution of the asynchronous power to ($\Delta P/\Delta t$) at the CSP will therefore be negative, making ($\Delta P/\Delta t$) more negative around the CSP area during stable power swings.

Inspection of the unstable, pole slipping ds/dt curve shows that it changes sign as the generator approaches and passes the CSP. The curve shown is for the case where stability is only just lost. If a more severe fault caused instability, then the ds/dt curve may change sign earlier because the generator would accelerate into the pole slip in a more severe manner. The effect of the asynchronous power in this case is therefore to increase the value of ($\Delta P/\Delta t$) at the CSP, i.e the asynchronous power makes ($\Delta P/\Delta t$) less negative at the CSP.

It can therefore be concluded that neglecting steady state saliency and asynchronous power generation effects in the calculation of $(\Delta P/\Delta t)_{min}$, results in a value of $(\Delta P/\Delta t)_{min}$ which is less negative than it should be. This suggests that the rate of change of power trip setting derived by the algorithm would tend to be too sensitive, and may result in algorithm nuisance tripping during recoverable power swings. However, sections A5.2.1 and A5.2.2 both state that the methods used in deriving $(\Delta P/\Delta t)_{min}$ result in a value of $(\Delta P/\Delta t)_{min}$ which is more negative than it should be. This is especially true for the transient saliency calculation. These methods therefore help to cancel out the inaccuracies produced by neglecting asynchronous power effects and steady state saliency in the calculation of $(\Delta P/\Delta t)_{min}$. Tests show that the algorithm is stable during recoverable power swings, yet able to detect pole slipping. The settings are therefore satisfactory.

A5.2.4 Units Used in Equations

The units of the expressions found in this chapter require clarification. Slip, s is in fractional units, δ is in radians, and the units of time are in radians. In order to convert from this time domain into the conventional time domain of seconds, the following relationship is used;

$$t_{[rad]} = \omega_o * t_{[sec]} \qquad A(64)$$

The values of slip used in this work should therefore be entered in terms of $s * \omega_o$, rather than purely s, since slip is defined as the rate of change of load angle. ω_o is defined

as the angular power system frequency, and is equal to 2 π f_o. All voltages and machine reactances used in equations are in per unit, on the generator base, whilst the generator time constants also require conversion using equation A(64) [127] .

A5.3 DERIVATION OF LIMITS OF OPERATION OF ALGORITHM AS THE SYSTEM INFEED IS VARIED

Four operational limit graphs were constructed to show the value of source impedance where the reactive power trip criterion would fail to work properly. One graph was constructed to shows the effect of varying the reactance to resistance ratios in the tie line, the other to show the effect of varying the generator internal voltage, E. The quantities referred to are shown diagrammatically in Figure A7a. The following assumptions were made in order to derive the graphs. The results are also given in tabular from in Tables A2 and A3. Chapter 4 details the methods used when using these results to apply the power based pole slipping algorithm to a generator.

a) The direct axis reactance which should be used to determine if the algorithm will operate satisfactorily, is the direct axis transient reactance, Xd'. This is the lowest operational reactance likely to occur during pole slipping. Assuming the lowest operational reactance produces a worst case scenario. Using Xd' assumes that the generator is operating at 50 % slip[45]. A slip of 0.33 % results in the generator reactance equalling 2 Xd'.

b) The value of inter-tie reactance, X, quoted is the highest theoretical value for which the algorithm will operate. The value is derived such that 60° of the theoretical reactive power load angle curve falls below the reactive power trip criterion, Qtrip, where Qtrip = -1/Xq * Sgen.

c) The values of voltage behind generator reactance used were 1.25, 1.5 and 1.75 p.u. Although it is referred to as E, technically, it should be Eq', the voltage behind transient reactance, as defined in section A3.1.1. A value of 1.25 should be chosen if the AVR fitted to the generator is not a high performance fast AVR[79]. Normally a value of 1.5 is the highest value expected. However, if a very fast high performance AVR is used on a generator with a short field time constant, a value of 1.75 may occur due to field forcing

action. Section 3.1.3 contains methods for calculating Eq'.

d) The per unit resistance of the generator was assumed to be 0.03 p.u. A parametric study on the effect of varying the stator resistance showed that a 1000 % increase in this figure produced a 1.6 % variation in the number of degrees of the reactive power curve which were below Qtrip.

e) For the first graph, curves have been calculated for two different amounts of inter-tie resistance. The first amount was calculated for an inter-tie resistance of 10 % of the inter-tie reactance. For the second situation, the inter-tie resistance was set equal to the reactance. The effect of varying the inter-tie R/X ratio was found to be small.

f) The synchronous machine assumptions usually made apply for this analysis, i.e, a sinusoidal, balanced voltage supply, and sinusoidally distributed windings.

g) The value of V, the infinite bus voltage was set to 1 pu in all cases.

Table A2 - Limits of Operation of Algorithm for 50 % slip case (Xg = Xd' = 0.1Xq) - Effect of a Varying Tie Line Resistance .

criteria \ Xq (pu)	0.5	1.5	2.5
X(pu) for E = 1.25 , r = 0.1X,	0.0320	0.09295	0.1545
X(pu) for E = 1.25, r = X,	0.03545	0.09845	0.16215
X(pu) for E = 1.5, r = 0.1X,	0.02734	0.07942	0.13195
X(pu) for E = 1.5, r = X,	0.02968	0.083	0.13695

Table A3 - Limits of Operation of Algorithm for 50 % slip case (Xg = Xd', R = 0.1X)- Effect of a Varying Generator Internal Voltage, E, and Xd'.

criteria \ Xq (pu)	0.5	1.5	2.5
X(pu) for E = 1.25 , Xd' = 0.1Xq	0.03201	0.09295	0.15445
X(pu) for E = 1.25, Xd' = 0.2Xq	0.05590	0.16510	0.27470
X(pu) for E = 1.25, Xd' = 0.3Xq	0.07423	0.2207	0.3674
X(pu) for E = 1.25, Xd' = 0.6Xq	0.10525	0.3152	0.5255
X(pu) for E = 1.25, Xd' = 0.9Xq	0.1123	0.3374	0.5628
X(pu) for E = 1.5 , Xd' = 0.1Xq	0.02734	0.0794	0.13195
X(pu) for E = 1.5, Xd' = 0.2Xq	0.04890	0.1444	0.2402
X(pu) for E = 1.5, Xd' = 0.3Xq	0.06633	0.1971	0.3281
X(pu) for E = 1.5, Xd' = 0.6Xq	0.0994	0.2975	0.496
X(pu) for E = 1.5, Xd' = 0.9Xq	0.1117	0.3353	0.5593
X(pu) for E = 1.75 , Xd' = 0.1Xq	0.02382	0.0692	0.1150
X(pu) for E = 1.75, Xd' = 0.2Xq	0.04330	0.1279	0.2128
X(pu) for E = 1.75, Xd' = 0.3Xq	0.05970	0.1773	0.2952
X(pu) for E = 1.75, Xd' = 0.6Xq	0.09335	0.2793	0.4654
X(pu) for E = 1.75, Xd' = 0.9Xq	0.1092	0.3275	0.5465

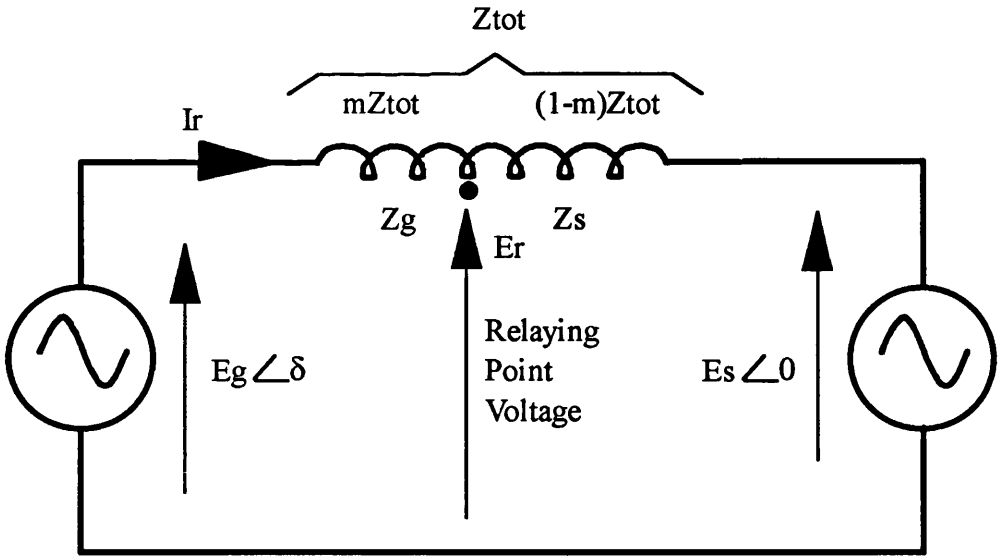

Figure A1
Two Machine Representation of Power System
Used in Analysing Swing Loci During Pole Slipping

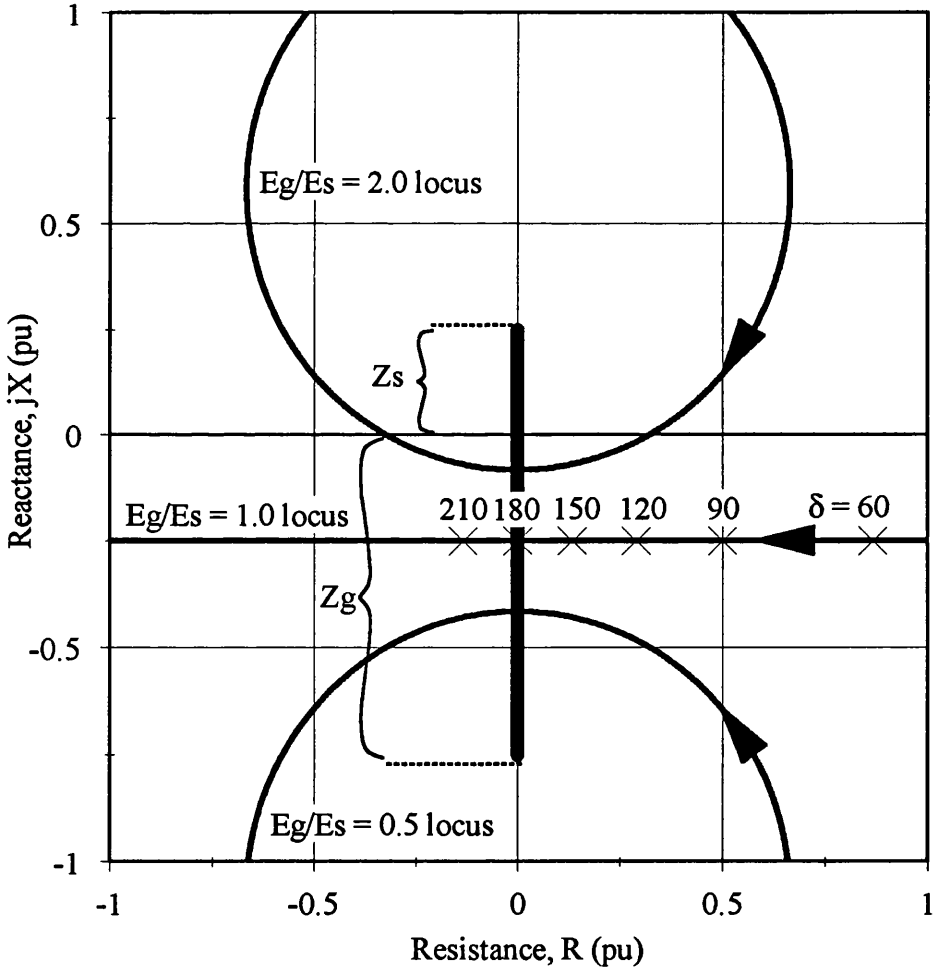

Figure A2
Impedance Plane Pole Slipping Loci for System Shown in Figure A1, m = 0.75, Z = j1 pu.

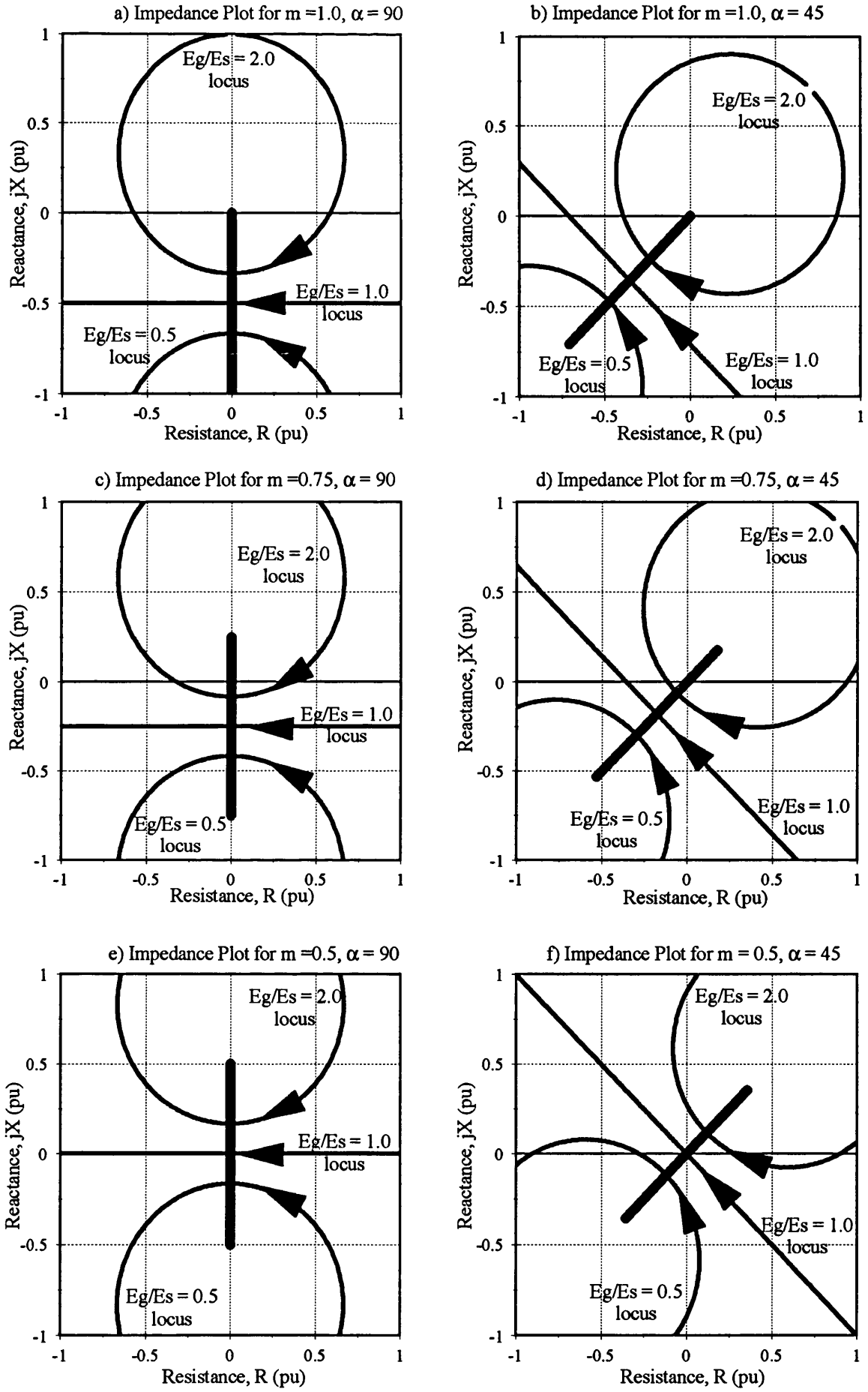

Figure A3

Impedance Plane Pole Slipping Loci for System Shown in Figure A1.

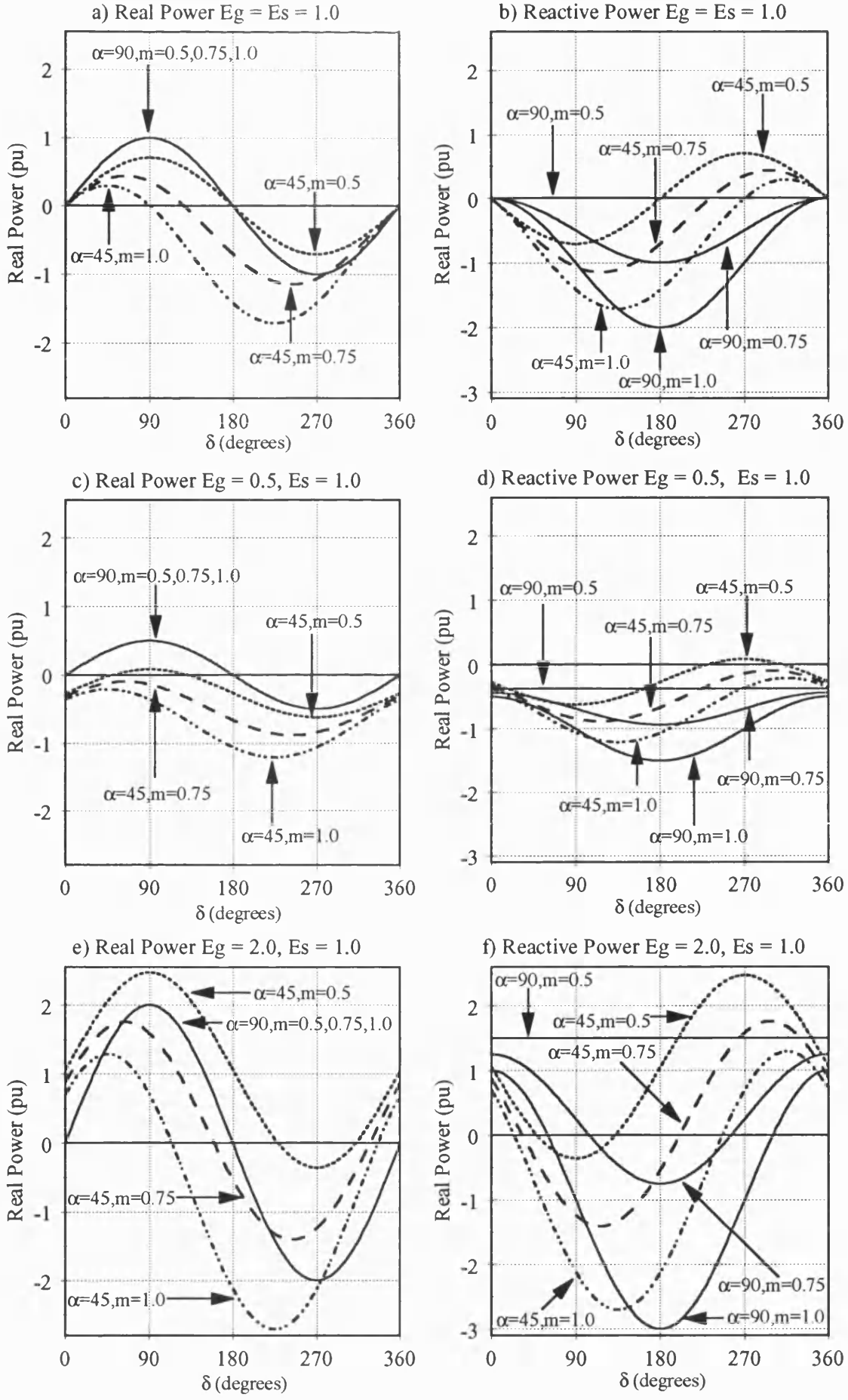

Figure A4 - Real and Reactive Power Load Angle Relationships for Figure A1.

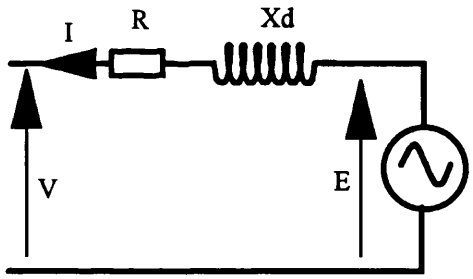

Figure A5a
Synhronous Machine Equivalent Circuit

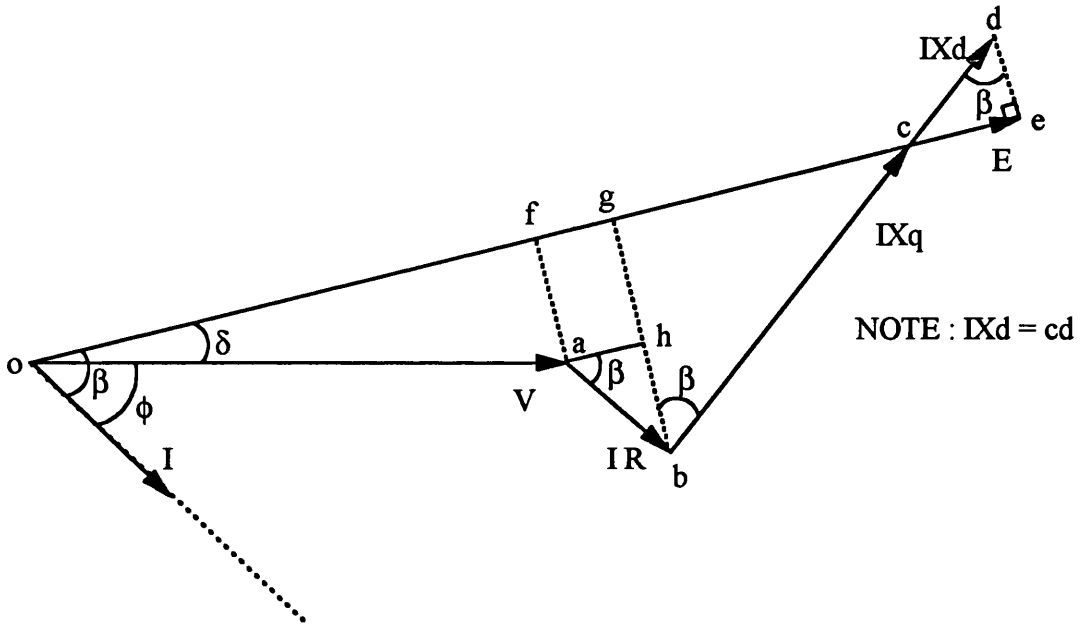

Figure A5b
Voltage Vector Consruction for Finding E and δ given V, I, ϕ, Xd, Xq, and R

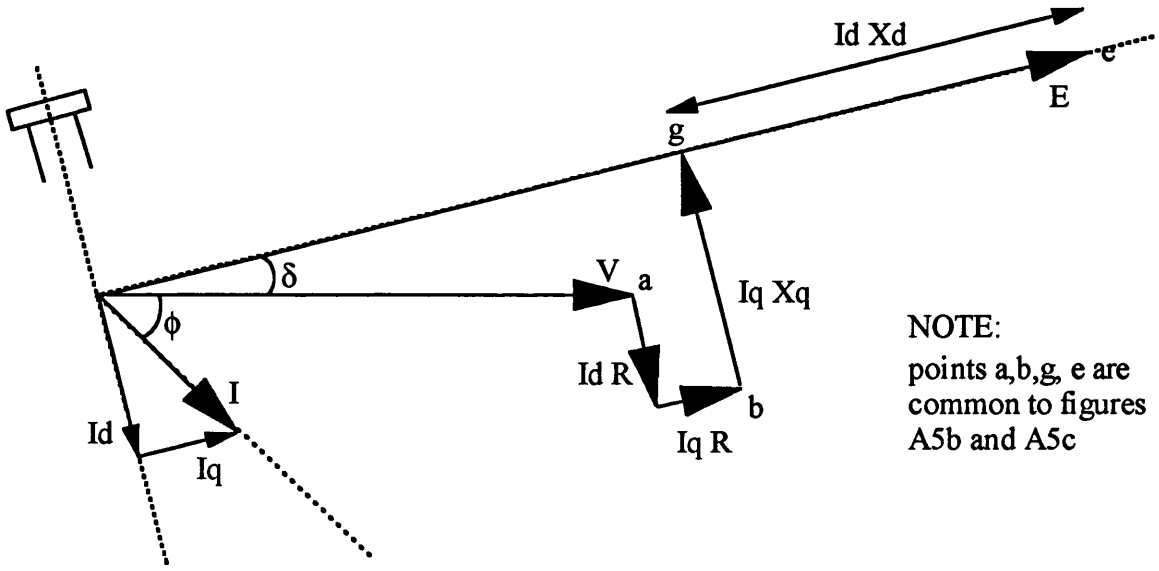

Figure A5c
Steady State Voltage Vector Diagram for Salient Pole Synchronous Generator

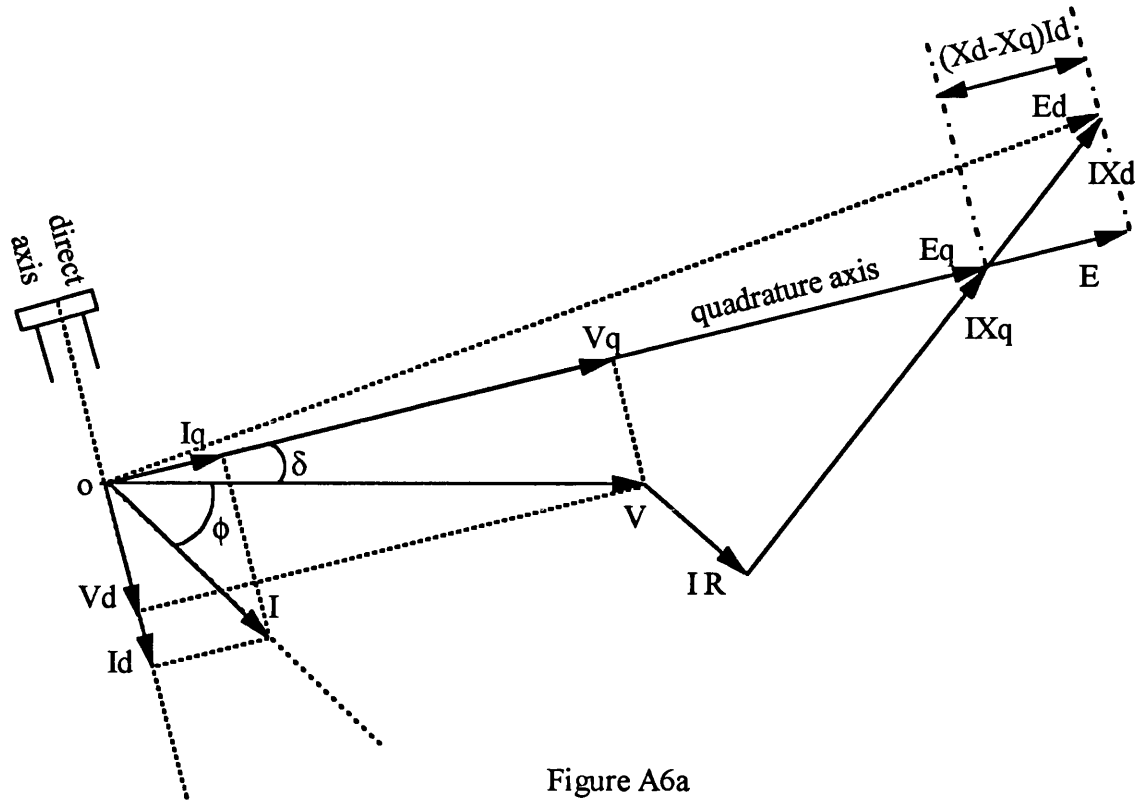

Figure A6a
Steady State Voltage Vector Diagram Showing Eq, Ed and E

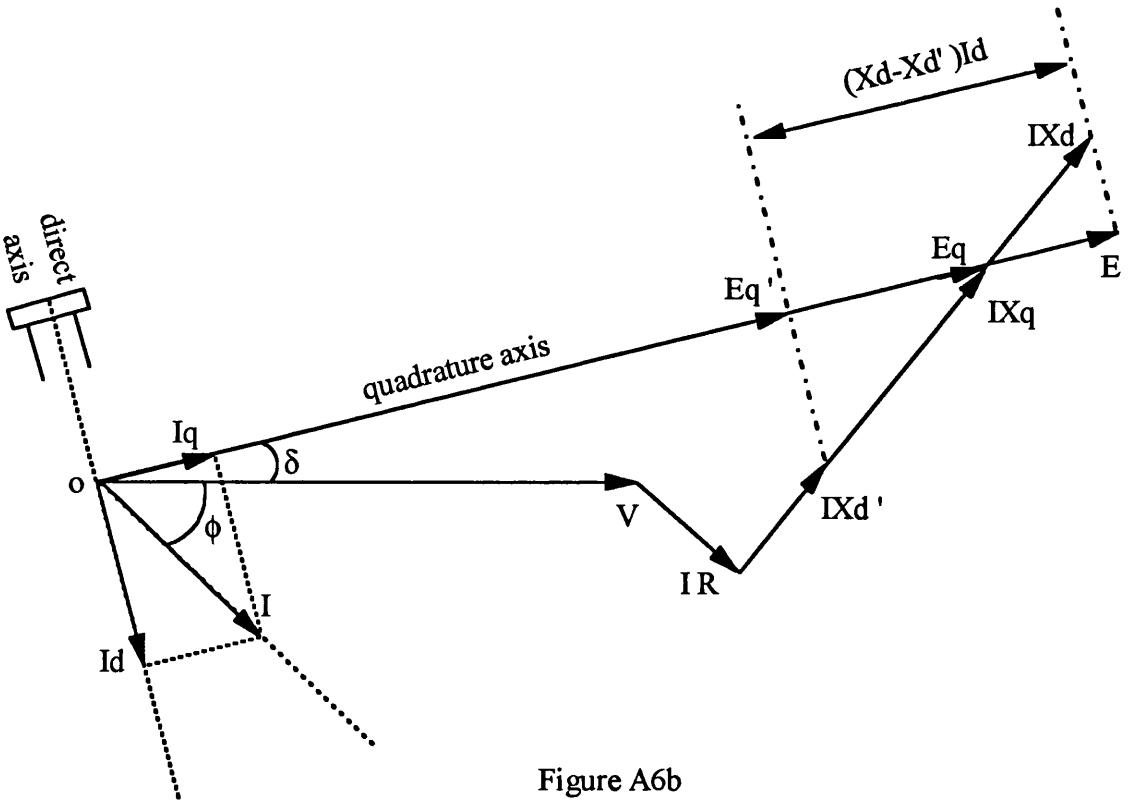

Figure A6b
Voltage Vector Diagram Showing Eq', Eq, and E

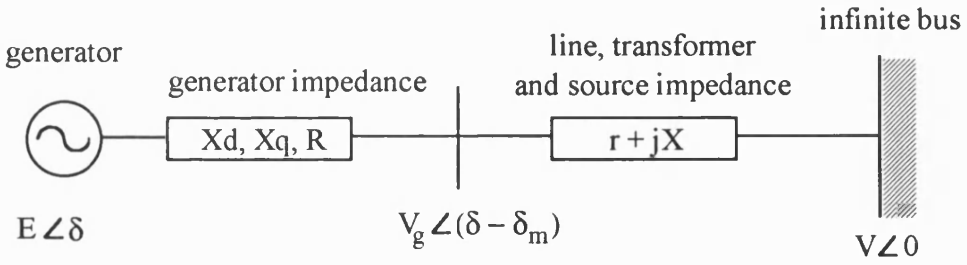

Figure A7a
Schematic Diagram Showing Generator Operating
Against an Infinite Bus Through an Inter-tie Impedance

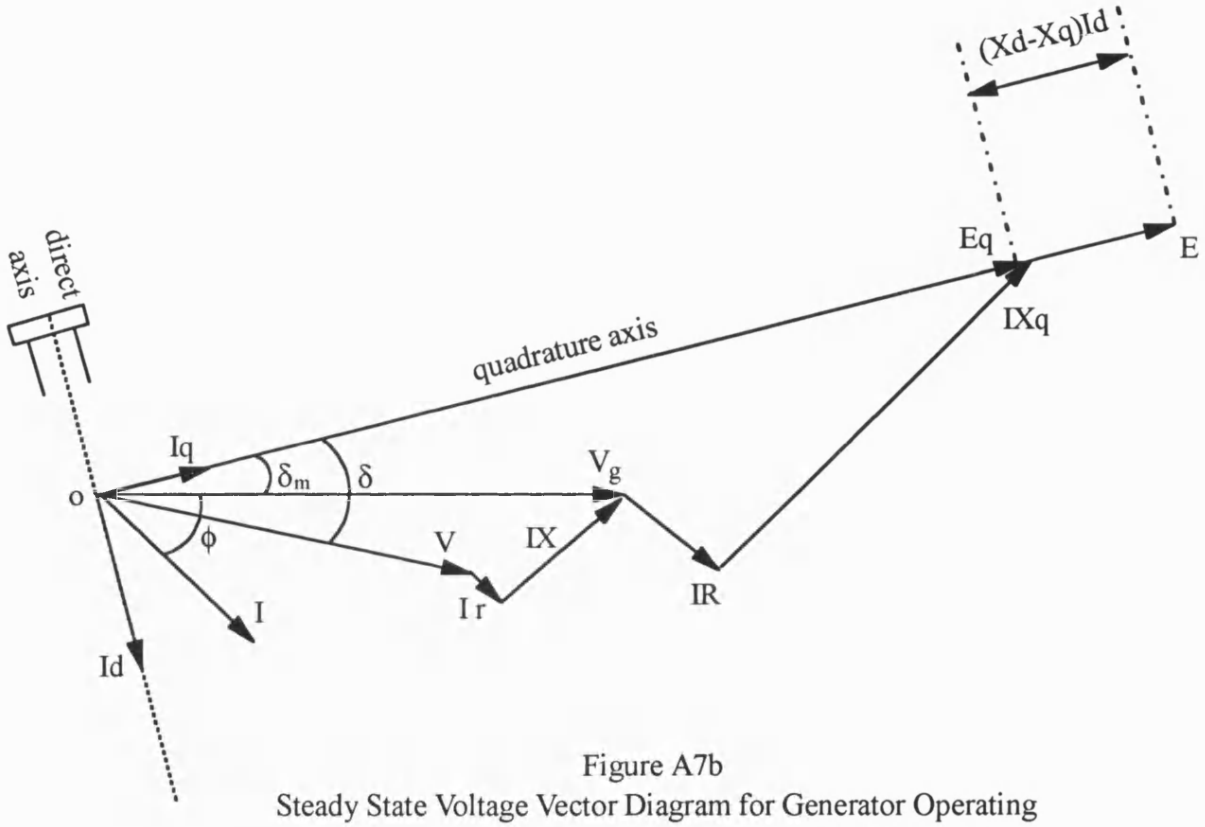

Figure A7b
Steady State Voltage Vector Diagram for Generator Operating
Against An Infinite Bus Through an Inter-tie Impedance

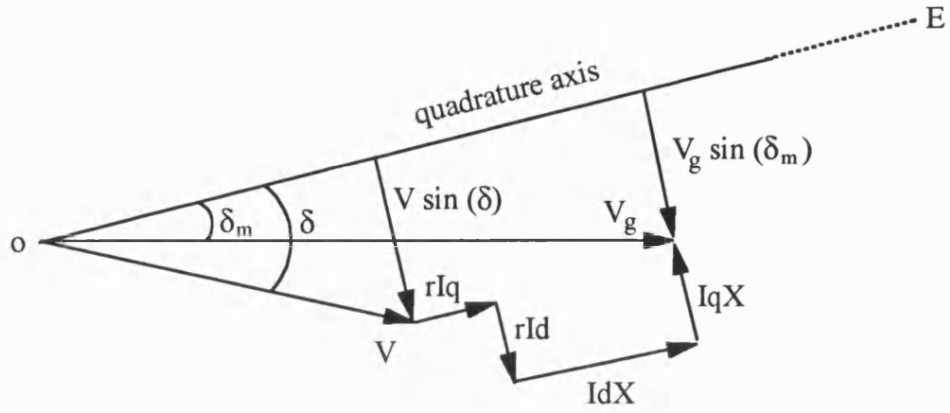

Figure A7c
Voltage Vector Diagram Showing Direct and Quadrature
Axis Voltages for the Inter-tie Impedance.

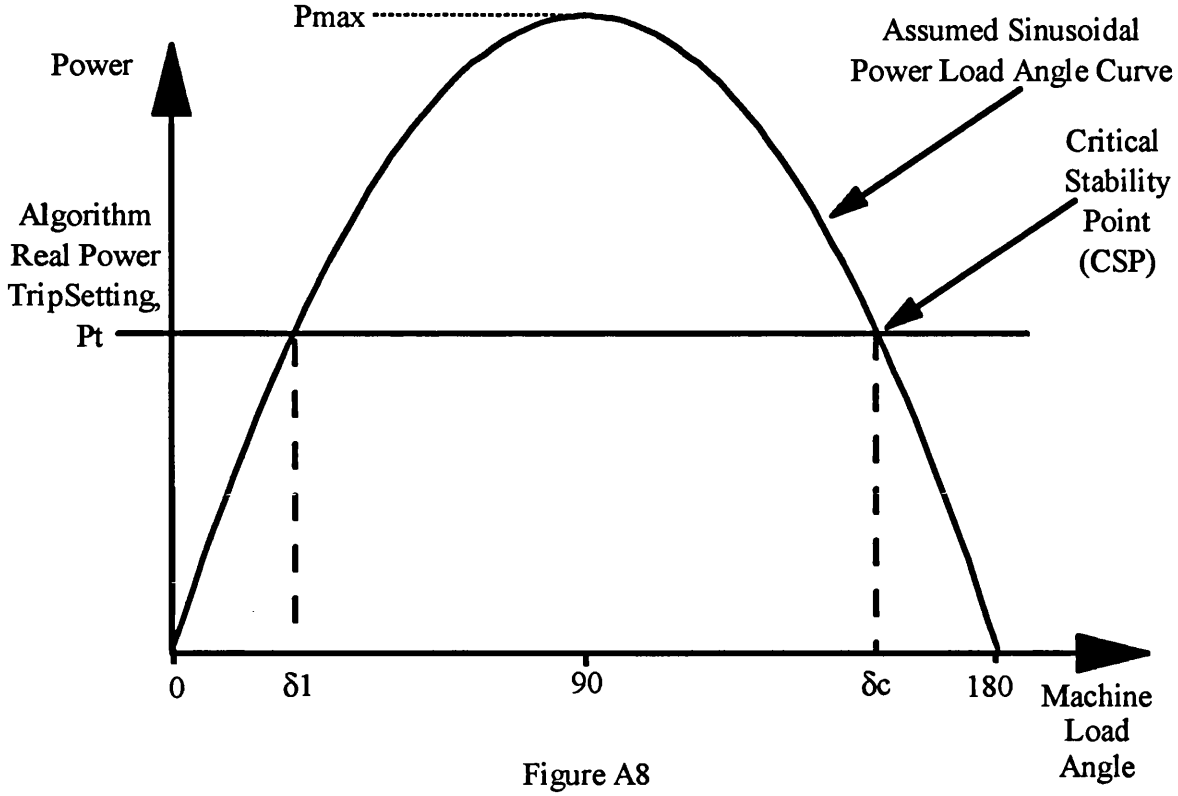

Figure A8
Diagram Showing Assumed Sinusoidal Power Load Angle Variation and the Pole Slipping Algorithm Variables, Pt and Pmax

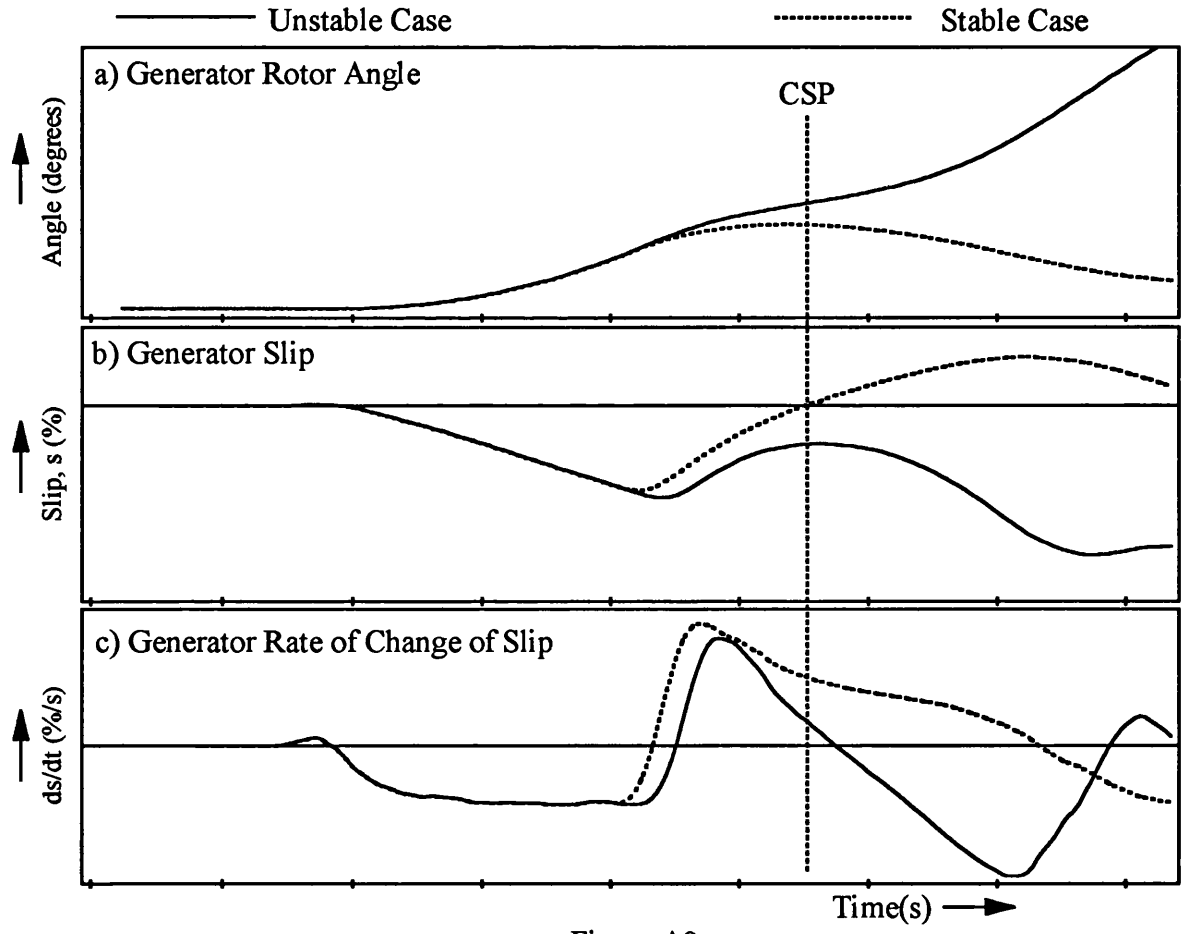

Figure A9
Rotor Angle, Slip, and Rate of Change of Slip for Stable and Unstable Power Swings.

Appendix B

SETTING OF CONVENTIONAL IMPEDANCE RELAYS

The procedures used to set conventional impedance based pole slipping schemes are contained in this chapter. Settings for the laboratory power system model 5 kVA generator, 625 kVA industrial diesel generator, and PPSS 200 MVA steam turbine generator are all included. Settings for the loss of field, mho, single blinder and double blinder schemes have been derived.

B1.1 LOSS OF FIELD SCHEME

The setting method used was based on recommendations taken from references [42,43,44,45,46,68,72,73,75,187]. The basic loss of field scheme used for embedded generators is the loss of field characteristic 1 shown in Figure 2.2. The recommended settings are;

mho offset = -Xd'/2

mho diameter = Xd

time delay of 0.5 to 0.6 seconds.

The offset referred to here is the distance from the origin of the R-X plane and the top of the loss of field characteristic.

B1.1.1 Loss of Field Settings for PPSS Test Generator

The 200 MVA PPSS generator specified in Appendix C will have the following loss of field settings;

offset = -Xd'/2 = -j0.23832pu/2 = -j0.120 pu

circle diameter = Xd = 1.7 pu , $\therefore$ centre = -j0.12 - j1.7/2 = -j0.97 pu

circle centre = -0.120 pu - 1.7 pu / 2 = -0.97 pu

time delay = 0.5 seconds.

Because the value of Xd is significantly larger than 1 pu, a time delay of 0.5 seconds is used in order to prevent nuisance tripping for stable swings that cause the offset mho element to pick up[44].

B1.1.2 Loss of Field Settings for 5 kVA Laboratory Generator

The data for the 5 kVA laboratory generator is given in Appendix C. The loss of field settings are as follows;

offset = -Xd'/2 = -j1.71 pu/2 = -j0.855 pu

circle diameter = Xd = 2.32 pu, $\therefore$ centre = -j0.855 - j2.32/2 = -j2.015 pu

time delay = 0.5 seconds.

B1.1.3 Loss of Field Settings for 625 kVA Diesel Generator

The available data for this generator is given in Appendix C. The loss of field settings are as follows;

offset = -Xd'/2 = -j0.22 pu/2 = -j0.110 pu

circle diameter = Xd = 2.25 pu, $\therefore$ centre = -j0.110 - j2.25/2 = -j1.235 pu

time delay = 0.5 seconds.

B1.2 MHO ELEMENT POLE SLIPPING SCHEME

The Mho element scheme is the simplest of the impedance based pole slipping projections. A trip signal is issued the instant the locus enters the circle, or after a time delay if the reach of the mho circle is large. There are various recommendations for the settings used. The IEEE (PR 3 & PR 64 section 9) recommend that the reach should be set short of the HV terminals of the generator transformer down to an impedance value which is equal to the direct axis transient reactance. If a larger mho characteristic than this is used, a time delay should be employed to ensure that nuisance tripping does not occur for faults or swings which appear beyond the high side terminals of the transformer. The IEEE recommend that the angle at which a swing is non-recoverable is 120°.

B1.2.1 Mho Element Settings for PPSS Test Generator

The pole slipping impedance loci for the 200 MVA PPSS generator were calculated using the procedure described in Appendix A. These impedance loci are shown in Figure B1. Initially the mho circle was set so that it covered the generator transient reactance and up to 80 % of the transformer. This meant that the swing locus entered the circle at a load angle of 110°. This was unacceptable because the protection scheme was not secure enough. The mho circle was therefore adjusted so that the Eg/Es = 1 locus entered the mho characteristic at an load angle just greater than 120°. This protected all of the

generator, but none of the transformer. A time delay of 20 ms was also used, in order to simulate delays inherent to an 'instantaneous relay' and to enhance relay security.

Figure B2 shows the mho characteristic (solid circle) with the impedance swing loci (dotted lines) also shown, along with the system and generator impedances (extra thick solid lines). This figure also contains part of the loss of field characteristic and shows where the protection zones of the two schemes overlap. The intersection of the mho circle and the Eg/Es = 1.0 impedance locus shows that the locus enters the circle at a load angle just greater than 120°. The diameter of the mho circle was set to 0.240 pu, its centre was located at 0, - j0.120 pu.

B1.2.2 Mho Element Settings for the 5 kVA Laboratory Generator

The pole slipping impedance loci for the 5 kVA laboratory generator are shown in Figure B5. If the mho circle was set to cover the whole of the transient reactance, the Eg/Es = 1.0 locus entered the circle at 92°. This was unacceptable, as the scheme would be likely to nuisance trip for recoverable swings. The mho circle was set so that the impedance locus entered it at 105°. This should provide cover for almost all impedance loci down to a ratio of Eg/Es of 0.19. The chosen characteristic is shown in Figure B6, as well as the loss of field characteristic. The two characteristics overlap providing an enhanced protection zone. It is important to not however, that the loss of field scheme has a 0.5 second time delay, it may therefore fail to detect fast pole slips whose impedance loci cross the area below the mho circle. In theory such impedance loci should occur rarely, since the effective generator voltage has to fall below 0.19 pu for this to happen. Since the 120° load angle criterion was not satisfied, a time delay of 40 ms was employed with the mho scheme to enhance security towards recoverable swings.

Assuming a uniform pole slipping rate, and using the Eg/Es = 1.0 impedance locus, the locus remains in the mho characteristic for 2 * (180°-105°) = 150°. The highest rate of pole slipping that the scheme can detect is therefore;

$$150°/(360° * 40 \text{ ms}) = 10.4 \text{ Hz}$$

The diameter of the mho circle equalled 1.402 pu, its centre was located at 0, - j0.709 pu.

B1.2.3 Mho Element Settings for the 625 kVA Industrial Diesel Generator

The pole slipping impedance loci for the 625 kVA diesel generator were calculated using the procedure described in Appendix A. These loci are shown in Figure B9. If the mho

circle was set to cover the whole of the transient reactance, then the Eg/Es = 1.0 impedance locus would enter the circle at 95°. This was unacceptable because the scheme may nuisance trip for recoverable swings. The mho circle was set so that the impedance locus entered at a load angle of 105°. This provided cover for swings down to a ratio of Eg/Es = 0.19. Figure B10 shows the mho circle characteristic, the loss of field characteristic, and the impedance loci lines. A time delay of 40 ms was employed to enhance scheme security towards recoverable power swings because the 120° criterion was not satisfied, . Assuming a uniform pole slipping rate, and using the Eg/Es = 1.0 locus, the locus remains inside the characteristic for 2 * (180°-105°) = 150°. The highest rate of pole slipping that the scheme can detect is therefore;

$$150°/(360° * 40 \text{ ms}) = 10.4 \text{ Hz}$$

The diameter of the mho circle equalled 0.1818 pu. The centre of the mho circle was located at -0.0076, -j0.0909 pu

B1.3 SINGLE BLINDER POLE SLIPPING PROTECTION SCHEME

With the single blinder scheme, tripping occurs after the pole slipping impedance locus has entered the mho circle, and crossed both of the blinder units in a specified time. The trip signal is issued after the locus has crossed the second blinder. Reference [68] recommends that the blinder reaches are set so that tripping occurs at a load angle of 90°. The angle of the blinder units should be set so that they are parallel with the overall equivalent system impedance line. The supervisory mho unit should be set so that impedance loci which pass though the generator transformer are detected. The minimum travel time between blinder units required for the scheme to trip is usually set to 40 ms[78].

B1.3.1 Single Blinder Settings for the PPSS Test Generator

The location of the right and left blinder units was chosen so that the Eg/Es = 1 swing impedance locus crossed them at 100° and 260° respectively. This was necessary in order to reduce the reach of the supervisory mho circle. This increases the security of the scheme towards recoverable swings which may pass underneath the transient reactance on the RX plane. An example of such as swing is shown in Figure 2.4. With the blinder characteristics set, the supervisory mho circle size was then selected so that it intersected the blinder units at the HV terminals of the generator transformer. This enables the scheme to trip for pole slips whose system centre appears in the generator transformer.

Pole Slips up to an Eg/Es ratio of 1.5 can be detected. The setting characteristics are shown in Figure B3, the transformer HV terminals are shown by the dash-dash line. The angle of the blinder units was set to the overall system impedance angle (86.4°). The left blinder crosses the R axis at a value of -0.152 pu, the right hand blinder crosses the R axis at a value of -0.159 pu. The supervisory mho element circle was centred at 0, -j0.120 pu with a diameter of 0.415 pu. The recommended impedance locus traverse time of 40 ms refers to blinder settings at 90° and 270°, this infers a mean pole slipping rate of ;

$$180/(360° * 40 \text{ ms}) = 12.5 \text{ Hz.}$$

Using this mean rate of pole slipping on the blinder settings of 100° and 260°, gives a setting time of;

$$160/(360° \ 12.5 \text{ Hz}) = 35.6 \text{ ms}$$

B1.3.2 Single Blinder Settings for the 5 kVA Laboratory Generator

The left and right blinders were set so that the Eg/Es = 1.0 swing locus crossed them at 270° and 90° respectively. The supervisory mho circle was then set so that swings appearing inside the generator were detected. The angle of the blinder units was set to the system impedance angle of 88.4°. The left blinder crosses the R axis at a value of -0.872 pu, the right blinder crosses the R axis at a value of 0.890 pu. The supervisory mho circle diameter was set to 2.43 pu, its centre located at 0, - j0.840 pu. Figure B7 shows the single blinder characteristic. Theoretically, the scheme should detect pole slips for an Eg/Es ratio of 1.5 to 0.67. The recommended traverse time of 40 ms was used as the minimum time the impedance locus could remain between the blinders. This corresponds to a pole slipping rate of 12.5 Hz (section B1.3.1).

B1.3.3 Single Blinder Settings for the 625 kVA Diesel Generator

The left and right blinders were set so that the Eg/Es = 1.0 swing locus crossed them at 270° and 90° respectively. The supervisory mho circle was then set so that swings appearing inside the generator were detected. The angle of the blinder units was set to the system impedance angle of 83°. The left blinder crosses the R axis at a value of -0.116 pu, the right blinder crosses the R axis at a value of 0.119 pu. The supervisory mho circle diameter was set to 0.306 pu, its centre was located at -0.009, - j0.100 pu. Figure B11 shows the single blinder characteristic along with the pole slipping loci and the supervisory mho circle. The recommended time of 40 ms was used as the minimum traverse time between blinders.

B1.4 DOUBLE BLINDER SCHEME

The inner blinder elements of this scheme should be set so that only pole slipping conditions will cause them to pick up[68]. A load angle of 130° was chosen for the inner element settings, this was 10° above the IEEE recommended value. This should therefore improve scheme security. The double blinder scheme produces a trip signal when the supervisory mho element resets. Before a trip signal will be issued, the impedance locus must first enter the mho circle, then cross the outer and inner blinder elements in a preset time, then stay in between the inner blinder elements for a preset time, and then cross the inner and outer blinders in a preset time. Unlike the single blinder scheme, a trip will result if the locus enters and leaves from the same side on the impedance plane.
The reach of the supervisory mho element should be chosen to cause the least stress on the generator circuit breaker. A load angle of 90° is therefore recommended as the optimum tripping point. The outer blinder element reach should be chosen so that the scheme operates for swings whose system centre appears inside the generator or its transformer.

B1.4.1 Double Blinder Settings for the PPSS Test Generator

The inner blinder elements were set so that the Eg/Es = 1 impedance locus crossed them at 230° and 130° respectively. The right inner blinder crosses the R axis at 0.090 pu, and the left inner blinder crosses at -0.083 pu.

The supervisory mho element was initially set so that tripping occurred at 90°. The location of the outer blinders was then chosen so that the scheme would operate for the Eg/Es = 1.5 pole slipping locus. The outer blinders were also placed so that the scheme would operate for swings whose system centre occurred inside the transformer. The location of the outer blinders was therefore fixed by the intersection of the supervisory mho element, the transformer terminals and the Eg/Es = 1.5 impedance locus.

Power systems analysis showed that with these settings, the scheme failed to operate for fast pole slips because the supervisory mho element dropped out before the impedance locus had crossed the left outer blinder unit. This problem could be remedied in two ways. The reach of the outer blinder elements could be reduced, or the reach of the supervisory mho relay could be increased. Decreasing the reach of the outer blinder elements would have produced too small a time setting (less than 5 ms) between the outer and inner

blinders, consequently the reach of the mho element was increased.

Further analysis showed that decreasing the reach of the outer and inner blinders elements and keeping the supervisory mho circle at a 90° load angle setting would have been more beneficial. Figure B4 shows the impedance plane representation of the double blinder scheme for the PPSS test system.

The adjustments to the scheme's settings highlight the difficulty in obtaining satisfactory settings for such a scheme. The settings used were as follows; the outer blinder elements cross the R axis at 0.156 pu and -0.150 pu. The supervisory mho centre was located at 0, - j 0.091 pu, its diameter equalled 0.410 pu. These figures were determined graphically. The mho element setting will make the scheme trip at a load angle of 85°.

No recommendations could be found on the timer settings required for the double blinder scheme. For the scheme to operate, the locus must take at least the preset time to travel from the outer blinders to the inner blinders. In addition to this time constraint, the locus must also stay in between the inner blinders for longer than a preset time, and must also take longer than a preset time to travel back from inner to outer blinder. The times used were based on the figures recommended for the single blinder scheme.

In the single blinder scheme, the mean rate of pole slipping is 12.5 Hz (Section B1.2.3). The double blinder scheme setting times were based on this rate. The inner elements are located at 130 and 230°, whilst the outer elements are located at 101 and 259°. The angular difference between the inner and outer elements is therefore 29°. The minimum traverse time for the locus entering and leaving the characteristic is therefore;

$$29°/360° * 1/12.5 \text{ Hz} = 6.4 \text{ ms}$$

This time applies to the blinders on both sides of the RX. The time setting for in between the inner blinders is dictated by an angular separation of 100°, the minimum time setting is therefore;

$$100°/360° * 1/12.5 \text{ Hz} = 22.2 \text{ ms}.$$

B1.4.2 Double Blinder Settings for the 5 kVA Laboratory Generator

The left and right inner blinder elements were set so that the Eg/Es = 1.0 impedance locus crossed them at load angles of 230° and 130°. The right inner blinder crosses the R axis at 0.419 pu, and the left inner blinder crosses at -0.410 pu.

The supervisory mho element was set so that tripping occurred when the Eg/Es = 1.0 locus crossed it at 90° or 270°. The diameter was therefore equal to 1.761 pu, its centre was located at 0, - j0.855 pu. The location of the outer blinders was then chosen so that the scheme detected the Eg/Es = 1.5 impedance locus was. This resulted in the Eg/Es = 1.0 locus crossing the outer blinder elements at 101° and 259°. The right outer blinder crosses the R axis at 0.769 pu, the left outer blinder crosses at -0.765 pu. Figure B8 shows the double blinder scheme for the 5 kVA laboratory generator.

The 12.5 Hz pole slipping rate was used as the basis for the double blinder schemes timer settings. The inner elements are located at 130 and 230 °, whilst the outer elements are located at 101 and 259°. The angular difference between the inner and outer elements is therefore 29°. the minimum traverse time for the locus entering and leaving the characteristic is therefore;

29°/360° * 1/12.5 Hz = 6.4 ms

This time applies for both sides. The time that the impedance locus must remain in between the inner blinders is dictated by an angular separation of 100°, the minimum time is therefore;

100°/360° * 1/12.5 Hz = 22.2 ms.

B1.4.3 Double Blinder Settings for the 625 kVA Diesel Generator

The inner blinder elements were set so that the Eg/Es = 1.0 locus crossed them at 230° and 130° respectively. The right inner blinder therefore crosses the R axis at 0.058 pu, and the left inner blinder crosses at -0.058 pu.

The supervisory mho element was set so that tripping occurred when the Eg/Es = 1.0 impedance locus crossed it at 90° or 270°. The mho element diameter was therefore 0.232 pu, its centre was located at -0.008, - j0.098. The location of the outer blinders was then chosen so that the scheme would operate for the Eg/Es = 1.5 locus. This resulted in the Eg/Es = 1.0 impedance locus crossing the outer blinder units at 106° and 254°. The right outer blinder crosses the R axis at 0.095 pu, the left outer blinder crosses at -0.092 pu. Figure B12 shows the impedance plane representation of the double blinder scheme for the 625 kVA diesel generator.

The 12.5 Hz pole slip rate criterion was used as the basis for providing the timer settings for the scheme. The inner elements are located at 130 and 230 °, whilst the outer elements

are located at 106 and 254°. The angular difference between the inner and outer elements is therefore 24°. The impedance locus must therefore remain between the inner and outer blinders for a time of least;

$$24°/360° * 1/12.5 \text{ Hz} = 5.3 \text{ ms}$$

This time applies for both sides of the scheme. The time that the locus must remain between the inner blinders is dictated by an angular separation of 100°, the minimum time is therefore;

$$100°/360° * 1/12.5 \text{ Hz} = 22.2 \text{ ms}.$$

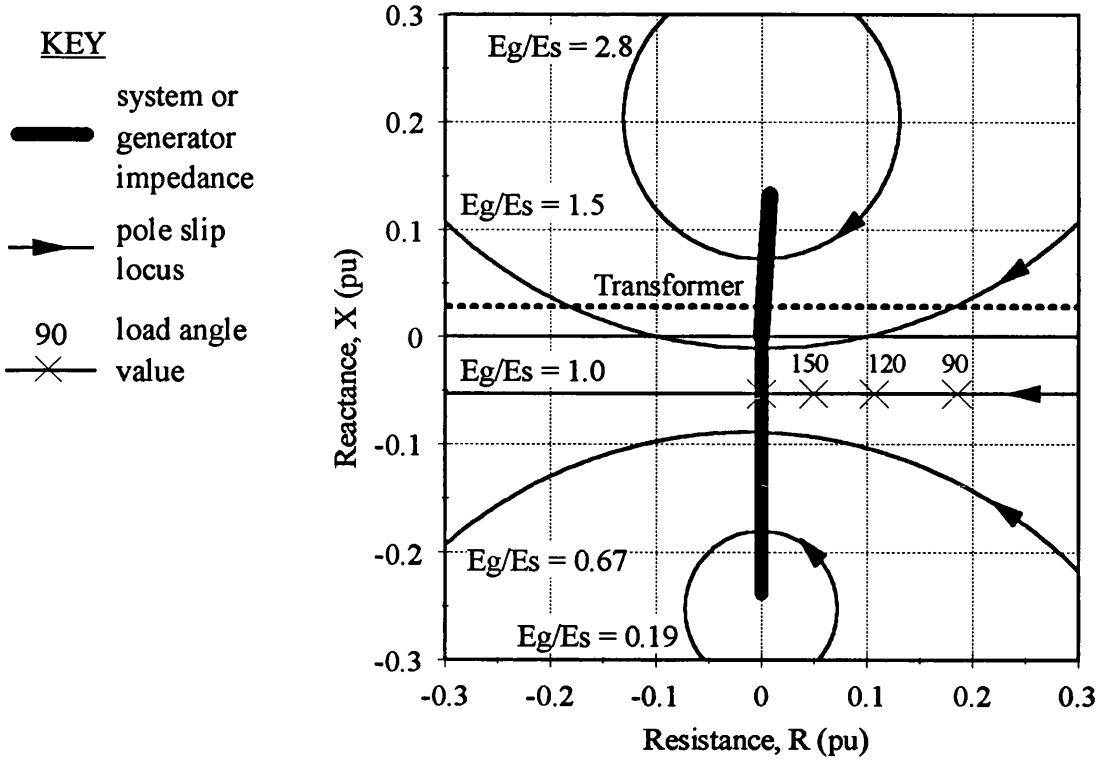

Figure B1
Pole Slipping Loci for ATP 200 MVA PPSS Test System.

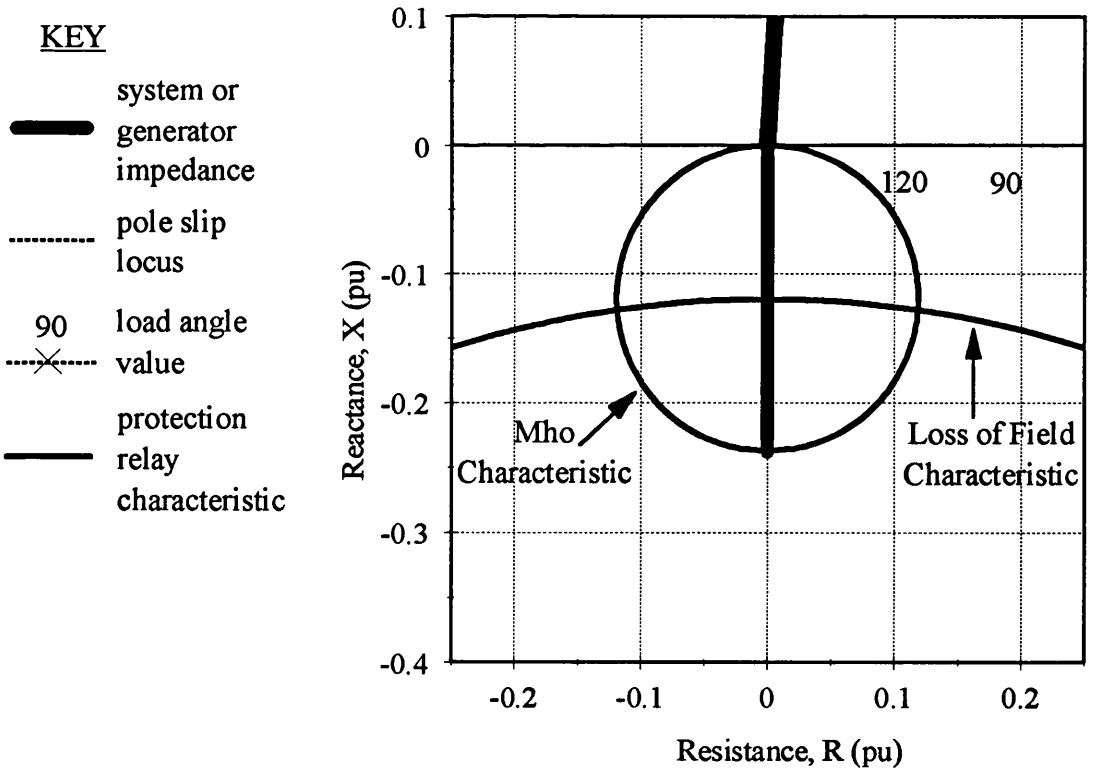

Figure B2
Single Mho Pole Slipping Protection Scheme for PPSS Test System

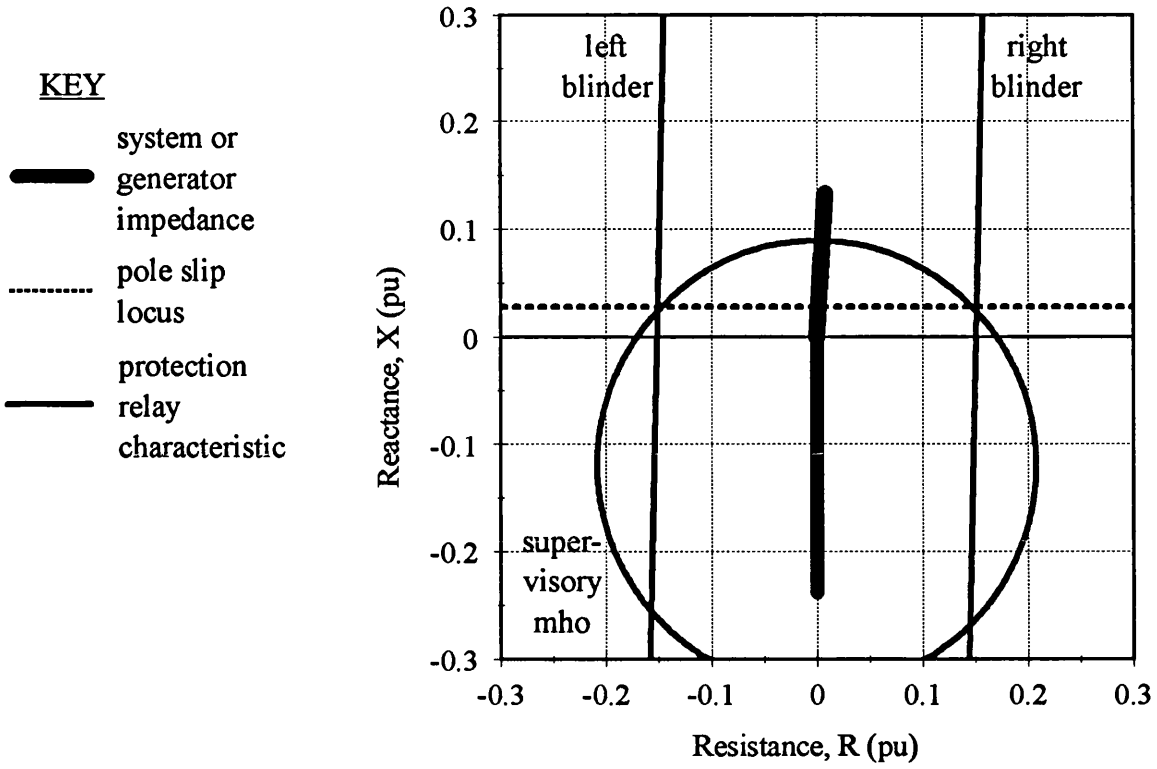

Figure B3
Single Blinder Pole Slipping Protection Scheme for 200 MVA PPSS Test System

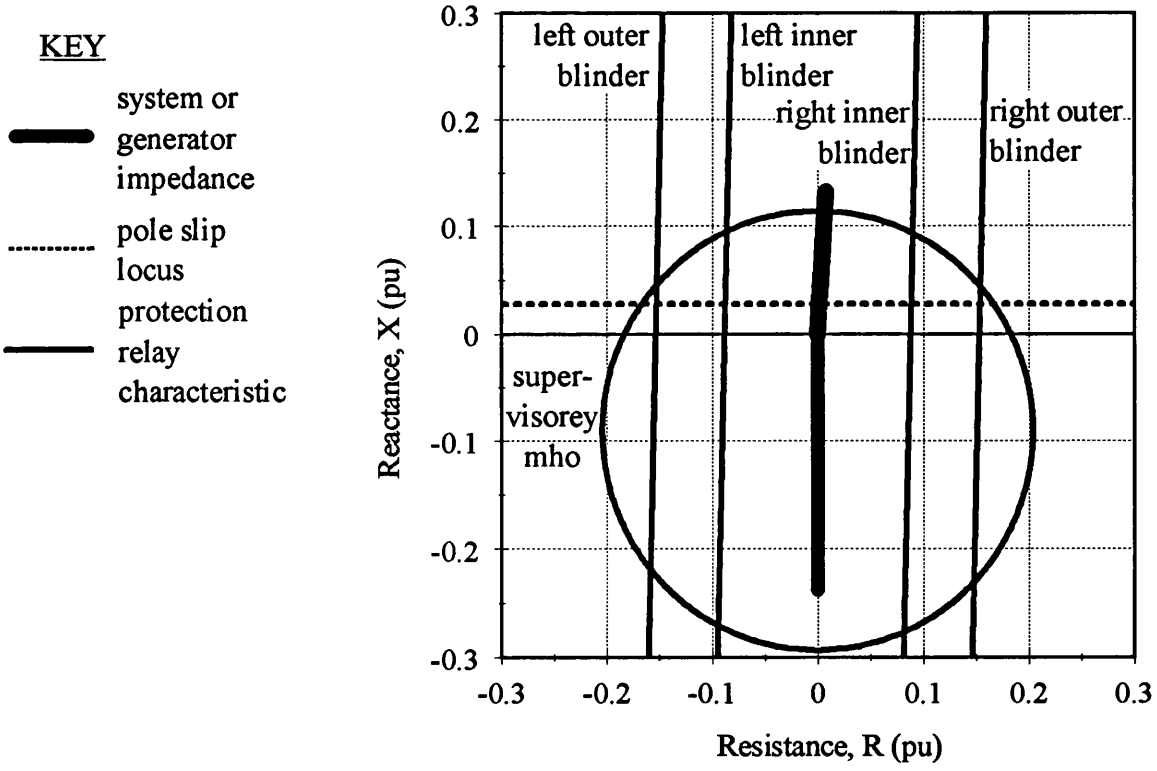

Figure B4
Double Blinder Pole Slipping Protection Scheme for 200 MVA PPSS Test System

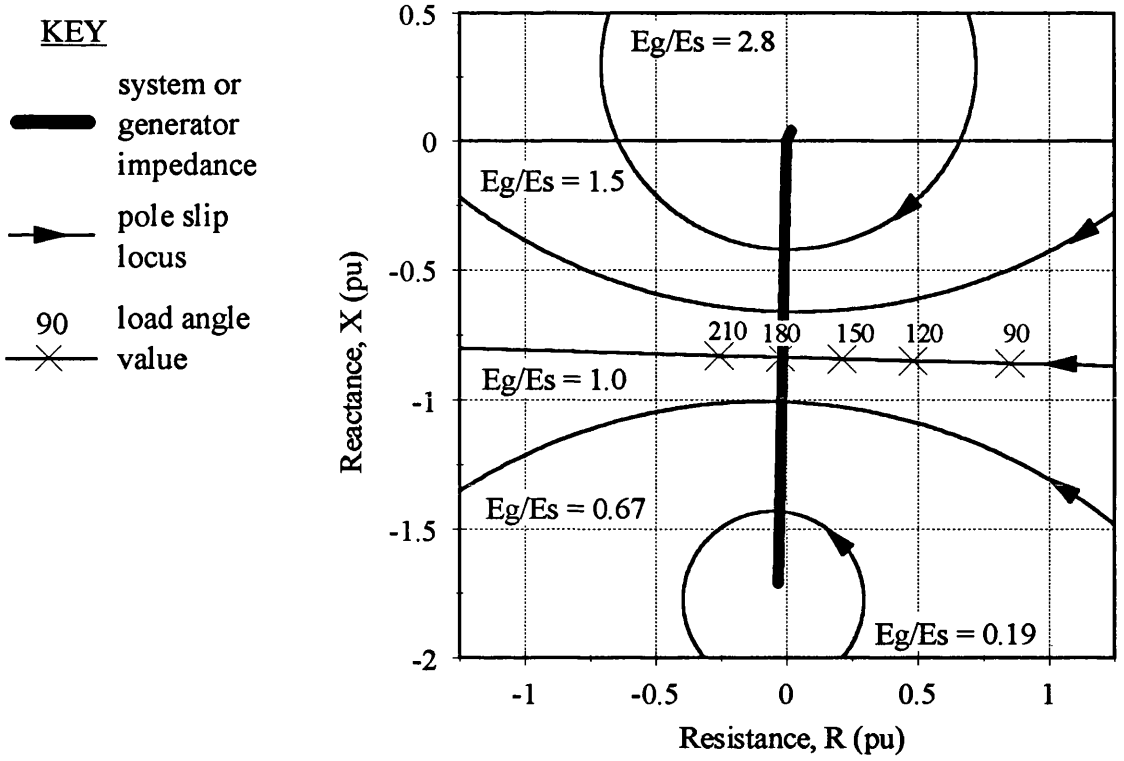

Figure B5
Pole Slipping Loci for the Laboratory 5 kVA Generator.

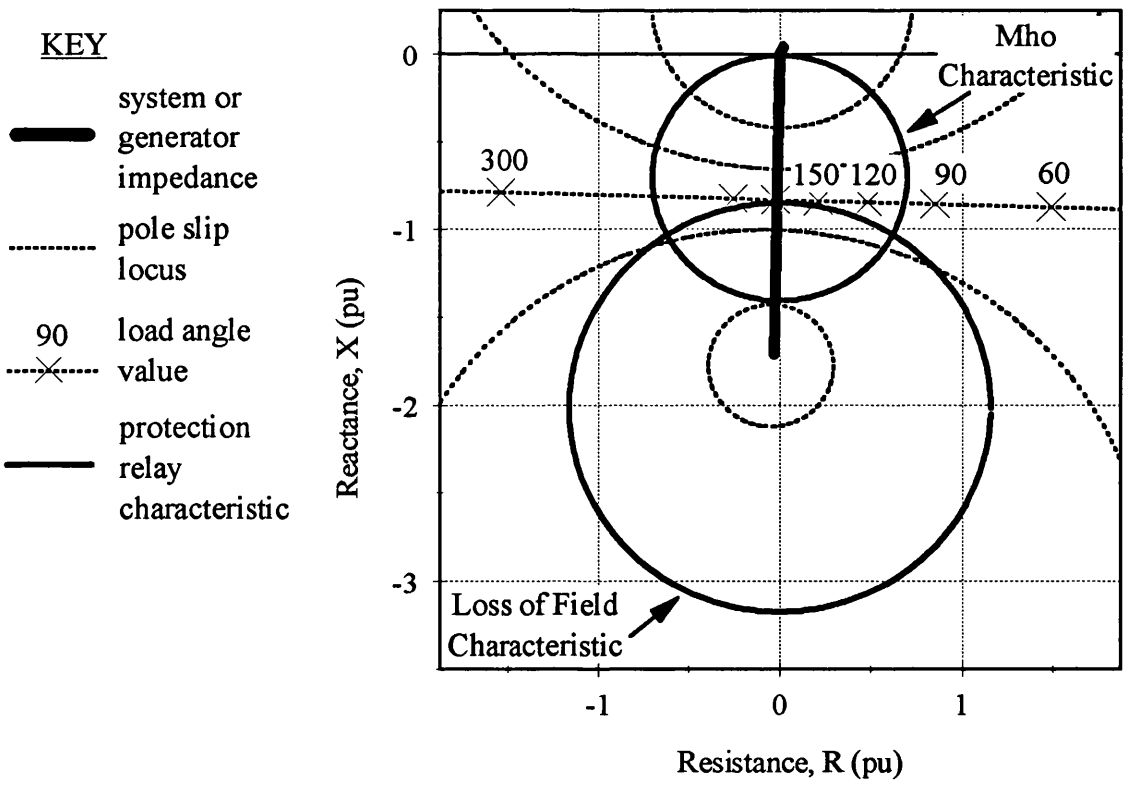

Figure B6
Single Mho Pole Slipping Protection Scheme &
Loss of Field Scheme for the Laboratory 5 kVA Generator.

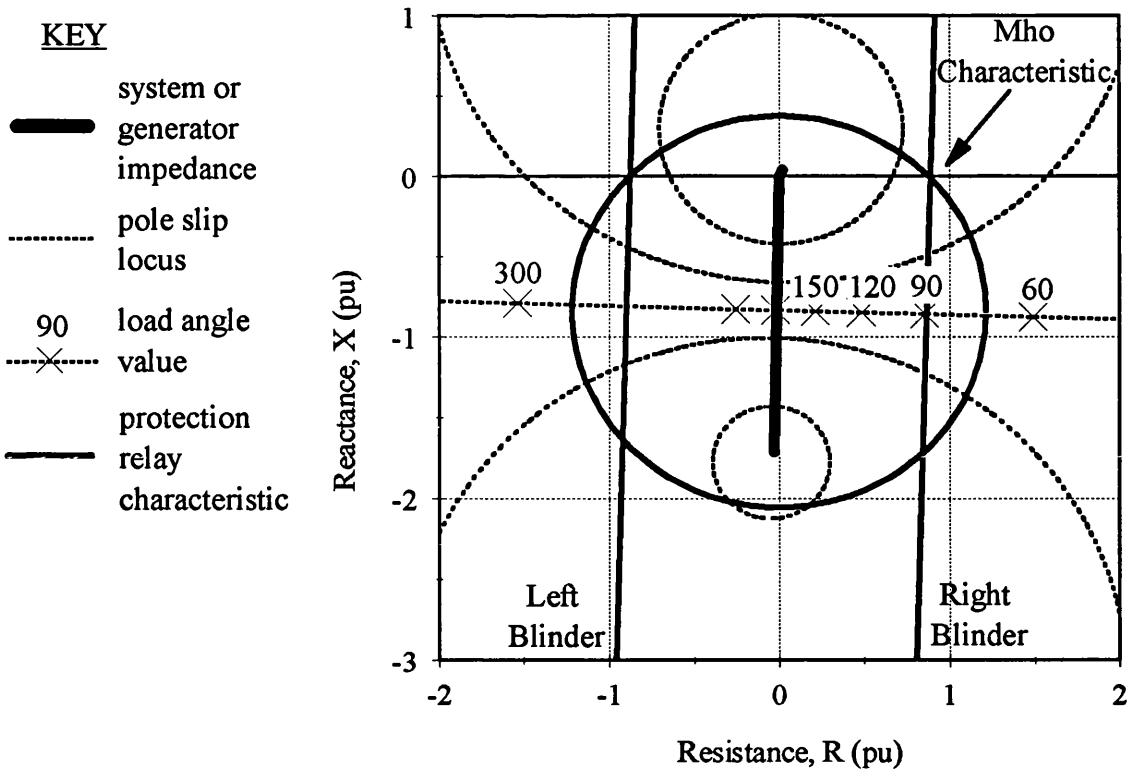

Figure B7
Single Blinder Pole Slipping Protection Scheme for the Laboratory 5 kVA Generator.

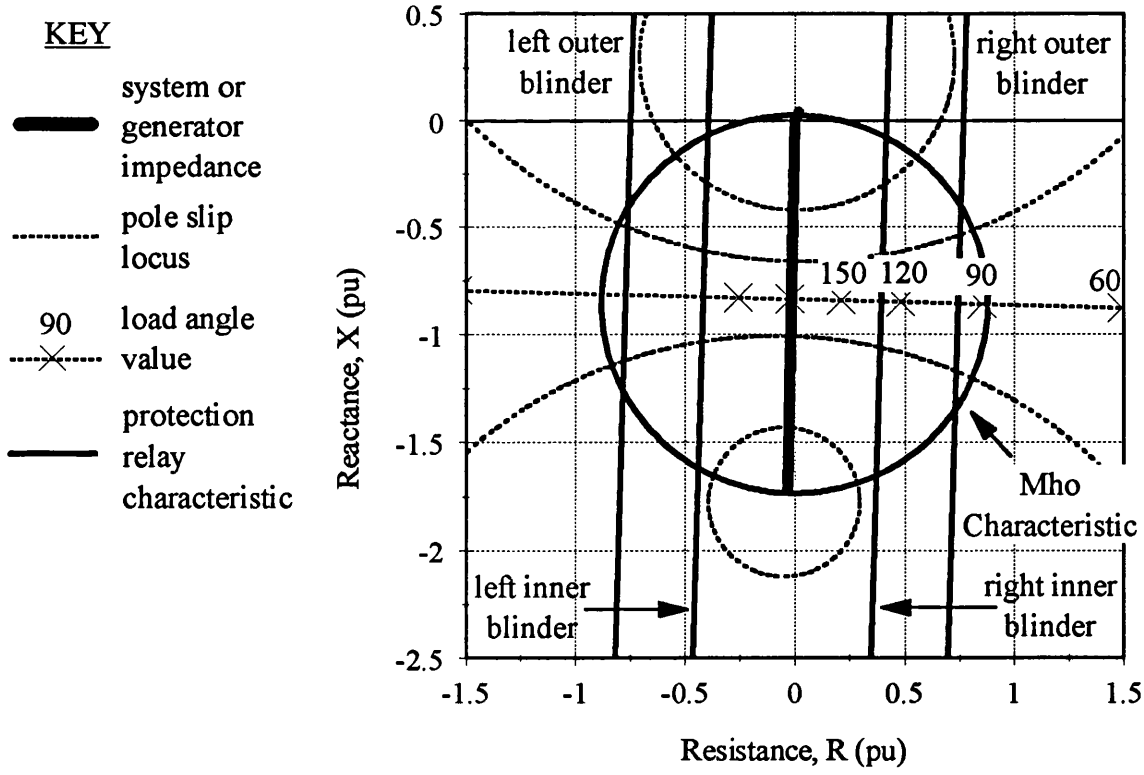

Figure B8
Double Blinder Pole Slipping Protection Scheme for the Laboratory 5 kVA Generator.

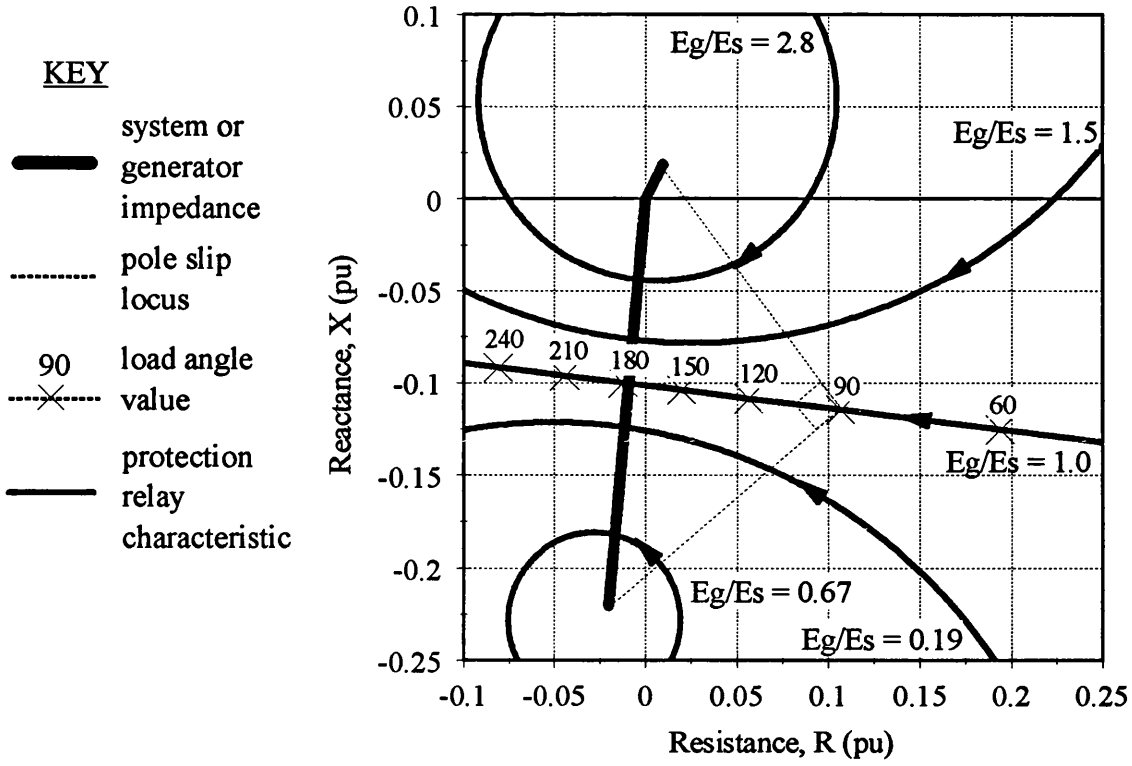

Figure B9
Pole Slipping Loci for the Industrial 625 kVA Diesel Generator.

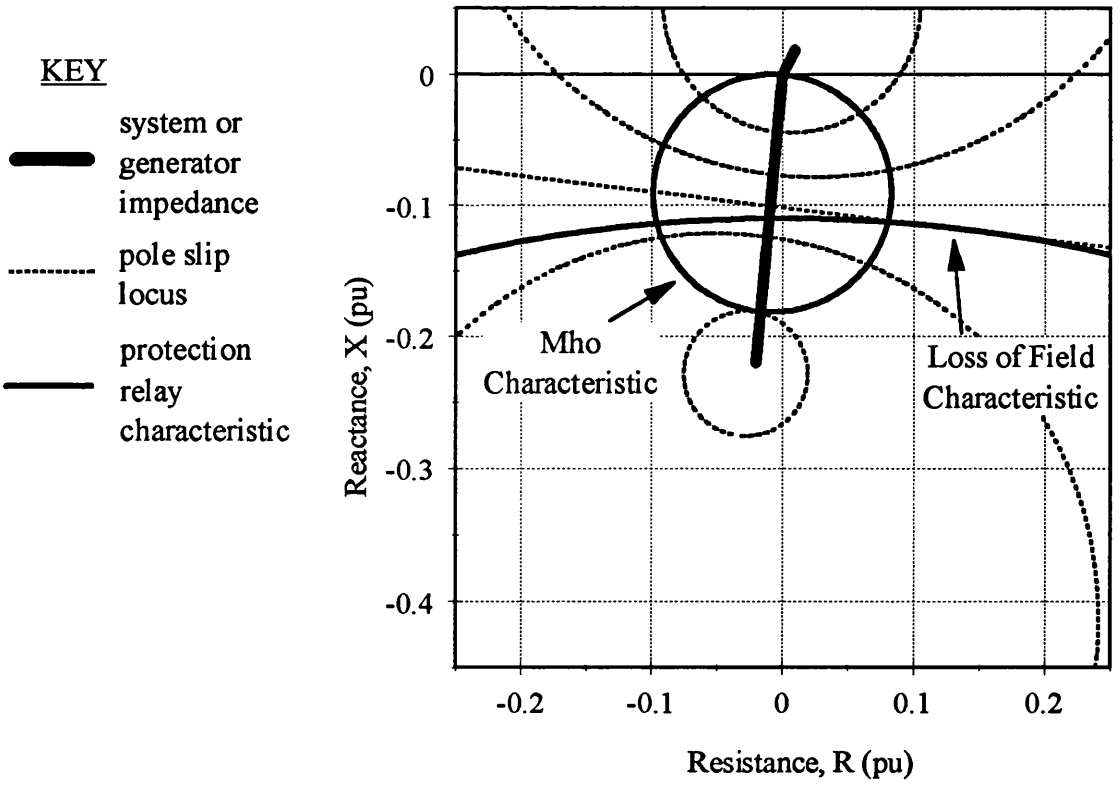

Figure B10
Single Mho Pole Slipping Protection Scheme & Loss of Field Scheme
for the Industrial 625 kVA Diesel Generator.

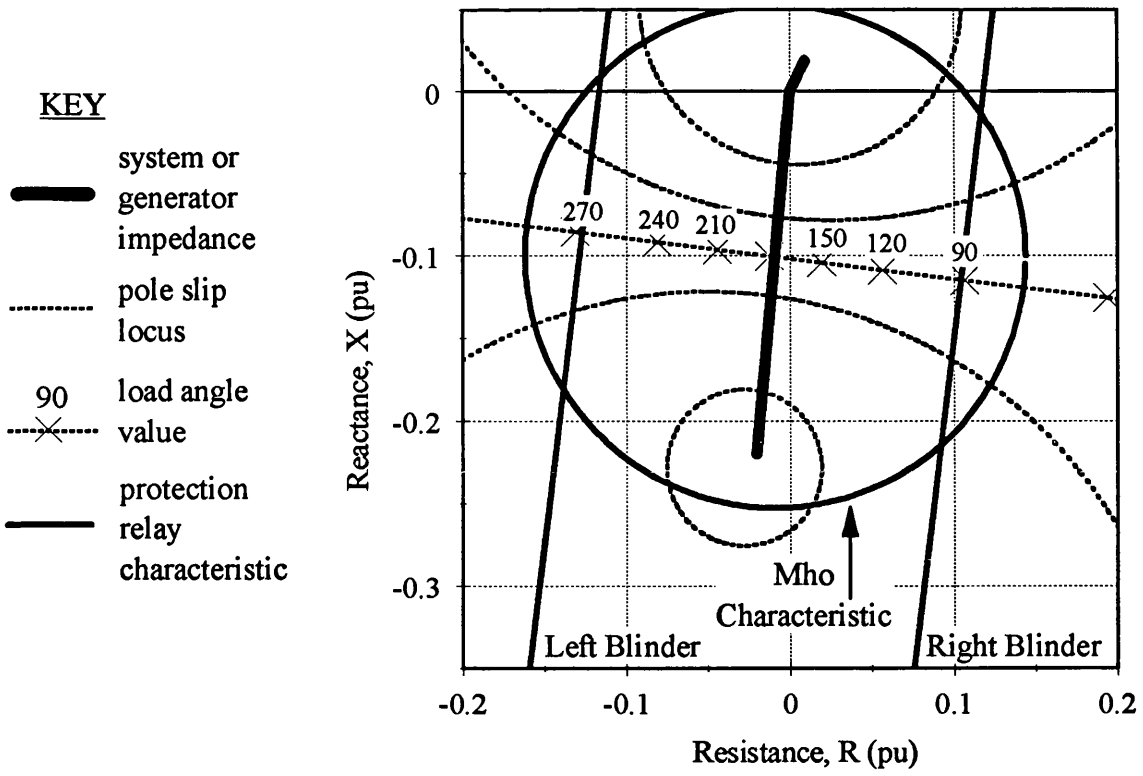

Figure B11
Single Blinder Pole Slipping Protection Scheme for the Industrial 625 kVA Diesel Generator.

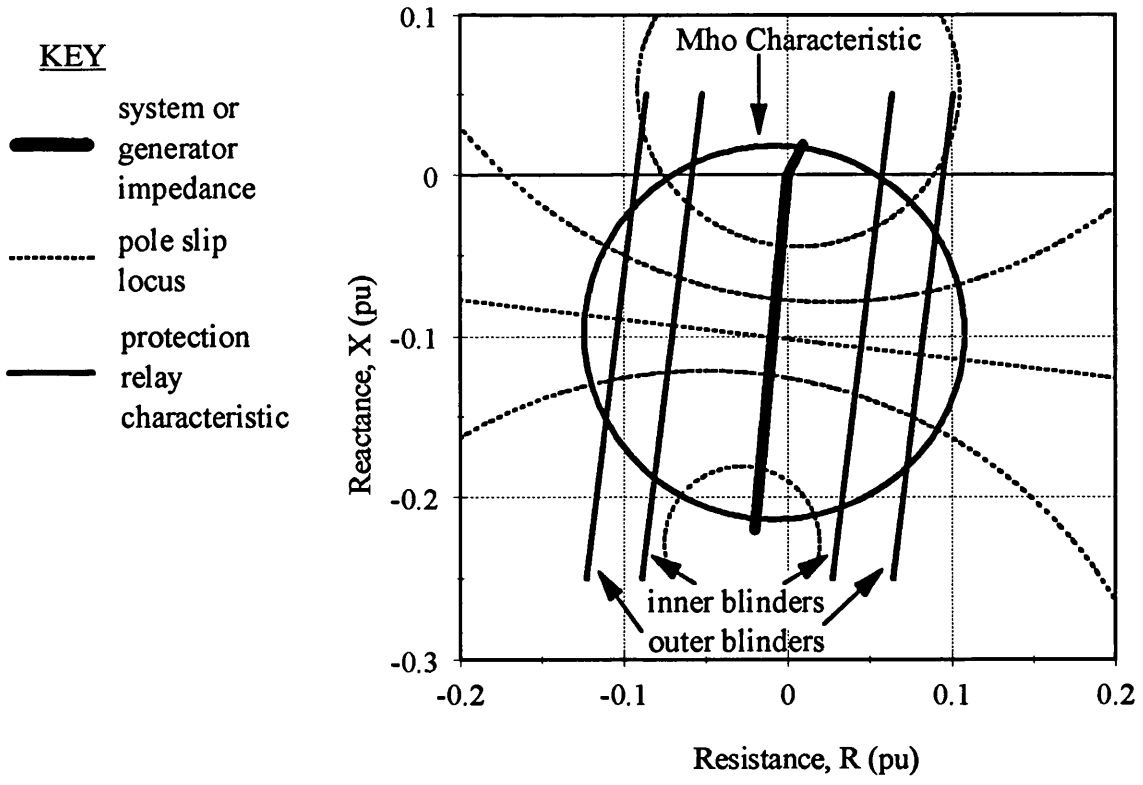

Figure B12
Double Blinder Pole Slipping Protection Scheme for the Industrial 625 kVA Diesel Generator.

Appendix C
DATA FOR GENERATORS AND SYSTEMS USED FOR ALGORITHM TESTS

This appendix contains data on the PPSS test system, the 5 kVA generator laboratory power system model, the diesel generator field test system, and typical embedded generator data.

C1.1 PPSS TEST SYSTEM

Figure C1 shows the power system model used for testing the power based pole slipping algorithm which had been installed in a commercially available generator protection relay[74]. The model was simulated using the ATP[166], and was based on a system used in an EPRI stability evaluation example[163]. Several modifications were made to this system so that all of the simulations required could be performed. The equivalent source impedance and interconnection impedances were reduced so the generator could operate at load angles in excess of 90 degrees[50]. The generator AVR was also adjusted for some of the tests. Chapter 5 contains details on the changes made to the AVR.

C1.1.1 Governor Model

The governor model was also changed from the original hydro governor unit to a tandem-compound single reheat model[164,188]. This model was faster than the original hydro unit, but does not constitute a 'fast' governor, such as the type found in a system with fast valving. The governor model was modified so that it would work for a 2 pole machine rather than a 4 pole, this involved changing the first multiplier unit which converts the velocity into per unit values. The block diagram for the governor is shown in Figure C2.

C1.1.2 AVR Model

The AVR model is shown in Figure C3. This is an IEEE type 1 model with no saturation. The limiter originally had infinite limits, these limits were changed to +/- 2 so that the maximum field voltage that the AVR could produce was equal to three times the full load value[109]. The AVR parameters had to be changed for the simulations where the generator was operated at machine angles of greater than 90 degrees. This was necessary because the generator damping was too low for the generator to remain operating in a stable

manner.

C1.1.3 Generator Model

The generator used in the simulation had the following parameters.

Rating	=	200 MVA
line to line terminal volts (rms)	=	13.8 kV
Frequency	=	50 Hz (3000 rpm, 2 pole)
Field current for rated volts on air gap line	=	935.016 Amps
Field current for rated volts on no load curve	=	1000 Amps
Field current for 1.2 pu volts on no load curve	=	1440 Amps
R - armature resistance	=	0.001096 pu
Xl - Leakage reactance	=	0.15 pu
Xd - direct axis synchronous reactance	=	1.70 pu
Xq - quadrature axis synchronous reactance	=	1.64 pu
Xd' - direct axis transient reactance	=	0.238324 pu
Xq' - quadrature axis transient reactance	=	1.64 pu (Xq)
Xd" - direct axis sub transient reactance	=	0.18469 pu
Xq" - quadrature axis sub transient reactance	=	0.185151 pu
Tdo' - o/c d-axis transient time constant	=	6.194876 s
Tqo' - o/c q-axis transient time constant	=	0. (No Q axis field winding)
Tdo" - o/c d-axis sub transient time constant	=	0.028716 s
Tqo" - o/c q-axis sub transient time constant	=	0.074960 s
Xo - zero sequence reactance	=	1.50 pu
HICO - inertia constant	=	.181128 million pound-feet^2

The inertia constant expressed in terms of H is given by[166];

$$WR^2\ (million\ lbf^2) = \frac{2 * H\ (s) * Sbase(MVA) * 23.7304}{Wbase^2\ (rads/s)} \qquad C(1)$$

The value of H for the generator is therefore;

$$H = 0.181128 * (100\ \pi)^2 / 2 * 200 * 23.7304 = 1.88 \text{ seconds.}$$

Some other useful formulae for converting between different units of inertia are given below[183];

$$H = \frac{J\ [\pi\ n]^2}{1800G} \qquad C(2)$$

Where J is the moment of Inertia in Kgm^2 and n is the shaft speed in rpm, G is the generator rating in VA.

$$J\ (units\ of\ Kgm^2) = \frac{WR^2}{23.74}\ \ (units\ of\ lbmft^2) \qquad C(3)$$

Another relationship between H and J is;

$$H = \frac{19.74\ J\ (\frac{freq}{N})^2}{G} \qquad C(4)$$

Where freq is the system frequency in Hz, N is the number of pole pairs. 'J' is sometimes referred to as GD^2. Generally J is specified in metric units and GD^2 in imperial, though physically they are a measure of the same quantity.

C1.1.4 Generator Infinite Bus Details

The generator was connected to an infinite bus via a 90 mile distributed parameter transmission line and a thevenin impedance. The thevenin impedance was modelled as a mutually coupled RL type (ATP type 51,52,53), this provides positive and zero phase sequence modelling so that unbalanced faults can be modelled correctly. The distributed parameter transmission line (ATP type -1,-2,-3) provides accurate simulation at frequencies other than the fundamental power system frequency. The generator transformer was modelled as a lossless transformer with no magnetising impedance, the leakage reactance values used were based on an assumed 3 % reactance divided between the windings. The impedance between the 'type 14' ideal voltage source and the generator is comprised of the following;

Thevenin impedance :	0.0075 Ω, 5 mH (= j 2*π *50 * 5 * 10^{-3} Ω)
	i.e 0.0075 + j1.57 Ω
Transmission Line :	0.0243 Ω/mile * 90 miles = 2.187 Ω
	0.92238 mH/mile * 90 miles = 83.142 mH
	i.e 2.187 + j26.12 Ω
Transformer :	11.69mH * 2 = 23.38 mH
	i.e j7.35
TOTAL:	2.195 + j35.04 Ω = 35.11 ∠86.4° Ω

The bus rating at the terminals of the generator is therefore;

$$(230 * 10^3)^2 / 35.11 = 1506.7\ MVA,$$

which in terms of multiples of the generator rating is 7.5. These values can be converted

into per unit values on the generator base using;

$$Z\ (pu) \quad = \quad \frac{Z(\Omega) * base\ VA}{base\ line\ voltage^{\ 2}} \qquad C(5)$$

The generator base impedance is given by its rating, 200 MVA. The base line voltage used for the above impedances is 230 kV. The per unit impedance is therefore;

$Z\ (pu) \quad = \quad 35.11 * 200 * 10^6 / (230 * 10^3)^2 \quad = \quad 0.13274\ pu$

Some pole slipping schemes require the zone of protection to cover the generator and its transformer. The per unit impedance of the transformer is therefore required, this is given by;

$X\ (pu) = 7.35 * 200 * 10^6 / (230 * 10^3)^2 \quad = \quad j\ 0.02779\ pu$

Referring to Figure A1, the parameters for the PPSS test system are;

$Ztot = 0.00833 + j\ 0.134278 \quad + \quad 0.001096\ pu + j\ 0.238324\ pu$

$Ztot = 0.009426 + j0.372602 = 0.37272\angle 88.6\ pu$

$m = 0.238324 / 0.37272 = 0.63941.$

C1.1.5 Load & Fault Information

The load located at bus 13 on Figure C1 is approximately 235.4 MW, 12.75 MVAr, when a voltage of 132 kV exists across it. The short circuit faults described for the PPSS test system were placed at BUS 12 of Figure C1. The generator therefore supplied the fault through its step up transformer, and 3.75 miles of mutually coupled line (ATP type 1,2,3). The short circuit faults were achieved by connecting the relevant phases to ground, they were cleared by disconnecting the load and the 3.75 mile line.

C1.2 LABORATORY POWER SYSTEM MODEL

Figure C4 shows a schematic diagram of the laboratory power system model. More information on this test system can be found in references [66,67,104]. The laboratory power system model has some inaccuracies. One inaccuracy is that the compound wound DC machine used as the generator prime mover does not behave like a regulated turbine. A regulated turbine will have a droop characteristic so that the turbine output will fall from full load to no load if the speed rises 4 % above synchronous speed[109]. This will typically occur with a time constant of 1 second. Below this 1 second region, the turbines torque will drop with an increase in speed, the turbine torque coefficient is approximately

equal to the loading of the machine in pu[109]. A compound DC machine on the other hand, will have a reasonably flat torque speed characteristic around synchronous speed[189]. It will therefore draw more power from its supply if there is an increase in speed, unlike a turbine.

The data available for the 5 kVA laboratory generator[67] is as follows;

Rating	=	5 kVA
line to line terminal volts (rms)	=	200 V
Frequency	=	50 Hz (3000 rpm, 2 pole)
Field current for rated volts on air gap line	=	3.75 Amps
Field current for rated volts on no load curve	=	4 Amps
Field current for 1.2 pu volts on no load curve	=	6.35 Amps
R - armature resistance	=	0.03 pu
Xl - Leakage reactance	=	≈ 0.24 pu *
Xd - direct axis synchronous reactance	=	2.32 pu
Xq - quadrature axis synchronous reactance	=	2.23 pu
Xd' - direct axis transient reactance	=	1.71 pu
Xq' - quadrature axis transient reactance	=	1.71 pu (Xq)
L_D- direct axis damper inductance	=	0 pu
L_Q - quadrature axis damper inductance	=	0 pu
L_F - field winding inductance	=	7.72 pu
Tdo' - o/c d-axis transient time constant = Lf/Rf	=	0.808 s
Tqo' - o/c q-axis transient time constant	=	0. (No Q axis field winding)
Tdo" - o/c d-axis sub transient time constant	=	0 s (no damper)
Tqo" - o/c q-axis sub transient time constant	=	0 s (no damper)
Xo - zero sequence reactance	=	0.24 pu
HICO - inertia constant, H	=	0.35 s

From the tests conducted, it was apparent that the machine had no damper windings. The inductance base for the machine is 0.025 H, the resistance base is 7.96 ohms.

* Leakage Reactance - This parameter can not be measured[110], it is the reactance resulting from the difference between the total flux produced by stator current acting alone, and the space fundamental of the flux in the air gap. It forms part of Xd and Xq, in addition to all other positive and negative sequence reactances. The value for Xl is typically between

5 and 10 % of Xd for generators with good coupling between stator and field. Generators with good coupling will have a large difference between Xd and Xd', this is typically an order of magnitude.

Other Laboratory Power System Model Data

Prime Mover → 8 Horse Power Compound DC motor (6 kW)

Bus Details → The laboratory is supplied by 0.5 km of cable from a 250 kVA source, i.e source impedance approximately equals j0.16 at 200 V, the approximate cable impedance is equal to $0.15 + j0.15\Omega$

Total source impedance → $0.15 + j0.31\ \Omega$

Converting into PU on generator base = $((0.15+j0.31\ \Omega)^* 5\ kVA)/200^2$

= $0.0188 + j0.0388$ pu

Referring to Figure A1, the parameters for the laboratory 5 kVA generator are;

Ztot = $0.0188 + j\ 0.0388$ + 0.03 pu + j 1.71 pu

Ztot = $0.0488 + j1.7488 = 1.7495\angle 88.40$ pu

m = 1.710 / 1.7495 = 0.9774.

C1.3 625 KVA INDUSTRIAL DIESEL GENERATOR

Data for the basic parameters of the generator was obtained from the manufacturer. The generator was manufactured over 40 years ago, the manufacturers therefore do not hold much of the data required for a full accurate simulation. The missing data has been estimated from inspection of the generator, or typical values have been used

Rating	=	625 kVA
Line to line terminal volts (rms)	=	415 V
Frequency	=	50 Hz (1500 rpm, 4 pole)
R - armature resistance	=	0.02 pu (estimated)
exciter current for rated volts on no load	=	0.625 Amps (13.5 Volts)
exciter current for rated volts at full load	=	1.75 Amps (48.0 Volts)
Xl - Leakage reactance	=	0.11 pu (estimated 5 % of Xd)
Xd - direct axis synchronous reactance	=	2.25 pu
Xq - quadrature axis synchronous reactance	=	1.1 pu (estimated)

Xd' - direct axis transient reactance	=	0.22 pu
Xq' - quadrature axis transient reactance	=	1.1 pu (no Q axis damper)
Xd" - direct axis sub transient reactance	=	0.15 pu
Xq" - quadrature axis sub transient reactance	=	0.20 pu (estimated)
Tdo' - o/c d-axis transient time constant	=	3.0 s (estimated)
Tqo' - o/c q-axis transient time constant	=	0. (No Q axis field winding)
Tdo" - o/c d-axis sub transient time constant	=	0.024 s (estimated)
Tqo" - o/c q-axis sub transient time constant	=	0.016 s (estimated)
Xo - zero sequence reactance	=	0.05 pu (estimated)
Inertia, WR^2 of generator rotor (not diesel engine)	=	853.43 pound-feet^2

Using equation C1, this value of WR^2 is equivalent to a value of H of 0.7 kWs/kVA.

Prime Mover → Dorman Diesel Engine.

Generator Bus Details → ratio of bus rating to generator rating = 48:1 i.e 30 MVA

BSP bus details 150 MVA i.e source impedance = $(11\ kV)^2/150\ MVA = j0.8067\ \Omega$

Interconnection impedance ≈ $1.8 + j1.8\ \Omega$

Total source impedance = 1.8 + j3.607

Converting into PU on generator base = $((1.8 + j3.607\ \Omega)*625\ kVA)/11\ kV^2$

= 0.0093 + j 0.0186 pu

Referring to Figure A1, the parameters for the 625 kVA generator are;

Ztot = 0.0093 + j 0.0186 + 0.02 pu + j 0.22 pu

Ztot = 0.0293 + j0.2386 = $0.240\angle 83.00$ pu

m = 0.2209 / 0.240 = 0.9204.

C1.4 DATA FOR DIFFERENT SIZED SYNCHRONOUS MACHINES

Tables C1 and C2 below contain parameters for a range of synchronous machine sizes. The tables provide information which can be used to compare small and large generators, whilst also providing information which can be used when simulating embedded generators.

Table C1 - Generator Data for Different Sized Synchronous Machines.

rating (kVA)	5 [67]	65 [173]	69 [87]	156 [87]	200 [175]	300 [175]	781 [87]	750
Xd (pu)	2.32	1.52	2.02	6.16	3.45	2.6	2.43	2.63
Xd' (pu)	1.71	0.289	0.171	0.347	0.24	0.22	0.254	0.21
Xd" (pu)	1.71	0.230	0.087	0.291	0.165	0.15	0.207	0.15
Xq (pu)	2.23	1.52	1.06	2.49	2.07	1.56	1.12	1.57
Xq" (pu)	2.23	0.230	0.163	0.503	0.248	0.225	0.351	0.18
Xl (pu)	0.12	0.15	-	-	-	-	-	-
Tdo' (sec)	0.808	3.36	0.950	1.87	1.725	1.182	1.9	2.35
Tdo" (sec)	0	0.06	0.078	0.013	0.015	0.015	0.024	0.025
Td' (sec)	0.596	0.639	0.08	0.105	0.12	0.10	0.199	0.188
Tqo" (sec)	0	0.06	0.045	0.020	-	-	0.016	-
R (pu)	0.03	0.008	0.011	0.034	0.095	0.067	0.017	0.032
H (sec)	0.35	0.82	0.329	0.205	1.5	1.8	0.5	0.22*
p.f.	0.85	0.8	0.8	0.8	0.8	0.8		0.8

* The inertia constant, H is for the generator only, it does not include the inertia of the prime mover system.

Table C2 - Generator Data for Different Sized Synchronous Machines.

rating (MVA)	1.044 [87]	4.51	9 [109]	17.5 [109]	25 [109]	35 [109]	75 [109]	384 [109]
Xd (pu)	2.38	2.95	0.911	1.07	1.25	1.0	1.05	1.798
Xd' (pu)	0.264	0.25	0.408	0.66	0.232	0.260	0.185	0.324
Xd" (pu)	0.201	0.17	0.329	0.330	0.120	0.235	0.130	0.260
Xq (pu)	1.1	1.35	0.580	0.66	1.220	0.620	0.980	1.778
Xq" (pu)	0.376	0.31	-	-	0.120	0.264	0.130	0.255
Xl (pu)	-	0.15	-	0.310	0.134	0.170	0.070	0.193
Tdo' (sec)	2.47	5.5	4.2	5.4	4.750	7.1	6.1	5.21
Tdo" (sec)	0.018	0.055	-	-	0.059	-	0.038	0.042
Td' (sec)	0.27	0.467	1.88	3.33	0.88	1.846	1.07	0.940
Tqo" (sec)	0.009	0.27	-	-	0.210	-	0.099	0.042
R (pu)	0.013	0.01	-	0.003	.0014	0.004	0.003	.0014
H (sec)	0.535	1.05	2.61	6.7	5.02	7.25	6.18	2.62
p.f.	0.8	-	0.9	0.8	0.8	0.9	0.8	0.85

* The inertia constant, H is for the generator only, it does not include the inertia of the prime mover system.

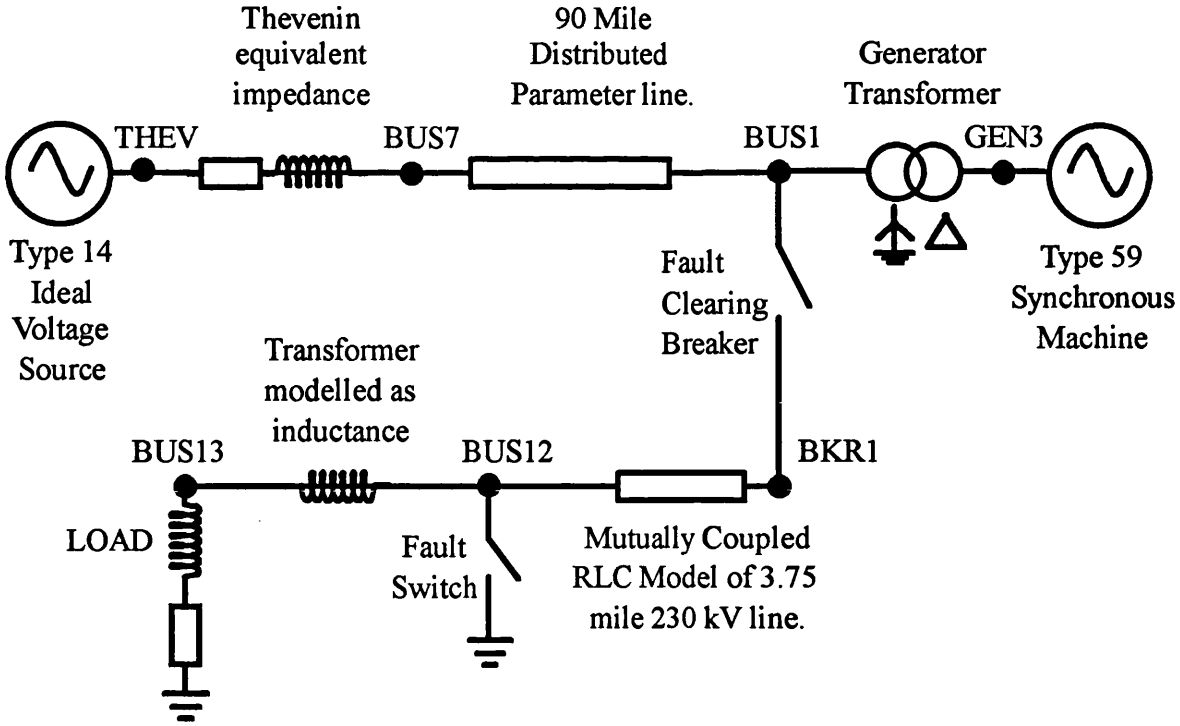

Figure C1
ATP Power System Model Used for Producing 200 MVA Generator PPSS Test Files.

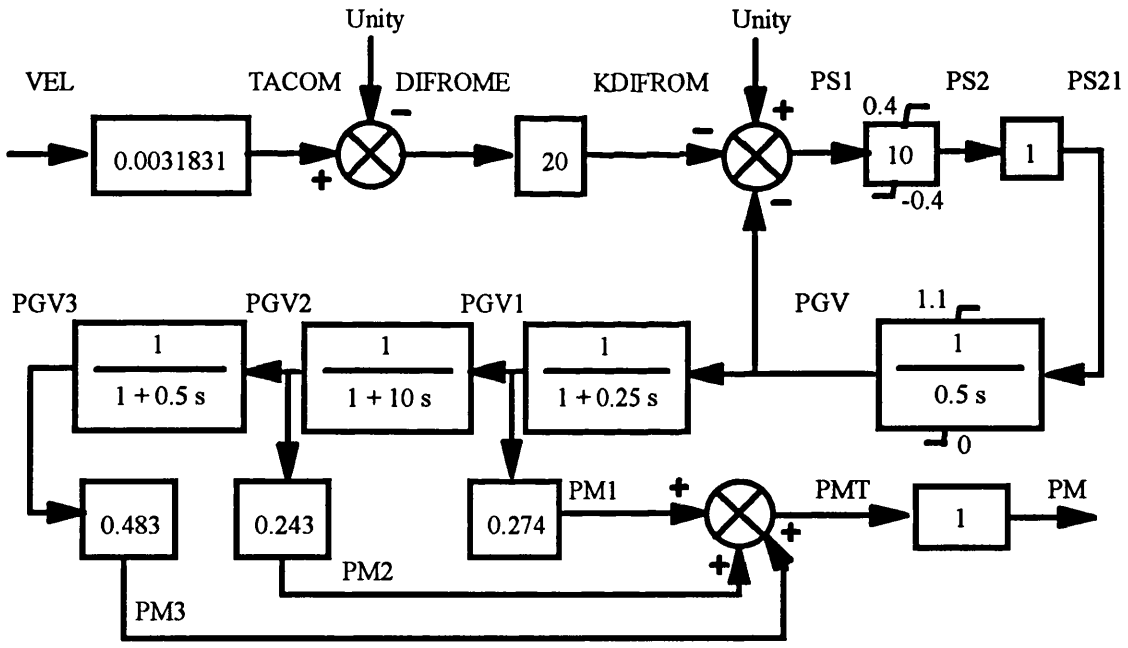

Figure C2
Steam Turbine Governor Model Used in
ATP Power System Simulations for 200 MVA Generator PPSS Test Files.

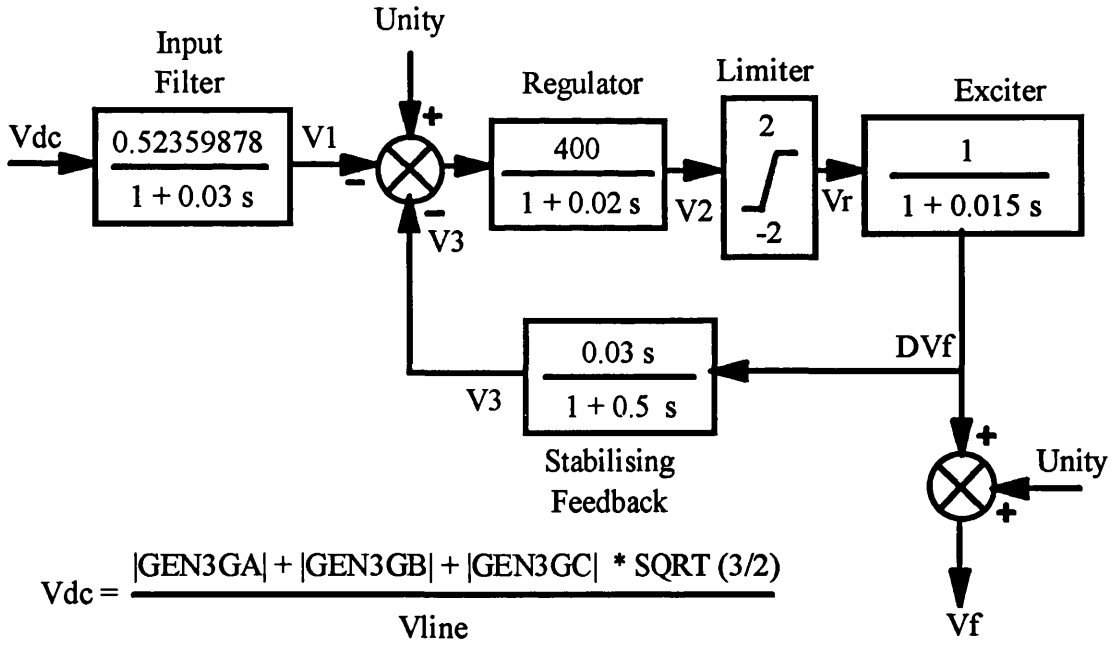

Figure C3
AVR Model Used in ATP Power System Simulations for 200 MVA Generator PPSS Test Files.

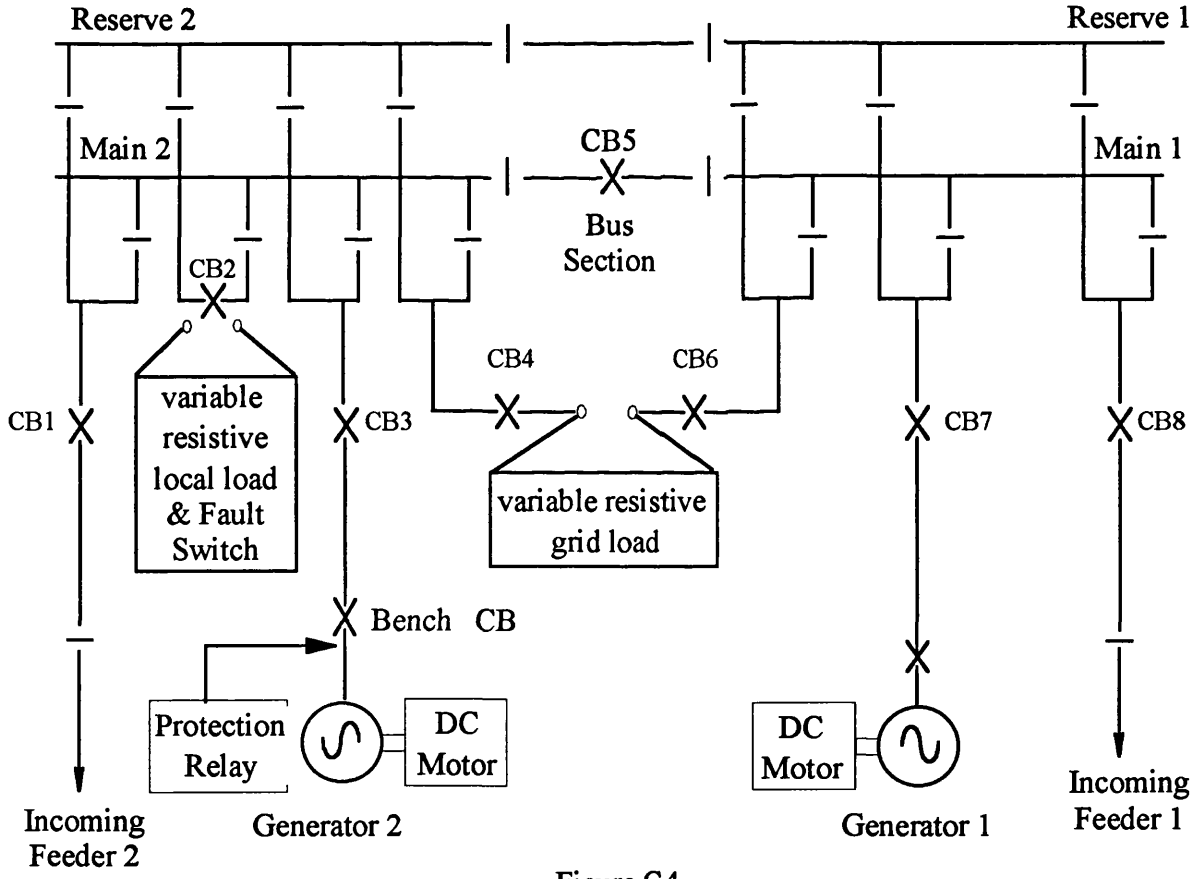

Figure C4
Schematic Diagram of Laboratory Model Power System
Used to Test Pole Slipping Algorithm in MPR.

Appendix D

PUBLISHED WORK

PAPER ONE

"AN INVESTIGATION INTO POLE SLIPPING PROTECTION FOR SMALL AND MEDIUM SIZED EMBEDDED GENERATION"

M J Checksfield and M A Redfern

Presented at :-
28th Universities Power Engineering Conference (UPEC),
September 1993, Stafford, UK, pp 957 - 960.

AN INVESTIGATION INTO POLE SLIPPING PROTECTION FOR SMALL AND MEDIUM SIZED EMBEDDED GENERATION.

M.J.Checksfield and M A Redfern

University of Bath, UK.

The probability of pole slipping of small and medium sized embedded generation is being viewed with concern. Research has therefore been directed at investigating new techniques for detecting pole slipping and the formulation of protection algorithms which can be included into an integrated protection scheme for these generators. This paper describes a method for detecting pole slipping using power measurements taken at the generator's terminals. This is shown to correctly detect pole slipping using both computer simulation and a laboratory model power system while remaining stable for excessive swing conditions and during power system faults.

1.1. INTRODUCTION.

Small and medium sized embedded generation sets are increasingly being connected to the utility power supply system. Transient stability problems, including those resulting from pole slipping, are being recognized as a cause for concern. The high clearance times associated with IDMT relays used to protect the system and the generator against short circuit faults together with the generator's low inertia and high resistance accentuate the probability of pole slipping.

Pole slipping is the process by which an imbalance between the mechanical input power and the electrical output power of a synchronous machine causes it to slip with respect to its primary magnetic flux which is synchronised to the electrical power system. The forces this produces within the machine can damage it in several ways. The high currents experienced can loosen stator windings, since these are generally only braced for three phase fault levels. If prolonged pole slipping is permitted, injurious heating of the stator and rotor will result. The high shaft stresses experienced can also endanger the shaft, if it does not have a sufficiently high safety margin to withstand the overload[1] and pulsating torques. From the power system viewpoint, if the generator is connected to a low capacity utility infeed, the resultant voltage fluctuations produced can cause considerable trouble to other consumers, and introduce risks of protection mal-operation. For these reasons it is therefore recommended that for a pole slipping condition, the generator is disconnected from the utility with no intentional delay and at least within the first slip cycle[2].

Investigations have therefore been undertaken into a new pole slipping protection algorithm which is suitable for a small or medium sized synchronous embedded generator and which can be included in an integrated protection scheme for these units. This project is an extension of other work into aspects of this protection package[3,4].

2.1. POLE SLIPPING.

Pole slipping of a synchronous machine occurs when there is insufficient electromagnetic torque to hold the rotor in synchronism with the stator magnetic flux compared to the mechanical input torque. This can arise due to an external disturbance on the system, a faulty excitation system, or an excess of prime mover input power.

The Equal Area Criterion is often used for stability assessment, and demonstrates the conditions where synchronism is lost and pole slipping occurs. Figure 1 shows the power/load angle relationship and the rate of change of load angle (slip, s) for a generator losing synchronism following an autoreclosure on a double circuit line[5]. The smaller of the power/load angle curves (points 0 to 3) represents the machine output when only one of the two feeder circuits is in operation. For synchronism to be lost, the acceleration energy resulting from a disturbance, represented by the area 1-2-3-3', must be larger than the retardation energy, represented by the area 3'-4-5, and hence there is a net acceleration of the rotor. If the rotor is still advancing when the load angle reaches point 5, then synchronism will be lost, and the rotor will continue to accelerate until one pair of poles has slipped and the generator has travelled through the motoring region back into a generating condition. If the accelerating forces are not absorbed, a further slip may occur. Figure 1 shows the slip increasing as synchronism is lost, as well as the asynchronous power output of the machine increasing due to induction generator action. If the governor reduces the input power to the generator, Pm, it is possible for stable asynchronous operation to occur or even synchronous operation to be restored.

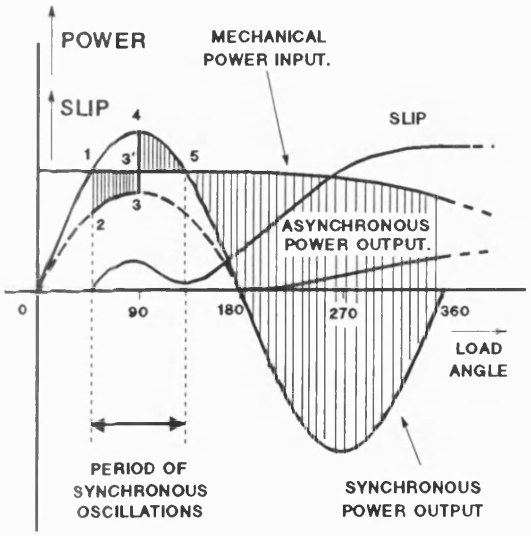

FIGURE 1. Equal Area Diagram for Generator Loss of Synchronism.

The above scenario illustrates that if a generator has sufficient load removed for a significant period of time, then pole slipping will occur, since the excess input power from the prime mover accelerates the rotor. The most severe disturbance for a generator is the close-up three phase fault, for which all of the generator's load is lost and therefore all of the prime mover power is used to accelerate the rotor. For less severe short circuit faults, a greater fault duration is required to incur pole slipping.

Pole slipping can also occur if the generator is under excited, since this reduces the maximum possible synchronous electrical power which can be taken out of the generator. If this maximum is less than

the prime mover input power, synchronism will not be maintained.

If excitation is lost completely then the machine runs asynchronously rather than pole slipping[6]. In this condition the output power pulsations will be significantly reduced to the amplitudes dictated by the machine's electric and magnetic characteristics.

3.1. CONVENTIONAL METHODS FOR DETECTING POLE SLIPPING.

The most widely used technique for detecting pole slipping is to monitor the path of the apparent impedance of the machine and its rate of change with distance type relays. As a generator falls out of step with the power system, the impedance falls to a minimum and then increases as the generator completes one slip cycle.

The basic scheme[2] uses two load blinder characteristics set either side of and parallel to the system impedance. When pole slipping occurs, the apparent impedance travels across the impedance plane, (R+jX), and a trip condition exists if the impedance crosses the two load blinder units in succession. If just one load blinder unit is tripped, as occurs for an internal or a close-up external fault, no pole slipping trip will occur. Refinements of this scheme use a MHO characteristic to prevent mal-operation due to disturbances else where or lenticular characteristics in place of the load blinders.

More sophisticated schemes[7] have been developed to predict the probability of pole slipping and to provide inputs into the generator's and prime mover's control system.

4.1. THE NEW APPROACH TO POLE SLIPPING PROTECTION.

Pole slipping is a power based phenomena and hence algorithms have been examined which are based on the Equal Area Criterion. In the design of the protection algorithm, the relay should trip when it observes the conditions which will produce a pole slip or correspond to an actual pole slip, but remain stable during fault conditions and other system abnormalities. By being able to recognise the conditions were a pole slip is inevitable, the algorithm offers the prospect of tripping before the actual pole slip and hence disconnecting the machine from the system before it can be damaged.

The instantaneous values of real and reactive power[8] used for the trip criterion were calculated using;-

$$P = v_a * i_a + v_b * i_b + v_c * i_c$$

$$Q = \frac{1}{\sqrt{3}}(v_a*(i_c - i_b) + v_b*(i_a - i_c) + v_c*(i_b - i_a))$$

where v_a, i_a, v_b, i_b, v_c, and i_c represent the sampled values of the terminal voltage and current. The sign convention used defines that for an under-excited generator, the reactive power is negative.

The Equal Area diagram, figure 1, shows that for a stable swing, the load angle cannot exceed the critical swing point, shown as point 5. For the generator to recover from the disturbance, the rate of change of load angle (slip) and hence the rate of change of electrical power output, $(\Delta P/\Delta t)$, must be zero at point 5. For an unstable generator, the load angle will continue to advance after point 5, and therefore $(\Delta P/\Delta t)$ will be negative at point 5. The measurement of $(\Delta P/\Delta t)$ therefore provides the first criterion for the pole slipping protection. The critical swing point can be identified as the point at which the electric power output of the machine, P, is equal to the mechanical shaft input power, Pm.

It is possible however, for a negative value of $(\Delta P/\Delta t)$ to occur during a stable swing. This would be the condition when the load angle is swinging back from point 4 towards point 1 as shown in figure 1. To differentiate between negative values of $(\Delta P/\Delta t)$ at the two points, reactive power is used. The steady state reactive power/load angle relationship for a round rotor machine is given by;

$$Q = \frac{E*V}{X_d}(\cos\ \delta) - \frac{V^2}{X_d}$$

This shows that for load angles between 90° and 270°, the reactive power, Q, will always be less than the load angle independent term. This value, Q_{trip}, is used to identify the stable negative derivative terms from the unstable derivative terms. The above equation is altered when transient conditions are taken into account, however this effect gives no detrimental effect in terms of algorithm stability.

In practice, a margin for error is allowed for in the rate expression $(\Delta P/\Delta t)$. A minimum value $(\Delta P/\Delta t)_{min}$ is designated, based on a minimum value of slip and an assumed sinusoidal power/load angle relationship. It can be seen that once the power output is less than the input power, then for load angles greater than the peak of the power/load angle curve, the trip criteria are defined by;

$$P \le P_t$$

AND

$$Q \le Q_{trip}$$

AND

$$\left(\frac{\Delta P}{\Delta t}\right)_{max} \le \left(\frac{\Delta P}{\Delta t}\right) \le \left(\frac{\Delta P}{\Delta t}\right)_{min}$$

where the value P_t is given by the expected output of the generator.

Embedded generators are generally operated at or close to their full rated load since they are used primarily to provide base load or peak lopping. Adaptive relaying would have to be considered if the generator operates with a range of output levels.

Faults cause considerable technical difficulties since they cause dramatic changes in the relay measurands. These transitions produce negative values of $(\Delta P/\Delta t)$ which are a potential source of instability to the algorithm. Fortunately, the faults generally introduce sinusoidal terms of twice the power system frequency into the power measurements. Since pole slipping is a relatively slow process in comparison to faults, then an imposed minimum tripping time of one power system cycle will inhibit most fault tripping. In addition, the rapid transitions experienced with faults produce negative values of $(\Delta P/\Delta t)$ far in excess of that possible due to pole slipping. This provides an additional mechanism to inhibit tripping during power system faults, whenever $(\Delta P/\Delta t)$ is less than $(\Delta P/\Delta t)_{max}$.

The relaying measurands were filtered to remove excessive harmonics and unbalance. A half cycle moving average filter was

used for the real and reactive powers, followed by a full cycle moving average for the derived rate of change of power signal.

5.1. SIMULATION STUDIES.

The performance of the protection algorithm was demonstrated using a computer based simulator[9] and a laboratory power system model[3].

The computer simulator modelled the behaviour of the machines, control systems and transmission network of an interconnected power system. To investigate the performance of the pole slipping protection algorithms, a simplified system was modelled which consisted of a grid network represented by a generator of 58.8 GVA connected by two parallel transmission lines to the protected generator of 588 MVA with an associated generator transformer. This model was similar to the laboratory model, since the ratio of utility to machine ratings was 100:1, although ideally a much smaller generator should have been used.

Pole slipping was triggered by applying a 3 phase fault on the generator transformer busbar with a fault duration just greater than that which would produce the critical conditions for stability. This technique was also used to trigger a power swing but for this the fault duration was chosen to be just less than the critical clearance time required for pole slipping.

The laboratory model[3] embedded generation system consisted of two 5kVA generators connected to a double bus system, 'local' load and a 200V laboratory three-phase 'utility' supply. The 5kVA generators were two pole, round rotor machines, driven by dc motors.

Pole slipping of the laboratory machine was induced by two methods. First by increasing the power into the dc machine, thus applying excess input torque, and second by reducing the generator's excitation to a level insufficient to maintain synchronism. Ideally pole slipping should have been induced by a long duration fault, but due to laboratory supply limitations this could not be done. The algorithm's security against faults was tested by applying a variety of faults to the local load busbar.

6.1. TEST RESULTS.

The response to pole slipping on the computer simulation is shown in figure 2. This shows pole slipping produced by a fault whose duration was 1 mS greater than the critical fault clearing time. The AVR and governor were both set to manual for this test. The algorithm detected the pole slip condition at a load angle of 167°, i.e. just before the machine actually slipped. Although the actual tripping time can be seen, the speed of pole slipping is dependent upon the degree of unbalance and will inherently vary from case to case. Expressing the tripping time in terms of load angle provides a more suitable measure for comparison.

The simulated power swing which produced the largest possible stable swing of 152° is shown in figure 3. For the period from 0.32 to 0.92 seconds, the reactive power is greater than Q_{trip}, since the load angle is less than 90°. However, during this time the real power is greater than P_t, which inhibits tripping. This indicates that the rotor is still retarding and the generator could remain stable. For the period when both P and $(\Delta P/\Delta t)$ satisfy their trip criterion, Q is greater than Q_{trip} restraining operation.

The response to a pole slip of the laboratory model is shown in figure 4. This slip was invoked using excess input shaft torque. The plots show the real output power increasing and the reactive power decreasing as the rotor angle begins to advance. Note that the maximum output power occurs just after the reactive power has fallen below Q_{trip}, as expected. Transient machine theory predicts that the peak power output would be produced at a load angle just greater than 90°. Once past the maximum value, the real power falls rapidly as the now unstable machine rotor accelerates into pole slipping.

Three pole slip cycles are shown in the diagram, of which the second and third cycles have a considerable amount of distortion on them. This was caused by the measured currents exceeding the maximum permitted for the microcomputer system's input circuits and by non-linearities in the power system model. As with the computer simulation, the algorithm tripped just before the machine actually slipped and before the machine would be damaged. Similar results were obtained for the insufficient excitation pole slip.

Of all fault types investigated, two phase to earth and three phase to earth faults presented the greatest threat to algorithm security. For these faults, both of the fault blocking mechanisms, the one cycle minimum operating time and the maximum negative value of $(\Delta P/\Delta t)$ were employed. The maximum negative value of $(\Delta P/\Delta t)$, i.e. $(\Delta P/\Delta t)_{max}$, was calculated to be 75 kW/s for the 5 kVA machine.

The results for a two phase to earth fault are shown in figure 5. The dangerous condition arises following removal of the fault which occurred at about 1.0 second in the record. At this time, the derivative, $(\Delta P/\Delta t)$, was not negative for the one cycle required for tripping, and was also less than $(\Delta P/\Delta t)_{max}$ indicating a fault condition. Tripping was therefore blocked for this fault condition.

7.1. CONCLUSIONS.

With the growing number of small and medium sized embedded generators, pole slipping protection is becoming more important. Machine winding damage, system problems, and shaft failure can all result if adequate protection is not provided. A power based algorithm, suitable for inclusion into an integrated protection scheme has therefore been developed.

Initial tests have shown that this algorithm can successfully detect pole slipping, whilst maintaining stability against faults and power swings. This approach has the advantage that it can detect when the machine has passed the point of no return and can therefore trip the breaker before the machine actually slips.

8.1. REFERENCES.

1. MASRUR M A, AYOUB A K and TIELKING J T. 'Studies on Asynchronous Operation of Synchronous Machines and Related Shaft Torsional Stresses.' IEE Proc. Part C, Vol 138, Jan 1991, pp 47-56.
2. IEEE Power System Relaying Committee. 'Out of Step Relaying for Generators Working Group Report,' IEEE Trans PAS, Vol 96, No.5, Sept 1977, pp 1556-1564.
3. REDFERN M A, BARRETT J, HEWINGS D, 'A Laboratory Facility For Research into Digital Protection Algorithms used for the Protection of Small and Medium Sized Synchronous Generators.' Proc. 27th UPEC, Vol 1, Sept 1992, pp16-19.
4. REDFERN MA, USTA O and FIELDING G, 'Protection against Loss of Utility Grid Supply for a Dispersed Storage and Generation Unit.' IEEE Paper 92 SM 376-4 PWRD presented to the PES Summer Meeting, Seattle, 1992.
5. VENIKOV V A. 'Transient Phenomena in Electrical Power Systems', Permagon Press, 1964.
6. CEGB. 'Modern Power Station Practice', Vol 4, 'Generator & Electrical Plant', Permagon Press, 1963.
7. SHIWEN S. 'Microcomputer Based Out-of-Step Protection for Large Generator', IEE APSCOM Hong Kong, Nov 1991, IEE Proc. No 348, Nov 1991, pp 839-842.
8. BONWICK W J and HESSION P J. 'Fast Measurement of Real and Reactive Power in Three Phase Circuits.' IEE Proc A, Vol 139, No 2, March 1992, pp 51-55.
9. DUNN R, BERRY T, CHAN K, NG F. 'Real Time Power System Training Simulator.' Proc.25th UPEC, 1990, pp 671-674.

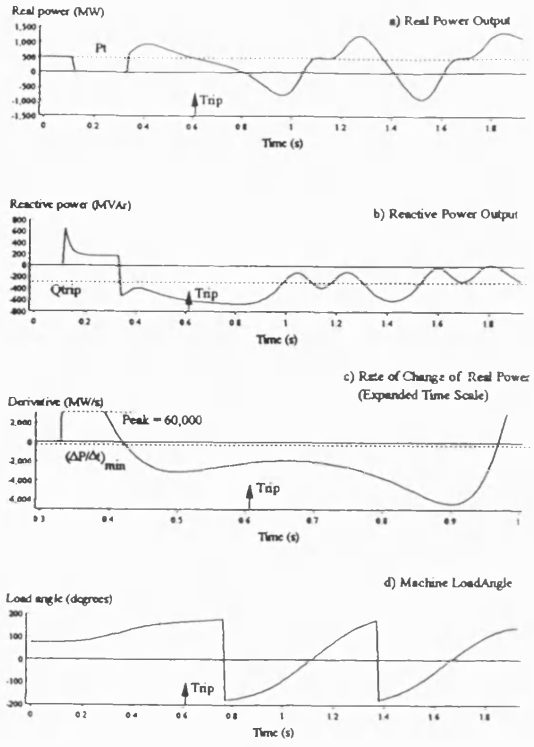

FIGURE 2 - Algorithm Quantities During Pole Slipping (Simulated).

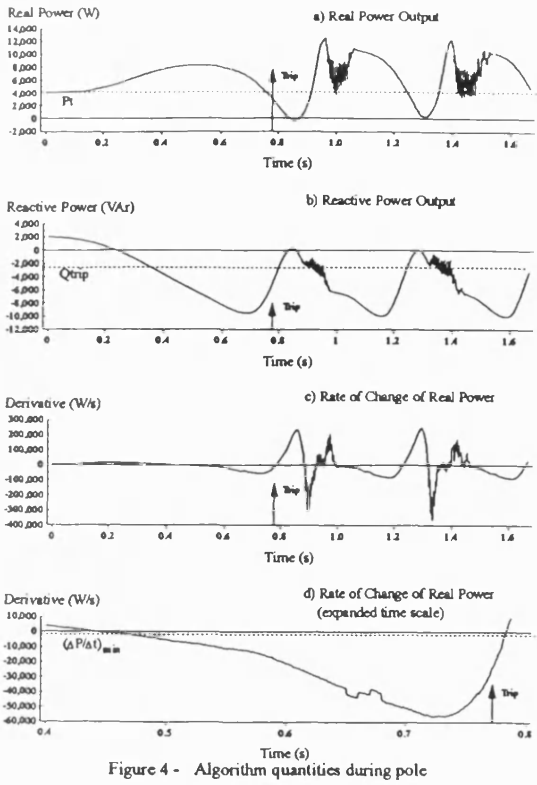

Figure 4 - Algorithm quantities during pole slipping of the 5 kVA machine.

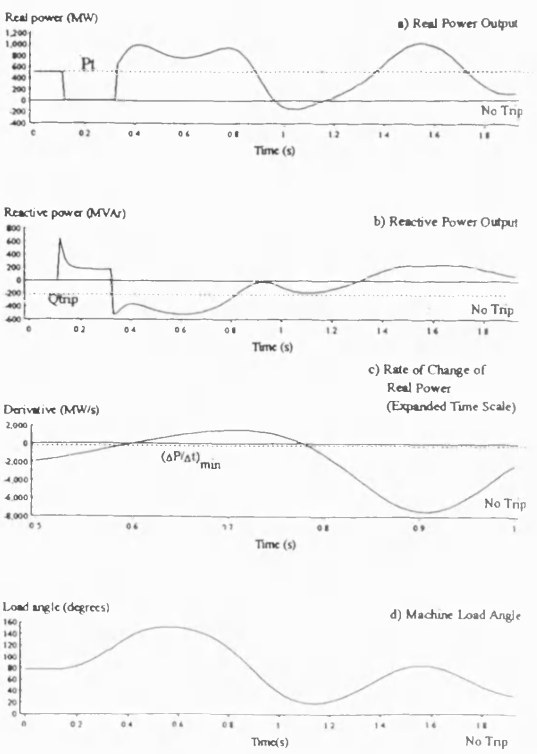

FIGURE 3 - Algorithm Stability Check Against a Power Swing (Simulated)

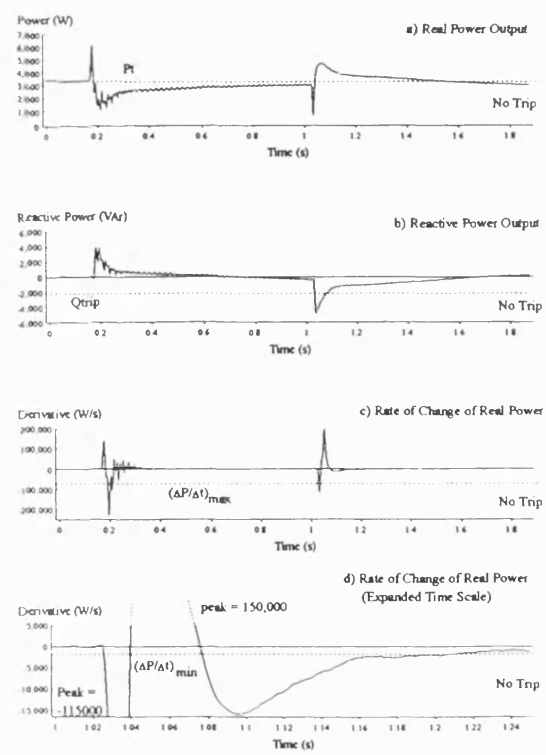

FIGURE 5 - Algorithm Stability Check for a Two Phase to Earth Fault.

PAPER TWO

"A NEW POLE SLIPPING PROTECTION ALGORITHM FOR DISPERSED STORAGE AND GENERATION USING THE EQUAL AREA CRITERION"

M A Redfern and M J Checksfield

Presented at :-
IEEE Power Engineering Society (PES) Summer Meeting,
July 1994, San Francisco,
Paper No. 94 SM 425-9 PWRD.

Published in :-
IEEE Transactions on Power Delievery,
Volume 10, Number 1, January 1995, pp 194 -202.

A NEW POLE SLIPPING PROTECTION ALGORITHM FOR DISPERSED STORAGE AND GENERATION USING THE EQUAL AREA CRITERION.

M. A. Redfern and M. J. Checksfield

School of Electronic and Electrical Engineering
University of Bath
Bath, BA2 7AY, UK.

Abstract - The probability of pole slipping of Dispersed Storage and Generation (DSG) synchronous machines is being viewed with concern, since this can damage the machine as well as promote power system instability. This is particularly the case for small and medium sized machines because their low inertias and high resistances make them inherently more unstable. Research has therefore been directed into new techniques for detecting pole slipping and the formulation of protection algorithms which can be included into an integrated microcomputer based protection scheme for these generators. This paper describes a method for detecting pole slipping using power measurements taken at the generator's terminals. This technique has been shown to correctly detect pole slipping using both computer simulation and a laboratory model power system. The algorithm remains stable for recoverable swing conditions and power system faults.

Keywords : - Power system protection, Dispersed storage and generation units, Pole slipping protection, Equal area criterion, Machine stability, Digital protection.

I. INTRODUCTION.

Pole slipping of any size of synchronous machine will always cause problems. The current trend of connecting an increasing number of small and medium sized synchronous generators to operate in parallel with the utility power supply puts such machines in a potentially damaging situation.

Generators on distribution systems using the widely adopted IDMT overcurrent relays can face fault clearance times of 0.5 to 1 second or more[1,2,3] which can cause generator instability. Future generator protection will be provided by microprocessor based integrated relaying schemes.

Since the protection functions are generally independent, there is little difficulty in using a common hardware system, thus providing the economy required to meet modern requirements. In addition to the required protection functions, disturbance and event recording, continuous self monitoring, ease of testing and SCADA interface are all possible features of this approach.

The algorithm described in this paper takes advantage of the processing capabilities of modern micro processor relaying platforms and has been designed to share sub-functions with other protection functions required for the protection of DSG synchronous generation[12,13,14]. The algorithm uses the Equal Area Criterion to assess the stability of the machine and determine when it is committed to a pole slip. This project is an extension of other work into aspects of this protection package[15,16].

Pole slipping is the process by which an imbalance between the mechanical input power and the electrical output power of a synchronous machine causes its rotor to accelerate, and hence the rotor magnetic flux to slip with respect to the stator flux which is synchronised to the electrical power system. The forces this produces within the machine can damage it in several ways. If the machine slips fast enough so that it operates past the peak of it's power/slip curve, the high currents experienced can loosen stator windings. These are generally only braced for three phase fault levels. Also, if prolonged pole slipping is permitted, injurious heating will result, the stator end teeth suffering the maximum temperature rise[4]. Induced slip frequency currents will flow in the rotor body, damping circuits and excitation windings. Their magnitude will be high since they must compensate the high stator mmf [5]. The rotor is therefore also at risk from overheating, pole slipping tests performed for one minute on a 60 MW turbo-generator[6] resulted in blueing of the rotor end rings, indicating that operation had come close to damaging the machine. If the generator uses an ac/dc excitation scheme, the induced voltage that results when the excitation rectifiers block the induced reverse rotor current can stress insulation and cause eventual breakdown if the exciter safety margins are not suitably specified[4].

The severe pulsating torques produced by pole slipping can torsionally excite sections of the shaft, exposing them to oscillatory stress[7]. Studies have found[8] that maximum torques and torsional stresses occur during the initial period of torsional oscillation after each torsional impulse, and that shaft damage generally occurs over this period. Additionally, it was found that the cumulative effects of smaller oscillations might in the long run lead to significant shaft damage also. If the shaft material is not sufficiently overdesigned, then its fatigue life can be used up after relatively few pole slipping events.

From the power system viewpoint, if the generator is connected to a low capacity utility infeed, the resultant voltage fluctuations produced can cause considerable trouble to other consumers, such as induction motor stalls and pole slipping of synchronous motors. Risks of protection mal-operation also result with overcurrent, undervoltage and distance relays being particularly at risk[9].

For these reasons it is therefore recommended that for a pole slipping condition, the generator is disconnected from the utility with no intentional delay[10] and at least within the first slip cycle[11].

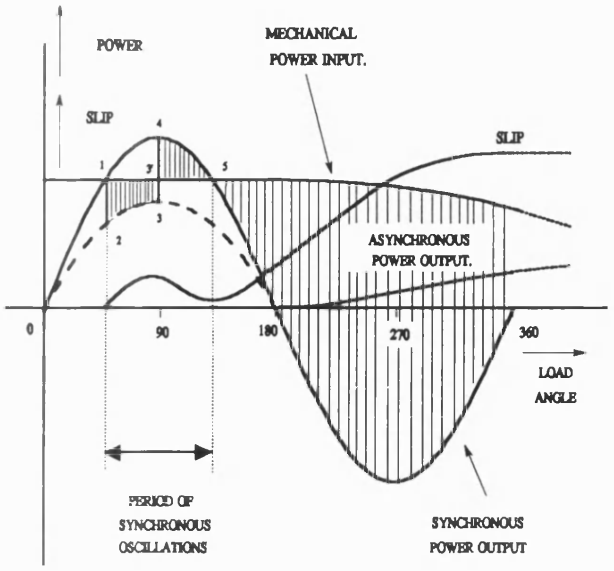

Fig. 1. Equal area diagram for generator loss of synchronism

II. POLE SLIPPING

Pole slipping of a synchronous machine occurs when there is insufficient electromagnetic torque to hold the rotor in synchronism with the stator magnetic flux. The loss of synchronism point can be defined as the point where the generator's real power output becomes zero. At this point, almost no flux links the stator and field windings, showing that the magnetic coupling between the two is at its weakest state[17].

Pole slipping can arise due to an external disturbance on the system such as an insufficiently cleared fault, a faulty excitation system, or an excess of prime mover input power caused by a sudden and large loss of load.

The Equal Area Criterion is often used for stability assessment, and demonstrates the conditions where synchronism is lost and pole slipping occurs. Fig.1 shows the power/load angle relationship and the rate of change of load angle (slip, s) for a generator losing synchronism following a loss of power transfer capability due to a disturbance on a double circuit line[18]. For this scenario, the generator is connected to a double circuit line and the disturbance is caused by switching one of the lines out of service temporarily.

The smaller of the power/load angle curves, the broken line, (points 0, 2, 3) represents the machine output when only one of the two feeder circuits is in operation. The larger of the power/load angle curves, the solid curve, represents the transfer capacity when both lines are in service.

For synchronism to be lost, the acceleration energy resulting from the loss of one line, represented by the area 1-2-3-3', must be larger than the retardation energy, represented by the area 3'-4-5, causing net acceleration of the rotor above synchronous speed. If the rotor is still above synchronous speed when the load angle reaches point 5, then synchronism will be lost, and the rotor will continue to accelerate until one pair of poles has slipped. The generator has travelled through the motoring region during this loss of synchronism before it returns to a generating condition. If the accelerating forces are not absorbed, a further slip may occur. Fig. 1 shows the slip increasing as synchronism is lost, as well as the asynchronous power output of the machine increasing due to induction generator action. If the governor reduces the input power to the generator, P_m, it is possible for stable asynchronous operation to occur or synchronous operation to be restored.

The above scenario illustrates that if a generator has sufficient load removed for a significant period of time, then pole slipping will occur, since the excess input power from the prime mover accelerates the rotor. The most severe disturbance for a generator is the close-up three phase fault, for which all of the generator's load is lost and therefore all of the prime mover power is used to accelerate the rotor. For less severe short circuit faults, a greater fault duration is required to incur pole slipping.

Pole slipping can also occur if the generator is under excited, since this reduces the maximum possible synchronous

electrical power which can be taken out of the generator. If this maximum is less than the prime mover input power, synchronism can not be maintained. If excitation is lost completely then the machine runs asynchronously rather than pole slipping[6], this is a loss of field condition. In this condition the output power pulsations will be significantly reduced to the amplitudes dictated by the machine's electric and magnetic characteristics.

III. CONVENTIONAL METHODS FOR DETECTING POLE SLIPPING.

The most widely used technique for detecting pole slipping is to monitor the path of the apparent impedance of the machine and its rate of change with distance type relays. Fig.2 shows the impedance characteristic for machine 'A' pole slipping due to a loss of load.

The impedance is not limited to just one trajectory, but is free to drift across the R/X plane according to variations in generator impedances and generator internal voltages. The point where the locus crosses the system impedance line AB corresponds to a load angle of 180°, i.e the point where loss of synchronism occurs.

The simplest scheme uses mho distance relay characteristics. The relay looks into the HV terminals of the generator step up transformer, a trip signal being given if the impedance enters the circle.

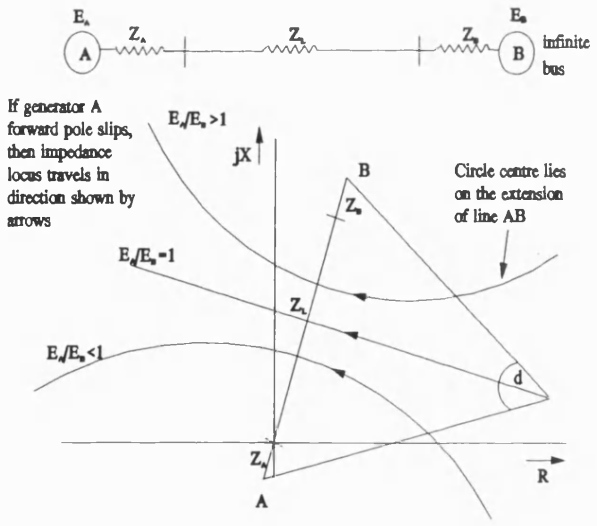

Fig. 2. Pole slipping impedance loci.

This scheme has the disadvantage that it can mal-operate for recoverable swings. Generally the relay is set to a sensitivity of 120° load angle, since return to stable operation is usually unattainable once this angle has been exceeded. The relay does provide fast back up protection for multiphase faults close to the generator.

A more secure distance type scheme[11] is shown in Fig. 3 This uses two load blinder characteristics set either side of and parallel to the system impedance, and a supervisory mho relay. When pole slipping occurs, the apparent impedance travels across the impedance plane, and a trip condition exists if the impedance enters the mho supervisory relay and then crosses the two load blinder units in succession. If just one load blinder unit is tripped, as occurs for an internal or a close-up external fault, the relay will not trip. The locus must enter from one side and leave from the other for tripping to occur.

Tripping is sometimes set to occur following reset of the mho element, enabling control of the angle at which tripping occurs for more favourable circuit breaker arc interruption. This is achieved by adjusting the diameter of the mho element, however, careful study of the mho setting must be made to prevent tripping for recoverable swings that cross both blinder elements.

Double blinder schemes with supervisory mho elements are also available, which allow the impedance to enter and leave on the same side. This makes for faster tripping than the single element scheme, but can mal-operate for recoverable swings unless very careful selection of the relay settings is made.

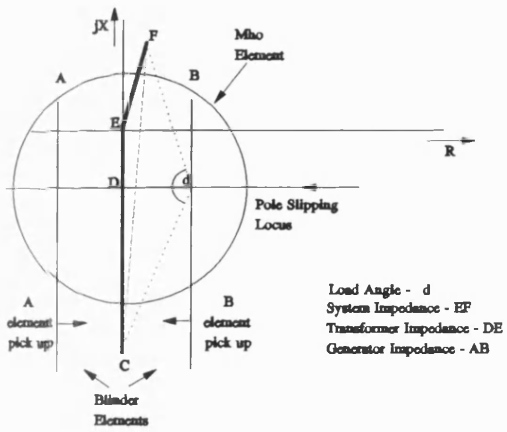

Fig. 3. Single blinder pole slipping protection.

More sophisticated schemes have been developed using lens characteristics[19] rather than circular mho or ohm characteristics. This type have similar operating characteristics to the single blinder scheme.

Microcomputer based schemes have been developed which sectionalise the R/X plane into multiple zones, making the scheme inherently more stable. Fig. 4 shows one such example described by Shiwen[20]. This scheme issues a trip signal after the locus has travelled through zone 0 to zone 4, staying in each zone for a time greater than that of the impedance characteristic associated with a short circuit fault, but less than the minimum time it would stay in any zone for the out of step condition. Again tripping does not occur until pole slipping has actually occurred, but the scheme does provide preventative control signals for fast valving or dynamic breaking if the locus travels through the first two zones in the correct manner.

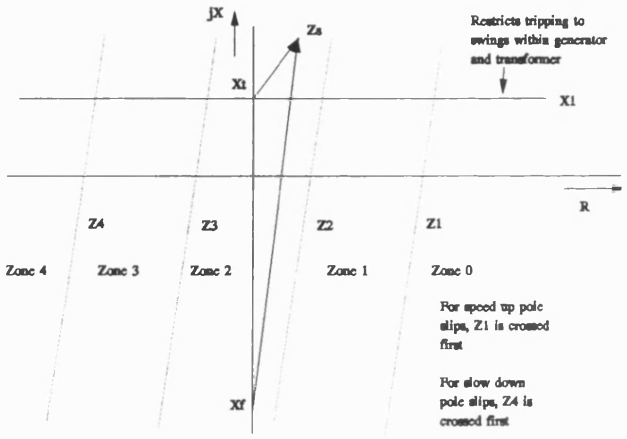

Fig. 4. Impedance microcomputer based pole slipping protection.

IV. THE NEW APPROACH TO POLE SLIPPING PROTECTION.

Pole slipping is a power based phenomena and hence power algorithms have been examined which are based on the Equal Area Criterion. In the design of the protection algorithm, the relay should trip when it observes the conditions which will produce a pole slip or correspond to an actual pole slip, but remain stable during fault conditions and other system abnormalities. By being able to recognise the conditions where a pole slip is inevitable, the algorithm offers the prospect of tripping before the actual pole slip and hence disconnecting the machine from the system before it can be damaged. This requires the circuit breaker to have adequate arc interruption capabilities.

The instantaneous values of real and reactive power[21] used for the trip criterion were calculated using;-

$$P = v_a * i_a + v_b * i_b + v_c * i_c \qquad (1)$$

$$Q = \frac{1}{\sqrt{3}}(v_a*(i_c - i_b) + v_b*(i_a - i_c) + v_c*(i_b - i_a)) \qquad (2)$$

where v_a , i_a , v_b , i_b , v_c , and i_c represent the sampled values of the terminal voltage and current. The sign convention used defines that for an under-excited generator, the reactive power is negative.

The Equal Area Diagram, Fig. 1, illustrates that for a stable swing, the machine operating point cannot exceed point 5. If point 5 can be identified in terms of machine terminal quantities, then machine stability can be determined. Point 5 corresponds to the electrical output of the machine, P, equalling the mechanical input from the prime mover, P_m. Instability occurs if the machine operates past point 5, and this can therefore be identified in terms of real power as the condition when

$$P < P_m \qquad (3)$$

The above criterion can also be satisfied for machine operating points between points 0 and 1 shown on Fig. 1. To differentiate between the two, reactive power measurement is used. The steady state reactive power/load angle relationship for a round rotor machine is given by :-

$$Q = \frac{E*V}{X_d}(\cos\ \delta) - \frac{V^2}{X_d} \qquad (4)$$

This shows that for load angles between 90° and 270°, the reactive power will always be less than the load angle (δ) independent term. Since point 5 of Fig. 1 occurs for load angles greater than 90°, then if :-

$$Q \leq \frac{-V^2}{Xd} \qquad (= Q_{trip}) \qquad (5)$$

the machine must be operating at point 5 and not point 1, and this forms the second criterion. The transient reactive power characteristics vary in magnitude from the above steady state

values. This does not corrupt the above method since the value of reactive power corresponding to a 90° load angle is identical to the steady state value. The transient reactive power characteristics above and below this load angle are such that in steady state terms it appears as if the load angle is correspondingly higher or lower.

Finally, it must be ascertained whether or not the load angle is still advancing. To determine this, rate of change of real power is used. It can be seen from the synchronous power output characteristic of Fig. 1, that if the load angle is still increasing when point 5 is reached, the machine output power will be decreasing, i.e. the rate of change of real power will be negative. This, therefore is the third criterion for determining machine stability and hence predicting pole slipping.

In practice a margin for error is allowed for in this rate expression ($\Delta P/\Delta t$), to ensure the algorithm does not mal-operate. A minimum negative value, $(\Delta P/\Delta t)_{min}$ is designated, based on a minimum value of slip and an assumed sinusoidal power/load angle relationship. The conditions which determine that a generator is about to pole slip are therefore :-

$$P \leq P_m$$
$$Q \leq Q_{trip} \qquad (6)$$
$$(\Delta P/\Delta t) \leq (\Delta P/\Delta t)_{min}$$

Dispersed storage and generation units are generally operated at, or close to their full rated load[22] to provide the greatest return on investment. A fixed value of P_m, designated as the trip setting P_t, can therefore be adopted for the algorithm real power setting which corresponds to the expected generator output.

If the synchronous machine is expected to operate over its full working range, an adaptive relaying technique would be used which utilises the mechanical power input. A technique similar to that used in [23], which uses an acceleration disturbance detector could easily be implemented.

Faults cause considerable technical difficulties since they cause dramatic changes in the relay measurands. These transitions produce negative values of ($\Delta P/\Delta t$) which are a potential source of instability to the algorithm. Fortunately, the faults generally introduce sinusoidal terms of twice the power system frequency into the power measurements. Since pole slipping is a relatively slow process in comparison to faults, then an imposed minimum tripping time of one power system cycle will inhibit fault tripping. In addition, the rapid transitions experienced with faults produce negative values of ($\Delta P/\Delta t$) far in excess of that possible due to pole slipping. This provides an additional mechanism to inhibit tripping during power system faults, whenever ($\Delta P/\Delta t$) is less than $(\Delta P/\Delta t)_{max}$, where $(\Delta P/\Delta t)_{max}$ is the maximum negative value expected from pole slipping, based on a maximum slip value and a sinusoidal power load angle relationship.

The relaying measurands are filtered to remove harmonics and unbalance present on the power system. A half cycle moving average filter is used for the real and reactive power measurements, followed by a full cycle moving average for the derived rate of change of power signal.

V. SIMULATION STUDIES.

The performance of the protection algorithm was investigated using a computer based simulator[24] and a laboratory power system model[15]. The computer based simulator was particularly useful in that the results it produces are of an 'ideal' nature and demonstrate the fundamental characteristics of pole slipping. The laboratory power system model provides a test bed for identifying problems with the algorithm not immediately evident from theory.

A. Computer Based Simulation Studies.

The power system simulation software was used to investigate the algorithm's performance with pole slipping and power swings. It lends itself especially to power swing analysis since the worst possible swing can be simulated. The computer simulator models the behaviour of the machines, control systems and transmission network of an interconnected power system. It uses a partitioned approach to solve the sets of equations, which describe the behaviour of the machines, control systems and transmission network. The differential equations for each machine group are solved independently to calculate the current injection into the transmission network. The algebraic network equations are then solved and the whole calculation repeated until the required accuracy is obtained. The machine model used is based on Park's transformation, the damper winding and eddy current effects being represented by a short circuited winding on both the direct and quadrature axis.

The classical single machine and infinite bus system was modelled, which consisted of a grid network represented by a generator of 58.8 GVA connected by two parallel transmission lines to the protected generator of 588 MVA with an associated generator transformer. This model is similar to the laboratory power system model used, in that the ratio of utility to machine ratings is 100:1. This computer model has characteristics much more akin to those of a grid system, since the machine is large, making the assumptions used in deriving

the Equal Area Criterion correct. For smaller machines, effects such as stator resistance have to be taken into account. These effects do not however affect the functioning of the algorithm since it is the principle of the Equal Area Criterion on which the algorithm is based and not absolute values.

Pole slipping was triggered by applying a 3 phase fault on the generator transformer busbar with a fault duration just greater than the critical clearance time (CCT). This is the maximum fault duration allowable before instability occurs. This technique was also used to trigger a power swing but for this the fault duration was chosen to be just less than the critical clearance time.

B. Laboratory Power System Model.

The laboratory model DSG system[15] consisted of two 5kVA generators connected to a double bus system, 'local' load and a 200V laboratory three-phase 'utility' supply. The 5kVA generators were two pole, round rotor machines, driven by dc motors. Although the transformer supplying the laboratory is rated at 500 kVA, giving a utility to machine rating of 100:1, the cable connecting the two has a relatively large impedance, making the system less 'stiff'. This makes the laboratory simulation more realistic for DSG machines, since in practice these may be located at the end of long distribution feeders.

Pole slipping of the laboratory machine was induced by two methods. In the first, a three phase fault was placed on the DSG utility intertie of sufficient duration to cause instability. The second method involved reducing the generator's excitation slowly until synchronism was lost.

The algorithm's security against faults was tested by applying phase to earth, phase to phase, twin phase to earth and three phase faults to the local load busbar. Full three phase fault current was not permitted and the fault current magnitude was therefore reduced using a current limiting resistor.

VI. ALGORITHM SETTINGS

The value for P_t is set by the expected steady state machine output power.

The value for Q_{trip} is given by :

$$Q_{trip} = -\frac{V^2}{Xd} \quad p.u. \tag{7}$$

The value of $(\Delta P/\Delta t)_{min}$ is derived as follows, if it is assumed that the power output of the generator can be expressed as the symmetrical function:

$$P = P_{max} \sin \delta \tag{8}$$

Where P_{max} is the maximum output of the machine at full load excitation, then the load angle at which P = Pm for load angles greater than 90° (unstable operation) is given by :

$$\delta_p = 180 - \sin^{-1}\left(\frac{P_m}{P_{max}}\right) \tag{9}$$

The derivative of real power with respect to time, can be expressed as :

$$\frac{dP}{dt} = \frac{dP}{d\delta}\frac{d\delta}{dt} \tag{10}$$

The derivative of load angle with respect to time is the slip, s and is defined as :

$$\frac{d\delta}{dt} = -s \tag{11}$$

i.e. negative values of slip exist for speeds above synchronous speed. If (8) is differentiated with respect to load angle then:

$$\frac{dP}{d\delta} = P_{max} \cos \delta \tag{12}$$

Hence the derivative of real power at the point where P = Pm can be expressed as :

$$\frac{dP}{dt} = -s\, P_{max} \cos \delta_p = (\Delta P/\Delta t)_{min} \tag{13}$$

A value for the margin for error can therefore be obtained by deciding on a minimum value of slip permitted at the point P = P_m. A value of 0.5 % was chosen as providing an adequate safety margin whilst still remaining lower than values expected from pole slipping generators. The above procedure can also be applied to find the value required for fault blocking $(\Delta P/\Delta t)_{max}$. Table I shows the algorithm settings for both of the machines tested.

A. Test Machine Settings.

TABLE I
ALGORITHM SETTINGS.

Machine Rating	5 kVA	588 MVA
Pmax	6.5 kW	720 MW
Xd	2.32 p.u.	2.77 p.u.
Qtrip	-2160 VAr	-260 MVAr
Pt	4 kW	500 MW
$(\Delta P/Dt)_{min}$	-2000 W/s	-260 MW/s
$(DP/Dt)_{max}$	-75 kW/s	-9500 MW/s

VII. TEST RESULTS.

A. Simulation Studies.

The response to pole slipping on the computer simulation is shown in Fig. 5. The algorithm detected the pole slip condition at a load angle of 167°, i.e. just before the machine actually slipped. It can be seen that the reactive power criterion was satisfied first, followed by the rate criterion, this indicates that the load angle was in excess of 90° and the rotor was travelling above synchronous speed. Tripping finally occurs once the real power falls below P_t, indicating that no further decelerating energy was available and that instability was unavoidable. Although the actual tripping time can be seen, the speed of pole slipping is dependent upon the degree of unbalance and will inherently vary from case to case. Expressing the tripping time in terms of load angle provides a more suitable measure for comparison.

The simulated power swing which produced the largest possible stable swing of 152° is shown in Fig. 6. For the time period between 0.3 and 0.8 seconds the reactive power is less than Q_{trip}, indicating that the load angle is greater than 90°, as the load angle plot confirms. However, during this time, real power is greater than P_t, restraining operation of the algorithm. This condition indicates that decelerating energy is still available. The section marked AB represents the portion 1-4-5 on the power/load angle curve of Fig. 1. Since this is a stable case, but close to the critical condition, point five is practically reached. Inspection of the derivative curve shows that a zero value of $\Delta P/\Delta t$ exists at this point, showing that the rotor is once again at synchronous speed (this can be ascertained from the load angle plot which is at its maximum at this point). The section BC then represents travel from point 5 to point 1 on Fig. 1, i.e. the rotor is backswinging towards a stable operating point. As it does so, the reactive power rises above Q_{trip}, restraining algorithm operation and ensuring no mal-operation. The relay therefore does not trip.

B Laboratory Studies.

Fig. 7 shows the 5 kVA laboratory machine pole slipping following a close up three phase fault. Inspection of the three phase fault section of the algorithm measurands confirms that the algorithm remains stable for such a disturbance. The critical point occurs at 1.4 seconds on the record, when the real and reactive criteria are satisfied but the fault is blocked by the extremely large negative value of $\Delta P/\Delta t$.

After the fault has cleared, it can be seen that the reactive power is less than Q_{trip}, i.e. the load angle has increased above 90° during the fault period. After this, real and reactive power gradually decrease as the generator slowly goes out of step. Tripping occurs when $\Delta P/\Delta t$ falls below the safety margin. It is interesting to note, that during the fault period, a significant amount of real power came from the generator. This was due to the high fault resistance present which was required to limit the fault current. Even with only 1 kW of load removed, the machine still lost synchronism. The algorithm successfully operated once the machine was committed to a pole slip.

Of all fault types investigated, the two phase to earth and three phase to earth faults presented the greatest threat to algorithm security. For these faults, both of the fault blocking mechanisms, the one cycle minimum operating time and the maximum negative value of $(\Delta P/\Delta t)$ were employed.

The results for a two phase to earth fault are shown in Fig. 8. The dangerous condition arises following removal of the fault which occurred just after 1.0 second in the record. At this time, the derivative, $(\Delta P/\Delta t)$, was not negative for the one cycle required for tripping, and was also more negative than $(\Delta P/\Delta t)_{max}$ indicating a fault condition. Tripping was therefore blocked for this fault condition.

VIII. CONCLUSIONS.

With the growing number of small and medium sized DSG generators, the probability of pole slipping is growing and therefore pole slipping protection is becoming more important. Machine winding damage, system problems, and shaft failure can all result if adequate protection is not provided. A power based algorithm, suitable for inclusion into an integrated protection scheme has therefore been developed using the Equal Area Criterion.

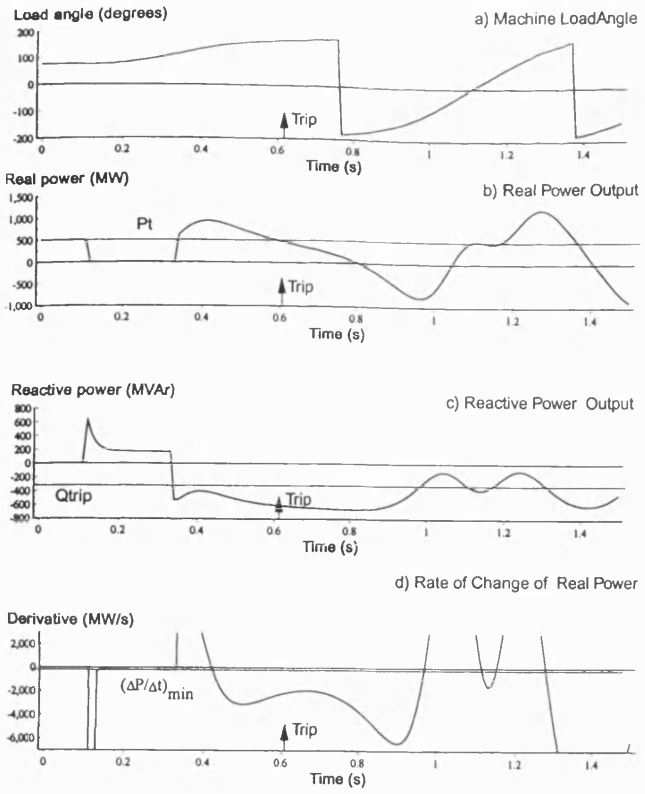

FIGURE 5 - Algorithm Quantities During Pole Slipping (Simulated).

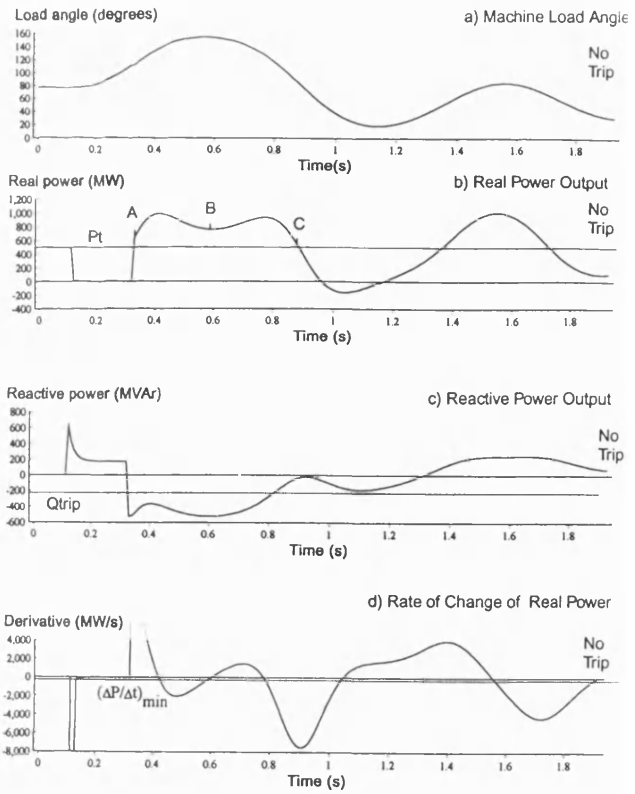

FIGURE 6 - Algorithm Stability Check Against a Power Swing (Simulated).

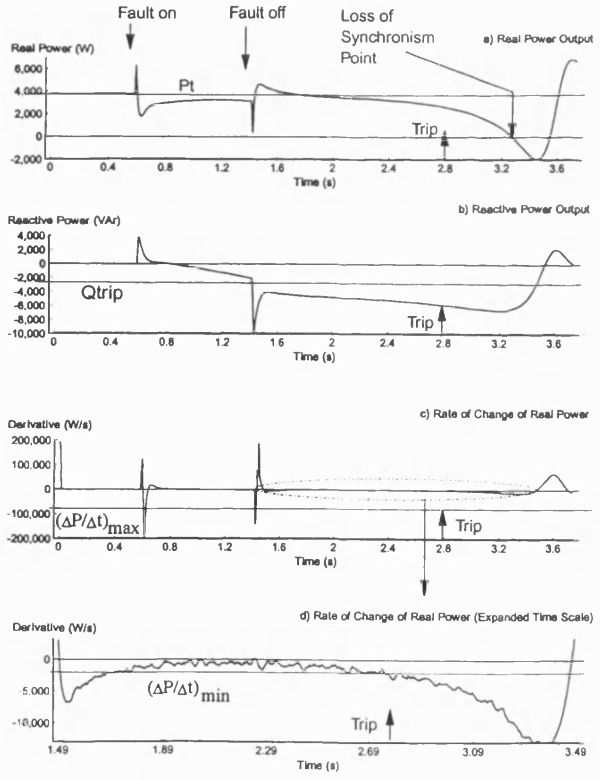

FIGURE 7 - Laboratory Machine Pole Slipping Due to Three Phase Fault.

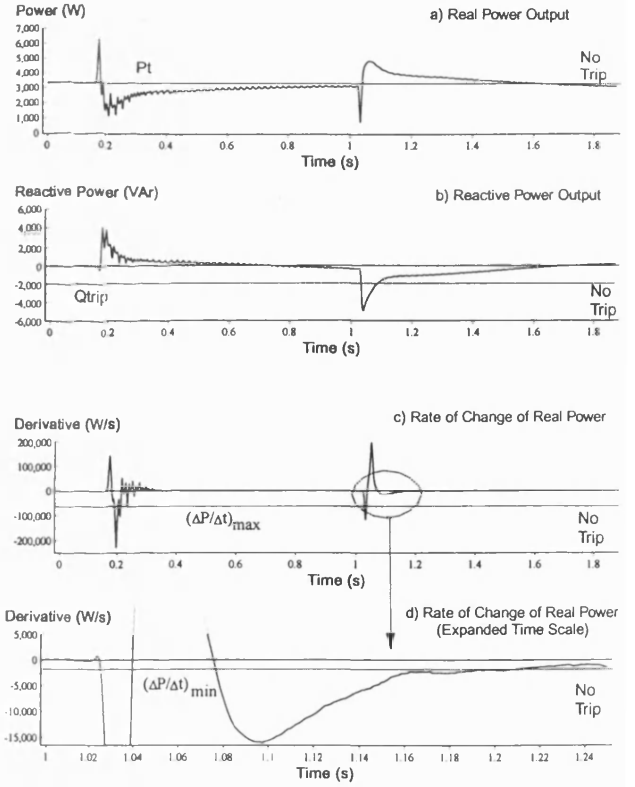

FIGURE 8 - Algorithm Stabilty Check for a Two Phase to Earth Fault.

Tests have shown that this algorithm can successfully detect pole slipping, whilst maintaining stability against faults and power swings. This approach has the advantage that it can detect when the machine has passed the point of no return and can therefore trip the breaker before the machine actually slips, preventing the pending damage.

IX. ACKNOWLEDGEMENTS.

The authors are pleased to acknowledge the help and encouragement provided by the University of Bath, GEC ALSTHOM Protection and Control and the Science and Engineering Research Council.

X. REFERENCES.

[1] N. Nichols, "The Electrical Considerations in Cogeneration," IEEE Transactions on Industry Applications, Vol.IA-21, No.4, May/June 1985, pp 754-761.

[2] Harrison K. Clark and James W. Feltes, "Industrial and Cogeneration Protection Problems Requiring Simulation," IEEE Transactions on Industry Applications, Vol IA-25, No.4, July/August 1989, pp 766-775.

[3] G. Fielding and G. W. Evans, "Industrial Feeder Protection," 10th International Conference on Electricity Distribution, Part 1, Subject Area 5 - Consumers Installations, IEE Conference Proceeding No. IEE 305, 1989, pp 460-466.

[4] T.H. Mason, W.Fairney, J. J.Arnold and M. J. Thelwell, "Asynchronous Operation of Turbo-Generators," CIGRE Vol.1 , 1972, Sec 11-02.

[5] C. B. Cooper, V. Easton, M. N. John, K. C. Parton, G. Shackshaft and T. M. Whitelegg, "Problems Associated with Limited Pole Slipping of Turbo-Generators Following System Faults," CIGRE 1966, Vol.3, No.306, pp 1-16.

[6] T. H. Mason, P. D. Aylett and F. H. Birch, "Turbo -Generator Performance Under Exceptional Operating Conditions," IEE Conf. Proc. Vol.106, Jan 1959, pp 357-373.

[7] A. Abolins, D. Lambrecht, J. S. Joyce and L. T. Rosenberg, "Effect of Clearing Short Circuits and Automatic Reclosing on Torsional Stress and Life Expenditure of Turbine-Generator Shafts," IEEE Transactions on Power Apparatus and Systems, Vol.PAS-97, No.1, Jan/Feb 1976, pp 14-25.

[8] M. A. Masrur, A. K. Ayoub, J. T. Tielking, "Studies on Asynchronous Operation of Synchronous Machines and Related Shaft Torsional Stresses," IEE Conf. Proc, Part-C, Vol.138, Jan 1991, pp 47-56.

[9] F. Ilar, "Innovations in the Detection of Power swings in Electrical Networks," Brown Boveri Revue, Part 2, 1981, pp 87-93.

[10] Summary Report of an IEEE Working Group Report, "Intertie Protection of Consumer-Owned Sources of Generation, 3 MVA or Less," IEEE Transactions on Power Delivery, Vol.5, No.2, April 1990, pp 924-929.

[11] J. A. Imhof (Chairman) et al, "Out of Step Relaying for Generators - Working Group Report," IEEE Transactions on Power Apparatus and Systems, Vol.PAS-96, No.5, Sep/Oct 1977, pp 1556-1564.

[12] J. H. Harlow, "A Multifunction Protective Relay for the Cogeneration Industry," IEEE Computer Applications in Power, Oct 1990, pp 25-30.

[13] F. Fromm, Z. Franc, B. Kulendik and C. Steiner, "Generator Protection with the Digital MODURES 216," Brown Boveri Review 1987, Vol.74, No.12, pp 693-700.

[14] M. V. V. S. Yalla, "A Digital Multifunction Protective Relay," IEEE Transactions on Power Delivery, Vol.7, No.1, Jan 1992, pp 193-200.

[15] M. A. Redfern, J. Barrett, D. Hewings, "A Laboratory Facility For Research into Digital Protection Algorithms used for the Protection of Small and Medium Sized Synchronous Generators." Proc. 27th UPEC, Vol 1, Sept 1992, pp 16-19.

[16] M. A. Redfern, O. Usta and G. Fielding, "Protection against Loss of Utility Grid Supply for a Dispersed Storage and Generation Unit." IEEE Transactions on Power Delivery, Vol. 8, No. 3, July 1993, pp 948-954.

[17] J. Matsuki, T.Okada and C. Uenosono, "Loss of Synchronism Process of a Synchronous Generator Described by its Internal Flux and Force Distributions," IEEE Transactions on Energy Conversion, Vol.7, No.1, March 1992, pp 177-181.

[18] V. A. Venikov, Transient Phenomena in Electrical Power Systems, Pergamon Press, 1964.

[19] A. Stalewski, J. L. H. Goody and J. A. Downes, "Pole Slipping Protection," Developments in Power System protection, IEE Conference Publication, No.185, pp 38-45.

[20] S. Shiwen, "Microcomputer Based Out-of-Step Protection for Large Generator," IEE APSCOM Hong Kong, Nov 1991, IEE Conf. Proc. No 348, Nov 1991, pp 839-842.

[21] J. W. Bonwick and P. J. Hession, "Fast Measurement of Real and Reactive Power in Three Phase Circuits," IEE Proc A, Vol 139, No 2, March 1992, pp 51-55.

[22] R. M. Rifaat, "Protection Scheme Considerations for Common Generator Bus Configurations used in Cogeneration Plants," IEEE Wescanex 93 - Communications, Computers and Power in the Modern Environment : Conference Proceedings 1993, Ch. 60, pp 1-6.

[23] William R. Roemish and Edward T. Wall, "A New Synchronous Generator Out-of-Step Relay Scheme," IEEE Transactions on Power Apparatus and Systems, Vol.PAS-104, No.3, March 1985, pp 563-582.

[24] R. Dunn, T. Berry, K. Chan and F. Ng, "Real Time Power System Training Simulator," Proc.25th UPEC, 1990, pp 671-674.

Miles A Redfern (M'79) received his BSc degree from Nottingham University and PhD degree from Cambridge University in 1970 and 1976 respectively. In 1970, he joined British Railways Research, and in 1975, moved to GEC measurements where he held various posts including Head of Research and Long Term Development and Overseas Sales Manager. In 1986, he joined Bath University with interests in Power Systems Protection and Management. He is currently a member of IEE Professional Group P11, Power System Measurement, Protection and Control, and is a corresponding member of the IEEE Line Protection Sub-Committee.

Matthew Checksfield received his B Eng degree from Bath University in 1993. He is currently studying for his PhD degree at Bath University and is sponsored by GEC ALSTHOM Protection and Control.

PAPER THREE

"A CONDITION MONITORING POLE SLIPPING PROTECTION ALGORITHM BASED ON THE EQUAL AREA CRITERION"

M J Checksfield and M A Redfern

Presented at :-
29th Universities Power Engineering Conference (UPEC),
September 1994, Galway, Ireland, pp 747 - 750.

A CONDITION MONITORING POLE SLIPPING PROTECTION ALGORITHM BASED ON THE EQUAL AREA CRITERION.

M. J. Checksfield and M. A. Redfern.

University of Bath, UK.

ABSTRACT

This paper introduces a new condition monitoring power based technique for detecting pole slipping of synchronous generators. The particular advantage of this approach is that it reduces the complexity of installation. As with techniques previously reported[1], the algorithm provides a trip signal 'on the way in' to a pole slip and hence before the pole slip actually occurs. In doing so, some of the undesirable effects produced by pole slipping can be avoided. A range of various operating conditions are used to demonstrate the algorithm's ability to restrain against faults and power swings and to operate when a pole slip is imminent.

1 INTRODUCTION.

Pole slipping relays have existed for over 50 years, and nearly all have been impedance based, relying on the variation in apparent impedance at the terminals of the protected generator. Pole slipping occurs when an imbalance between generator input and output powers causes the rotor to accelerate and lose synchronism from the stator magnetic flux.

Impedance relays generally work by detecting when the apparent impedance of the machine crosses the equivalent system impedance line in a specified time limit[2]. Choosing the correct settings makes the installation of these types of relays difficult[3]. Research is therefore being conducted into a new type of pole slipping algorithm which does not require such careful analysis before installation.

2 REASONS FOR USING POLE SLIPPING PROTECTION.

Pole slipping protection is necessary to minimize the disturbance pole slipping can cause to other consumers connected to the power system and to prevent damage to the generator. The extent of the damage is dependent on the rating of the bus that the generator is connected to, the speed of the pole slip, and the overcapacity rating of the machine. When the utility infeed capacity is high in comparison to the generator rating, the currents experienced during pole slipping can be greater than three phase fault levels. Since machine windings are only braced for three phase fault levels, pole slipping could therefore loosen and deteriorate the windings[3].

The induced slip frequency currents that flow in the rotor body, damping circuits and excitation windings can result in serious overheating if prolonged operation is permitted.

Pole slipping can also cause damage to excitation systems due to the large induced currents that flow in the field winding, which try to reverse in direction every pole slip cycle. Rectifier excitation systems will not permit the rotor current to reverse, thus producing a rapid flux change which produces a large reverse voltage across the rectifiers. This can cause reverse breakdown of the semiconductor devices if they are not sufficiently over rated[4].

Generator shafts are also at risk due to the pulsating torques produced torsionally exciting them and exposing them to oscillatory stress. Particularly at risk are turbine generator shafts since the bladed rotating parts of the turbine interact with the couplings and reduced diameter shaft extensions to form a torsionally resonant system. One study[5], found that the generator-exciter shaft section experiences the highest stresses. It was found that 100 % of the fatigue life of this shaft section was used up after one pole slip for a shaft over design rating of two.

The study indicated that the maximum torques and torsional stresses occur during the first period of oscillation caused by pole slipping, and it is this period where the shaft damage usually occurs. It is therefore advantageous to disconnect the generator from the system *before* a pole slipping event occurs in the hope that the torsional impulse will be prevented. It was also indicated that the cumulative effects of smaller disturbances taken together, due to less severe transients, might in the long run lead to significant shaft damage.

The effect of pole slipping on the rest of the system can result in plant outages and even a cascading loss of synchronism of machines nearby. The voltage fluctuations produced can cause motor starter contactors to open, causing unnecessary loss of plant. If a serious voltage depression is experienced, induction motors could stall, depressing system voltage further. Synchronous motors may also pole slip as a result of the voltage depression, suffering all of the ill effects of generators. The lowest voltages will occur at the location where the contribution from the pole slipping generator is equal to the contribution from the rest of the system, referred to as the system centre. If the system centre occurs inside the generator, the resultant voltage fluctuations will not be severe. However, if the utility infeed is of low capacity compared to the generator rating, the voltage fluctuations will be centred in the system, causing disturbances to other users.

Power system protection also suffers from the effects of pole slipping, since the voltage and current variations at the electrical centre are similar to those caused by a three phase short circuit. The relays most affected are undervoltage, overcurrent and impedance type relays. If adequate blocking is not applied to these relays then unnecessary system outages will occur.

3 TIIE EQUAL AREA CRITERION.

If the power/load angle characteristic of a generator operating on an infinite bus is known, then the Equal Area Criterion is often used to determine which conditions cause transient instability[6]. Consider the case where a generator is initially operating with a prime mover input power of Pm, and the prefault electrical load curve as shown in Figure 1, giving an initial load angle of $\delta 1$. If a three phase fault occurs near to the generator, then the generator terminal voltage will collapse and the generator will be less able to export power. The electrical output from the generator is now characterised by the 'fault duration' power/load angle curve. This reduction in output power results in an imbalance between generator input and output powers, which accelerates the rotor causing an increase in load angle. If subsequently, at a load angle of $\delta 2$, the fault is removed by disconnecting the faulty line, therefore restoring the voltage, the electrical output is characterised by the post fault load curve.

The post fault load/angle curve differs from the pre-fault, due to the system transfer impedance increasing on removal of the faulty line. The generator output power will now be higher than the input power, causing a decelerating force on the rotor. It can be shown that for a given load angle swing, the area between the shaft power input line, Pm, and the electrical output power of the machine, is proportional to the total energy involved in that swing. Area 'A' in Figure 1, therefore represents the *accelerating* energy into the rotor, and area 'B' the *decelerating energy*. Even though a retarding force is now acting on the rotor, the load angle still continues to advance since the rotor is travelling above synchronous speed. If area A were

equal to area B, the rotor would once again be a synchronous speed on reaching load angle δ3. The load angle would then begin to decrease as shown, due to the retarding force acting on the rotor still.

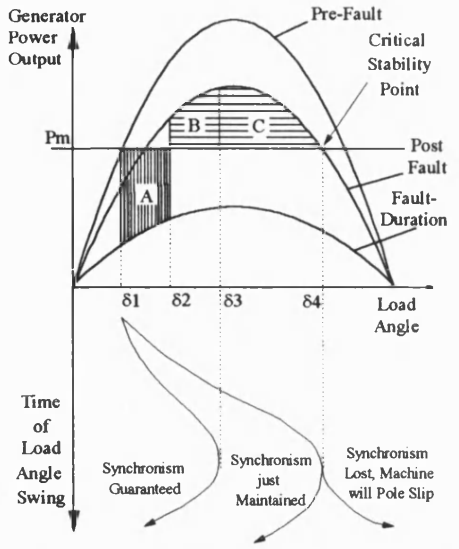

Figure 1. Equal Area Diagram Showing Load Angle

However, if area 'A' were equal to area 'B + C' then the retardation energy produced by the machine when swinging from δ2 to δ4 would only just be sufficient to counteract the accelerating energy absorbed by the rotor in swinging from δ1 to δ2. In this instance, stability would have just been maintained. The load angle would swing up to a value δ4, this is known as the *critical stability point* [6] (CSP). Above this, synchronism would have been lost, i.e. if area 'A' were larger than area 'B + C' .

This point forms the basis for the new power based algorithm. Once the CSP is exceeded, the rotor will again start to accelerate and the machine will slip one pair of poles. If the excess kinetic energy is not removed from the rotor by the next time the CSP is reached, another pole slip will occur.

4 THE POWER BASED TECHNIQUE.

A pole slipping algorithm must be capable of detecting when a pole slip is about to occur, or actually is occurring. It must remain stable for all other power system conditions. The two situations which most commonly cause difficulties are external faults and power swings.

Figure 1 demonstrates that once the machine has passed the CSP, a pole slip will occur. The power based algorithm functions by detecting if the load angle is still increasing once the CSP has been reached. In order to determine when the machine has reached the CSP, both real and reactive power are used. The reactive power characteristics of a generator are such that at a load angle of 90°, the machine's reactive power demand is always given by :

$$Q = -\frac{V^2}{Xq} \qquad (1)$$

Where V is the terminal voltage, Xq is the quadrature axis synchronous reactance. If the generator reactive power falls below this value, then it can be concluded that the generator load angle is greater than 90°. This therefore provides a trip criteria in that if the reactive power falls below the level corresponding to the load angle being 90° (Qtrip) then the machine is operating in an area where pole slipping is likely. Also at the CSP, the generator real output power equals the prime mover input power, Pm. Operation at the CSP can therefore be identified when:

$$Q \le Qtrip \quad And \quad P \le Pm \quad (= Pt) \qquad (2)$$

Where Pt is the algorithm setting for Pm. Since in theory it is possible to just reach the CSP and still maintain stability, a third criterion, the rate of change of real power is used to detect that the load angle is still increasing. From the power/load angle characteristics in Figure 1, it can be seen that at the CSP, if the load angle is still increasing, then the real power output will be decreasing, i.e the rate of change of power (ΔP/Δt) will be negative. This forms the final criterion:

$$(\Delta P/\Delta t) \le (\Delta P/\Delta t)_{min} \qquad (3)$$

Where $(\Delta P/\Delta t)_{min}$ is a margin for error, allowed for in this expression to ensure secure reliable relay operation. Derivation of this margin for error will be discussed later.

Extra constraints are also necessary to eliminate mal-operation due to faults. Faults introduce oscillations in power of double system frequency, which will produce a change in sign in (ΔP/Δt) every half cycle. Since pole slipping is a slow process compared with faults, if the above three criteria (equations 2 and 3) must be satisfied for at least one cycle, faults will be blocked due to the change in sign occurring every half cycle.

5. CONDITION MONITORING TECHNIQUES.

This algorithm is primarily intended for inclusion in a microprocessor based integrated generator protection package[7]. The only information available to the relay is the three voltage and three current signals that are produced by the relay's VT's and CT's. Since no prime mover input power signal is available, a method is required which estimates the prime mover input power, Pm from these voltage and current signals, in order to provide an algorithm setting, Pt. This is achieved using the following algorithm:

$$if \quad |P - P_{n*lag}| \le P_{tol} \quad ; then \; Pt = P \qquad (4)$$

where lag is a predefined time, and n is an integer varied from 0 to n, P_{tol} is the expected oscillation in output power due to irregular prime mover torque, chosen as nominally 5 % of machine rating. P is the present value of real power, this evaluation is performed every lag seconds. The value of lag and n are chosen to provide a compromise between reliable evaluation of Pm, and expeditious update times. A value of lag of 1 second was chosen in conjunction with a value for n of 3, resulting in 3 seconds of steady state operation within P_{tol} being required before Pt is updated.

Adaptive $(\Delta P/\Delta t)_{min}$ Setting.

As well as a continuously changing real power setting, an adaptive $(\Delta P/\Delta t)_{min}$ is used in order that algorithm performance be optimised for both steady state and transient loss of synchronism pole slips. A value for $(\Delta P/\Delta t)_{min}$ is derived by assuming that the power output of the generator can be expressed as the symmetrical function;

$$P = P_{max} \sin \delta \qquad (5)$$

Where P_{max} is the maximum machine output just before pole slipping. The load angle at the CSP is given by (using Pm = Pt):

$$\delta_p = 180 - \sin^{-1}\left(\frac{P_t}{P_{max}}\right) \qquad (6)$$

The derivative of real power can be expressed as:

$$\frac{dP}{dt} = \frac{dP}{d\delta}\frac{d\delta}{dt} \qquad (7)$$

The derivative of load angle with respect to time is the slip, s and is expressed as:

$$\frac{d\delta}{dt} = -s \qquad (8)$$

i.e. negative values of slip exist for speeds above synchronous speed. If equation 5 is differentiated with respect to load angle then ;

$$\frac{dP}{d\delta} = P_{max} \cos \delta \qquad (9)$$

Hence the derivative of real power at the CSP can be expressed as;

$$\left.\frac{dP}{dt}\right|_{CSP} = -s\, P_{max} \cos\left(180 - \sin^{-1}\left(\frac{P_t}{P_{max}}\right)\right) = (\Delta P/\Delta t)_{min} \qquad (10)$$

A value for the margin for error can therefore be obtained by deciding on a minimum value of slip permitted at the CSP. This value will not ultimately be the minimum value of slip at which a trip signal will be issued due to the errors introduced in assuming a constant sinusoidal power/load angle characteristic. In reality, errors will be introduced by non-adherence of the machine to the constant flux linkage theorem, asynchronous induction generator effects, and transient saliency. Only transient saliency can be accounted for, however to do this requires more generator data, which is often not available to the commissioning engineer. The errors will cause a decrease in the observed negative value of $(\Delta P/\Delta t)$, so the value of slip chosen can be selected accordingly. Equation 10 is used by the algorithm to continuously adjust the value of $(\Delta P/\Delta t)_{min}$ according to what the variables Pt and P_{max} dictate.

Determination of P_{max}.

If the generator pole slips due to a steady state loss of synchronism, no peak will occur in the real power before the event, as shown in Figure 2b. If the pole slip is due to a transient loss of synchronism (due to a fault, or line switching etc) then a peak will occur before the pole slip, as shown in Figure 4b. This will cause larger values of $(\Delta P/\Delta t)$. The value of P_{max} used in deriving $(\Delta P/\Delta t)_{min}$ is nominally set to 1.25*Pt, in order that the cosine expression in (10) does not fall below -0.6, giving a minimum value of $(\Delta P/\Delta t)_{min}$ of $0.6*s*P_{max}$. An absolute minimum value of P_{max} must also be chosen to ensure $(\Delta P/\Delta t)_{min} = 0$ never occurs. If generator output power does rise above 1.2*Pt for more than half a power system cycle, then the value for P_{max} used in deriving $(\Delta P/\Delta t)_{min}$ is updated to this value for a time of 1 second, which ensures that the correct value of P_{max} is used if a pole slip does occur. The half cycle constraint ensures that P_{max} is not incorrectly updated for short spikes in power produced by disturbances such as faults.

6. SIMULATION STUDIES.

The protection algorithm was tested using a computer based dynamic simulation package and a laboratory embedded generation model.

The laboratory embedded power system was comprised of two 5 kVA generators driven by 8 hp dc machines, connected to a 'local' load and a 200 V laboratory 'utility' supply. Pole slipping was induced in the protected machine by suddenly inserting a resistor in parallel with the field supply, so that the field was weakened sufficiently to cause pole slipping within the time frame of the micro-computer based relay being used for data recording. The full range of fault types were also placed on the local load busbar to test the algorithms stability against such disturbances.

The computer based simulation package was used to model power swings and pole slips. A simplified one machine (588 MVA) and infinite bus (58.8 GVA) power system model was used, which possessed 'ideal' power system characteristics. For the power swing, the generator power was first reduced from rated power (500 MW) to half rated power. A three phase fault was then placed on the generator transformer to trigger a power swing that came close to the CSP. This technique was used to test the adaptive Pt algorithm.

The Pole slip started with a change in output power from 250 MW to 500 MW, and was triggered also by a three phase fault, the duration of which pushed the generator far beyond the CSP, therefore producing a very fast and violent pole slip.

7. TEST RESULTS.

Figure 2 shows the algorithm results for the laboratory pole slipping test. The machine was initially operating at it's minimum value of excitation, indicated by the initial negative value of reactive power. The field was weakened by inserting the parallel resistor at a time of 0.8 seconds, which caused a glitch in the real power signal. The reactive power progressively decreased as the load angle increased due to the rotor's field not being strong enough to hold it in synchronism.

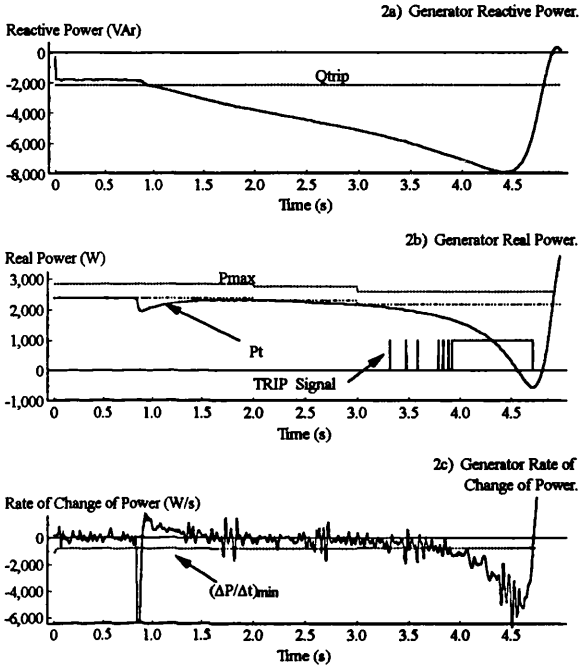

Figure 2. Generator Pole Slipping Due to Weak Field.

An update in Pt occurs just before the real power starts to drop away suddenly, this was due to the power staying within the tolerance, P_{tol} of equation 4. Once the real power started to drop suddenly with further load angle increase, only the rate of change of power criterion was blocking algorithm operation. This was finally satisfied at a time of 3.3 seconds, which was the first time $(\Delta P/\Delta t)$ was less than $(\Delta P/\Delta t)_{min}$ for one cycle. The algorithm therefore produced a trip signal a significant time before the pole slip had occurred, with the real power output of the machine still high at a value of 2 kW. The trip signal produced by the algorithm was intermittent until 3.9 seconds, this was due to a noisy $(\Delta P/\Delta t)$ signal. This distortion was due to noise being induced in the data acquisition system, due to inadequate levels of shielding. The action of differentiating increases these noise levels to an observable magnitude and provided an opportunity to test the algorithm in extreme noise conditions, where it successfully functioned.

Other tests using a variety of fault types did not cause any mal-operations. The two phase to earth and three phase faults provided the most testing conditions for the algorithm.

Using results from the simulator, Figure 3 shows that the algorithm remained stable for the simulated three phase fault induced power swing, which caused the load angle to rise to 160°. Figure 3a shows that the reactive power increased from 0 to 250 MVAr over the fault period (5.5 to 5.8 seconds), and then jumped to -500 MVAr when the fault was removed. This satisfied the first criterion for the algorithm, since Q < Qtrip, indicating a load angle of greater than 90°. Figure 3b shows that the active power criterion was not satisfied over this period, indicating that decelerating power was still

available and thus blocking algorithm operation. Inspection of the adaptive prime mover setting, Pt in Figure 3b shows the three second update time taken in adjusting from the old value of 500 MW to the new value of 250 MW. After this update at 5 seconds on the record no changes occurred in Pt, indicating that the algorithm used (equation 4) functioned correctly.

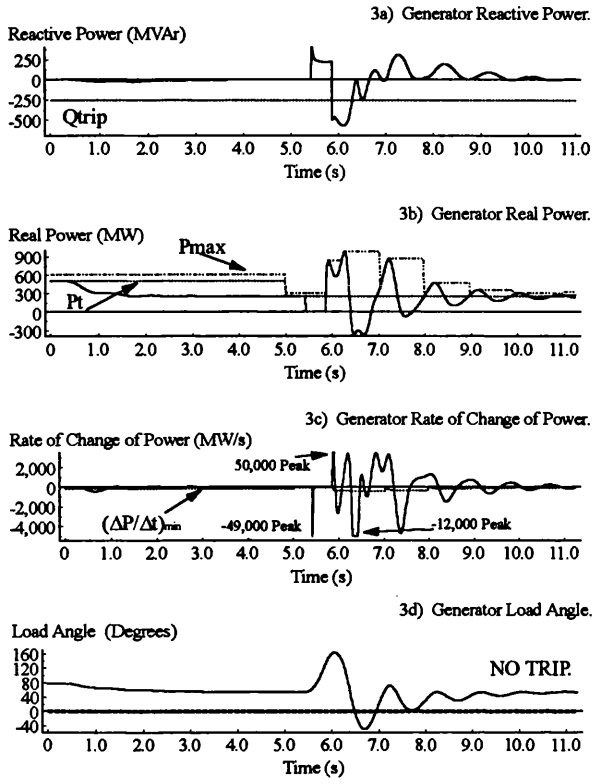

Figure 3. Generator Power Swing Due to Three Phase Fault.

Figure 4 shows the algorithm measurands for the simulated pole slip using the computer model, which caused the algorithm to correctly operate. Observation of Pt in Figure 4b shows that it was updated from 250 MW to 500 MW and then no further change occurred. Also at this time, P_{max} increased to satisfy the P_{max} = 1.2*Pt requirement. Before this time it can be seen that P_{max} tracked the output power of the machine, since this was higher than 1.2*250 MW, i.e. the old Pt setting. This resulted in an increase in inherent stability of the algorithm, due to the trip setting for the rate of change of power criterion $(\Delta P/\Delta t)_{min}$, becoming progressively more negative as Pt/P_{max} decreased.

At a time of 5.7 seconds the reactive power, Q falls below Qtrip. Shortly after this the real power, P falls below the Pt setting, and the rate of change of power signal $(\Delta P/\Delta t)$ falls below $(\Delta P/\Delta t)_{min}$, resulting in the algorithm producing a trip signal. The algorithm produced a trip signal at a load angle of 170°. Inspection of P_{max} also shows the temporary 1 second update to the value dictated by the peak in real power just before the pole slip.

This action can also be seen in Figure 3c, where P_{max} can be seen to be returning to the nominal value of 1.2*Pt, shortly before being updated by the next peak. Inspection of the $(\Delta P/\Delta t)_{min}$ signal of Figure 4c shows how it decreases when P_{max} is increased due to a peak. This de-sensitises the $(\Delta P/\Delta t)$ part of the algorithm for large swings in power, thus improving algorithm security. However, if a peak does not occur, as in the case of steady state loss of synchronism, $(\Delta P/\Delta t)_{min}$ is at it's lowest value for a given value of Pt, providing a more sensitive algorithm when required.

8. CONCLUSIONS.

The new power based algorithm successfully operated for pole slipping conditions, providing a trip signal before the machine actually slipped. It successfully restrained for power swings and external faults. The use of condition monitoring methods simplifies the settings of the algorithm. This only requires the generator rating and quadrature axis synchronous reactance. Monitoring the prime mover input power and maximum output power also provides a means of adjusting the algorithm settings depending upon the type of pole slip that could be potentially occurring and thus optimising the algorithm's performance.

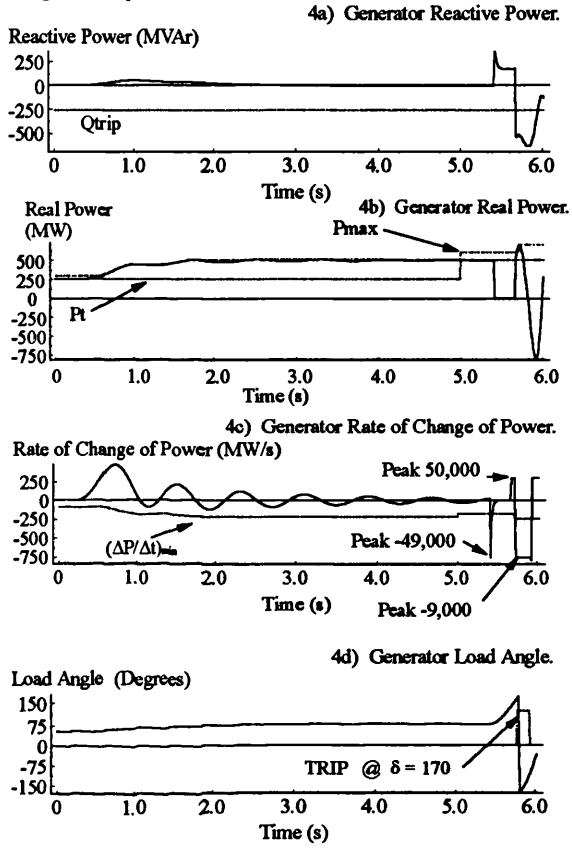

Figure 4. Generator Pole Slipping Due to a Three Phase Fault.

9. REFERENCES.

[1] REDFERN M A and CHECKSFIELD M J, 'An Investigation into Pole Slipping Protection for Small and Medium Sized Embedded Generation', Proc. 28th UPEC, Stafford, Sept 1993, pp 957- 960.

[2] IMHOF J. A. (Chairman) et al, "Out of Step Relaying for Generators - Working Group Report," IEEE Trans. on Power App. and Systems, Vol.PAS-96, No.5, Sep/Oct 1977, pp 1556-1564.

[3] CLARK H K and FELTES J W, 'Industrial and Cogeneration Protection Problems Requiring Simulation', IEEE Transactions on Industry Applications, Vol 25, No.4, July/August 1989, pp 766-775.

[4] GUILE A E and PATERSON W. 1977. Electrical Power Systems Volume 2: Pergamon Press.

[5] MASRUR M A, AYOUB A K and TIELKING J T, 'Studies on Asynchronous Operation of Synchronous Machines and Related Shaft Torsional Stresses', Proc.IEE, Part-C, Vol.138,Jan '91, pp47-56.

[6] CEGB: Modern Power Station Practice - Vol.4 - Generator and Electrical Plant, 1963 - Permagon Press, pp 126-153.

[7] ZIEGLER G, 'Developments in Generator Protection - Design and Application Aspects of a New Numerical Relay Range', IEE Conference Publication No. 368, 1993, pp 111-114.

PAPER FOUR

"A POWER BASED CONDITION MONITORING ALGORITHM FOR DETECTING DISPERSED GENERATOR LOSS OF SYNCHRONISM"

M J Checksfield and M A Redfern

Presented at :-
International Power Engineering Conference (IPEC) 1995,
Singapore, February 1995, Volume 1, pp 328 - 333.

A POWER BASED CONDITION MONITORING ALGORITHM FOR DETECTING DISPERSED GENERATOR LOSS OF SYNCHRONISM.

M. J. Checksfield and M. A. Redfern.
University of Bath, UK.

Abstract

This paper introduces a new loss of synchronism (LOS) relay which uses condition monitoring and adaptive techniques to reduce the complexity of installation. As previously reported [1] this approach uses the Equal Area Criterion as its basis to provide a trip signal *before* the LOS occurs. By doing this, it reduces the likelihood of machine damage and voltage disturbances due to generator LOS. The algorithm's derivation is given and its performance tested using a variety of system operating scenarios from power swings to faults.

Keywords

Loss of synchronism, pole slipping, dispersed generator protection, microprocessor based relay.

1 INTRODUCTION

The majority of traditional LOS relays use the variation in 'apparent' impedance at the generator's terminals to detect a LOS condition[2]. If the impedance crosses two measurement characteristics on an impedance plane within a specified time limit, a trip signal is issued.

However, there are two problems with this approach. The relays function by observing the impedance variation produced by the complete LOS condition, and therefore only provide a trip signal once the LOS has occurred. This means that an unstable generator may already have undergone damage and would cause voltage disturbances before it was disconnected from the system.

Choosing the correct boundaries and time limits on the impedance plane can also be a difficult process, especially when dispersed generators are being considered since they can produce unpredictable impedance variations [3]. If the wrong relay settings are chosen, the LOS condition may go undetected, or worse still, the relay may mal-operate due to a power swing or power system fault.

For these reasons, research has been carried out into a new LOS algorithm which can be included in a modern microprocessor based integrated protection scheme for dispersed generators. The new approach reduces the complexity of installation and provides a trip signal before the LOS actually occurs.

2 LOSS OF SYNCHRONISM PROTECTION

LOS protection is required to reduce the damage caused to the generator by the LOS or pole slipping condition, and to ensure that the quality of supply of consumers connected electrically close to the effected generator remains acceptable. The degree of these ill-effects depends upon the relative rating of the bus to which the generator is connected, the speed with which the generator loses synchronism, and the overcapacity rating of the generator.

When the dispersed generator is connected to an infinite utility bus, then the currents experienced during LOS can be in excess of those experienced during three phase faults. Generator windings are normally designed to withstand three phase fault levels, and the higher current levels experienced therefore loosen and abrade the windings [3].

High utility infeeds also increase the risk of generator shaft damage during LOS. Turbine generators are especially vulnerable since the pulsating torques experienced can torsionally excite resonant sections of the turbine shaft. One study [4] found that the generator-exciter section was most at risk after the *first* torsional oscillation produced by a LOS. It can therefore be concluded that if shaft damage due to LOS is to be minimised, the generator must be disconnected from the power system *before* the LOS occurs, in the hope that the torsional impulse will be avoided.

Synchronous machines are not designed to operate asynchronously, the resulting induced currents experienced during a LOS can cause stator and rotor

overheating. Induced field winding currents can stress the generator exciter insulation and semiconductor devices due to the excessive voltages they produce. The semiconductor devices do not allow reverse field current flow, therefore when the field current tries to reverse during the LOS, it is blocked and a high voltage results.

The effect of LOS on other consumers connected close to the effected generator is most pronounced if the utility infeed is of a relatively low capacity. The 'system centre' is an expression often used to describe the point in the power system where the contribution from the generator equals that from the rest of the system. At this point the voltage fluctuations experienced will be at their most severe, the voltage may even fall to zero. For the normal generator/infinite bus situation the system centre appears inside the generator. However, if the utility infeed is low, then the system centre may appear in the load network.

The voltage fluctuations at the system centre can cause plant outages, and in extreme cases, cause a cascading LOS of nearby machines [5], including both generators and motors. If the voltage depressions last for too long a period, then induction motors may stall depressing system voltage further.

If the system centre occurs in the zone of a distance relay, LOS may cause it to mal-operate since the system centre takes on the appearance of a fault, i.e a low voltage and high current. The LOS condition can also cause other protection relays to mal-operate, such as undervoltage and overcurrent relays. If adequate blocking is not applied to the effected relays, then unnecessary outages could occur.

3 GENERATOR STABILITY ASSESSMENT

The Equal Area Criterion is one of the simplest methods for assessing generator stability for a given transient disturbance. If the power/load angle curves for all states of power system operation are known, then generator stability and hence the possibility of LOS can be ascertained for a given disturbance. The disturbances most likely to cause LOS are severe faults, large load switching operations, and excitation system faults.

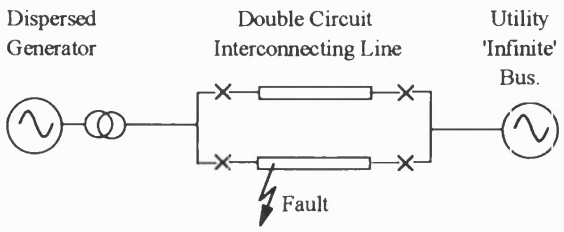

Figure 1 - Dispersed Generator Utility Connection.

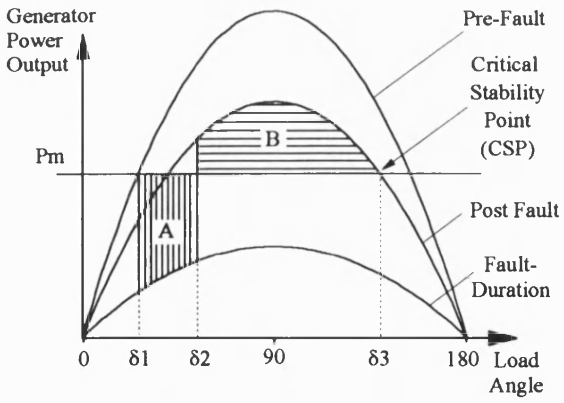

Figure 2 - The Equal Area Criterion.

Consider the case where a transient disturbance results from a three phase fault on one side of a double circuit line as shown in Figure 1. The fault is removed by disconnecting the faulty circuit, leaving the healthy side of the line to transfer power at a reduced capacity. The Equal Area Representation of this scenario is shown in Figure 2.

The Pre-fault curve corresponds to the initial operating condition, where both lines are transferring power, in this condition the dispersed generator's power transfer capability is at its maximum. The fault duration curve represents the generator's power/load angle characteristic during the fault period. The three phase fault severely reduces system voltage so that power transfer is impaired. The post fault curve depicts the power transfer capability once the faulty line has been disconnected, the power transfer capability is reduced due to the increase in the interconnecting impedance.

The generator's prime mover input power is given by the line Pm. The interception of the prefault output curve and prime mover input curve gives the initial load angle $\delta 1$. When the fault occurs the generator's output characteristic falls down to the fault duration curve. The resulting discrepancy between input and output powers produces a net accelerating torque on the generator rotor. As the rotor accelerates the load angle increases, until the fault is removed, which in this example corresponds to a load angle of $\delta 2$.

At the instant the fault is removed, the generator's output characteristic jumps up above the line Pm to the post fault curve. This results in a net retarding force on the generator rotor, but because the rotor is now travelling above synchronous speed, the initial retarding force is used to remove kinetic energy from the rotor, in order to return the rotor to synchronous speed. If this is achieved before the rotor reaches load angle $\delta 3$, then the retarding force will slow the rotor to below synchronous speed, thus causing the load angle to decrease back

towards a stable operating value. If however, the rotor does not reach synchronous speed by load angle δ3, then it will again start to accelerate, due to the output power characteristic of the generator falling below the input power line Pm, causing an accelerating torque once more. This is the unstable situation which results in LOS.

The Equal Area Criterion states that the accelerating energy on the rotor due to a disturbance can be represented by area 'A', whilst the decelerating energy is represented by area 'B'. For synchronism to be lost, the net accelerating energy for a given disturbance must exceed the net decelerating energy, i.e a LOS will occur if area 'A' is greater than area 'B'. It can be seen from Figure 2 that the limiting point for stability occurs when the generators output power falls below its input power, this point is referred to as the *Critical Stability Point* (CSP). If the generator operates past this point, then stability cannot be maintained, and a LOS will occur.

4 THE NEW LOS ALGORITHM

The algorithm predicts LOS by detecting if the load angle is still increasing once the CSP has been exceeded. In designing a LOS algorithm, it must be able to predict when a generator is committed to a LOS. It must also remain stable for all other power system conditions, including faults and power swings.

Figure 2 shows that once the CSP has been exceeded, the load angle is greater than 90°. The reactive power output characteristics of a generator are such that at a load angle of 90°, the reactive power demand of the machine is always given by :

$$Q = -\frac{V^2}{Xq} \qquad (1)$$

where V is the machine terminal voltage, and Xq is the quadrature axis synchronous reactance. This value is denoted as the reactive trip criteria, *Qtrip*. If the generator's reactive power demand falls below this negative value, then it's load angle must be greater than 90°, indicating that it is operating in a potentially unstable area.

Generator real power is used in conjunction with the reactive criterion to determine whether or not the generator is operating at, or beyond the CSP. From Figure 2 it can be seen that when the CSP has been exceeded, the generators real power output, P is less than the prime mover input power level, *Pm* indicating that no more decelerating power is available. Operation at, or beyond the CSP is therefore recognised when :

$$\begin{aligned} &Q \leq Qtrip \\ &\quad and \\ &P \leq Pm \quad (= Pt) \end{aligned} \qquad (2)$$

where *Pt* is the algorithm's trip setting for the prime mover input power, *Pm*.

The third criterion uses the rate of change of power $(\Delta P/\Delta t)$ to deduce that the load angle is still increasing in an unstable manner at the CSP. If the machine had maintained stability after just reaching the CSP, the load angle would be decreasing.

From Figure 2 it can be seen that at and beyond the CSP, the real power output of the machine decreases with load angle increase. Therefore, if the rate of change of power, $(\Delta P/\Delta t)$ is negative at the CSP it can be concluded that the load angle is still increasing and that the generator is unstable and a LOS will occur. This forms the third and final criterion for detecting LOS :

$$(\Delta P/\Delta t) \leq (\Delta P/\Delta t)_{min} \qquad (3)$$

where $(\Delta P/\Delta t)_{min}$ is a margin for error allowed for in this expression to ensure algorithm mal-operation due to measurement errors or noise does not occur.

4.1 Fault Blocking

With the criteria set out in Equations (2 & 3) the algorithm successfully predicts LOS. However it mal-operates for power system faults. To overcome this fault blocking constraints are required. Unbalanced faults introduce oscillations in power of twice power system frequency, which produce a corresponding change in sign of $(\Delta P/\Delta t)$ every half cycle. A LOS condition is slow compared to faults and so if the criteria of Equations (2 & 3) have to be satisfied for one power system cycle continuously, unbalanced faults will be blocked due to the change in sign of $(\Delta P/\Delta t)$, whilst the algorithm is only delayed from tripping by one cycle for a LOS condition.

In addition to this, faults also produce values of $(\Delta P/\Delta t)$, which are far in excess of those witnessed due to LOS. If a maximum negative magnitude is chosen such that a LOS condition will never produce it, but faults will, then this can be used as another form of fault blocking. If $(\Delta P/\Delta t)$ falls below this limit, referred to as $(\Delta P/\Delta t)_{max}$ then algorithm operation can be blocked.

5 CONDITION MONITORING TECHNIQUES

In a dispersed generator microprocessor based relaying environment, the only information normally available to the relay is the 3 Voltage and 3 Current signals provided by the relay's transducers. Dispersed generators may be operated over a range of output powers and so a method of monitoring the prime mover input power, *Pm* is

necessary in order to determine the algorithm trip setting, *Pt*. The algorithm has been designed with a microprocessor relaying platform in mind, a limited amount of processing power is therefore available to achieve this goal. The input power, *Pm* is effectively found by monitoring the power output of the generator, if this remains constant for a sufficient amount of time, then the input value must approximately equal this value, the only discrepancy being produced by the losses in the generator. The following algorithm performs this function :

$$if \quad |P - P_{n*lag}| \leq P_{tol} \quad ; then \; Pt = P \qquad (4)$$

where *lag* is a predefined time, and *n* is an integer varied from 0 to *n*. P_{tol} is the expected oscillation in generator output power, due to irregular input torque, chosen as nominally 5% of machine rating and *P* is the machine output power. This evaluation is performed every *lag* seconds. The value of *n* and *lag* are chosen so that update times are satisfactorily short and accuracy is sufficiently high.

5.1 Adaptive Trip Settings

5.1.1 $(\Delta P/\Delta t)_{min}$ Setting. Assuming a sinusoidal power load angle curve, then for a given value of slip at a given power input level, $(\Delta P/\Delta t)_{min}$ can be calculated using :

$$\frac{dP}{dt}_{@CSP} = -s\, P_{max}\cos(180 - \sin^{-1}(\frac{Pt}{P_{max}})) = (\Delta P/\Delta t)_{min} \qquad (5)$$

It should be stressed that the value of slip chosen will not be the exact value at which the relay produces a trip output, due to the assumptions used in deriving Equation (5). Inaccuracies due to transient saliency and induction generator action will cause $(\Delta P/\Delta t)$ to be more negative than predicted by Equation (5).

Equation (5) is used by the algorithm to continuously update the trip setting $(\Delta P/\Delta t)_{min}$ depending on what the variables P_{max} and *Pt* dictate.

5.1.2 Determination of P_{max} . The maximum power output of the generator is monitored so that the algorithm can adjust its setting according to whether a transient or steady state LOS will occur. For a transient LOS, the generator's output during the first swing will be much greater than its nominal output. This results in a greater magnitude in the signal $(\Delta P/\Delta t)$, the algorithm therefore adjusts its setting $(\Delta P/\Delta t)_{min}$ accordingly. For a steady state LOS, no peak will occur in the power output before the LOS, the algorithm trip setting should therefore be at its most sensitive level to detect the LOS in the shortest time possible.

The value of P_{max} used by Equation (5) is nominally set to *1.25*Pt*, so that Equation (5) evaluates to minimum setting level of *0.6*s*Pmax* (*= 0.75*s*Pt)*. If the generator's output rises above *1.25*Pt* for greater than a half a power system cycle, then the value of P_{max} is updated to the new maximum for a duration of one second. The one second limit is used so that the new value of P_{max} is only used for the period where a LOS associated with that value is likely to occur. The half cycle constraint is necessary so that incorrect values of P_{max} do not result due to spikes on the power waveform.

6.0 SIMULATION STUDIES

A laboratory dispersed generation model and a computer based dynamic simulation package were used to test the algorithm's performance at predicting LOS and restraining for faults and power swings.

The laboratory dispersed generation model consisted of two 5 kVA synchronous generators driven by 8 horse power dc motors. These were connected to a 'local' load and a 200 V laboratory 'Utility' supply. This was useful for testing the algorithm in a real life situation, since harmonics and heavily alternating loads nearby made the supply far from ideal. To test the condition monitoring section of the algorithm the generator was ran initially at low power, when data recording started, the input power was then increased. A short while after, the LOS was forced by quickly inserting a resistor in parallel with the generator field winding which weakened the field sufficiently to cause a LOS.

The laboratory model was also used to test the algorithm during power system fault conditions. All of the fault types possible were placed temporarily on the local load busbar by switching in a 'fault' resistance.

The computer based dynamic simulation package was used to test the algorithm's performance against power swings and LOS. The model used was the simple one machine (588 MVA), infinite bus model (58.8 GVA). A power swing was caused by placing a fault on the generator transformer terminals of sufficient duration to cause the generator rotor to swing up to the CSP and back down to a stable operating area.

To test the algorithm for detecting LOS, the simulated generator was initially set to run at maximum output power. The input power was then reduced to half rating in order to test the condition monitoring section of the algorithm. A three phase fault of slightly longer duration than the one used to trigger the power swing was then used to cause a LOS.

7 TEST RESULTS

Figure 3 shows the algorithm variations for the laboratory system weak field LOS test. Inspection of plots a and b show that the generator was initially operating overexcited at very low power. At a time of 1s on the record the power input to the generator was increased so that the machine operated at approximately 2.5 kW. Observation of the $(\Delta P/\Delta t)_{min}$ curve in plot c shows that because *Pt* was not updated during this period, the trip setting $(\Delta P/\Delta t)_{min}$ gradually decreased, resulting in a de-sensitising of the algorithm. This is beneficial since the likelihood of LOS is higher during adjustment to a higher output level.

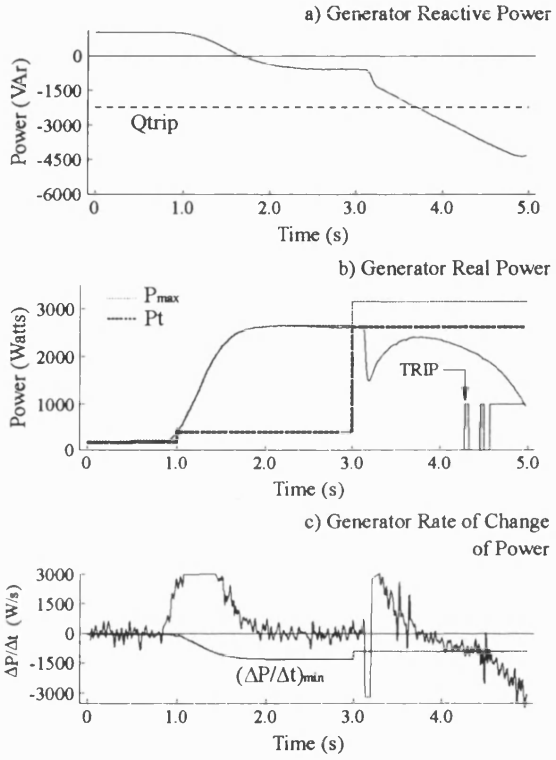

Figure 3 - 5 kVA Generator Loss of Synchronism (LOS).

At a time of 3s on the record, the condition monitoring part of the algorithm updates the value of *Pt* to the new operating level. This caused a drop in magnitude of $(\Delta P/\Delta t)_{min}$, but it did not drop back to the initial value, due to *Pt* being at a higher level. This is the desired effect since at higher input powers, more severe LOS can occur and more negative values of $(\Delta P/\Delta t)$ are produced.

Shortly after the update, the resistor was connected in parallel with the field, causing the LOS to occur. Inspection of the reactive power plot shows that this criterion was satisfied at 3.75 s, when the reactive power fell below the trip setting, *Qtrip* indicating that the load angle had increased to a value above 90°. Inspection of the real power plot shows that after insertion of the parallel resistor, the generators field was weakened sufficiently so that the generator could not maintain the level of output required, the real power criterion was therefore satisfied on inserting the resistor.

The final criterion ($\Delta P/\Delta t$) , can be seen to fall below its trip setting $(\Delta P/\Delta t)_{min}$ at a time of 4.3s. This meant that all three criteria were satisfied for the one cycle required and a trip signal was therefore produced. The trip signal can be found on the real power plot, it can be seen that the trip was issued a significant time before the LOS occurred. The usual point where LOS is said to have occurred is when the machine goes from generator to motor action, i.e when the power output of the machine goes negative. Unfortunately, in this case the whole LOS could not be recorded, due to limitations in the data acquisition system.

Figure 4 shows the algorithm's response to a two phase to earth fault. Of all the fault types tested, this and the three phase faults provided the toughest conditions for testing algorithm stability. The reactive power criterion was satisfied for a small period on removal of the fault, at 1.4 s on the record. During this time the real power criterion is satisfied for a very short amount of time, before the real power output of the generator jumps above the trip setting *Pt*. It is this short interval where algorithm mal-operation is most likely. However, inspection of the $(\Delta P/\Delta t)$ plot shows that during this period, the $(\Delta P/\Delta t)$ signal jumps to a negative value off of the scale for a very short time, before escalating to a very high positive value for a short time. These oscillations took less than one power system cycle, and so the algorithm was continually restrained.

The algorithm also successfully restrained for all of the other fault types tested.

Figure 5 shows the dynamic simulator results. Initially the generator was operated at full power, it was then reduced to half rated operation. The condition monitoring part of the algorithm updated at a time of 3.75s on the record. Inspection of the $(\Delta P/\Delta t)_{min}$ curve shows that until the update it stayed at its high power level, resulting in the algorithm being de-sensitised for a small duration. This is unavoidable, but is of no great concern since in the event of a LOS it would just result in the algorithm producing a trip signal delayed by a small time. At 4.75 s on the record the fault was placed on transformer bus, and removed again at 5.2s.

On removal of the fault the generator's reactive power was less than *Qtrip*, satisfying the reactive criterion indicating that the load angle was above 90°. At the same time, the real power output is much greater than the nominal value before the fault.

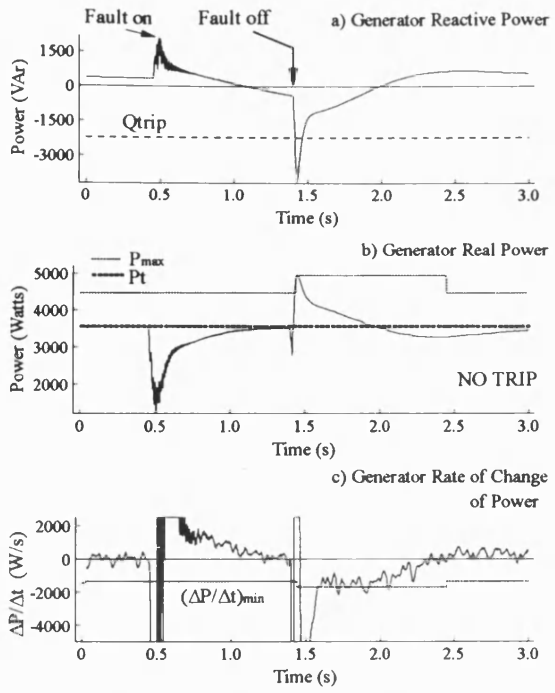

Figure 4 - 5 kVA Generator 2 Phase to Earth Fault Test.

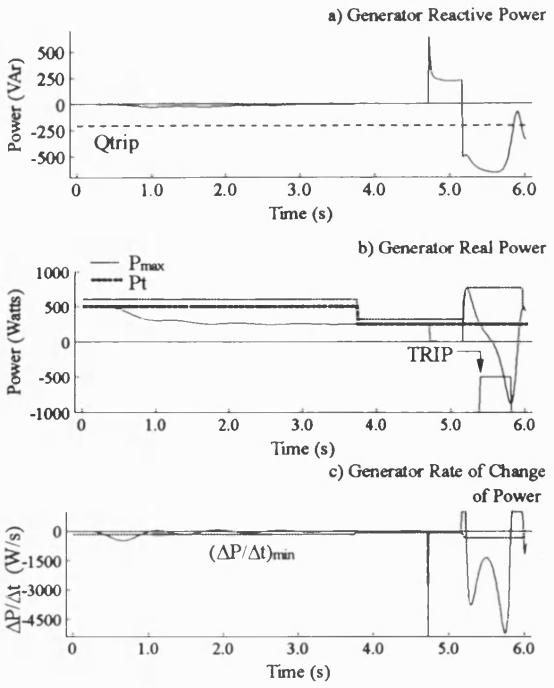

Figure 5 - 588 MVA Generator Loss of Synchronism Due to a Three Phase Fault.

This invoked the adaptive P_{max} part of the algorithm, which tracked the real power output up to its maximum value, and then held this value for 1 second before returning back to *1.25*Pt*.

This action resulted in $(\Delta P/\Delta t)_{min}$ falling to a lower level, thus desensitising the algorithm to the pending transient LOS. The $(\Delta P/\Delta t)$ signal still fell below the trip setting $(\Delta P/\Delta t)_{min}$ for one cycle, and during this time the other two criteria were satisfied. A trip signal therefore resulted.

The algorithm successfully restrained for the power swing test, which produced a severe swing in load angle up to a value of 160°.

8 CONCLUSIONS

The new algorithm successfully predicted LOS before it actually occurred. In doing so the new algorithm offers the advantage over traditional relays of disconnecting the generator before the LOS, minimising the potential damage. It successfully restrained for all of the fault types and for power swings. The algorithm's adaptive nature helps improve algorithm performance for steady state and transient LOS by monitoring the input and maximum powers. In addition to this, it simplifies the installation procedure. Since only the q-axis synchronous reactance and the machine rating are required to set the LOS protection function.

9 REFERENCES

[1] M. A. Redfern and M. J. Checksfield. A New Pole Slipping Protection Algorithm for Dispersed Storage and Generation Using the Equal Area Criterion. Presented at the *IEEE PES Summer Meeting, San Francisco*, 94 SM 425-9 PWRD, July 1994.

[2] J. A. Imhof et al. Out of Step Relaying for Generators - Working Group Report. *IEEE Trans. Power Apparatus and Systems*. Vol PAS-96, No.5, Sep/Oct 1977, pp 1556 - 1564.

[3] H. K. Clark and J. W. Feltes. Industrial and Cogeneration Protection Problems Requiring Simulation. *IEEE Trans. Industry Applications*. Vol IA-25, No.4, July/August 1989, pp766-775.

[4] M. A. Masrur et al. Studies on Asynchronous Operation of Synchronous Machines and Related Shaft Torsional Stresses. *IEE Conf. Proc.* Part C, Vol.138, Jan 1991, pp 47-56.

[5] L. J. Powell. An Industrial View of Utility Cogeneration Protection Requirements. *IEEE Transactions on Industry Applications*, Vol IA-24, No.1, Jan/Feb 1988, pp 75-81.

PAPER FIVE

"ASSESSMENT OF EMBEDDED GENERATOR STABILITY WHEN CONNECTED TO A HV UTILITY DISTRIBUTION SYSTEM"

M J Checksfield and M A Redfern

Presented at :-
30th Universities Power Engineering Conference (UPEC),
September 1995, Greenwich, UK, pp 219 - 222.

ASSESSMENT OF EMBEDDED GENERATOR STABILITY WHEN CONNECTED TO A HV UTILITY DISTRIBUTION SYSTEM.

M J Checksfield & M A Redfern.

University of Bath, UK.

ABSTRACT.

Concern is mounting about the likelihood of instability of embedded generators which are being installed to operate in parallel with utility distribution systems. This is due to their low inertias, high resistances and low time constants. A stability assessment of a 625 kVA embedded generator connected to an 11 kV distribution system is used to illustrate the factors affecting stability.

1. INTRODUCTION.

The installation of small and medium sized synchronous generators to operate in parallel with a Regional Electricity Companies (REC) distribution system has become commonplace. These embedded generators pose technical problems which normally do not have to be considered with the large grid generators connected to transmission circuits. One concern is the transient stability margins of these machines. Transient stability is the ability of the generator to produce forces which act to restore the generator back to a state of equilibrium following a transient disturbance. Transient disturbances can be produced by load changes, switching operations and electrical faults.

A transient disturbance, such as a fault will reduce a generator's ability to provide output power. The input power from the prime mover will not follow this change however. This mismatch between input and output results in an accelerating torque on the generator's rotor which causes the load angle of the generator to increase. If the load angle increases beyond a certain angle, called the critical clearing angle, δc, then the generator will not be able to provide the necessary decelerating forces to return the generator back to a stable operating point. A further increase in load angle will cause the generator to lose stability and 'slip poles' until either it's rotor returns to synchronous speed and re-synchronises to the REC's power system, or the generator is disconnected by protective relays.

The time taken for the load angle to swing from its initial value to the critical clearing angle (δc) for a 3 phase short circuit fault, is referred to as the Critical Clearing Time (CCT). Faults must therefore be cleared within this time in order to maintain stability. In most cases of transient stability assessment, if the machine does not lose stability during the first swing in load angle, it will maintain stability for that disturbance.

For most embedded generators, the point of connection to the REC's distribution system can be thought of as a connection to an infinite bus, that is a bus whose frequency and voltage remain un-affected by the embedded generator's operation. This simplifies the discussion of stability greatly since the one machine - infinite bus is the most basic system from a stability analysis viewpoint. If the REC's bus is not infinite, then the system can be represented as a two machine system, which is also relatively simple to analyze.

2. FACTORS AFFECTING GENERATOR STABILITY.

The factors which affect synchronous generator stability can be split into two different categories, those which are determined by the generator and its control equipment, and those which are dependent upon the configuration and operation of the system to which the generator is connected.

2.1 The Generator and It's Control Equipment.

The two main generator parameters which have the most affect on stability are the inertia of the generator, and the direct axis transient reactance. The most useful measure of generator inertia is the inertia constant, H in units of kW-s/kVA. The main advantage of using H compared with other measures of rotational inertia is that its value is fairly constant for a wide range of generator sizes and types, and it therefore makes comparisons between machines much easier.

2.1.1 Inertia Constant, H & Transient Reactance Xd'.

From a stability viewpoint the higher the generator's value of H, the more stable it will be. For a given fault clearing time, the machine load angle at which the fault is cleared decreases with an increase in inertia. The machine requires more acceleration energy to make its rotor advance and therefore appears less responsive and more able to withstand a mismatch between generator input and output powers.

The direct axis transient reactance, denoted Xd' is also a vital measure of transient stability because it determines the amplitude of the generator's power output - load angle characteristic. For the simplest case of a round rotor machine with resistance neglected, the transient P δ curve is given by;

$$P = \frac{EV}{Xd'} \sin(\delta) \qquad (1)$$

where E is the voltage behind transient reactance, V is the infinite bus voltage which the generator is connected to, and δ is the rotor angle. As can be seen from equation (1), the lower the transient reactance, the more output power the generator can produce. This serves to provide a greater decelerating force on the generator rotor following a transient disturbance.

2.1.2 Open Circuit Time Constant, Tdo' & Resistances.

To a lesser extent than H and Xd', other synchronous machine parameters have an effect on stability. One of these is the direct axis open circuit time constant Tdo'. Following a transient disturbance, the reactance of the generator goes from the normal steady state synchronous value, Xd to the transient value, Xd'. This can be explained using the constant flux linkage theorem. Following an increase in stator current, and therefore armature reaction, a decrease in the flux flowing from the stator to the rotor occurs, the field current therefore changes so that it can maintain constant flux linkage in the field circuit. This increased field current decays eventually, the time it takes to decay is given by the time constant Tdo', where;

$$Tdo' = \frac{Lff}{Rf} \qquad (2)$$

Lff is the field winding self inductance and Rf is the field resistance[1]. The field circuit parameters are dictated by the values given by the combination of fielding winding, rheostat and exciter armature. Tdo' determines the time taken for the reactance of the machine to change from the transient value Xd' back to the synchronous value Xd. With this change comes a corresponding decrease in the output power capabilities of the generator and hence its potential to produce decelerating forces in response to a disturbance. It follows that the higher the resistance compared with the inductance of the field, the shorter the time constant, and the less time the generator has for producing high output powers. The

average value of the time constant is around 6 seconds, and when this is compared with the mechanical period of interest for stability of 1 second the condition of constant flux linkage is valid. However, if the generator is exposed to a severe fault, which is cleared in a time of around a few hundred milliseconds[1] the constant flux theorem does not hold due to the decrease in flux which the fault causes. Embedded generators tend to have high per unit resistances, which results in them having smaller time constants.

2.1.3 Damping Power.
Another factor which can influence stability is the damping power produced by the generator. This is dependent mainly upon the type of damper winding in the machine, and the magnitude of armature resistance. As the amount of resistance increases, the damping torque produced by the machine decreases, the synchronous torque also decreases, but not by as much[2]. As well as enhancing stability by acting like an induction machine and providing positive damping, the damper windings also serve to improve stability by providing negative sequence damping and enhancing positive sequence damping during unbalanced faults, in addition to producing some DC braking[1].

2.1.4 Automatic Voltage Regulator (AVR)
As mentioned in section 2.1.2, the effect of armature reaction during a fault tends to decrease flux linkage, especially if the reactive power output of the generator is large[3]. If the generator has an AVR in operation the action of the AVR would tend to force the excitation system to boost the exciters mmf and therefore maintain flux levels. Anderson[3], states that the dominant factor with AVR's in maintaining stability is the ability to offset the affects of armature reaction during faults. Even though AVR's can significantly improve the flux levels during faults, their effect on the magnitude of the first swing in load angle is generally only a reduction of a few degrees. The situations where they are most beneficial is where the faults have long clearance times.

One possible drawback to using high performance fast AVR's is their effect on the damping of the generator. A fast AVR may reduce the magnitude of the first swing, but in doing so reduces the damping (section 2.1.3) for subsequent swings. If the reduction is severe enough the generator may maintain stability for the first swing and then lose synchronism in subsequent swings. This is known as dynamic instability, and additional stabilising feedback signals need to be incorporated into the AVR to avoid it[4].

2.1.5 Generator Governors.
Depending upon the type of prime mover/governor set used, the governor may offer a significant improvement in the CCT. If the governing system has a small overall time lag, then the CCT will be increased by its effect. Studies conducted in reference [5] show that the governor can increase the critical clearance time by approximately 40 ms. If, however, the governor and prime mover system has a long time lag, it's time constants will render it practically in-active during the first swing of a transient disturbance, and it will therefore have little effect on the CCT[6].

2.2 The System Connected to the Generator.
The two main factors which can affect the transient stability margins of a generator are the effective transfer impedance between generator and infinite bus and the protection clearance times for faults.

2.2.1 Protection Clearance Times.
Protection clearance time is the most important factor in maintaining stability, since the longer the fault exists on the system, the longer the power transfer capabilities of the generator are disrupted. The protection clearance times normally associated with high power transfer transmission circuits are usually in the region of several power system cycles, this means that only a small amount of accelerating energy is produced as a consequence of the fault. With the protection associated with distribution feeders, the clearance time can be in excess of one second if graded inverse definite minimum time overcurrent relays are employed[7,8]. With this amount of time the load angle increases so much so that the likelihood of the generator maintaining stability is low.

2.2.2 Transfer Reactance Between Generator and Infinite Bus.
The value of connecting impedance between the generator and the infinite bus has a crucial affect on generator stability. A study conducted on a 4.5 MVA generator [5] revealed that the CCT was reduced by 40 ms when the ratio of the bus at the generator terminals to the generator rating was reduced from 100:1 to 5:1. This can be explained using equation (1). Any reactance between the terminals of the generator and the infinite bus can be added to the reactance of the generator, including that of a step up transformer. Therefore it can be seen from equation (1) that an increase in connection impedance results in a decrease of the maximum output power of the generator, and therefore the amount of decelerating torque it can produce. As a general rule[5], the critical clearing time is related to inertia and reactance in the following manner;

$$CCT \;\alpha\; \sqrt{\frac{H}{(Xd' + Xt)\,(Xd + Xt)}} \qquad (3)$$

Where Xt is the transfer reactance. The situation may be made worse following the clearance of a fault since one of a set of parallel interconnections would have to be disconnected in order to clear the fault, resulting in a higher transfer impedance.

2.2.3 Effect of Resistance on Stability.
As well as the reactance of the generator and interconnection altering the stability limits, the resistance of the generator and interconnection can also adversely effect it. Normally, with large synchronous machines, the per unit values of resistance can be neglected. However, with smaller embedded machines the value of resistance both in the generator and the interconnection becomes more appreciable. As with reactance the resistance of the interconnection can be added to that of the armature circuit of the generator. In section 2.1.3 it was stated that resistance reduces the damping capabilities of the generator, lessening the stability margin. The greatest concern with high resistance values in an embedded generation environment is the affect on dynamic stability. It is possible that a high value of resistance found in a long length of cable, combined with an already lowly damped machine, low performance AVR and poorly damped governor could result in a negative value of damping[9,10,11]. This could potentially cause the machine to oscillate at its natural frequency, with the amplitudes of the oscillations increasing until the generator dynamically loses stability. The only situation where increased resistance in beneficial to stability is with a close up three phase fault, where the power dissipated in the resistance reduces the accelerating power going into the rotor.

2.2.4 Affect of Fault Type on Stability.
As the impedance of a fault decreases, so does the amount of power transfer possible from the generator, causing a lower stability limit for a given fault duration. In order of fault severity, the most severe fault is the 3 phase fault followed by 2 phase to earth, two phase, and single phase to earth. The difference in severity of faults becomes smaller as the fault duration is decreased, however, with a fault of 200 ms there is an appreciable difference[6].

2.2.5 Affect of Grounding on Stability.
The grounding of a system affects it's zero sequence impedance, Zo which in turn affects the impedance of unbalanced faults and hence the level of power mismatch caused by the fault. As Zo increases with reference to the fault location, the severity of the fault decreases. Taking it to the extreme of an infinite value of Zo, it can easily be seen that this would transform a two phase to earth fault

into a two phase fault. It is therefore beneficial from a stability viewpoint to ground through impedances rather than using solid grounding techniques. Grounding resistors close to generators are more beneficial than reactors since they provide an additional breaking effect to the generator during unbalanced faults. Embedded generators are generally resistively earthed in order to keep ground fault currents low and to reduce third harmonics, this therefore improves stability with respect to unbalanced faults.

2.2.6 Affect of Local Load on Stability.

The type of load must also be considered since loads such as induction motors can continue to depress system voltage after a fault has been cleared[12]. If an induction motor is braked sufficiently during the fault due to the voltage dip, then the machine's reactive load will increase as the machine attempts to regain speed. The voltage reduction produced will reduce the generator's power transfer capabilities, and hence the amount of decelerating torque produced will be lower.

2.3 Comparison of Stability Parameters of Typical Embedded and Grid Synchronous Generators.

Table 1 illustrates how the constants which affect the stability of a generator vary for embedded generators[13] and conventional 'grid' size machines[3].

Analysis of the inertia constants show that for embedded generators, the value for H is generally 10 times less than it is for grid machines. This highlights the responsiveness of embedded machines to disturbances, an embedded machine will swing much further than a conventional grid machine for a given disturbance.

Examination of armature resistance (ra) values reveals that this also tends to be 10 times larger for embedded machines, resulting in embedded machines theoretically having less damping. Damping however is dependent on numerous factors so this does not necessarily mean the damping will be proportionally 10 times less.

Inspection of the reactances and time constants shows that although the transient values are practically the same whatever the size of the generator, the open circuit time constants for embedded generators are over 2.5 times shorter. This means the flux levels will not be maintained for long in the embedded machines following a disturbance, unless a high response ratio, high performance AVR is fitted [3], which will keep the flux high by field forcing action.

3.0 EMBEDDED GENERATOR STABILITY ASSESSMENT.

The industrial embedded generation system, shown in Figure 1, was modelled using the Electromagnetic Transients Program (EMTP). The data used in the simulation is in Appendix A. The generator only uses an AVR when operating on its own, when it is paralleled with the REC system, the AVR is taken out of service. Due to insufficient data, the governor model was not simulated.

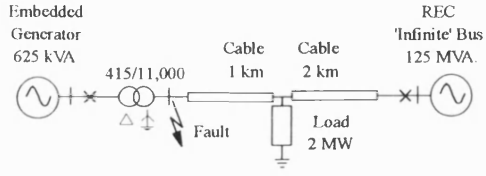

Figure 1: Embedded Generator/Utility Connection.

A three phase fault was placed at the HV terminals of the step up transformer and the fault duration gradually increased until the generator went unstable. For a fault clearance time of 270 ms the generator remained stable, for a clearance time of 280 ms, it was unstable and pole slipping resulted. The machine load angle curves for these simulations can be found in Figure 2. The value for the CCT of 280 ms is very alarming since to obtain satisfactory grading, the REC's generally set their overcurrent relays to clear faults in a time of 0.5 to 1 second [7,8]. With clearance times far in excess of the CCT, generator instability is very likely.

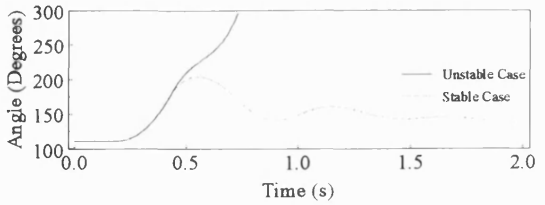

Figure 2: Machine Angle for Stable & Unstable Simulations

Also of interest, in terms of quality of supply are the fluctuations experienced in the load and generator terminal voltages following loss of stability. These can be seen in Figures 3 & 4. It is evident from Figure 3 that the mean load voltage for the unstable case is lower than for the stable case. The severity of the depression is of the order of 2 %.

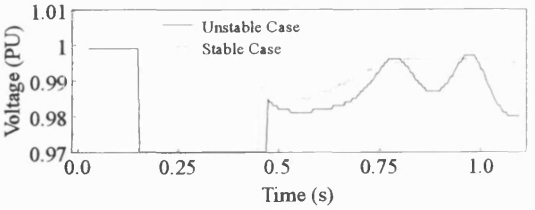

Figure 3: Load Voltage for Stable and Unstable Simulations.

This scenario has a high 'infinite' bus to generator ratio of 200:1. The infinite bus therefore maintains the load voltage within acceptable limits. If the ratio of infinite bus to machine ratings dropped, or the impedance between the 'infinite' bus and load increased, the magnitude of the voltage fluctuations would increase. This can be explained if the generator and infinite bus are each thought of as contributing to the load voltage. Their respective contributions to the voltage depend upon their apparent rating from the load's viewpoint, the higher the rating the more they contribute. When the generator pole slips, it's contribution to the voltage is 180° out of phase, and therefore its effect is to decrease the voltage. The higher its rating in proportion to the infinite bus, the more it will decrease the load voltage.

In this simulation, the load was static, and did not have any sensitivity to voltage variations. If the load had been an induction motor load for example, the decreased voltage may have caused it to stall, or it's starter contactors to open.

It can be seen from Figure 4 that the generator terminal voltage suffers more severe voltage depressions, and if a local load was connected, the voltage depressions would have severely disrupted it. As well as induction motor loads suffering from voltage disturbances, thought must be borne over to the effect on undervoltage protection relays which may operate if the voltage is depressed for long enough.

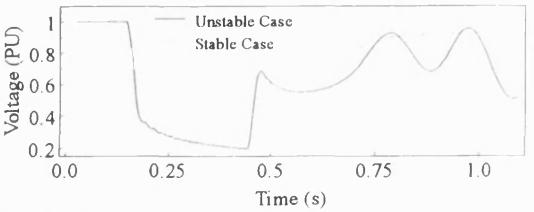

Figure 4: Generator Voltage for Stable and Unstable Simulations.

3.1 Effects of Embedded Generation System Configuration on Stability.

Some embedded configurations have multiple embedded generators located within one site. If the generators are connected to the same bus, they can usually be grouped together, there behaviour appearing as though they were one larger generator. From a stability viewpoint adding extra generation to a site will reduce the ratio of infinite bus to machine ratios, if the ratio becomes too low, then the generators will not receive enough synchronising power following disturbances and will be more prone to instability. On the other hand, the inertias of the two machines combine to make a larger inertia, which makes the 'group' of generators less 'twitchy'.

The effect of step up transformers also affects stability, since the impedance of the transformer can be added to that of the generator's stator circuit. If the transformer has a high impedance then the interchange of synchronising power between generator and grid will be reduced. The transformer may improve stability for close up terminal faults, since the transformer will partially load the generator.

3.2 Availability of Data and Use of Computerised Techniques for Stability Analysis.

If it is possible to obtain manufacturers data on the generator, transformer & connecting lines, then a comprehensive stability evaluation can be performed using one of the many transient stability evaluation packages available. However, in many cases, it may be impossible to obtain the full set of data. In these instances, an estimate of the CCT can be found using just the inertia, synchronous and transient reactances and bus capacity. If a computer based technique is used, then the other parameters required by the package will have to be estimated. If a computer package is not available, then a fair estimate of the CCT can be found using the Equal Area Criterion and step by step calculations, as described in reference [6].

4.0 CONCLUSIONS.

Embedded generators connected to distribution systems using overcurrent protection can be prone to instability. The long fault clearance times associated with overcurrent protection, coupled with low generator inertias, short time constants, high resistances and high reactance values in the generator and interconnection make them much less stable than traditional 'grid' generators.

Prolonged disturbance to the surrounding power system may result following a fault, due to the effects of a synchronous generator operating in an unstable manner. These problems can only be remedied by either reducing fault clearance times so that the generator remains stable, or installing protective relays to disconnect the generator when it is operating unstably.

The Critical Clearance Time (CCT) for the typical case studied was 270 ms, when this is compared with the 0.5 to 1 second fault clearance times typically produced by overcurrent relays, then it can be concluded that there is a high likelihood that embedded generators will go unstable.

5.0 REFERENCES.

[1] Kimbark, E W : 1956. "Power System Stability - Synchronous Machines" Vol 3, Chapman & Hall Ltd, London.

[2] Gupta, S & Lynn J : 1980. "Electrical Machine Dynamics" The Macmillan Press Ltd, London.

[3] Anderson, P M & Fouad, AA : 1977. "Power System Control and Stability" The Iowa State University Press, Iowa, USA.

[4] Demello F P & Concordia C : "Concepts of Synchronous Machine Stability as Affected by Excitation Control" IEEE Trans. Vol. PAS-88, No.4, April 1969, p 316.

[5] Electricity Council : "Notes of Guidance for the Protection of Private Generating Sets for Operation in Parallel with Electricity Board Distribution Networks" Engineering Technical Report 113, London, 1989.

[6] Kimbark, E W : 1964. "Power System Stability - Elements of Stability Calculations" Vol 1, 5th edition, John Wiley & Sons, London.

[7] Clark H K & Feltes J W : "Industrial and Co-generation Protection Problems Requiring Simulation" IEEE Trans. on Industry Applications, Vol 25, No.4, July 1989, pp766 - 775.

[8] Fielding G & Evans G W : "Industrial Feeder Protection" Tenth international Conference on Electricity Distribution, Part1, 5 - Consumers Installations, 1989, pp 460 - 466.

[9] Concordia C : "Effect of Prime Mover Speed Control Characteristics on Electric Power System Perfomance" IEEE Trans. Vol. PAS-88, No. 5, May 1969, p 752.

[10] Nickle C A & Pierce C A : "Stability of Synchronous Machines - Effect of Armature Circuit Resistance" AIEE Transactions, Vol. 49, 1930, pp 338-351.

[11] Concordia C & Carter G K : "Negative Damping of Electrical Machinery" AIEE Trans. Vol. 60, March 1941, p 116.

[12] Arcidiacono V : "Studies on Damping of Electromechanical Oscillations in Multimachine Systems with Longitudinal Structure" IEEE Trans. Vol. PAS-95, No. 2, March 1976, p 450.

[13] Gish W : "Small Induction Generator and Synchronous Generator Constants for DSG Isolation Studies" IEEE Trans. Power Systems, Vol PWRD - 1, No. 2, April 86, pp 231 - 239

APPENDIX A DATA USED FOR TRANSIENT STABILITY EVALUATION.

All per unit values given on generator base (625 kVA)

Generator : S = 625 kVA, H = 2.84 s, Xd = 2.25 pu, Xd' = 0.22 pu, Xd" = 0.15 pu, Xq = 2.15 pu, Xq' = 2.15 pu (No q axis damper modelled), Xq" = 0.225 pu, Tdo' = 1.9 s, Tqo' = 0 s, Tdo" = 0.024 s, Tqo" = 0.018 s, Xo = 0.051 pu, Ra = 0.017 pu, Xl = 0.1 pu

Transformer Parameters : S = 625 kVA, X = 0.1, ratio 415 V/11 kV.
REC parameters : S = 125 MVA, 11 kV.
Load Parameters : P = 2 MW, Q = 0.2 MVAr
Interconnection : R = .00655 pu, X = .00689 pu (for 1 km)

Table 1 - Typical Stability Analysis Data for Embedded and Grid Type Machines

Type	Embedded	Embedded	Embedded	Embedded	Grid	Grid	Grid	Grid
Rating	156 kVA	781 kVA	1044 kVA	4510 kVA	100 MVA	233 MVA	414 MVA	552 MVA
ra (pu)	0.011	0.034	0.017	0.013	0.0035	0.0016	0.0019	0.0047
H(seconds	0.329	0.205	0.500	0.535	4.985	4.122	3.704	5.453
Tdo' (pu)	0.950	1.87	1.90	2.47	5.90	5.14	5.43	3.65
Xd (pu)	2.02	6.16	2.43	2.38	1.18	1.57	1.77	1.78
Xd' (pu)	0.171	0.347	0.254	0.264	0.220	0.324	0.274	0.258

PAPER SIX

"THE EFFECTIVENESS OF STANDARD SCHEMES FOR THE PROTECTION OF DISPERSED GENERATORS FROM ABNORMAL OPERATING CONDITIONS"

M A Redfern and M J Checksfield

Presented at :-

3rd International Conference on Advances in Power System Control, Operation and Management (APSCOM)

November 1995, Hong Kong, pp 506 - 511.

THE EFFECTIVENESS OF STANDARD SCHEMES FOR THE PROTECTION OF DISPERSED GENERATORS FROM ABNORMAL OPERATING CONDITIONS.

M A Redfern & M J Checksfield.

University of Bath, UK.

ABSTRACT.

Questions are increasingly being asked about the response of standard protection schemes used for protecting embedded synchronous generators during abnormal operating conditions. Loss of grid and pole slipping are two such abnormal operating conditions, both of which can cause potentially damaging shaft torques and disturbances to the power supply system. This paper discusses a standard protection scheme and highlights the operating conditions where standard schemes may not operate as expected. It then presents new protection techniques which have been developed and compares these to the standard schemes.

1.0 INTRODUCTION.

When a small embedded synchronous generator is connected to operate in parallel with a utility distribution supply, the protective relay schemes normally used for protecting large synchronous generators are generally too expensive. The size and hence cost of an embedded generator dictates that a low cost protection scheme is required.

In the United Kingdom, the minimum protection requirements for connecting a synchronous generator to operate in parallel with the distribution system are detailed in 'Engineering recommendation G59' [1] and 'Engineering Technical Report ET 113' [2]. These documents stipulate that the generator be disconnected from the utility supply whenever an operating condition exists which will produce an unacceptable deviation in the voltage or frequency at the point of supply.

Loss of grid and pole slipping can both cause unacceptable deviations in the supply voltage and frequency.

1.1 Loss of Grid.

Loss of Grid protection is required to protect against an accidental isolation of the utility supply and the embedded generator systems. This isolation can result in a portion of the utility's load being left connected to the embedded generator alone. In this condition the isolated part of the system may continue to operate independently of the utility, forming its own power island.

Two problems can result following the loss of grid. The embedded generator may not be able to maintain the voltage and frequency within acceptable limits, thus disrupting consumer loads which are still connected to the power island. Additionally, the embedded generator is at great risk from an out of synchronism re-closure, reconnecting it to the utility supply.

Depending upon the degree that the two systems are out of phase at the time of re-closure, the resulting shaft torques may cause mechanical shaft failure. It is therefore vital that the loss of grid condition be detected before the utility circuit breakers are re-closed. Since automatic re-closure schemes can operate in as little as 0.5 seconds, the loss of grid condition must be detected and the generator disconnected within 0.5 seconds.

1.2 Pole Slipping.

Pole slipping occurs when there is an imbalance between the generator's input and output powers. This imbalance causes the generator rotor to accelerate, and to try to operate at a speed which is above that of the electrical supply to which it is connected.

The imbalance can occur due to delays in clearing short circuit faults, faulty excitation systems, faulty governing systems, or sudden losses of load.

The power surges associated with pole slipping can have a detrimental affect on the quality of supply of the system to which the generator is connected. They can also damage the generator. If the utility system does not have infinite bus characteristics, then as the generator pole slips, the utility voltage will fluctuate. If voltage sensitive loads such as induction motors are connected nearby, the voltage depressions may cause them to stall, depressing system voltage further.

Pole slipping can also cause rotor and stator over heating due to the eddy currents which are produced when the machine is operating asynchronously. The currents and shaft torques experienced during pole slipping can exceed those produced by three phase fault levels. Since generators are generally only designed to withstand three phase fault levels, the extra forces produced during pole slipping may loosen the stator windings and cause permanent damage.

2.0 A STANDARD PROTECTION SCHEME.

There are several suggested protection schemes for embedded generation. The scheme used for this study is based on G 59 and is shown in Figure 1. The technical details are listed in Table 1. The time delays have been calculated with the assumption that it takes 100 ms for the circuit breaker to operate. The performance of the relays shown was analysed using protection algorithm versions of the functions in a digital computing environment.

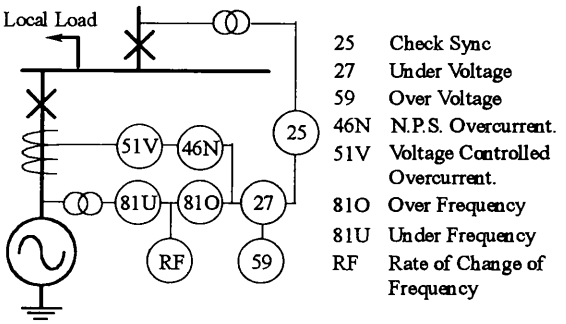

Fig 1 - Standard Embedded Generator Protection Scheme

Since loss of grid and pole slipping are both balanced phenomena, the negative phase sequence protection function was not analysed.

Table 1 - Protection Settings.

PROTECTION	SETTING	DELAY
UNDER VOLTAGE	- 10 %	0.4 seconds
OVER VOLTAGE	+ 10 %	0.4 seconds
UNDER FREQUENCY	- 4 %	0.4 seconds
OVER FREQUENCY	+ 1 %	0.4 seconds
VOLTAGE CONTROLLED OVERCURRENT	PSM = 2 * In	TMS = 0.1
RATE OF CHANGE OF FREQUENCY	0.3 Hz/s	0.25 seconds

2.1 Under/Over Voltage Protection.

This protection operates when the relaying voltage exceeds the preset limits for the specified time. The rms phase voltage which was used as the input to the relay was derived from the instantaneous voltage samples using;

$$Vrms_k = \frac{1}{N} \sum_{r=0}^{N-1} Z^2_{(k-r)} \qquad (1)$$

where N is the number of samples per power system cycle, and Z is the voltage sample value.

2.2 Under/ Over Frequency Relays.

This protection operates when the measured frequency exceeds the preset limits for the specified time. In this study, the frequency was measured using a zero crossing technique and linear interpolation to determine the length of each half cycle.

The sampled values of voltage used for the frequency measurement were first pre-filtered with a two cycle cosine filter. This removes dc offsets and any half multiples of the fundamental frequency present in the raw sampled data. A sampling rate of 1000 Hz was used. Following the calculation of the frequency, an half cycle moving average filter was applied to remove any high frequency components which may have corrupted the rate of change of frequency measurement.

2.3 Voltage Controlled Overcurrent Protection.

Voltage controlled overcurrent protection is necessary for synchronous embedded generators, due to their decaying fault current characteristics. This type of protection has two characteristics, one long IDMT characteristic for overloads or internal faults where the terminal voltage is maintained, the other a faster IDMT characteristic for faults which severely depress the terminal voltage. The standard inverse IDMT characteristic was simulated using the RMS phase current as the actuating quantity. A reset characteristic was also modelled such that the integrand exponentially reset over a time of five power system cycles.

The voltage control characteristic was set such that if the rms voltage dropped below 30 % of its nominal value, then the plug scale multiplier (PSM) setting was multiplied by a factor of 0.4.

2.4 Rate of Change of Frequency Protection.

This protection operates when the rate of change of frequency exceeds the preset limits for the preset time. The rate of change of frequency was calculated using;

$$(\Delta F/\Delta t) = (F_n - F_{n-1}) * 1 /dt \qquad (2)$$

where F_n is the present sample value of frequency, and F_{n-1} is the previous sample value of frequency, dt is the time between samples. After the rate of change signal had been calculated, a full cycle moving average filter was applied to the signal to remove short fluctuations.

3.0 THE NEW PROTECTION ALGORITHMS.

New types of generator protection are increasingly using microcomputer based relays and integrated protection functions. Instead of having one individual relay for each function of the protection scheme, one microprocessor relay is used which contains all of the necessary protection functions required by the scheme. There are numerous advantages to this approach, such as disturbance and event recording, SCADA interface, self monitoring and alternative setting groups.

New algorithm's have been developed that take advantage of the processing capability provided by these microprocessor relays, and offer the advantage of improved protection performance over conventional techniques.

Research has been conducted into two such algorithms for detecting loss of grid and pole slipping [3,4]. The new algorithms developed, both use real time power measurements and the rate of change of power in their algorithms.

Using power measurements offers advantages over impedance measurements since precise synchronisation of the voltage and current samples and hence phasors is not required. Power measurement is also more convenient than frequency measurement since it is much less prone to input waveform distortion and can tolerate low sampling rates.

In sharing the same measuring quantities the algorithm's also reduce the processing burden placed on the microprocessor.

3.1 Power Based Loss of Grid Protection.

This technique [3] detects the loss of grid by monitoring the behaviour of the power system to load disturbances. It detects a loss of grid by differentiating between the responses produced when the embedded generator is connected to the utility supply, and when the embedded generator operates in isolation.

3.2 Power Based Pole Slipping Protection.

This technique [4] uses real power, it's rate of change, and reactive power to predict when a generator is about to, or actually is pole slipping. It works by monitoring the operating point of the generator to see if the point of no return has been passed. Once the point of no return has been passed, a pole slip is inevitable.

4.0 SIMULATION STUDIES.

The performance of the protection schemes was assessed using the Alternative Transients Program (ATP). The test model contained a 625 kVA synchronous generator connected to a utility distribution system through parallel 11 kV cables, as shown in Figure 2.

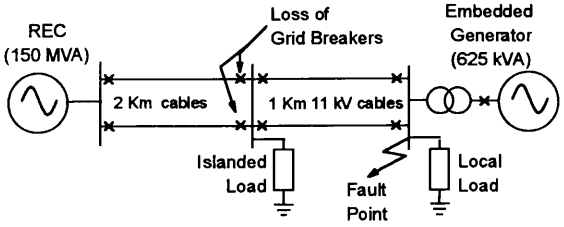

Fig. 2 Embedded Generation System Used for Tests.

The generator's inertia constant, H was 2.84 s, its open circuit time constant , Tdo' was 1.9 s, its synchronous reactance, Xd was 2.25 p.u., whilst it's transient reactance was 0.15 p.u. The impedance per km of the interconnecting lines was 0.0066 + j0.0069 p.u., and the transformer's reactance was j0.1 p.u. All per unit values have the generator rating as their base.

When the generator is operating in parallel with the utility system, its AVR is disabled. The AVR was not modelled in these simulations. The governor present on the generator was of a slow acting type and hence would not have affected the simulations in the period of interest.

4.1 Simulation of Loss of Grid.

Two different loss of grid situations were simulated in order to evaluate the standard protection scheme and the new power based loss of grid algorithm's performance. For both tests, the generator was initially operating at 470 kW.

For the first test, following the loss of grid, the load connected to the embedded generator was 940 kW. The generator therefore experienced a 100 % increase in loading when the loss of grid breakers were opened.

For the second test, following the loss of grid, the load connected to the embedded generator was 420 kW. The generator therefore experienced a 10 % decrease in loading following the loss of grid. For both tests, the loss of grids occurred after 0.1 seconds from the start of the simulation.

4.2 Pole Slipping Simulations.

Two different tests were used to evaluate the standard scheme and the power based pole slipping algorithm. The generator was initially operated at full power.

For the first test, a three phase fault of 255 ms duration was applied at the terminals of the generator

step up transformer at a time of 0.1 s. This caused the generator rotor to accelerate and the generator to pole slip. The generator was permitted to slip 6 pairs of poles before the simulation was stopped.

For the second test, a three phase fault of 235 ms duration was again applied at the terminals of the generator step up transformer. This was not sufficient to cause the generator to pole slip, however it did cause a large swing in power output from the generator. This power swing tested the protection's ability to remain stable during large power system disturbances.

5.0 SIMULATION RESULTS.

5.1 Loss of Grid Simulations.

100 % Load Increase Test The results from this test are presented in Figure 3. For this test, the power based LOG tripped 33 ms after the loss of grid occurred. The rate of change of frequency tripped 0.344 s after the loss of grid, and the under voltage protection tripped after 0.641 s.

The increased loading, coupled with the slowing down of the generator caused the voltage to fall below the undervoltage trip level.

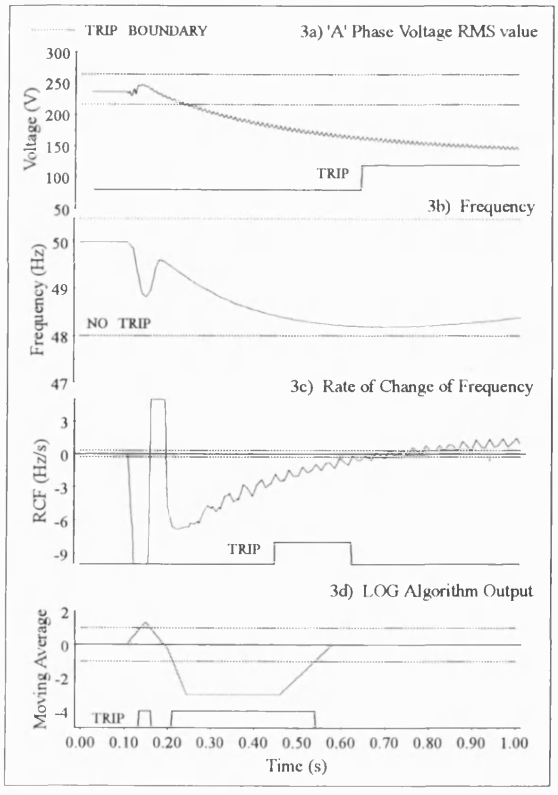

Figure 3 Results to 100 % Load Increase Loss of Grid Simulation.

Under and over voltage relays will generally only detect a loss of grid if the real or reactive power demands resulting from the loss of grid are severe enough to cause an appreciable excursion in voltage. The time delay of 0.4 seconds is used so that the protection can ride through disturbances which cause short term voltage fluctuations.

With this dramatic change in load following the loss of grid, both the undervoltage and rate of change of frequency relays tripped. Although the rate of change of frequency relay is designed to operate for a loss of grid, the undervoltage relay's operation shows that the quality of supply was compromised.

Observation of the under frequency plot shows why this protection did not operate. This was due to the generator terminal voltage dropping to a value which made the electrical load equal to the initial load on the generator of 470 kW. Once this condition occurred the generator stopped slowing down since its input and output powers were matched.

The voltage controlled overcurrent algorithm did not operate. A very high overload level would be required to make this protection operate, at such a high level of overload, the under voltage and frequency algorithms would definitely operate.

10 % Load Decrease Test. The results from this test can be seen in Figure 4. The first protection function to trip was the power based LOG, which operated 55 ms after the event. After this, the rate of change of frequency tripped 0.369 s after the event. The over frequency tripped last, 0.883 s after the loss of grid.

The standard scheme successfully detected the loss of grid condition within the time specified by Engineering recommendation G 59. The power based LOG offered improved performance since it detected the loss of grid condition 0.314 s before the rate of change of frequency function.

Very careful setting of the rate of change of frequency relay is required, as too low a setting will result in mal-operation due to everyday system disturbances, while too high a setting will result in small load change loss of grids going undetected.

The change in loading of the generator was not sufficient to cause the over voltage algorithm to operate.

5.2 Pole Slip Simulations.

Pole Slip Test The results from the pole slipping test can be seen in Figure 5. The first pole slip occurred between 0.75 and 1.25 s. The first protection function to trip was the rate of change of frequency, at a time of 0.357 s.

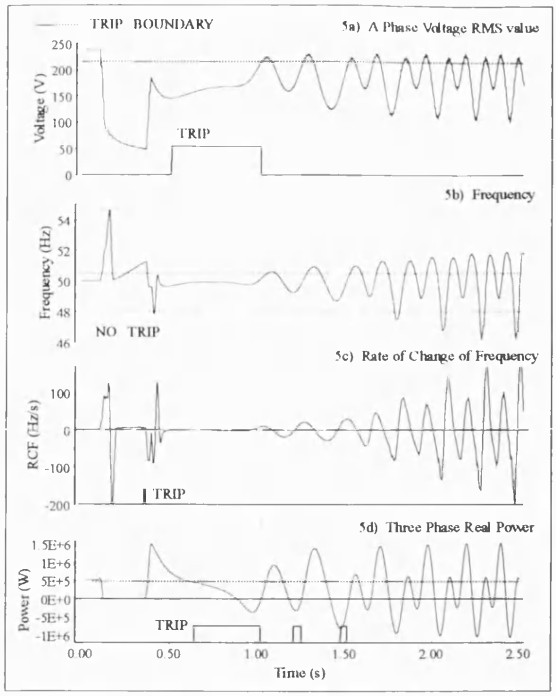

Figure 4 Results to 10 % Load Decrease Loss of Grid Simulation

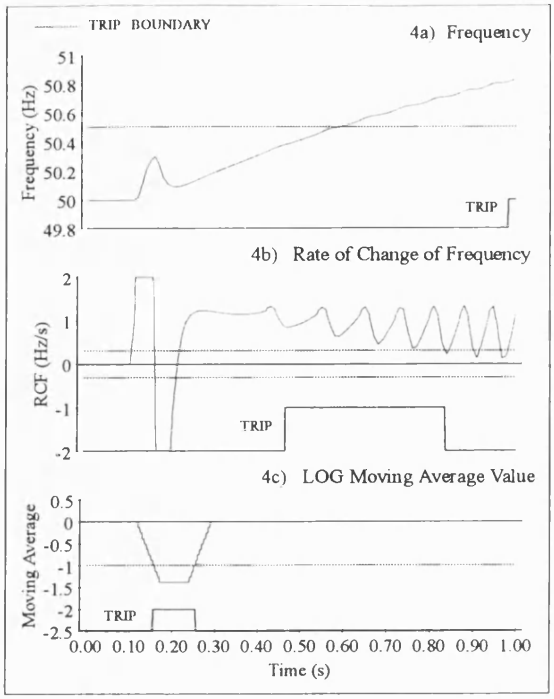

Figure 5 Results to Pole Slipping Simulation.

Inspection of the plot shows that this relay responded to the fault, and operated before the first pole slip.

The under voltage protection tripped next, at a time of 0.502 s. This again was not due to the pole slipping, but the system voltage being depressed after the fault was cleared.

When a generator pole slips, it's reactive power demand oscillates wildly. When the generator is demanding large amounts of reactive power, a voltage depression results, which may cause the undervoltage relay to operate. The undervoltage algorithm did not respond to the pole slipping in this case however, the time delay enabled the relay to ride through the voltage dips.

The new power based algorithm successfully tripped at a time of 0.640 s, before the pole slip occurred. The generator was committed to a pole slip, and as designed, the algorithm predicted the pole slip before it occurred.

Examination of the frequency plot shows that the frequency measurement jumps at the fault on and fault off points. This was a result of the zero crossing method used to measure frequency, however, it did not cause the relay to trip because the under and over frequency protection's time setting enabled it to ride through the glitches

The voltage phase of the generator as it pole slips swings through 360 °, and this affects the location of the zero crossings of the voltage waveform. The net result was that the location of the zero crossings moved forwards and backwards as the pole slip occurred, resulting in the observed frequency fluctuating up and down. This fluctuation in the frequency repeatedly reset the over frequency algorithm and prevented it from operating.

If a frequency measurement technique had been employed which only measured the frequency of the generator, then the over frequency algorithm would have detected the pole slip.

Although the current exceeded three phase fault levels during the pole slipping, the voltage controlled overcurrent algorithm did not operate. This was due to the relay being reset between the current maximums. If a longer reset time had been used, and the pole slips had been faster, then the algorithm may have integrated the current over several slip cycles and tripped.

The most important task of the overcurrent relay with reference to pole slipping, is that of disconnecting the generator from the utility supply when a fault occurs whose duration is long enough to causing pole slipping. For these tests, the fault was cleared before the overcurrent relay could operate.

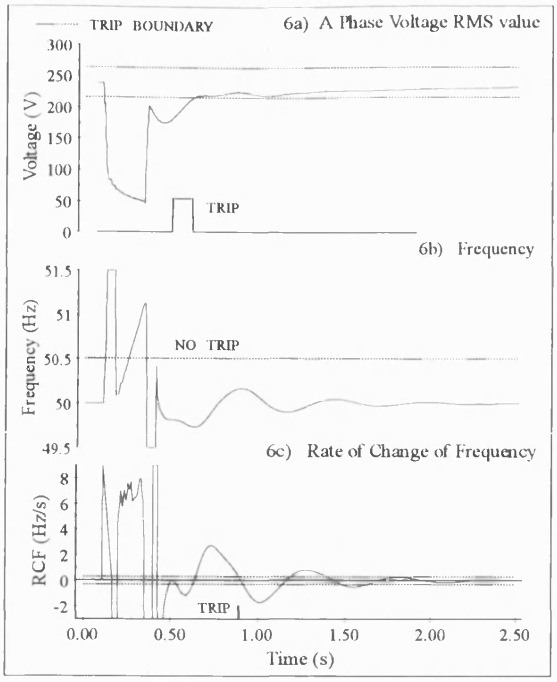

Figure 6 Results to Power Swing Simulation.

Power Swing Test. The results from the power swing test can be seen in Figure 6. None of the functions should have tripped for this simulation since the generator would have returned back to normal operation.

The undervoltage did trip, this was due to the generators reactive power demand depressing the system voltage long enough for it to operate.

The rate of change of frequency function also operated when the generator swung following the fault. The oscillations in real and reactive power experienced during the power swing caused the frequency to fluctuate and hence the rate of change of frequency relay to operate.

The other functions, including the power based pole slipping function remained stable.

6.0 CONCLUSIONS.

The standard schemes used for protecting synchronous embedded generators detect the majority of loss of grid conditions satisfactorily. The new power based loss of grid algorithm offers the prospect of enhanced performance over the standard scheme, whilst being simple enough to be included in an in-expensive integrated protection relay.

The standard scheme can however, mal-operate during stable swings in power following power system faults. If the generator should be disconnected for power system faults then this is not a problem. If the generator should remain connected, then the undervoltage relay settings used would have to be re-considered.

Of more concern, is the rate of change of frequency relay, which may also operate during stable swings in power. This is due to the oscillations in the generator's voltage phase angle causing the observed frequency to oscillate. It may be possible for the generator to swing for reasons other than faults, concern must therefore be given to the operation of such relays.

The time delays associated with the standard scheme have been found to prevent several relays detecting pole slipping conditions, while not preventing relay operation during power swings produced by faults. The new power based pole slipping algorithm successfully detected the pole slipping condition while remaining stable during the power swing.

7.0 REFERENCES.

[1] The Electricity Council. "Recommendations for the Connection of Private Generating Plant to the Electricity Board's Distribution Systems - Engineering Recommendation G 59." June 1985.

[2] The Electricity Council. "Notes of Guidance for the Protection of Private Generating Sets for Operation in Parallel with Electricity Board Distribution Networks" Engineering Technical Report 113, London 1989.

[3] Redfern M A, Usta O, & Fielding G, "Protection Against Loss of Utility Grid Supply For a Dispersed Storage And Generation Unit", Paper Ref 92 SM 376-4 PWRD, Presented at the IEEE Power Engineering Society 1992 Summer Meeting, Seattle, July 12 - 16.

[4] Redfern M A & Checksfield M J, "A New Pole Slipping Protection Algorithm for Dispersed Storage and Generation Using the Equal Area Criterion.", IEEE Transactions on Power Delivery, Vol. 10, No.1, pp 194 - 202, January 1995.

PAPER SEVEN

"A STUDY INTO A NEW SOLUTION FOR THE PROBLEMS EXPERIENCED WITH POLE SLIPPING PROTECTION"

M A Redfern and M J Checksfield

To be presented at :-
IEEE Power Engineering Society (PES) Winter Meeting,
New York, USA, February 1997.

Accepted for Publication in the
IEEE Transactions on Power Delievery
Reference PE-486-PWRD-0-11-1996.

A STUDY INTO A NEW SOLUTION FOR THE PROBLEMS EXPERIENCED WITH POLE SLIPPING PROTECTION.

M. A. Redfern and M. J. Checksfield

School of Electronic and Electrical Engineering
University of Bath, Bath, BA2 7AY, UK.

Abstract - Pole slipping of synchronous generators operating in parallel with a utility supply system is a complex phenomenon. This paper provides an overview of a new solution for pole slipping protection, together with a review of conventional techniques. Immediate advantages of the new approach are that it simplifies relay settings and avoids the need for extensive simulation studies. Results from simulation studies and field tests are used to demonstrate the performance of these systems. The new technique is shown to offer a significant improvement in performance over conventional schemes.

Keywords: Power system protection, Pole slipping protection, Out-of-step protection, Digital protection, Numeric protection.

I. INTRODUCTION

Pole slipping is a concern for all synchronous generation designed to operate in parallel with utility systems. Recent trends in power systems have meant that synchronous generators are being operated close to their stability limits[1]. This together with the lower generator inertias, higher machine reactances and the long fault clearance times especially encountered on distribution systems, increases the likelihood of synchronous generator pole slipping.

Pole slipping causes dramatic fluctuations of the generator's currents and as a result can cause fluctuations in power system voltages. The mechanical forces and heating effects produced during pole slipping can damage the machine and associated transformers. Pole slipping protection is required to initiate disconnection of the generator from its supply as soon as possible after it loses synchronism with the utility supply to which it is connected.

The new approach to pole slipping protection uses power measurements to determine the status of the generator, whereas conventional schemes monitor the system's impedance. An immediate difficulty with the impedance techniques is that they are difficult to set [1,3,4]. This problem is avoided with the new relay. Most techniques require detailed power system simulations to determine a reliable setting and performing a detailed computer simulation is time consuming and therefore expensive. Unfortunately most techniques for calculating the impedance locus for pole slipping and stable swing conditions do not take into account effects such as generator damping, non-constant flux linkage, and control system operation[5]. This can therefore be a constraint on the choice of pole slipping protection.

II. POLE SLIPPING

Pole slipping can be caused by an external disturbance on the system such as slow fault clearance, line switching operations which increase the transfer impedance, a faulty excitation system, or an excess of prime mover input power. The phenomenon is likely to occur when the generator is under excited, since this reduces the maximum electrical power which can be taken out of the generator. Unfortunately, generators are occasionally operated in an under-excited manner when the system is lightly loaded to prevent high system voltages.

From a machine view point, pole slipping occurs when the mechanical torque produced by the prime mover is greater than the electromagnetic torque used to produce the power output. If this condition persists for too long the rotor is unable to stay in synchronism with the stator magnetic flux. The loss of synchronism point can be defined as the point where the generator's real power output becomes zero. Once this point has been reached the generator will briefly accelerate into a motoring condition, during which time it will absorb power from both the prime mover and the system. It will then return to a generating condition. If it cannot then produce the synchronising forces necessary to pull itself back into a synchronous state of operation, it will repeat the cycle again and again.

Pole slipping can damage the generator in several ways. If it is connected to a high capacity infeed, the currents experienced can exceed three phase fault levels. Machine windings are generally designed to withstand three phase fault levels. These high currents cause damage both through mechanical forces on the conductors and overheating. The generator's unit transformer windings are also exposed to high mechanical stresses and overheating and can therefore be damaged as well.

Pole slipping also produces severe pulsations in shaft torque, and if the speed of the pole slip is such that the pulsations excite resonance in the shaft, shaft failure may result. The magnitude of the shaft torque pulsation builds up if the generator is allowed to continue to pole slip, and the generator should therefore be tripped immediately when a pole slip occurs [1,3].

The high currents associated with pole slipping can cause voltage fluctuations to the local supply which in turn can cause motor starter contactors to open and induction motors to stall, further depressing the system voltage. In severe cases, pole slipping of a generator can lead to a cascading loss of synchronism of machines nearby.

III. NEW POLE SLIPPING PROTECTION

A new pole slipping algorithm has been developed[2] to take advantage of the capabilities provided by modern numeric microprocessor relays. Using real time power measurements and the rate of change of power, the algorithm trips when the generator is committed to a pole slip, rather than when a pole slip has actually occurred. The new approach can therefore disconnect the machine from the power system before it can be damaged, or severe voltage disturbances are caused.

The algorithm uses the generator parameters, Xq - the quadrature axis synchronous reactance, Xd - the direct axis transient reactance, along with the generator rating, $Sgen$, and generator operating point to derive the trip levels. By dynamically adjusting the trip settings according to the current operating point, the algorithm can use sensitive trip levels to quickly detect pole slips which occur due to steady state or dynamic instability. During transient disturbances, larger trip levels are automatically used, ensuring that there are no false trips during stable power swings.

Fig. 1 shows the Equal Area Diagram commonly used to assess stability for a given disturbance[5]. The disturbance in this case is the clearance of a short circuit fault on one of two transmission lines which connect the generator to the main utility supply. The fault is cleared at load angle $\delta 2$. The limiting case for stability is when area 'A', the accelerating energy into the rotor is equal to area 'B', the decelerating energy. When this condition occurs, the load angle will swing up to the Critical Stability Point, ***CSP***. If the fault clearance time is slightly longer, then area 'A' will be greater than area 'B', and the load angle will swing *past* the ***CSP*** and instability and hence pole slipping will occur. The algorithm predicts that pole slipping will occur by detecting if the load angle is still increasing once the ***CSP*** has been exceeded [2]. If the generator operates past the ***CSP***, stability cannot be maintained and a pole slip is inevitable.

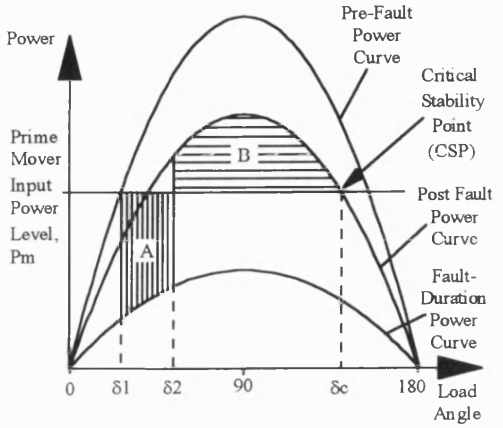

Fig. 1 Equal Area Diagram Showing Critical Stability Point (***CSP***) for Clearance of a Fault on a Double Circuit Transmission Line

In designing a pole slipping algorithm, it must be able to predict when a generator is committed to a pole slip, or detect when a pole slip is actually occurring. It must also remain stable for all other power system conditions, including short circuit faults and recoverable power swings. The algorithm uses reactive power, real power, and rate of change of real power to detect operation past the ***CSP***. Reactive power is used to tell if the generator is operating at load angles of greater than 90°. The trip criteria are:-

TRIP WHEN:-

$$\left.\begin{array}{l} Q < Qtrip \\ \quad and \\ P < Pt \\ \quad and \\ (\Delta P/\Delta t) < (\Delta P/\Delta t)_{min} \end{array}\right\} \begin{array}{l} \text{All must} \\ \text{be satisfied} \\ \text{continuously} \\ \text{for 1.5 power} \\ \text{system cycles.} \end{array} \qquad (1)$$

Where Q is the three phase reactive power, P is the three phase real power, and $(\Delta P/\Delta t)$ is the rate of change of real power. The reactive power trip level, $Qtrip$ is calculated from Xq, and is entered as an external setting;

$$Qtrip = -\frac{1}{Xq} * Sgen \qquad (2)$$

The real power trip level, Pt is derived by the algorithm, and is automatically adjusted according to the generator operating point. The rate of change of power trip setting, $(\Delta P/\Delta t)_{min}$ is also continuously adjusted by the algorithm according to the

generator operating point.

The 1.5 power system cycle time constraint is introduced to ensure that the algorithm remains stable during short circuit faults. The majority of faults will not satisfy all of the trip criteria, but the few that do only cause the criteria to be satisfied for less than one power system cycle.

A - Condition Monitoring Techniques

The algorithm is designed for a commercially available microprocessor based relaying environment, and hence the only information available to the relay is 2 phase voltages and 3 current signals provided by the relay's transducers. Since generators may be operated over a wide range of output powers, a method of estimating the prime mover input power is required so that the real power trip setting, ***Pt*** can be dynamically derived. The input power, ***Pm*** is estimated by observing the power output of the generator, and if this remains within a pre-defined tolerance band for a sufficient amount of time, then the input power is approximately equal to the output power, the only discrepancy being produced by the losses in the generator. Pt is derived from;

$$\text{if } |P_n - P_{(n-del)}| \text{ and } |P_n - P_{n-(2*del)}| < Ptol \text{ ;} \quad \text{then } Pt = P_n * Pfact \tag{3}$$

where P_n is the present real power sample value, P_{n-del} is the sample value of '*del*' samples ago, $P_{n-(2*del)}$ is the sample value of '*2*del*' samples ago, P_{tol} is the tolerance band, chosen as nominally 5% of machine rating, and ***Pfact*** is a coefficient to take into account the losses and inaccuracies inherent in measuring machine input power from output power.

The protection algorithm is also designed to be accommodated in the finite processing resources of a multi-function microprocessor relay and is executed 4 times per power system cycle. The value of '*del*' typically chosen is 200 which equates to 1 second, ***Pfact*** is nominally set to 0.9.

B - Adaptive Trip Setting $(\Delta P/\Delta t)_{min}$

The adaptive trip setting, $(\Delta P/\Delta t)_{min}$ is the theoretical value of $(\Delta P/\Delta t)$ at the ***CSP***. The algorithm calculates this value using an assumed sinusoidal power load angle curve[2], which gives;

$$(\Delta P/\Delta t)_{min} = -s * Pmax * \cos(180 - \sin^{-1}(\frac{Pt}{Pmax})) \tag{4}$$

Note that the value of slip, *s* used in (4) will not be the exact value at which the relay produces a trip output, due to damping power and other effects not taken into account in the derivation of (4). This equation is used to continuously update the trip setting $(\Delta P/\Delta t)_{min}$ depending on the variables ***Pmax*** and ***Pt***.

Since ***Pmax*** is a measure of the maximum output power that the generator has produced in the last second, it enables the algorithm to adjust its setting according to whether a 'transient' or 'steady state' pole slip will occur. A 'steady state' pole slip occurs due to control system malfunction, or loss of steady state stability, whereas a 'transient' pole slip occurs after the generator has been severely disturbed, after a fault for example. If the generator has been transiently disturbed, its output power during the first swing of its load angle, be it stable or unstable, will be much greater than its nominal output. This results in a greater magnitude in $(\Delta P/\Delta t)$ at the ***CSP***, the algorithm therefore needs to adjust its setting $(\Delta P/\Delta t)_{min}$ accordingly. The algorithm adjusts this setting using;

$$If \ \frac{Pt}{Pmax} < 0.6; \quad then \ (\Delta P/\Delta t)_{min} = (\Delta P/\Delta t)_{min} + (\Delta P/\Delta t)_{tran} \tag{5}$$

where $(\Delta P/\Delta t)_{tran}$ is an external relay setting based on the degree of transient saliency in the generator. Transient saliency arises due to differences in the values of ***Xd'*** and ***Xq'***. Normally ***Xq'*** is equal to ***Xq***. $(\Delta P/\Delta t)_{tran}$ is given by;

$$(\Delta P/\Delta t)_{tran} = \left(\frac{1}{Xq} - \frac{1}{Xd'}\right) * S_{gen} \tag{6}$$

For a steady state pole slip, no peak will occur in the power output before the pole slip, the algorithm trip setting should therefore be at its most sensitive level to detect the pole slip since low values of $(\Delta P/\Delta t)$ will result.

During steady state conditions the value of ***Pmax*** used by equations (4) and (5) is nominally *1.4 * Pt*. The ratio ***Pt/Pmax*** therefore is 0.71, and ***Pt/Pmax > 0.6***. $(\Delta P/\Delta t)_{tran}$ is therefore not included in the calculation of $(\Delta P/\Delta t)_{min}$ during steady state conditions. If the generator's power output rises above the existing value of ***Pmax*** for greater than one power system cycle, then the value of ***Pmax*** is updated to the new maximum for a duration of one second. The one second limit is used so that the new value of ***Pmax*** is only used for the period where a pole slip or power swing associated with that value is likely to occur. The one cycle constraint is necessary so that incorrect values of ***Pmax*** do not result from spurious spikes on the power waveform. This mechanism also de-sensitises the algorithm during the period where generator output power is being increased.

IV. CONVENTIONAL POLE SLIPPING PROTECTION

A - Generator Pole Slipping Impedance Characteristics.

Conventional methods of detecting pole slipping use impedance relays to monitor the variations in apparent impedance at the generator or its unit transformer terminals during the pole slip. The theoretical variations in impedance during pole slipping were studied by Edith Clarke[7] and are

simplistically shown in Fig. 2. These loci are derived using the assumption that the ratio of generator to source voltages, ***Eg/Es*** remains constant. The analysis also assumes that generator saliency is neglected, generator damper effects are neglected, transient fault impedance effects have decayed, shunt loads and shunt capacitance effects are ignored, effects of automatic voltage regulators and governors are neglected, and the source voltages behind their equivalent impedances are sinusoidal and at fundamental frequency [1,3,5,7].

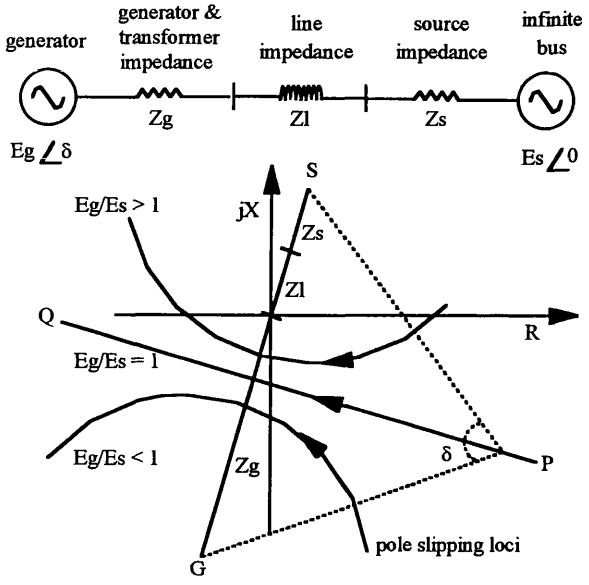

Fig. 2 Classical Pole Slipping Impedance Loci.[7]

When a pole slip occurs and the two generator voltages are the same, the load angle δ increases causing the impedance to travel from right to left across the R-X plane. When the load angle reaches 180°, the loss of synchronism point has been reached and the impedance will lie on the system impedance line ***GS***. This is known as the system centre, and at this point the impedance presented to the generator appears to be a three phase fault. As the pole slip cycle is completed and δ approaches an in-phase value of 360°, the impedance locus will travel to the left of the system impedance line before returning to the load area of the R-X plane.

Fig. 2 also shows impedance loci for the cases where the ratio ***Eg/Es*** < 1 and ***Eg/Es*** > 1. The effect is to cause the impedance locus to take on a circular arc form. These curves show that as the generator internal voltage is increased the system centre is pushed away from the generator. AVR field forcing action has this effect.

B - MHO Relay Scheme.

This is the simplest type of impedance based pole slipping protection and uses a single MHO characteristic[1,3]. The main advantages are that tripping occurs before δ= 180°, and hence before the most damaging current conditions. It also provides back-up protection for faults occurring in the transformer and generator. Careful selection of the MHO circle's reach is required to avoid nuisance tripping during recoverable and hence stable swings.

The relay is normally set to cover the generator transient reactance, ***Xd'*** plus the reactance of the unit transformer. It is recommended that the angle of swing where the impedance locus enters the characteristic is at least 120° [3].

C - Single Blinder Scheme.

This is the most secure of the impedance based techniques for detecting pole slipping and uses a pair of blinder characteristics as well as a supervisory MHO circle[1,2,3]. The MHO supervisory element restricts operation to swings appearing inside the generator and its transformer. For the scheme to operate, the impedance locus must enter the MHO circle and its trajectory must take longer than a specified time to cross from one blinder unit to the other. This time constraint is typically set to two power system cycles.

The scheme has the advantage over the MHO scheme that the diameter of the supervisory MHO element can be increased in order to provide better sensitivity to pole slipping conditions without introducing nuisance tripping for stable swings.

D - Double Blinder Scheme.

The double blinder scheme uses two pairs of blinder characteristics together with a supervisory MHO element[1,3]. For the scheme to operate, the MHO element must first pick up, and then the locus must then stay between the inner and outer blinders for greater than a preset time. It must then stay between the inner blinder elements for greater than a second time setting. Finally when the locus leaves the inner characteristics, it must stay between the inner and outer blinder elements for greater than a preset time. When all of these stages have been satisfied, a trip signal is issued when the supervisory MHO resets.

The main difference between the single and double blinder schemes is that with the double blinder scheme, the locus can enter and leave the characteristic from any direction. With the single blinder scheme the locus must enter from one side and leave from the other for a trip to occur. The inner elements of the double blinder scheme must therefore be set so that they will only respond to non recoverable swings.

V. SIMULATION STUDIES

The performance of the new and conventional protection schemes was investigated using computer simulations of a 200 MVA generator using the Electro-Magnetic Transients Program (EMTP) [6] and field trial tests using an industrial 625 kVA diesel generator.

The three phase impedance used to demonstrate the impedance based relays' responses to the tests was derived from three phase real and reactive power, and voltage signals with a moving average filter to reproduce the averaging techniques used in an impedance relay.

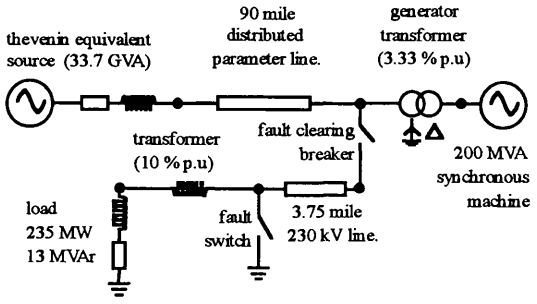

Fig 3 EMTP Power System Model.

A. Computer Based Simulation Studies.

The EMTP used the power system model shown in Fig. 3. This model was based on the EPRI transient stability study model[8]. Stable swings were generally initiated by using a fault whose duration was just short of the critical clearing time of the generator. This produces the most severe stable swing possible. Pole slips were triggered using a range of faults whose duration was longer than the critical clearing time.

B. 625 kVA Diesel Generator Field Trial Test.

In order to demonstrate the algorithm's operation in anger, limited tests were conducted using a diesel generator. The 625 kVA industrial generator was connected to the utility network via a 415/11,000 volt unit transformer and 2 km of 11 kV cable. The utility infeed capacity at the cable termination was 150 MVA and the local load connected to the generator was approximately 500 kW.

Performing practical pole slipping tests on a generator was particularly difficult because of the damage pole slipping could cause. The operator would not allow the use of short circuit faults on the power system to induce pole slipping. A steady state pole slip was therefore induced by increasing the diesel engine's output torque with the generator under-excited for one test as shown later. This produced a 2.5 MW power surge in the machine. Although contrived, this scenario is not unknown and would result from a generator control system malfunction or inexperienced operators.

VI. DISCUSSION OF SIMULATION STUDIES

A. Computer Based Simulation Study Results.

An extensive series of simulation studies was conducted including both pole slipping tests and recoverable or stable swings of the system. For these tests, the power based algorithm operated for all of the pole slipping tests and successfully restrained for all stable swing tests. The MHO pole slipping scheme operated for all of the pole slipping simulations, but it also operated for 30 % of the stable swing tests. The single blinder scheme operated for 75 % of the pole slipping tests, and successfully restrained for all of the stable swing tests. The double blinder scheme also operated for 75 % of the pole slipping tests, but also operated for 15 % of the stable swing tests.

A.1 Power Based Pole Slipping Protection Scheme

Fig. 4 shows the algorithm's response to a classical pole slip, for which it trips after 1.52 s. The pole slip was induced by a two phase fault which was cleared at a time of 1.495 s. The algorithm detected the pole slip 25 ms after fault clearance. Note that the units are in relay secondary quantities, the secondary rating of the generator was 190 VA.

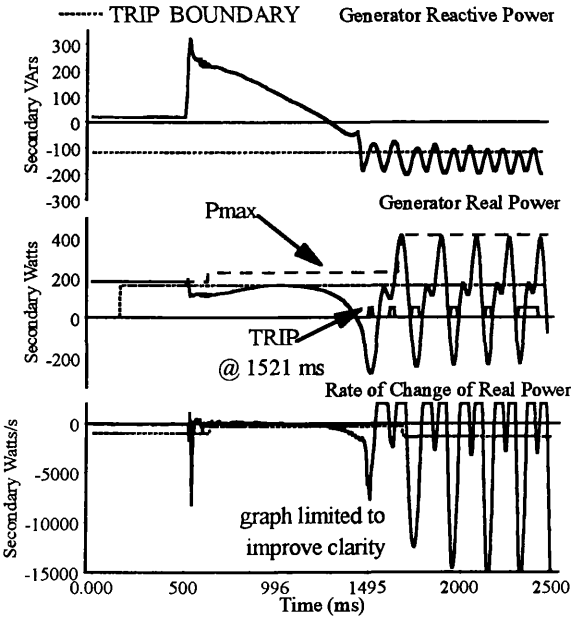

Fig. 4 Power Based Pole Slipping Algorithm Response to 200 MVA Generator Pole Slip.

The algorithm's ability to remain stable during a stable swing is shown in Fig. 5. Following the disturbance, parts of the trip criteria could be satisfied, but not all of them together and hence the algorithm did not trip. At the 1.0 s point, the rate of change of power satisfies its trip level, as does the reactive power, but the algorithm does not trip because the real power is above its trip level. At 1.4 s, the rate of change of power satisfies its trip level once more, as does the real power, but here, the reactive power is above its trip level. By the time the reactive trip criteria is once again satisfied, the rate of change of power trip level is not satisfied and the algorithm therefore remains stable.

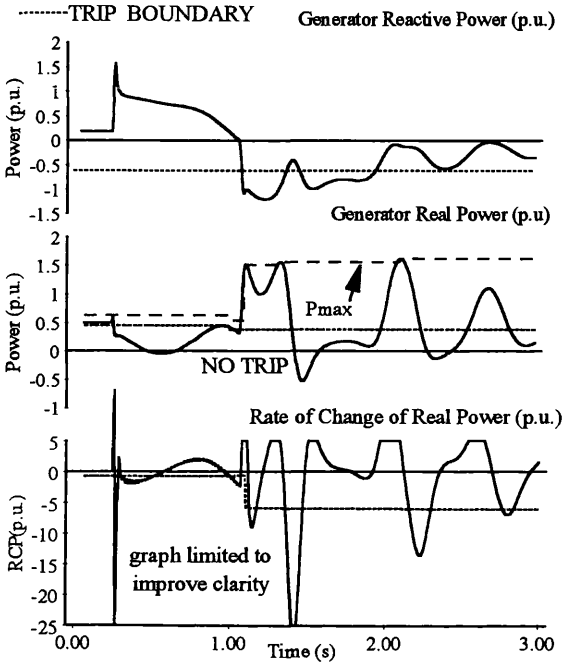

Fig. 5 Power Based Pole Slipping Algorithm Response to 200 MVA Generator Stable Swing.

A.2 MHO Scheme

The MHO characteristic reach was set such that the theoretical swing locus entered at 120°. It therefore included all of the generator's impedance, but none of the transformer's. A time delay of 20 ms was used to increase the stability of the scheme.

Fig. 6 shows the MHO characteristic and the impedance trajectory for a stable swing test which resulted in a nuisance trip. This swing was set up using a 2 phase to earth fault, with the generator initially at 50 % load, its governor was included, but the AVR was modelled as being on manual control. Immediately after the fault was cleared, at 1.07 s, the impedance trajectory jumps into the MHO circle, and then leaves temporarily at 1.11 s. It then re-enters the circle and remains inside the characteristic for a total time of 140 ms. The scheme tripped at 1.16 s.

If the scheme's time delay had been increased to 140 ms, the nuisance tripping would have been avoided, but the scheme would fail to detect fast pole slips, whose locus may travel through the relay characteristic in less than 140 ms.

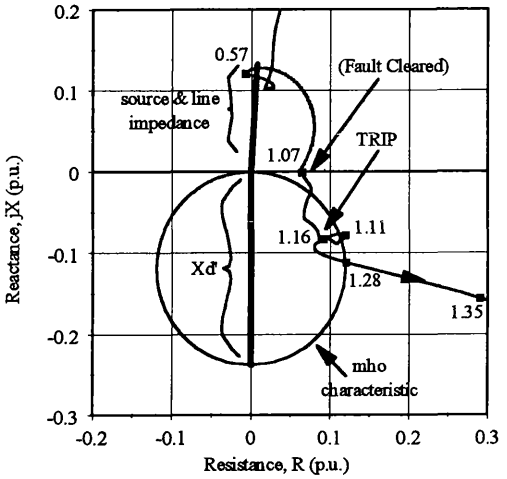

Fig 6 MHO Scheme Characteristic for 200 MVA Generator Stable Swing Simulation.

A.3 Single Blinder Scheme

The settings for the single blinder scheme were chosen so that the theoretical swing locus crossed the right and left blinders at 100 and 260° respectively. The MHO was set so that the scheme would operate for pole slips appearing on the generator side of the high voltage transformer terminals. The minimum permitted travel time between left and right blinders for this scheme to operate was set to 40 ms, two cycles at 50 Hz.

Fig. 7 shows the single blinder scheme characteristic and the impedance locus for a typical pole slipping condition. The pole slip was caused by a 3 phase fault, with the generator initially at 50 % load, and both the AVR and governor were modelled.

As a result of the fault, the impedance locus travels between the two blinder units and moves down the impedance plane towards the origin, this can be seen at 0.27 s on Fig. 7. When the fault is cleared, the impedance enters the supervisory MHO characteristic as the generator is part way through its first pole slip cycle, this corresponds to 0.94 s in Fig 7. The first stage of the single blinder logic is not satisfied, since the impedance locus must first enter the MHO circle before crossing the blinder unit. If the fault had been cleared when the system angle was at a lower value, then the impedance would have

jumped to the right of the right hand blinder and the scheme would have operated successfully. After fault clearance, the impedance locus then moves to the left of the R-X plane, and leaves the MHO circle just before 1.12 s. The single blinder scheme therefore did not trip for the first pole slip.

For the series of tests, the scheme failed to trip for 25 percent of the pole slipping conditions. In all of these tests, the generator was initially operating at low power, and as a result only slipped one pair of poles. The scheme therefore did not detect these conditions as it requires a complete pole slipping cycle to operate. This increases the potential for damage to the generator, since for pole slips following faults, the scheme may require two complete pole slipping cycles before tripping. This may be seen as desirable in some instances, however it is more flexible to have a facility built into the relay which delays tripping until the second pole slip cycle if required.

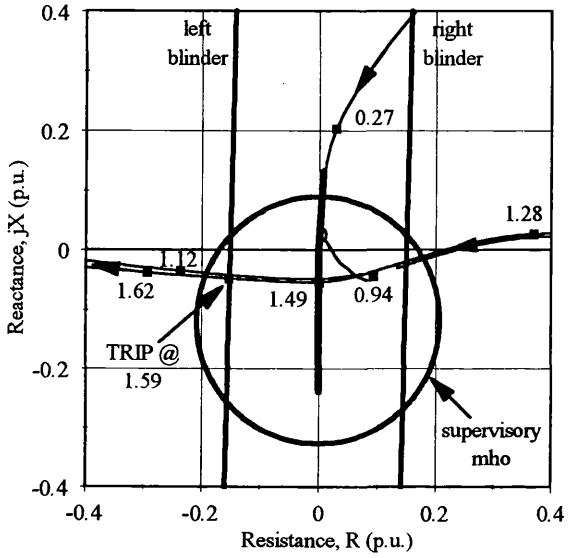

Fig 7 Single Blinder Scheme Characteristic for 200 MVA Generator Pole Slip.

The impedance trajectory for the second pole slip cycle enters the diagram at 1.28 s as shown in Fig. 7, and then enters the MHO circle and crosses the right hand blinder unit, sealing in the first stage of the single blinder logic. The impedance locus then travels across from right to left and crosses the left blinder unit, causing the scheme to trip at a time of 1.59 s. The scheme therefore successfully trips for the second pole slip.

A.4 Double Blinder Scheme

The double blinder scheme also failed to trip for 25 percent of the pole slipping simulations for similar reasons to the single blinder scheme. The double blinder scheme requires a complete pole slipping cycle to operate, and could therefore fail to operate for the first pole slip following a close up fault.

Fig. 8 shows part of the double blinder characteristic and an impedance locus for a stable swing produced by a 3 phase fault. The generator was initially operating at 100 % load, and the AVR was included in the model, but not the governor.

The inner elements of a double blinder scheme should be set so that only non-recoverable swings should cross them [1], and they were therefore set to 130°. To reduce the stress on the breaker, tripping is delayed until the supervisory MHO element resets. The MHO characteristic was therefore set to a value of 85°. The outer blinder elements were then set so that the swings with a ratio of *Eg/Es* of up to 1.5 would be detected. The timing constraints were calculated assuming the maximum mean rate of pole slipping to be 8 Hz.

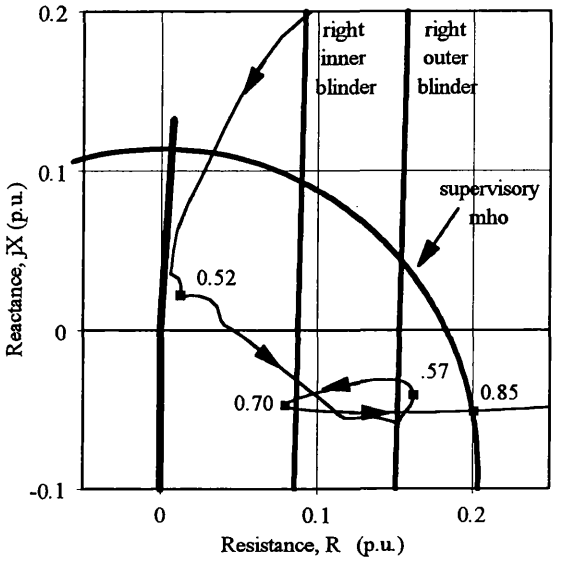

Fig. 8 Double Blinder Scheme Characteristic for 200 MVA Generator Stable Swing Simulation.

As shown in Fig. 8, the fault is cleared at 0.52 s. The impedance trajectory then travels from inside the two inner elements to the outside of the right outer blinder element. At 0.57 s, the supervisory MHO is picked up, but the two right blinder units are not. The locus then heads back to the left and crosses both of the blinders with a time delay of approximately 0.13 s. This satisfies the first stage of the double blinder logic. The locus then stays in between the inner blinder elements for long enough to seal the next stage of the scheme's logic. It then crosses back over the two right hand blinder units in 0.12 s, satisfying the final stage of the scheme logic, and a trip signal is produced at a time of 0.85 s.

B. 625 KVA Diesel Generator Pole Slip Test.

The performance of the generator and the new power based algorithm was monitored by the disturbance recorder function included in the microprocessor relay package together with a second package. During the test the operator permitted the generator to complete two entire pole slipping cycles before reducing the diesel engine torque to allow the generator to pull back into synchronism.

In the most dramatic of the tests, the new power based pole slipping algorithm successfully detected both of the pole slips, however, analysis showed that the impedance based schemes all failed to trip.

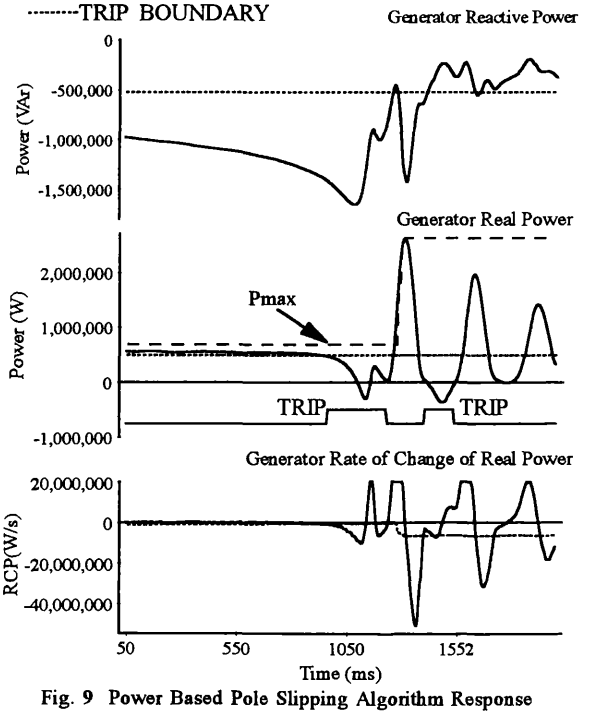

Fig. 9 Power Based Pole Slipping Algorithm Response to 625 kVA Diesel Generator Pole Slip.

Fig. 9 shows the power based pole slipping algorithm's response to this test. The real power plot shows where the algorithm tripped, which for the first pole slip occurred just before 1000 ms on the record. Allowing for a circuit breaker operating time of 100 ms, this would have isolated the generator before the pole slip. The real power plot also reveals the potentially damaging effects of pole slipping, since the peak in power output after the first pole slip reaches 2.7 MW, five times rated power. By tripping before the pole slip occurred, the new algorithm would have avoided this dangerous surge in the power output. Due to the finite disturbance recording time, the transition from normal to underexcited generator operation was not captured.

The conventional impedance based schemes were set so that they would operate for swings appearing on the generator side of the transformer high voltage terminals for a range of values of ***Eg/Es*** from 0.66 to 1.5. The value of ***Xd'*** for the generator was 0.22 p.u., the transformer reactance was 0.03 p.u. The MHO scheme was set so that the swing locus for a value of ***Eg/Es*** of 1 entered the characteristic at an angle of 120°. If the characteristic had been set to reach from the transformer high voltage terminals all the way into the generator, the theoretical locus would have entered at a value of 102°, making the scheme liable to operate for recoverable power swings.

The MHO scheme's failure to trip further highlights the difficulty in using it. Covering the whole of the generator ***Xd'*** can lead to too large a MHO characteristic, and this makes the scheme prone to nuisance tripping. Adding a time delay increases the stability of the scheme to recoverable swings, but as the time delay is increased, the scheme may fail to detect fast pole slips whose locus travels through the characteristic quickly. If the circle size is decreased in order to increase stability, the scheme can fail to detect pole slips whose impedance does not take the classical trajectory.

The single blinder scheme was set using the recommended blinder settings of 90° and 270°. The supervisory MHO circle was set so that theoretical swings appearing in the transformer and generator could be detected. The scheme characteristics and the impedance locus of the pole slipping generator are shown in Fig. 10. It must be noted that the time records are not the same as used in Fig. 9 since the disturbance recorders were not synchronised.

The first pole slip occurred between 0.2 and 0.3 s, and the second occurred between 0.5 and 0.6 s. The first pole slip was not detected because the impedance trajectory did not enter the supervisory MHO characteristic. However, even if the supervisory MHO had been made larger, the scheme would still have failed to trip since the trajectory did not cross the left hand blinder. For the second pole slip, the swing impedance travelled across the impedance plane from right to left as predicted by theory, but again it did not enter the supervisory MHO characteristic. This was due to the speed at which the generator pole slipped. If the generator pole slips at a slow speed, then the impedance of the generator is much larger. At a slip of 0.33 %, the effective impedance of the generator becomes ***2*Xd'*** [9].

The double blinder scheme suffered similar problems to the other impedance based techniques and failed to trip.

A loss of field protection included in the relay did however trip. Its MHO characteristic was set to a value of ***Xd + Xd'/2***, which for this generator was -j 2.26 pu. This relay had a 0.5 s delay.

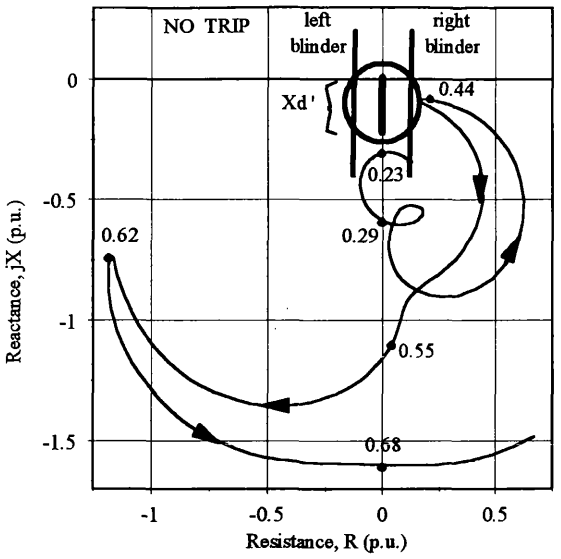

Fig **10** Single Blinder Protection Scheme Characteristic for 625 kVA Generator Pole Slip Test.

VII. CONCLUSIONS

The growth in microprocessor relaying has enabled new adaptive pole slipping algorithms to be developed which automatically adjust their settings according to the generator operating point. The power based scheme discussed in this paper successfully detected all of the pole slipping conditions and restrained for all of the stable swings. In addition a major advantage is the simplicity of setting the relay.

Conventional impedance based pole slipping protection requires detailed simulations of the system to be protected in order to derive reliable settings. Unfortunately, pole slipping impedance loci predicted from theory are not always reflected in reality and complicate the choice of reliable settings.

The MHO scheme was shown to mal-operate for stable swings if the characteristic was set too large, and failed to detect some pole slips if time delays were used in order to prevent nuisance tripping during stable swings.

The single blinder scheme is the most secure of the conventional schemes, but the price for this extra security against relay mal-operation is that a complete pole slip cycle is required for the scheme to operate.

The double blinder scheme is less secure than the single blinder scheme, and may fail to detect the first pole slip following a fault. Like the single blinder scheme, it requires a complete pole slip cycle to operate properly.

VIII. ACKNOWLEDGEMENTS

The authors are pleased to acknowledge the help and encouragement provided by the University of Bath, GEC ALSTHOM Protection and Control and the Engineering and Physical Science Research Council.

IX. REFERENCES

[1] D.W. Smaha, "Out-of-Step Relay Protection of Generators," *IEEE Tutorial on the Protection of Synchronous Generators*, Section 8, 95-TP-102, Power System Relaying Committee 1995.

[2] M.A. Redfern & M.J. Checksfield, "A New Pole Slipping Protection Algorithm for Dispersed Storage and Generation Using the Equal Area Criterion," *IEEE Trans. Power Delivery*, Vol.10, No.1, Jan 1995, pp 194 - 202.

[3] J.A. Imhof (Chairman) et al, "Out of Step Relaying for Generators - Working Group Report," *IEEE Trans. Power Apparatus and Systems*, Vol. PAS-96, No.5, Sept 1977, pp 1556 - 1564.

[4] H.K. Clark and J.W. Feltes, "Industrial and Co-generation Protection Problems Requiring Simulation," *IEEE Trans. Industry Applications*, Vol. IA 25, No.4, July 89, pp 766-775.

[5] E.W. Kimbark, *Power System Stability - Power Circuit Breakers and Protective Relays*, Vol - II, New York: Wiley & Sons, 1964, Chapter X.

[6] *Alternative Transients Program (ATP) Rule Book*, July 1987 Edition, Leuven EMTP Centre (LEC), Belgium.

[7] Clarke E, "Impedances Seen by Relays During Power Swings With and Without Faults" AIEE Trans. Vol 64, 1945, pp 372 - 384.

[8] Alvarado F L, "Electromagnetic Transients Program (EMTP), Volume 3: Workbook III", EPRI EL-4651, Research Project 2149-6, Chapters 7 & 8, June 1989.

[9] Stalewski A, "Pole Slipping Protection", Developments in Power System Protection Conf, IEE Conf. Pub. No. 185, pp 3845.

Miles A Redfern (M'79) received his BSc degree from Nottingham University and PhD degree from Cambridge University in 1970 and 1976 respectively. In 1970, he joined British Railways Research, and in 1975, moved to GEC measurements where he held various posts including Head of Research and Long Term Development and Overseas Sales Manager. In 1986, he joined Bath University with interests in Power Systems Protection and Management. He is chairman of the organising committee for the 1997 IEE conference "Developments in Power System Protection", and is a member of IEE Professional Group P11, Power System Measurement, Protection and Control. He is a corresponding member of the IEEE Line Protection Sub-Committee.

Matt Checksfield received his B Eng degree from the University of Bath in 1993. He is currently studying for his PhD degree at the University of Bath and is sponsored by GEC ALSTHOM Protection and Control. His research interests are embedded generation, protection, power system stability, and renewable energy systems.

PAPER EIGHT

"PROTECTION AGAINST POLE SLIPPING AND LOSS OF EXCITATION FOR EMBEDDED GENERATORS"

M J Checksfield and M A Redfern

Presented at :-
31st Universities Power Engineering Conference (UPEC),
September 1996, Crete, pp 9 - 12.

PROTECTION AGAINST POLE SLIPPING AND LOSS OF EXCITATION FOR EMBEDDED GENERATORS.

M J Checksfield & M A Redfern.

University of Bath, UK.

ABSTRACT.

With the increasing amount of embedded generators being installed, concern has arisen regarding pole slipping and loss of excitation. Both conditions can cause machine damage and system problems. Protection which disconnects the machine as quickly as possible for either conditions is therefore required. This paper presents new algorithms for detecting both loss of excitation and pole slipping which are simple to set and detect both conditions quickly and securely. Results from industrial generator field trials are used to verify the new algorithms.

1.0 INTRODUCTION.

With the growing number of embedded generation sets being installed to operate in parallel with utility distribution systems, synchronous generator pole slipping and loss of excitation are increasingly being recognised as areas of concern.

The likelihood of pole slipping for embedded generators is high[1], due to the low values of generator inertia, short transient time constants, high reactances, and long fault clearance times associated with distribution systems. Stability studies have shown [1] that the critical clearance time for embedded generators is generally below 300 ms. Since the fault clearance times associated with the overcurrent type protection schemes are normally in the 400 to 1000 ms range, generator instability and hence pole slipping is highly probable following clearance of a fault which does not cause the generator itself to be disconnected [2].

Pole slipping can cause utility voltage disruptions which can create problems for other consumers close to the affected generator [3]. Induction motor stalls, motor tripping, synchronous motor pole slipping and nuisance tripping of other protection relays can also be caused. Pole slipping may damage the machine due to rotor and stator overheating, shaft fatigue, excitation system damage and mechanical damage to the windings. It is therefore recommended, that when a generator pole slips, it is dis-connected as soon as possible[4].

Loss of excitation like pole slipping, results in the synchronous generator operating asynchronously. However, since the generator has very little, if any excitation during loss of excitation, the resultant fluctuations in machine power and torque are less. As with pole slipping, loss of excitation imposes a very high reactive power demand on the system, which may depress system voltage and cause problems for adjacent machines and other consumers. The generator stator winding can become over loaded by the high reactive currents, and may overheat due to the induced currents in the field winding and rotor body. The permissible time before damage occurs varies according to the type of machine, prime mover governor characteristics, type of excitation loss, and system conditions. The maximum permitted time before damage may be as low as 10 seconds [2]. Another consideration is when the loss of excitation condition is due to a failure of one of the components of the excitation system. Prompt tripping of the generator and any associated equipment will ensure that any additional damage to other components and adjacent equipment will be minimised[5].

Loss of excitation may be caused by a short in the excitation system, failure of the excitation power source, a faulty Automatic Voltage Regulator (AVR), and personnel errors. Pole slipping is generally due to a system problem, whereas loss of excitation is a machine problem. Although both conditions require immediate tripping, it may be possible to re-synchronise and re-load the generator directly after pole slipping. It is therefore useful to know which phenomenon caused the generator disconnection.

2.0 ASYNCHRONOUS OPERATING CHARACTERISTICS.

The synchronous real power, Ps and reactive power, Qs characteristics for a disturbed synchronous generator operating against an infinite bus[6] are given in (1) and (2);

$$Ps = \frac{Eq' V}{Xd'} \sin(\delta) + \left[\frac{1}{Xq} - \frac{1}{Xd'}\right] \frac{V^2}{2} \sin(2\delta) \quad (1)$$

$$Qs = \frac{Eq'V}{Xd'} \cos(\delta) - \left[\frac{1}{Xq} + \frac{1}{Xd'}\right]\frac{V^2}{2} + \left[\frac{1}{Xq} - \frac{1}{Xd'}\right]\frac{V^2}{2} \cos(2\delta) \quad (2)$$

Where Eq' is the voltage behind transient reactance, Xq is the Q axis synchronous reactance, Xd' is the D axis transient reactance, V is the generator terminal voltage, and δ is the generator load angle. The first term containing Eq' in both equations is due to the excitation supply on the field winding. The (2δ) terms are due to the effects of rotor saliency. The middle term of (2) is a result of the magnetisation energy that the machine requires to produce an air gap flux. The dominant terms during stable synchronous operation are the first terms. During asynchronous operation additional components of power are produced due to induction generator action. The mean values [7] of these terms are given by (3) and (4);

$$Pas = -s \frac{V^2}{2} \left[\frac{Xd-Xd'}{Xd.Xd'} \frac{Td'}{1+(sTd')^2} + \frac{Xd'-Xd''}{Xd'.Xd''} \frac{Td''}{1+(sTd'')^2} + \frac{Xq-Xq''}{Xq.Xq''} \frac{Tq''}{1+(sTq'')^2} \right] \quad (3)$$

Where Pas is the average component of real power generated due to rotor slip, s, Xd is the D axis synchronous reactance, Xd" is the D axis sub-transient reactance, Xq" is the Q axis sub transient reactance, Td' is the D axis short circuit transient time constant, Td" is the D axis sub-transient time constant, and Tq" is the Q axis sub transient time constant.

$$Qas = -s^2 \frac{V^2}{2} \left[\frac{Xd-Xd'}{Xd.Xd'} \frac{(Td')^2}{1+(sTd')^2} + \frac{Xd'-Xd''}{Xd'.Xd''} \frac{(Td'')^2}{1+(sTd'')^2} + \frac{Xq-Xq''}{Xq.Xq''} \frac{(Tq'')^2}{1+(sTq'')^2} \right] \quad (4)$$

Where Qas is the average component of reactive power due to rotor slip. Note that a negative value of slip is produced when the rotor is travelling above synchronous speed. The machine reactances are in per unit, the time constants in radians, ($t_{[rad]} = \omega_o t_{[sec]}$) and the slip has no units, it is relative (1% slip => 0.01).

Equation (3) shows that a significant amount of real power generation is possible during asynchronous operation.

2.1 Pole Slipping Characteristics.

During pole slipping the dominant characteristics are determined by (1) and (2). The real and reactive power both take on sinusoidal characteristics with increase in load angle during the pole slip. These

sinusoidal characteristics make the apparent impedance locus track from right to left across the RX plane, and it is this characteristic which the majority of impedance based pole slipping protection schemes rely upon to detect pole slipping.

Asynchronous power is also generated during pole slipping as shown by (3) and (4). Equation (3) shows that an extra component of real power will be generated, and this can significantly change the real power characteristic during pole slipping in some machines. It is possible that during times of low excitation, where Eq' is small, the contribution to generator output power by asynchronous operation results in a power output characteristic which does not reverse during pole slipping[8]. This will increase the difficulty in setting some impedance based relays which rely on the apparent impedance crossing from right to left across the impedance plane.

Equations (2) and (4) show that the reactive power demand that the generator places on the system during pole slipping can be very high. The worst point occurs when the load angle travels from 180 to 270°. During this period the synchronous terms of (2) will cause the generator to import reactive power. In addition the slip of the generator will be approaching its highest value since the generator will be motoring, and (4) shows that asynchronous reactive power demand varies approximately with the square of slip. The amount of reactive power imported during pole slipping is important when considering the stability of pole slipping and loss of excitation protection schemes during recoverable power swings. The 'ideal' reactive power demand outlined in (2) can become highly distorted by the induction machine action described in (4). The high asynchronous reactive power demand occurs for positive (motoring) as well as negative (generating) slips. The overall effect on generator reactive power demand during recoverable power swings is therefore to increase it. This brings the apparent impedance locus closer to the operating characteristics of impedance based relays.

2.2 Loss of Excitation Characteristics.

When a generator loses its field, the Eq' terms in (1) and (2) gradually fall to zero in a time determined by the open circuit transient time constant, Tdo'. Following the loss of excitation, some of the generator real power output will be provided by the second term in (1). This is the 'transient saliency' term, and for the duration of the period where the generator is losing its main field, this term will help maintain real output power and prevent load angle increase. After the transient period of the generator has died away, the Xd' term in (1) becomes an Xd term.

Most of the literature concerning loss of excitation deals with characteristics for turbo - generator units. These are round rotor machines and therefore have Xd ≈ Xq. A round rotor machine will begin to accelerate at this point since it can no longer produce synchronising forces to keep the machine load angle at a constant value. As the generator slip begins to increase, the machine will begin to function as an induction generator and it is possible for the prime mover governor characteristics to intersect the asynchronous torque curve. When this occurs the generator operates as a stable asynchronous generator. Some loss of excitation schemes may fail to detect this condition due to the impedance locus settling to the right of their protection characteristic. This is more likely to occur for loss of excitation conditions which occur at low generator loadings. At full load stable asynchronous operation may not occur and the generator may be forced to operate past the peak of its power slip curve. This is a more onerous condition since the machine may overheat quickly due to the high level of induced currents in the rotor structure. The generator therefore needs disconnecting as quickly as possible when a loss of excitation occurs at full load.

In contrast to the commonly discussed round rotor generators, embedded generators are often salient pole machines. Diesel generators and hydro sets are two examples. With salient pole machines, the loss of excitation characteristics can be different to round rotor characteristics. At low loads it is possible that the generator may function as a reluctance generator. The maximum amount of power which the machine can provide due to reluctance action, Pr(max) is given by (5);

$$Pr(max) = \left[\frac{1}{Xq} - \frac{1}{Xd}\right]\frac{V^2}{2} \qquad (5)$$

Typical values for Xd and Xq are 2.25 and 1.1 pu respectively, a reluctance power output of 23 % pu may therefore be achieved at 1 pu terminal voltage. If the generator functions as a reluctance generator, synchronous operation will be maintained and no overheating due to induced currents will occur. The generator should still be tripped however, as a fault will still exist in the excitation system. If the initial generator output power is greater than the maximum reluctance torque, then asynchronous operation will occur once that the generator field flux has decayed. This condition will appear to be more severe than with a round rotor machine due to the rotor saliency. The 2δ terms of (1) and (2) will cause oscillations in the generator real and reactive power at twice slip frequency. These variations will superimpose oscillations onto the terminal voltage. If the embedded generator is connected to a weak source, the voltage oscillations in addition to the voltage depression caused by the loss of excitation will compromise the quality of supply of adjacent consumers. It is therefore essential that the generator is tripped as quickly as possible.

3.0 PROTECTION ALGORITHMS FOR DETECTING POLE SLIPPING AND LOSS OF EXCITATION.

The algorithm used to detect pole slipping and loss of excitation from high initial powers uses the Critical Stability Point (CSP)[3,9]. Once the critical stability point has been past, stability can not be maintained and pole slipping, or asynchronous running will occur. The algorithm predicts that pole slipping will occur by detecting if the load angle is still increasing once the CSP has been exceeded. In designing an algorithm for detecting generator asynchronous conditions, it must be able to predict when a generator is about to, or actually is running asynchronously. It must also remain stable for all other power system conditions, including faults and recoverable power swings.

The algorithm uses reactive power, real power, and rate of change of real power to detect operation past the CSP. The algorithm is;

$$\text{TRIP IF} \quad \begin{array}{rcll} Q & < & Q_{trip} & \} \text{ Continuously} \\ \text{and} & & & \} \\ P & < & P_t & \} \text{ For 1.5 Power} \\ \text{and} & & & \} \\ (\Delta P/\Delta t) & < & (\Delta P/\Delta t)_{min} & \} \text{ System Cycles} \end{array} \qquad (6)$$

Where Q is the generator three phase reactive power, Qtrip is the reactive power trip setting, based on the Q axis synchronous reactance. P is the generator real power output, Pt is the real power trip setting which is derived by the algorithm. (ΔP/Δt) is the rate of change of real power, $(\Delta P/\Delta t)_{min}$ is the rate of change of power trip setting which is derived by the algorithm. The 1.5 power system cycle time constraint is to ensure the algorithm does not operate for faults. The majority of faults will not satisfy all of the criteria of equation (6), the few that do only cause the criteria to be satisfied during fault clearance for less than one power system cycle.

3.1 Condition Monitoring Techniques.

The algorithm is designed for a microprocessor based relaying, where the only information available to the relay is 2 phase voltages and 3 current signals provided by the relay's input transducers. Since generators may be operated over a range of output powers, a method

of estimating the prime mover input power, Pm is required so that the real power trip setting, Pt can be derived. The input power is estimated by observing the power output of the generator and using the following algorithm;

$$\text{if } |P_n - P_{n-lag}| \text{ and } |P_n - P_{n-(2*lag)}| < Ptol ; \quad \text{then } Pt = P_n * Pfact \tag{7}$$

where P_n is the present real power sample value, P_{n-lag} is the sample value of 'lag' samples ago, $P_{n-(2*lag)}$ is the sample value of '2*lag' samples ago, P_{tol} is the tolerance band, chosen as nominally 5% of machine rating, and Pfact is a coefficient to take into account the losses and inaccuracies inherent in measuring machine input power from output power. The algorithm processing rate is 4 times per power system cycle, the value of 'lag' typically chosen is 200 which equates to 1 second, Pfact is nominally set to 0.9.

3.2 Adaptive Trip Setting $(\Delta P/\Delta t)_{min}$

The margin for error, $(\Delta P/\Delta t)_{min}$ used in the $(\Delta P/\Delta t)$ criterion is based on the theoretical value of $(\Delta P/\Delta t)$ at the CSP[3,9], it is given by;

$$(\Delta P/\Delta t)_{min} = -s * Pmax * \cos\left\{180 - \sin^{-1}\left(\frac{Pt}{Pmax}\right)\right\} \tag{8}$$

The value of slip chosen will not be the exact value at which the relay trips, due to effects not taken into account in the derivation of (8), such as damping power. Equation (8) is used by the trip algorithm to continuously update the trip setting $(\Delta P/\Delta t)_{min}$ depending on what the variables Pmax and Pt dictate.

Pmax is a measure of the maximum output power that the generator has produced in the last second. It is used so that the algorithm can adjust its setting according to whether transient or steady state conditions are prevailing. With loss of excitation or steady state pole slips, a gradual loss of synchronism occurs, and the resulting power output waveforms change gently to begin with. This produces low values of $(\Delta P/\Delta t)$, a sensitive trip setting is therefore required. If the generator has been transiently disturbed, its output during the first swing in load angle, be it stable or unstable, will be much greater than its nominal output. This results in a greater magnitude in $(\Delta P/\Delta t)$ at the CSP, the algorithm therefore needs to adjust its setting $(\Delta P/\Delta t)_{min}$ accordingly. The algorithm adjusts the setting, $(\Delta P/\Delta t)_{min}$ according to (9);

$$\text{If } \frac{Pt}{Pmax} < 0.6 \text{ then; } (\Delta P/\Delta t)_{min} = (\Delta P/\Delta t)_{min} + (\Delta P/\Delta t)_{tran} \tag{9}$$

where $(\Delta P/\Delta t)_{tran}$ is an external relay setting based on the degree of transient saliency in the generator. Transient saliency arises due to differences in the values of Xd' and Xq'. $(\Delta P/\Delta t)_{tran}$ is given by;

$$(\Delta P/\Delta t)_{tran} \text{ (pu)} = \left(\frac{1}{Xq} - \frac{1}{Xd'}\right) \tag{10}$$

For a steady state pole slip or loss of excitation, no peak will occur in the power output before the pole slip, the algorithm trip setting should therefore be at its most sensitive level to detect the pole slip since low values of $(\Delta P/\Delta t)$ will result.

The value of Pmax used by equations (8) and (9) is nominally set to 1.4 * Pt, so that the ratio Pt/Pmax equals 0.71, $(\Delta P/\Delta t)_{tran}$ is therefore not included in the calculation of $(\Delta P/\Delta t)_{min}$ during steady state conditions. If the generator's power output rises above the existing value of Pmax for greater than one power system cycle, then the value of Pmax is updated to the new maximum for a duration of one second. The one second limit is used so that the new value of Pmax is only used for the period where a pole slip or recoverable power swing associated with that value is likely to occur. The one cycle constraint is necessary so that incorrect values of Pmax do not result from spurious spikes on the power waveform.

3.3 Detection of Loss of Excitation at Low Powers.

The above algorithm will successfully detect pole slipping and will also detect loss of excitation from high initial powers. It may fail to detect loss of excitation from low initial powers. For a round rotor machine, the drop in real power and resultant size of the $(\Delta P/\Delta t)$ signal may not be sufficient to cause it to trip. The small amount of saliency also means that once asynchronous operation occurs, the pulsations in power will not be sufficient to cause it to operate. Salient pole machines will cause the algorithm to trip if they operate asynchronously following loss of excitation, due to the pulsations in real and reactive power. If the machine remains in synchronism due to reluctance torque action, no power pulsation will result and the algorithm will not trip.

To provide full loss of excitation protection at these lower power ranges, a real power limited VAr relay is used. Figure 1 shows its operating characteristic on the underexcited portion of a salient pole generator operating chart[10]. The VAr limit setting, Qset is set according to V^2/Xd, whilst the Watt setting, Pset is based on the saliency term V^2 (1/Xq - 1/Xd). This introduces a margin for error since the generator can only operate as a reluctance generator at half this value.

If the generator is a round rotor machine, Pset is set to half machine VA rating. The purpose of Pset is to ensure the scheme does not nuisance trip during recoverable power swings. During such swings the reactive power may fall below Qset, but this only occurs when the power is at high values, i.e above Pset. The 1 second time delay enhances algorithm security. The operating characteristic is located just at the edge of the practical stability limit. It is very unlikely that an embedded generator would be operated in this region since this mode of operation is only required if the local load is predominantly capacitive, or the system voltage is too high. These conditions occur very rarely. In addition, operation in this area would further decrease the machines stability margins increasing the chance of instability and pole slipping. If the generator was required to operate in this area from, the reactive setting, Qset would have to scaled up by a safety factor of 1.2.

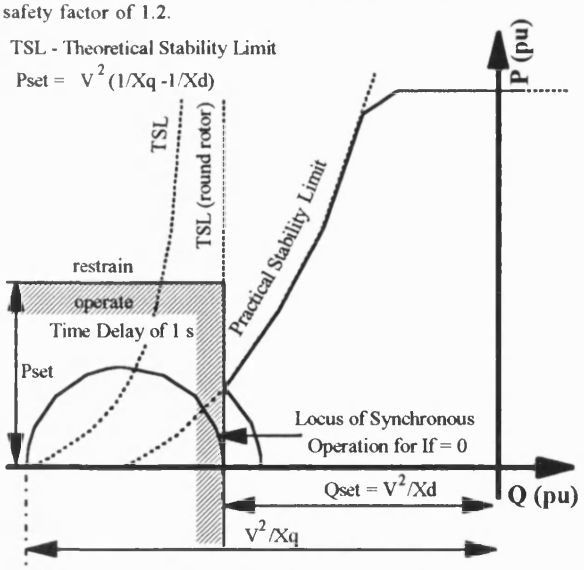

Figure 1: Under-Excited Section of Salient Pole Generator Operating Chart and Loss of Excitation Var Relay Characteristic.

4.0 ALGORITHM VALIDATION STUDIES.

The algorithms were tested using field trials on a 625 kVA industrial diesel generator connected to the utility network via a 415/11,000 volt unit transformer and two parallel 2 km 11 kV cables. The fault capacity at the generator terminals was 30 MVA. 500 kW of local

load was connected to the generator. The field trial tests were performed in order to validate the operation of the new power based pole slipping algorithm within a commercial relaying platform. It was not possible to place faults on the power system to induce pole slipping, and hence a pole slip was induced by increasing the diesel engine's output torque with the generator under-excited. This scenario could happen due to operator error, or if the diesel engine control system mal-functioned. Loss of excitation tests were also performed at 20, 50 and 100 % load at under-excited and over-excited initial excitations.

5.0 FIELD TRIAL RESULTS.

The combination of algorithms successfully detected all of the pole slipping and loss of excitation conditions. The rate of change of power algorithm detected all of the high power loss of excitation whilst the power restrained VAr relay detected all of the low and medium power loss of excitations.

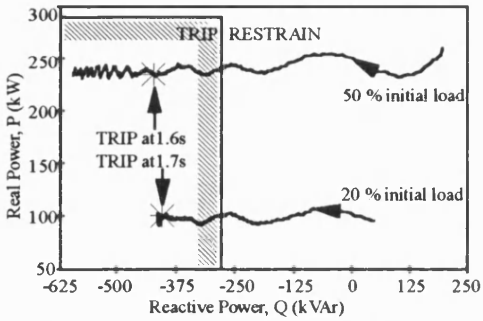

Figure 2: PQ plane Showing Power restrained VAr relay Operating Characteristicand Two Loss of Excitation Loci.

Figure 2 shows two PQ loci for loss of excitations from 20 % and 50 % load. For the 20 % load loss of excitation, the VAr relay tripped 1.7 s after the field was short circuited, for the 50 % loss of excitation, the VAr relay tripped 1.6 s after short circuiting the field. Due to the time delay, the protection did not operate the instant the PQ locus entered the tripping zone. Note that in both cases the generator had not lost synchronism, if it had, there would be significant pulsations in the real and reactive power.

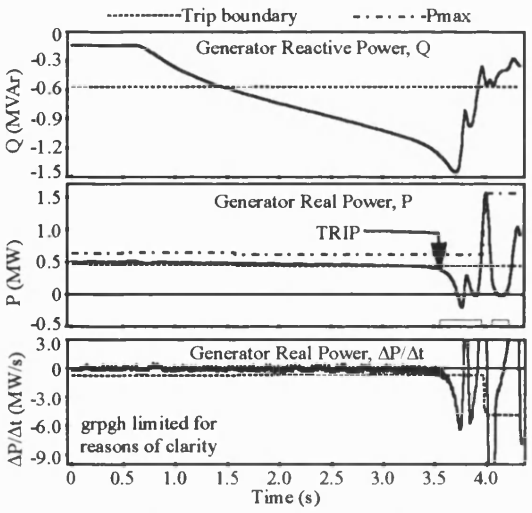

Figure 3: Rate of Change of Power Algorithm Response to Underexcited Full Load Loss of excitation.

Figure 3 shows the rate of change of power algorithm measurands for a loss of excitation from 100 % initial load. The algorithm tripped 2.85 s after the field was short circuited. The real power waveform of Figure 3 shows that the algorithm tripped before the generator operated asynchronously. This would have prevented any damage due to overheating. The VAr relay did not operate for this as the real power did not stay below Pset for 1 s.

References [3,9] provide details of the rate of change of power algorithm's response to pole slipping. Further facilities could be placed into the algorithms to enable the system to diagnosis what caused the trip conditions. The VAr relay will only trip for loss of excitation, unless a very slow pole slip at a rate of 0.5 Hz occurs. If the maximum real power monitor, Pmax is greater than its nominal value of 1.4 * Pt, before the pole slip occurs, then the pole slip would have been caused by a transient disturbance, rather than generator control system failure. Another approach would be to monitor the level of $\Delta P/\Delta t$, if the amplitude of this signal exceeds a level before the before the algorithm trips, then the pole slip was probably due to a transient disturbance. Inspection of the disturbance recording also provides another means of diagnosis, all of which help the protection engineer to ascertain what if anything is wrong with the generator.

6.0 CONCLUSIONS.

Pole slipping and Loss of excitation are two concerns which need to be addressed when considering the protection of embedded generators. Machine damage and system problems may result if protection is not provided.

The power based algorithms presented successfully detect pole slipping and loss of excitation, whilst restraining for all other power system conditions. The power restrained VAr relay is used to detect low power loss of excitations in both salient pole and round rotor generators, whilst the other power based algorithm detect loss of excitation from high powers and all types of pole slipping.

Additional features can be added to the algorithms to provide the protection engineer with diagnostic information. This information will help to ascertain whether the algorithms tripped due to problems with the generator or problems with the power system, such as faults.

7.0 REFERENCES.

[1] Checksfield M J & Redfern M A, "Assessment of Embedded Generator Stability When Connected to a HV Utility Distribution System", 30th UPEC, 1996, Greenwich, pp 219 - 222.

[2] Clark H K & Feltes J W, "Industrial and Co-generation Protection Problems Requiring Simulation," IEEE Trans. Industry Applications, Vol.IA-25, No.4, July 89, pp 766 - 775.

[3] Redfern M A & Checksfield M J, "A New Pole Slipping Protection Algorithm for Dispersed Storage and Generation Using the Equal Area Criterion," IEEE Trans. Power Delivery, Vol.10, No.1, Jan 1995, pp 194 - 202.

[4] J.A. Imhof (Chairman) et al, "Out of Step Relaying for Generators - Working Group Report," IEEE Trans. Power Apparatus and Systems, Vol. PAS-96, No.5, Sept 1977, pp 1556 - 1564.

[5] Mackenzie W F, "Loss of Field Relay Operation During System Disturbances", IEEE Trans, Vol PAS-94, No.5, Sept 1975, pp 1464 - 1472.

[6] CONCORDIA C. 1951, Synchronous Machines: London: J Wiley & Sons, Inc, Ch 2 & 3.

[7] VENIKOV V A. 1964. Transient Phenomena in Electrical Power Systems: Permagon Press.

[8] GUILE A E. Electrical Power Systems,Vol 2.PP106 - 141.

[9] Checksfield M J & Redfern M A, "A Condition Monitoring Pole Slipping Protection Algorithm Based on the Equal Area Criterion", 29th UPEC, Galway, 1994, pp 747 - 750.

[10] Walker J H, "Operating Characteristics of Salient Pole Machines", IEE. Proc. 1953, Vol 100 Pt 2, pp 13 - 23.

PAPER NINE

"A REVIEW OF POLE SLIPPING PROTECTION"

by M A Redfern and M J Checksfield

Published in :-
IEE Colloquim Digest 1996/265 - Generator Protection,
October 1996, Newcastle, UK, pp 6/1-6/9.

A REVIEW OF POLE SLIPPING PROTECTION.

M A Redfern and M J Checksfield
School of Electronic and Electrical Engineering
University of Bath, BATH, UK.

1. INTRODUCTION.

Pole slipping protection, also referred to as loss of synchronism protection, is required when a generator loses synchronism with the utility's main source of power and is subjected to high fluctuations in the current passing through it. When a machine pole slips, it is desirable to disconnect it from the utility supply as quickly as possible, thus preventing possible damage to the generator, disturbance to the local power system, and system instability.

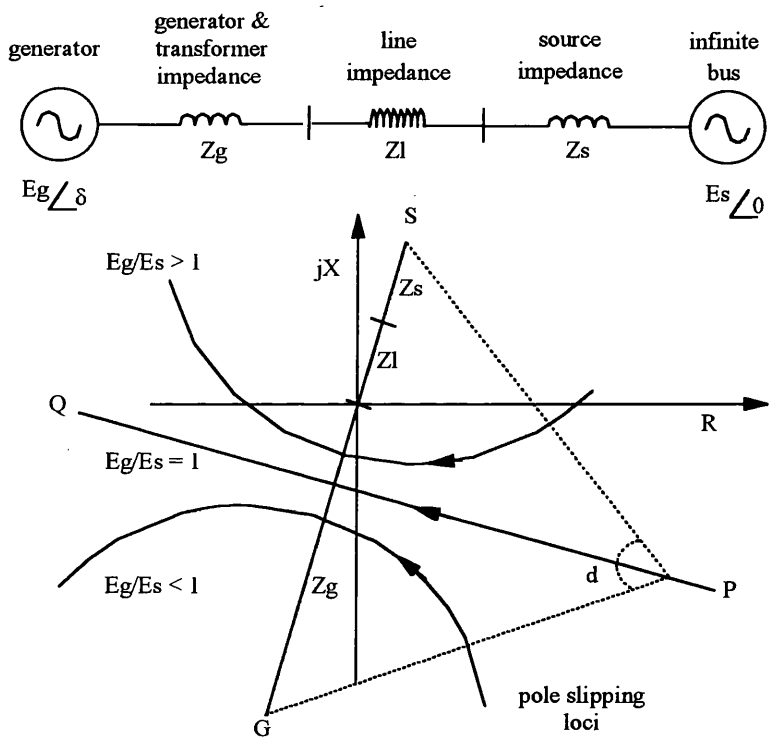

FIGURE 1. THE CLASSICAL POLE SLIPPING IMPEDANCE LOCI.

Pole slipping of a synchronous generator connected to a power supply system can be caused by short circuit faults, general disturbances to the power supply network, or problems with the generator's prime mover or control system. Although system performance criteria for transmission systems have become more stringent over the last few decades and as such the probability of pole slipping on main generation units is very low, the connection of embedded generation to sub-transmission and distribution systems has raised new interest in this type of protection. Some of the factors which promote pole slipping are long fault clearance times, low system voltages, reduced excitation, high impedances between the generator and the supply network, and system switching operations. All of these can be found in sub-transmission and distribution systems.

2. TRADITIONAL TECHNIQUES FOR DETECTING POLE SLIPPING IN GENERATORS.

The traditional technique for detecting pole slipping is to examine the variations in the apparent impedance of the generator as seen from its terminals. Several schemes are commercially available which are based on distance type relays[1,2,3], and use combinations of mho and linear characteristics.

The variations in the impedance seen at the terminals of the generator during pole slipping[4] are shown in figure 1. These impedance loci are derived using the assumptions that the ratio of generator to source impedances, Eg/Es remains constant, generator saliency is neglected, generator damper effects are neglected, transient fault impedance effects have decayed, shunt loads and shunt capacitance effects are ignored, effects of automatic voltage regulators and governors are neglected, and the source voltages behind their equivalent impedances are sinusoidal and at fundamental frequency[1,4,5,7].

For the case where the ratio Eg/Es = 1, the impedance locus will be a straight line, PQ, which is the perpendicular bisector of the system impedance line GS. When a pole slip occurs, the load angle δ increases causing the impedance to travel from right to left across the R-X plane. When the load angle reaches 180°, the loss of synchronism point has been reached and the impedance will lie on the system impedance line GS. The point on the system impedance line where the impedance locus appears for $\delta = 180°$ is known as the system centre, at this point the impedance gives the appearance of a three phase fault. As the pole slip cycle is completed and δ approaches an in-phase value of 360° the impedance locus will travel to the left of the system impedance line before returning to the load area of the R-X plane.

Figure 1 also shows impedance loci for the cases where the ratio Eg/Es < 1 and Eg/Es > 1. The effect is to cause the impedance locus to become a circular arc. These curves show that as the generator internal voltage is increased, the system centre is pushed away from the generator. AVR field forcing action will have this effect.

For the majority of situations, the combined impedance of the generator and its transformer will be larger than the combination of line and equivalent source impedances. This will result in the system centre appearing inside the generator or its transformer during pole slipping.

The simplest type of impedance based pole slipping protection is the single MHO relay scheme[1,5]. Its main advantages are that tripping can occur before the load angle $\delta = 180°$, and that it provides a degree of back up protection for faults occurring in the transformer and generator. Its main disadvantage is that very careful selection of the mho reach is necessary to avoid tripping during power swings for which the pole slipping protection should remain stable.

The relay is normally set to cover the generator transient reactance, Xd' and most of the generator transformer. This may produce a characteristic which is too large and hence be prone to nuisance tripping. Another recommendation is that the angle of swing where the impedance locus enters the characteristic is set to be at least 115°.

The single blinder scheme[1,5] is the most secure of the impedance based techniques for detecting pole slipping. The mho supervisory element restricts operation to swings appearing inside the generator and its transformer. For the scheme to operate, the impedance locus must

enter the mho circle and its trajectory must take longer than a specified time to cross from one blinder unit to the next. The time constraint is normally set to two power system cycles.

The scheme has the advantage over the mho scheme that the diameter of the supervisory mho element can be increased in order to provide better sensitivity to pole slipping conditions without the scheme tripping for stable swings.

The double blinder scheme[1,5] also uses a supervisory mho characteristic to stop the scheme tripping for stable swings. For the scheme to operate, the mho element must first pick up, then the locus must then stay between the inner and outer blinders for a preset time. This will satisfy the first stage of the scheme logic. It then must stay between the inner blinder elements for a short time, and then when leaving the inner characteristics, it must again stay between the inner and outer blinder elements for greater than a preset time. This satisfies the final stage of the scheme logic, a trip signal is then issued when the supervisory mho resets.

The main difference between the single and double blinder schemes is that with the double blinder scheme, the locus can enter and leave the characteristic from any direction. With the single blinder scheme the locus must enter from one side and leave from the other for a trip to occur. The inner elements of the double blinder scheme must therefore be set so that they will only pick up for non recoverable swings.

Unfortunately, the impedance of a generator is not as predicable as would be expected and it depends on the prevailing situation. Hence the concept of the sub-transient, transient and dynamic impedance. It is therefore generally recommended[1,5,6] that transient stability studies are performed so that the location of the impedance loci are known and the most appropriate relaying scheme can be selected. These simulations are necessary to enable correct setting of conventional impedance relays, and they can be time consuming and expensive.

3. Power Based Technique for Detecting Pole Slipping in Generators.

Pole slipping is a power based phenomena and an alternative approach[10] to detecting pole slipping has been developed which uses the Equal Area diagram as a basis to assess the stability of the machine and determine when it is committed to a pole slip. This approach has the potential of tripping before the pole slip actually occurs and hence offers the best prospect of preventing damage to the generator and the adjacent power system.

The technique takes advantage of the processing capabilities of modern multi-function microprocessor relaying platforms and has been designed to share sub-functions with other protection functions required for the protection of embedded generation.

The Equal Area Criterion demonstrates the conditions where synchronism is lost and pole slipping occurs. Figure 2 shows the power/load angle relationship and the rate of change of load angle (slip, s) for a generator losing synchronism with the utility supply to which it is connected following a loss of power transfer capability due to a disturbance on a double circuit line[8]. For this scenario, the generator is connected to a double circuit line and the power system disturbance is caused by switching one of the lines out of service for a short period. Removing the electrical load from the generator, while keeping the mechanical power constant, causes the generator to accelerate and eventually pole slip.

The Equal Area Diagram, figure 2, illustrates that for a stable swing, the machine operating point cannot exceed point 5, the critical stability point. This corresponds to the point where the electrical output of the machine, P, equals the mechanical input from the prime mover, P_m. When the machine becomes insrable, it moves beyond the critical stability point, which can be identified in terms of real power as the condition when:-

$$P < P_m$$

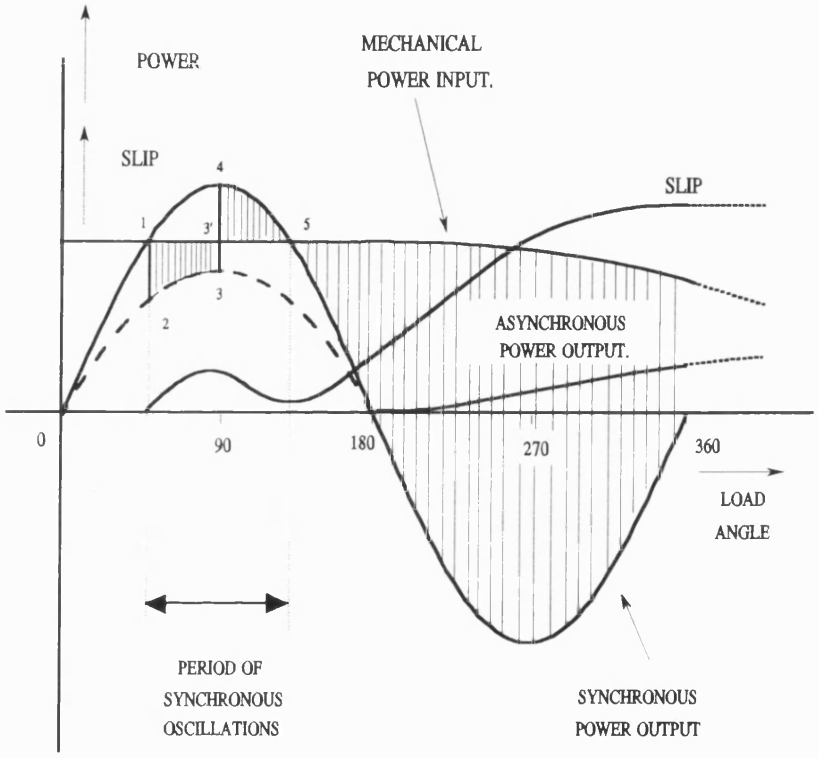

FIGURE 2. EQUAL AREA DIAGRAM FOR GENERATOR LOSS OF SYNCHRONISM.

Since this criterion can also be satisfied for machine operating points between points 0 and 1 shown on figure 2, the reactive power measurement is used to differentiate between the two. The steady state reactive power/load angle relationship for a round rotor machine is given by:-

$$Q = \frac{E*V}{X_d}(\cos(\ \delta\ )) - \left(\frac{1}{X_q} + \frac{1}{X_d}\right)\frac{V^2}{2} + \left(\frac{1}{X_q} - \frac{1}{X_d}\right)\frac{V^2}{2}\ (\cos(\ 2\ \delta\ ))$$

This shows that for load angles between 90° and 270°, the reactive power will always be less than Q_{trip}. Since point 5 of figure 2 occurs for load angles greater than 90°, then if :-

$$Q \leq \frac{-V^2}{X_q} \qquad (= Q_{trip})$$

the machine must be operating at point 5 and not point 1.

The transient reactive power characteristics vary in magnitude from the above steady state values. This does not corrupt the above method since the value of reactive power corresponding to a 90° load angle is identical to the steady state value. The transient reactive power characteristics above and below this load angle are such that in steady state terms it appears as if the load angle is correspondingly higher or lower.

Finally, it must be ascertained whether or not the load angle is still advancing. To determine this, rate of change of real power is used. It can be seen from the synchronous power output characteristic of figure 2, that if the load angle is still increasing when point 5 is reached, the machine output power will be decreasing, i.e. the rate of change of real power will be negative.

In practice a margin for error is allowed for in this rate expression ($\Delta P/\Delta t$), to ensure the algorithm does not mal-operate. A minimum negative value, $(\Delta P/\Delta t)_{min}$ is designated, based on a minimum value of slip and an assumed sinusoidal power/load angle relationship. The conditions which determine that a generator is about to pole slip are therefore :-

$$P < P_t, \quad where \quad P_t \propto P_m$$

$$Q < Q_{trip}$$

$$(\Delta P/\Delta t) < (\Delta P/\Delta t)_{min}$$

These conditions are used to give the trip criteria for the algorithm. The real power trip level, P_t is derived from the generator's monitored power output and is proportional to the mechanical power input P_m. This setting is adjusted periodically. The rate of change of power trip setting, $(\Delta P\backslash\Delta t)_{min}$ is also continuously adjusted by the algorithm according to the generator operating point.

Short circuit faults cause added complications since they cause dramatic changes in the relay measurands. These transitions produce negative values of ($\Delta P/\Delta t$) which are a potential source of instability to the algorithm. Fortunately, the faults generally introduce sinusoidal terms of twice the power system frequency into the power measurements. Since pole slipping is a relatively slow process in comparison to faults, then an imposed minimum tripping time of one and a half power system cycles will inhibit fault tripping.

4. PERFORMANCE TESTS

The performance of the various pole slipping algorithms, including the power based algorithm, have been tested using computer simulation, laboratory machines and field tests. The field tests were the most enlightening and witnessing the pole slipping of a 'real' machine was itself an education.

In the most dramatic of the tests using a 625 KVA diesel generator, the power based pole slipping algorithm successfully detected both of the pole slips, whereas, analysis showed that the impedance based schemes all failed to trip.

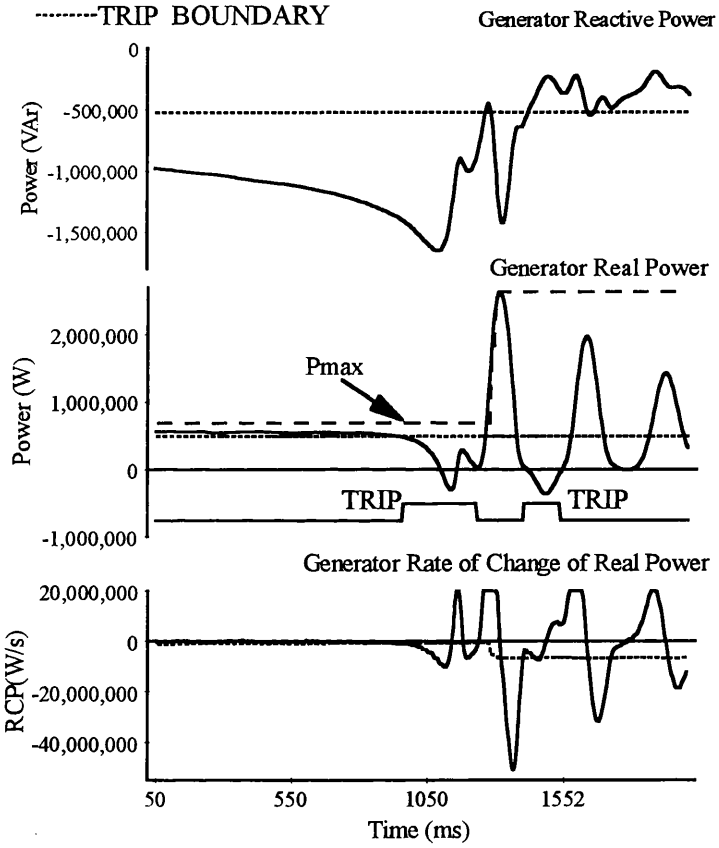

FIGURE 3. POWER BASED ALGORITHM RESPONSE TO 625 KVA DIESEL GENERATOR POLE SLIP.

Figure 3 shows the power based pole slipping algorithm's response to this test. The real power plot shows where the algorithm tripped, which for the first pole slip occurred just before 1000 ms on the record. Allowing for a circuit breaker operating time of 100 ms, this would have isolated the generator before the pole slip. The real power plot also reveals the potentially damaging effects of pole slipping, since the peak in power output after the first pole slip reaches 2.7 MW, five times rated power. By tripping before the pole slip occurred,

the new algorithm would have avoided this dangerous surge in the power output. Due to the finite disturbance recording time, the transition from normal to underexcited generator operation was not captured.

The conventional impedance based schemes were set so that they would operate for swings appearing on the generator side of the transformer high voltage terminals for a range of values of ***Eg/Es*** from 0.66 to 1.5. The value of ***Xd'*** for the generator was 0.22 p.u., the transformer reactance was 0.03 p.u. The MHO scheme was set so that the swing locus for a value of *Eg/Es* of 1 entered the characteristic at an angle of 120°. If the characteristic had been set to reach from the transformer high voltage terminals all the way into the generator, the theoretical locus would have entered at a value of 102°, making the scheme liable to operate for recoverable power swings.

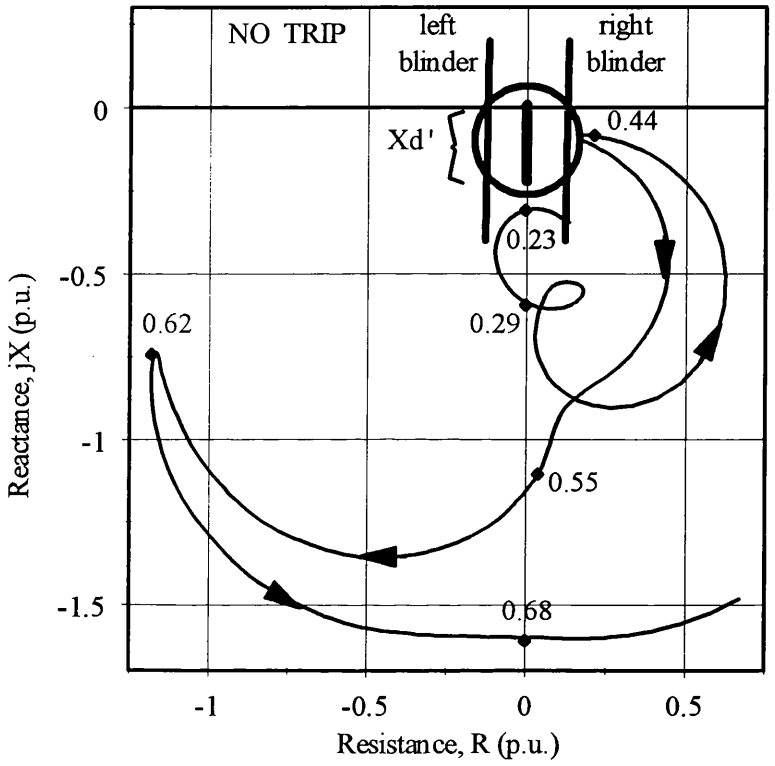

FIGURE 4. SINGLE BLINDER PROTECTION SCHEME CHARACTERISTIC FOR 625 KVA GENERATOR POLE SLIP TEST.

The MHO scheme's failure to trip further highlights the difficulty in using it. Covering the whole of the generator *Xd'* can lead to too large a MHO characteristic, and this makes the scheme prone to nuisance tripping. Adding a time delay increases the stability of the scheme to recoverable swings, but as the time delay is increased, the scheme may fail to detect fast pole slips whose locus travels through the characteristic quickly. If the circle size is decreased in order to increase stability, the scheme can fail to detect pole slips whose impedance does not take the classical trajectory.

The single blinder scheme was set using the recommended blinder settings of 90° and 270°. The supervisory MHO circle was set so that theoretical swings appearing in the transformer and generator could be detected. The scheme characteristics and the impedance locus of the pole slipping generator are shown in figure 4. It must be noted that the time records are not the same as used in figure 3 since the disturbance recorders were not synchronised.

The first pole slip occurred between 0.2 and 0.3 s, and the second occurred between 0.5 and 0.6 s. The first pole slip was not detected because the impedance trajectory did not enter the supervisory MHO characteristic. However, even if the supervisory MHO had been made larger, the scheme would still have failed to trip since the trajectory did not cross the left hand blinder. For the second pole slip, the swing impedance travelled across the impedance plane from right to left as predicted by theory, but again it did not enter the supervisory MHO characteristic. This was due to the speed at which the generator pole slipped. If the generator pole slips at a slow speed, then the impedance of the generator is much larger. At a slip of 0.33 %, the effective impedance of the generator becomes $2*Xd'$ [11].

The double blinder scheme suffered similar problems to the other impedance based techniques and failed to trip.

A loss of field protection included in the relay did however trip. Its MHO characteristic was set to a value of $Xd + Xd'/2$, which for this generator was -j 2.26 pu. This relay had a 0.5 s delay.

5. CONCLUSIONS.

Protecting an embedded generator against abnormal operating conditions is rarely as simple as detecting short circuit faults, but is as important to the safe and secure operation of the machine and the associated power system.

With the growing number of small and medium sized synchronous generators embedded in sub-transmission and distribution systems, the probability of pole slipping is growing and therefore pole slipping protection is becoming more important. Machine winding damage, system problems, and shaft failure can all result if adequate protection is not provided.

The availability of powerful microprocessor based relay hardware has enabled new techniques to be considered to provide protection against pole slipping. These include a new power based pole slipping protection algorithm. This has been shown to be effective in detecting the onset of pole slipping and hence is able to disconnect the generator before the dramatic current surges can occur.

The pole slip used to illustrate the operation of pole slipping protection was not designed to be particularly testing for any technique and considerable effort was put into choosing the most appropriate settings for the impedance based relays so that they provided the effective protection. The results, however, clearly demonstrated the difficulties of using impedance based pole slipping relays and the immediate advantages of the power based algorithm. The setting data for which is normally supplied with the generator. Using power as the basis for the detection of pole slipping proved advantageous.

6. REFERENCES.

1. J. A. Imhof et al, 'Out of Step Relaying for Generators - Working Group Report,' IEEE Transactions PAS-96, No.5, Sep/Oct 1977, pp 1556-1564.
2. A. Stalewski, J. L. H. Goody and J. A. Downes, 'Pole Slipping Protection,' Developments in Power System protection, IEE Conf. Publication, No.185, pp 38-45.
3. S. Shiwen, 'Microcomputer Based Out-of-Step Protection for Large Generator,' IEE APSCOM Hong Kong, Nov 1991, IEE Conf. Proc. No 348, Nov 1991, pp 839-842.
4. E Clark, 'Impedances Seen by Relays During Power Swings with and without Faults.' AIEE Trans Vol 64, 1945, pp 372-384.
5. D.W. Smaha, 'Out-of-Step Relay Protection of Generators.' IEEE Tutorial on the Protection of Synchronous Generators, Section 8, 95-TP-102, Power System Relaying Committee 1995.
6. H.K. Clark & J.W. Feltes, 'Industrial and Cogeneration Protection Problems Requiring Simulation.' IEEE Trans. Industry Applications, Vol. IA-25, No.4, July 89, pp 766-775.
7. E.W. Kimbark, 'Power System Stability - Power Circuit Breakers and Protective Relays.' Vol - II, New York, Wiley & Sons, 1964, Chapter X.
8. V. A. Venikov, 'Transient Phenomena in Electrical Power Systems', Pergamon Press, 1964.
9. T. H. Mason, P. D. Aylett and F. H. Birch, 'Turbo-Generator Performance Under Exceptional Operating Conditions,' IEE Conf. Proc. Vol.106, Jan 1959, pp 357-373.
10. M A Redfern and M J Checksfield, 'A New Pole Slipping Protection Algorithm for Dispersed Storage and Generation using the Equal Area Criterion.' IEEE Transactions on Power Delivery PWRD Vol 10, No 1, Jan 1995, pp 194-202.
11. GEC Measurements, 'Protective Relay Applications Guide.' GEC Measurements, Stafford.

PAPER TEN

"POLE SLIPPING PROTECTION: PROBLEMS AND SOLUTIONS"

M A Redfern, M J Checksfield, J Gosalia and G K Clough

Presented at :-

23rd Western Protection Relay Conference

Spokane, USA, October 1996, pp5/1-5/5.

POLE SLIPPING PROTECTION: PROBLEMS AND SOLUTIONS.

M. A. Redfern, M. J. Checksfield

School of Electronic and Electrical Engineering
University of Bath, BATH, BA2 7AY, UK.

J Gosalia and G K Clough

GEC ALSTHOM T&D Protection and Control
Hawthorne, New York, USA.

1. INTRODUCTION.

With the growing number of Dispersed Storage and Generation units (DSG) being installed to operate in parallel with utility distribution systems, synchronous generator instability is increasingly being recognized as an area of concern. Generator instability, pole slipping, can damage the machine and disturb the local power system. Unfortunately, DSG generators generally have high per unit impedances, low inertia and small transient time constants. These together with the long fault clearance times associated with distribution networks all contribute to the increased probability of pole slipping.

Pole slipping of a synchronous generator connected to a supply system is the process by which an imbalance between the mechanical power input to the machine and its electrical power output causes the rotor to accelerate and eventually slip with respect to the power system frequency. This can be caused by short circuit faults, general disturbances on the power system, or problems with the generator's prime mover, its excitation or its control system.

Traditional techniques for detecting pole slipping examine the variations in the apparent impedance of the generator as seen from its terminals. Several schemes are commercially available which are based on distance type relays [1,2,3,4], and use combinations of mho and linear characteristics. Some of these schemes are able to trip before the pole slip occurs, whereas others rely on the pole slip having taken place before they will disconnect the generator from the network.

Unfortunately, the impedance of a generator is not as predicable as would be expected and depends on the type of disturbance. Hence the concept of the sub-transient, transient and dynamic impedance. It is therefore generally recommended [1,4,5] that transient stability studies are performed so that the location of the impedance loci are known and the most appropriate relaying scheme and its settings can be selected. These simulations can be time consuming and expensive, and due to the vagaries of pole slipping do not guarantee reliable tripping or the absence of nuisance tripping.

Pole slipping is a power based phenomena and an alternative approach to detecting pole slipping has been developed which uses the Equal Area diagram as a basis to assess the stability of the machine and determine when it is committed to a pole slip. The settings for this technique rely on data which is generally available from the generator's manufacturer and stability studies are not required. Since this approach [6] is able to recognise the conditions where a pole slip is inevitable, it therefore offers the prospect of tripping before the actual pole slip and hence disconnecting the machine from the system before it can be damaged and before there is a major disturbance to the adjacent power system.

The technique takes advantage of the processing capabilities of modern multi-function microprocessor numeric relaying platforms and has been designed to share sub-functions with other protection functions required for the protection of Dispersed Storage and Generation units.

2. POWER BASED TECHNIQUE FOR DETECTING POLE SLIPPING.

The Equal Area Criterion demonstrates the conditions where synchronism is lost and pole slipping occurs. Figure 1 shows the power/load angle relationship and the rate of change of load angle (slip, s) for a generator losing synchronism with the utility supply to which it is connected following a loss of power transfer capability due to a disturbance on a double circuit line [7]. For this scenario, the generator is connected to a double circuit line and the power system disturbance is caused by switching one of the lines out of service for a short period. Removing the electrical load from the generator, while keeping the mechanical power constant, causes the generator to accelerate and eventually pole slip.

The most severe disturbance for a generator is the close-up three phase fault, for which all of the generator's load is lost and therefore all of the prime mover power is used to accelerate the rotor. For less severe short circuit faults, a greater fault duration is required to cause pole slipping.

The Equal Area Diagram, figure 1, illustrates that for a stable swing, the machine operating point cannot exceed point 5, the critical stability point. This corresponds to the point at which the electrical output of the machine, P, equals the mechanical input from the prime mover, P_m. Instability occurs if the machine moves beyond the critical stability point. This point can be identified in terms of real power as the condition when:-

$$P < P_m$$

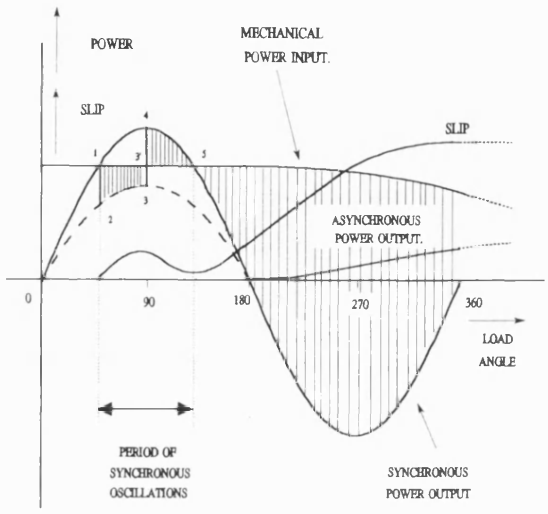

FIGURE 1. EQUAL AREA DIAGRAM FOR GENERATOR LOSS OF SYNCHRONISM.

Since this criterion can also be satisfied for machine operating between points 0 and 1 shown on figure 1, the reactive power measurement is used to differentiate between the two. The steady state reactive power/load angle relationship for a round rotor machine is given by:-

$$Q = \frac{E*V}{X_d}(\cos(\delta)) - \left(\frac{1}{X_q} + \frac{1}{X_d}\right)\frac{V^2}{2} + \left(\frac{1}{X_q} - \frac{1}{X_d}\right)$$

This shows that for load angles between 90° and 270°, the reactive power will always be less than Q_{trip}. Since point 5 of figure 1 occurs for load angles greater than 90°, then if :-

$$Q < \frac{-V^2}{X_q} \qquad (Q = Q_{trip})$$

the machine must be operating at point 5 and not point 1.

The transient reactive power characteristics vary in magnitude from the above steady state values. This does not corrupt the above method since the value of reactive power corresponding to a 90° load angle is identical to the steady state value. The transient reactive power characteristics above and below this load angle are such that in steady state terms, it appears as if the load angle is correspondingly higher or lower.

Finally, it must be ascertained whether or not the load angle is still advancing. To determine this, the rate of change of real power is used. It can be seen from the synchronous power output characteristic of figure 1, that if the load angle is still increasing when point 5 is reached, the machine output power will be decreasing, i.e. the rate of change of real power will be negative.

In practice a margin for error is allowed for in this rate expression $(\Delta P/\Delta t)$, to ensure the algorithm does not mal-operate. A minimum negative value, $(\Delta P/\Delta t)_{min}$ is designated, based on a minimum value of slip and an assumed sinusoidal power/load angle relationship. The conditions which determine that a generator is about to pole slip are therefore :-

$$P < P_t, \quad where \quad P_t \propto P_m$$

$$Q < Q_{trip}$$

$$(\Delta P/\Delta t) < (\Delta P/\Delta t)_{\min}$$

These conditions are used to give the trip criteria for the algorithm. The real power trip level, P_t, is derived from the generator's monitored power output and is proportional to the mechanical power input P_m. This setting is automatically adjusted periodically. The rate of change of power trip setting, $(\Delta P/\Delta t)_{min}$ is also continuously adjusted by the algorithm according to the generator operating point.

Short circuit faults cause added complications since they cause dramatic changes in the relay measurands. These transitions produce negative values of $(\Delta P/\Delta t)$ which are a potential source of instability to the algorithm. Fortunately, the faults generally introduce sinusoidal terms of twice the power system frequency into the power measurements. Since pole slipping is a relatively slow process in comparison to faults, then an imposed minimum tripping time of one and a half power system cycles will inhibit fault tripping.

3. Simulation Studies.

The performance of the pole slipping algorithm was tested using a laboratory dispersed generation model, computer based dynamic simulation and field tests.

The laboratory dispersed generation model used two 5 kVA synchronous generators driven by 8 horse power dc motors. These were connected to a 'local' load and a 200 V, 3 phase laboratory 'Utility' supply. This was useful for testing the algorithm in a real life situation, since harmonics and heavily alternating loads nearby made the supply far from ideal.

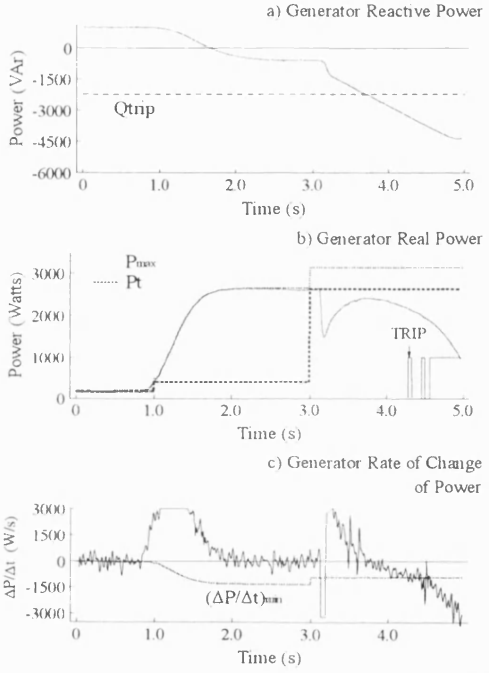

FIGURE 2 - 5 kVA GENERATOR POLE SLIP.

The laboratory model was also used to test the algorithm during power system fault conditions. All of the fault types possible were placed temporarily on the local load busbar by switching in 'fault' resistance.

The computer based dynamic simulation package was used to test the algorithm's performance against power swings and pole slipping. The model used was based on the simple one machine model (588 MVA) connected to an infinite bus model (58.8 GVA). A stable swing was caused by placing a fault on the generator transformer terminals of sufficient duration to cause the generator rotor to swing up to the critical stability point and back down to a stable operating area.

To test the algorithm for detecting a pole slip, the simulated generator was initially set to run at maximum output power. The input power was then reduced to half rating to test the adaptive setting section of the algorithm. A three phase fault of slightly longer duration than the one used to trigger the power swing, was then used to cause a pole slip.

4. Simulation Test Results.

Figure 2 shows the algorithm variations for the laboratory system weak field pole slipping test. Inspection of plots (a) and (b) show that the generator was initially operating overexcited at very low power. At a time of 1s on the record the power input to the generator was increased so that the machine operated at approximately 2.5 kW. Observation of the $(\Delta P/\Delta t)_{min}$ curve in plot (c) shows that because Pt was not updated during this period, the trip setting $(\Delta P/\Delta t)_{min}$ gradually decreased, resulting in a de-sensitising of the algorithm. This is beneficial since the likelihood of a pole slip is higher during adjustment to a higher output level.

At a time of 3s on the record, the adaptive setting part of the algorithm updates the value of Pt to the new operating level. This caused a drop in magnitude of $(\Delta P/\Delta t)_{min}$, but it did not drop back to the initial value, due to Pt being at a higher level. This is the desired effect since at higher input powers, more severe pole slip can occur and more negative values of $(\Delta P/\Delta t)$ are produced.

Shortly after the update, the resistor was connected in parallel with the field, causing the pole slip to occur. Inspection of the reactive power plot shows that this criterion was satisfied at 3.75 s, when the reactive power fell below the trip setting, *Qtrip*, indicating that the load angle had increased to a value above 90°. Inspection of the real power plot shows that after insertion of the parallel resistor, the generator's field was weakened sufficiently so that the generator could not maintain the level of output required, the real power criterion was therefore satisfied on inserting the resistor.

The final criterion ($\Delta P/\Delta t$) , can be seen to fall below its trip setting $(\Delta P/\Delta t)_{min}$ at a time of 4.3s. This meant that all three criteria were satisfied for the one and a half cycle required and a trip signal was therefore produced. The trip signal can be found on the real power plot, it can be seen that the trip was issued a significant time before the pole slip occurred. The usual point where pole slip is said to have occurred is when the machine goes from generator to motor action, i.e when the power output of the machine goes negative. Unfortunately, in

this case the whole pole slip could not be recorded, due to limitations in the data acquisition system.

Figure 3 shows the algorithm's response to a two phase to earth fault. Of all the fault types tested, this and the three phase faults provided the toughest conditions for testing algorithm stability. The reactive power criterion was satisfied for a small period on removal of the fault, at 1.4 s on the record. During this time the real power criterion is satisfied for a very short amount of time, before the real power output of the generator jumps above the trip setting *Pt*. It is this short interval where algorithm mal-operation is most likely. However, inspection of the $(\Delta P/\Delta t)$ plot shows that during this period, the $(\Delta P/\Delta t)$ signal jumps to a negative value off the scale for a very short time, before escalating to a very high positive value for a short time. These oscillations took less than one power system cycle, and so the algorithm was continually restrained.

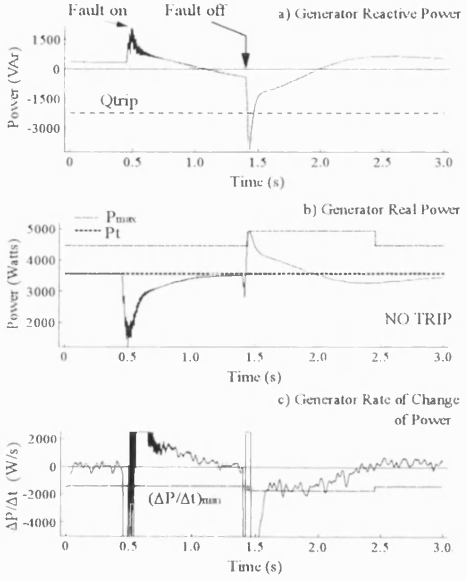

FIGURE 3 - 5 kVA GENERATOR 2 PHASE TO EARTH FAULT TEST.

The algorithm also successfully restrained for all of the other fault types tested.

Figure 4 shows the results to a test using the dynamic simulator. Initially the generator was operated at full power, it was then reduced to half rated operation. The condition monitoring part of the algorithm updated at a time of 3.75s on the record.

Inspection of the $(\Delta P/\Delta t)_{min}$ curve shows that until the update, it stayed at its high power level, resulting in the algorithm being de-sensitised for a small duration. This is unavoidable, but is of no great concern since in the event of a pole slip it would just result in the algorithm producing a trip signal delayed by a small time. At 4.75 s on the record the fault was placed on transformer bus, and removed again at 5.2s.

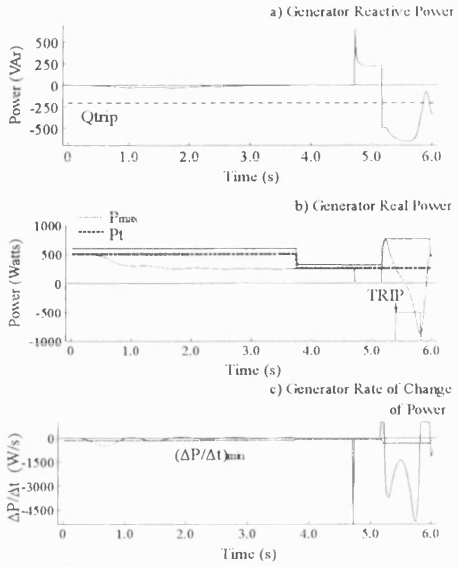

FIGURE 4 - 588 MVA GENERATOR POLE SLIPPING DUE TO A THREE PHASE FAULT.

On removal of the fault the generator's reactive power was less than *Qtrip*, satisfying the reactive criterion indicating that the load angle was above 90°. At the same time, the real power output is much greater than the nominal value before the fault.

This invoked the adaptive P_{max} part of the algorithm, which tracked the real power output up to its maximum value, and then held this value for 1 second before returning back to *1.25*Pt*.

This action resulted in $(\Delta P/\Delta t)_{min}$ falling to a lower level, thus desensitising the algorithm to the pending transient pole slip. The $(\Delta P/\Delta t)$ signal still fell below the trip setting $(\Delta P/\Delta t)_{min}$ for one cycle, and during this time the other two criteria were satisfied. A trip signal therefore resulted.

The algorithm successfully restrained for the power swing test, which produced a severe swing in load angle up to a value of 160°.

4. FIELD TESTS.

A series of field tests were conducted using a 625 kVA diesel generator connected via a transformer to the 11 kV network supply. In the most dramatic of the tests, a pole slip was induced by quickly ramping the diesel power at a rate faster than the generator controls could respond.

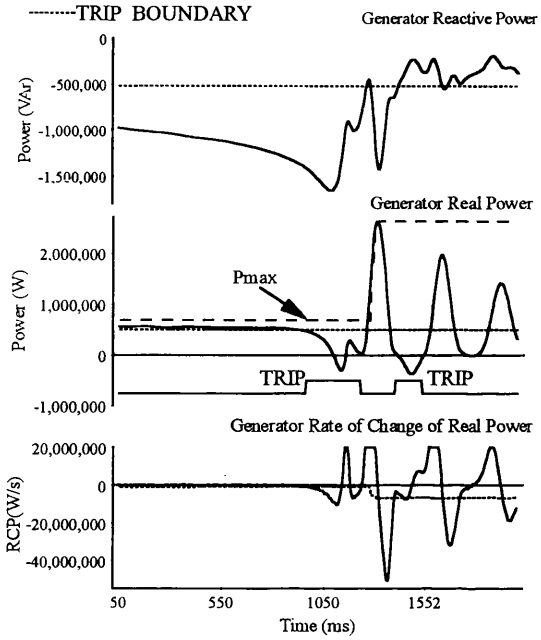

FIGURE 5. POWER BASED ALGORITHM RESPONSE TO 625 KVA DIESEL GENERATOR POLE SLIP.

Figure 5 shows the power based pole slipping algorithm's response to this test. The real power plot shows where the algorithm tripped, which for the first pole slip occurred just before 1000 ms on the record. Allowing for a circuit breaker operating time of 100 ms, this would have isolated the generator before the actual pole slip. The real power plot also reveals the potentially damaging effects of pole slipping, since the peak in power output after the first pole slip reaches 2.7 MW, five times rated power. By tripping before the pole slip occurred, the new algorithm would have avoided this dangerous surge in the power output. Due to the finite disturbance recording time, the transition from normal to underexcited generator operation was not captured.

5. CONCLUSIONS.

During laboratory model, computer simulation and field tests, the power based pole slipping algorithm has proven to be very successful in detecting pole slips while remaining stable during periods of other types of power system disturbances.

It offers the immediate advantage of detecting when the synchronous Dispersed Storage and Generation unit is committed to a pole slip rather than has actually slipped and therefore offers the opportunity of disconnecting the machine from the network before possible damage or major disturbance to the power system.

The relay's settings are determined by readily available generator data and thus the need for simulation studies is avoided.

6. REFERENCES.

1. J. A. Imhof et al, 'Out of Step Relaying for Generators - Working Group Report,' IEEE Transactions PAS-96, No.5, Sep/Oct 1977, pp 1556-1564.
2. A. Stalewski, J. L. H. Goody and J. A. Downes, 'Pole Slipping Protection,' Developments in Power System protection, IEE Conf. Publication, No.185, pp 38-45.
3. S. Shiwen, 'Microcomputer Based Out-of-Step Protection for Large Generator,' IEE APSCOM Hong Kong, Nov 1991, IEE Conf. Proc. No 348, Nov 1991, pp 839-842.
4. D.W. Smaha, 'Out-of-Step Relay Protection of Generators.' IEEE Tutorial on the Protection of Synchronous Generators, Section 8, 95-TP-102, Power System Relaying Committee 1995.
5. H.K. Clark & J.W. Feltes, 'Industrial and Cogeneration Protection Problems Requiring Simulation.' IEEE Trans. Industry Applications, Vol. IA-25, No.4, July 89, pp 766- 775.
6. M A Redfern and M J Checksfield, 'A New Pole Slipping Protection Algorithm for Dispersed Storage and Generation using the Equal Area Criterion.' IEEE Transactions on Power Delivery PWRD Vol 10, No 1, Jan 1995, pp 194-202.
7. V. A. Venikov, 'Transient Phenomena in Electrical Power Systems', Pergamon Press, 1964.

PAPER ELEVEN

"A NEW POLE SLIPPING PROTECTION FOR NUMERICAL RELAYING"

by M A Redfern and M J Checksfield

Presented at :-
11th CEPSI 96, Paper 12-29
Kuala Lumpur, Malaysia,
November 1996, pp12.29/1-12.29/10.

A NEW POLE SLIPPING PROTECTION FOR NUMERICAL RELAYING.

Miles A Redfern Matthew J Checksfield

University of Bath
Claverton Down
Bath
BA2 7AY
United Kingdom

ABSTRACT

With the increasing number of synchronous generators at risk of damage from pole slipping, pole slipping protection is a concern. Machine and system problems can result if a generator is permitted to pole slip continuously. The present impedance based methods can be difficult to set, and detailed computer based simulations are required to derive reliable relay settings, due to the unpredictable nature of the apparent impedance locus during pole slipping. This paper presents a new technique which simplifies the setting procedure for pole slipping protection whilst offering improved performance over conventional schemes. Results from field trials on a 625 kVA industrial diesel generator and simulations using the ATP programme are used to compare the performance of the new algorithm with the existing impedance based schemes.

1.0 INTRODUCTION

Generator pole slipping protection is necessary because when a generator looses synchronism with the utility supply to which it is connected, machine damage and system problems can result. The trend to low transmission system reactances compared to the high reactances of synchronous generators increases the likelihood of the electrical system centre appearing inside the generator during pole slipping rather than out in the transmission system. This requires generator pole slipping protection relaying to detect this out of step situation, rather than transmission line relaying [1]. Generators are also being operated closer to their stability limits, especially during light load periods. They are therefore more prone to instability and hence pole slipping[2].

Pole slipping is a particular concern for embedded generation units installed to operate in parallel with utility distribution systems. The electrical centre almost always appears inside the generator or its transformer due to the small rating of the generator compared to the utility system to which it is connected. The probability of pole slipping on distribution systems is increased since they often have long fault clearance times due to the IDMT overcurrent protection commonly employed [3] . Due to grading considerations, fault clearance times of up to one second are possible. If the generator protection scheme is not configured to disconnect the generator for all fault conditions that occur, then the probability of pole slipping is very high [4].

Pole slipping protection has existed for many years. The conventional impedance based forms of protection can be difficult to set [1,2,4]. Most schemes therefore require detailed power system simulations if they are to be set properly. Unfortunately most techniques for calculating the impedance locus for pole slipping and stable swing conditions do not take into account effects such as generator damping, non-constant flux linkage, and control system operation. All of these complicate the situation. The process of performing a detailed computer simulation can be time consuming and expensive. It can therefore be a constraint on the choice of pole slipping protection.

1.1 Pole Slipping

Pole slipping occurs due to an imbalance between the mechanical input power and the electrical output power of a synchronous machine, which causes its rotor to accelerate. If the rotor accelerates too far, the machine will not be able to produce the synchronising forces necessary to keep its rotor in synchronism with the stator magnetic flux, and the excess mechanical forces will cause a pole slip to occur.

The power imbalance can be caused by an external disturbance on the system such as a slow fault clearance, line switching operations which increase the system's transfer impedance, or a faulty generator control system. The loss of synchronism point at which pole slipping occurs is defined as the point where the generator's real power output becomes zero. Once this point has been reached the generator will briefly accelerate into a motoring condition, where it will absorb power from the electrical system. It will then go back into a generating condition. If it cannot produce the synchronising forces necessary to pull it back into synchronous operation, it will repeat the pole slipping cycle again and again.

Pole slipping can cause generator damage in numerous ways. Generators can experience currents in excess of three phase fault levels for periods much longer than the sub-transient fault period. Machine windings are generally designed to withstand three phase fault levels. The mechanical forces produced by the higher current levels experienced during pole slipping can therefore damage the windings. The unit transformer windings may also be exposed to high mechanical stresses because of these high current levels. If prolonged pole slipping is permitted, then the high current levels in the stator, and resultant induced slip frequency currents in the rotor can cause over-heating. AC/DC excitation systems can suffer insulation breakdown due to the excitation rectifiers blocking the field current as it tries to reverse during the pole slip cycle. High transient shaft torques also result, especially in steam turbine units. If the slip frequency of the generator coincides with a torsional natural frequency in the shaft system, the resultant torques can break the shaft if it is not suitably over-rated.

System voltage problems can also occur during pole slipping. In extreme cases the voltage depressions produced can cause plant outages, and even a cascading loss of synchronism of adjacent machines [5]. The worst voltage fluctuations occur at the system centre. The system centre is the point where the contribution from the generator equals that from the rest of the system. At the system centre, the voltage will be low whilst the current will be high, giving the appearance of a three phase short circuit fault. Distance protection, under voltage and over current protection may all operate during pole slipping.

2.0 CONVENTIONAL POLE SLIPPING PROTECTION

There are numerous impedance based schemes for detecting pole slipping[6]. The loss of field, mho and the single blinder schemes are the most commonly used techniques[1].

2.1 Generator Pole Slipping Impedance Characteristics.

The majority of conventional methods for detecting pole slipping use impedance relays to sense the variations in apparent impedance at the generator or high voltage transformer terminals during the pole slip. Using non computer based simulation techniques, the impedance loci can be derived using the assumption that the ratio of generator to source impedances, Eg/Es remains constant. Generator saliency and generator damper effects are also neglected, transient fault impedance effects are assumed to have decayed, shunt loads and shunt capacitance effects are ignored, effects of automatic voltage regulators and governors are neglected, and the source voltages behind their equivalent impedances are assumed to be sinusoidal and at fundamental frequency [1,2,7]. Once the theoretical loci have been calculated, the setting of the impedance schemes can be derived. Unfortunately, deriving the settings based on theoretical impedance loci can result in protection schemes which either fail to detect all pole slipping conditions, or nuisance trip for recoverable power swings or faults. Further information can be found in literature [1,2,6,8,9].

It is therefore strongly recommended that computer based simulation studies are performed for each specific generator so that improved settings can be chosen [1,2,6,8].

2.2 Generator Loss of Field Protection Scheme

Loss of field relaying inherently provides a degree of pole slipping protection. Due to the time delays employed to prevent nuisance tripping, loss of field schemes may fail to detect some pole slips because

the time delay may prevent the scheme tripping for pole slips whose impedance locus travels through the characteristic faster than the time delay. Modern loss of field relays have the facility to adjust the reset delay, and this helps to improve the range of pole slipping frequencies which can be detected. The problem is that several pole slips may occur before the relay operates.

2.3 The Mho Element Scheme

This is the simplest type of impedance based pole slipping protection, it uses a mho characteristic which reaches into the transformer and generator transient reactance. The scheme's main advantages are that tripping can occur before the pole slip has occurred, and that it provides a degree of back up protection for faults occurring in the transformer and generator. Its main disadvantage is that very careful selection of the mho reach is necessary to avoid tripping during power swings for which the pole slipping protection should remain stable. The mho circle reach is often set so that the impedance locus enters the mho circle at a system load angle of 120°. If this can not be achieved, a time delay is often included to increase the scheme's stability [2].

2.4 The Single Blinder Scheme

There are many possible variations of this scheme [6,8,10]. The basic scheme consists of two blinder elements which track the pole slipping impedance locus as it moves across the RX plane from right to left. To restrict the operation of the scheme to swings appearing in the generator or transformer, and to prevent operation for recoverable swings that pass through both blinder elements[1,11], the relay is supervised by a mho element. This also stops tripping for oscillations in reactive flow after synchronising[1, 9,10].

The blinder units are set parallel to the generator and transformer impedance. This scheme operates when the impedance locus enters the relay characteristic from one side of the R-X plane, and leaves from the other, taking longer than a preset time. The recommended settings for the blinders are 90° and 270°, which relieves the circuit breaker from a high out of phase arc interruption duty. Although, the scheme is inherently more stable against recoverable power swings and faults, detailed computer based simulations should still be performed in order to find the correct blinder, mho, and timer settings [1,2, 4,11]. Details of the scheme logic used in this paper are given by Goody [8].

3.0 THE NEW POWER BASED POLE SLIPPING ALGORITHM

The algorithm predicts that pole slipping will occur by detecting if the load angle is still increasing once the Critical Stability Point (CSP) has been exceeded [12,13]. If the generator operates past the CSP, stability cannot be maintained and a pole slip is inevitable. In designing a pole slipping algorithm, it must be able to predict when a generator is committed to a pole slip, or detect when a pole slip is actually occurring. It must also remain stable for all other power system conditions, including faults and recoverable power swings.

The algorithm uses reactive power, real power, and rate of change of real power to detect operation past the CSP. The algorithm is shown in equation (1).

$$\text{TRIP if:} \quad \left.\begin{array}{l} Q < Qtrip \\ \quad and \\ P < Pt \\ \quad and \\ (\Delta P/\Delta t) < (\Delta P/\Delta t)_{min} \end{array}\right\} \begin{array}{l} \text{Continuously} \\ \\ \text{For 1.5 Power} \\ \\ \text{System Cycles} \end{array} \qquad (1)$$

Where Q is the generator three phase reactive power, Qtrip is the reactive power trip setting, based on the quadrature axis synchronous reactance. P is the generator real power output, Pt is the real power trip setting which is derived by the algorithm. $(\Delta P/\Delta t)$ is the rate of change of real power, $(\Delta P/\Delta t)_{min}$ is the rate of change of power trip setting which is derived by the algorithm. The 1.5 power system cycle time constraint is to ensure that the algorithm remains stable during short circuit faults. The majority of faults will not satisfy all of the criteria of equation (1), the few that do only cause the criteria to be satisfied for less than one power system cycle.

3.1 Condition Monitoring Techniques

The algorithm is designed to be included into a microprocessor based relaying environment. The only information available to the relay is 2 phase voltages and 3 current signals provided by the relay's transducers. Since generators may be operated over a range of output powers, a method of estimating the prime mover input power, Pm is required so that the real power trip setting, Pt can be derived. The microprocessor relaying platform has a limited amount of processing power available to achieve this goal. The input power, Pm is found by observing the power output of the generator, and if this remains within a pre-defined tolerance band for a sufficient amount of time, then Pm must approximately equal this value, the only discrepancy being produced by the losses in the generator[13].

3.2 Adaptive Trip Setting $(\Delta P/\Delta t)_{min}$

Using an assumed sinusoidal power load angle curve[12], a value for $(\Delta P/\Delta t)$ at the CSP can be estimated for a given value of slip at a given value of Pt by;

$$(\Delta P/\Delta t)_{@CSP} = -s * Pmax * \cos\left(180 - \sin^{-1}\left(\frac{Pt}{Pmax}\right)\right) = (\Delta P/\Delta t)_{min} \qquad (2)$$

Note that the value of slip chosen will not be the exact value at which the relay produces a trip output, due to effects not taken into account in the derivation of (2), such as damping power. Equation (2) is used by the algorithm to continuously update the trip setting $(\Delta P/\Delta t)_{min}$ depending on the variables Pmax and Pt.

Pmax is a measure of the maximum output power that the generator has produced in the last second. It is used so that the algorithm can adjust its setting according to whether a transient or steady state pole slip will occur. A steady state pole slip occurs due to control system mal-function, whereas a transient pole slip occurs after the generator has been severely disturbed, after a fault for example. If the generator has been transiently disturbed, its output power during the first swing in load angle, be it stable or unstable, will be much greater than its nominal output. This results in a greater magnitude in $(\Delta P/\Delta t)$ at the CSP, the algorithm therefore needs to adjust its setting $(\Delta P/\Delta t)_{min}$ accordingly. The algorithm adjusts the setting, $(\Delta P/\Delta t)_{min}$ according to (3);

$$\text{If } \frac{Pt}{Pmax} < 0.6 \text{ then; } \quad (\Delta P/\Delta t)_{min} = (\Delta P/\Delta t)_{min} + (\Delta P/\Delta t)_{tran} \qquad (3)$$

where $(\Delta P/\Delta t)_{tran}$ is an external relay setting based on the degree of transient saliency in the generator. Transient saliency arises due to differences in the values of Xd' and Xq. $(\Delta P/\Delta t)_{tran}$ is given by;

$$(\Delta P/\Delta t)_{tran} = \left(\frac{1}{Xq} - \frac{1}{Xd'}\right) * S_{gen} \qquad (4)$$

Where S_{gen} is the generator rating. For a steady state pole slip, no peak will occur in the power output before the pole slip, the algorithm trip setting should therefore be at its most sensitive level to detect the pole slip since low values of $(\Delta P/\Delta t)$ will result.

During steady state conditions the value of Pmax used by equations (2) and (3) is nominally set to 1.4 * Pt. The ratio Pt/Pmax equals 0.71, $(\Delta P/\Delta t)_{tran}$ is therefore not included in the calculation of $(\Delta P/\Delta t)_{min}$ during steady state conditions. If the generator's power output rises above the existing value of Pmax for greater than one power system cycle, then the value of Pmax is updated to the new maximum for a duration of one second. The one second limit is used so that the new value of Pmax is only used for the period where a pole slip or power swing associated with that value is likely to occur. The one cycle constraint is necessary so that incorrect values of Pmax do not result from spurious spikes on the power waveform.

4.0 ALGORITHM VALIDATION

The pole slipping algorithm was validated and tested against the impedance based techniques detailed in section two using results from field trials on a 625 kVA industrial diesel generator, and from computer simulations on

the Alternative Transients Program (ATP) [14].

4.1 625 kVA Industrial Diesel Generator Field Trials

The 625 kVA generator is an industrial diesel generator connected to the utility network via a 415/11,000 volt unit transformer and two parallel 2 km 11 kV cables. The fault capacity at the generator terminals is 30 MVA. During normal service, there is 500 kW of local load connected to the generator. The field trials used a commercial microprocessor relaying platform. It was not possible to place faults on the power system to induce pole slipping, and hence a pole slip was induced by increasing the diesel engine's output torque with the generator under-excited. This scenario could happen due to operator error, or due to a mal-function of the diesel engine control system.

4.2 ATP Computer Based Simulation Studies.

The ATP was used to simulate both recoverable power swings and pole slips. The simulations were based on the power system described above. Pole slips and recoverable power swings were simulated by placing a fault in the middle of one of the 2 km inter-connection cables. The fault was cleared by disconnecting the faulty line. The generator AVR and governor system were included in the model.

5.0 SIMULATION STUDIES

5.1 625 KVA Diesel Generator Field Trial Pole Slip Test.

The generator was permitted to complete two entire pole slipping cycles before the diesel engine torque was reduced, and the generator allowed to pull back into synchronism. The new power based pole slipping algorithm successfully detected both of the pole slips, however, both the mho and single blinder schemes failed to detect them. The loss of field scheme did detect the pole slip.

The single blinder scheme characteristic, and the impedance locus of the pole slipping generator are shown in figure 1. The first pole slip occurred between 0.2 and 0.3 s, whilst the second occurred between 0.55 and 0.65 s. The first pole slip was not detected due to the impedance falling outside the supervisory mho relay. If the supervisory mho characteristic had been made larger, the scheme would still have failed to detect the first pole slip as it did not cross the left hand blinder.

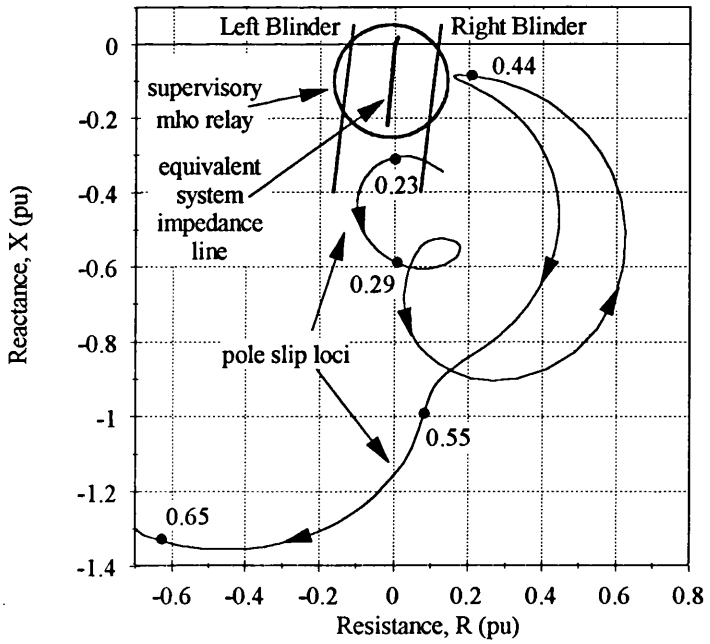

Figure 1: : Single Blinder Pole Slipping Protection Scheme for Industrial 625 kVA Diesel Generator Field Trial Pole Slip.

For the second pole slip, the swing impedance travelled across the impedance plane from right to left as predicted by theory, but was again significantly below the supervisory mho characteristic. This was due to the impedance of the generator being larger than the value of Xd'. In fact the impedance of the generator appeared to be closer to the synchronous value Xd. This observation is consistent with slow pole slip rates. At a slip rate of 0.1 % the generator reactance becomes 0.75 Xd [8].

The swing impedance of figure 1 also shows why the mho scheme failed to detect the pole slip. The size of the mho characteristic is smaller than that of the single blinder scheme supervisory mho circle, and so both of the pole slip impedance loci travelled under the relay characteristic. The mho scheme's failure to trip highlights one of the constraints of the mho scheme. Covering the whole range of possible pole slip generator reactances, from Xd' to 0.75 Xd can lead to too large a mho characteristic, which is prone to nuisance tripping during recoverable power swings. Adding a time delay increases the stability of the scheme to recoverable swings, but as the time delay is increased, the scheme may fail to detect fast pole slips whose locus travels through the characteristic too quickly. If the circle size is decreased in order to increase stability, the scheme may fail to detect pole slips whose impedance does not take the classical trajectory. The problem may be alleviated to some extent by co-ordinating the scheme with an impedance based loss of field scheme.

All of the purpose designed pole slipping detection impedance based schemes failed to detect the pole slip, due to the impedance falling below the mho relay characteristics. However, the loss of field relay used did detect the pole slip, since its mho characteristic was set to a value of Xd + Xd'/2, which for the diesel generator equals a value of -j 2.26 pu. Figure 1 highlights the degree to which the impedance locus produced by pole slipping can vary from the locus predicted by theory. If conventional schemes are set using theoretical impedance loci, then a high degree of confidence in the settings cannot be justified.

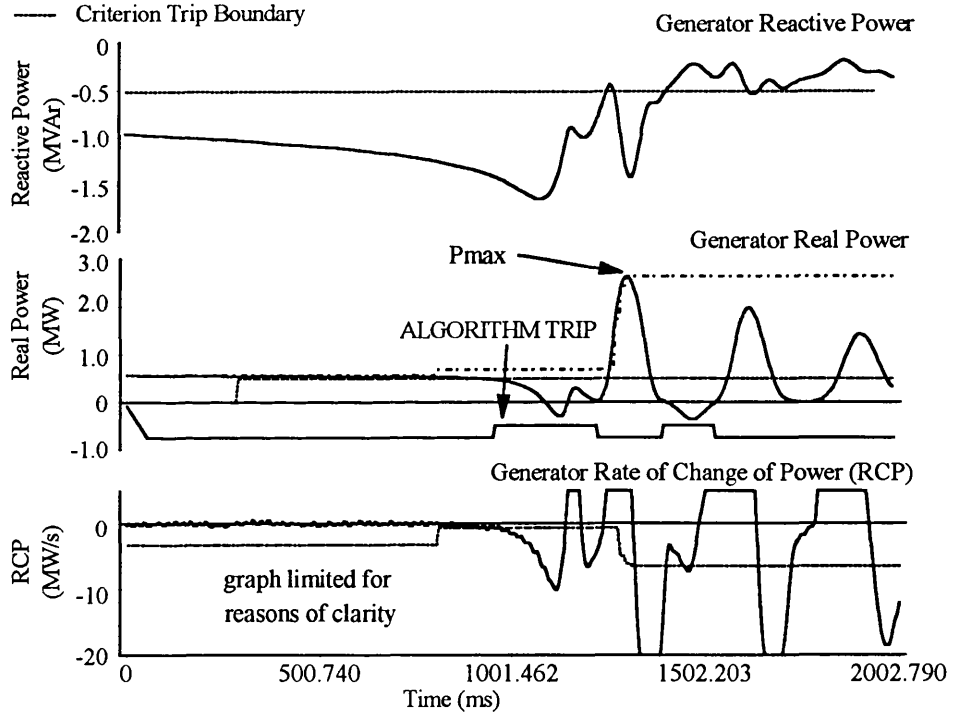

Figure 2: Power Based Pole Slipping Algorithm Response to 625 kVA Diesel Generator Field Trial Pole Slip.

Figure 2 shows the response of the power based pole slipping algorithm to the same test. Note that the times used in this figure are not the same as in figure 1 due to a different disturbance recorder being used. The real power plot shows where the algorithm tripped, which for the first pole slip occurred just before 1000 ms on the record. Allowing for a circuit breaker operating time of 100 ms, the protection would still have disconnected the generator before the pole slip.

The real power plot shows the potentially damaging effects of pole slipping. The peak in power output after the first pole slip reaches 2.7 MW, over five times rated power. By detecting the pole slip before it occurred, the new algorithm would have avoided this dangerous deviation in power output.

5.2 ATP Computer Based 625 KVA Diesel Generator Simulation Results.

The simulation of fault induced pole slipping of the diesel generator showed that the mho and power based pole slipping algorithms both tripped for the pole slipping simulation, whilst the single blinder scheme failed to trip. The mho scheme tripped at a time of 386 ms, and the power based scheme tripped at a time of 410 ms. The fault occurred at 100 ms and was cleared at 340 ms.

The mho scheme incorrectly tripped for the recoverable power swing simulation, at a time of 376 ms, for this simulation, the fault was cleared at 330 ms. The power based and single blinder pole slip schemes both remained stable during the recoverable power swing. The loss of field scheme did not trip for any of the simulations performed due to the time delay employed in the scheme of 0.5 s.

Figure 3 shows the single blinder scheme characteristic, and the solid impedance locus shows the pole slip impedance for the simulated pole slip. At fault clearance, the impedance locus changes rapidly due to the effects of pole scatter. After this, the impedance locus moves downwards rather than right to left across the RX plane as would be expected from a classical pole slip. The downwards movement causes the mho element to drop out before the impedance locus crosses the left hand blinder unit, the scheme therefore fails to detect the pole slip.

The predominant downwards movement of the impedance locus is due to the short time constant, Tdo' of the generator. Another simulation was performed with Tdo' increased from 2.0 to 6.0 seconds, and the resultant impedance locus is shown as the dotted line in figure 3. This impedance locus takes a more conventional trajectory. A short time constant means that the flux linkage of the generator is not constant during the pole slip. The fault causes the flux linkage to decay, which reduces the effective generator voltage so the impedance locus produced moves from a curve with a high value of the ratio Eg/Es to a curve with a low ratio of Eg/Es. Where Eg is the effective generator emf, and Es is the effective system source emf. Embedded generators will often have values of Tdo' of around 2 seconds due to their higher per unit resistances.

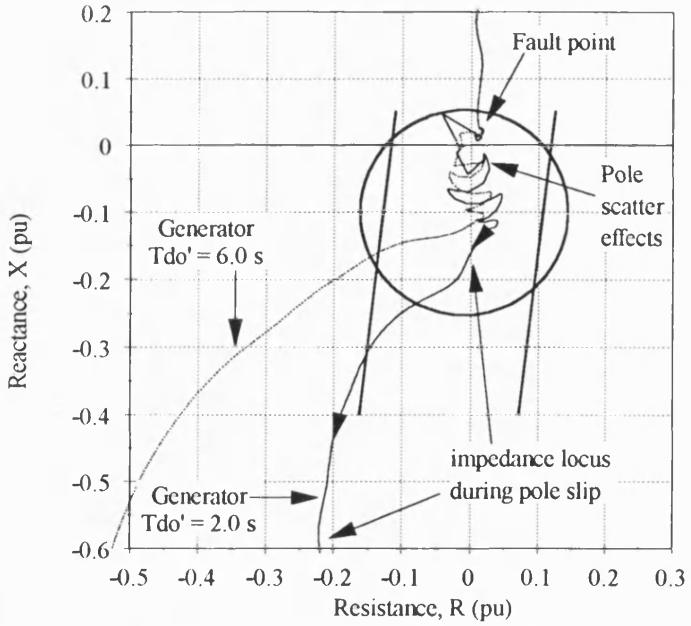

Figure 3: Single Blinder Pole Slipping Protection Scheme for Industrial 625 kVA Diesel Generator Simulated Pole Slip.

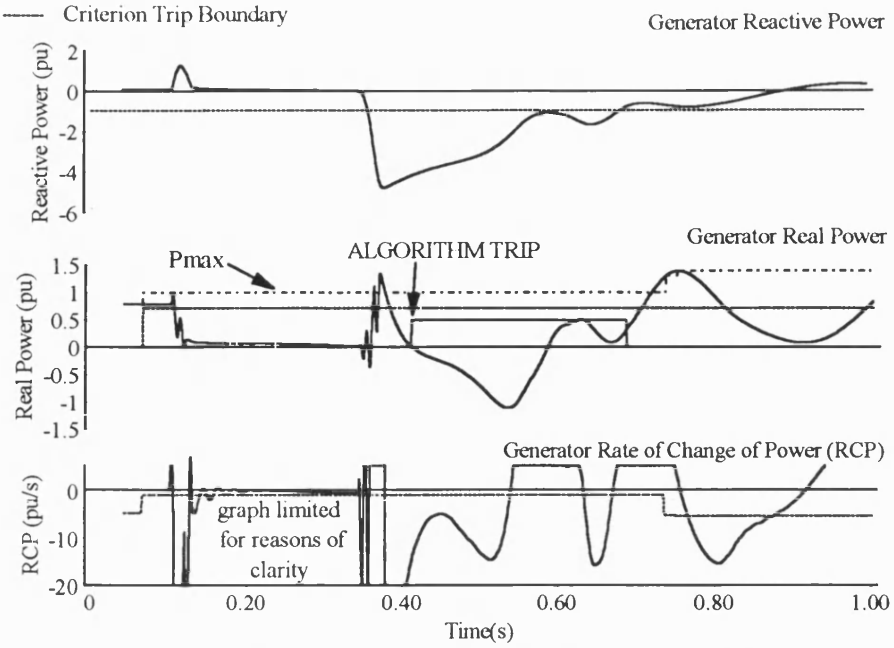

Figure 4: Power Based Algorithm Response to Simulated Pole Slip on 625 kVA Industrial Generator.

Figure 4 shows the response of the power based algorithm for the simulated pole slip. The algorithm tripped at a time of 0.41 s on the record, which corresponds to the point where the power output of the generator is zero. Note the non-sinusoidal nature of the generator real power waveform following fault clearance, which is due to the generator flux decaying. The algorithm does not reset until the reactive criterion is reset, thus preventing relay output chatter. The algorithm function Pmax fails to update to the peak in power output following fault clearance due to the spiky nature of the power waveform. The effect on the rate of change of power trip criterion of an update in Pmax to a greater than nominal value can be seen at a time of 0.73 s on the record. This action enhances algorithm security towards recoverable power swings, whilst still enabling fast tripping during pole slipping.

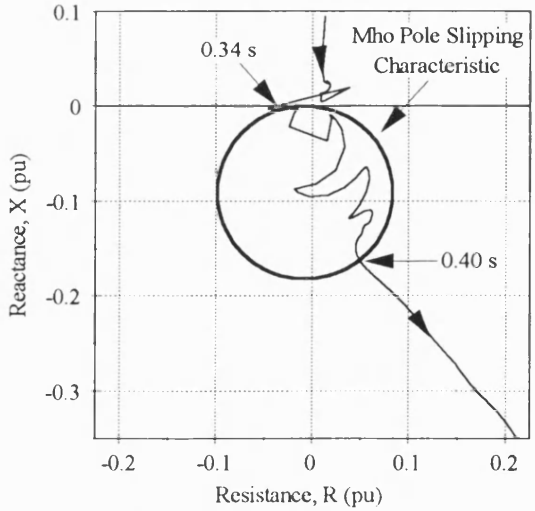

Figure 5: Single Mho Pole Slipping Protection Scheme for Industrial 625 kVA Diesel Generator Recoverable Power Swing.

Figure 5 shows the impedance locus for the recoverable power swing simulation, and the characteristic for the mho circle scheme. The impedance locus was inside the characteristic for 60 ms, and since the timer on the scheme was set to 40 ms an incorrect trip condition resulted. If the impedance locus had

taken the conventional trajectory, as predicted by basic theory, then it would have left the circle moving from left to right and a trip would not have occurred. The reason for the downwards component in the impedance locus is again due to the short time constant of the generator rendering the constant flux linkage assumption used in deriving the impedance loci for setting purposes invalid.

Figure 6 shows the power based algorithm measurands for the simulated recoverable power swing test. During the time when the reactive criterion is satisfied, between 0.35 and 0.5 s, the real power criterion is not satisfied for long enough to cause tripping. The fault used in this simulation was just shorter than the critical clearance time, and the resultant recoverable power swing is therefore the most severe possible.

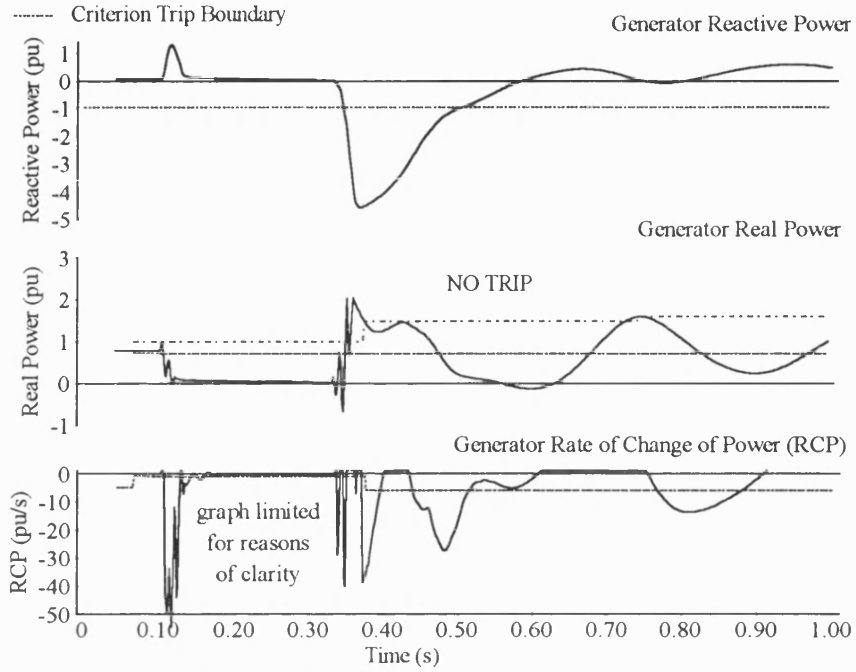

Figure 6: Power Based Algorithm Response to Simulated Recoverable Power Swing on 625 kVA Industrial Generator.

6.0 CONCLUSIONS

Microprocessor relaying technology has meant that new adaptive pole slipping algorithms can be developed which adjust their settings according to the generator operating point. The power based scheme discussed in this paper successfully detected all of the pole slipping conditions whilst restraining for stable swings and faults. In addition to the performance of the scheme, another advantage compared with conventional techniques is the scheme's simplicity to set. The new approach only requires the generator transient reactance Xd', synchronous reactance, Xq and generator rating to be set. The rest of the trip points are derived internally by the algorithm.

Conventional impedance based pole slipping protection requires detailed simulations of the system to be protected to derive reliable settings. Unfortunately, pole slipping impedance loci predicted from theory are sometimes not accurate enough to provide reliable setting of impedance based pole slipping schemes.

The mho scheme can mal-operate for stable swings if set too large, and can fail to detect some pole slips if time delays are used in order to prevent nuisance tripping during stable swings.

The single blinder scheme is the most secure of the conventional schemes. The price for this extra security is that the blinders and supervisory mho settings must be carefully set to detect all pole slips. To confidently set such a scheme, detailed computer based simulations of the system to be protected are required, which cost the applications engineer time and also money.

Embedded generators are very prone to instability and hence pole slipping, and do not have very predictable

impedance loci. Their short time constants and nearby plant can radically alter the path of the apparent impedance locus predicted by theory. Computer based simulations are therefore the only guaranteed way of finding settings which will work for the impedance based protection.

7.0 REFERENCES

[1] J.A. Imhof (Chairman) et al, "Out of Step Relaying for Generators - Working Group Report," IEEE Trans. Power Apparatus and Systems, Vol. PAS-96, No.5, Sept 1977, pp 1556 - 1564.

[2] D.W. Smaha, "Out-of-Step Relay Protection of Generators," IEEE Tutorial on the Protection of Synchronous Generators, Section 8, 95-TP-102, Power System Relaying Committee 1995.

[3] M.M.Elkateb & G Fielding, "Coordinating Protection and Control of Dispersed Generators",Tenth International Conf. on Electricity Distribution, Part1, 5 - Consumers Installations, 1989, pp131 - 135.

[4] H.K. Clark & J.W. Feltes, "Industrial and Cogeneration Protection Problems Requiring Simulation," IEEE Trans. Industry Applications, Vol.IA-25, No.4, July 89, pp 766 - 775.

[5] L J Powell, "An Industrial View Of Utility Cogeneration Protection Requirements", IEEE Trans, Vol IA-23, No.5, Sep/Oct 1987, pp777-785.

[6] P Kundur, *Power System Stability and Control*, , EPRI Power System Engineering Series, McGraw-Hill Inc, London 1993.

[7] E.W. Kimbark, *Power System Stability - Power Circuit Breakers and Protective Relays*, Vol - II, New York: Wiley & Sons, 1964, Chapter 10.

[8] J.L.H. Goody, "Overcoming Problems Associated With Impedance Measurement in Pole Slipping Protection for Dinorwig", IEE Proc. Vol 133, Pt.C, No.1, Jan 1986, pp 44-48.

[9] Westinghouse Electric Corporation, *Applied Protective Relaying*, 1979, Ch.19, Silent Sentinels Publication.

[10] W.C.Morris, "One Slip Cycle Out of Step Relay" AIEE Trans, 1949, Vol 68 pp 1246 - 1249.

[11] A. Stalewski, J.L.H.Goody, & J.A.Downes, "Pole Slipping Protection", Developments in Power System Protection, IEE Conf. Publication No.185, pp 38 - 45.

[12] M.A. Redfern & M.J. Checksfield, "A New Pole Slipping Protection Algorithm for Dispersed Storage and Generation Using the Equal Area Criterion," IEEE Trans. Power Delivery, Vol.10, No.1, Jan 1995, pp 194 - 202.

[13] M.J. Checksfield & M.A.Redfern, "A Power Based Condition Monitoring Algorithm for Detecting Dispersed Generator Loss of Synchronism", IPEC 95, Singapore, Feb 1995. Vol 1, pp 328 - 333.

[14] *Alternative Transients Program (ATP) Rule Book*, July 87 Ed, Leuven EMTP Centre (LEC), Belgium

8.0 ACKNOWLEDGEMENTS

The authors would like to thank the University of Bath for the use of facilities. Special thanks is also given to the Engineering and Physical Sciences Research Council (EPSRC) and GEC Alsthom T & D Protection and Control Limited for their support of this project.

9.0 BIOGRAPHY

Miles A Redfern (M'79) received his BSc degree from Nottingham University and PhD degree from Cambridge University in 1970 and 1976 respectively. In 1970, he joined British Railways Research, and in 1975, moved to GEC measurements where he held various posts including Head of Research and Long Term Development and Overseas Sales Manager. In 1986, he joined The University of Bath with interests in Power Systems Protection and Management. He is chairman of the organising committee for the 1997 IEE conference "Developments in Power System Protection", and is a member of IEE Professional Group P11, Power System Measurement, Protection and Control.

Matt J Checksfield received his B Eng degree from the University of Bath in 1993. He is currently studying for his PhD degree at the University of Bath and is sponsored by GEC ALSTHOM Protection and Control. His interests are in embedded generation, renewable energy, and protection systems.

PAPER TWELVE

"FIELD TRIALS TO DEMONSTRATE THE PERFORMANCE OF A NEW POLE SLIPPING PROTECTION"

M A Redfern, M J Checksfield and H T Yip

To be presented at :-

6th International IEE Conference on 'Developments in Power System Protection',

25 - 27 March 1997, Nottingham, UK.

FIELD TRIALS TO DEMONSTRATE THE PERFORMANCE OF A NEW POLE SLIPPING PROTECTION.

M A Redfern, M J Checksfield, H T Yip

University of Bath, UK GEC ALSTHOM T & D Protection and Control Ltd, UK.

ABSTRACT

This paper presents a new approach to pole slipping protection which eliminates the need for simulations, thus greatly simplifying the setting process. The new adaptive algorithm uses power measurements to ascertain if the generator is committed to a pole slip. In doing so it offers the prospect of detecting the pole slip before it occurs. The paper shows that this new approach works successfully by using results from field trials performed on an industrial diesel generator.

INTRODUCTION

The majority of conventional pole slipping relays use the variation in 'apparent' impedance as seen at the generator's terminals to detect pole slipping, as described by Imhof et al (1). If the impedance crosses two measurement characteristics on an impedance plane within a specified time limit, a trip signal is issued.

There are two problems with this approach. With the more secure of the impedance relay schemes, such as the single blinder scheme, the relay trips after observing a complete pole slip. This means that an unstable generator may already have been damaged and the pole slip could have caused voltage disturbances before the generator was disconnected from the system. Also, additional problems could result if the pole slipping impedance locus does not take the 'ideal' trajectory across the impedance plane and the relay fails to detect the phenomena. Small embedded generators and industrial generators located close to induction motors can suffer from this problem, Clarke & Feltes (2).

Choosing the correct trip boundaries and relay timer settings for the impedance based schemes can therefore be a difficult process. If the wrong relay settings are chosen, the pole slip may go undetected. If the settings are too sensitive, the relay may mal-operate due to a power swing or a power system fault.

The MHO scheme is a simpler scheme and can trip following the start of the pole slip thus reducing the potential for both damage to the generator and disturbance to the system. However it is a less secure scheme, still suffering from the above setting dilemmas.

For these reasons together with the opportunities offered by numeric relays, research has been carried out into a new pole slipping algorithm. The new approach reduces the complexity of setting, can provide a trip signal before the pole slip actually occurs and can be included in a modern microprocessor based protection scheme.

POLE SLIPPING PROTECTION

Pole slipping protection is required to reduce the damage caused to the generator by the pole slipping condition, and to ensure that the quality of supply for consumers connected electrically close to the effected generator remains acceptable. The severity of the problems produced by pole slipping depends upon the relative rating of the bus to which the generator is connected, the speed with which the generator pole slips, and the overcapacity rating of the generator.

If the generator is connected to an infinite bus, the currents experienced during pole slipping can be in excess of those experienced during three phase faults. Generator windings are normally designed to withstand three phase fault levels, the higher current levels experienced can therefore damage the windings (2).

Turbine generators may suffer shaft damage since the pulsating torques experienced, can torsionally excite resonant sections of the turbine shaft. Masrur et al (3) found that the generator-exciter section was most at risk after the *first* torsional oscillation produced by a pole slip. The cumulative effects of smaller oscillations may also lead to significant shaft damage. It can therefore be concluded that if shaft damage due to pole slipping is to be minimised, the generator must be disconnected from the power system *before* the pole slip occurs, in the hope that the torsional impulse will be avoided.

Synchronous machines are not designed to operate asynchronously, the resulting induced currents experienced during pole slipping can cause stator and rotor overheating. Induced field winding currents can stress the exciter insulation and semiconductor devices due to the high voltages they produce. The semiconductor devices block reverse field current flow, a high voltage therefore results when the field current cannot reverse during the pole slip.

The effect of pole slipping on other consumers connected close to the effected generator is most pronounced if the generator is connected to a weak system.

The voltage fluctuations can cause plant outages, and in extreme cases, cause a cascading loss of synchronism of nearby machines, including both generators and motors, Powell (4). If the voltage depressions last for too long a period, then induction motors may stall depressing system voltage further.

Transmission line and other feeder protection relays may also mal-operate during pole slipping, since at one location in the system, a pole slip appears as a three phase fault, i.e a low voltage and high current. The pole slipping condition can also cause other protection relays to mal-operate, such as under-voltage and over-current relays.

THE EQUAL AREA CRITERION

The Equal Area Criterion is one of the simplest methods for assessing generator stability for a given transient disturbance. If the power/load angle curves for all states of power system operation are known, then stability and hence the likelihood of a pole slip can be estimated for a given disturbance. The disturbances most likely to cause a pole slip are severe faults, large load switching operations, and generator control system faults.

Figure 1 shows the Equal Area Diagram for clearance of a three phase fault on one side of a double circuit line. The fault was removed by disconnecting the faulty circuit, leaving the healthy side of the line to transfer power at a reduced capacity.

It can be seen from Figure 1 that the limiting point for stability occurs when the generators output power falls below its input power, this point is referred to as the *Critical Stability Point* (*CSP*). If the generator operates past this point, then stability cannot be maintained, and a pole slip will occur.

THE NEW POLE SLIPPING ALGORITHM

The algorithm predicts that pole slipping will occur by detecting if the load angle is still increasing once the *CSP* has been exceeded, Redfern & Checksfield (5). If the generator operates past the *CSP*, stability cannot be maintained and a pole slip is inevitable. In designing a pole slipping algorithm, it must be able to predict when a generator is committed to a pole slip, or detect when a pole slip is actually occurring. It must also remain stable for all other power system conditions, including faults and recoverable power swings.

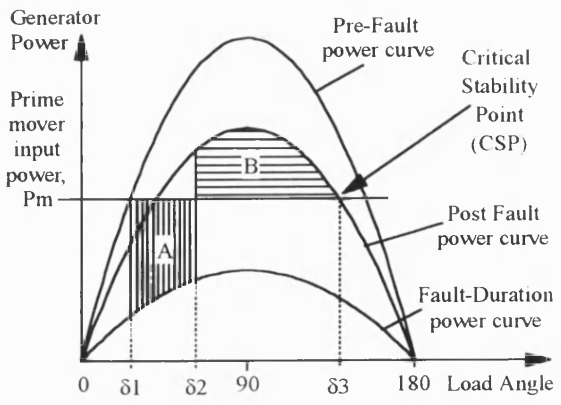

Figure 1: Equal Area Criterion Diagram.

The algorithm uses reactive power, real power, and rate of change of real power to detect operation past the *CSP*. The algorithm is shown in equation (1).

TRIP IF :-

$$\left.\begin{array}{l} Q < Qtrip \\ \quad and \\ P < Pt \\ \quad and \\ (\Delta P/\Delta t) < (\Delta P/\Delta t)_{min} \end{array}\right\} \text{ All criteria must be satisfied for 1.5 power system cycles continuously} \qquad (1)$$

Where Q is the generator reactive power, $Qtrip$ is the reactive power trip setting, P is the generator real power output, Pt is the real power trip setting, which is derived by the algorithm. $(\Delta P/\Delta t)$ is the generator rate of change of real power, $(\Delta P/\Delta t)_{min}$ is the rate of change of power trip setting which is also derived by the algorithm. The 1.5 power system cycle time constraint is to ensure that the algorithm remains stable during short circuit faults. The majority of faults will not satisfy all of the criteria of equation (1), the few that do only cause the criteria to be satisfied for less than one power system cycle.

The reactive power trip criterion, $Qtrip$, is calculated using the generator quadrature axis synchronous reactance, Xq. The reactive power output characteristics of a generator are such that at a load angle of 90°, the reactive power demand is given by;

$$Q = -\frac{V^2}{Xq} = Qtrip \qquad (2)$$

Figure 1 shows that the *CSP* occurs at load angles greater than 90°. The reactive power criterion is therefore used to indicate when the generator is operating in a potentially unstable region.

Condition Monitoring Techniques

The algorithm is designed to be included into a microprocessor based relaying environment. The only information available to the relay is the voltage and current signals provided by the relay's transducers. Since generators may be operated over a range of output powers, a method of estimating the prime mover input power, *Pm* is required so that the real power trip setting, *Pt* can be derived. The microprocessor relaying platform has a limited amount of processing power available to achieve this goal. The input power, *Pm* is found by observing the power output of the generator, and if this remains within a pre-defined tolerance band for a sufficient amount of time, then *Pm* must approximately equal this value, the only discrepancy being produced by the losses in the generator. A safety factor is also included, by making *Pt* equal to 90 % of the estimated value of *Pm*.

Adaptive Trip Setting $(\Delta P/\Delta t)_{min}$

Using an assumed sinusoidal power load angle curve (5), a value for $(\Delta P/\Delta t)$ at the *CSP* can be estimated for a given value of slip, s at a given value of *Pt* by;

$$(\Delta P/\Delta t)_{min} = -s * Pmax * \cos(\delta)$$
$$where \quad \delta = 180 - \sin^{-1}\left(\frac{Pt}{Pmax}\right) \qquad (3)$$

Note that the value of slip chosen will not be the exact value at which the relay produces a trip output, due to effects not taken into account in the derivation of (3), such as damping power. Equation (3) is used by the algorithm to continuously update the trip setting $(\Delta P/\Delta t)_{min}$ depending on the variables *Pmax* and *Pt*.

Pmax is a measure of the maximum output power that the generator has produced in the last second. It is used so that the algorithm can adjust its setting according to whether a transient or steady state pole slip will occur. A steady state pole slip may occur due to control system mal-function, whereas a transient pole slip occurs after the generator has been exposed to a disturbance such as a fault. If the generator has been transiently disturbed, its output power during the first swing in load angle, be it stable or unstable, will generally be much greater than its nominal output. This results in a greater magnitude in $(\Delta P/\Delta t)$ at the *CSP*, the algorithm therefore needs to adjust its setting $(\Delta P/\Delta t)_{min}$ accordingly. The algorithm adjusts the setting, $(\Delta P/\Delta t)_{min}$ according to;

$$If \quad \frac{Pt}{Pmax} < 0.6 \quad then; \qquad (4)$$
$$(\Delta P/\Delta t)_{min} = (\Delta P/\Delta t)_{min} + (\Delta P/\Delta t)_{tran}$$

where $(\Delta P/\Delta t)_{tran}$ is an external relay setting based on the degree of transient saliency in the generator. Transient saliency arises due to differences in the values of *Xd'* and *Xq*. $(\Delta P/\Delta t)_{tran}$ is given by;

$$(\Delta P/\Delta t)_{tran} = \left(\frac{1}{Xq} - \frac{1}{Xd'}\right) * S_{gen} \qquad (5)$$

Where S_{gen} is the generator rating. For a steady state pole slip, no peak will occur in the power output before the pole slip, the algorithm trip setting should therefore be at its most sensitive level to detect the pole slip since low values of $(\Delta P/\Delta t)$ will result.

During steady state conditions the value of *Pmax* used by equations (3) and (4) is nominally set to *1.4 * Pt*. The ratio *Pt/Pmax* equals 0.71, $(\Delta P/\Delta t)_{tran}$ is therefore not included in the calculation of $(\Delta P/\Delta t)_{min}$ during steady state conditions. If the generator's power output rises above the existing value of *Pmax* for greater than one power system cycle, then the value of *Pmax* is updated to the new maximum for a duration of one second. The one second limit is used so that the new value of *Pmax* is only used for the period where a pole slip or power swing associated with that value is likely to occur. The one cycle constraint is necessary so that incorrect values of *Pmax* do not result from spurious spikes on the power waveform.

ALGORITHM VALIDATION

The pole slipping algorithm was validated and tested using results from computer simulation, laboratory tests and field trials on a 625 kVA industrial diesel generator. The industrial generator was connected to the utility network via a 415/11,000 volt unit transformer and two parallel 2 km 11 kV cables. The fault capacity at the generator terminals is 30 MVA. During normal service, 500 kW of local load is connected to the generator.

The series of tests included large local load changes, synchronisation, generator run up, and one very interesting pole slip scenario.

It was not possible to place faults on the power system to induce pole slipping, and hence pole slips were induced by increasing the diesel engine's output torque with the generator under-excited. This scenario could happen due to operator error, or due to a mal-function of the diesel engine control system. A range of pole slips and loss of excitations were performed in order to fully test the algorithm.

Diesel Generator Field Trial Test Results.

The new algorithm successfully restrained for the load change, run up and synchronisation tests. The generator was permitted to complete two entire pole slipping cycles before the diesel engine torque was reduced, and

the generator allowed to pull back into synchronism. The new power based pole slipping algorithm successfully detected both of the pole slips.

Figure 2 shows the response of the power based pole slipping algorithm to a pole slipping test. The real power plot shows where the algorithm tripped, which for the first pole slip was at 1000 ms on the record. Allowing for a circuit breaker operating time of 100 ms, the new algorithm would still have disconnected the generator before the actual pole slip occurred.

The reactive power plot shows that when the disturbance recorder was triggered, the reactive power trip criterion had already been satisfied. This indicates that the generator was already operating with a potentially unstable load angle of greater than 90°. The real power plot shows that the generator was at its maximum power output of 550 kW when the disturbance recorder was triggered.

At a time of 1000 ms on the record, the real power begins to decrease, indicating the onset of instability. This is a steady state loss of stability, brought on by having too much input power for the level of excitation. The low level of excitation means that the generator was unable to transfer the mechanical input power to electrical output power. The mismatch in power caused the generator rotor to accelerate and the machine to eventually lose synchronism and pole slip.

Shortly after the real power begins to decrease, the algorithm detects that the generator is operating past its *CSP* and therefore trips. Allowing 100 ms for circuit breaker operation would result in the generator being disconnected just before the real power went negative. This would place a high switching duty on the generator circuit breaker since it would have to disconnect as the voltages across its poles approached 180 ° out of phase.

The real power plot shows the potentially damaging effects of pole slipping. The peak in power output after the first pole slip reaches 2.7 MW, over five times rated power. By detecting the pole slip before it occurred, the new algorithm would have avoided this dangerous deviation in power output..

CONCLUSIONS

Microprocessor technology has meant that adaptive, condition monitoring pole slipping algorithms can be developed which adjust their settings according to the generator operating point. The approach presented in this paper can use sensitive settings to detect pole slips which occur due to a loss of steady state stability, whilst automatically selecting more secure settings when recoverable power swings occur.

Results from field trial tests on a 625 kVA industrial diesel generator have proved that the algorithm successfully detects pole slipping *before* the actual pole slip occurs. The new approach also has the added advantage that it is simple to set, the generator transient reactance, the quadrature axis synchronous reactance, and the generator rating are required to derive settings which will detect the whole range of pole slipping conditions.

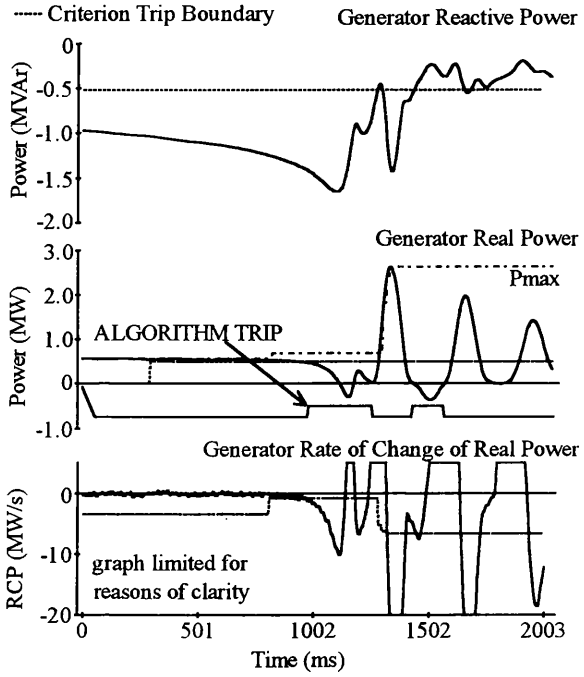

Figure 2: Pole Slipping Algorithm Response to 625 kVA Diesel Generator Field Trial Pole Slip.

REFERENCES

1. Imhof J A et al, "Out of Step Relaying for Generators - Working Group Report", IEEE Transactions in Power Apparatus and Systems, Vol PAS-96, No.5, September 1977, pp 1556 - 1564.
2. Clark H K, and Feltes J W, " Industrial and Co-generation Protection Problems Requiring Simulation", IEEE Transactions in Industrial Applications, Vol IA25, No.4, July 89, pp 766 - 775
3. Masrur M A, Ayoub A K, and Tielking J T, "Studies on Asynchronous Operation of Synchronous Machines and Related Shaft Torsional Stresses", IEE Conference Proc. Part-C, Vol.138, Jan 91, pp 47-56
4. Powell L J, "An Industrial View of Utility Co-generation Protection Requirements", IEEE Trans. Ind. App., Vol IA-23, No.5, Sep 87, pp 777-785.
5. Redfern M A and Checksfield M J, "A New Pole Slipping Protection Algorithm for Dispersed Storage and Generation Using the Equal Area Criterion", IEEE Trans. Power Delivery, Vol.10, No.1, January 1995, pp 194-202.

PAPER THIRTEEN

"TRANSIENT STABILITY CONSIDERATIONS ASSOCIATED WITH CONNECTING EMBEDDED GENERATION TO UTILITY NETWORKS"

M A Redfern and M J Checksfield

Proceedings of the second ERA International Conference
"Protecting Electrical Networks and Quality of Supply"
London, January 1997, pp 6.3.0-6.3.10

TRANSIENT STABILITY CONSIDERATIONS ASSOCIATED WITH CONNECTING EMBEDDED GENERATION TO UTILITY NETWORKS.

M. A. Redfern and M. J. Checksfield

School of Electronic and Electrical Engineering
University of Bath, BATH, UK.

1. INTRODUCTION.

With the growing number of embedded generators being installed to operate in parallel with utility distribution systems, transient instability is increasingly becoming recognized as an area of concern. Generator instability, can damage the embedded generator and compromise the quality of supply of the local power system. Unfortunately, embedded generators generally have high per unit impedances, low inertia and short transient time constants. These together with the long fault clearance times associated with the types of protection used on distribution networks all contribute to the increased probability of transient instability.

Transient instability of an embedded generator results in loss of synchronism between the embedded generator and the supply to which it is connected. This causes the embedded generator to pole slip with respect to the utility network's grid supply. This pole slipping is accompanied by dramatic fluctuations in the currents both absorbed and provided by the embedded generator.

The classical cause of transient instability is a three phase short circuit fault close to the terminals of the embedded generator. The typical clearance time for this type of fault on distribution networks is governed by the response of inverse definite minimum time delay overcurrent relaying, IDMT, and can be of the order of one second or more. Coupled with the critical clearance time for a typical embedded generator being of the order of 300 milliseconds, transient instability can be expected following such a fault. Fortunately, three phase faults are not prevalent on distribution systems, and the critical clearance times for an embedded generator increases as the distance between the generator and the fault increases. The generator may also be disconnected from the grid supply as a result of the circuit breaker tripping.

It is not feasible to design generators which have a greater tolerance to transient instability problems. These problems could be avoided by replacing the distribution network's IDMT relays with high speed protection, but the costs involved for existing distribution systems can rarely be justified. An alternative solution is to use pole slipping protection for the embedded generator, such that when transient instability is detected, the embedded generator is disconnected from the network before it is damaged or the system is disturbed.

2. POLE SLIPPING PROTECTION.

Pole slipping of a synchronous generator connected to a supply system is the process by which an imbalance between the mechanical power input to the machine and its electrical power output causes the rotor to accelerate and eventually slip with respect to the power system frequency. This can be caused by short circuit faults, general disturbances on the power system, or problems with the generator's prime mover, its excitation or its control system.

Traditional techniques for detecting pole slipping examine the variations in the apparent impedance of the generator as seen from its terminals. Several schemes are commercially available which are based on distance type relays [1,2,3,4], and use combinations of mho and linear characteristics. Some of these schemes are able to trip before the pole slip occurs, whereas others rely on the pole slip having taken place before they will disconnect the generator from the network.

Unfortunately, the impedance of a generator is not as predictable as would be expected and it depends on the type of disturbance to which the generator is subjected. Hence the concept of the sub-transient, transient and synchronous impedance. It is therefore generally recommended [1,4,5] that transient stability studies are performed so that the trajectory of the impedance loci due to the disturbance is known and the most appropriate relaying scheme and its settings can be selected. These simulations can be time consuming and expensive, and due to the vagaries of pole slipping do not guarantee reliable tripping or the absence of nuisance tripping.

Pole slipping is a power based phenomena and an alternative approach for detecting pole slipping has been developed which uses the Equal Area diagram as a basis to assess the stability of the machine and determine when it is committed to a pole slip. The settings for this technique rely on data which is generally available from the generator's manufacturer and therefore stability studies are not required. Since this approach [6] is able to recognise the conditions where a pole slip is inevitable, it offers the prospect of tripping before the actual pole slip and hence disconnecting the machine from the system before it can be damaged and before there is a major disturbance to the quality of supply to the adjacent power system.

The technique takes advantage of the processing capabilities of modern multi-function microprocessor numeric relaying platforms and has been designed to share sub-functions with other protection functions required for the protection of embedded generation.

3. POWER BASED TECHNIQUE FOR DETECTING POLE SLIPPING.

The Equal Area Criterion demonstrates the conditions where synchronism is lost and pole slipping occurs. Figure 1 shows the power/load angle relationship and the rate of change of load angle (slip, s) for a generator losing synchronism with the utility supply to which it is connected following a loss of power transfer capability due to a disturbance on a double

circuit line [7]. For this scenario, the generator is connected to a double circuit line and the power system disturbance is caused by switching one of the lines out of service for a short period. Removing the electrical load from the generator, while keeping the mechanical power constant, causes the generator rotor to accelerate and eventually pole slip.

The most severe disturbance for a generator is the close-up three phase fault, for which all of the generator's load is lost and therefore all of the prime mover power is used to accelerate the rotor. For less severe short circuit faults, a greater fault duration is required to cause pole slipping.

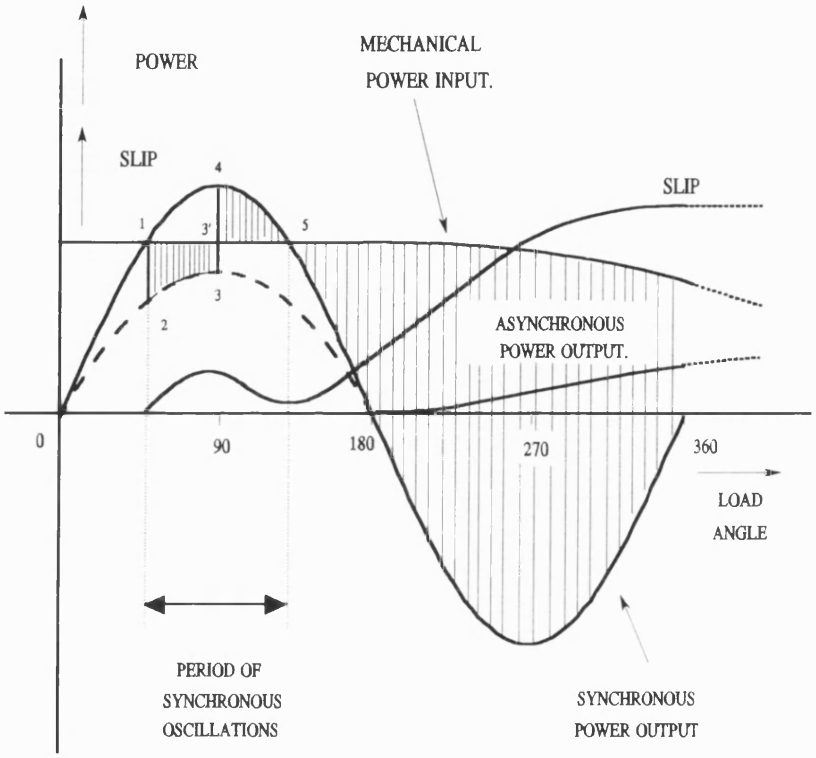

FIGURE 1. EQUAL AREA DIAGRAM FOR GENERATOR LOSS OF SYNCHRONISM.

The Equal Area Diagram, figure 1, illustrates that for a stable swing, the machine operating point cannot exceed point 5, the critical stability point. This corresponds to the point at which the electrical output of the machine, P, equals the mechanical input from the prime mover, P_m . Instability occurs if the machine moves beyond the critical stability point, which is point 5 of figure 1. This condition can be identified in terms of real power as when:-

$$P < P_m$$

6.3.3

Since this criterion can also be satisfied for machine operating between points 0 and 1 shown on figure 1, a reactive power measurement is used to differentiate between the two. The steady state reactive power/load angle relationship for a synchronous machine operating connected to an infinite bus is given by:-

$$Q = \frac{E*V}{X_d}(\cos(\delta)) - \left(\frac{1}{X_q} + \frac{1}{X_d}\right)\frac{V^2}{2} + \left(\frac{1}{X_q} - \frac{1}{X_d}\right)\frac{V^2}{2}(\cos(2\delta))$$

where E is the machine internal voltage and V is its terminal voltage.

This shows that for load angles between 90° and 270°, the reactive power will always be less than Q_{trip}, where Q_{trip} is given by the equation below. Since point 5 of figure 1 occurs for load angles greater than 90°, then if :-

$$Q < \frac{-V^2}{X_q} \qquad (Q = Q_{trip})$$

the machine must be operating at point 5 and not point 1.

The transient reactive power characteristics vary in magnitude from the above steady state values. However, this does not corrupt the above method since the value of reactive power corresponding to a 90° load angle is identical to the steady state value. The transient reactive power characteristics above and below this load angle are such that in steady state terms, it appears as if the load angle is correspondingly higher or lower.

Finally, it must be ascertained whether or not the load angle is still advancing. To determine this, the rate of change of real power is used. It can be seen from the synchronous power output characteristic of figure 1, that if the load angle is still increasing when point 5 is reached, the machine output power will be decreasing, i.e. the rate of change of real power will be negative.

In practice a margin for error is allowed for in this rate expression $(\Delta P/\Delta t)$, to ensure the algorithm does not mal-operate. A minimum negative value, $(\Delta P/\Delta t)_{min}$ is designated, based on a minimum value of slip and an assumed sinusoidal power/load angle relationship. The conditions which determine that a generator is about to pole slip are therefore :-

$$P < P_t, \quad where \quad P_t \propto P_m$$

$$Q < Q_{trip}$$

$$(\Delta P/\Delta t) < (\Delta P/\Delta t)_{min}$$

6.3.4

These conditions are used to give the trip criteria for the algorithm. The real power trip level, P_t , is derived from the generator's monitored power output and is proportional to the mechanical power input P_m. This setting is automatically adjusted periodically. The rate of change of power trip setting, $(\Delta P \backslash \Delta t)_{min}$ is also continuously adjusted by the algorithm according to the generator operating point.

Short circuit faults cause added complications since they cause dramatic changes in the relay measurands. These transitions produce negative values of $(\Delta P/\Delta t)$ which are a potential source of instability to the algorithm. Fortunately, the faults generally introduce sinusoidal terms of twice the power system frequency into the power measurements. Since pole slipping is a relatively slow process in comparison to faults, an imposed minimum tripping time of one and a half power system cycles will inhibit fault tripping.

4. Simulation Studies.

The performance of the pole slipping algorithm was tested using a laboratory generator, computer based dynamic simulation and field tests using an industrial diesel generator.

The laboratory generator system used two 5 kVA synchronous generators driven by 8 horse power dc motors. These were connected to a 'local' load and a 200 V, 3 phase laboratory 'Utility' supply. This was useful for testing the algorithm in a real life situation. The system was subjected to harmonics from other research projects and to heavily alternating loads nearby which made it far from an ideal text book system.

Pole slipping tests were conducted by inserting a resistance in parallel with the generator's field winding and therefore weakening the excitation. The laboratory model was also used to test the algorithm during power system fault conditions, and all of the fault types possible were placed on the local load busbar by switching in 'fault' resistance.

The computer based dynamic simulation package was used to test the algorithm's performance against power swings and pole slipping. The model used was based on the simple one machine model using a 588 MVA generator connected to an 'infinite bus' model rated at 58.8 GVA. A stable swing was caused by placing a fault on the generator transformer terminals of sufficient duration to cause the generator rotor to swing up to the critical stability point and back down to a stable operating area. Transient instability was caused by using a fault of duration greater than the critical clearance time.

Other tests to demonstrate the algorithm's ability to detect a pole slip were simulated by initially setting it to run at maximum output power, and then reducing the input power to half rated power. This tested the adaptive setting section of the algorithm.

5. Simulation Test Results.

Figure 2 shows the algorithm variations for the laboratory system weak field pole slipping test. Inspection of plots (a) and (b) show that the generator was initially operating overexcited at very low power. After one second on the record, the power input to the generator was

increased so that the machine operated at approximately 2.5 kW. Observation of the $(\Delta P/\Delta t)_{min}$ curve in plot (c) shows that because P_t was not updated during this period, the trip setting $(\Delta P/\Delta t)_{min}$ gradually decreased to a lower negative value, resulting in a de-sensitising of the algorithm.

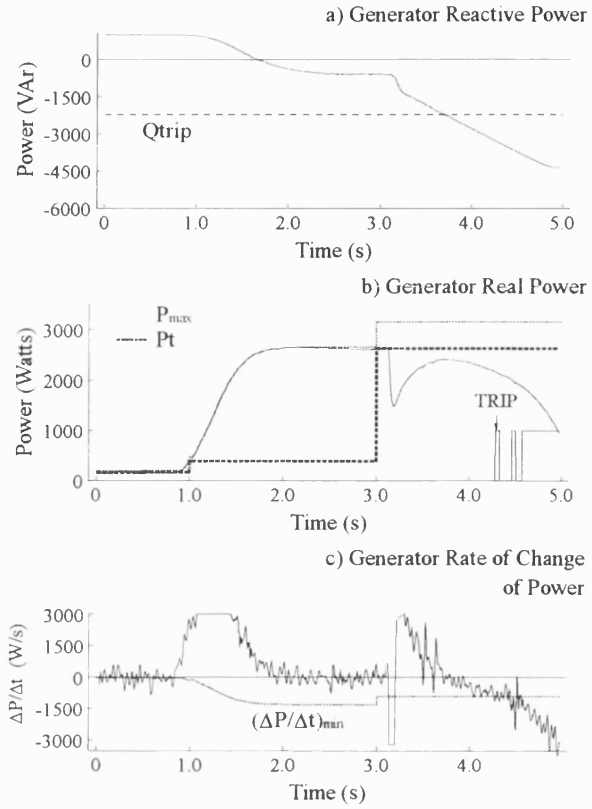

FIGURE 2 - 5 kVA GENERATOR POLE SLIP.

At a time of three seconds on the record, the adaptive setting part of the algorithm updates the value of P_t to the new operating level. This caused a drop in magnitude of $(\Delta P/\Delta t)_{min}$, but it did not drop back to the initial value, due to P_t being at a higher level. This is the desired effect since at higher input powers, more severe pole slips can occur and therefore more negative values of $(\Delta P/\Delta t)$ are produced.

Shortly after the update, the resistor was connected in parallel with the field, causing the pole slip to occur. Inspection of the reactive power plot shows that this criterion was satisfied at 3.75 seconds, when the reactive power fell below the trip setting, Q_{trip}, indicating that the load angle had increased to a value above 90°. Inspection of the real power plot shows that after insertion of the parallel resistor, the generator's field was weakened sufficiently so that the generator could not maintain the level of output required to match the mechanical power input. The real power criterion was therefore satisfied on inserting the resistor.

The final criterion $(\Delta P/\Delta t)$, can be seen to fall below its trip setting $(\Delta P/\Delta t)_{min}$ at a time of

4.3 seconds. All three criteria were then satisfied for the one and a half cycle required and a trip signal was produced. The trip signal can be found on the real power plot and it can be seen that the trip signal was issued a significant time before the pole slip occurred. The usual point where pole slip is said to have occurred is when the machine goes from generator to motor action, i.e when the power output of the machine goes negative. Unfortunately, in this case the whole pole slip could not be recorded, due to limitations in the data acquisition system.

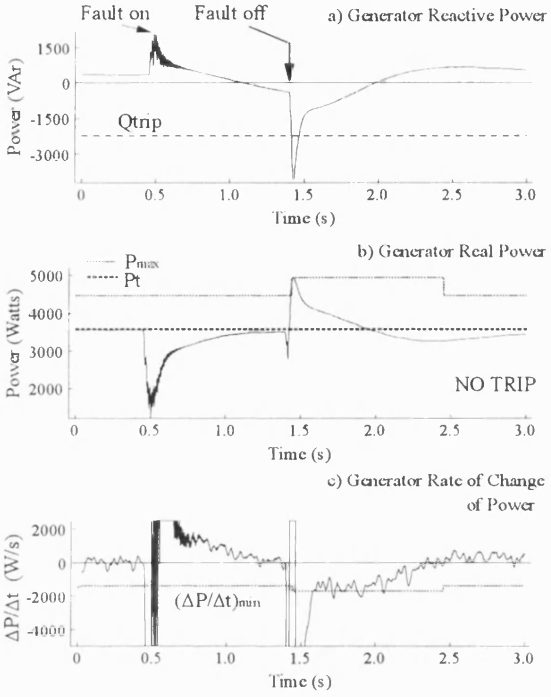

FIGURE 3 - 5 kVA GENERATOR 2 PHASE TO EARTH FAULT TEST.

Figure 3 shows the algorithm's response to a two phase to earth fault. Of all the fault types tested, this and the three phase faults provided the toughest conditions for testing algorithm stability. The reactive power criterion was satisfied for a small period after removal of the fault at 1.4 seconds on the record. During this time the real power criterion was satisfied for a very short time, before the real power output of the generator jumps above the trip setting P_t . However, inspection of the $(\Delta P/\Delta t)$ plot shows that during this period, the $(\Delta P/\Delta t)$ signal jumps to a negative value off the scale for a very short time, before escalating to a very high positive value for a short time. These oscillations took less than one and a half power system cycles, and so the algorithm was continually restrained.

The algorithm also successfully restrained for all of the other fault types tested.

Figure 4 shows the results to a test using the dynamic simulator. Initially the generator was operated at full power, it was then reduced to half rated operation. The condition monitoring

part of the algorithm updated at a time of 3.75 seconds on the record.

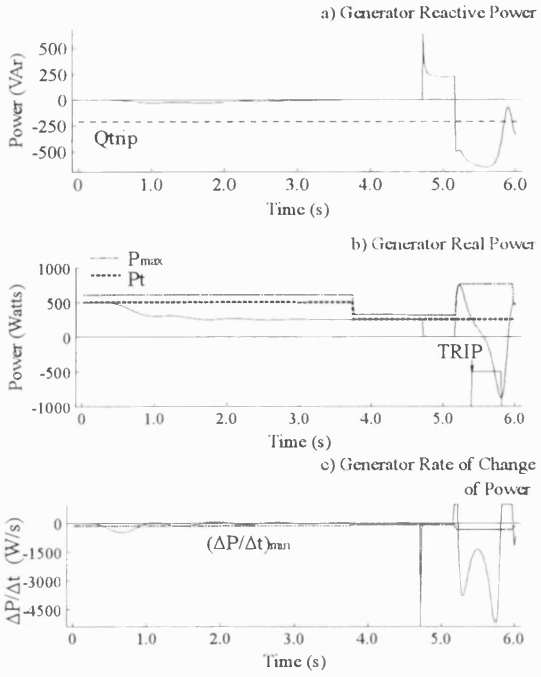

FIGURE 4 - 588 MVA GENERATOR POLE SLIPPING DUE TO A THREE PHASE FAULT.

Inspection of the $(\Delta P/\Delta t)_{min}$ curve shows that until the update, it stayed at its high power level, resulting in the algorithm being de-sensitised for a small duration. This is unavoidable, but is of no great concern since in the event of a pole slip it would just result in the algorithm producing a trip signal which is subject to a short time delay. The fault was applied to the transformer busbar at 4.75 seconds and removed again at 5.2 seconds.

On removal of the fault, the generator's reactive power was less than Q_{trip} , satisfying the reactive criterion indicating that the load angle was above 90°. At the same time, the real power output is much greater than the nominal value before the fault. This invoked the adaptive P_{max} part of the algorithm, which tracked the real power output up to its maximum value, and then held this value for 1 second before returning back to its default value of $1.25*P_t$.

This action resulted in $(\Delta P/\Delta t)_{min}$ falling to a lower level, thus desensitising the algorithm to the pending transient pole slip. The $(\Delta P/\Delta t)$ signal still fell below the trip setting $(\Delta P/\Delta t)_{min}$ for one and a half cycles, and during this time the other two criteria were satisfied. A trip signal therefore resulted.

The algorithm successfully restrained for the power swing test, which produced a severe swing in load angle up to a value of 160° before recovering to the stable condition.

6.3.8

6. FIELD TESTS.

A series of field tests were conducted using a 625 kVA diesel generator connected via a transformer to the 11 kV network supply. In the most dramatic of the tests, a pole slip was induced by quickly ramping the diesel engine's output power at a rate faster than the generator controls could respond.

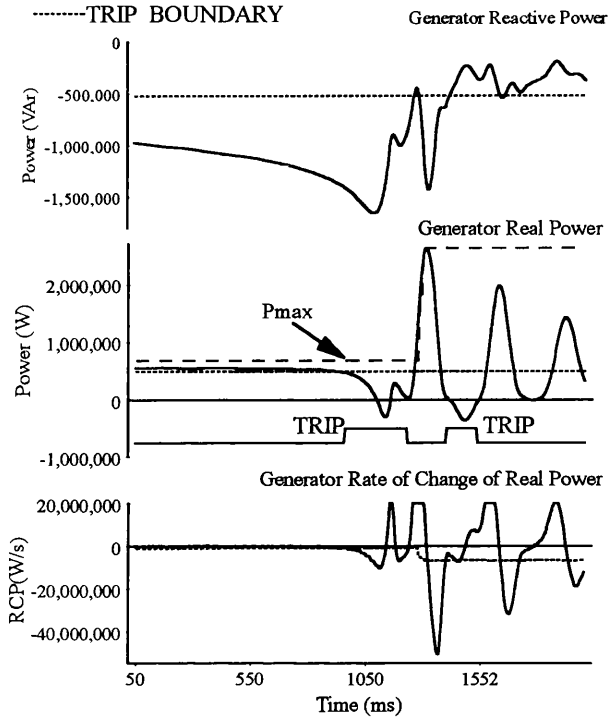

FIGURE 5. POWER BASED ALGORITHM RESPONSE TO 625 KVA DIESEL GENERATOR POLE SLIP.

Figure 5 shows the power based pole slipping algorithm's response to this test. The real power plot shows where the algorithm tripped, which for the first pole slip occurred just before 1000 ms on the record. Allowing for a circuit breaker operating time of 100 ms, this would have isolated the generator before the actual pole slip. The real power plot also reveals the potentially damaging effects of pole slipping, since the peak in power output after the first pole slip reaches 2.7 MW, five times rated power. By tripping before the pole slip occurred, the new algorithm would have avoided this dangerous surge in the power output. Due to the finite disturbance recording time, the transition from normal to underexcited generator operation was not captured.

7. CONCLUSIONS.

Transient instability is a point of concern for embedded generation connected to utility distribution networks. Typical short circuit fault clearance times obtained with the protection

used on these systems are in excess of the critical stability times associated with typical embedded generation units. Loss of stability can weaken or damage the embedded generator and the disturbance to the local supply network can compromise the quality of supply.

It has to be accepted that it is not feasible to design generators which are immune to transient instability and therefore there is an increased role for pole slipping protection. The traditional approach is to use impedance type relaying, however, there are complications in the choice of settings and power system simulation studies are recommended.

These complications can be avoided by using a power based technique to detect when the embedded generator is committed to pole slipping. Relay settings for this algorithm are determined from general machine data provided by manufacturers and the trip levels are automatically adjusted to the current loading on the machine.

This new technique is suited to modern numeric relay platforms and can be integrated into a multi-function generator protection package.

Laboratory tests, computer simulation and field tests have all demonstrated that the power based pole slipping algorithm is successful in detecting pole slips while remaining stable during periods of other types of power system disturbances.

It offers the immediate advantage of detecting when the synchronous embedded generator is committed to a pole slip rather than has actually slipped and therefore offers the opportunity of disconnecting the machine from the network before possible damage or major disturbance to the power system.

8. REFERENCES.

1. J. A. Imhof et al, 'Out of Step Relaying for Generators - Working Group Report,' IEEE Transactions PAS-96, No.5, Sep/Oct 1977, pp 1556-1564.
2. A. Stalewski, J. L. H. Goody and J. A. Downes, 'Pole Slipping Protection,' Developments in Power System protection, IEE Conf. Publication, No.185, pp 38-45.
3. S. Shiwen, 'Microcomputer Based Out-of-Step Protection for Large Generator,' IEE APSCOM Hong Kong, Nov 1991, IEE Conf. Proc. No 348, Nov 1991, pp 839-842.
4. D.W. Smaha, 'Out-of-Step Relay Protection of Generators.' IEEE Tutorial on the Protection of Synchronous Generators, Section 8, 95-TP-102, Power System Relaying Committee 1995.
5. H.K. Clark & J.W. Feltes, 'Industrial and Cogeneration Protection Problems Requiring Simulation.' IEEE Trans. Industry Applications, Vol. IA-25, No.4, July 89, pp 766-775.
6. M A Redfern and M J Checksfield, 'A New Pole Slipping Protection Algorithm for Dispersed Storage and Generation using the Equal Area Criterion.' IEEE Transactions on Power Delivery PWRD Vol 10, No 1, Jan 1995, pp 194-202.
7. V. A. Venikov, 'Transient Phenomena in Electrical Power Systems', Pergamon Press, 1964.

Appendix E

THE PRACTICAL IMPLEMENTATION OF THE POWER BASED POLE SLIPPING ALGORITHM INTO A COMMERCIAL MICROPROCESSOR RELAY

The following report contains the information which was used to implement the power based pole slipping algorithm in a commercially available microprocessor relay. The symbols used in this report refer only to this report, and are defined in the report's symbols list.

INCLUSION OF THE POWER BASED POLE SLIPPING ALGORITHM INTO THE LGPG 111 GENERATOR PROTECTION RELAY.

Author	M Checksfield (University of Bath)
Project Leader	H T Yip (GEC Alsthom T & D, Protection & Control Ltd)
Supervisor	M A Redfern (University of Bath)

Table of Contents.

LIST OF SYMBOLS

$(\Delta P/\Delta t)_{tran}$	generator transient saliency component used in the calculation of $(\Delta P/\Delta t)_{min}$ (W/s)
$(\Delta P/\Delta t)_{fact}$	maximum value for rate of change of power trip level, $(\Delta P/\Delta t)_{min}$ (W/s)
$(\Delta P/\Delta t)_{min}$	rate of change of power trip level (W/s)
$(\Delta P/\Delta t)$	rate of change of power measurand (W/s)
δ_c	angle used in calculating $(\Delta P/\Delta t)_{min}$ (degrees)
dt	length of time between the two samples used in calculating $(\Delta P/\Delta t)$ (seconds)
i_a	instantaneous phase value of current (cosine fourier filtered A-Phase current) (Amps)
i_b	instantaneous phase value of current (cosine fourier filtered B-Phase current) (Amps)
i_c	instantaneous phase value of current (cosine fourier filtered C-Phase current) (Amps)
In	relay secondary nominal current (rms value) (Amps)
lag	time between calculations of the real power trip setting, Pt (seconds)
N	number of samples used in half cycle moving average window (2)
P	real power (W)
Pfact	scaling factor used in Pt calculation to introduce a margin for error in the estimation
Pmax	generator maximum output power in the last 1 second (W)
P_n	present sample value of moving average filtered real power (W)
P_{n-2}	previous but one (half a cycle ago) value of moving average filtered real power (W)
Pt	real power trip setting (W)
Ptol	tolerance band used in calculation of Pt (W)
Q	reactive power (VAr)
Qtrip	reactive power trip level
Sgen	3 phase VA rating of generator (VA)
slip	external setting used in calculation of $(\Delta P/\Delta t)_{min}$ (%)
Sn	relay secondary rating of generator = $\sqrt{3}$ * Vn * In (W)
V_{ab}	instantaneous line value of voltage (cosine fourier filtered AB voltage) (Volts)
V_{bc}	instantaneous line value of voltage (cosine fourier filtered BC voltage) (Volts)
Vn	relay secondary nominal voltage (rms value) (Volts)
$x_{(n)}$	present sample input value to moving average filter
Xq	generator quadrature axis synchronous reactance (per unit value)
$y_{(n)}$	present sample output value from moving average filter.

Variables Used in Pole Slipping Algorithm Computer Code.

cnt_pmax	counter used to check if powerP >= pmax for one power system cycle (4 counts)
cnt_pmax_off	counter used to check if pmax should be reset to nominal value (reset after 1 second)
COS_DELTA_SCALE	scaling value used gor cos (δc) term in Dmin calculation.
count	counter used to see if pt calculation should be performed (every 'lag' seconds)

deriv	$(\Delta P/\Delta t)$
DERIV_OF	number of counts that powerP - last_p_val is limited to in deriv calculation
DERIV_MULT	multiplier used in deriv calculation (multiplier at 50 Hz)
DMIN_SCALE	internal scaling factor from Dmin calculation
DMIN_MAX_PMAX	maximum value that pmax is allowed to be in Dmin calculation
Dfact	$(\Delta P/\Delta t)_{fact}$
Dmin	$(\Delta P/\Delta t)_{min}$
Dtran	$(\Delta P/\Delta t)_{tran}$
Ia_oc.Fcos	i_a
Ib_oc.Fcos	i_b
Ic_oc.Fcos	i_c
LAG_SCALE	scaling used for 'lag' term used in Pt calculation.
last_p_val	P_{n-2} - stored moving average filter value of real power - used to calculate deriv
last_powP	previous sample of 'raw' real power required for 2 point (half cycle) moving average calculation
last_powQ	previous sample of 'raw' reactive power required for 2 point (half cycle) moving average calculation
lookup[i]	look up table equal to cos(δc) * slip, i , the look up index ranges, from 0 to 7
lookup_val	value looked up from lookup table used in calculating Dmin
master_look_up[i]	look up table value equal to cos(δc), i , the look up index ranges from 0 to 7
on_off_switch	variable used to see whether pole slipping function is enabled within LGPG
P	'raw' value of real power
p1	value of moving average filtered real power stored by pt calculation function. this is the value used by the function 2*lag seconds ago
p2	value of moving average filtered real power stored by pt calculation function. this is the value used by the function lag seconds ago
pen_p_val	P_{n-1} - stored moving average filter value of real power - used to calculate deriv in the following sample where it will become P_{n-2}
Pfact	multiplying factor used in pt calculation.
pmax	generator maximum power output - pmax.
PMAX_OF1	maximum value pt is allowed to be in pmax calculation.
PMAX_OF2	maximum value powerP is allowed to be in pmax calculation.
powerP	2 point half cycle moving average filter value of real power
powerQ	2 point half cycle moving average filter value of reactive power
pt	real power trip setting, Pt.
pt_pmax	variable equal to pt_x100 / pmax - used to find look up index, i
pt_x100	real power trip setting scaled up by 100 (note Pmax is internally scaled by 10)
PU_I	'per unit' internal value of current = 800 counts / Amp for 1 amp relay
PU_POLE_SLIP_DMIN	Dmin scaling factor = 30518 counts/W/s
PU_POLE_SLIP_P	'per unit' internal value of power = PU_V * PU_I = 8000 counts/VA

PU_POLE_SLIP_POW	powerP, (real power) scaling factor = 4000 counts/W
PU_POLE_SLIP_PMAX	pmax scaling factor = 400,000 counts/W/s
PU_POLE_SLIP_PT	pt scaling factor = 40,000 counts/W/s
PU_POLE_SLIP_Q	'per unit' internal value of real power = PU_V * PU_I * $\sqrt{3}$ = 8000 counts/VA
PU_V	'per unit' internal value of voltage = 10 counts / Volt
Q	'raw' value of reactive power
Qtrip	reactive power trip setting.
root3	square root of 3 = 1.732050808
SLIP_SCALE	scaling used for slip value used in Dmin calculation.
trip	boolean flag used to show whether algorithm has tripped
trip_count	counter used to check that P, Q, ($\Delta P/\Delta t$) trip criteria are all satisfied for one power system cycle
Vab_1_poleslip.Fcos	V_{ab}
Vbc_1.Fcos	V_{bc}

1.0 INTRODUCTION

The power based pole slipping algorithm measures three different power system quantities in order to establish if a pole slipping condition exists. These are the Reactive Power, Q, the Real Power, P, and the Rate of Change of Power, ($\Delta P/\Delta t$).

The trip settings for P and ($\Delta P/\Delta t$) are derived internally, and the algorithm adjusts these settings according to the operating point of the generator. The reactive power trip setting, Qtrip is entered as an external setting. The precise nature of the trip conditions will be explained later.

Section Two explains how the algorithm uses P, Q & ($\Delta P/\Delta t$) to determine when a pole slipping condition exists.

Section Three discusses the scaling values used in implementing the algorithm within the LGPG 111 relay, it also discusses the intricacies of getting the algorithm to work over the operating range of the relay, as well as the disturbance recording requirements of the algorithm.

2.0 THE POLE SLIPPING ALGORITHM.

The algorithm produces a trip output if the following conditions exist at the terminals of the generator.

$Q < Qtrip$ }

and } ALL OF THESE NEED TO BE

$P < Pt$ } SATISFIED FOR 1.5

and } POWER SYSTEM CYCLES.

$(\Delta P/\Delta t) < (\Delta P/\Delta t)_{min}$ }

The algorithm is frequency dis-abled if the system frequency does not lie between 40 and 70 Hz. This allows for 10 Hz either side of the 50/60 Hz operating frequencies. The algorithm processing rate is synchronously locked to the power system frequency and is at a rate of 4 samples per power system cycle, i.e at a frequency of 50 Hz, the above criteria are checked every 5 ms. The above criteria must therefore be satisfied over 6 successive sample instants in order for the algorithm to produce a trip output. The flowchart for the algorithm can be found in Figure 1.

The function which calculates the real power trip setting, Pt is run asynchronously. It is not called at the same time as the rest of the algorithm. Since it is asynchronous the exact time at which it is calculated may vary by a small amount. This is due to its priority being lower than other tasks in the multi-tasking executive priority level. A tolerance of +/- 10 % of the 'lag' setting is acceptable.

Including Hysteresis in the Pole Slipping Algorithm.

In most protection algorithms, a hysteresis facility is provided in order to avoid 'chatter' of the trip output. Chatter occurs when the algorithm measurand is at the trip level, and is therefore crossing to and fro between 'trip' and 'no trip'. The problem is usually overcome by reducing the trip level when a trip first occurs, so that a trip condition exists continuously after the initial trip.

With the pole slipping algorithm, it would be most desirable to stay 'tripped' until the generator is back in a stable generating condition (or is dis-connected), the algorithm would then be reset. This is achieved by latching the trip signal the first time it occurs, and only resetting it once the reactive power trip criterion is NOT satisfied. With this arrangement, the algorithm will produce one trip output per slip cycle. This should work for both pole slipping and loss of excitation. The algorithm structure used to achieve this can be found at the bottom half of Figure 1.

Algorithm Initialisation Values

Before the algorithm runs, some variables need to be initialised. This is to ensure that the algorithm does not mal-operate in the first few seconds when it is calculating it's settings according to the generator operating point. The total time the algorithm takes to initialise is given by '2 * lag' seconds. This is the time it takes for the real power trip setting Pt to be derived. Initialisation is also necessary to ensure no maths errors occur due to dividing by zero. Specific details of what each variable will be initialised to can be found in section 3.5

2.1 THE REACTIVE POWER TRIP CRITERION.

2.1.1 Calculation of Reactive Power Measurand, Q.

The reactive power is calculated using the 2 watt meter method, i.e ;

$$Q = \frac{1}{\sqrt{3}} \left(V_{ab} * (i_c - i_b) + V_{bc} * (i_a - i_b) \right) \quad \textit{(units of VArs)} \qquad 1$$

where V_{ab} , V_{bc} are the instantaneous fourier filtered line voltages, and i_a , i_b , i_c are the instantaneous fourier filtered phase currents. Note that the sign convention used for reactive power is that reactive power is negative at the terminals of an under excited generator. This is the opposite of the standard IEE definition for reactive power.

Once the reactive power has been calculated, a half cycle moving average filter is applied to it. This is done in order to remove any power system frequency unbalance in the signal.

2.1.2 Calculation of the Half Cycle Moving Average Filter Values.

The moving average filter is expressed mathematically as;

$$y_{(n)} = \frac{1}{N} \sum_{r=0}^{N-1} x_{(n-r)} \qquad 2$$

Where $y_{(n)}$ and $x_{(n)}$ are the n^{th} output and input respectively, N is the window size.
Since the number of samples per cycle to be used is 4, the value of N required for a half cycle moving average is 2. The above expression therefore simplifies to;

$$y_{(n)} = x_{(n)} + x_{(n-1)} / 2 \qquad 3$$

Note from this expression that the previous sample value is required for this calculation, this must therefore be stored between function calls.

2.1.3 Calculation of Reactive Power Trip Level, Qtrip.

The reactive power trip level 'Qtrip' is entered as an external setting. In absolute values, Qtrip is determined from;

$$Qtrip = - \frac{1}{Xq} * Sgen \qquad 4$$

Where Sgen is the generator three phase VA rating, and Xq is the per unit quadrature axis synchronous reactance of the generator. The value of 'Xq' is expected to vary between 0.3 and 2.5 PU on generator rating.

2.2 THE REAL POWER TRIP CRITERION.

2.2.1 Calculation of Real Power, P.

The real power is calculated using the 2 watt meter method, i.e ;

$$P = V_{ab} * i_a - V_{bc} * i_c \quad (units\ of\ Watts) \qquad 5$$

where V_{ab} , V_{bc} are the instantaneous fourier filtered line voltages, and i_a , i_c are the instantaneous fourier filtered phase currents. Once the real power has been calculated, a half cycle moving average filter is applied to it. This is done in order to remove any unbalance in the signal. (see section 2.1.2). As well as having to store the previous 'raw' value of power for the moving average calculation, the previous two values of moving average filtered power also need to be stored so that the ($\Delta P/\Delta t$) calculation can be performed (see section 2.3.1).

2.2.2 Calculation of Real Power Trip level, Pt.

The real power trip level, Pt is derived internally by the algorithm. The trip setting is an estimate of the generator mechanical input power. It is estimated using the assumption that in the steady state, the generator electrical output power is equal to the generator's mechanical input power. Detection of operation in the steady state is detected by checking that the generator's real output power stays within a pre-defined tolerance band (Ptol) for a specified time of (2*lag) seconds. Both 'lag' and 'Ptol' are entered as external settings.

A safety margin is included in this estimation which ensures the estimate will always be an under estimate. The estimation process is performed by comparing the most resent value of real power with two other previously stored values. The estimation process is performed nominally every 1 second, there is a setting provided in the algorithm called 'lag' which can change this time span between 0.1 and 10 seconds. The flowchart for this function can be found in Figure 2.

External Settings of 'Ptol' and 'lag'.

Both 'lag' and 'Ptol' are entered as external settings. 'Lag' can be set between 0.1 and 10 seconds, in 0.1 second intervals, whilst 'Ptol' can be entered between 1 % and 20 % of generator rating.

2.3 THE RATE OF CHANGE OF POWER TRIP CRITERION.

2.3.1 Calculation of (ΔP/Δt) Signal.

The rate of change of power is calculated using;

$$(\Delta P / \Delta t) = (P_n - P_{n-2}) * 1 / dt \quad (\text{units of Watts / second}) \qquad 6$$

P_n is the present moving average filtered sample value of real power. P_{n-2} is the previous but one sample, dt is the time between P_n and P_{n-2} , which is every half a power system cycle. This technique is used to prevent any double frequency terms present in the real power signal being transferred into the (ΔP/Δt) signal.

2.3.2 Calculation of Rate of Change of Power Trip Level, $(\Delta P/\Delta t)_{min}$.

The rate of change of power trip level is calculated from an external setting value of 'slip' and two real power measurements, namely Pt (see section 2.2.2) and Pmax (see below). It should be noted that all of the rate of change of power tripping and blocking levels will be negative.

Minimum Setting Value for $(\Delta P/\Delta t)_{min}$

In addition to the calculation mentioned above for finding $(\Delta P/\Delta t)_{min}$, a check is performed on the calculated value, if it's magnitude is below a certain value, a minimum setting value is assigned. This minimum

setting value is entered as the external setting, '$(\Delta P/\Delta t)_{fact}$' . It can be set between -10 % and -50 % of generator rating.

Calculation of Pmax

Pmax is a measure of the maximum output power which the generator has produced in the last second. A default value of 1.4 * Pt exists to ensure a minimum value for the rate of change of power trip level.
Measuring the generator maximum output power allows the algorithm to differentiate between 'transient' and 'steady state' generator operation. During transient operation, the rate of change of power trip setting should be very negative, to ensure stable swings in power are blocked. For steady state pole slips, the trip setting should be at a less negative level in order to provide the earliest detection possible.

It is important to note that the Pmax function should only track slow changes in generator output power. If the generator produces a high value of output power for a short time (less than one power system cycle) then this value should be rejected. The function should only track swings in generator output power which are a consequence of the generator rotor dynamics (i.e in the 1-10 Hz region).

The flowchart describing how Pmax is obtained can be found in Figure 3.

Calculation of $(\Delta P/\Delta t)_{min}$

The trip level $(\Delta P/\Delta t)_{min}$ is calculated using the following formula;

$$(\Delta P / \Delta t)_{min} = - slip * P\max * \cos(\delta_c)$$

if ratio Pt / Pmax < 0.6 then

$$(\Delta P / \Delta t)_{min} = (\Delta P / \Delta t)_{min} + (\Delta P / \Delta t)_{tran} \qquad 7$$

where $(\Delta P/\Delta t)_{tran}$ is entered as an external setting, derived from the generator quadrature axis synchronous reactance, Xq, and direct axis transient reactance, Xd'. This term is used to take into account the effects of transient saliency in the generator. Note that

$$\delta_c = 180° - \sin^{-1}\left(\frac{Pt}{P\max}\right) \qquad 8$$

Trigonometric functions require a relatively large amount of computation, the expression ' cos δc' is therefore found using a look up table. This look up table is split into 8 different levels, as defined in Table 1.

Table 1 - Lookup Table Used For Finding the Value 'cos (δc)'

lookup index	ratio Pt/Pmax	ratio Pmax/Pt	δc	cos (δc)
0	0 - 0.1	10 - infinity	180	-1
1	0.1 - 0.2	5 - 10	174.26	-0.99498
2	0.2 - 0.3	3.33 - 5	168.46	-0.97980
3	0.3 - 0.4	2.5 - 3.33	162.54	-0.95394
4	0.4 - 0.5	2 - 2.5	156.42	-0.91652
5	0.5 - 0.6	1.66 - 2	150.00	-0.86603
6	0.6 - 0.7	1.43 - 2	143.13	-0.80000
7 (nominal)	0.7 - 0.8	1.25 - 1.43	135.57	-0.71414

NOTE: The nominal value for Pmax = 1.4 * Pt, when this condition exists, then the ratio of Pt/Pmax = 1/1.4 = 0.714. This therefore falls into look up index 7. As the ratio of Pmax to Pt becomes greater than 1.4 a more negative value of cos (δc) is selected. The most negative value of cos (δc) is therefore -1 when the ratio of Pmax to Pt lies between 10 and infinity.

The Externally Set Value for Slip.

The value of slip used in calculating $(\Delta P/\Delta t)_{min}$ can vary between 0.1 % and 5 %, in 0.1 % intervals. The nominal setting used is 0.5 %.

The Externally Set Value $(\Delta P/\Delta t)_{tran}$

The formula for calculating $(\Delta P/\Delta t)_{tran}$ is given below;

$$(\Delta P / \Delta t)_{tran} = \left(1/Xq - 1/Xd'\right) * Sgen \qquad 9$$

Where Sgen is the generator three phase rating, Xq is the quadrature axis synchronous reactance, and Xd' is the direct axis transient reactance. The value of Xq is expected to vary between 0.3 and 2.5 PU, whilst Xd' is expected to vary between 0.1 and 2 PU on generator base. Note that Xd' < Xq. $(\Delta P/\Delta t)_{tran}$ is therefore always negative.

3.0 INCLUSION OF POLE SLIPPING ALGORITHM IN LGPG.

This section details the settings and scaling factors required for the implementation of the power based pole slipping algorithm in the LGPG111 generator protection relay. These settings have been designed with the following conversion values from relay secondary volts and amps to internal ' counts'.

1 Volt = 10 counts;
1 Amp = 800 counts (1 Amp relay), or 5 Amps = 800 counts (5 Amp relay);
1 VA = 8000 counts (1 Amp relay), or 5 VA = 8000 counts (5 Amp relay);
PU_POLE_SLIP_P = 800 * 10 = 8000 counts.

In - Nominal input current = 1 A (1 Amp relay) or 5A (5 Amp relay) (RMS phase value);
Vn - Nominal input voltage = 100 to 120 Volts. (RMS line to line value)
Sn - Three phase rated apparent power = Vn * In * $\sqrt{3}$

The value Sn can be considered as equivalent to the generator rating in terms of relaying secondary quantities. All variables referred to in section 3 which are used in the code (and are not constants) will have the prefix 'pole_slip_prot.' since they belong to a data type structure called pole_slip_prot. This section will refer to all variables by their computer code names. Most variable names are defined in file 'data_13.h', however, some are defined in poleslip.c.

The setting and scaling values in the following section *have been calculated for the 1 Amp relay.* The minimum and maximum setting values have been calculated using the following minimum and maximum values of Vn and In;
Vn (max) = 120 Volts, Vn (min) = 100 Volts,
In (min) = 0.5 Amps, In (max) = 1.5 Amps

3.1 REACTIVE POWER VARIABLES - powerQ, Qtrip.

3.1.1 Calculation of Raw Reactive Power, Q.

The reactive power is calculated using the formula below;

$$Q = \frac{Vab\_1\_poleslip.F\cos * (Ic\_oc.F\cos - Ib\_oc.F\cos) + Vbc\_1.F\cos * (Ia\_oc.F\cos - Ib\_oc.F\cos)}{2} \quad \mathbf{10}$$

where Vab_1_poleslip.Fcos, Vbc_1.Fcos are the relay instantaneous fourier filtered line voltages, which have been scaled down by the relays internal hardware by a factor of $\sqrt{2}$, and ia_oc.Fcos, ib_oc.Fcos, ic_oc.Fcos are the instantaneous fourier cosine filtered phase currents which have also been scaled down by the relays internal hardware by a factor of $\sqrt{2}$.

NOTE that the factor $\sqrt{3}$ shown in section 2.1.1 has not been included, this would result in an unnecessary division. The expression is divided by 2 in order to a) introduce a scaling factor of 1/2 to avoid numerical overflow. b) avoid having to perform another division by 2 when calculating the half cycle moving average value. Note that it is effectively divided by an additional factor of 2 due to the relays internal hardware scaling.

The half cycle moving average calculation of reactive power, powerQ, is therefore reduced to a simple addition of the present (Q) and previous (last_powQ) raw values of reactive power, i.e the moving average filtered value, called powerQ is given by 'Q + last_powQ'.

To scale from internal 'counts' into VAr, Q should be
SCALED BY (PU_POLE_SLIP_P * $\sqrt{3}$) /2 = 6928.2 $\Rightarrow$ 6928 counts/VAr
This variable is referred in the code as PU_POLE_SLIP_Q.

NOTE the factor of $\sqrt{3}$ has been included since it was not used in the reactive power calculation. The reactive power, Q was therefore $\sqrt{3}$ times too big. The factor of 2 comes from the scaling down used in the calculation of Q.

3.1.2 Setting ' Qtrip'.

Qtrip is given by equation 4, Xq varies between 0.3 PU and 2.5 PU.

The minimum and maximum setting values in terms of relay secondary quantities are therefore;
MINIMUM QTRIP = -1/0.3 * 120 V * 1.5 A * $\sqrt{3}$ = -1039 VAr $\Rightarrow$ -1100 VAr
MAXIMUM QTRIP = -1/2.5 * 100 V * 0.5 A * $\sqrt{3}$ = -35 VAr $\Rightarrow$ -30 VAr
in INCREMENTS OF 1 VAr

To scale into internal 'counts' these input values should be
SCALED BY 'PU_POLE_SLIP_Q', i.e (8000 counts/VA* $\sqrt{3}$) /2 = 6928.2 $\Rightarrow$ 6928 counts/VAr

NOTE the factor of $\sqrt{3}$ has been included since it was not used in the reactive power calculation. The reactive power, Q was therefore $\sqrt{3}$ times too big. The factor of 2 comes from the scaling down used in the calculation of Q.

3.2 REAL POWER VARIABLES - powerP, Pfact, pt, pmax, Ptol

3.2.1 Calculation of Raw Real Power, P.

The real power is calculated using the formula below;

$$P = \frac{Vab\_1\_poleslip.F\cos^{*}(Ia\_oc.F\cos) - Vbc\_1.F\cos^{*}Ic\_oc.F\cos)}{2}$$

where Vab_1_poleslip.Fcos, Vbc_1.Fcos are the relay instantaneous fourier cosine filtered line voltages, which have been scaled down by the relays internal hardware by a factor of $\sqrt{2}$, and ia_oc.Fcos, ic_oc.Fcos are the instantaneous fourier filtered phase currents which have also been scaled down by the relays internal hardware by a factor of $\sqrt{2}$.

The expression is divided by 2 in order to a) introduce a scaling factor of 1/2 to avoid numerical overflow, b) avoid having to perform another division by 2 when calculating the half cycle moving average value. Note that it is effectively divided by an additional factor of 2 due to the relays internal hardware scaling.

The half cycle moving average calculation of real power, powerP, is therefore reduced to a simple addition of the present (P) and previous (last_powP) raw values of real power, i.e the moving average filtered value, called powerP is given by 'P + last_powP'.

To scale from counts into Watts, these values should be
SCALED BY PU_POLE_SLIP_P/2 = 8000 counts/VA /2 = 4,000 counts/W

This variable is referred in the code as PU_POLE_SLIP_POW = 4000 counts/W.

3.2.2 Setting 'Pfact'.

This setting is used by the algorithm in the pt calculation purely as a means of scaling by a factor which varies between 0.7 and 1.0. Since floating point maths is not permitted, the actual multiplication by Pfact in the pt calculation function must be using integers between 7 & 10. The minimum and maximum setting values for Pfact are;

MINIMUM PFACT = 0.7
MAXIMUM PFACT = 1.0
in INCREMENTS OF 0.1

To scale into internal 'counts' these input values should be
SCALED BY 10 counts/unit

3.2.3 Calculation of Real Power Trip Setting, pt.

The value of pt is derived in the algorithm by the formula;

$$pt = powerP * Pfact \qquad 12$$

Note that the variable Pfact varies between 7 and 10, it should actually vary between 0.7 and 1.0, it has been scaled up by a factor of 10 to accommodate the integer mathematics requirement. pt is therefore

internally SCALED by 10/2 = 5. The factor of 10 comes from the Pfact scaling, the factor of 2 comes from the real power scaling.

To scale from counts into W these values should be
SCALED BY PU_POLE_SLIP_P * 10 /2 = PU_POLE_SLIP_POW * 10 = 40,000 counts/W
This variable is called PU_POLE_SLIP_PT.

3.2.4 Calculation of pmax.

The value of 'pmax' is derived in the algorithm by either one of the following formulae;

$$pmax = 14 * pt \qquad (14 \text{ used instead of } 1.4) \qquad 13$$

or

$$pmax = 10 * (10 * powerP) \qquad (10 \text{ used instead of } 1.0) \qquad 14$$

however, before multiplying by pt, a numerical overflow check needs to be performed. The number in counts which 'pt' should not exceed to prevent numerical overflow of pmax, denoted PMAX_OF1 is given by;

$$PMAX\_OF1 = 2^{31}/14 = 153391689$$

before multiplying by the moving average filtered real power, powerP, a numerical overflow check should be performed. The number in counts which 'powerP' should not exceed to prevent numerical overflow of pmax, denoted PMAX_OF2 is given by;

$$PMAX\_OF2 = 2^{31} / 100 = 21474836$$

If either of these numerical overflow checks are exceeded, pmax should be set equal to 2147483600 counts, ie the value PMAX_OF2 * 100.

pmax is internally SCALED by (10*10)/2 = 50. One factor of 10 comes from the pt scaling, the other comes from using 14 instead of 1.4, the 2 comes from the real power calculation.

To scale from counts into Watts these values should be
SCALED BY PU_POLE_SLIP_PT * 10 = 400,000 counts/W
This variable is called PU_POLE_SLIP_PMAX.

3.2.5 Setting ' Ptol'.

Section 2.2.2 stated that Ptol should be entered between 1% and 20 % of the generator rating.

Minimum and maximum setting values in terms of relay secondary quantities are therefore ;
MINIMUM PTOL = 1% /100 * 100 V * 0.5 A * $\sqrt{3}$ = 0.866 W $\Rightarrow$ 1 W

MAXIMUM PTOL = 20 % / 100 * 120 V * 1.5 A * √3 = 62.35 W ⇒ 70 W
in INCREMENTS OF 0.1 W

To scale into internal 'counts' these input values should be scaled by the same factor as the real power, powerP, i.e they should be SCALED BY
PU_POLE_SLIP_P /2 = PU_POLE_SLIP_POW = 4000 counts/W

The factor of 2 comes from the scaling down used in the calculation of powerP.

3.3 RATE OF CHANGE OF POWER VARIABLES
Dmin, deriv, Dfact, Dtran

3.3.1 Calculation of Rate of Change of Power Setting Dmin.

Dmin is calculated using equations 7 & 8. The external setting, slip, should vary between 0.1 and 5.0 %, due to the integer maths requirement this is scaled up by 10 to range from 1 to 50. The slip setting value has to be converted into actual units. These units need to be referenced to the frequency of the generator, the % slip setting should therefore be scaled up by;

2 * pi * freq (Hz) / 100

In the actual code the slip setting is scaled up when the lookup table, 'lookup' is initialised, the slip is scaled up by a factor of 2 * pi. The scaling by freq(Hz)/100 is performed later on in the code. As described in section 3.2.4, pmax is internally scaled by the factor (10*10)/2 = 50. The values for cos (δ_c) are not calculated trigonometrically, instead they are stored in an 8 point lookup table (Table 1).

Initialisation of the Look Up Table.

To avoid the slip * Pmax calculation in equation 7, the look up table is actually initialised with values of cos (δ_c) * slip * 2 * pi. The multiplication by the system frequency, and the division by 100 is performed when the look up value is taken from the lookup table, just before the Dmin calculation is performed. The cos (δ_c) values have been scaled up by 1000, this is referred to as COS_DELTA_SCALE, this preserves three decimal places of accuracy. The lookup table therefore takes the form shown in Table 2, in the code , the initialised look up table is referred to as 'lookup[pt_pmax]', where pt_pmax is the lookup index;

Table 2 - Look Up Table Used in the Pole Slipping Algorithm LGPG Code.

lookup index	ratio Pt/Pmax	cos (δc) * slip
0	0 - 0.1	-6283 * slip
1	0.1 - 0.2	-6252 * slip
2	0.2 - 0.3	-6156 * slip
3	0.3 - 0.4	-5994 * slip
4	0.4 - 0.5	-5759 * slip
5	0.5 - 0.6	-5441 * slip
6	0.6 - 0.7	-5027 * slip
7	0.7 - 0.8	-4487 * slip

NOTE:

1) When calculating the ratio pt/pmax, pt is first multiplied so that its scaling is ten times bigger than that of pmax , this variable is denoted as 'pt_x100' in the code. The ratio for pt/pmax then varies between 0 and 7, and can be used as the index to the lookup table, the variable name which is equal to pt_x100/pmax is called 'pt_pmax' in the code. The variable name is called pt_x100 because the pmax scaling is such that it is already 10 times greater than pt, this is why pt needs to be multiplied by 100 to make it ten times bigger than pmax.

Any remainder left from the division of pt_x100 and pmax is always discarded, the ratio pt/pmax is therefore rounded down. This results in the larger value of cos (δ_c) always being selected. Several checks are performed in the code to ensure numerical overflow does not occur. If pmax is equal to 0, then the division pt/pmax is not performed, the quantity pt_pmax is set to 0. A further check is performed to see if the quantity pt_pmax is between 0 and 7, if it is not, no look up value will exist, and the code may fail. To overcome this the lookup index is set to 0.

2) In the actual formula for Dmin, there is a negative sign in the formula. Since the sign of cos(δ_c) is also negative, and the slip should technically be negative (it is entered as positive), the sign from the formula has been omitted.

The essential requirement is that the overall sign of Dmin is negative.

Due to the scaling in pmax, slip, and cos (δc), the value for Dmin has to be scaled back down to prevent numerical overflow. The value chosen was 131072 which corresponds to a value 2^{17}. This value was chosen, as were all of the other scaling values which involve a factor of two, to reduce the computational burden since a division by 2 can be implemented by one shift right operation. To ensure that a minimal loss of resolution occurs, the look up table value is scaled down by 2, and Pmax is scaled down by 65536.

The procedure used for calculating Dmin is as follows;

1) Dmin = (pole_slip_prot.pmax / 2^{16}) * (lookup_val/2)
2) if pt_pmax < 6 then Dmin = Dmin + Dtran
3) if Dmin > Dfact then Dmin = Dfact.

Numerical Overflow

Before step 1 in the above calculation is performed, a numerical overflow check is performed. The numerical overflow checking is performed on pmax. If this is above a certain magnitude, it is set to that magnitude in order to limit the magnitude of Dmin. The maximum permitted magnitude of pmax which will not cause numerical overflow of Dmin is calculated from the following variables. The other variables in the Dmin calculation have maximum magnitudes of;

Dtran = -3000 W/s = -3000 * 30518 counts/W/s = -91554000, (section 3.3.4)

slip = 5% * 70 Hz * 2 * pi * 10 /100 = 250 counts, (70 Hz maximum operating frequency)

cos(δc) = -1000.

pmax is divided by 2^{16} in the code whilst the term 'slip * cos(δc)' or 'lookup_val' in the code is divided by 2, Dmin will overflow at -2^{31} counts , the maximum value pmax can be (denoted as DMIN_MAX_PMAX) without the variable Dmin overflowing is therefore given by;

-2^{31} = (-1000 * 220)/2 * (DMIN_MAX_PMAX/2^{16}) - 91554000

DMIN_MAX_PMAX = 1,224,885,504 counts. The magnitude of pmax is checked first before the Dmin calculation, if it is greater than 1,224,885,504 counts, then step 1 of the Dmin calculation is simplified to;

1) Dmin = 18690 * lookup_val/2

The number 18690 comes from DMIN_MAX_PMAX / 2^{16} . This should be implemented in the code in this format.

Calculation of lookup_val

The lookup_val is calculated in the code in the following manner;

1) lookup_val = lookup[pt_pmax] (this takes value from lookup table)
2) lookup_val = ((lookup_val * psfreq) + 5000) / 10000 (this adjust value according to frequency)

The variable psfreq is the current system frequency (Hz) , which has been scaled up by a factor of 100. 5000 is added to it here in order to round it up. It is then divided by 10000, in order to a) scale the frequency down to the correct value, and b) scale the lookup_val down by a factor of 100, this effectively scales the slip used in calculating the lookup table 'lookup' from % into absolute units. (see 3.3.1)

Including the Effects of Transient Saliency

The second line in the Dmin calculation is so that the algorithm can take into account the effects of generator transient saliency in the calculation of Dmin. Dtran is entered as an external setting. Dtran should only be used in the calculation of Dmin when the generator is in a transient, rather than steady state mode of operation. Dtran is only added to the Dmin calculation if the ratio of pt/pmax < 0.6, since this implies that the generator is in a transient state. Under steady state conditions, the ratio of pt/pmax is set by the pmax = 1.4 * pt criterion, which makes the ratio of pt/pmax = 1/1.4 = 0.714, i.e lookup index 7 will be used during steady state conditions.

Minimum Setting Value for Dmin

As described in section 2.3.2 an absolute minimum negative value for Dmin is implemented via the external setting Dfact. This is step 3 of the Dmin calculation shown above. If the value calculated by the above formula is greater than the value set by Dfact (recall Dfact is negative), then the setting Dmin is made equal to Dfact.

Overall Dmin Scaling

The resultant amount by which Dmin is scaled in the code is given by;

SLIP_SCALE * PU_POLE_SLIP_PMAX * COS_DELTA_SCALE/2^{17}

i.e (10 * 50 * 1000) * 8,000 / 131072 = 30517.57 counts/W/s

= 30518 counts/W/s

This scaling value is called PU_POLE_SLIP_DMIN = 30518 counts/W/s

The internal scaling is given by;

SLIP_SCALE * PU_POLE_SLIP_PMAX * COS_DELTA_SCALE / (PU_POLE_SLIP_P * 2^{17} = 3.81469727, this value is denoted as 'DMIN_SCALE'

3.3.2 Setting Dfact

Section 2.3.2 stated that Dfact should be entered between -10% and -50 % of the generator rating. Minimum and maximum setting values in terms of relay secondary quantities are therefore;

MINIMUM Dfact = -50% / 100 * 120 V * 1.5 A * $\sqrt{3}$ = -155.9 W/s $\Rightarrow$ -160W/s

MAXIMUM Dfact = -10% /100 * 100 V * 0.5 A * $\sqrt{3}$ = -8.7 W/s $\Rightarrow$ -5 W/s

in INCREMENTS OF 0.1 W/s

To scale into internal 'counts' these input values should be

SCALED BY PU_POLE_SLIP_DMIN = 30518 counts/W s^{-1}

3.3.3 Calculation of deriv Inside the Algorithm.

deriv is calculated using equation 6. With a sampling rate of 4 samples per cycle and a nominal operating frequency of 50 Hz, dt = 10 ms. Therefore 1/dt = 100 s^{-1}. In order to get the value of rate of change of power to the same scaling as Dmin, the following formula has been used;

deriv = (powerP - last_p_val) * DERIV_MULT * (psfreq /5000);

where DERIV_MULT = DMIN_SCALE * 100 * PU_POLE_SLIP_P/PU_POLE_SLIP_POW =
= 3.81469727 * 100 * 8000/4000 = 763

DMIN_SCALE comes from the scaling in the Dmin calculation, the 100 comes from the nominal value of 1/dt at 50 Hz. The factor of 2 (8000/4000) comes from the real power scaling.

The deriv calculation is actually split into three separate steps.

Step1 The first step is to calculate the quantity ' powerP - last_p_val'. Once this has been done, numerical saturation checks are performed on it to ensure that the deriv signal does not overflow.

Step2 The magnitude of the quantity 'powerP - last_p_val' is checked to see whether it is greater than a pre-determined value called DERIV_OF, if it is, then it is set equal to DERIV_OF. DERIV_OF is given by;

DERIV_OF = 2^{31} / MAX_DERIV_MULT

where MAX_DERIV_MULT = DERIV_MULT * 70/50 = DMIN_SCALE * 100 * 2 * 70/50 = 3.81469727 * 100 * 2 * 70/50 = 1069 counts. DERIV_OF = 2^{31} / 1069 = 2008871 counts, this value is set by the fact that the algorithm does not have to work at frequencies above 70 Hz.

Step3 The term 'powerP - last_p_val' is then multiplied by DERIV_MULT * (psfreq/5000) if the frequency is below 70 Hz. If the frequency is above 70 Hz, the term is multiplied by MAX_DERIV_MULT. Note that the protection is only enabled to provide a trip output between 40 and 70 Hz.

3.3.4 Setting Dtran

Dtran is calculated from equation 9, i.e

Dtran = (1/Xq - 1/ Xd') * Sgen

The maximum and minimum values of Xq and Xd' are given by;

0.3 < Xq < 2.5 pu
0.1 < Xd' < 2 pu Xq > Xd'

MINIMUM Dtran = (1/2.5 - 1/0.1) * 120 V * 1.5 A * $\sqrt{3}$
= -2993 W/s $\Rightarrow$ -3000 W/s
MAXIMUM Dtran = (1/2 - 1/2) * 100 V * 0.5 A * $\sqrt{3}$
= 0 W/s
in INCREMENTS OF 1 W/s

To scale into internal 'counts' these input values should be
SCALED BY PU_POLE_SLIP_DMIN = 30518 counts/W s^{-1}

3.4 OTHER SETTINGS - LAG, SLIP.

3.4.1 Setting 'Lag'.

The external setting 'lag' is used in the calculation of Pt, and can be varied between 0.1 and 10 seconds in 0.1 second intervals.

MINIMUM LAG = 0.1 s
MAXIMUM LAG = 10 s
in INCREMENTS OF 0.1 s

Pt is calculated in it's own function 'pole_slip_pt_calc', which is called every 20 ms (asynchronously). In order to get 'lag' working correctly within this function, a counter is used to count the number of function calls, when this counter is equal to 'lag' * 50, a new value of Pt is calculated.

To scale into internal 'counts' the input value for 'lag' should be
SCALED BY LAG_SCALE, which = 50 counts/sec .

3.4.2 Setting 'Slip'

The external setting 'slip' is used in the calculation of Dmin

MINIMUM SLIP = 0.1 %
MAXIMUM SLIP = 5 %
in INCREMENTS OF 0.1 %

Due to the integer maths requirement, scaling is required, to scale into internal 'counts' the input value for 'slip' should be SCALED BY 10 counts/% . This is referred to as SLIP_SCALE.

3.5 INITIALISATION OF VALUES.

3.5.1 Initialising the cos (δ_c) Look Up Table.

When the algorithm is being initialised, the look up table containing the terms 'slip * cos (δc)' should be initialised. This is necessary since 'slip' is entered as an external input, and therefore the look up table values vary according to this setting. The Slip setting is also part converted from percentage to absolute values at this stage.

3.5.2 Initialising Other Variables.

The programming language 'C' will initialise all static type variables to zero if no other initial value is specified. Most variables therefore need to be initialised in order to prevent divide by zero errors, and algorithm mal-operation. The algorithm takes ' 2 * lag' seconds to initialise fully.

Variables 'PU_POLE_SLIP_? etc' These variables are stored in the include file 'dconst.h' and are given by;

DERIV_MULT = DMIN_SCALE * 100 * PU_POLE_SLIP_P/PU_POLE_SLIP_POW = 763 counts
DERIV_OF = 2^{31} / MAX_DERIV_MULT = 2008871 counts
DMIN_MAX_PMAX = see section 3.3.1 = 1,224,885,504 counts
DMIN_SCALE =
SLIP_SCALE * PMAX_SCALE * COS_DELTA_SCALE / (2^{17} * PU_POLE_SLIP_P)
= 3.81469727
MAX_DERIV_MULT = DERIV_MULT * 70/50 = 1069 counts
PFACT_SCALE = 10 counts (Pfact setting scaled by 10)
PMAX_OF1 = 2^{31} / 14 = 153391689 counts
PMAX_OF2 = 2^{31} / (PU_POLE_SLIP_PMAX/PU_POLE_SLIP_POW) = 2^{31} / 100
= 21474836 counts
PU_POLE_SLIP_P = PU_I * PU_V = 800 * 10 = 8000 counts/VA
PU_POLE_SLIP_Q = PU_I * PU_V * root3 / 2 = 800 * 10 * 1.732050808/2 = 6928 counts/VAr
PU_POLE_SLIP_POW = PU_POLE_SLIP_P/2 = 4,000 counts/W
PU_POLE_SLIP_PT = PU_POLE_SLIP_POW * PFACT_SCALE = 40,000 counts/W
PU_POLE_SLIP_PMAX = PU_POLE_SLIP_POW * PFACT_SCALE * 10 = 400,000 counts/W
PU_POLE_SLIP_DMIN = PU_POLE_SLIP_P * DMIN_SCALE = 8000 * 3.81469727
= 30518 counts/W/s
SLIP_SCALE = 10 counts/% (slip setting scaled up by 10)
LAG_SCALE = 50 counts/s

'Pt', & Variable 'P2' The variable Pt should be initialised to a value of 1 'count' this means in secondary values, that the algorithm Pt setting is at it's most secure value of zero Watts. This will also occur during generator run up where the machines output power should be practically zero (neglecting transformer losses).

The variable 'P2' which is used within the Pt estimation function should also be set to 1 count. The other variable 'P1' used in this function should be set to a larger value so that the terms |P - P2| & |P - P1| are not identical and one will at least be greater than Ptol.

Pt = 1 count, P2 = 1 count.

Variable 'P1' As mentioned above, P1 should be set to a high value of power, so that it's difference compared to P2 is always greater than Ptol. This ensures that Pt is not incorrectly estimated until a true steady state condition has been reached. The chosen value of real power is two times nominal rated power therefore I = 2 Amps, V = 120 Volts;

P1 = 120 V * 2 A * PU_POLE_SLIP_Q = 3,325,538 counts

The PU_POLE_SLIP_Q value was used since this contains the root3 factor which is necessary in calculating the true generator per unit power.

Variable 'Pmax' Pmax should be set to a value equivalent to the generator rating, the ratio Pt/Pmax will then be in the region 0 to 0.1 thus resulting in a large, secure setting value for $(\Delta P/\Delta t)_{min}$ of -1 * slip * Pmax.

Pmax should therefore be initialised to ;

Pmax = 120V * 1A * PU_POLE_SLIP_Q * PU_POLE_SLIP_PMAX/PU_POLE_P
= 83,138,439 counts.

The PU_POLE_SLIP_Q value was used for the same reason as in P1.

Variables 'last_p_val' & 'pen_p_val' The variables 'last_p_val' and 'pen_p_val' are the stored values of moving average filtered power used to calculate $(\Delta P/\Delta t)$. If they are set to 0 counts, then the first two values of $(\Delta P/\Delta t)$ calculated will be positive if power is positive, or will be zero if the power is zero.

last_p_val = pen_p_val = 0 counts.

Variables 'last_powP' & 'last_powQ' These variables are the stored values of 'raw' real and reactive power used in calculating the respective moving average values. If both of these are set to rated generator output power, then they will make the first value of real and reactive power calculated more positive than it should be, this results in more secure values from an algorithm stability viewpoint.

last_powP & last_powQ = 120V * 1A * PU_POLE_SLIP_Q /2 = 415680 counts.

The division by 2 is due to the algorithm's internal scaling value.

Counter Variables 'trip_count', 'cnt_pmax_off', 'cnt_pmax', & 'count' All counter variables should be initialised to zero.

Variables 'Dmin', 'deriv', 'powerP' & 'powerQ' These variables can be initialised to a value of 1 count, their initialisation is not important since they will be calculated in the first time step. Since the algorithm requires 1.5 power system cycles to operate, it is unlikely that it will nuisance trip on start up anyway.

3.6 NUMERICAL OVERFLOW CONSIDERATIONS & RESOLUTION.

The maximum input values of voltage and current are 204.8 Volts (rms line) and 20.4 Amps (rms phase). These figures are given as rms quantities due to the hardware scaling which is used in the relay so that the phasors calculated are in rms quantities. These therefore set the overflow considerations for the power variables. In calculating the maximum power from the maximum voltage and current inputs, a factor of $\sqrt{3}$ is included since the voltage used is a line voltage.

Reactive power, Q The scaling of this value is set to 6,928 counts/VAr (PU_POLE_SLIP_Q). The maximum generator power is;

204.8 V * 20.4 A * $\sqrt{3}$ = 7236.37 VAr. $\Rightarrow$ 50133570 counts

This uses log (50133570) / log (2) = 25.6 $\Rightarrow$ 26 bits required for magnitude.

The resolution for a 1 Amp relay is 1/6928 = 144 .34 μVAr (721.71 μVAr for 5 Amp)

Real power, P The scaling of this value is set to 4,000 counts/W (PU_POLE_SLIP_POW). The maximum generator power is ;

204.8 V * 20.4 A * $\sqrt{3}$ = 7236.37 W $\Rightarrow$ 28945480 counts

This uses log (28945480) / log (2) = 24.8 $\Rightarrow$ 25 bits required for magnitude.

The resolution for a 1 Amp relay is 1/4000 = 250 μW (1.25 mW for 5 Amp)

Real Power Trip Level, Pt The scaling of this value is set to 40,000 counts/W (PU_POLE_SLIP_PT). The maximum generator power is ;

204.8 V * 20.4 A * $\sqrt{3}$ = 7236.37 W $\Rightarrow$ 289454800 counts

This uses log (289454800) / log (2) = 28.11 $\Rightarrow$ 29 bits required for magnitude.

The resolution for a 1 Amp relay is 1/40000 = 25 μW (125 μW for 5 Amp).

Real Power Maximum Output Level, Pmax The scaling of this value is set to 400,000 counts/W (PU_POLE_SLIP_PMAX). The maximum value of pmax is limited by numerical saturation and is equal to

PMAX_OF2 * 100 = (2^{31} / 100) * 100 = 2147483600 counts

The maximum value of pmax in terms of secondary watts is therefore given by;

PMAX_OF2 * 100 / PU_POLE_SLIP_PMAX = 2,147,483,600/400,000 = 5368.7 Watts

The resolution for a 1 Amp relay is 1/400000 = 2.5 μW (12.5 μW for 5 Amp).

Rate of Change of Power (ΔP/Δt) The scaling of this value is set to 30518 counts/W/s (PU_POLE_SLIP_DMIN) . The maximum number that this can reach is limited within the algorithm code, it is equal to;

DERIV_OF * MAX_DERIV_MULT = 2008871 * 1069 = 2,147,483,099 counts

This in terms of secondary Watts/second is equivalent to;

2,147,483,099/30518 = 70,367.8 W/s

The resolution for a 1 Amp relay is 1/30518 = 32.7 μW/s (163.8 μW/s for 5 Amp).

Rate of Change of Power trip level $(\Delta P/\Delta t)_{min}$ The scaling of this value is set to 30518 counts/W/s (PU_POLE_SLIP_DMIN). The maximum number that this can reach is limited in the code by the variables Pmax, slip, and cos(δc) (see equation 7).

The maximum value for lookup_val term in the Dmin calculation is -1000 * 220 counts, the maximum value Dtran is -91554000 counts. The maximum value for pmax is limited in the Dmin calculation to is DMIN_MAX_PMAX / 2^{16} = 18690 counts. Recall that the lookup_val is scaled down by a factor of two in the Dmin calculation.. The maximum number is therefore ;

((-1000*220)/2 * 18690) - 91554000 = -2,147,454,000 counts.

This uses log (2,147,454,000) / log (2) = 30.999 ⇒ 31 bits required for magnitude. This will not overflow even if Pmax and all of the other settings were at their maximum value. This in terms of secondary Watt/s is; -2,147,454,000/30518 = 70366.8 W/s

The resolution for a 1 Amp relay is 1/30518 = 32.7 μW/s (163.8 μW/s for 5 Amp).

3.7 DISTURBANCE RECORDING.

3.7.1 Disturbance Recorder Requirements.

The LGPG 111 is capable of storing 2 disturbance records in its volatile memory. Once these two records have been filled up, no further disturbance recording will be performed until the records in the buffer have been uploaded to a PC. For the Scottish field trials, interrogation of the relay can be achieved remotely the University of Bath.

The LGPG 111 is capable of storing 8 channels, each channel having a capacity to store 768 samples, which at 4 samples per cycle produces a disturbance record of 3.84 seconds at 50 Hz. In addition to these 8 channels the relay also stores all of the digital inputs and relay status outputs. The variables which need to be recorded are powerP, pt, pmax, powerQ, deriv, Dmin. In addition to these 6 algorithm variables, if possible it is hoped that the spare two channels can be used to store one voltage magnitude and voltage phase angle.

Within the algorithm code 3 additional 'relay status' outputs will be formed which will flag when each of the three algorithm criterions are satisfied ((powerP < pt), (powerQ < Qtrip), & (deriv < Dmin)). This will help with the debugging of the algorithm. The relay status outputs will be named as follows;

1)	Pole slipping algorithm trip	function_details name > POLE_SLIP
2)	Reactive power criterion	function_details name > QTRIP_CRITERION
3)	Real power criterion	function_details name > PT_CRITERION
4)	Rate of Change of power criterion	function_details name > DMIN_CRITERION

Disturbance Recorder Trigger Conditions.

There are two different conditions which should trigger the disturbance recorder. The first trigger is provided by the pole slipping algorithm relay output, POLE_SLIP. This is the normal way that the disturbance recorder is triggered. The second trigger condition is provided when the pole slipping algorithm's reactive trip criterion is satisfied (powerQ < Qtrip), the relay status QTRIP_CRITERION will provide the trigger. Disturbance records triggered in this manner should provide an indication of conditions which may potentially cause algorithm mal-operation if settings are incorrect. The trigger conditions can be selected from the LGPG's front end menu system. An overcurrent trip will also be used for the field trials to provide a higher likelihood of capturing data during a disturbance.

In summary the disturbance recorder should be triggered if;

1) Q < Qtrip (within pole slipping algorithm)

or

2) Pole slipping algorithm produces trip output

or

3) Overcurrent algorithm produces a trip.

Disturbance Recorder Pre & Post Fault Time Allocations.

The amount of pre trigger and post trigger time in the disturbance record can be adjusted from the relays front end. The amount of pre-trigger, and post - trigger time should be allocated as follows;

pre-trigger period	=	2.34 seconds (117 power system cycles)
post trigger period	=	1.50 seconds (75 power system cycles)
total disturbance record	=	3.84 seconds

These times will ensure that with pole slipping events, the disturbance record will capture the pole slip. For events such as stable power swings, which should not cause the algorithm to trip, the 1.5 second post trigger period should be adequate to allow analysis of the algorithm measurands.

Frequency Measurement.

Since the disturbance record results are frequency locked, it is impossible to derive the frequency measurement in the usual way, (zero crossings). The disturbance record contains the time at which each sample was stored however, and this information can therefore be used to calculate the frequency to an accuracy of around 0.02 Hz.

3.7.2 Scaling from 32 Bit Precision to 16 Bit Precision.

The disturbance recorder requires that the variables it stores are of 16 bit precision. Eventually, the whole algorithm will probably be implemented in 16 bit format, since this will improve the operation speed greatly. This conversion will be performed when the algorithm is optimised.

NOTE : the values calculated below are for the 1 Amp relay

Reactive power, powerQ The scaling of this value is set to PU_POLE_SLIP_Q, 6,928 counts/VAr. If the internal 32 bit variable is divided by $2^9 = 512$, then the above scaling figure becomes;

$$6928/512 = 13.53125 \text{ counts/VAr}$$

The resolution is therefore $1/13.53125 = 73.90$ mVAr.

The reactive power disturbance record may therefore overflow at a value of;

$$2^{15} \text{ counts}/ 13.53125 \text{ counts/VAr} = 2421.65 \text{ VAr}$$

Section 3.6 states that the maximum input level is 7236.4 Var. If you consider a machine of secondary rating $120 * 1 * \sqrt{3} = 207.84$ VA, then the maximum possible reactive power measurement is $2421.65/207.84 = 11.7$ * rating of generator, this is very unlikely. This resolution therefore provides 207.84 VAr/73.9 mVAr = 2812 discrete levels between zero and nominal rated power.

Real power, powerP The scaling of this value is set to PU_POLE_SLIP_POW, 4,000 counts/W. If the internal 32 bit variable is divided by $2^9 = 512$, then the above scaling figure becomes;

4000/512 = 7.8125 counts/W

The resolution is therefore 1/7.8125 = 128 mW.

The real power disturbance record may therefore overflow at a value of;

2^{15} counts/ 7.8125 counts/W = 4194.3 W.

Section 3.6 states that the maximum input level is 7236.4 W. If you consider a machine of secondary rating 120 * 1 * $\sqrt{3}$ = 207.84 VA, then the maximum possible real power measurement is 4194.3/207.84 = 20.0 * rating of generator.

Real Power Trip Setting , pt The scaling of this value is set to PU_POLE_SLIP_PT, 40,000 counts/W. If the internal 32 bit variable is divided by 2^{12} = 4096, then the above scaling figure becomes;

40000/4096 = 9.765625 counts/W

The resolution is therefore 1/9.765625 = 102.4 mW.

The real power trip setting disturbance record may therefore overflow at a value of;

2^{15} counts/ 9.765625 counts/W = 3355.44 W.

Section 3.6 states that the maximum input level is 7236.4 W. If you consider a machine of secondary rating 120 * 1 * $\sqrt{3}$ = 207.84 VA, then the maximum possible real power trip level measurement is 3355.44/207.84 = 16.1 * rating of generator.

Real Power Maximum Output Monitor, pmax The scaling of this value is set to PU_POLE_SLIP_PMAX, 400,000 counts/W. If the internal 32 bit variable is divided by 2^{15} = 32768, then the above scaling figure becomes;

400000/32768 = 12.207 counts/W

The resolution is therefore 1/12.207 = 81.9 mW.

pmax is limited in the code to 2,147,483,600 counts, this converts to;

2,147,483,600 / 2^{15} counts = 65536 counts. This requires log(65536) /log(2) = 15.99 bits and will therefore overflow at 2^{15} /12.207 = 2684.36 Watts (secondary)

If you consider a machine of secondary rating 120 * 1 * $\sqrt{3}$ = 207.84 VA, then the maximum possible value of Pmax measurement is 2684.36/207.84 = 12.9 * rating of generator.

Rate of Change of Real Power Measurement , ($\Delta P/\Delta t$)

The scaling of this value is set to PU_POLE_SLIP_DMIN, 30,518 counts/W/s. The maximum magnitude that this variable is permitted to reach by the algorithm code is

DERIV_OF * MAX_DERIV_MULT = 2,008,871 * 1069 = 2,147,483,099 counts

This needs to be scaled down by 2^{15} to achieve 16 bit precision. The above scaling figure therefore becomes

30,518 / 2^{15} = 0.93133545 counts/W/s

The resolution is therefore 1/0. 93133545 = 1.0737 W/s.

The ($\Delta P/\Delta t$) measurement has a maximum of;

2,147,483,099 counts / 2^{15} = 65536 counts.

this requires log (65536) / log (2) = 16 bits. It may therefore overflow.

Overflow will occur at 2^{15} / 0.93133545 = 35183 W/s (secondary)

Rate of Change of Real Power Trip Setting , $(\Delta P/\Delta t)_{min}$

The scaling of this value is the same as above (30,518 counts/W/s). It will therefore require the same scaling down as the above to get it into 16 bit format. i.e it needs scaling down by 2^{15} = 32,768. The maximum value of Dmin is limited in the code to 2,147,454,000 counts. The maximum value if therefore given by

2,147,454,000/2^{15} = 65535 counts this requires log(65535) / log(2) = 15.9 bits and may therefore overflow !

Overflow will occur at 2^{15} / 0.93133545 = 35183 W/s (secondary)

Summary of Scaling Values Used in Converting from 32 bit to 16 bit Format.

Tables 3 and 4 detail the scaling, overflow points and resolution for the 1 and 5 amp relays.

Table 3 - Scaling values for 1 Amp Relay (32 bit to 16 bit conversion for data capture)

Variable	Scaling Factor	Overflow point	Resolution	Comment
Q	2^9 = 512	2421.7 VAr	73.9 mVAr	numerical overflow possible
P	2^9 = 512	4194.3 W	128 mW	numerical overflow possible
Pt	2^{12} = 4096	3355.4 W	102.4 mW	numerical overflow possible
Pmax	2^{15} = 32768	2684.4 W	81.9 mW	numerical overflow possible
($\Delta P/\Delta t$)	2^{15} = 32768	35183 W/s	1.0737 W/s	numerical overflow possible
$(\Delta P/\Delta t)_{min}$	2^{15} = 32768	35183 W/s	1.0737 W/s	numerical overflow possible

Table 4 - Scaling values for 5 Amp Relay (32 bit to 16 bit conversion for data capture)

Variable	Scaling Factor	Overflow point	Resolution	Comment
Q	$2^9 = 512$	12108.5 VAr	369.5 mVAr	
P	$2^9 = 512$	20971.5 W	640 mW	
Pt	$2^{12} = 4096$	16777.2 W	512 mW	
Pmax	$2^{15} = 32768$	13422 W	409.5 mW	should be an unsigned int
$(\Delta P/\Delta t)$	$2^{15} = 32768$	175915 W/s	5.3685 W/s	saturation definitely required
$(\Delta P/\Delta t)_{min}$	$2^{15} = 32768$	175915 W/s	5.3685 W/s	saturation definitely required

VERSION CONTROL

Issue	Author	Reason for Change	Date
PA	Matt Checksfield	Original	30/6/95
PB	Matt Checksfield	Addition of disturbance recorder information & Corrections to scaling values.	14/9/95
PC	Matt Checksfield	Modification of algorithm (Dtran etc) and addition of symbolic constants to replace 'magic numbers' in code	10/5/96

4.0 SUMMARY OF ALL SCALING FACTORS IN ALGORITHM

The table belows contains a summary of the user interface pole slipping variables for display and setting. The default values given on the 1 Amp tables are for the SLOY Scottish generator. The dafault values for the 5 Amp tables are 5 times those for the 1 amp.

SETTINGS 1 AMP RELAY

Setting	Minimum	Maximum	Step	Default	Menu Scaling	Protection Mapping	Total Scaling	Affected by xformer ratios and In
Qtrip	-1100 VAr	-30 VAr	1 VAr	-272 VAr [(-1/0.7) *110V*1A*√3]	1VAr = 1	6928 [PU_POLE_SLIP_Q]	1VAr = 6928 PU_POLE_SLIP_Q	Yes
Ptol	1.0 W	70 W	0.1 W	6.9 W [5%*138VA]	1W = 10	400 [PU_POLE_SLIP_POW/10]	1W = 4000 PU_POLE_SLIP_POW	Yes
Pfact	0.7	1.0	0.1	0.9	1=10	NONE	1=10	No
Dfact [(ΔP/Δt)fact]	-160.0 W/s	-5.0 W/s	0.1 W/s	-47.6 W/s [-0.25s^{-1}*110V*1A*√3]	1W/s = 10	3051.8 [PU_POLE_SLIP_DMIN/10]	1W/s = 30518 PU_POLE_SLIP_DMIN	Yes
Dtran [(ΔP/Δt)tran]	-3000 W/s	0 W/s	1 W	-572 W/s [-3s^{-1}*110V*1A*√3]	1W/s = 1	30518 [PU_POLE_SLIP_DMIN]	1W/s = 30518 PU_POLE_SLIP_DMIN	Yes
Slip	0.1%	5%	0.1 %	0.5 %	1%=10	NONE	1%=10	No
Lag	0.1s	10.0 s	0.1 s	1.0 s	1s=10	5	1s=50 (20ms resolution)	No

SETTINGS 5 AMP RELAY

The table below was derived from the 1 Amp table by multiplying all setting values which are dependent upon current input levels by a factor of 5 , and dividing all scaling values by a factor of 5

Setting	Minimum	Maximum	Step	Default	Menu Scaling	Protection Mapping	Total Scaling	Affected by xformer ratios and In
Qtrip	-5500 VAr	-150 VAr	5 VAr	-1360 VAr [(-1/0.7) *110V*5A*√3]	1VAr = 1	1386 [PU_POLE_SLIP_Q/5]	1VAr = 1386 PU_POLE_SLIP_Q/5	Yes
Ptol	5.0 W	350 W	0.5 W	34.5 W [5%*5*138 VA]	1W = 10	80 [PU_POLE_SLIP_POW/ (10*5)]	1W = 800 PU_POLE_SLIP_POW/5	Yes
Pfact	0.7	1.0	0.1	0.9	1=10	NONE	1=10	No
Dfact [(ΔP/Δt)fact]	-800.0 W/s	-25.0 W/s	0.5 W/s	-238.0 W/s [-0.25s^{-1}*110V*5A*√3]	1W/s = 10	610.35 [PU_POLE_SLIP_DMIN/ (10 * 5)]	1W/s = 6104 PU_POLE_SLIP_DMIN/5	Yes
Dtran [(ΔP/Δt)tran]	-15,000 W/s	0 W/s	5 W	-2858 W/s [-3s^{-1}*110V*5A*√3]	1W/s = 1	6103.5 [PU_POLE_SLIP_DMIN/ 5]	1W/s = 6104 PU_POLE_SLIP_DMIN/5	Yes
Slip	0.1%	5%	0.1 %	0.5 %	1%=10	NONE	1%=10	No
Lag	0.1s	10.0 s	0.1 s	1.0 s	1s=10	5	1s=50 (20ms resolution)	No

CALCULATION OF SETTINGS

The table below details the methods and maximum and minimum setting limits

Setting	Formula	Minimum setting	Maximum setting
Qtrip	**-1/Xq * Vn * In* √3**	**Xq = 2.5 pu**	**Xq = 0.3 pu**
Ptol	**'x %'/100 * Vn * In * √3**	**x = 1 %**	**x = 20 %**
Pfact	**none**	**0.7**	**1.0**
Dfact $(\Delta P/\Delta t)_{fact}$	**'y %'/100 * Vn * In * √3**	**y = - 10 %**	**y = - 50 %**
Dtran $(\Delta P/\Delta t)_{tran}$	**(1/Xq - 1/Xd') * Vn *In *√3**	**Xq = 2.5 pu Xd' = 0.1 pu**	**Xq = 2 pu Xd' = 2 pu**
slip	**none**	**0.1 %**	**5 %**
lag	**none**	**0.1 seconds**	**10 seconds**

MEASUREMENTS 1 AMP RELAY

Measurement	Resolution (1 Amp)	Maximum Magnitude Internally.	Menu Scaling	Comments	Affected by xformer ratios and In
Pt	25 μW	7236.37 W	PU_POLE_SLIP_PT 40,000 counts/W	maximum magnitude due to V & I input limits being reached	Yes
P	250 μW	7236.37 W	PU_POLE_SLIP_POW 4000 counts/W	maximum magnitude due to V & I input limits being reached	Yes
Pmax	2.5 μW	5368.7 W	PU_POLE_SLIP_PMAX 400,000 counts/W	maximum magnitude limited by code - max magnitude is PMAX_OF2 * 100	Yes
Q	144.34 μVAr	7236.37 VAr	PU_POLE_SLIP_Q 6928 counts/W	maximum magnitude due to V & I input limits being reached	Yes
Dmin [(ΔP/Δt)min]	32.7 μW/s	70,366.8 W/s	PU_POLE_SLIP_DMIN 30518 counts/W/s	maximum magnitude limited by code - max magnitude limited by DMIN_MAX_PMAX, and slip setting max	Yes
Deriv [(ΔP/Δt)]	32.7 μW/s	70,367.8 W/s	PU_POLE_SLIP_DMIN 30518 counts/W/s	maximum magnitude limited by code - max magnitude set by DERIV_OF * MAX_DERIV_MULT	Yes

MEASUREMENTS 5 AMP RELAY

Measurement	Resolution (5 Amp)	Maximum Magnitude Internally.	Menu Scaling	Comments	Affected by xformer ratios and In
Pt	125 μW	36181.9 W	PU_POLE_SLIP_PT/5 8,000 counts/W	maximum magnitude due to V & I input limits being reached	Yes
P	1.25 mW	36181.9 W	PU_POLE_SLIP_POW/5 800 counts/W	maximum magnitude due to V & I input limits being reached	Yes
Pmax	12.5 μW	26843.5 W	PU_POLE_SLIP_PMAX/5 80,000 counts/W	maximum magnitude limited by code - max magnitude is PMAX_OF2 * 100	Yes
Q	721.7 μVAr	36181.9 VAr	PU_POLE_SLIP_Q/5 1386 counts/W	maximum magnitude due to V & I input limits being reached	Yes
Dmin [(ΔP/Δt)min]	163.5 μW/s	351,834 W/s	PU_POLE_SLIP_DMIN/5 6104 counts/W/s	maximum magnitude limited by code - max magnitude limited by DMIN_MAX_PMAX, and slip setting max	Yes
Deriv [(ΔP/Δt)]	163.5 μW/s	351,839 W/s	PU_POLE_SLIP_DMIN/5 6104 counts/W/s	maximum magnitude limited by code - max magnitude set by DERIV_OF * MAX_DERIV_MULT	Yes

The Power Based Pole Slipping Algorithm.

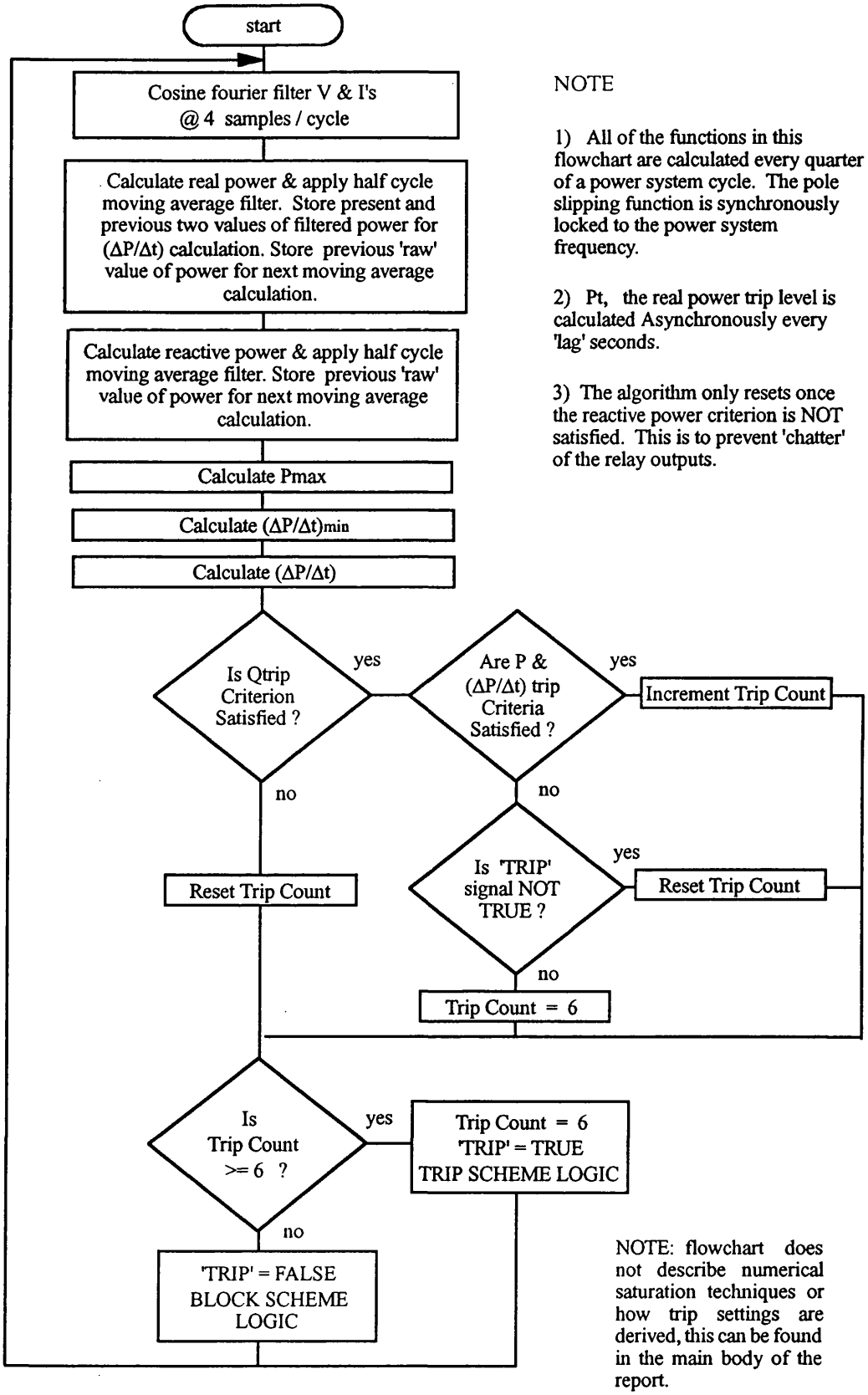

NOTE

1) All of the functions in this flowchart are calculated every quarter of a power system cycle. The pole slipping function is synchronously locked to the power system frequency.

2) Pt, the real power trip level is calculated Asynchronously every 'lag' seconds.

3) The algorithm only resets once the reactive power criterion is NOT satisfied. This is to prevent 'chatter' of the relay outputs.

NOTE: flowchart does not describe numerical saturation techniques or how trip settings are derived, this can be found in the main body of the report.

Figure 1
Flowchart Showing Operation of The Pole Slipping Algorithm

Pt Calculation Function.

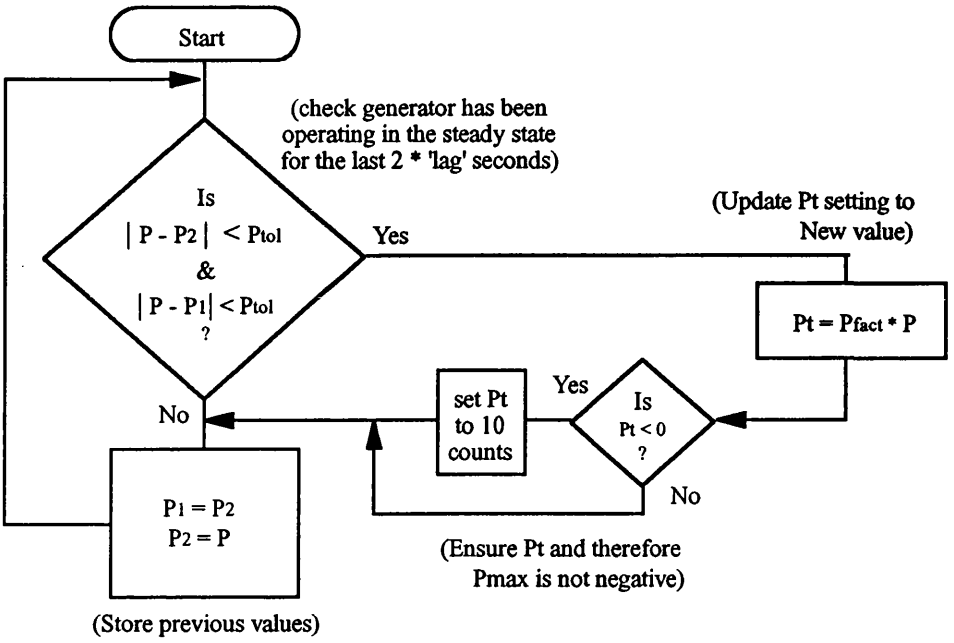

NOTE

1) The Pt calculation function is called every 'lag' seconds, the most recent value of moving average filtered real power calculated at the time the function is called is set to 'P'. This function is separate from the rest of the algorithm and is performed asynchronously, all of the other algorithm functions are called synchronously every quarter of a power system cycle.

2) P_1 is the value of P used '2*lag' seconds ago, whilst P_2 is the value of P used 'lag' seconds ago.

3) Pfact is the scaling factor used to introduce a safety margin in the Pt estimation. Nominally, it is set to 0.9 in absolute terms. It can be externally set from 0.7 to 1.0 in 0.1 increments.

4) Ptol is the tolerance band which the generator output power must stay within over the time period ' 2 * lag' seconds for the value of Pt to be updated.

5) The Pt function is actually called every 20 ms. The menu scaling on variable lag is therefore set so that menu scaled lag * 20 ms = actual lag in seconds, i.e the menu scaling is 50, this is so a counter within the Pt calculation function can count when Pt should be calculated. The Pt calculation function although called every 20 ms, therefore only runs through the above flowchart every 'lag' seconds.

Figure 2

The Generator Input Power Estimation Function (Calculates Trip Setting, Pt.)

Pmax Calculation Function.

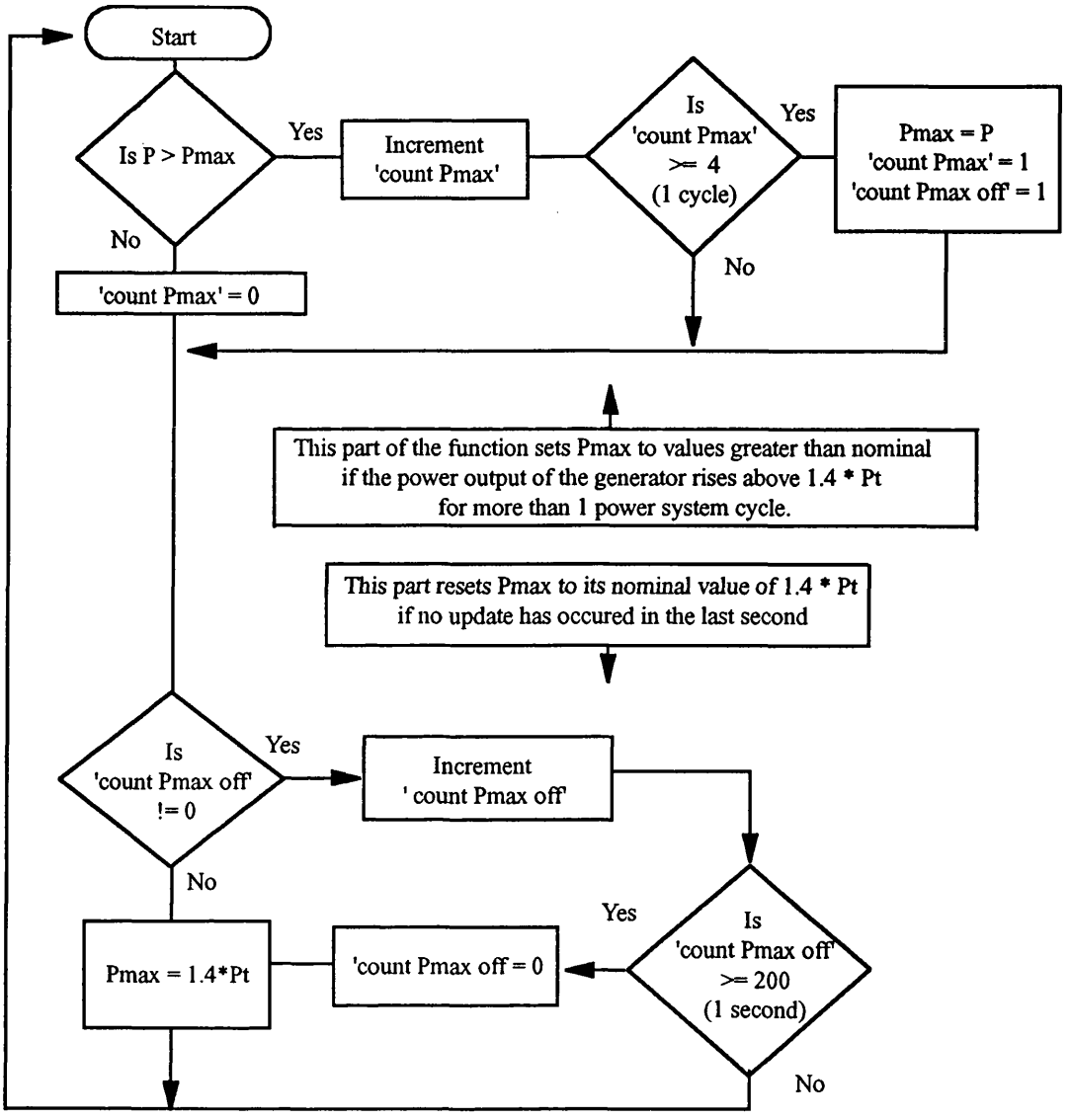

NOTE

1) With reference to the boxes which check whether 'count Pmax' is greater than or equal to one cycle, the criterion is that it should be in terms of power system cycles, not absolute time. This will therefore work as intended over the complete frequency operating range.

2) The function tracks any slow changes in power output from the generator which are greater than the nominal value of 1.4 * Pt. It will reject any spikes produced by disturbances such as faults, this is why the power, P has to be greater than Pmax for one power system cycle before an update occurs. Once an update occurs, the updated value is 'held' for one second, Pmax is then reset to its nominal value.

3) The algorithm has to successfully detect pole slipping over the operating range of 40 - 70 Hz. Since the Pmax off counter is counted in numbers of quarter cycles, the time of one second will vary with frequency. The actual 'Pmax off' time will vary between 1.25 and 0.714 seconds. The amount of time required to reset is approximately inversely proportional to the square of the system frequency. It is dictated by the natural frequency of swinging of the generator rotor.

4) Flowchart does not contain any details of the numerical saturation employed, this can be found in the main body of the report.

Figure 3

Generator Maximum Power Output Monitor (Pmax Measuring Function).

Appendix F
EXAMPLES OF COMPUTER FILES USED TO TEST THE POLE SLIPPING ALGORITHM.

F1.1 PPSS Simulation File PSL3GA - Pole Slip From Full Load, Governor & AVR Included

This is the ATP file used to produce test 'PSL3GA'.

```
C File    :-  PSL3GA.DAT
C Details :-  POLE slipping induced by 2 Phase to earth Fault,
C             Generator control details;
C             AVR (YES)
C             GOVERNOR (YES)
C             INITIAL LOAD 100 % (200 MW)
C
C Source  :-  System taken from example given on Page 7-18 of the
C             EMTP Vol 3, Wookbook 3, June 1989, a research project
C             report made by the EPRI, Poject 2149-6, Vol EL-4651
C             Source capacity and transformer impedance both decreased
C
C System  :-  200 MVA syncheonous generator using type SM 59 model,
C             13.8 kV (line-line rms), No saturation modelling.
C             Transformer has 3.5 % PU leakage reactance (200 MVA base).
C             Infinite bus seperated from machine by 144 Km dist param line.
C             Load is 235.4 MW 0.9985 power factor lagging (@ 132 kV)
C             When fault cleared, load and feeder are also cleared.
C             Fault separated from generator by type 1,2,3 line. (unbalanced)
C             Load seperated from fault by inductance.(transformer)
C             System frequency changed from 60 to 50 Hz.
C
C      The Governor model has been changed to the one given in DC47.DAT (and
C      also in LEC EMTP Summer Course, Leuven 15 july 91, Rotating machines)
C      This is faster than the original hydro governor.
C
C      M Checksfield 10/8/95
C
BEGIN NEW DATA CASE
POWER FREQUENCY                      50.0      {special request card
C .............Set up I/O to write to correct file.............................
$CLOSE, UNIT=4 STATUS=DELETE
$OPEN, UNIT=4 FILE=C:\atp\gecptl\psl3ga.pl4 FORM=FORMATTED STATUS=UNKNOWN !
C ........................Misc Data.........................................
C <DELTA<---TMAX<---XOPT<---COPT<-EPSILN<-TOLMAT<-Tstart
200.0E-6     6.0
C <-IOUT<--IPLOT<-IDOUBL<-KSSOUT<-MAXOUT<---IPUN<-MEMSAV<---ICAT<-NERERG<-IPRSUP
     500       5              1                                  1
```

```
TACS HYBRID
C opName  s<--ip1 s<--ip2 s<--ip3 s<--ip4 s<--ip5 <-gain<-FxLo<-FxHi<-NmLo<-NmHi
C <--No,Do<----N1,D1<----N2,D2<----N3,D3<----N4,D4<----N5,D5<----N6,D6<----N7,D7
C Zero_block
  VR      +V2                                          1.  -2.0   2.0
  VF      +DVF    +UNITY                               1.
C Laplace S blocks
 1V2      -V1     +UNITY  -V3                        400.
        1.
        1.       .02
 1V1      +VDC                                         1.
 .52359878
        1.       .03
 1DVF     +VR                                          1.
        1.
        1.      .015
 1V3      +DVF                                         1.
        0.       .03
        1.        .5
C  SPEED GOVERNOR SYSTEM
92VEL1
C  CONVERSION OMEGA TO PER UNIT SYSTEM
99TACOM   = .0031831 * VEL1
C Speed Governor System.
 0DIFOME  -UNITY  +TACOM
 0KDIFOM  +DIFOME                                    20.
 0PS1     +UNITY  -KDIFOM -PGV
 0PS2     +PS1                                       10.    -.4   .4
88PS21    = PS2
 1PGV     +PS21                                      1.0     0.   1.1
        1.
                0.5
 1PGV1    +PGV                                       1.
        1.
        1.      0.25
 1PGV2    +PGV1                                      1.
        1.
        1.       10.
 1PGV3    +PGV2                                      1.
        1.
        1.       0.5
88PM1     = 0.274 * PGV1
88PM2     = 0.243 * PGV2
88PM3     = 0.483 * PGV3
88PMT     = PM1 + PM2 + PM3
88PM      = 1.0 * PMT
C NODE_V
90BUS1A                  50.
90GEN3GA                 50.
90GEN3GB                 50.
90GEN3GC                 50.
C  emtp switch current defined as flowing left node to rgt
91GEN3A                                                          -1.0     9999.
91GEN3B                                                          -1.0     9999.
```

```
91GEN3C                                                              -1.0     9999.
C RMS_VALUE
88VT_A  66+GEN3GA                                    50.
88VRMS1A66+BUS1A                                     50.
88VDC     =(ABS(GEN3GA)+ABS(GEN3GB)+ABS(GEN3GC))*SQRT(3/2)/13800
88WREF    =2*PI*50
C tacs algebraic & logical fortran expressions for calculating P and Q etc
C OPNAME  =<-------------------------------------FREE FORMAT FORTRAN EXPRESSION
88REAL    = (GEN3GA*GEN3A) + (GEN3GB*GEN3B) + (GEN3GC*GEN3C)
88QA      =  GEN3GA * (GEN3C - GEN3B)
88QB      =  GEN3GB * (GEN3A - GEN3C)
88QC      =  GEN3GC * (GEN3B - GEN3A)
88REACT   =  (QA + QB + QC) * 0.57735027
C TACS_OUTPUT
C <-Name<-Name<-Name<-Name<-Name<-Name<-Name<-Name<-Name<-Name<-Name
33GEN3GAGEN3GBGEN3GCGEN3A GEN3B GEN3C
C TACS_IC
77VDC       1.732051
77VF              1.
77DVF             0.
77V2              0.
77VR              0.
77V1              1.
77V3              0.
C
77VEL1     314.15926
77TACOM          1.0
77PS1            0.0
77PGV            1.0
77PGV1           1.0
77PGV2           1.0
77PGV3           1.0
77PMT            1.0
77PM             1.0
BLANK card terminates TACS data
C ..............................Circuit_Data.................................
C Bus-->Bus--><----------><----R<----------L<----R<----------L<----R<----------L
51THEVA BUS7A               .0163      2.9638                                  0
52THEVB BUS7B               .0075       4.999                                  0
53THEVC BUS7C                                                                  0
C Bus-->Bus-->Bus-->Bus--><----R<----L<----C<----R<----L<----C<----R<----L<----C
 1BKR1A BUS12A            0.728510.209.06562
 2BKR1B BUS12B            0.59274.8968-.01510.748410.179.06834
 3BKR1C BUS12C            0.57954.0768-.00380.59274.8968-.01510.728610.209.06562
C Bus-->Bus-->Bus-->Bus--><---R'<---L'<---C'<--len 0 0 0<-------Blank--------->O
-1BUS7A BUS1A             0.3167 3.222.00787 144.4 0 0 0                       0
-2BUS7B BUS1B             0.0243 .9238 .0126 144.4 0 0 0                       0
-3BUS7C BUS1C                                                                  0
C Bus-->Bus-->Bus-->Bus--><----R<----L<----C                                   O
  BUS12ABUS13A                   70.16                                         0
  BUS12BBUS13BBUS12ABUS13A                                                     0
  BUS12CBUS13CBUS12ABUS13A                                                     0
  BUS13A                  221.41 38.26                                         0
  BUS13B      BUS13A                                                           0
```

```
  BUS13C      BUS13A                                                    0
C Saturable_transformer_components.
C ----------><-Bus3<----><----I<--Phi<BusSt<-Rmag<-------------------------->O
  TRANSFORMER                          DELTAB                            0
C -------current<-----------flux
            9999
C <-Bus1<-Bus2<----------><---Rk<---Lk<---Nk<--------------------------------->O
 1GEN3A GEN3B                     .0421  13.8                              0
 2BUS1A                          11.69132.79
C Note.- These Leakage values were calculated assuming a 3.5 % p.u reactance at
C        200 MVA for the transformer, divided in half between the two windings.
C <---------><-Bus3<---------------><BusSt
  TRANSFORMER DELTAB                   DELTBC
C <-Bus1<-Bus2
 1GEN3B GEN3C
 2BUS1B
  TRANSFORMER DELTAB                   DELTCA
 1GEN3C GEN3A
 2BUS1C
BLANK card terminates circuit data
C ................................Switch_data.................................
C BUS-->BUS--><---Tclose<----Topen<-------Ie                               O
  BUS1A BKR1A        -1.   580.E-3         0                               0
  BUS1B BKR1B        -1.   580.E-3         0                               0
  BUS1C BKR1C        -1.   580.E-3         0                               0
C Fault switch, duration is 330 ms
  BUS12A         250.E-3     9999.         0                               0
  BUS12B         250.E-3     9999.         0                               0
  BUS12C       99999.E-3     9999.         0                               0
C  Generator circuit breaker switch
  GEN3GAGEN3A        -1.     9999.  9999999.                               0
  GEN3GBGEN3B        -1.     9999.  9999999.                               0
  GEN3GCGEN3C        -1.     9999.  9999999.                               0
BLANK card terminates switch data
C ..................................Source Data.............................
C Bus--><I<Amplitude<Frequency<--TO|Phio<---O=PhiO<---Ignore<---Tstart<----Tstop
14THEVA     187.79E3       50.        0.        0.                 -1.     9999.
14THEVB     187.79E3       50.     -120.        0.                 -1.     9999.
14THEVC     187.79E3       50.      120.        0.                 -1.     9999.
C Dynamic Synchronous Machine
C Terminal connection for phase "a"
C Bus-->  <-----Volt<-----Freq<----angle
59GEN3GA    11267.65       50.    -30.43
  GEN3GB
  GEN3GC
C Machine Parameter Cards (Optional)
C ---------------------><-----FM
PARAMETER FITTING             1.
C Electrical Parameters of Machine
C <-<-<-NP<---SMOutP<---SMOutQ<-----RMVA<------RkV<---AGLINE<-------S1<-------S2
 1 1     2        1.        1.      200.      13.8   935.016     1000.     1440.
C Col: (1-2) NuMas, (3-4) KMac, (5-6) Kexc
C Note: AGLine is used to get the real magnitude in AMP of the field current
C                   in principle any value can be used here.
```

```
C ------->------AD1<------AD2<------AQ1<------AQ2<-----AGLQ<------S1Q<------S2Q
BLANK
C If S.M. is not saturable (AGLine >= 0), leave S1 -> S2Q Blank
C Manufacturer supplied pu data (if PARAMETER FITTING used)
C When transient data not available for Q-axis, make Xq' = Xq, TqO'=0
C This will eliminate the 'G' winding form the SM model.
C ------Ra<-------Xl<-------Xd<-------Xq<------X'd<------X'q<------X"d<------X"q
  0.001096      0.15      1.70      1.64   .238324      1.64   .184690   .185151
C ----T'dO<-----T'qO<-----T"dO<-----T"qO<-------XO<-------Rn<-------Xn<-------Xc
  6.194876        0.  0.028716  0.074960      1.40
C Mechanical parameters for the shaft system (mass card) .
C <------><----ExTrs<-----HICO<------DSR<------DSM<------HSP<------DSD
 1                1.   .181128
C col: (1-2) ML
BLANK card terminates mass data
C output requests
C GA<-->N1<---N2<---N3<---N4<---N5<---N6<---N7<---N8<---N9<--N10<--N11<--N12
  10
  21
  30
C Col: (3) Group, (4) All
BLANK card terminates synchronous machine output requests
C TACS input cards
C Exciter (EMTP assumes that the exciter is regulating to 1 pu = Vf-TACS = 1)
C Bus--><----><KI
71VF
72PM            1
74VEL1          2
  FINISH
BLANK card terminates source data
C ........................Output Request Data.............................
C Bus-->Bus-->Bus-->Bus-->Bus-->Bus-->Bus-->Bus-->Bus-->Bus-->Bus-->Bus-->
BLANK card terminates output requests
$CLOSE, UNIT=4 STATUS=KEEP
BLANK card terminates plot requests
BLANK card terminates EMTP solution-mode
```

F1.2 Example of BCTRAN Calculation file for 1.5 MVA Delta Star Transformer

```
BEGIN NEW DATA CASE
C ATP file tr_1_5dy.dat  tr-transformer, 1_5m - 1.5MVA, dy- delta star
C ------------------------------------------------------------------------
C transformer model used for CEPSI Paper.
C  11 kV/415 V  1.5 MVA transformer
C GEN1T?  high voltage delta winding
C GEN1?  low voltage star winding
C GEN1N  star point - connect earthing resistor here if required
C 25/4/96
C FILE TO DERIVE A LINEAR REPRESENTATION FOR A TRANSFORMER
C ------------------------------------------------------------------------
C        1         2         3         4         5         6         7         8
```

```
C 3456789-123456789-123456789-123456789-123456789-123456789-123456789-123456789-
ACCESS MODULE BCTRAN  { request for BCTRAN overlay
$ERASE   {Emtpy punch buffer, in case data already there from previous simu
C -- EXCITATION TEST DATA
C cols 1-2 no of windings/core leg|| NP - 0 true 3 phase trans, NP-1 singlephase
C let Exlos(kw) = 0.15 % -> 0.15/100 * 1.5 MVA = 2.25 kW (positive sequence)
C let Exlos(kw) = 0.30 % -> 0.30/100 * 1.5 MVA = 4.50 kW (zero sequence)
C <------POSITIVE SEQUENCE TEST PARAMETERS<--ZERO SEQ TST,D-WINDINGOPEN <-IT--IP
C <-----Freq<--Iex1(%)<--SN(MVA)<ExLos(kW)<--Iex0(%)<--SN(MVA)(ExLos(kW)NP--IW--
 2      50.0       1.3     1.500      2.25      100.     1.500       4.5 0 2 2-1
C Rated Line Voltaeges & Node names
C  first card - HV winding || second card MV or LV winding... (cols 1-2 wind no)
C ]<-Vrat(kV)<--WindRes <-IN A<-OUTA<-IN B<-OUTB<-IN C<-OUTC
  1      11.0           GEN1TAGEN1TBGEN1TBGEN1TCGEN1TCGEN1TA
  2    0.2396           GEN1A GEN1N GEN1B GEN1N GEN1C GEN1N
C -- SHORT CIRCUIT TEST
C Let short ciruit loss = 2% -> 2/100 * 1.5 MVA = 30 kW
C   <-POSITIVE SEQ TEST PARAMETERS<------ZERO SEQ TEST  IL
C <J<--LOS(kW)<--Zpos(%)<Spos(MVA)<--Zzer(%)<Szer(MVA)ID--
 1 2      30.0       5.5     1.500       4.5     1.500 0 1
BLANK card terminates input of short circuit test data
$PUNCH
BLANK card ends BCTRAN case
BEGIN NEW DATA CASE
BLANK card to end EMTP solution mode
```

BCTRAN OUTPUT FILE - tr_1_5dy.pch

```
$VINTAGE, 1,
 1GEN1A GEN1N              76.628252798683
 2GEN1B GEN1N              0.0
                           76.628252798683
 3GEN1C GEN1N              0.0
                           0.0
                           76.628252798683
  USE AR
 1GEN1TAGEN1TB             27.626520962479            2.42
 2GEN1A GEN1N              -1268.329426491             0.0
                           59164.519802098     .0011481632
 3GEN1TBGEN1TC             2.2886655921248             0.0
                           -105.0722934615             0.0
                           27.626520962479            2.42
 4GEN1B GEN1N              -105.0722934615             0.0
                           5724.2256543802             0.0
                           -1268.329426491             0.0
                           59164.519802098     .0011481632
 5GEN1TCGEN1TA             2.2886655921248             0.0
                           -105.0722934615             0.0
                           2.2886655921248             0.0
                           -105.0722934615             0.0
                           27.626520962479            2.42
 6GEN1C GEN1N              -105.0722934615             0.0
                           5724.2256543802             0.0
```

```
                          -105.0722934615             0.0
                          5724.2256543802             0.0
                          -1268.329426491             0.0
                          59164.519802098     .0011481632
$VINTAGE, 0,
$UNITS, -1.,-1.
  USE RL
C ----------------- << case separator >>> -----------
$VINTAGE, 1,
 1GEN1A GEN1N             76.628252798683
 2GEN1B GEN1N             0.0
                          76.628252798683
 3GEN1C GEN1N             0.0
                          0.0
                          76.628252798683
  USE RL
$UNITS, 0.50E+02 , 0.
 1GEN1TAGEN1TB                      2.42 12585.505242951
 2GEN1A GEN1N                        0.0 273.88431155028
                           .0011481632 5.9656982770407
 3GEN1TBGEN1TC                       0.0 -6166.886509987
                                     0.0 -134.3068074521
                                    2.42 12585.505242951
 4GEN1B GEN1N                        0.0 -134.3068074521
                                     0.0 -2.925446460501
                                     0.0 273.88431155028
                           .0011481632 5.9656982770407
 5GEN1TCGEN1TA                       0.0 -6166.886509987
                                     0.0 -134.3068074521
                                     0.0 -6166.886509987
                                     0.0 -134.3068074521
                                    2.42 12585.505242951
 6GEN1C GEN1N                        0.0 -134.3068074521
                                     0.0 -2.925446460501
                                     0.0 -134.3068074521
                                     0.0 -2.925446460501
                                     0.0 273.88431155028
                           .0011481632 5.9656982770407
$VINTAGE, 0,
$UNITS, -1.,-1.
  USE RL
C ----------------- << case separator >>> -----------
```

F1.3 ATP File Simulation Including a Fast Governor for Test 'FG2'

```
BEGIN NEW DATA CASE
$LISTOFF
POWER FREQUENCY                    50.0     {special request card
FIX SOURCE                                  {declaraction of EMTP Load Flow
AVERAGE OUTPUT
$COMMENT
C <DELTA<---TMAX<---XOPT<---COPT<-EPSILN<-TOLMAT<-Tstart
```

```
90.91E-6     1.0     50.     50.
C <-IOUT<--IPLOT<-IDOUBL<-KSSOUT<-MAXOUT<---IPUN<-MEMSAV<---ICAT<-NERERG<-IPRSUP
    1500      11       0       0                                    1
TACS HYBRID
C opName  s<--ip1 s<--ip2 s<--ip3 s<--ip4 s<--ip5 <-gain<-FxLo<-FxHi<-NmLo<-NmHi
C <--No,Do<----N1,D1<----N2,D2<----N3,D3<----N4,D4<----N5,D5<----N6,D6<----N7,D7
C NOTE-because the Tacs variuable Vf is scaled according to the initial value
C      the effective gain of the AVR will vary with loading, the gain may be
C      three times or more, the amount at full load compared to no load.
C      the _1 refers to PI1 , _2 on the variable name refers to PI2
C note the limiter function is set to -1 so that Vf can drop to zero, the
c highest it can be is 3 times initial value (i.e 3 times full load possibly ?)
C Anderson appendix D - typically 3 to 4  times full load
c
c AVR parameters for GEN1G - 0.750 MVA generator
C opName  s<--ip1 s<--ip2 s<--ip3 s<--ip4 s<--ip5 <-gain<-FxLo<-FxHi<-NmLo<-NmHi
C <--No,Do<----N1,D1<----N2,D2<----N3,D3<----N4,D4<----N5,D5<----N6,D6<----N7,D7
C Zero_block
 0VR_1    +V2_1                                        1.  -1.0   2.0
 0VF_1    +DVF_1  +UNITY                               1.
C S_block
 1V2_1    -V1_1   +UNITY  -V3_1                      700.
       1.0
       1.0       .10
 1V1_1    +VDC_1                                       1.
       1.0
       1.0       .03
 1DVF_1   +VR_1                                        1.
       1.0
       1.0       .50
 1V3_1    +DVF_1                                       1.
       0.0      .180
       1.0       .50
C  Speed Governor System for PI1 - Diesel governor first order approximation
C opName  s<--ip1 s<--ip2 s<--ip3 s<--ip4 s<--ip5 <-gain<-FxLo<-FxHi<-NmLo<-NmHi
C <--No,Do<----N1,D1<----N2,D2<----N3,D3<----N4,D4<----N5,D5<----N6,D6<----N7,D7
92VEL_1
C  CONVERSION OMEGA TO PER UNIT SYSTEM ( 4 pole 50 Hz -> w = pi*50)
99W_1     = .0031830988 * VEL_1
C Speed Governor System. value of 25 gives 4 % droop, 12 gives 8 %
 0DIF_W1  -UNITY  +W_1                              1.0
 0KDIFW1  +DIF_W1                                   25.
 0PS1_1   +UNITY  -KDIFW1                           1.0
 0PM_1    +PMD_1  +PMDEL1                           1.0      0.0  1.10
 1PS2_1   +PS1_1                                    1.0
       1.0
       1.0      0.04
C  governor main lag ranges from .04 to 0.4 (ATP wookbook 3, ch8)
c  Diesel Engine Firing Delay - 15 ms constant assumed for modelling purposes
C <-nameCDs<--IN1 s<--IN2 s<--IN3 s<--IN4 s<--IN5 <----A<----B<----C<----D<----E
98PMD_1 53+PS2_1                                        0.015
c  this block is necesary to fill
C <op-nmXX<--------A<--------B<--------CXXXXXXXXXXXXXXXXXXX<--T_start<---T_stop
11PMDEL1         1.0                                                0.     0.015
```

```
C <-NAME  <--------A<--------B<--------C                    <--T-START<---T-STOP
90GEN1GA                  50.
90GEN1GB                  50.
90GEN1GC                  50.
C  emtp switch current defined as flowing left node to rgt
91GEN1A                                                        -1.0
91GEN1B                                                        -1.0
91GEN1C                                                        -1.0
C tacs algebraic & logical fortran expressions for calculating P and Q etc
C OPNAME  =<-------------------------------------FREE FORMAT FORTRAN EXPRESSION
88REAL    = ((GEN1GA*GEN1A) + (GEN1GB*GEN1B) + (GEN1GC*GEN1C)) / 750.E3
88REACTA  = (GEN1GA*(GEN1C-GEN1B))
88REACTB  = (GEN1GB*(GEN1A-GEN1C))
88REACTC  = (GEN1GC*(GEN1B-GEN1A))
88REAC    = ((REACTA + REACTB + REACTC)*0.57735027) / 750.E3
C per unit impedance calculation
88IRMS    = SQRT( (GEN1A*GEN1A) + (GEN1B*GEN1B) + (GEN1C*GEN1C) )
88VDC_1   = SQRT( (GEN1GA*GEN1GA) + (GEN1GB*GEN1GB) + (GEN1GC*GEN1GC) ) / 415.0
88VRMS    =  VDC_1 * 415.
88R       = (REAL * VDC_1 * VDC_1) / ((REAL * REAL) + (REAC * REAC))
88X       = (REAC * VDC_1 * VDC_1) / ((REAL * REAL) + (REAC * REAC))
C TACS_output
c <-NAME<-NAME<-NAME<-NAME<-NAME<-NAME<-NAME<-NAME<-NAME<-NAME<-NAME<-NAME
33GEN1GAGEN1GBGEN1GCGEN1A GEN1B GEN1C
C 33REAC  REAL  PM_1
C R     X     VRMS  IRMS
C <-NAME  <-INIT_VAL
C AVR for GEN1 IC's
77VDC_1          1.0
77V1_1           1.0
77V2_1           0.0
77V3_1           0.0
77VR_1           0.0
77DVF_1          0.0
77VF_1           1.0
C Governor for PI1 IC's
77VEL_1    314.15926
77W_1            1.0
77PS1_1          1.0
77PS2_1          1.0
77PM_1           1.0
77PMDEL1         1.0
BLANK card terminates TACS data
C ..............................Circuit_Data.................................
C Thevenin Source Impedance - 70 MVA at 11 kV
C Bus-->Bus--><----------><----R<----------L<----R<----------L<----R<----------L
51GSPA  THVA              1.386       4.942
52GSPB  THVB              0.104       1.728
53GSPC  THVC
C recall Z11 = 1/3 (Z0 + 2 Z1) = 0.333 * (4.942 + 2(1.728)) = 2.79 ohms
C Numerical damping resistors for above Rp = 171.87 * XL(11)
  THVA  GSPA              380.6
  THVB  GSPB              380.6
  THVC  GSPC              380.6
```

```
C CABLES FROM GRID SUPPLY POINT TO GENERATOR TRANSFORMER
C Bus-->Bus-->Bus-->Bus--><----R<----L<----C<----R<----L<----C<----R<----L<----C
C feeder THVA to BUS1 (2 km of 20 kv  150 mm2 cable )
 1BUS3A BUS2A                .42   .26  220.
 2BUS3B BUS2B               .308 .1804  -10.   .42   .26  220.
 3BUS3C BUS2C               .308 .1804  -10.  .308 .1804  -10.   .42   .26  220.
C Numerical damping resistors for above Rp = 171.87 * XL(11)
  BUS2A BUS3A              34.68
  BUS2B BUS3B              34.68
  BUS2C BUS3C              34.68
C feeder THVA to BUS5 (2 km of 20 kv  150 mm2 cable)
 1THVA  BUS5A                .42   .26  220.
 2THVB  BUS5B               .308 .1804  -10.   .42   .26  220.
 3THVC  BUS5C               .308 .1804  -10.  .308 .1804  -10.   .42   .26  220.
C Numerical damping resistors for above Rp = 171.87 * XL(11)
  BUS5A THVA               34.68
  BUS5B THVB               34.68
  BUS5C THVC               34.68
C Bus-->Bus-->Bus-->Bus--><----R<----L<----C<----R<----L<----C<----R<----L<----C
C feeder BUS1 to BUS2 (2 km of 20 kv  150 mm2 cable)
 1BUS1A BUS2A                .42   .26  220.
 2BUS1B BUS2B               .308 .1804  -10.   .42   .26  220.
 3BUS1C BUS2C               .308 .1804  -10.  .308 .1804  -10.   .42   .26  220.
C Numerical damping resistors for above Rp = 171.87 * XL(11)
  BUS2A BUS1A              34.68
  BUS2B BUS1B              34.68
  BUS2C BUS1C              34.68
C Bus-->Bus-->Bus-->Bus--><----R<----L<----C<----R<----L<----C<----R<----L<----C
C feeder BUS5 to GEN1T (2 km of 20 kv  150 mm2 cable)
 1BUS5A GEN1TA               .42   .26  220.
 2BUS5B GEN1TB              .308 .1804  -10.   .42   .26  220.
 3BUS5C GEN1TC              .308 .1804  -10.  .308 .1804  -10.   .42   .26  220.
C Numerical damping resistors for above Rp = 171.87 * XL(11)
  GEN1TABUS5A              34.68
  GEN1TBBUS5B              34.68
  GEN1TCBUS5C              34.68
C
C LOCAL LOAD1 - 500 kW, 0.9 pf @ 11 kV RMS line to line
C Bus1->Bus2->            <----R<----L<----C
  GEN1TA                  196.16  94.8
  GEN1TB                  196.16  94.8
  GEN1TC                  196.16  94.8
C GENERATOR TRANSFORMER - 1.5 MVA 5.5% impedance
C .415/11 kV star delta transformer taken from BCTRAN output tr_1_5dy.pch
$VINTAGE, 1,
C Bus-->Bus-->Bus-->Bus--><--------------R<--------------L
 1GEN1A GEN1N             76.628252798683
 2GEN1B GEN1N             0.0
                          76.628252798683
 3GEN1C GEN1N             0.0
                          0.0
                          76.628252798683
  USE AR
 1GEN1TAGEN1TB            27.626520962479           2.42
```

```
 2GEN1A GEN1N              -1268.329426491            0.0
                           59164.519802098     .0011481632
 3GEN1TBGEN1TC             2.2886655921248            0.0
                           -105.0722934615            0.0
                           27.626520962479           2.42
 4GEN1B GEN1N              -105.0722934615            0.0
                           5724.2256543802            0.0
                           -1268.329426491            0.0
                           59164.519802098     .0011481632
 5GEN1TCGEN1TA             2.2886655921248            0.0
                           -105.0722934615            0.0
                           2.2886655921248            0.0
                           -105.0722934615            0.0
                           27.626520962479           2.42
 6GEN1C GEN1N              -105.0722934615            0.0
                           5724.2256543802            0.0
                           -105.0722934615            0.0
                           5724.2256543802            0.0
                           -1268.329426491            0.0
                           59164.519802098     .0011481632
$VINTAGE, 0,
$UNITS, -1.,-1.
  USE RL
C Generator Transformer Earthing Point - Solidly Earthed
C Bus1->Bus2->            <----R<----L<----C
  GEN1N                      0.1
  GEN1N                      0.1
  GEN1N                      0.1
BLANK card terminates circuit data
C ................................Switch_data.................................
C Generator Circuit Breaker
C BUS-->BUS--><---Tclose<----Topen<-------Ie                                 O
  GEN1GAGEN1A        -1.     9999.        0.                                 0
  GEN1GBGEN1B        -1.     9999.        0.                                 0
  GEN1GCGEN1C        -1.     9999.        0.                                 0
C GEN1T - BUS1 Circuit Breaker
C BUS-->BUS--><---Tclose<----Topen<-------Ie                                 O
  GEN1TABUS1A        -1.   440.E-3        0.                                 0
  GEN1TBBUS1B        -1.   440.E-3        0.                                 0
  GEN1TCBUS1C        -1.   440.E-3        0.                                 0
C GEN1T - BUS1 Circuit Breaker
C BUS-->BUS--><---Tclose<----Topen<-------Ie                                 O
  THVA  BUS3A        -1.   440.E-3        0.                                 0
  THVB  BUS3B        -1.   440.E-3        0.                                 0
  THVC  BUS3C        -1.   440.E-3        0.                                 0
C Fault Switch
  BUS2A          100.E-3   470.E-3        0.                                 0
  BUS2B          100.E-3   470.E-3        0.                                 0
  BUS2C          100.E-3   470.E-3        0.                                 0
BLANK card terminates switch data
C ..................................Source Data..............................
C Bus--><I<Amplitude<Frequency<--TO|Phio<---O=PhiO<---Ignore<---Tstart<----Tstop
14GSPA       8981.46       50.        0.        0.                -1.     9999.
14GSPB       8981.46       50.     -120.        0.                -1.     9999.
```

```
14GSPC       8981.46       50.      120.        0.                  -1.      9999.
C Dynamic Synchronous Machine - "generator"
C Terminal connection for phase "a"
C voltage has to be set differently to get right reactive flow
C Bus-->  <-----Volt<-----Freq<----angle
59GEN1GA     338.846       50.     -00.0
  GEN1GB
  GEN1GC
C ---------------------><-----FM
PARAMETER FITTING             1.
C Electrical Parameters of Machine
C <-<-<-NP<---SMOutP<---SMOutQ<-----RMVA<------RkV<---AGLINE<-------S1<-------S2
 1 1     2        1.        1.     0.750     0.415      -5.0     5.297     8.472
C ------->------AD1<------AD2<------AQ1<------AQ2<-----AGLQ<------S1Q<------S2Q
                                                          -1.
C ------Ra<-------Xl<-------Xd<-------Xq<------X'd<------X'q<------X"d<------X"q
    0.0322      0.10      2.63      1.57      0.21      1.57      0.15      0.18
C ----T'd0<-----T'q0<-----T"d0<-----T"q0<-------XO<-------Rn<-------Xn<-------Xc
       3.0       0.0     0.035     0.028     0.024
C Mechanical parameters for the shaft system (mass card) .
C 0.18E-3 --> an H of 0.5 s
C <------><----ExTrs<-----HICO<------DSR<------DSM<------HSP<------DSD
 1                1.   0.18E-3
C col: (1-2) ML
BLANK card terminates mass data
C output requests
C GA<-->><---N1<---N2<---N3<---N4<---N5<---N6<---N7<---N8<---N9<--N10<--N11<--N12
  10
  21
  30
C Col: (3) Group, (4) All
BLANK card terminates synchronous machine output requests
C Bus-->><---->KI
71VF_1          1
72PM_1          1
74VEL_1         2
  FINISH
BLANK card terminates source data
C EMTP LOAD FLOW         0 - P,Q     1 - P,V  2 - Q, THETA
C <-bus1<-bus2<-bus3<-------Pk-or-Qk<-------Qk-or-Vk<---Vmin<---Vmax<THmin<Thmax
0 GEN1GAGEN1GBGEN1GC          600.E3          450.E3    328.    348.
C         NNNOUT  NITERA  NFLOUT  NPRINT  RALCHK  CFITEV  CFITEA  VSCALE  KTAPER
               0    2000      20       0 0.00001     0.1     2.0               2
BLANK card terminates output requests
BLANK card terminates plot requests
BLANK card terminates EMTP solution-mode
```

F1.4 ATP Simulation File of Slow Loss of Synchronism During Loss of Field

```
C emtp simulation for thesis based on  625 Diesel gen at GEC Stafford
c The saturable transformer model has been used, instead of BCTRAN.
C Generator loss of field from 225 kW, showing effect of transient saliency.
```

```
C generator voltage is 415 V, (rating  625 kVA)
C contains full governor model.
C also contains a DY transformer at genertaor terminals
C Local load - 0.5 MW
C                                                    Matt Checksfield 10.12.96
BEGIN NEW DATA CASE
POWER FREQUENCY                      50.0     {special request card
FIX SOURCE                                    {declaraction of EMTP Load Flow
AVERAGE OUTPUT
$COMMENT
C <DELTA<---TMAX<---XOPT<---COPT<-EPSILN<-TOLMAT<-Tstart
125.0E-6    15.0     50.     50.
C             if Iplot every 5 --> 1600 Hz output (32 samps/cyc).
C                Iplot every 9 --> 888.8 Hz output (17.7 samps/cyc).
C                Iplot every 13 --> 615.4 Hz output (12.3 samp/cyc).
C <-IOUT<--IPLOT<-IDOUBL<-KSSOUT<-MAXOUT<---IPUN<-MEMSAV<---ICAT<-NERERG<-IPRSUP
    4500      81       1       1                                  1
TACS HYBRID
c  this block 'simulates' loss of field by ramping Vf to zero
C opName  s<--ip1 s<--ip2 s<--ip3 s<--ip4 s<--ip5 <-gain<-FxLo<-FxHi<-NmLo<-NmHi
0 VF_1    +LOE_1  +LOE_2                              1.   0.0   1.0
C <op-nmXX<--------A<--------B<--------CXXXXXXXXXXXXXXXXXXXX<--T_start<---T_stop
11LOE_1          1.0                                                -0.       0.3
24LOE_2         -1.0       0.1                                      0.2       0.3
c  Speed Governor System for PI1 - Diesel governor first order approximation
92VEL_1
C  CONVERSION OMEGA TO PER UNIT SYSTEM ( 4 pole 50 Hz -> w = pi*50)
99W_1     = .0063662 * VEL_1
C Speed Governor System. value of 25 gives 4 % droop, 12 gives 8 %
C droop settings on governors are notoriously variable (DAB)
 0DIF_W1  -UNITY  +W_1                            1.0
 0KDIFW1  +DIF_W1                                 25.
 0PS1_1   +UNITY  -KDIFW1                         1.0
 0PM_1    +PMDEL1 +PMD_1                          1.0      0.0  1.10
 1PS2_1   +PS1_1                                  1.0
       1.0
      1.0      0.10
c  Diesel Engine Firing Delay - 15 ms constant assumed for modelling purposes
C <-nameCDs<--IN1 s<--IN2 s<--IN3 s<--IN4 s<--IN5 <----A<----B<----C<----D<----E
98PMD_1 53+PS2_1                                        0.015
c  this block is necesary to fill in gap from delay
C <op-nmXX<--------A<--------B<--------CXXXXXXXXXXXXXXXXXXXX<--T_start<---T_stop
11PMDEL1         1.0                                                 0.     0.015
C Node_Voltage
C <-NAME  <--------A<--------B<--------C                    <--T-START<---T-STOP
90GEN1GA                  50.
90GEN1GB                  50.
90GEN1GC                  50.
C  emtp switch current defined as flowing left node to rgt
91GEN1A                                                          -1.0
91GEN1B                                                          -1.0
91GEN1C                                                          -1.0
C tacs algebraic & logical fortran expressions for calculating P and Q etc
C OPNAME  =<-----------------------------------FREE FORMAT FORTRAN EXPRESSION
```

```
88REAL    = ((GEN1GA*GEN1A) + (GEN1GB*GEN1B) + (GEN1GC*GEN1C))
88REACTA  = (GEN1GA*(GEN1C-GEN1B))
88REACTB  = (GEN1GB*(GEN1A-GEN1C))
88REACTC  = (GEN1GC*(GEN1B-GEN1A))
88REAC    = ((REACTA + REACTB + REACTC)*0.57735027)
88VRMSGA66+GEN1GA                                    50.
88IRMSA 66+GEN1A                                     50.
C control system input_fcns - normalise voltage to 1 pu using Vline to line RMS
88VDC_1   =SQRT( (GEN1GA*GEN1GA) + (GEN1GB*GEN1GB) + (GEN1GC*GEN1GC) ) / 415.0
88VRMS    =  VDC_1 * 415
C per unit impedance calculation
88R       = (REAL * VDC_1 * VDC_1) / ((REAL * REAL) + (REAC * REAC))
88X       = (REAC * VDC_1 * VDC_1) / ((REAL * REAL) + (REAC * REAC))
C TACS_output
c <-NAME<-NAME<-NAME<-NAME<-NAME<-NAME<-NAME<-NAME<-NAME<-NAME<-NAME<-NAME
33REAC  REAL  VRMS  IRMSA
C TACS_I.C.
C <-NAME  <-INIT_VAL
C AVR for GEN1 IC's
77VF_1           1.0
C Governor for PI1 IC's
77VEL_1    157.07963
77W_1            1.0
77PS1_1          1.0
77PS2_1          1.0
77PM_1           1.0
BLANK card terminates TACS data
C ..............................Circuit_Data.................................
C Thevenin Source Impedance
C Bus-->Bus--><----------><----R<----------L<----R<----------L<----R<----------L
51GSPA  THVA              1.386       4.942
52GSPB  THVB              0.104       1.728
53GSPC  THVC
C recall Z11 = 1/3 (Z0 + 2 Z1) = 0.333 * (4.942 + 2(1.728)) = 2.79 ohms
C Numerical damping resistors for above Rp = 171.87 * XL(11)
  THVA  GSPA              380.6
  THVB  GSPB              380.6
  THVC  GSPC              380.6
C CABLES FROM GRID SUPPLY POINT TO GENERATOR TRANSFORMER
C Bus-->Bus-->Bus-->Bus--><----R<----L<----C<----R<----L<----C<----R<----L<----C
C feeder THVA to BUS1 (2 km of 150 mm2 cable)
 1BUS3A BUS2A               .42   .26  220.
 2BUS3B BUS2B              .308 .1804  -10.   .42   .26  220.
 3BUS3C BUS2C              .308 .1804  -10.  .308 .1804  -10.   .42   .26  220.
C Numerical damping resistors for above Rp = 171.87 * XL(11)
  BUS2A BUS3A             34.68
  BUS2B BUS3B             34.68
  BUS2C BUS3C             34.68
C feeder THVA to BUS5 (2 km of 150 mm2 cable)
 1THVA  BUS5A               .42   .26  220.
 2THVB  BUS5B              .308 .1804  -10.   .42   .26  220.
 3THVC  BUS5C              .308 .1804  -10.  .308 .1804  -10.   .42   .26  220.
C Numerical damping resistors for above Rp = 171.87 * XL(11)
  BUS5A THVA              34.68
```

```
  BUS5B THVB               34.68
  BUS5C THVC               34.68
C Bus-->Bus-->Bus-->Bus--><----R<----L<----C<----R<----L<----C<----R<----L<----C
C feeder BUS1 to BUS2 (2 km of 150 mm2 cable)
 1BUS1A BUS2A               .42   .26  220.
 2BUS1B BUS2B              .308 .1804  -10.   .42   .26  220.
 3BUS1C BUS2C              .308 .1804  -10.  .308 .1804  -10.   .42   .26  220.
C Numerical damping resistors for above Rp = 171.87 * XL(11)
  BUS2A BUS1A              34.68
  BUS2B BUS1B              34.68
  BUS2C BUS1C              34.68
C Bus-->Bus-->Bus-->Bus--><----R<----L<----C<----R<----L<----C<----R<----L<----C
C feeder BUS5 to GEN1T (2 km of 150 mm2 cable)
 1BUS5A GEN1TA              .42   .26  220.
 2BUS5B GEN1TB             .308 .1804  -10.   .42   .26  220.
 3BUS5C GEN1TC             .308 .1804  -10.  .308 .1804  -10.   .42   .26  220.
C Numerical damping resistors for above Rp = 171.87 * XL(11)
  GEN1TABUS5A              34.68
  GEN1TBBUS5B              34.68
  GEN1TCBUS5C              34.68
C LOCAL LOAD1 - 500 kW, 0.9 pf @ 11 kV RMS line to line
C Bus1->Bus2->            <----R<----L<----C
  GEN1TA                  196.16  94.8
  GEN1TB                  196.16  94.8
  GEN1TC                  196.16  94.8
C Saturable_transformer_components.
C ----------><-Bus3<----><----I<--Phi<BusSt<-Rmag<--------------------------->O
  TRANSFORMER                        DELTAB                                  0
C -------current<----------flux
           9999
C <-Bus1<-Bus2<----------><---Rk<---Lk<---Nk<---------------------------------->O
 1GEN1A GEN1B             .7E-3 .00315 0.415                                  0
 2GEN1TA                   .198 2.218 6.3508
C Note.- These Leakage values were calculated assuming a 5.5 % p.u reactance at
C        1.5 MVA for the transformer, divided in half between the two windings.
C <---------><-Bus3<---------------><BusSt
  TRANSFORMER DELTAB                 DELTBC
C <-Bus1<-Bus2
 1GEN1B GEN1C
 2GEN1TB
  TRANSFORMER DELTAB                 DELTCA
 1GEN1C GEN1A
 2GEN1TC
BLANK card terminates circuit data
C ................................Switch_data.................................
C Generator Circuit Breaker
C BUS-->BUS--><---Tclose<----Topen<-------Ie                                  O
  GEN1GAGEN1A        -1.     9999.        0.                                  0
  GEN1GBGEN1B        -1.     9999.        0.                                  0
  GEN1GCGEN1C        -1.     9999.        0.                                  0
C GEN1T - BUS1 Circuit Breaker - fault clearing
C BUS-->BUS--><---Tclose<----Topen<-------Ie                                  O
  GEN1TABUS1A        -1.     9999.        0.                                  0
  GEN1TBBUS1B        -1.     9999.        0.                                  0
```

```
  GEN1TCBUS1C        -1.     9999.        0.                                    0
C GEN1T - BUS1 Circuit Breaker - fault clearing
C BUS-->BUS-->&lt;---Tclose&lt;----Topen&lt;-------Ie                                    O
  THVA  BUS3A        -1.     9999.        0.                                    0
  THVB  BUS3B        -1.     9999.        0.                                    0
  THVC  BUS3C        -1.     9999.        0.                                    0
C Fault Switch
  BUS2A          100.E-0  -440.E-3        0.                                    0
  BUS2B          100.E-0  -440.E-3        0.                                    0
  BUS2C          100.E-0  -440.E-3        0.                                    0
BLANK card terminates switch data
C .....................................Source Data.............................
C Bus-->&lt;I&lt;Amplitude&lt;Frequency&lt;--TO|Phio&lt;---O=PhiO&lt;---Ignore&lt;---Tstart&lt;----Tstop
14GSPA       8981.46       50.        0.        0.                  -1.     9999.
14GSPB       8981.46       50.     -120.        0.                  -1.     9999.
14GSPC       8981.46       50.      120.        0.                  -1.     9999.
C Dynamic Synchronous Machine - "generator"
C Terminal connection for phase "a"
C Bus-->  &lt;-----Volt&lt;-----Freq&lt;----angle
59GEN1GA     338.846       50.     -00.0
  GEN1GB
  GEN1GC
C  TOL    &lt;---EPSUBA&lt;---EPOMEG&lt;---EPDGEL----------&lt;---NIOMAX
C TOLERANCES              1.E-16                          20
C **EPSUBA is the built in damping value see p 8-5 of ref manual
C **EPOMEG is the tolerance for rotor speed iteration, if blank then the
C **default used.  Only minor benefits gained from tight convergence Criteria.
C Machine Parameter Cards (Optional)
C ---------------------><-----FM
PARAMETER FITTING             1.
C Electrical Parameters of Machine
C <-<-<-NP<---SMOutP<---SMOutQ<-----RMVA<------RkV<---AGLINE<-------S1<-------S2
 1 1     4        1.        1.     0.625     0.415      -5.0     5.297     8.472
C Col: (1-2) NuMas, (3-4) KMac, (5-6) Kexc
C Note: AGLine is used to get the real magnitude in AMP of the field current
C in principle any value can be used here.
C ------->&lt;------AD1&lt;------AD2&lt;------AQ1&lt;------AQ2&lt;-----AGLQ&lt;------S1Q&lt;------S2Q
                                                          -1.
C If S.M. is not saturable (AGLine >= 0), leave S1 -> S2Q Blank
C Manufacturer supplied pu data (if PARAMETER FITTING used)
C When transient data not available for Q-axis, make Xq' = Xq, TqO'=0
C This will eliminate the G winding form the SM model.
C Xq'' made up  = 1.5 * Xd'' , also Tqo'' = 0.75 * Tdo'' (kimbark III)
C ------Ra<-------Xl<-------Xd<-------Xq<------X'd<------X'q<------X"d<------X"q
      0.03      0.10      2.25      1.10      0.22      1.10      0.15      0.18
C ----T'dO<-----T'qO<-----T"dO<-----T"qO<-------XO<-------Rn<-------Xn<-------Xc
       4.5       0.0     0.035     0.028     0.051
C Mechanical parameters for the shaft system (mass card) .
C 0.9E-3 --> an H of 0.7 kWs/kVA ish ???
C <------><----ExTrs<-----HICO<------DSR<------DSM<------HSP<------DSD
 1                1.    0.9E-3
C col: (1-2) ML
BLANK card terminates mass data
C output requests
```

```
C GA<-->&lt;---N1<---N2<---N3<---N4<---N5<---N6<---N7<---N8<---N9<--N10<--N11<--N12
  10
  21
  30
C Col: (3) Group, (4) All
BLANK card terminates synchronous machine output requests
C TACS input cards
C Exciter (EMTP assumes that the exciter is regulating to 1 pu = Vf-TACS = 1)
C Bus-->&lt;---->&lt;KI
71VF_1          1
72PM_1          1
74VEL_1         2
  FINISH
BLANK card terminates source data
C EMTP LOAD FLOW         0 - P,Q     1 - P,V  2 - Q, THETA
C <-bus1<-bus2<-bus3<-------Pk-or-Qk<-------Qk-or-Vk<---Vmin<---Vmax<THmin<Thmax
0 GEN1GAGEN1GBGEN1GC          225.E3         -150.E3    328.    348.
C          NNNOUT  NITERA  NFLOUT  NPRINT  RALCHK  CFITEV  CFITEA  VSCALE  KTAPER
               0   10000      20       0 0.00001     0.1     2.0               2
C .........................Output Request Data.............................
C Bus-->Bus-->Bus-->Bus-->Bus-->Bus-->Bus-->Bus-->Bus-->Bus-->Bus-->Bus-->Bus-->
c  GSPA  GEN1A BUS1A BUS2A
BLANK card terminates output requests
BLANK card terminates plot requests
BLANK card terminates EMTP solution-mode
```

F2.1 C Code for PC Based Simulation of Single Blinder Scheme

```
int sngBldr (void)
{
/* trip signal issued if imp causes 'left' element to drop out */
/* trip output file is 2 for motor pole slip, 1 for gen pole slip */

    extern int sng_bldr_p, samp_cyc, per_unit;
    extern Real rating, vbase, sng_bldr_x_offset, sng_bldr_r_offset;
    extern Real sng_bldr_diam, sng_bldr_l_grad, sng_bldr_r_grad;
    extern Real sng_bldr_l_intcpt, sng_bldr_r_intcpt, sng_bldr_del;
    Real rad_sqrd, mod_term, r_offset, x_offset, pu_base;
    Real left_val, right_val;
    int l_bldr_pick, r_bldr_pick, trip = 0;
    static int flag_a = 0, flag_b = 0, old_l_pick = 0, old_r_pick = 0;
    static Real t1 = 0, t2 = 0;

    /*** is function enabled or not ? ****/
    if (sng_bldr_p == 0) return -1;
    pu_base = (vbase*vbase)/rating;

    /***  scale per unit values accordingly ***/
```

```
        if (per_unit == 0) {
        x_offset = sng_bldr_x_offset * pu_base;
        r_offset = sng_bldr_r_offset * pu_base;
        sng_bldr_diam = sng_bldr_diam * pu_base;
        sng_bldr_l_intcpt = sng_bldr_l_intcpt * pu_base;
        sng_bldr_r_intcpt = sng_bldr_r_intcpt * pu_base;
}
else {
        x_offset = sng_bldr_x_offset;
        r_offset = sng_bldr_r_offset;
}

left_val = ( (value(X)/sng_bldr_l_grad) + sng_bldr_l_intcpt);
right_val = ( (value(X)/sng_bldr_r_grad) + sng_bldr_r_intcpt);

/***** check which blinders have picked up ****/
if ( value(R) > left_val) l_bldr_pick = 1;
else l_bldr_pick = 0;
if ( value(R) < right_val) r_bldr_pick = 1;
else r_bldr_pick = 0;

/**** check if mho has picked up ****/
rad_sqrd = (sng_bldr_diam/2)*(sng_bldr_diam/2);
mod_term =  ( (value(X)-x_offset) * (value(X)-x_offset) ) +
                ( (value(R)-r_offset) * (value(R)-r_offset) );

if ( mod_term < rad_sqrd ) {
                /**** gen pole slip, cross first blinder (right) ******/
                if (old_r_pick == 0 && r_bldr_pick == 1){
                        t1 = value(TIME);
                        flag_a = 1;
                        flag_b = 0;
                }

                /***** motor pole slip, cross first blinder (left) *****/
                if (old_l_pick == 0 && l_bldr_pick == 1){
                        t1 = value(TIME);
                        flag_a = 0;
                        flag_b = 1;
                }

                /****** check if generator pole slip has happpened ******/
                if ( old_l_pick == 1 && l_bldr_pick == 0 && flag_a == 1 &&
                                                        flag_b == 0 && r_bldr_pick == 1){
```

```
                t2 = value(TIME);
                if ( (t2 - t1) >= sng_bldr_del){
                        trip = 1;
                        flag_a = flag_b = 0;
                        t1 = t2 = 0;
                }
                else {
                        flag_a = flag_b = 0;
                        t1 = t2 = 0;
                }
        }

        /***** check if motor pole slip has happened ******/
        if ( old_r_pick == 1 && r_bldr_pick == 0 && flag_a == 0 &&
                                                        flag_b == 1 && l_bldr_pick == 1){
                t2 = value(TIME);
                if ( (t2 - t1) >= sng_bldr_del){
                        trip = 2;
                        flag_a = flag_b = 0;
                        t1 = t2 = 0;
                }
                else {
                        flag_a = flag_b = 0;
                        t1 = t2 = 0;
                }
        }
    }
    else {
        trip = 0;
        flag_a = flag_b = 0;
        t1 = t2 = 0;
    }

/* update stored values of blinder outputs */
    old_r_pick = r_bldr_pick;
    old_l_pick = l_bldr_pick;

    set (SNG_T, trip);
    if (trip != 0) return 1;
    else return 0;
}
```

F2.2 C Code for PC Based Simulation of Power Based Pole Slipping Algorithm

```
/* ---------- POLE SLIPPING FUNCTION PROTOTYPES ----------*/

PRIVATE void init_pole_slip_lookup_tab (void);
PRIVATE void init_pole_slip_protection (void);
PRIVATE void pole_slip_pt_calc (void);

/*-------------------------------------------------------------------------
                    Pole Slipping Protection Data Structure
-------------------------------------------------------------------------*/
typedef struct
{
  /* Settings */
  int on_off_switch;                /* Flag indicates whether the */
                                    /* function is enabled or disabled. */
                                    /* 1 = enabled, 0 = disabled */

  Real Qtrip;   /** reactive trip level **/
  Real Ptol;  /* real power tolerance band in calc of Pt **/
  Real Pfact; /* input power estimation factor in Pt calc **/
  Real Dfact; /* maximum size of Dmin **/
  Real Dtran;  /* transient saliency */
  Real slip; /* used in Dmin calc **/
  int lag;  /* time setting used in Pt calc */

  /* Private */
  Real p1;   /* used in Pt calc - previous value of power */
  Real p2;   /* used in Pt calc - previous value of power */
  int  trip_count;              /** trip counter, trip at 6  */
  int  cnt_pmax_off;            /* counter used to reset Pmax to nominal */
  int  cnt_pmax;               /* counter used in pmax calc */
  Real lookup[8];       /* lookup index used in Dmin calc = ratio 10*pt/Pmax */
  int  count;             /* used in Pt calc function */
  int  trip;   /* 1 = true */

  /* Public Measurements */
  Real pt;  /* real power trip level */
  Real pmax;  /* maximum power output in last second */
  Real powerP; /* moving average value of power */
  Real powerQ; /* moving average value of power */
  Real Dmin;   /* rate of change of power trip level */
  Real deriv; /* rate of change of power */
```

```
} pole_slip_struct;

pole_slip_struct pole_slip_prot;

static float const master_look_up[8] = {
  /* Idx  Angle     Cos(Angle)*1000 */
  /*  0    180.000 */    -1.00000,
  /*  1    174.268 */          -0.99498,
  /*  2    168.522 */          -0.97980,
  /*  3    162.554 */          -0.95394,
  /*  4    156.491 */          -0.91652,
  /*  5    149.997 */          -0.86603,
  /*  6    143.130 */          -0.80000,
  /*  7    135.561 */          -0.71414
};

void init_pole_slip_lookup_tab(void)
{
  int i;
  /** initialsie lookup table based on the slip value **/
  for(i=0; i < 8; i++)
  pole_slip_prot.lookup[i] = pole_slip_prot.slip * master_look_up[i];
}

void init_pole_slip_protection(void)
{

  extern Real admit_trip, lg_ptol, lg_p_fact, dp_fact, dp_tran;
  extern Real rating, slip, lg_lag;
  extern int lgpg_p, samp_cyc, per_unit;

  if((samp_cyc != 4) && (samp_cyc != 8) && (samp_cyc != 12) &&
     (samp_cyc != 16) && (samp_cyc != 20) && (samp_cyc != 24) )
   {
   fatal("samples per cycle must be a multiple of 4 for power based pole slip function");
   }

    /** modify trip settings from  % rating actual values **/

  /*************** CHANGE VALUES ACCORDING TO PER UNIT SETTING *************/
  if (per_unit == 0)
  {
     pole_slip_prot.Qtrip = (-1/admit_trip) * rating;
     pole_slip_prot.Ptol = lg_ptol * rating;
```

```
    pole_slip_prot.Dfact = dp_fact * rating;
    pole_slip_prot.Dtran = dp_tran * rating;
    pole_slip_prot.pt = 0.01 * rating;  /* low so algorithm most secure */
    pole_slip_prot.pmax = 2 * rating;

  }
  else
  {
    pole_slip_prot.Qtrip = (-1/admit_trip);
    pole_slip_prot.Ptol = lg_ptol;
    pole_slip_prot.Dfact = dp_fact;
    pole_slip_prot.Dtran = dp_tran;
    pole_slip_prot.pt = 0.01;  /* low so algorithm most secure */
    pole_slip_prot.pmax = 2;

  }

  pole_slip_prot.Pfact = lg_p_fact;
  pole_slip_prot.slip = slip * 3.141593; /* scale slip up into proper units */
                                         /* i.e units of t radians 18/10/95 */
  pole_slip_prot.lag = lg_lag * 50;


/** initialise all other varaibles **/

  pole_slip_prot.on_off_switch = lgpg_p;
  pole_slip_prot.p1 = rating;
  pole_slip_prot.p2 = 0;   /* need p1 and p2 different so Pt does not */
                           /* incorrectly update */
  pole_slip_prot.trip_count = 0;
  pole_slip_prot.cnt_pmax_off = 0;
  pole_slip_prot.cnt_pmax = 0;
  pole_slip_prot.powerP = rating;
  pole_slip_prot.powerQ = 0;
  pole_slip_prot.Dmin = pole_slip_prot.Dfact;
  pole_slip_prot.deriv = 0;  /* will be initialised from
                             ** powerP and last_p_val */
  pole_slip_prot.count = 0;
  pole_slip_prot.trip  = 0;
}

int lgpg (void)
{ /* function needs to be processed 4 times per cycle */
  extern int samp_cyc, lgpg_p, per_unit;
```

```
extern Real rating;
Real pt_x10;
int pt_pmax;
Real lookup_val;
static int i = 0, k = 0;

if (lgpg_p == 0) return -1;

/*** initialise variables ***/
if (i == 0) {
   init_pole_slip_protection();
   init_pole_slip_lookup_tab();
}

if(i == samp_cyc/4)   /* so that function is processed @ 4 times/cyc */
{
    i = 0;              /* reset counter */
    pole_slip_prot.powerP = value(P);   /* half cycle moving average value of power */
    pole_slip_prot.powerQ = value(Q);   /* half cycle moving average value of power */

    /** call Pt calculation function every 20 ms ( 1 cycle )**/
    if (k == 4)
    {
          pole_slip_pt_calc();
          k = 0;
    }
    k++;

    /* Calculate adaptive Pmax every 5 ms (quarter cycle) */
    if ((pole_slip_prot.powerP) > pole_slip_prot.pmax)
    {  /* need 1 cycles worth of conditions before pmax re-calc'ed */
          pole_slip_prot.cnt_pmax ++;
          if (pole_slip_prot.cnt_pmax >=4)
          {
              pole_slip_prot.pmax = pole_slip_prot.powerP;
              pole_slip_prot.cnt_pmax = 1;
              pole_slip_prot.cnt_pmax_off = 1;
          }
    }
    else pole_slip_prot.cnt_pmax = 0;          /* reset counter */
    if (pole_slip_prot.cnt_pmax_off != 0)
    {
          pole_slip_prot.cnt_pmax_off ++;
          if (pole_slip_prot.cnt_pmax_off >= 200)
```

```
        {
            pole_slip_prot.cnt_pmax_off = 0;
            pole_slip_prot.pmax = 1.4 * pole_slip_prot.pt;
        }
    }
    else pole_slip_prot.pmax = 1.4 * pole_slip_prot.pt;

    /* Calculate dp/dt (dt = 1/(4xFsys) = 5ms for Fsys=50Hz) */
    pt_x10 = pole_slip_prot.pt * 10;  /* pt*10 to get lookup index
                                         ** (between 0 & 7) */

    /* pmax bombproofing if pmax = 0 then pt_pmax = 0  **/
    /* (0 is most secure trip level)  */
    if(pole_slip_prot.pmax == 0)
    {
        pt_pmax = 0;
        printf("warning function lgpg, Pmax = 0\n");
    }
    else
    {
        pt_pmax = (int)(pt_x10 / pole_slip_prot.pmax);
        /* pt/Pmax bombproofing incase pt_pmax > 7 or < 0  */
        if((pt_pmax > 7) || (pt_pmax < 0))
        {
            pt_pmax = 0;
            printf("warning function lgpg, Pt/Pmax = %d\n",pt_pmax);
        }
    }
    lookup_val = pole_slip_prot.lookup[pt_pmax];

    if(pt_pmax < 6) /* if in transient state add transient saliency */
        pole_slip_prot.Dmin = (pole_slip_prot.pmax * lookup_val) +
                                                        pole_slip_prot.Dtran;
    else
        pole_slip_prot.Dmin = (pole_slip_prot.pmax * lookup_val);

    if(pole_slip_prot.Dmin > pole_slip_prot.Dfact)
         pole_slip_prot.Dmin = pole_slip_prot.Dfact;

    pole_slip_prot.deriv = value(DP);

    /* Trip Determination hysteresis has been Implemented */
    if (pole_slip_prot.on_off_switch == 1)
    {
```

```
            if (pole_slip_prot.powerQ < pole_slip_prot.Qtrip)
            { /* if starter satisfied... */
                if ((pole_slip_prot.deriv  < pole_slip_prot.Dmin) &&
                        (pole_slip_prot.powerP < pole_slip_prot.pt  ))
                { /* if all pole slipping criteria met... */
                        pole_slip_prot.trip_count++;  /* inc trip counter */
                }
                else if (pole_slip_prot.trip != 1)
                {   /* else if started, but not tripped; reset */
                        pole_slip_prot.trip_count = 0;  /* reset counter */
                }
//          else  /* Implicit code: remain tripped while Q<Qtrip */
//          { /* else if started AND tripped; stay tripped */
//                  pole_slip_prot.trip_count = 6; /* hold counter at 6 */
//          }
            }
            else
                pole_slip_prot.trip_count = 0;      /* reset counter */

            if (pole_slip_prot.trip_count >= 6)
            {
                pole_slip_prot.trip_count = 6;      /* hold counter at 6 */
                pole_slip_prot.trip = 1;
                /** function_details |= POLE_SLIP; **/ /* SET OUTPUT */
            }
            else
            {
                pole_slip_prot.trip = 0;
                /** function_details &= ~POLE_SLIP;  **/ /* Reset Output */
            }
        }
        else
        {
            pole_slip_prot.trip = 0;
            pole_slip_prot.trip_count = 0;
            /** function_details &= ~POLE_SLIP; **/  /* Reset Output */
        }
    }
    i++;  /** variable i also used to get function working every 5 ms **/


    /** write to output file **/
    set (LG_DPMIN, pole_slip_prot.Dmin);
    set (LG_PT, pole_slip_prot.pt);
```

```
    set (LG_PMAX, pole_slip_prot.pmax);
    if(per_unit == 1) set (LG_T, (pole_slip_prot.trip*0.5) );
    else set (LG_T, (pole_slip_prot.trip*0.5*rating) );
    return pole_slip_prot.trip;
}

void pole_slip_pt_calc(void)
{ /* designed to be called every 20ms */
  extern Real rating;
  static int i = 0;

  /** only 3 sec of test data, initialise Pt & Pmax after two cycles **/
  if (i == 2)
  {
     pole_slip_prot.pt = pole_slip_prot.powerP * pole_slip_prot.Pfact;
     pole_slip_prot.p1 = pole_slip_prot.p2 = pole_slip_prot.powerP;
     pole_slip_prot.pmax = 1.4 * pole_slip_prot.pt;
  }
  i++;

  if (pole_slip_prot.on_off_switch == 1)
  {
    if (++pole_slip_prot.count >= pole_slip_prot.lag)
    {

      /* Pt calculation (done every lag*20ms) */
      if ((ABS(pole_slip_prot.powerP - pole_slip_prot.p2) <
                                                  pole_slip_prot.Ptol) &&
           (ABS(pole_slip_prot.powerP - pole_slip_prot.p1) <
                                                  pole_slip_prot.Ptol))
      {
          pole_slip_prot.pt = pole_slip_prot.powerP *
                                          pole_slip_prot.Pfact;

          if(pole_slip_prot.pt < 0) pole_slip_prot.pt = 10;
      }
      pole_slip_prot.p1 = pole_slip_prot.p2;
      pole_slip_prot.p2 = pole_slip_prot.powerP;

      pole_slip_prot.count = 0;          /* reset count */
    }
  }
  else /* pole_slip_prot.on_off_switch == 0 */
  {
```

```
    pole_slip_prot.p1 = rating;
    pole_slip_prot.p2 = 0;
    pole_slip_prot.pt = 0.01* rating;
    pole_slip_prot.count = 0;            /* reset count */
  }
}

/*================================-E-N-D-=====================================*/
```

2.3 IDMT OverCurrent Relay Simulation 'C' Code

```
int idmtOc (void)
{   /* qauntity P * In entered in config file as PU  (idmt_psm) */
    /* this is a voltage controlled o/c , unless idmt_vc set to -1 */
    /* when voltage drops below idmt_vc setting, then the current setting */
    /* (psm) is reduced by a factor of 0.4 (as in GEC CDV 22 & 62) */

    extern int idmt_p, idmt_type, samp_cyc, per_unit;
    extern Real idmt_psm, idmt_tms, idmt_vc, rating, vbase;
    static int reset_timer_a =  0, reset_timer_b = 0, reset_timer_c = 0;
    static Real integ_a = 0, integ_b = 0, integ_c = 0;
    int trip = 0, trip_a = 0, trip_b = 0, trip_c = 0;
    Real psm, volt_con, numer, timestep;
    double curr_a, curr_b, curr_c, power_of;

    if (idmt_p == 0) return -1;
    if (per_unit == 1) {
        psm = idmt_psm;
        volt_con = idmt_vc;
    } else {
        psm = idmt_psm * (rating/(1.73205*vbase));
        volt_con =  idmt_vc * (vbase * 0.5773502);
    }
    timestep = 1/(50*(Real)samp_cyc);

    /* set numerator and 'to the power of' expressions */
    if (idmt_type == 0) {
    numer = 13.5;
    power_of = 1;
    } else if (idmt_type == 1) {
    numer = 0.14;
    power_of = 0.02;
    } else if (idmt_type == 2) {
```

```
    numer = 80;
    power_of = 2;
    } else fatal("Invalid idmt_type '%d' in config file", idmt_type);

    /******************** Phase A element ************************/
    /* voltage control element */
    if (value(VRMS_A) < volt_con)
    {
        /* derive current in multiples of the tap setting */
        curr_a = value(IRMS_A) / (0.4 * psm);
    }
    else
        curr_a = value(IRMS_A) / psm;

    /* check whether to start integration process (current > 1)  */
    /* reset is done over 5 cycles as an exponential */
    if (curr_a >= 1 ) {
        integ_a += ( (pow(curr_a, power_of) - 1) * (timestep/numer) );
        reset_timer_a = 1;
    } else {
        if (reset_timer_a != 0) {
                integ_a = integ_a * exp ( -reset_timer_a/samp_cyc );
                reset_timer_a++;
                if (reset_timer_a == ((5 * samp_cyc) + 2) ) {
                        integ_a = 0;
                        reset_timer_a = 0;
                }
        }
    }

    /* check to see whether to trip or not */
    if (integ_a >= idmt_tms) {
    trip_a = 2;
    }
    else trip_a = 0;

/* note: the phase b and c elements have been removed for the thesis as they are identical to the phase a element */

    set (IDMT_T, (trip_a * psm));
    if (trip >= 2) return 1;
    else return 0;
}
```

2.4 Frequency Measuring Algorithm 'C' Code

```
PRIVATE Real calcFreq ()
{
   /** this function caluclates frequency using the zero crossing
   *  method outlined in 'MO17'
   *  NB: val[0] & val[1] are sample values either side of zero crossing
   *      at beginning, whilst val[2] & val[3] are values either side of
   *      zero crossing at end of measuring period (half cycle).
   *      fourier cosine components used.  2 CYCLE Cosine fourier
   *      filter used to smooth waveform
   **/

   /** variables for freq measurement **/
   extern int samp_cyc, per_unit;
   extern Real rcf_set;
   static int c_count = 0, timer = 0, reject = 1, i = 0;
   static Real val_c[4] = {0,1,2,3}, z_cc[2] = {1,2}, val[20];
   static Real c_freq_old = 0, c_freq_new = 50, old_freq = 50, movavg;
   static Real rej_lev;
   Real c_period = 0, freq, mvg;

   /** variables for 2 cycle cosine filter */
   static Real val_cos[85];
   static int x = 0;
   int z, n = 1;
   Real twopiN, lastval = 0, result = 0;

   if(samp_cyc > 40) fatal ("Function calcFreq, samp_cyc > 40");
   twopiN = (2 * 3.14159)/samp_cyc;
   lastval = val_cos[x];
   val_cos[x] = value(V_A);
   z = x - 1;

   while (z >= 0)
   {
     result += val_cos[z] * cos(twopiN * n);
     z--;
     n++;
   }
   z = (2*samp_cyc) - 1;

   while (z > x)
   {
```

```
    result += val_cos[z] * cos(twopiN * (Real)n);
    z--;
    n++;
  }
  result += ( (val_cos[x]/2) + (lastval/2) );
  result /= ((Real)samp_cyc * 0.5);

  if (x == ((2*samp_cyc) - 1)) x = 0;
  else x++;

  if (timer == 0) rej_lev = rcf_set/( (Real)samp_cyc * 5);
    /** NB mult by 5 , not 50 cos freq only changes every half cycle **/

  /** set new samples to  z_cc[1] **/
  z_cc[1] = result;

  /** check to see if zero crossing has just happened **/
  if(((z_cc[0] <= 0)&&(z_cc[1] > 0)) || ((z_cc[0] >= 0)&&(z_cc[1] < 0))){
        val_c[3]  = z_cc[1];
        val_c[2]  = z_cc[0];
        c_period = c_count + 1 - (val_c[0] / (val_c[0] - val_c[1]))
                               - (val_c[3] / (val_c[3] - val_c[2]));
        c_freq_old = c_freq_new;
        c_freq_new = (Real)samp_cyc * 12.5 / c_period;

        /** set values ready for next half cycle **/
        val_c[0] = val_c[2];
        val_c[1] = val_c[3];
        c_count = 1;
  }
  else c_count++;

  /** reset zero crossing detector values **/
  z_cc[0] = z_cc[1];
  timer++;

 /** check that max rate of change has not been exceeded **/

  if( timer > (int)((float)samp_cyc * 2.5) ) /* to ensure filter settled */
  {
          freq = c_freq_new + c_freq_old;
          if ( ABS(freq - old_freq) >= (rej_lev * reject/10) )
          {
           freq = old_freq;
```

```
            reject++;
            }
            else
            {
             old_freq = freq;
             reject = 1;
            }

            if (per_unit == 1) freq = freq/50;
    }
    else
    {
            if (per_unit == 1) freq = c_freq_new = 1;
            else freq = c_freq_new = 50;
    }

/** half cycle moving average filter (for smoothing, mainly for ROCOF) **/
    movavg -= val[i];
    val[i] = freq;
    movavg += val[i];
    mvg = movavg / ((Real)samp_cyc/2);

    if (i == ( (int)(samp_cyc/2) - 1)) i = 0;
    else i++;

    if (timer >= (2*samp_cyc) ) return mvg;
    else return c_freq_new;
}
```